

# INSIGHTS INTO BROWN ADIPOSE TISSUE FUNCTIONS AND BROWNING PHENOMENON

EDITED BY: Rita De Matteis, Paula Oliver and Assunta Lombardi  
PUBLISHED IN: Frontiers in Physiology



# frontiers

## Frontiers eBook Copyright Statement

The copyright in the text of individual articles in this eBook is the property of their respective authors or their respective institutions or funders. The copyright in graphics and images within each article may be subject to copyright of other parties. In both cases this is subject to a license granted to Frontiers.

The compilation of articles constituting this eBook is the property of Frontiers.

Each article within this eBook, and the eBook itself, are published under the most recent version of the Creative Commons CC-BY licence.

The version current at the date of publication of this eBook is CC-BY 4.0. If the CC-BY licence is updated, the licence granted by Frontiers is automatically updated to the new version.

When exercising any right under the CC-BY licence, Frontiers must be attributed as the original publisher of the article or eBook, as applicable.

Authors have the responsibility of ensuring that any graphics or other materials which are the property of others may be included in the CC-BY licence, but this should be checked before relying on the CC-BY licence to reproduce those materials. Any copyright notices relating to those materials must be complied with.

Copyright and source acknowledgement notices may not be removed and must be displayed in any copy, derivative work or partial copy which includes the elements in question.

All copyright, and all rights therein, are protected by national and international copyright laws. The above represents a summary only. For further information please read Frontiers' Conditions for Website Use and Copyright Statement, and the applicable CC-BY licence.

ISSN 1664-8714

ISBN 978-2-88963-657-0

DOI 10.3389/978-2-88963-657-0

## About Frontiers

Frontiers is more than just an open-access publisher of scholarly articles: it is a pioneering approach to the world of academia, radically improving the way scholarly research is managed. The grand vision of Frontiers is a world where all people have an equal opportunity to seek, share and generate knowledge. Frontiers provides immediate and permanent online open access to all its publications, but this alone is not enough to realize our grand goals.

## Frontiers Journal Series

The Frontiers Journal Series is a multi-tier and interdisciplinary set of open-access, online journals, promising a paradigm shift from the current review, selection and dissemination processes in academic publishing. All Frontiers journals are driven by researchers for researchers; therefore, they constitute a service to the scholarly community. At the same time, the Frontiers Journal Series operates on a revolutionary invention, the tiered publishing system, initially addressing specific communities of scholars, and gradually climbing up to broader public understanding, thus serving the interests of the lay society, too.

## Dedication to Quality

Each Frontiers article is a landmark of the highest quality, thanks to genuinely collaborative interactions between authors and review editors, who include some of the world's best academicians. Research must be certified by peers before entering a stream of knowledge that may eventually reach the public - and shape society; therefore, Frontiers only applies the most rigorous and unbiased reviews.

Frontiers revolutionizes research publishing by freely delivering the most outstanding research, evaluated with no bias from both the academic and social point of view. By applying the most advanced information technologies, Frontiers is catapulting scholarly publishing into a new generation.

## What are Frontiers Research Topics?

Frontiers Research Topics are very popular trademarks of the Frontiers Journals Series: they are collections of at least ten articles, all centered on a particular subject. With their unique mix of varied contributions from Original Research to Review Articles, Frontiers Research Topics unify the most influential researchers, the latest key findings and historical advances in a hot research area! Find out more on how to host your own Frontiers Research Topic or contribute to one as an author by contacting the Frontiers Editorial Office: [researchtopics@frontiersin.org](mailto:researchtopics@frontiersin.org)

# INSIGHTS INTO BROWN ADIPOSE TISSUE FUNCTIONS AND BROWNING PHENOMENON

Topic Editors:

**Rita De Matteis**, University of Urbino Carlo Bo, Italy

**Paula Oliver**, University of the Balearic Islands, Spain

**Assunta Lombardi**, University of Naples Federico II, Italy

**Citation:** De Matteis, R., Oliver, P., Lombardi, A., eds. (2020). Insights Into Brown Adipose Tissue Functions and Browning Phenomenon. Lausanne: Frontiers Media SA. doi: 10.3389/978-2-88963-657-0

# Table of Contents

- 05 Editorial: Insights Into Brown Adipose Tissue Functions and Browning Phenomenon**  
Paula Oliver, Assunta Lombardi and Rita De Matteis
- 08 Brown Adipose Tissue and Skeletal Muscle <sup>18</sup>F-FDG Activity After a Personalized Cold Exposure is not Associated With Cold-Induced Thermogenesis and Nutrient Oxidation Rates in Young Healthy Adults**  
Guillermo Sanchez-Delgado, Borja Martinez-Tellez, Yolanda Garcia-Rivero, Juan M. A. Alcantara, Francisco M. Acosta, Francisco J. Amaro-Gahete, Jose M. Llamas-Elvira and Jonatan R. Ruiz
- 18 Brown Adipose Tissue—A Therapeutic Target in Obesity?**  
Paul Trayhurn
- 23 Dietary Proteins, Brown Fat, and Adiposity**  
Lise Madsen, Lene Secher Myrmel, Even Fjære, Jannike Øyen and Karsten Kristiansen
- 36 Environmental Pollutants Effect on Brown Adipose Tissue**  
Ilaria Di Gregorio, Rosa Anna Busiello, Mario Alberto Burgos Aceves, Marilena Lepretti, Gaetana Paoletta and Lillà Lionetti
- 44 High Fat Diet Increases Circulating Endocannabinoids Accompanied by Increased Synthesis Enzymes in Adipose Tissue**  
Eline N. Kuipers, Vasudev Kantae, Boukje C. Eveleens Maarse, Susan M. van den Berg, Robin van Eenige, Kimberly J. Nahon, Anne Reifel-Miller, Tamer Coskun, Menno P. J. de Winther, Esther Lutgens, Sander Kooijman, Amy C. Harms, Thomas Hankemeier, Mario van der Stelt, Patrick C. N. Rensen and Mariëtte R. Boon
- 54 Regulation of Adaptive Thermogenesis and Browning by Prebiotics and Postbiotics**  
Bàrbara Reynés, Mariona Palou, Ana M. Rodríguez and Andreu Palou
- 69 Opposing Actions of Adrenocorticotrophic Hormone and Glucocorticoids on UCP1-Mediated Respiration in Brown Adipocytes**  
Katharina Schnabl, Julia Westermeier, Yongguo Li and Martin Klingenspor
- 83 Autophagy in Adipocyte Browning: Emerging Drug Target for Intervention in Obesity**  
Seung-Hyun Ro, Yura Jang, Jiyoung Bae, Isaac M. Kim, Cameron Schaecher and Zachery D. Shomo
- 94 Brown and Brite: The Fat Soldiers in the Anti-obesity Fight**  
Shireesh Srivastava and Richard L. Veech
- 107 Neuregulin 4 is a Novel Marker of Beige Adipocyte Precursor Cells in Human Adipose Tissue**  
Ferran Comas, Cristina Martínez, Mònica Sabater, Francisco Ortega, Jessica Latorre, Francisco Díaz-Sáez, Julian Aragonés, Marta Camps, Anna Gumà, Wifredo Ricart, José Manuel Fernández-Real and José María Moreno-Navarrete



- 116 *Beta 3 Adrenergic Receptor Activation Rescues Metabolic Dysfunction in Female Estrogen Receptor Alpha-Null Mice***  
Stephanie L. Clookey, Rebecca J. Welly, Dusti Shay, Makenzie L. Woodford, Kevin L. Fritsche, R. Scott Rector, Jaume Padilla, Dennis B. Lubahn and Victoria J. Vieira-Potter
- 131 *Fibroblast Growth Factor 21 and Browning of White Adipose Tissue***  
Daniel Cuevas-Ramos, R. Mehta and Carlos A. Aguilar-Salinas
- 140 *Secretory Proteome of Brown Adipocytes in Response to cAMP-Mediated Thermogenic Activation***  
Joan Villarroya, Rubén Cereijo, Marta Giralt and Francesc Villarroya
- 148 *Neonatal Resveratrol and Nicotinamide Riboside Supplementations Sex-Dependently Affect Beige Transcriptional Programming of Preadipocytes in Mouse Adipose Tissue***  
Madhu Asnani-Kishnani, Ana M. Rodríguez, Alba Serrano, Andreu Palou, M. Luisa Bonet and Joan Ribot
- 161 *Mechanisms of Impaired Brown Adipose Tissue Recruitment in Obesity***  
Martín Alcalá, María Calderon-Dominguez, Dolors Serra, Laura Herrero and Marta Viana
- 171 *Housing Temperature Modulates the Impact of Diet-Induced Rise in Fat Mass on Adipose Tissue Before and During Pregnancy in Rats***  
Layla Albustanji, Gabriela S. Perez, Enas AlHarethi, Peter Aldiss, Ian Bloor, Jairza M. Barreto-Medeiros, Helen Budge, Michael E. Symonds and Neele Dellschaft
- 182 *Important Trends in UCP3 Investigation***  
Elena E. Pohl, Anne Rupprecht, Gabriel Macher and Karolina E. Hilse
- 198 *Cold Induced Depot-Specific Browning in Ferret Aortic Perivascular Adipose Tissue***  
Bàrbara Reynés, Evert M. van Schothorst, Jaap Keijer, Enzo Ceresi, Paula Oliver and Andreu Palou



# Editorial: Insights Into Brown Adipose Tissue Functions and Browning Phenomenon

Paula Oliver<sup>1,2,3</sup>, Assunta Lombardi<sup>4</sup> and Rita De Matteis<sup>5\*</sup>

<sup>1</sup> Nutrigenomics and Obesity Group, University of the Balearic Islands, Palma, Spain, <sup>2</sup> Health Research Institute of the Balearic Islands (IdISBa), Palma, Spain, <sup>3</sup> CIBER de Fisiopatología de la Obesidad y Nutrición, Madrid, Spain, <sup>4</sup> Department of Biology, University of Naples Federico II, Naples, Italy, <sup>5</sup> Department of Biomolecular Sciences, University of Urbino Carlo Bo, Urbino, Italy

**Keywords:** thermogenesis, mitochondria, uncoupling proteins (UCPs), obesity, metabolic disease, adipocytes, dietary components

## Editorial on the Research Topic

### Insights Into Brown Adipose Tissue Functions and Browning Phenomenon

Originally identified as part of the thermogenic system in mammals, researchers were quick to perceive the potential of brown adipose tissue (BAT) to increase energy expenditure and to control energy homeostasis. Experimental evidence regarding the thermogenic capacity of BAT made it a plausible therapeutic target for inducing weight loss, increasing energy expenditure, and contributing to whole-body energy balance.

The recent discovery of functional BAT in humans has generated enormous interest, based on the already clear acceptance that the tissue is present, thermogenically active, and exhibits plasticity. The ability to recruit so-called brite/beige adipocytes within white adipose tissue (WAT) has further added to the focus on BAT. WAT browning represents a particularly intriguing concept in humans given the extreme amount of excess WAT in obese individuals. Moreover, the obesity pandemic and its metabolic complications have focused attention on adipose tissue and the molecular mechanisms underlying energy homeostasis, raising important questions concerning the metabolic proprieties of thermogenic fat.

This Research Topic aims to provide a thorough overview of research progress on BAT biology, exploring unexpected putative roles for brown/brite cells, and presenting new activators and physiological conditions promoting the browning process.

The Opinion article of Traythurn provides a comprehensive historical overview of the key role of BAT thermogenesis in the control of energy homeostasis and identifies the viability of therapeutic applications for obesity treatment, in the light of human metabolism. Although substantive evidence points to BAT activation and browning as interesting obesity therapeutic strategies, there are also substantive arguments against the realistic usefulness of this therapeutic approach in humans. Thus, in spite of the fact that active BAT contributes to glucose uptake and triglyceride clearance, its contribution to total energy expenditure is as yet not clear.

In this line, conflicting data about the contribution of BAT to cold-induced thermogenesis (CIT) in humans raise the question of the importance of BAT as a realistic therapeutic target to induce weight loss. The provocative original paper of Sanchez-Delgado et al. describes the effect of a personalized cold protocol on young adults. Contrary to what could be expected, their data show no contribution of either BAT or muscle activity to CIT or to cold-induced nutrient oxidation. Lack of a physiological plausible association could be due to experimental variability/technological limitations for human metabolism quantification, which is an important

## OPEN ACCESS

### Edited by:

Brian G. Drew,  
Baker Heart and Diabetes  
Institute, Australia

### Reviewed by:

Kazuhiro Nakamura,  
Nagoya University, Japan

### \*Correspondence:

Rita De Matteis  
rita.dematteis@uniurb.it

### Specialty section:

This article was submitted to  
Integrative Physiology,  
a section of the journal  
Frontiers in Physiology

**Received:** 30 January 2020

**Accepted:** 25 February 2020

**Published:** 06 March 2020

### Citation:

Oliver P, Lombardi A and De Matteis R  
(2020) Editorial: Insights Into Brown  
Adipose Tissue Functions and  
Browning Phenomenon.  
Front. Physiol. 11:219.  
doi: 10.3389/fphys.2020.00219

limitation in thermogenesis research. However, these results could also point to a marginal role of BAT in human CIT and, therefore, the energy metabolism.

Meanwhile, beyond their controversial role in energy waste and body weight control, it is now evident that brown/brite cells are involved in new functions that could transform the perspective of the tissue and its potential therapeutic application. Some contributions to this knowledge are published in this Research Topic. In recent years, in research mainly performed in rodents, browning of periaortic adipose tissue has been linked to cardiovascular protection. Reynés, van Schothorst et al. analyse cold response in adipose tissue of ferrets, a model closer to humans than rodents, and demonstrate clear adipose remodeling specifically in perivascular in comparison to subcutaneous fat. This browning induction along with the decreased expression of immune-related genes could be relevant for cardiovascular protection.

Moreover, the new concept of “metabolically active” BAT suggests that the beneficial effects of brown/brite activation could be due to UCP1 independent mechanisms, in both physiological and pathological conditions, associated with enhanced mitochondrial oxidative machinery. In the review of Pohl et al. the spotlight is focused on the emerging yet still enigmatic role played by UCP3 in BAT, the only tissue that simultaneously expresses two homologous proteins, with a similar proton transport rate but with UCP3 expression being 400-fold less than UCP1. The review also focuses on the molecular mechanism by which purine nucleotides differently inhibit UCP1 and UCP3, and on the direct correlation between UCP3 abundance and degree of cell fatty acid oxidation.

In addition, the emerging concept of a specific brown fat secretoma provides a physiologically significant link between adipose tissue, systemic metabolism, and health status. In this Research Topic, Villarroya et al. describe the brown adipocyte secretome in a cell culture medium in response to cAMP to mimic thermogenic activation. Surprisingly, most of the up-regulated secreted proteins correspond to extracellular matrix components, which could therefore play a key role in BAT remodeling. Unexpectedly, complement-related proteins are also secreted, probably contributing to signaling properties mediated by brown adipocytes. All the functions carried out by these secreted proteins are worth exploring in order to understand the metabolic roles of BAT. In this regard, Neuregulin 4 is a batokine that has become clinically relevant as a marker of metabolic health in murine models. Comas et al. show that, in humans, Neuregulin 4 may be considered a novel browning marker as its expression in adipose tissue correlates with that of brown/brite adipocyte markers and insulin action.

All in all, recent discoveries highlight the relevance of research concerning the physiological and pharmacological tools promoting brown/brite appearance of fat to thwart both excessive fat accumulation and consequent metabolic dysregulation.

The chronic effects of high-fat eating are more difficult to ignore, as an interesting article of Kuipers et al. describes in this Research Topic. In both white and brown fat of mice, the intake of a high-fat diet rapidly increases the synthesis pathways and circulating levels of endocannabinoids, which can

have autocrine and even paracrine effects on adipose tissue by inhibiting noradrenergic signaling through activation of the G-protein-coupled receptor CB1R. Activation of CB1R decreases lipolysis in WAT and thermogenesis in BAT, leading to a greater positive energy balance and contributing to the development of obesity. Therefore, selective inhibition of CB1R on brown adipocytes or inhibition of endocannabinoid synthesis appears as a potential anti-obesity strategy.

Another important topic is nutritional programming during pregnancy. The article of Albustanji et al. mainly focuses on the impact of housing temperature on fat mass gain during pregnancy, and confirms the confounding effect of temperature on the outcome of metabolic studies. The obesogenic capacity of diets at different housing temperatures may contribute to an understanding of the mechanisms by which diet influences obesity development during pregnancy, which is reflected in adipose tissue features (adipogenesis) and metabolic alterations in the pups.

An obesogenic environment contributes to the whitening of brown fat and to the pathological processes associated with obesity. This may influence the correct differentiation/recruitment of BAT through different processes, such as catecholamine resistance, inflammation, oxidative stress, and endoplasmic reticulum stress, as described in the review article by Alcalá et al.

On the other hand, the innovative article of Asnani-Kishnani et al. demonstrates that intake of specific food bioactives in early postnatal life can influence the fate of preadipocytes in WAT toward a brown-like adipogenesis transcriptional program. Particularly, the authors analyse the role of resveratrol and of the vitamin B3 form nicotinamide riboside orally administered to post-natal mice. These results point toward metabolic programming which could program a protection to developmental obesity, with sexual dimorphism.

Meanwhile, there is a case for emerging obesogenic stimuli coming from the environment. In this context, Di Gregorio et al. point attention to the opposite effects elicited by different environmental pollutants on body energy homeostasis and BAT thermogenic activity.

Unfortunately, the modern lifestyle puts pressure on the homeostatic system responsible for the regulation of body weight and metabolism. Redirecting nutritional, environmental, and behavioral (daily) habits could help us discover new physiological stimuli to unlock the therapeutic potential of brown/brite fat. For this purpose, three intriguing reviews are presented in this Research Topic: Srivastava and Veech present evidence from recent literature concerning the regulation of BAT activity and browning by endocrine factors, dietary- and phyto-derived components. The effect of physical exercise on BAT activity and browning is also analyzed, pointing toward the divergent response elicited by rodents and humans. Furthermore, Madsen et al. suggest that high protein diets may modulate the energy metabolism, including the possible role of activating brown and brite adipocytes, futile cycles, and UCP1-independent mechanisms. Intriguing data from rodent and human trials are discussed, pointing attention to the lack of consistence when comparing both species. Last but not least, Reynés, Palou et al.

suggest a key link between prebiotics and the regulation of adaptive thermogenesis and lipid metabolism (in both BAT and WAT). Thus, a connection is established between prebiotic consumption, microbiota selection (especially gut microbiota), production of microbiota metabolites, and regulation of the energy metabolism in adipose tissue, particularly regarding the effects on browning promotion, or on BAT recruitment.

This emerging dietary- and metabolite-mediated control of BAT activity and WAT browning could occur either directly or indirectly through specific modulation of traditionally noradrenergic regulation via  $\beta$ -adrenergic signaling. Adrenergic agonists are commonly considered to be inductors of WAT and BAT thermogenesis. In their original article, Clookey et al., by using a rodent model of menopause associated metabolic dysfunction [estrogen receptor alpha (ER $\alpha$ ) null mice], show that adrenergic activation mitigates the metabolic dysfunction associated to the loss of ER $\alpha$  signaling through WAT browning and UCP1 induction.

On the other hand, Schnabl et al. reveal novel non-adrenergic activators of brown adipocytes. They identify six non-adrenergic targets to activate and recruit UCP1 in BAT. Among these ligands, the adrenocorticotrophic hormone is described as one of the most potent activators of respiration and UCP-1 dependent thermogenesis in adipocytes, suggesting that, in physiological situations, it could mediate an acute effect of stress on BAT.

An important player in WAT browning induction is FGF21. The review of Cuevas-Ramos et al. describes the molecular pathways of browning induced by FGF21 and the UCP1-dependent and independent mechanisms by which FGF21 integrates metabolic pathways to regulate human energy balance and metabolism.

Finally, the review of Ro et al. focuses on the relevance of a proper regulation of autophagy in obesity prevention. In fact, obesity has been associated to autophagic dysregulation in adipose tissues. Therefore, as reviewed by the authors, an unexplored manipulation of the autophagic pathways could be considered in order to regulate WAT browning and adipogenesis reprogramming.

## CONCLUSIONS

Beyond the controversial contribution of BAT/browning to human whole-body energy expenditure, the new face/aspects presented in this Research Topic confirm the unequivocal evidence of the benefits conferred by the promotion of brown/brite phenotype of adipose tissue and give further evidence for its therapeutic role. Taking into consideration the available information, brown/brite adipocytes emerge as key players of metabolic homeostasis; therefore, new therapeutic perspectives, based on drugs, diet compounds/dietary and behavioral habits, and not necessarily focused on UCP1 activation, should be considered. Finally, a more profound understanding of the underlying mechanisms involved in browning promotion of energy homeostasis, which remains poorly understood, would help design health-promoting therapies.

## AUTHOR CONTRIBUTIONS

All authors have made a substantial, direct and intellectual contribution to the work, and approved it for publication.

## ACKNOWLEDGMENTS

We would like to thank all the Authors and Reviewers for their contributions to this collection of articles.

**Conflict of Interest:** The authors declare that the research was conducted in the absence of any commercial or financial relationships that could be construed as a potential conflict of interest.

*Copyright © 2020 Oliver, Lombardi and De Matteis. This is an open-access article distributed under the terms of the Creative Commons Attribution License (CC BY). The use, distribution or reproduction in other forums is permitted, provided the original author(s) and the copyright owner(s) are credited and that the original publication in this journal is cited, in accordance with accepted academic practice. No use, distribution or reproduction is permitted which does not comply with these terms.*



# Brown Adipose Tissue and Skeletal Muscle $^{18}\text{F}$ -FDG Activity After a Personalized Cold Exposure Is Not Associated With Cold-Induced Thermogenesis and Nutrient Oxidation Rates in Young Healthy Adults

Guillermo Sanchez-Delgado<sup>1\*</sup>, Borja Martinez-Tellez<sup>1,2</sup>, Yolanda Garcia-Rivero<sup>3,4</sup>, Juan M. A. Alcantara<sup>1</sup>, Francisco M. Acosta<sup>1</sup>, Francisco J. Amaro-Gahete<sup>1,5</sup>, Jose M. Llamas-Elvira<sup>3,4</sup> and Jonatan R. Ruiz<sup>1</sup>

## OPEN ACCESS

### Edited by:

Rita De Matteis,  
Università degli Studi di Urbino  
Carlo Bo, Italy

### Reviewed by:

Mueez U. Din,  
Turku PET Centre, Finland  
Kristin Stanford,  
The Ohio State University,  
United States

### \*Correspondence:

Guillermo Sanchez-Delgado  
gsanchezdelgado@ugr.es

### Specialty section:

This article was submitted to  
Integrative Physiology,  
a section of the journal  
Frontiers in Physiology

**Received:** 27 July 2018

**Accepted:** 22 October 2018

**Published:** 16 November 2018

### Citation:

Sanchez-Delgado G, Martinez-Tellez B, Garcia-Rivero Y, Alcantara JMA, Acosta FM, Amaro-Gahete FJ, Llamas-Elvira JM and Ruiz JR (2018) Brown Adipose Tissue and Skeletal Muscle  $^{18}\text{F}$ -FDG Activity After a Personalized Cold Exposure Is Not Associated With Cold-Induced Thermogenesis and Nutrient Oxidation Rates in Young Healthy Adults. *Front. Physiol.* 9:1577. doi: 10.3389/fphys.2018.01577

<sup>1</sup> PROFITH (PROmoting FITness and Health through Physical Activity) Research Group, Department of Physical Education and Sports, Faculty of Sport Sciences, University of Granada, Granada, Spain, <sup>2</sup> Department of Medicine, Division of Endocrinology and Einthoven Laboratory for Experimental Vascular Medicine, Leiden University Medical Center, Leiden, Netherlands, <sup>3</sup> Nuclear Medicine Department, "Virgen de las Nieves" University Hospital, Granada, Spain, <sup>4</sup> Nuclear Medicine Department, Biohealth Research Institute in Granada (ibs.GRANADA), Granada, Spain, <sup>5</sup> Department of Medical Physiology, School of Medicine, University of Granada, Granada, Spain

Cold induced thermogenesis (CIT) in humans results mainly from the combination of both brown adipose tissue (BAT) and skeletal muscle thermogenic activity. The relative contribution of both tissues to CIT and to cold induced nutrient oxidation rates (CI-NUTox) remains, however, to be elucidated. We investigated the association of BAT and skeletal muscle activity after a personalized cold exposure with CIT and CI-NUTox in 57 healthy adults ( $23.0 \pm 2.4$  years old;  $25.1 \pm 4.6$  kg/m<sup>2</sup>; 35 women). BAT and skeletal muscle (paracervical, sternocleidomastoid, scalene, longus colli, trapezius, parathoracic, supraspinatus, subscapular, deltoid, pectoralis major, and triceps brachii) metabolic activity were assessed by means of a  $^{18}\text{F}$ Fluorodeoxyglucose positron emission tomography-computed tomography scan preceded by a personalized cold exposure. The cold exposure consisted in remaining in a mild cold room for 2 h at  $19.5\text{--}20^\circ\text{C}$  wearing a water perfused cooling vest set at  $3.8^\circ\text{C}$  above the individual shivering threshold. On a separate day, we estimated CIT and CI-NUTox by indirect calorimetry under fasting conditions for 1 h of personalized cold exposure. There was no association of BAT volume or activity with CIT or CI-NUTox (all  $P > 0.2$ ). Similarly, the skeletal muscle metabolic activity was not associated either with CIT or CI-NUTox (all  $P > 0.2$ ). The results persisted after controlling for sex, the time of the day, and the date when CIT was assessed. Our results suggest that human BAT activity and skeletal muscle  $^{18}\text{F}$ -FDG activity are not associated to CIT in young healthy adults. Inherent limitations of the available radiotracers for BAT detection and muscle activity quantification may explain why we failed to detect a physiologically plausible association.

**Keywords:** brown fat, non-shivering thermogenesis, energy expenditure, energy balance, obesity, mild cold



## INTRODUCTION

Obesity is considered a public health problem of epidemic proportions (Ng et al., 2014). In simple terms, obesity results from a positive energy balance, and establishing a negative energy balance is a requisite for achieving weight loss. However, compensatory mechanisms, both physiological and behavioral, in response to short-term negative energy balance make it very difficult to establish a long-term energy deficit and sustainable weight loss (Palmer and Clegg, 2017). Thus, there are currently no non-invasive therapies capable of inducing sustainable weight loss, and developing new therapeutic strategies is, therefore, necessary (Palmer and Clegg, 2017).

Brown adipose tissue (BAT) was thought to be metabolically irrelevant or even absent in most human adults (Cannon and Nedergaard, 2004). However, recent evidence has shown that BAT is present and active in most, if not all, human adults (Nedergaard et al., 2007; Cypess et al., 2009; Saito et al., 2009; van Marken Lichtenbelt et al., 2009; Virtanen et al., 2009; Zingaretti et al., 2009). During the last decade, BAT has been regarded as a promising therapeutic target to tackle the obesity pandemic (Lee et al., 2013; Palmer and Clegg, 2017; Ruiz et al., 2018). Brown adipocytes are highly specialized thermogenic cells capable of taking up large quantities of energy substrates for producing heat by means of uncoupling mitochondrial respiration (Cannon and Nedergaard, 2004). In murine, BAT is responsible for a large proportion of both resting metabolic rate (RMR) and adaptive thermogenesis [i.e., diet-induced thermogenesis and cold-induced thermogenesis (CIT)] (Garland et al., 2011). However, although the total BAT volume in humans is still unknown (Martinez-Tellez et al., 2018), it is clear that adult humans present a considerable lower proportional amount (i.e., in relation to body weight) of BAT than murine (Leitner et al., 2017). Furthermore, murine and human BAT seem to have different molecular signatures and functionalities (Cypess et al., 2013; Muzik et al., 2013; Peirce et al., 2014). Therefore, it is still not clear whether human BAT is able to produce a relevant increase in the energy expenditure in adult humans (Marlatt et al., 2018).

The main reason why BAT contribution to human energy expenditure is still unknown is the lack of technology to properly assess its contribution *in vivo* (Ong et al., 2018). The most used technique to assess BAT volume and activity is the  $^{18}\text{F}$ -fluorodeoxyglucose ( $^{18}\text{F}$ -FDG) positron-emission tomography and computed tomography (PET-CT) scan (Carpentier et al., 2018). Besides implicating high ionizing radiation exposure, one of the  $^{18}\text{F}$ -FDG-PET-CT scan's main limitation relates to the substrate preference of BAT. The  $^{18}\text{F}$ -FDG radiotracer is a glucose analog. However, several studies have shown that brown adipocyte's energy expenditure mainly relies on fatty acid oxidation (Schilperoort et al., 2016; Blondin et al., 2017). Although other alternatives to the  $^{18}\text{F}$ -FDG-PET-CT scan are being used, several limitations preclude the existence of a real gold-standard for *in vivo* BAT assessments in humans (Ong et al., 2018). Among the alternatives to  $^{18}\text{F}$ -FDG-PET-CT, the skin temperature of the supraclavicular area has been used as an indirect marker of BAT activity, which would allow non-invasive

and continuous assessments (Boon et al., 2014; van der Lans et al., 2016).

Besides the technical limitations to study the BAT contribution to human energy expenditure, it has been suggested that BAT could just be a minor contributor to CIT in humans, while skeletal muscle, by means of both shivering and non-shivering thermogenesis, could be the main effector of CIT (Muzik et al., 2013; Blondin et al., 2015b; Jensen, 2015; U Din et al., 2016; Palmer and Clegg, 2017). Moreover, it has been suggested that not only skeletal muscle, but also white adipose tissue, could play a role in CIT (Blondin et al., 2015b; Betz and Enerbäck, 2017). To date, there are contradictory findings regarding the relative contribution of both human BAT and skeletal muscle to CIT (Muzik et al., 2013; van der Lans et al., 2013; Bakker et al., 2014; Chondronikola et al., 2014; Blondin et al., 2015b; Jensen, 2015; U Din et al., 2016; Yoneshiro et al., 2016; Palmer and Clegg, 2017; Porter, 2017), and more studies are needed to fully understand the relation of BAT and skeletal muscle activity with CIT. The relation of BAT and skeletal muscle activity with cold-induced nutrient oxidation rates (CI-NUTox) has received much less attention and remains to be elucidated. Changes in the pattern of nutrient oxidation are related to overall metabolic health (Galgani et al., 2008; Goodpaster and Sparks, 2017; Fernández-Verdejo et al., 2018). Thus, even if BAT or skeletal muscle non-shivering thermogenesis had a small impact on energy expenditure, they would still be very interesting therapeutic targets for human metabolic health improvements if they modify the substrate oxidation.

This study aimed to investigate the association of BAT and skeletal muscle  $^{18}\text{F}$ -FDG activity after a personalized cold exposure with CIT and CI-NUTox in young healthy adults. Additionally, we examined the association of supraclavicular skin temperature as a proxy of BAT activity with CIT and CI-NUTox rates.

## MATERIALS AND METHODS

### Participants

We used data from two different cohorts. The participants were young (18–25 years old), healthy, did not smoke or take any medication, had had a stable body weight in the previous 3 months ( $< 3$  kg change), and were not regularly exposed to cold. A total of 57 young healthy adults ( $23.0 \pm 2.4$  years old;  $25.1 \pm 4.6$  kg/m<sup>2</sup>; 35 women) participated in the present study (Table 1). Forty-four participants (29 women) were part of the ACTIBATE study (Study 1), a randomized controlled trial aiming to study the effect of exercise on BAT volume and activity (clinicaltrials.gov: NCT02365129) (Sanchez-Delgado et al., 2015). Only 18 out of these 44 participants met the required fasting time (6–8 h) to be included in the analyses referred to CI-NUTox (Table 1). The data for Study 1 was collected between October and November 2016. In addition, 13 participants were enrolled (Table 1) in Study 2, which was conducted between December 2017 and January 2018.

The participants signed a written informed consent, and both the informed consent and the whole study were approved by

the Human Research Ethics Committee of the University of Granada (n°924) and of the Servicio Andaluz de Salud (Centro de Granada, CEI-Granada), and was performed following the Declaration of Helsinki (last revision).

## Procedures

**Study 1.** The data were collected on three days. The participants were always required to come to the research center by bus or by car (i.e., with the minimum possible physical activity), in a fasting state (>6 h), after having slept as usual, and having refrained from stimulant beverages and any moderate (within the previous 24 h) or vigorous (within the previous 48 h) physical activity.

On the first day, we assessed the participants' shivering threshold (i.e., the lowest tolerable temperature without external observed or auto-reported shivering) (Martinez-Tellez et al., 2017c). After having checked that they met the previous conditions, the participants rested in a warm room for 30 min while wearing standardized clothes (Flip-flops, shorts, and a T-shirt; clo-value: 0.20). Later, the participants entered a mild cold room (19.5–20°C) and were equipped with a water-perfused cooling vest (Polar Products Inc., Ohio, United States) set at 16.6°C. They were required to remain seated and relaxed while the water temperature was progressively decreased (approximately 2°C every 10 min) until a temperature of 3.8°C was reached (at which the participants remained exposed for 45 additional minutes) or shivering occurred. We determined shivering visually and by asking the participants if they were experiencing shivering. The water temperature at which shivering occurred was considered the shivering threshold.

On the second day, we assessed BAT and skeletal muscle  $^{18}\text{F}$ -FDG activity by a static  $^{18}\text{F}$ -FDG PET-CT scan after a personalized cold exposure (Martinez-Tellez et al., 2017c). Prior to the PET-CT scan, the participants were exposed to a 2-h

personalized cooling protocol, using the same water-perfused vest as in the shivering threshold test but set at 3.8°C above the individual shivering threshold, in a mild cold room (19.5–20°C). One hour after starting the cooling protocol, a bolus of approximately 5 mCi ( $\approx 185$  MBq) of  $^{18}\text{F}$ -FDG was injected through a peripheral catheter, and the water temperature was increased by 1°C to avoid shivering. Immediately after the cooling protocol, we performed the static PET-CT scan and obtained PET-CT images from the atlas vertebrae (Cervical 1) to the thoracic vertebrae 6, approximately.

On the third day, we assessed CIT and CI-NUTox. After voiding their bladders, the participants wore the same standardized clothes (clo: 0.20) as on the other testing days and moved into a warm ( $23.2 \pm 0.7^\circ\text{C}$ ) quiet room. Before the evaluation, the participants lay down on a reclined bed, in supine position, and covered by a sheet for 20 min. Later, RMR was assessed using indirect calorimetry for 30 min following the current methodological recommendations (Fullmer et al., 2015). They were instructed to breathe normally and not to talk, fidget, or sleep. After assessing RMR, the participants were moved into the cold room (19.5–20°C). They once again wore the temperature-controlled water perfused cooling vest set at the lowest tolerable temperature on the second day (i.e., 3.8°C above the individual's shivering threshold, except for those who required changes in water temperature to avoid shivering during the cold-exposure previous to the PET-CT) (Study 1). Then, they lay down on a bed with the same reclined position as the one used for the RMR assessment and were instructed to breathe normally and not to talk, fidget, or sleep. Then, the CIT measurement was performed during two consecutive 30-min periods, separated by a 5-min pause to recalibrate the metabolic cart, during which they continued exposed to cold.

Additionally, on a different day, we measured the participant's body composition by dual-energy x-ray absorptiometry scan (Discovery Wi, Hologic, Inc., Bedford, MA, United States). Weight and height were also measured by a Seca scale and a stadiometer (model 799, Electronic Column Scale, Hamburg, Germany).

**Study 2.** This study followed a similar procedure to Study 1, except for some minor differences. BAT and skeletal muscle  $^{18}\text{F}$ -FDG activity was not assessed, so Study 2 only included two testing days. On the shivering threshold test (day 1) the participants lay on a bed instead of being seated, and the fasting time before the CIT assessment was 10 h. Additionally, the time between the shivering threshold test and the CIT assessment was 48 h instead of 5–7 days.

## $^{18}\text{F}$ -FDG-PET-CT Scan Analysis

We performed and analyzed the  $^{18}\text{F}$ -FDG-PET-CT scan (Siemens Biograph 16 PET-CT, Siemens, Germany) following the protocol extensively described elsewhere (Martinez-Tellez et al., 2017c, 2018) and in agreement with current methodological recommendations for human BAT assessment (Chen et al., 2016). We analyzed the images using the Beth Israel plugin for FIJI software (Schindelin et al., 2012). For the BAT assessment we applied a fixed range of Hounsfield units (HU, -190 to -10) (Chen et al., 2016) and an individualized SUV threshold: 1.2/(lean

**TABLE 1 |** Descriptive characteristics of the participants included in the energy expenditure analyses.

	CIT analyses (Study 1) (n = 44)	NUTox analyses (Study 1) (n = 18)	No PET-CT (Study 2) (n = 13)
Sex (women, %)	29 (65.9)	13 (72.2)	6 (46.2)
Age (years)	22.2 (2.2)	21.9 (2.0)	25.6 (3.0)
BMI ( $\text{kg}/\text{m}^2$ )	25.6 (5.3)	24.3 (4.6)	23.6 (2.4)
Lean mass (kg)	42.7 (10.4)	40.4 (8.0)	45.7 (13.3)
Fat mass (kg)	27.2 (10.6)	25.0 (9.6)	18.4 (3.8)
Fat mass percentage (%)	37.0 (8.0)	36.1 (7.0)	28.4 (6.6)
RMR (kcal/day)	1565 (278)	1554 (227)	1484 (286)
BAT volume (ml)	94.4 (59.6)	74.29 (49.7)	
BAT SUV mean	4.29 (1.60)	4.24 (1.11)	
BAT SUV peak	14.13 (7.22)	13.40 (6.08)	
Muscle SUV peak	1.67 (0.33)	1.63 (0.33)	
Descending aorta SUV peak	0.92 (0.21)	0.83 (0.20)	

Data are presented as means (standard deviation). BMI: Body mass index; RMR: Resting metabolic rate; BAT: Brown adipose tissue; SUV: Standardized uptake value; CIT: Cold-induced thermogenesis; NUTox: Nutrient oxidation rates.

body mass/body mass) (Chen et al., 2016). We calculated BAT volume, BAT mean activity (SUV mean), and BAT maximal activity (SUV peak). In addition, we calculated the SUVpeak of several skeletal muscles (paracervical, sternocleidomastoid, scalene, longus colli, trapezius, parathoracic, supraspinatus, subscapular, deltoid, pectoralis major, and triceps brachii), and averaged the obtained value from all muscles in both sides of the body. Furthermore, we grouped these muscles into deep (paracervical, scalene, longus colli, paravertebral, subscapular), cervical (paracervical, sternocleidomastoid, scalene, longus colli), and cold sensitive (sternocleidomastoid, scalene, longus colli, pectoralis major) muscles, since it has been shown that these muscle groups could have a different behavior than others upon cold exposure (Blondin et al., 2015b). Additionally, a ROI was drawn in the descending aorta to be used as a reference tissue.

### CIT and CI-NUTox Estimations

The indirect calorimetry measurements for both RMR and CIT were performed using a neoprene face-mask connected to a CCM Express/Ultima CardiO2 metabolic cart (Medgraphics Cardiorespiratory Diagnostic, Saint-Paul, MN, United States) equipped with a directconnect<sup>TM</sup> metabolic flow sensor (Medgraphics Corp, Minnesota, United States) (Sanchez-Delgado et al., 2017; Alcantara et al., 2018). The flow calibration was performed by a 3-L calibration syringe at the beginning of every test day, and the gas analyzers were calibrated using 2 standard gas concentrations before every 30-min bout of indirect calorimetry measurement following the manufacturers' instructions. We used the same metabolic cart for RMR and CIT in all participants.

Indirect calorimetry data were averaged every minute and downloaded from the Breeze Suite 8.1.0.54 SP7 software (Medgraphics Cardiorespiratory Diagnostic, Saint-Paul, MN, United States). For RMR, we selected the most stable 5-min period (i.e., the one with the lowest average coefficients of variance of oxygen consumption, carbon dioxide production, minute ventilation, and respiratory exchange ratio), after excluding the first 5 min recorded (Sanchez-Delgado et al., 2017). To obtain a single representative value of CIT, we divided the 60 min recorded into 4 periods (i.e., 15 min each). We then selected the most stable 5-min period within every 15-min period (using the same criteria than for RMR). Finally, we used the 4 selected 5-min periods together with the RMR to calculate the area under the curve (trapezoidal rule), expressing it as a percentage of RMR (Sanchez-Delgado et al., 2018a).

Oxygen consumption and carbon dioxide production for each selected data point were used to estimate energy expenditure, carbohydrates (CHO<sub>ox</sub>), and fat oxidation (FAT<sub>ox</sub>). Energy expenditure was estimated through Weir's abbreviated equation (Weir, 1949). For CHO<sub>ox</sub> and FAT<sub>ox</sub> estimations, we used Frayn's equations (Frayn, 1983). We did not include urinary nitrogen data into the equations.

In addition to indirect calorimetry, we also recorded the skin temperature of several body locations (Martinez-Tellez et al., 2017a) throughout the CIT assessment by iButtons (DS-1922 L, Thermochron; resolution 0.0625°C; Maxim, Dallas, United States). All iButtons were attached to the skin with

adhesive tape (Fixomull, Beiersdorf AG, Hamburg, Germany), and we estimated the mean skin temperature (ISO-standard 9886:2004, 2004). Finally, we calculated the difference between the warm value and the temperature for the subclavicular and supraclavicular skin temperature at the end of the cooling protocol. All data recorded by the devices were processed and analyzed by the Temperatus<sup>®</sup> software<sup>1</sup>

### Statistical Analyses

The distribution of the variables was verified using the Shapiro-Wilk test, skewness and kurtosis values, visual check of histograms, Q-Q, and box plots. The descriptive statistics are presented as mean  $\pm$  standard deviation, unless otherwise stated. The analyses were conducted using the Statistical Package for Social Sciences (SPSS, v. 21.0, IBM SPSS Statistics, IBM Corporation), and the level of significance was set at  $< 0.05$ .

We used simple linear regression analyses to test the association of BAT and skeletal muscle <sup>18</sup>F-FDG activity after a personalized cold-exposure and supraclavicular temperature with CIT and CI-NUTox. We also used multiple linear regression models to test these associations adjusting by sex, BMI, the time of the day, and the date when CIT was assessed. Furthermore, we used repeated-measures analyses of variance (ANOVA) to study the cold-induced changes on skin temperature parameters. BAT and skeletal muscle <sup>18</sup>F-FDG activity after a personalized cold-exposure was only assessed in Study 1. Therefore, Study 2 was only included in the analyses studying the association of the supraclavicular skin temperature with CIT and CI-NUTox.

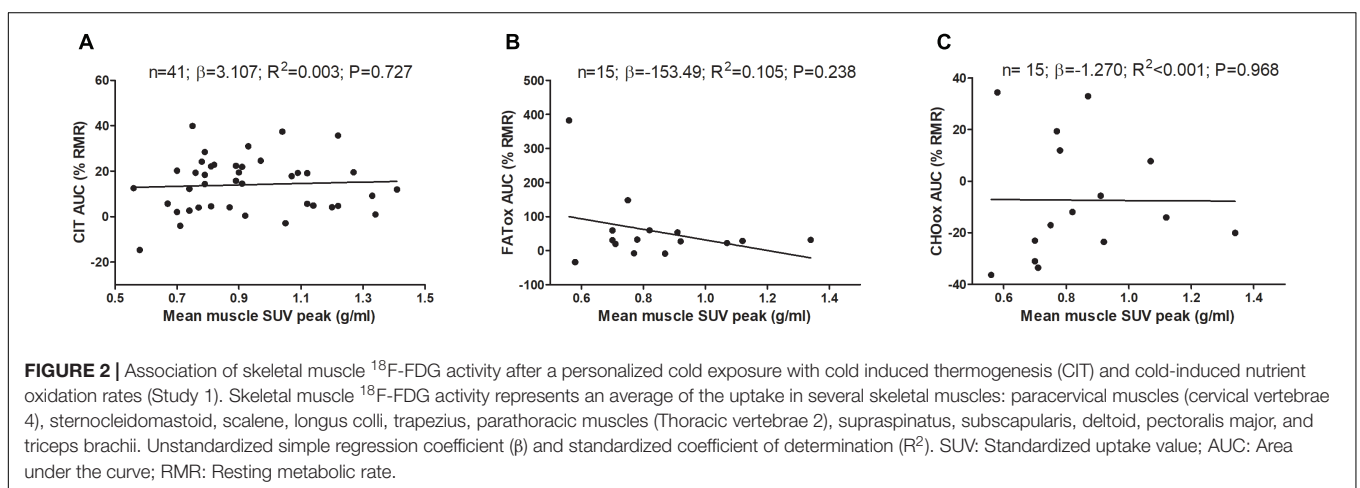
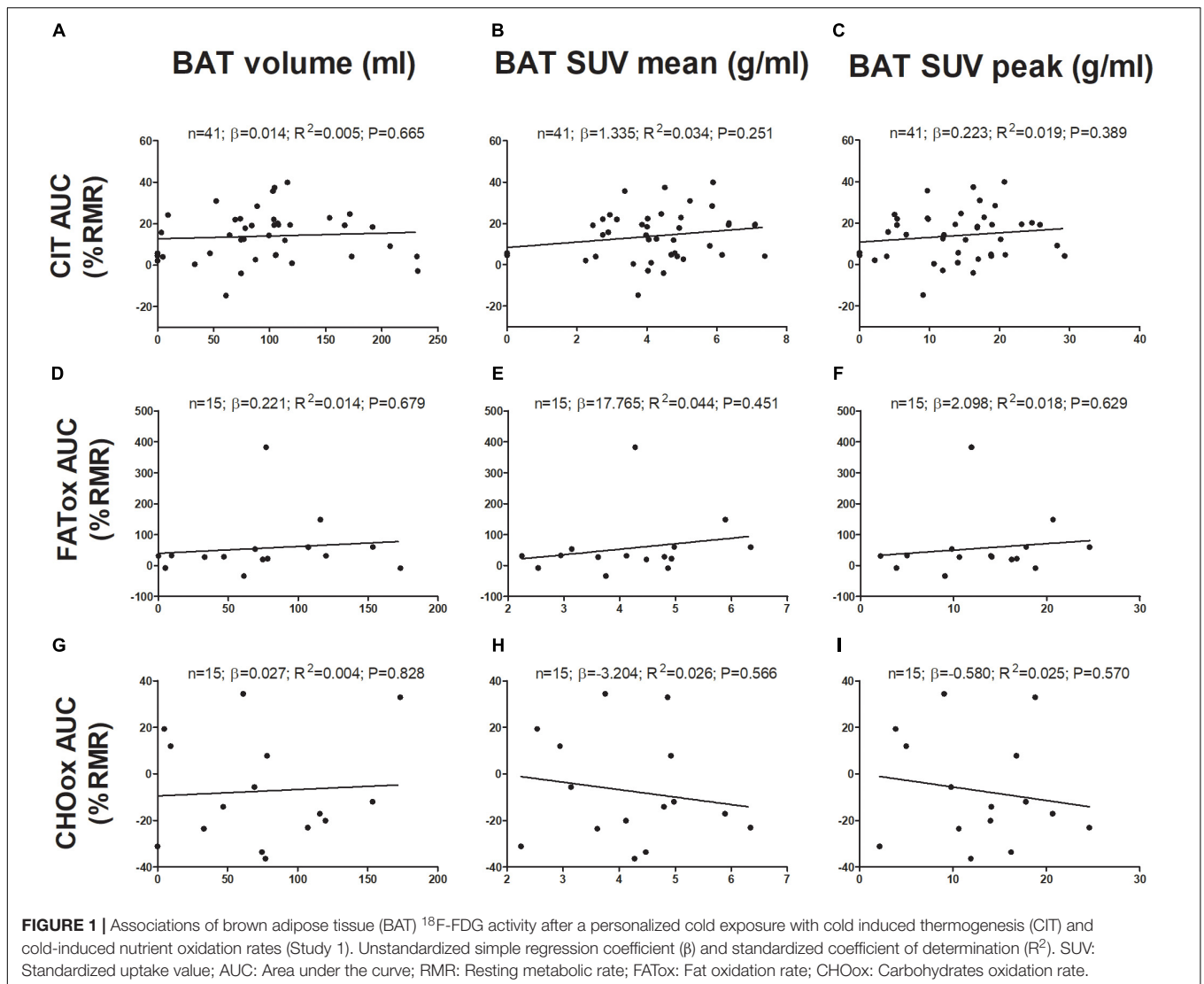
### RESULTS

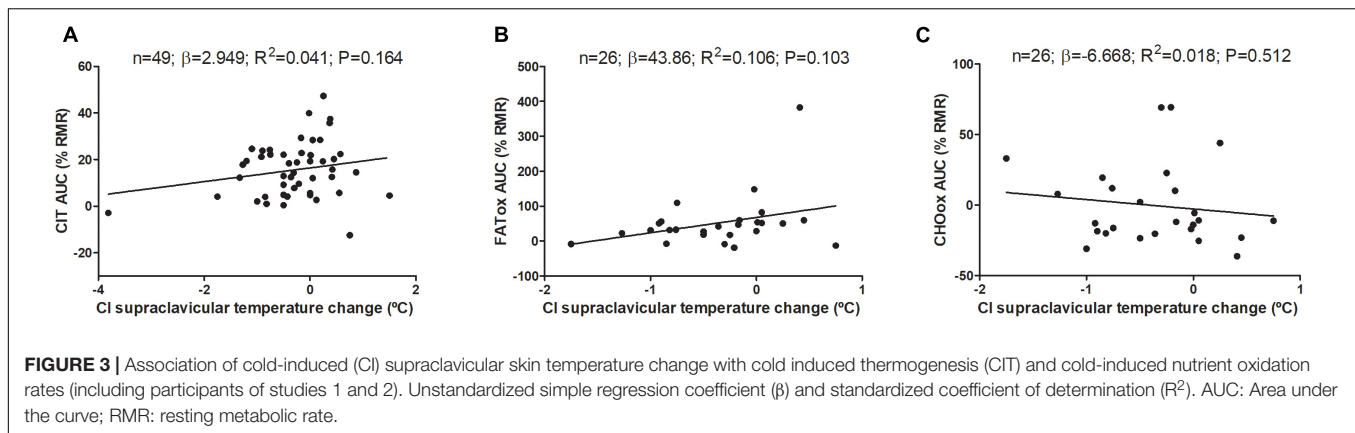
The associations of BAT with CIT and CI-NUTox are shown in **Figure 1**. There was no association of BAT (volume: all  $P > 0.68$ ; mean activity: all  $P > 0.25$ ; maximal activity: all  $P > 0.39$ ) with CIT and NUTox. The results persisted after adjusting by sex, BMI, the time of the day, or the date when CIT was assessed. In addition, we analyzed whether using SUV expressed as a function of lean body mass (SUV<sub>LBM</sub>), instead of body mass (SUV<sub>BM</sub>), influenced the results (Leitner et al., 2017), and no differences were found (data not shown).

**Figure 2** shows the association of skeletal muscle <sup>18</sup>F-FDG activity after a personalized cold exposure with CIT and CI-NUTox. There were no associations either when using SUV<sub>BM</sub> (all  $P > 0.23$ ) or SUV<sub>LBM</sub> (data not shown). Adjusting the analyses by sex, BMI, the time of the day, and the date when CIT was assessed did not modify the results. Furthermore, we tested the association of CIT and CI-NUTox with the deep, cervical, and cold sensitive muscles activity, as they have been shown to respond differently to cold (Blondin et al., 2015b; Martinez-Tellez et al., 2017c). We found no significant association with any criteria for grouping muscles (i.e., deep muscles, cervical muscles, and cold sensitive muscles). All these results remained when using skeletal muscle SUVmean instead of SUVpeak (data not shown).

<sup>1</sup><http://profith.ugr.es/temperatus?lang=en>







Changes on mean, subclavicular, and supraclavicular skin temperature during CIT assessment are shown in **Supplementary Figure S1**. The associations of cold-induced changes in supraclavicular skin temperature with CIT and CI-NUTox are shown in **Figure 3** (including data of studies 1 and 2). We failed to observe any significant association (all  $P > 0.09$ ), which was unaffected when adjusting by sex, BMI, the time of the day, or the date when CIT was assessed. Similar results were found when using the skin temperature data at the end of the test instead of the cold-induced change ( $\Delta$ ). Moreover, neither the mean nor subclavicular skin temperature were associated with CIT or CI-NUTox.

Finally, we also tested the above-mentioned associations using the difference between energy expenditure at the end of the cooling protocol and RMR, instead of the area under the curve calculation, and with % of energy expenditure coming from FATox instead of CI-NUTox. We found no significant associations in any of these analyses (data not shown).

## DISCUSSION

This study analyzed the association of BAT and skeletal muscle  $^{18}\text{F}$ -FDG activity after a personalized cold exposure with CIT and CI-NUTox in young healthy adults. We also examined the association of supraclavicular skin temperature, an indirect marker of BAT activity (Boon et al., 2014; van der Lans et al., 2016), with CIT and CI-NUTox. No significant associations were found of BAT, skeletal muscle  $^{18}\text{F}$ -FDG activity, or supraclavicular skin temperature with CIT and CI-NUTox. This lack of association was consistent across different methodologies for BAT and CIT assessment, and independent of several potential confounders. These findings are partially in line with other studies which used different methodologies (Muzik et al., 2013; Blondin et al., 2015b; U Din et al., 2016), suggesting a negligible contribution of BAT to human CIT. On the other hand, the observed associations of skeletal muscle  $^{18}\text{F}$ -FDG activity after a personalized cold exposure with CIT and CI-NUTox should be considered with caution, since not having  $^{18}\text{F}$ -FDG activity in warm conditions might impair the ability to effectively assess cold-induced skeletal muscle metabolism.

The relation between BAT and CIT in humans has been extensively studied during the last years, yet, controversial results still exist. Several studies showed that individuals with detectable BAT (BAT + in  $^{18}\text{F}$ -FDG-PET-CT scan) present higher CIT levels (Vijgen et al., 2011; Yoneshiro et al., 2011; Chondronikola et al., 2014), and that only BAT + individuals present seasonal variation of CIT, being higher in winter than in summer (Yoneshiro et al., 2016). Moreover, other studies showed positive and significant associations between BAT (assessed by  $^{18}\text{F}$ -FDG-PET-CT) and CIT (van Marken Lichtenbelt et al., 2009; Ouellet et al., 2012; Chen et al., 2013). In contrast, other studies did not observe any significant association between BAT and CIT (Vosselman et al., 2012; Bakker et al., 2014; Blondin et al., 2015b), and BAT activation induced by cold acclimation was not accompanied by changes in CIT (Lee et al., 2014), which concur with our findings. Of note is that the lack of association observed in our study between CIT and supraclavicular skin temperature, as an indirect marker of BAT activity (Boon et al., 2014; van der Lans et al., 2016), further reinforces this finding.

Importantly, studies using  $[(15\text{O})\text{O}_2]$ , instead of  $^{18}\text{F}$ -FDG, as the radiotracer for PET-CT scans, have demonstrated that the direct contribution of BAT to CIT is rather small (i.e., only 1% of the increase of CIT) (Muzik et al., 2013; U Din et al., 2016). Of note is that although  $[(15\text{O})\text{O}_2]$  presents limitations due to a very short half-life (e.g., only a small anatomical area can be assessed) among others, it is able to effectively quantify energy expenditure of different tissues and it is not affected by changes in substrate preference, as  $^{18}\text{F}$ -FDG is. According to these studies, BAT in the cervical and upper thorax area (most human BAT) would account for only 10–15 kcal/day if fully activated for 24 h. However, paradoxically, some of the studies using radiotracers different from  $^{18}\text{F}$ -FDG consistently showed a positive association of BAT perfusion and volume with CIT (Orava et al., 2011; U Din et al., 2016). This, together with the observations showing higher glucose uptake and energy expenditure in skeletal muscles close to BAT depots (Blondin et al., 2015b; U Din et al., 2016), suggest that BAT may influence human CIT by indirect, rather than direct, mechanisms (U Din et al., 2016), such as endocrine signaling (Villarroya et al., 2017).

The hypothesis of an indirect effect of BAT over CIT could explain the controversy in the studies investigating the relation

between BAT assessed by  $^{18}\text{F}$ -FDG-PET-CT and CIT. Moreover, it is known that different methodological approaches for both PET-CT acquisition and analysis can profoundly influence the outcome (Martinez-Tellez et al., 2017b, 2018). Most studies examining the relation between BAT and CIT were conducted before a consensus was reached on how to perform PET-CT scans for BAT assessment and quantification (Chen et al., 2016), and thus, applied different methodologies. Therefore, methodological issues regarding cold exposure prior to PET-CT and PET-CT analyses might explain the observed discrepancies. Here, we investigated the association between BAT and CIT in a larger sample size than previous studies, and strictly following state-of-the-art methodology for BAT assessment. However, it is to note that we measured BAT and CIT on different days, and, therefore, intra-individual day-to-day variance in energy expenditure may have prevented us from finding an existing association (Bader et al., 2005; Schoeller, 2007; Cooper et al., 2009; Alcantara et al., 2018).

There is cumulating evidence supporting the idea that skeletal muscle is the main thermogenic organ upon cold exposure in humans (Blondin et al., 2015b; Jensen, 2015; U Din et al., 2016; Betz and Enerbäck, 2017), even at mild cold exposure. For instance, upon cold stimulation, energy expenditure of muscles in the cervical and upper thorax is  $\approx 8$  times higher than energy expenditure of BAT (U Din et al., 2016). Interestingly, skeletal muscle contribution to CIT seems to be higher in deep and centrally located muscles than in superficial and bigger muscle groups (Blondin et al., 2015b; U Din et al., 2016). Moreover, it is not clear whether the muscle energy expenditure during mild cold exposure relies upon shivering (Blondin et al., 2015b) or non-shivering mechanisms (Betz and Enerbäck, 2017). In contrast with this strong evidence, we found no association between skeletal muscle  $^{18}\text{F}$ -FDG activity after a personalized cold exposure and CIT. However, it should be considered that we did not assess the skeletal muscle  $^{18}\text{F}$ -FDG activity in warm conditions, and, therefore, we could not determine whether the cold-induced change in glucose uptake was associated with CIT. This issue might not be of importance where BAT is concerned (Chen et al., 2016), since BAT glucose uptake in warm conditions is rather low (Cypess et al., 2009). However, differences between muscle  $^{18}\text{F}$ -FDG activity in warm conditions and upon cold exposure are much smaller, and, therefore, not having skeletal muscle warm  $^{18}\text{F}$ -FDG activity might have considerably limited the ability to detect an existing association. In addition to the skeletal muscle  $^{18}\text{F}$ -FDG activity, we also tested the association between lean mass (as a subrogate of muscle mass) and CIT, which did not show significance (data not shown).

Moreover, it should be noted that skeletal muscle thermogenesis, even during shivering, relies mainly on fatty acid oxidation (Blondin et al., 2014; Haman and Blondin, 2017), and, therefore, the glucose analog  $^{18}\text{F}$ -FDG might not be a valid marker of muscle thermogenesis or metabolic activity. Similarly, BAT thermogenesis also relies mainly on fat oxidation (Blondin et al., 2017), and it has recently been shown that glucose uptake is not mandatory for human BAT thermogenesis (Blondin et al.,

2015a). Therefore, inherent limitations of  $^{18}\text{F}$ -FDG for BAT detection and muscle activity quantification may explain why we failed to detect a physiologically plausible association. There is a need to develop new radiotracers for BAT detection and muscle activity quantification with more metabolic significance than  $^{18}\text{F}$ -FDG and with a larger half-life than others such as  $[(15\text{O})\text{O}_2]$ .

We also studied the associations of BAT and skeletal muscle  $^{18}\text{F}$ -FDG activity with CI-NUTox. Since both BAT and skeletal muscle thermogenesis relies on fatty acid oxidation, it is plausible to expect a positive association of BAT and skeletal muscle activity with FATox. In contrast, we observed no association, which could be partially explained by the inherent limitations of  $^{18}\text{F}$ -FDG as a radiotracer. However, since BAT and skeletal muscle thermogenesis seem to compensate each other (Blondin et al., 2016) and both mainly depend on FATox, it is also plausible that no relation with FATox exists. Finally, it should be considered that we recorded CI-NUTox in a cold exposure of only 1 h. Longer cold exposures result in different contributions of both CHOx and FATox (Blondin et al., 2014), and, therefore, new studies examining the relation of BAT and muscle thermogenesis with CI-NUTox during longer cold exposures are needed.

Our results should be considered with caution since some limitations are present. It should be noted that BAT and skeletal muscle  $^{18}\text{F}$ -FDG activity was assessed on a different day than CIT and CI-NUTox, and, therefore, day-to-day variation may have influenced our results. Moreover, as stated above, whereas  $^{18}\text{F}$ -FDG PET-CT after a personalized cold exposure is currently considered the gold standard for BAT *in vivo* quantification (Chen et al., 2016; Carpentier et al., 2018), it is not the best method to assess skeletal muscle metabolism upon cold exposure, which could explain the lack of association with CIT. Moreover, we quantified skeletal muscle  $^{18}\text{F}$ -FDG activity (SUVpeak) in one image slice, and therefore it might be influenced by the blood vessels eventually contained in the ROI. Using skeletal muscle SUVmean did not change the results, probably because muscle SUVmean and SUVpeak are highly correlated (all  $r > 0.976$ ; all  $P < 0.001$ ). Of note is also that the cooling protocol applied to assess both BAT and skeletal muscle  $^{18}\text{F}$ -FDG activity and CIT and CI-NUTox is based on the individuals' shivering threshold, which was assessed by subjective methods (self-reported and direct observation), rather than by objective methods (electromyography) (Acosta et al., 2018). Another relevant issue is that the cold-exposure used to assess CIT and CI-NUTox was only 1 h long, and, therefore, we cannot know whether a longer cold exposure would provide different results. In addition, it should be noted that we studied young healthy adults, hence we do not know whether these findings extend to older or unhealthy individuals. Finally, due to a lack of homogeneity in the fasting time of Study 1, we conducted the NUTox analyses with a relatively small sample size (only 18 out of 44 participants in Study 1). However, we performed a second study which allowed us to study the association of supraclavicular temperature with CIT and CI-NUTox in a larger sample size.

## CONCLUSION

We found, in a larger sample size than previous studies and strictly following the most updated methodological recommendations, that BAT and skeletal muscle thermogenic activity (assessed by means of  $^{18}\text{F}$ -FDG activity after a personalized cold exposure) is not associated with CIT or CI-NUTox. These findings support the hypothesis of BAT having a marginal role in human CIT, although important limitations inherent to the available technology for BAT and skeletal muscle metabolism *in vivo* quantification precludes us from drawing firm conclusions from the present data.

## AUTHOR CONTRIBUTIONS

GS-D, BM-T, and JR designed the research. GS-D, BM-T, YG-R, JA, FA, FA-G, and JL-M conducted the research. GS-D, BM-T, and JM analyzed the data. GS-D wrote the paper. GS-D and JR had primary responsibility for the final content. GS-D, BM-T, YG-R, JA, FA, FA-G, JL-M, and JR, discussed the results and approved the final version of the manuscript.

## FUNDING

The study was supported by the Spanish Ministry of Economy and Competitiveness (PTA 12264-I), Fondo de Investigación Sanitaria del Instituto de Salud Carlos III (PI13/01393), and Retos de la Sociedad (DEP2016-79512-R), Fondos Estructurales

de la Unión Europea (FEDER), by the Spanish Ministry of Education (FPU 13/04365, FPU14/04172, and FPU15/04059), by the Fundación Iberoamericana de Nutrición (FINUT), by the Redes temáticas de investigación cooperativa RETIC (Red SAMID RD16/0022), by AstraZeneca HealthCare Foundation and by the University of Granada, Plan Propio de Investigación 2016, Excellence actions: Units of Excellence; Scientific Unit of Excellence on Exercise and Health (UCEES).

## ACKNOWLEDGMENTS

We are grateful to Ms. Carmen Sainz-Quinn for assistance with the English language. Parts of this study (preliminary data of study 1) were presented as an oral presentation at the European Congress of Obesity (ECO), Vienna, Austria, May 23–26, 2018 (Sanchez-Delgado et al., 2018b). This study is part of a Ph.D. thesis conducted in the Biomedicine Doctoral Studies of the University of Granada, Spain.

## SUPPLEMENTARY MATERIAL

The Supplementary Material for this article can be found online at: <https://www.frontiersin.org/articles/10.3389/fphys.2018.01577/full#supplementary-material>

**FIGURE S1 |** Skin temperature parameters during cold-induced thermogenesis. *P* for one-way analysis of variance. min: minute.

## REFERENCES

- Acosta, F. M., Martinez-Tellez, B., Sanchez-Delgado, G., Alcantara, J. M. A., Acosta-Manzano, P., Morales-Artacho, A. J., et al. (2018). Physiological responses to acute cold exposure in young lean men. *PLoS One* 13:e0196543. doi: 10.1371/journal.pone.0196543
- Alcantara, J. M. A., Sanchez-Delgado, G., Martinez-Tellez, B., Merchán-Ramirez, E., Labayen, I., and Ruiz, J. R. (2018). Congruent validity and inter-day reliability of two breath by breath metabolic carts to measure resting metabolic rate in young adults. *Nutr. Metab. Cardiovasc. Dis.* 28, 929–936. doi: 10.1016/j.numecd.2018.03.010
- Bader, N., Bosy-Westphal, A., Dilba, B., and Müller, M. J. (2005). Intra- and interindividual variability of resting energy expenditure in healthy male subjects – biological and methodological variability of resting energy expenditure. *Br. J. Nutr.* 94, 843–849. doi: 10.1079/BJN20051551
- Bakker, L. E., Boon, M. R., van der Linden, R. A., Arias-Bouda, L. P., van Klinken, J. B., Smit, F., et al. (2014). Brown adipose tissue volume in healthy lean south Asian adults compared with white Caucasians: a prospective, case-controlled observational study. *Lancet. Diabetes Endocrinol.* 2, 210–217. doi: 10.1016/S2213-8587(13)70156-6
- Betz, M. J., and Enerbäck, S. (2017). Targeting thermogenesis in brown fat and muscle to treat obesity and metabolic disease. *Nat. Rev. Endocrinol.* 14, 77–87. doi: 10.1038/nrendo.2017.132
- Blondin, D. P., Daoud, A., Taylor, T., Tingelstad, H. C., Bézaire, V., Richard, D., et al. (2016). Four-week cold acclimation in adult humans shifts uncoupling thermogenesis from skeletal muscles to BAT. *J. Physiol.* 6, 2099–2113. doi: 10.1113/JP273395
- Blondin, D. P., Frisch, F., Phoenix, S., Guérin, B., Turcotte, É. E., Haman, F., et al. (2017). Inhibition of intracellular triglyceride lipolysis suppresses cold-induced brown adipose tissue metabolism and increases shivering in humans. *Cell Metab.* 25, 438–447. doi: 10.1016/j.cmet.2016.12.005
- Blondin, D. P., Labbé, S. M., Noll, C., Kunach, M., Phoenix, S., Guérin, B., et al. (2015a). Selective impairment of glucose but not fatty acid or oxidative metabolism in brown adipose tissue of subjects with type 2 diabetes. *Diabetes Metab. Res. Rev.* 64, 2388–2397. doi: 10.2337/db14-1651
- Blondin, D. P., Labbé, S. M., Phoenix, S., Guérin, B., Turcotte, É. E., Richard, D., et al. (2015b). Contributions of white and brown adipose tissues and skeletal muscles to acute cold-induced metabolic responses in healthy men. *J. Physiol.* 593, 701–714. doi: 10.1113/jphysiol.2014.283598
- Blondin, D. P., Tingelstad, H. C., Mantha, O. L., Gosselin, C., and Haman, F. (2014). Maintaining thermogenesis in cold exposed humans: relying on multiple metabolic pathways. *Compr. Physiol.* 4, 1383–1402. doi: 10.1002/cphy.c130043
- Boon, M. R., Bakker, L. E., van der Linden, R. A., Pereira Arias-Bouda, L., Smit, F., Verberne, H. J., et al. (2014). Supraclavicular skin temperature as a measure of  $^{18}\text{F}$ -FDG uptake by BAT in human subjects. *PLoS One* 9:e98822. doi: 10.1371/journal.pone.0098822
- Cannon, B., and Nedergaard, J. (2004). Brown adipose tissue: function and physiological significance. *Physiol. Rev.* 84, 277–359. doi: 10.1152/physrev.00015.2003
- Carpentier, A. C., Blondin, D. P., Virtanen, K. A., Richard, D., Haman, F., and Turcotte, É. E. (2018). Brown adipose tissue energy metabolism in humans. *Front. Endocrinol.* 9:447. doi: 10.3389/fendo.2018.00447
- Chen, K. Y., Brychta, R. J., Linderman, J. D., Smith, S., Courville, A., Dieckmann, W., et al. (2013). Brown fat activation mediates cold-induced thermogenesis in adult humans in response to a mild decrease in ambient temperature. *J. Clin. Endocrinol. Metab.* 98, 1218–1223. doi: 10.1210/jc.2012-4213
- Chen, K. Y., Cypress, A. M., Laughlin, M. R., Haft, C. R., Hu, H. H., Bredella, M. A., et al. (2016). Brown adipose reporting criteria in imaging studies (BARCIST 1.0): recommendations for standardized FDG-PET/CT experiments in humans. *Cell Metab.* 24, 210–222. doi: 10.1016/j.cmet.2016.07.014



- Chondronikola, M., Volpi, E., Børsheim, E., Porter, C., Annamalai, P., Enerbäck, S., et al. (2014). Brown adipose tissue improves whole-body glucose homeostasis and insulin sensitivity in humans. *Diabetes Metab. Res. Rev.* 63, 4089–4099. doi: 10.2337/db14-0746
- Cooper, J. A., Watras, A. C., O'Brien, M. J., Luke, A., Dobratz, J. R., Earthman, C. P., et al. (2009). Assessing validity and reliability of resting metabolic rate in six gas analysis systems. *J. Am. Diet. Assoc.* 109, 128–132. doi: 10.1016/j.jada.2008.10.004
- Cypess, A. M., Lehman, S., Williams, G., Tal, I., Rodman, D., Goldfine, A. B., et al. (2009). Identification and importance of brown adipose tissue in adult humans. *N. Engl. J. Med.* 360, 1509–1517. doi: 10.1056/NEJMoa0810780
- Cypess, A. M., White, A. P., Vernochet, C., Schulz, T. J., Xue, R., Sass, C. A., et al. (2013). Anatomical localization, gene expression profiling and functional characterization of adult human neck brown fat. *Nat. Med.* 19, 635–639. doi: 10.1038/nm.3112
- Fernández-Verdejo, R., Bajpeyi, S., Ravussin, E., and Galgani, J. E. (2018). Metabolic flexibility to lipid availability during exercise is enhanced in individuals with high insulin sensitivity. *Am. J. Physiol. Endocrinol. Metab.* 315, E715–E722. doi: 10.1152/ajpendo.00126.2018
- Frayn, K. N. (1983). Calculation of substrate oxidation rates in vivo from gaseous exchange. *J. Appl. Physiol.* 55, 628–634. doi: 10.1152/jap.1983.55.2.628
- Fullmer, S., Benson-Davies, S., Earthman, C. P., Frankenfield, D. C., Gradwell, E., Lee, P. S. P., et al. (2015). Evidence analysis library review of best practices for performing indirect calorimetry in healthy and non-critically ill individuals. *J. Acad. Nutr. Diet.* 115, 1417.e2–1446.e2. doi: 10.1016/j.jand.2015.04.003
- Galgani, J. E., Moro, C., and Ravussin, E. (2008). Metabolic flexibility and insulin resistance. *AJP Endocrinol. Metab.* 295, E1009–E1017. doi: 10.1152/ajpendo.90558.2008
- Garland, T., Schutz, H., Chappell, M. A., Keeney, B. K., Meek, T. H., Copes, L. E., et al. (2011). The biological control of voluntary exercise, spontaneous physical activity and daily energy expenditure in relation to obesity: human and rodent perspectives. *J. Exp. Biol.* 214, 206–229. doi: 10.1242/jeb.048397
- Goodpaster, B. H., and Sparks, L. M. (2017). Metabolic flexibility in health and disease. *Cell Metab.* 25, 1027–1036. doi: 10.1016/j.cmet.2017.04.015
- Haman, F., and Blondin, D. P. (2017). Shivering thermogenesis in humans: origin, contribution and metabolic requirement. *Temperature* 4, 217–226. doi: 10.1080/2328940.2017.1328999
- ISO-standard 9886:2004 (2004). *ISO-standard 9886:2004 Ergonomics – Evaluation of Thermal Strain by Physio- Logical Measurements*. Geneva: International Standards Organization.
- Jensen, M. D. (2015). Brown adipose tissue—not as hot as we thought. *J. Physiol.* 593:489. doi: 10.1113/jphysiol.2014.287979
- Lee, P., Smith, S., Linderman, J., Courville, A. B., Brychta, R. J., Dieckmann, W., et al. (2014). Temperature-acclimated brown adipose tissue modulates insulin sensitivity in humans. *Diabetes Metab. Res. Rev.* 177, 1–59. doi: 10.2337/db14-0513
- Lee, P., Swarbrick, M. M., and Ho, K. K. Y. (2013). Brown adipose tissue in adult humans: a metabolic renaissance. *Endocr. Rev.* 34, 413–438. doi: 10.1210/er.2012-1081
- Leitner, B. P., Huang, S., Brychta, R. J., Duckworth, C. J., Baskin, A. S., McGehee, S., et al. (2017). Mapping of human brown adipose tissue in lean and obese young men. *Proc. Natl. Acad. Sci. U.S.A.* 114, 6–11. doi: 10.1073/pnas.1705287114
- Marlatt, K., Chen, K., and Ravussin, E. (2018). Is activation of human brown adipose tissue a viable target for weight management? *Am. J. Physiol. Integr. Comp. Physiol.* 315, R479–R483. doi: 10.1152/ajpregu.00443.2017
- Martinez-Tellez, B., Nahon, K. J., Sanchez-Delgado, G., Abreu-Vieira, G., Llamas-Elvira, J. M., van Velden, F. H. P., et al. (2018). The impact of using BARCIST 1.0 criteria on quantification of BAT volume and activity in three independent cohorts of adults. *Sci. Rep.* 8:8567. doi: 10.1038/s41598-018-26878-4
- Martinez-Tellez, B., Sanchez-Delgado, G., Acosta, F. M., Alcantara, J. M. A., Boon, M. R., Rensen, P. C. N., et al. (2017a). Differences between the most used equations in BAT-human studies to estimate parameters of skin temperature in young lean men. *Sci. Rep.* 7:10530. doi: 10.1038/s41598-017-10444-5
- Martinez-Tellez, B., Sanchez-Delgado, G., Boon, M. R., Rensen, P. C. N., and Ruiz, J. R. (2017b). Activation and quantification of human brown adipose tissue: methodological considerations for between studies comparisons: comment on: hot heads & cool bodies: the conundrums of human BAT activity research. *Eur. J. Intern. Med.* 40, e19–e21. doi: 10.1016/j.iejim.2017.02.006
- Martinez-Tellez, B., Sanchez-Delgado, G., Garcia-Rivero, Y., Alcantara, J. M. A., Martinez-Avila, W. D., Muñoz-Hernandez, M. V., et al. (2017c). A new personalized cooling protocol to activate brown adipose tissue in young adults. *Front. Physiol.* 8:863. doi: 10.3389/fphys.2017.00863
- Muzik, O., Mangner, T. J., Leonard, W. R., Kumar, A., Janisse, J., and Granneman, J. G. (2013). 150 PET measurement of blood flow and oxygen consumption in cold-activated human brown fat. *J. Nucl. Med.* 54, 523–531. doi: 10.2967/jnumed.112.111336
- Nedergaard, J., Bengtsson, T., and Cannon, B. (2007). Unexpected evidence for active brown adipose tissue in adult humans. *Am. J. Physiol. Endocrinol. Metab.* 293, E444–E452. doi: 10.1152/ajpendo.00691.2006
- Ng, M., Fleming, T., Robinson, M., Thomson, B., Graetz, N., Margono, C., et al. (2014). Global, regional, and national prevalence of overweight and obesity in children and adults during 1980–2013: a systematic analysis for the global burden of disease study 2013. *Lancet* 384, 766–781. doi: 10.1016/S0140-6736(14)60460-8
- Ong, F. J., Ahmed, B. A., Oreskovich, S. M., Blondin, D. P., Haq, T., Konyer, N. B., et al. (2018). Recent advances in the detection of brown adipose tissue in adult humans: a review. *Clin. Sci.* 132, 1039–1054. doi: 10.1042/CS20170276
- Orava, J., Nuutila, P., Lidell, M. E., Oikonen, V., Noponen, T., Viljanen, T., et al. (2011). Different metabolic responses of human brown adipose tissue to activation by cold and insulin. *Cell Metab.* 14, 272–279. doi: 10.1016/j.cmet.2011.06.012
- Ouellet, V., Labbé, S. M., Blondin, D. P., Phoenix, S., Guérin, B., Haman, F., et al. (2012). Brown adipose tissue oxidative metabolism contributes to energy expenditure during acute cold exposure in humans. *J. Clin. Invest.* 122, 545–552. doi: 10.1172/JCI60433
- Palmer, B. F., and Clegg, D. J. (2017). Non-shivering thermogenesis as a mechanism to facilitate sustainable weight loss. *Obes. Rev.* 18, 819–831. doi: 10.1111/obr.12563
- Peirce, V., Carobbio, S., and Vidal-Puig, A. (2014). The different shades of fat. *Nature* 510, 76–83. doi: 10.1038/nature13477
- Porter, C. (2017). Quantification of UCP1 function in human brown adipose tissue. *Adipocyte* 6, 167–174. doi: 10.1080/21623945.2017.1319535
- Ruiz, J. R., Martinez-Tellez, B., Sanchez-Delgado, G., Osuna-Prieto, F. J., Rensen, P. C. N., and Boon, M. R. (2018). Role of human brown fat in obesity, metabolism and cardiovascular disease: strategies to turn up the heat. *Prog. Cardiovasc. Dis.* 61, 232–245. doi: 10.1016/j.pcad.2018.07.002
- Saito, M., Okamatsu-Ogura, Y., Matsushita, M., Watanabe, K., Yoneshiro, T., Nio-Kobayashi, J., et al. (2009). High incidence of metabolically active brown adipose tissue in healthy adult humans: effects of cold exposure and adiposity. *Diabetes Metab. Res. Rev.* 58, 1526–1531. doi: 10.2337/db09-0530
- Sanchez-Delgado, G., Alcantara, J. M. A., Acosta, F. M., Martinez-Tellez, B., Amaro-Gahete, F. J., Ortiz-Alvarez, L., et al. (2018a). Estimation of non-shivering thermogenesis and cold-induced nutrient oxidation rates: Impact of method for data selection and analysis. *Clin. Nutr.* 1–7. doi: 10.1016/j.clnu.2018.09.009
- Sanchez-Delgado, G., Alcantara, J. M. A., Ortiz-Alvarez, L., Xu, H., Martinez-Tellez, B., Labayen, I., et al. (2017). Reliability of resting metabolic rate measurements in young adults: Impact of methods for data analysis. *Clin. Nutr.* 37, 1618–1624. doi: 10.1016/j.clnu.2017.07.026
- Sanchez-Delgado, G., Garcia-Rivero, Y., Rodriguez-Perez, L., Martinez-Tellez, B., Alcantara, J. M. A., Amaro-Gahete, F. J., et al. (2018b). *Association of Brown Adipose Tissue, Skeletal Muscle Glucose Uptake and Supraclavicular Skin Temperature, with Cold-Induced Thermogenesis and Nutrient Oxidation Rates*, ed. S. A. G. Karger (Vienna: European Congress on Obesity).
- Sanchez-Delgado, G., Martinez-Tellez, B., Olza, J., Aguilera, C. M., Labayen, I., Ortega, F. B., et al. (2015). Activating brown adipose tissue through exercise (ACTIBATE) in young adults: rationale, design and methodology. *Contemp. Clin. Trials* 45, 416–425. doi: 10.1016/j.cct.2015.11.004
- Schilperoort, M., Hoeke, G., Koopman, S., and Rensen, P. C. N. (2016). Relevance of lipid metabolism for brown fat visualization and quantification. *Curr. Opin. Lipidol.* 27, 242–248. doi: 10.1097/MOL.0000000000000296

- Schindelin, J., Arganda-Carreras, I., Frise, E., Kaynig, V., Longair, M., Pietzsch, T., et al. (2012). Fiji: an open-source platform for biological-image analysis. *Nat. Methods* 9, 676–682. doi: 10.1038/nmeth.2019
- Schoeller, D. A. (2007). Making indirect calorimetry a gold standard for predicting energy requirements for institutionalized patients. *J. Am. Diet. Assoc.* 107, 390–392. doi: 10.1016/j.jada.2007.01.030
- U Din, M., Raiko, J., Saari, T., Kudomi, N., Tolvanen, T., Oikonen, V., et al. (2016). Human brown adipose tissue [(15)O]O<sub>2</sub> PET imaging in the presence and absence of cold stimulus. *Eur. J. Nucl. Med. Mol. Imaging* 43, 1878–1886. doi: 10.1007/s00259-016-3364-y
- van der Lans, A. A., Hoeks, J., Brans, B., Vijgen, G. H., Visser, M. G., Vosselman, M. J., et al. (2013). Cold acclimation recruits human brown fat and increases nonshivering thermogenesis. *J. Clin. Invest.* 123, 3395–3403. doi: 10.1172/JCI68993
- van der Lans, A. A., Vosselman, M. J., Hanssen, M. J., Brans, B., and van Marken Lichtenbelt, W. D. (2016). Supraclavicular skin temperature and BAT activity in lean healthy adults. *J. Physiol. Sci.* 66, 77–83. doi: 10.1007/s12576-015-0398-z
- van Marken Lichtenbelt, W. D., Vanhommerig, J. W., Smulders, N. M., Drossaerts, J. M., Kemerink, G. J., Bouvy, N. D., et al. (2009). Cold-activated brown adipose tissue in healthy men. *N. Engl. J. Med.* 360, 1500–1508. doi: 10.1056/NEJMoa0808718
- Vijgen, G. H., Bouvy, N. D., Teule, G. J., Brans, B., Schrauwen, P., and van Marken Lichtenbelt, W. D. (2011). Brown adipose tissue in morbidly obese subjects. *PLoS One* 6:e17247. doi: 10.1371/journal.pone.0017247
- Villarroya, F., Cereijo, R., Villarroya, J., and Giral, M. (2017). Brown adipose tissue as a secretory organ. *Nat. Rev. Endocrinol.* 13, 26–35. doi: 10.1038/nrendo.2016.136
- Virtanen, K. A., Lidell, M. E., Orava, J., Heglind, M., Westergren, R., Niemi, T., et al. (2009). Functional brown adipose tissue in healthy adults. *N. Engl. J. Med.* 360, 1518–1525. doi: 10.1056/NEJMoa0808949
- Vosselman, M. J., van der Lans, A. A. J. J., Brans, B., Wierds, R., van Baak, M. A., Schrauwen, P., et al. (2012). Systemic  $\beta$ -adrenergic stimulation of thermogenesis is not accompanied by brown adipose tissue activity in humans. *Diabetes Metab. Res. Rev.* 61, 3106–3113. doi: 10.2337/db12-0288
- Weir, J. B. (1949). New methods for calculating metabolic rate with special reference to protein metabolism. *J. Physiol.* 109, 1–9. doi: 10.1113/jphysiol.1949.sp004363
- Yoneshiro, T., Aita, S., Matsushita, M., Kameya, T., Nakada, K., Kawai, Y., et al. (2011). Brown adipose tissue, whole-body energy expenditure, and thermogenesis in healthy adult men. *Obesity* 19, 13–16. doi: 10.1038/oby.2010.105
- Yoneshiro, T., Matsushita, M., Nakae, S., Kameya, T., Sugie, H., Tanaka, S., et al. (2016). Brown adipose tissue is involved in the seasonal variation of cold-induced thermogenesis in humans. *Am. J. Physiol. Regul. Integr. Comp. Physiol.* 310, R999–R1009. doi: 10.1152/ajpregu.00057.2015
- Zingaretti, M. C., Crosta, F., Vitali, A., Guerrieri, M., Frontini, A., Cannon, B., et al. (2009). The presence of UCP1 demonstrates that metabolically active adipose tissue in the neck of adult humans truly represents brown adipose tissue. *FASEB J.* 23, 3113–3120. doi: 10.1096/fj.09-133546

**Conflict of Interest Statement:** The authors declare that the research was conducted in the absence of any commercial or financial relationships that could be construed as a potential conflict of interest.

Copyright © 2018 Sanchez-Delgado, Martinez-Tellez, Garcia-Rivero, Alcantara, Acosta, Amaro-Gahete, Llamas-Elvira and Ruiz. This is an open-access article distributed under the terms of the Creative Commons Attribution License (CC BY). The use, distribution or reproduction in other forums is permitted, provided the original author(s) and the copyright owner(s) are credited and that the original publication in this journal is cited, in accordance with accepted academic practice. No use, distribution or reproduction is permitted which does not comply with these terms.



# Brown Adipose Tissue—A Therapeutic Target in Obesity?

Paul Trayhurn<sup>1,2\*</sup>

<sup>1</sup> Clore Laboratory, University of Buckingham, Buckingham, United Kingdom, <sup>2</sup> Obesity Biology Unit, University of Liverpool, Liverpool, United Kingdom

**Keywords: brown adipocyte, beige adipocyte, obesity, thermogenesis, uncoupling protein-1**

## OPEN ACCESS

### Edited by:

Rita De Matteis,  
Università degli Studi di Urbino Carlo  
Bo, Italy

### Reviewed by:

Giovanni Solinas,  
University of Gothenburg, Sweden  
Catalina Pico,  
Universidad de les Illes Balears, Spain  
Marta Giralt,  
University of Barcelona, Spain

### \*Correspondence:

Paul Trayhurn  
p.trayhurn@liverpool.ac.uk

### Specialty section:

This article was submitted to  
Integrative Physiology,  
a section of the journal  
Frontiers in Physiology

**Received:** 31 August 2018

**Accepted:** 07 November 2018

**Published:** 23 November 2018

### Citation:

Trayhurn P (2018) Brown Adipose  
Tissue—A Therapeutic Target in  
Obesity? *Front. Physiol.* 9:1672.  
doi: 10.3389/fphys.2018.01672

Since brown adipose tissue (BAT) was first identified in the interscapular area of marmots by Gessner in 1551 (Smith and Horwitz, 1969), views on its functions have continued to evolve (Table 1). The initial proposition was that it was linked to hibernation, reflecting the fact that marmots are hibernating animals. This was followed sequentially by the view that BAT was part of the thymus (1670–1817), an endocrine gland active in the formation of blood (1817–63), a modified form of fat tissue providing a reservoir for food substances (1863–1902), and again as an endocrine gland (1902–61) (Afzelius, 1970). It was only in 1961 that the tissue was finally identified as an effector of non-shivering thermogenesis (NST) and the “metabolic power” of brown adipocytes recognized (Smith and Horwitz, 1969).

There were three situations where BAT was understood to be highly active—during arousal from hibernation, in the response to cold-exposure of certain adult mammals, and in cold-stressed mammalian neonates (Smith and Horwitz, 1969). The quantitative importance of BAT to NST was initially unclear. However, in the late 1970's it was clarified in the case of cold-acclimated rodents by employing radioactively microspheres to map regional blood flow, these studies demonstrating that brown fat may account for up to two-thirds of heat from NST (Foster and Frydman, 1978, 1979). The mechanism for heat generation in brown adipocytes was also being explored, and the uncoupling of oxidative phosphorylation through proton leakage across the inner mitochondrial membrane was established as the pathway by which thermogenesis occurs (Nicholls and Locke, 1984). This proton conductance pathway was shown to be dependent on, and regulated by, a cold-inducible mitochondrial uncoupling protein—UCP1 (Ricquier and Kader, 1976; Nicholls and Locke, 1984; Ricquier, 2017).

Since these pivotal advances, perspectives on the physiology of BAT have continued to evolve. Here, recent views on the role of the tissue are summarized and the potential implications for the treatment of obesity considered.

## BAT AND NUTRITIONAL ENERGETICS

A major new dimension emerged in the late 1970's with the establishment of a link between BAT and energy balance (Table 1). This resulted from two key observations, one of which was that rats exhibiting high rates of diet-induced thermogenesis on a cafeteria diet are characterized by an activation of BAT (Rothwell and Stock, 1979), including increased mitochondrial GDP binding indicative of an activation of the proton conductance pathway (Brooks et al., 1980). The other major observation was of decreased BAT activity, with a reduction in GDP binding, in obese (*ob/ob*) mice; this was proposed as a causative factor in the development of their obesity (Himms-Hagen and Desautels, 1978).

These pioneering observations resulted in a new paradigm in the etiology of obesity (Rothwell and Stock, 1981; Himms-Hagen, 1983, 1989; Trayhurn, 1989). A tissue and molecular basis for the reduced energy expenditure on facultative thermogenesis proposed as an important factor in the development of obesity had been identified. Abnormalities in BAT activity were subsequently

**TABLE 1** | Evolution of perspectives on the physiological functions and characteristics of brown adipose tissue.

Year	Function
1551	Description by Gessner—role in hibernation
1670–1817	Part of the thymus
1817–1863	An endocrine gland—and active in the formation of blood
1863–1902	Modified form of fat tissue which serves as a reservoir for food substances
1902–1961	An endocrine gland once more
1961–	Thermogenic organ—non-shivering thermogenesis
1974–7	Elucidation of unique bioenergetic properties of brown fat mitochondria (proton leak)
1976–8	Discovery of UCP1
1978	Demonstration of quantitative importance to non-shivering thermogenesis in cold-acclimated rodents
1978/9–	Involved in energy balance (diet-induced thermogenesis) and obesity
2009–	Definitive identification of BAT in adult humans and its metabolic plasticity
2010/12	Discovery of “beige”/“brite” adipocytes
2011/12	Role in glucose disposal and triglyceride clearance – metabolic homeostasis

Based partly on Afzelius (1970).

reported in a range of animal obesities, including *db/db* mice and Zucker (*fa/fa*) rats, and in rodents with experimentally-induced obesity (Himms-Hagen, 1989; Trayhurn, 2017). The central role of BAT in nutritional energetics and body fat regulation was further evident from studies demonstrating changes in thermogenic activity in a range of physiological conditions—from fasting to lactation and photoperiod-induced seasonal changes in body weight (Trayhurn, 2017).

## BROWN ADIPOSE TISSUE IN MAN

A widely debated question in the 1980's was the extent to which studies on laboratory rodents were relevant to energetics and obesity in humans. This was effectively two questions—whether reduced expenditure on thermogenesis underpins the development of human obesity, and whether BAT is present in adults and thus the potential locus of impaired thermogenesis. The first question has been the source of continuing debate, but what seems clear is that thermogenesis is not a major component of expenditure in adult humans (Wijers et al., 2007; van Marken Lichtenbelt and Schrauwen, 2011)—certainly compared with small rodents such as mice in the cold where it accounts for up to two-thirds of total expenditure (Trayhurn and James, 1978; Trayhurn, 1979).

In the early 1980's, BAT was considered, essentially on histological criteria, to be absent in humans after the first years of life. This parallels precocial species such as goats and sheep in which BAT, while abundant at birth, rapidly loses UCP1 and thermogenic capacity over the first weeks of postnatal life being replaced by white fat (Casteilla et al., 1987; Trayhurn et al., 1993).

Until 2009, the widely held view was that BAT (or thermogenic adipocytes) is absent from adult humans, despite anatomical studies identifying multi-locular adipocytes (Heaton, 1972), and more critically: (i) UCP1 being identified in adipose tissue depots of adults, including elderly subjects (Lean et al., 1986a), (ii) activation of BAT being demonstrated in pheochromocytoma patients (Ricquier et al., 1982; Lean et al., 1986b), and (iii) *UCP1* gene expression in adipose tissue of adults, particularly in pheochromocytoma (Bouillaud et al., 1988).

The lack of recognition that adults do contain active BAT was a key element in the decline of interest in the tissue by the 1990's. However, over the past decade several major developments have led to a renewed focus on BAT. First, studies from the late 2000's utilizing FDG-PET (fluorodeoxyglucose positron emission tomography), commonly employed to track tumor metastasis, have mapped areas of high glucose uptake which also contain UCP1, thereby firmly identifying active BAT in adults (Cypess et al., 2009; Virtanen et al., 2009; Moonen et al., 2019). Through such studies, increased BAT activity has been observed in response to multiple stimuli, including cold exposure (as in rodents), and administration of insulin and the  $\beta_3$ -adrenoceptor agonist mirabregon (van Marken Lichtenbelt et al., 2009; Virtanen et al., 2009; Orava et al., 2011; Ouellet et al., 2012; Cypess Aaron et al., 2015). Importantly, the thermogenic activity of the tissue has been shown to decline with age and increasing BMI (Cypess et al., 2009; van Marken Lichtenbelt et al., 2009; Pfannenberger et al., 2010; Moonen et al., 2019).

## RECENT DEVELOPMENTS IN BAT PHYSIOLOGY

An important development over the past decade, although not on BAT as such, is the discovery of a third form of adipocyte—“brite” or “beige” (Petrovic et al., 2010; Wu et al., 2012; Carobbio et al., 2019). These fat cells contain UCP1, providing the potential for thermogenesis, and have some of the other molecular signatures of brown adipocytes (Petrovic et al., 2010; Wu et al., 2012). Beige adipocytes are found primarily within WAT depots, and are recruited particularly during cold-exposure and following  $\beta$ -adrenergic stimulation resulting in the “browning” of white fat (Carobbio et al., 2019).

A further advance comes from evidence suggesting that BAT plays an important role in metabolic homeostasis, the tissue being a major site of glucose disposal, insulin action and triglyceride clearance (Bartelt et al., 2011; Stanford et al., 2013; Bartelt and Heeren, 2014). A high capacity for glucose uptake, which can be stimulated by insulin and cold, is evident from FDG-PET studies. Roles for BAT in glucose homeostasis and triglyceride clearance have led to the proposition that reduced activity in the tissue may underlie the metabolic syndrome (Nedergaard et al., 2011; Bartelt and Heeren, 2014; Moonen et al., 2019).

An additional dimension is the function of BAT as a secretory organ. Apart from the release of fatty acids, brown adipocytes synthesize and secrete multiple peptide/protein factors, these “brown adipokines” paralleling the adipokines of white adipocytes (Villarroya et al., 2013, 2017). While the



adipokinome of white fat cells numbers several hundred entities (Trayhurn, 2013), it is unclear whether the secretome from brown adipocytes is as extensive. The brown adipokinome includes classical adipokines such as leptin and IL-6 (Villarroya et al., 2013, 2017), but brown adipocytes are unlikely to be an important source of these factors.

## BAT AS A THERAPEUTIC TARGET—IS IT REALISTIC?

A major driver behind the renewed interest in BAT relates to its potential as a therapeutic target to treat obesity. This reflects the revival of a concept current in the 1980's, but it is now based on the firm acceptance that the tissue is present, thermogenically active and exhibits plasticity in adults. The ability to recruit beige adipocytes within WAT has further added to the focus on BAT (Petrovic et al., 2010; Wu et al., 2012; Jespersen Naja et al., 2013; Sacks et al., 2013), or more strictly on UCP1-dependent adipocyte thermogenesis, as a therapeutic route in obesity. But how realistic is this?

### The Case in Favor

There are substantive points in favor of BAT as a target—which in principal can be through increasing the thermogenic activity/capacity of pre-existing brown adipocytes, by recruitment of new brown adipocytes, or a combination of the two. Additionally, there is the potential to recruit beige cells through “browning.” BAT has the conceptual attraction of being a clearly defined target with a precise molecular end-point in the amount and activity of UCP1. It also centres on one specific element of energy balance—adaptive energy expenditure—so augmentation is a logical approach. Furthermore, as well as increasing expenditure it has the potential of improving metabolic homeostasis through its role in glucose utilization and lipid clearance (Nedergaard and Cannon, 2010; Bartelt and Heeren, 2014; Moonen et al., 2019).

### The Case Against

There are, nevertheless, also substantive arguments against BAT as a realistic target. A key requirement is that the stimulation of energy expenditure through BAT does not lead to a compensatory increase in energy intake, which would be counter-productive. It is uncertain whether compensation would occur under normal circumstances; however, increased intake is very evident in rodents in the cold, with for example mice consuming three times more food at 4°C than at thermoneutrality (Trayhurn, 1981), suggesting that increased BAT activity is linked to higher intake.

A critical issue is the quantitative importance of BAT thermogenesis to energy expenditure in adults. Clearly, if the contribution is minimal then it is a less obvious target for modulating energy balance—though a small, but sustained, imbalance between expenditure and intake would be effective. Estimates of the importance of BAT in energy expenditure range from 1 to 5% of RMR, but these are in effect basal values and it is argued that with stimulation the value will be higher at up to 16%

of RMR (van der Lans et al., 2013; Moonen et al., 2019)—this can be viewed as part of the “case in favor.”

A number of approaches to increasing the thermogenic activity and capacity of BAT have been proposed. The initial route was to design selective  $\beta_3$ -agonists, reflecting the centrality of the  $\beta_3$ -adrenoceptor in the regulation of thermogenesis, and several were developed (Arch, 2002). However, although the first generation compounds were effective in stimulating expenditure and reversing obesity in rodents, their efficacy and potency in humans is poor due to a combination of factors including sequence differences between the human and rodent  $\beta_3$ -adrenoceptor (Arch, 2002). Nevertheless, selective  $\beta_3$ -agonists continue to be of interest with mirabegron having recently been shown to stimulate RMR and glucose uptake by BAT (Cypess Aaron et al., 2015). Alternative strategies have been proposed and these include central stimulation of the sympathetic innervation to BAT, brown fat transplantation and stem cell therapy (Gunawardana and Piston, 2012; Nishio et al., 2012; Guénantin et al., 2017; Carobbio et al., 2019). While potentially feasible, it is difficult to regard transplantation and stem cell therapy as practical approaches to obesity treatment.

Recruitment of beige cells would augment the number of thermogenic adipocytes, and multiple factors can facilitate this process (Bartelt and Heeren, 2014; Nedergaard and Cannon, 2014; Carobbio et al., 2019). There are, however, potential constraints on whether beige adipocytes may provide significant amounts of heat—apart from any intracellular limitation. To make a significant contribution to NST, close proximity to an extensive vascular network would be expected, both to rapidly dissipate the heat generated and to provide oxygen and other nutrients to fuel high rates of thermogenesis. Furthermore, thermogenesis requires noradrenergic stimulation, and the recruitment of beige adipocytes needs to be accompanied by local growth of the sympathetic innervation. A report that alternatively activated macrophages stimulate thermogenesis in BAT through the secretion of catecholamines (Nguyen et al., 2011) has not been supported subsequently (Fischer et al., 2017); however, the hormone meteronin-like promotes browning through M2 macrophage activation (Rao et al., 2014).

The final reservation to treating obesity through the stimulation of BAT thermogenesis lies in the potential cardiovascular risk. While this may be small, and needs to be balanced against the risks associated with obesity itself, regulatory agencies are likely to be ultra-cautious given the readiness with which previous anti-obesity drugs have been withdrawn following evidence of adverse effects.

## CONCLUDING COMMENTS

Our understanding of the functions of BAT has continued to evolve and it is evident that the tissue has multiple actions beyond a core thermoregulatory role. Recognition of its involvement in nutritional energetics and the etiology of obesity in the late 1970's transformed perspectives on the tissue. Over the past decade there has been a renaissance of interest in BAT, following clear

evidence of its presence and metabolic plasticity in adult humans. There is currently considerable focus on BAT as a therapeutic target in the treatment of obesity and its associated metabolic disorders, aided by the identification of beige adipocytes and the phenomenon of browning of WAT. However, it is suggested that in totality there are formidable barriers to this approach and that the stimulation and recruitment of thermogenic adipocytes

is unlikely to provide a realistic anti-obesity/anti-metabolic syndrome strategy in the near-future.

## AUTHOR CONTRIBUTIONS

The author confirms being the sole contributor of this work and has approved it for publication.

## REFERENCES

- Afzelius, B. A. (1970). "Brown adipose tissue: its gross anatomy, histology, and cytology," in *Brown Adipose Tissue*, ed. O. Lindberg (New York, NY: American Elsevier), 1–31.
- Arch, J. R. (2002).  $\beta_3$ -Adrenoceptor agonists: potential, pitfalls and progress. *Eur. J. Pharmacol.* 440, 99–107. doi: 10.1016/S0014-2999(02)01421-8
- Bartelt, A., Bruns, O. T., Reimer, R., Hohenberg, H., Ittrich, H., Peldschus, K., et al. (2011). Brown adipose tissue activity controls triglyceride clearance. *Nat. Med.* 17, 200–205. doi: 10.1038/nm.2297
- Bartelt, A., and Heeren, J. (2014). Adipose tissue browning and metabolic health. *Nat. Rev. Endocrinol.* 10, 24–36. doi: 10.1038/nrendo.2013.204
- Boullaud, F., Villarroja, F., Hentz, E., Raimbault, S., Cassard, A. M., and Ricquier, D. (1988). Detection of brown adipose tissue uncoupling protein mRNA in adult humans by a genomic probe. *Clin. Sci.* 75, 21–27. doi: 10.1042/cs0750021
- Brooks, S. L., Rothwell, N. J., Stock, M. J., Goodbody, A. E., and Trayhurn, P. (1980). Increased proton conductance pathway in brown adipose tissue mitochondria of rats exhibiting diet-induced thermogenesis. *Nature* 286, 274–276. doi: 10.1038/286274a0
- Carobbio, S., Guénantin, A.-C., Samuelson, I., Bahri, M., and Vidal-Puig, A. (2019). Brown and beige fat: from molecules to physiology and pathophysiology. *Biochim. Biophys. Acta Mol. Cell Biol. Lipids.* 1864, 37–50. doi: 10.1016/j.bbalip.2018.05.013
- Casteilla, L., Forest, C., Robelin, J., Ricquier, D., Lombet, A., and Ailhaud, G. (1987). Characterization of mitochondrial-uncoupling protein in bovine fetus and newborn calf. *Am. J. Physiol. Endocrinol. Metab.* 252, E627–E636. doi: 10.1152/ajpendo.1987.252.5.E627
- Cypess Aaron, M., Weiner Lauren, S., Roberts-Toler, C., Elia Elisa, F., Kessler Skyler, H., Kahn Peter, A., et al. (2015). Activation of human brown adipose tissue by a  $\beta_3$ -adrenergic receptor agonist. *Cell Metab.* 21, 33–38. doi: 10.1016/j.cmet.2014.12.009
- Cypess, A. M., Lehman, S., Williams, G., Tal, I., Rodman, D., Goldfine, A. B., et al. (2009). Identification and importance of brown adipose tissue in adult humans. *N. Engl. J. Med.* 360, 1509–1517. doi: 10.1056/NEJMoa0810780
- Fischer, K., Ruiz, H. H., Jhun, K., Finan, B., Oberlin, D. J., van der Heide, V., et al. (2017). Alternatively activated macrophages do not synthesize catecholamines or contribute to adipose tissue adaptive thermogenesis. *Nat. Med.* 23, 623–630. doi: 10.1038/nm.4316
- Foster, D. O., and Frydman, M. L. (1978). Nonshivering thermogenesis in the rat. II. Measurements of blood flow with microspheres point to brown adipose tissue as the dominant site of the calorogenesis induced by noradrenaline. *Can. J. Physiol. Pharmacol.* 56, 110–122. doi: 10.1139/y78-015
- Foster, D. O., and Frydman, M. L. (1979). Tissue distribution of cold-induced thermogenesis in conscious warm- or cold-acclimated rats re-evaluated from changes in tissue blood flow: the dominant role of brown adipose tissue in the replacement of shivering by non-shivering thermogenesis. *Can. J. Physiol. Pharmacol.* 57, 257–270. doi: 10.1139/y79-039
- Guénantin, A.-C., Briand, N., Capel, E., Dumont, F., Morichon, R., Provost, C., et al. (2017). Functional human beige adipocytes from induced pluripotent stem cells. *Diabetes* 66, 1470–1478. doi: 10.2337/db16-1107
- Gunawardana, S. C., and Piston, D. W. (2012). Reversal of type 1 diabetes in mice by brown adipose tissue transplant. *Diabetes* 61, 674–682. doi: 10.2337/db11-0510
- Heaton, J. (1972). The distribution of brown adipose tissue in the human. *J. Anatol.* 2, 35–39.
- Himms-Hagen, J. (1983). Brown adipose tissue thermogenesis; energy balance; and obesity. *Can. J. Biochem. Cell Biol.* 62, 610–617.
- Himms-Hagen, J. (1989). Brown adipose tissue thermogenesis and obesity. *Prog. Lipid Res.* 28, 67–115.
- Himms-Hagen, J., and Desautels, M. (1978). A mitochondrial defect in brown adipose tissue of the obese (*ob/ob*) mouse: reduced binding of purine nucleotides and a failure to respond to cold by an increase in binding. *Biochem. Biophys. Res. Commun.* 83, 628–634. doi: 10.1016/0006-291X(78)91036-7
- Jespersen Naja, Z., Larsen Therese, J., Peijs, L., Dagaard, S., Homøe, P., Loft, A., et al. (2013). A Classical brown adipose tissue mRNA signature partly overlaps with brite in the supraclavicular region of adult humans. *Cell Metab.* 17, 798–805. doi: 10.1016/j.cmet.2013.04.011
- Lean, M. E., James, W. P., Jennings, G., and Trayhurn, P. (1986a). Brown adipose tissue uncoupling protein content in human infants, children and adults. *Clin. Sci.* 71, 291–297. doi: 10.1042/cs0710291
- Lean, M. E. J., James, W. P. T., Jennings, G., and Trayhurn, P. (1986b). Brown adipose tissue in patients with pheochromocytoma. *Int. J. Obesity* 10, 219–27.
- Moonen, M. P. B., Nascimento, E. B. M., and van Marken Lichtenbelt, W. D. (2019). Human brown adipose tissue: underestimated target in metabolic disease? *Biochim. Biophys. Acta Mol. Cell Biol. Lipids.* 1864, 104–112. doi: 10.1016/j.bbalip.2018.05.012
- Nedergaard, J., Bengtsson, T., and Cannon, B. (2011). New powers of brown fat: fighting the metabolic syndrome. *Cell Metab.* 13, 238–240. doi: 10.1016/j.cmet.2011.02.009
- Nedergaard, J., and Cannon, B. (2010). The changed metabolic world with human brown adipose tissue: therapeutic visions. *Cell Metab.* 11, 268–272. doi: 10.1016/j.cmet.2010.03.007
- Nedergaard, J., and Cannon, B. (2014). The browning of white adipose tissue: some burning issues. *Cell Metab.* 20, 396–407. doi: 10.1016/j.cmet.2014.07.005
- Nguyen, K. D., Qiu, Y., Cui, X., Goh, Y. P., Mwangi, J., David, T., et al. (2011). Alternatively activated macrophages produce catecholamines to sustain adaptive thermogenesis. *Nature* 480, 104–108. doi: 10.1038/nature10653
- Nicholls, D. G., and Locke, R. M. (1984). Thermogenic mechanisms in brown fat. *Physiol. Rev.* 64, 1–64. doi: 10.1152/physrev.1984.64.1.1
- Nishio, M., Yoneshiro, T., Nakahara, M., Suzuki, S., Saeki, K., Hasegawa, M., et al. (2012). Production of functional classical brown adipocytes from human pluripotent stem cells using specific hemopoietin cocktail without gene transfer. *Cell Metab.* 16, 394–406. doi: 10.1016/j.cmet.2012.10.011
- Orava, J., Nuutila, P., Lidell, M. E., Oikonen, V., Noponen, T., Viljanen, T., et al. (2011). Different metabolic responses of human brown adipose tissue to activation by cold and insulin. *Cell Metab.* 14, 272–279. doi: 10.1016/j.cmet.2011.06.012
- Ouellet, V., Labbé, S. M., Blondin, D. P., Phoenix, S., Guérin, B., Haman, F., et al. (2012). Brown adipose tissue oxidative metabolism contributes to energy expenditure during acute cold exposure in humans. *J. Clin. Invest.* 122, 545–552. doi: 10.1172/JCI60433
- Petrovic, N., Walden, T. B., Shabalina, I. G., Timmons, J. A., Cannon, B., and Nedergaard, J. (2010). Chronic peroxisome proliferator-activated receptor  $\gamma$  (PPAR $\gamma$ ) Activation of epididymally derived white adipocyte cultures reveals a population of thermogenically competent, UCP1-containing adipocytes molecularly distinct from classic brown adipocytes. *J. Biol. Chem.* 285, 7153–7164. doi: 10.1074/jbc.M109.053942
- Pfannenberger, C., Werner, M. K., Ripkens, S., Stef, I., Deckert, A., Schmadl, M., et al. (2010). Impact of age on the relationships of brown adipose tissue with sex and adiposity in humans. *Diabetes* 59, 1789–1793. doi: 10.2337/db10-0004

- Rao, R. R., Long, J. Z., White, J. P., Svensson, K. J., Lou, J., Lokurkar, I., et al. (2014). Meteorin-like is a hormone that regulates immune-adipose interactions to increase beige fat thermogenesis. *Cell* 157, 1279–1291. doi: 10.1016/j.cell.2014.03.065
- Ricquier, D. (2017). UCP1, the mitochondrial uncoupling protein of brown adipocyte: a personal contribution and a historical perspective. *Biochimie* 134, 3–8. doi: 10.1016/j.biochi.2016.10.018
- Ricquier, D., and Kader, J. C. (1976). Mitochondrial protein alterations in active brown fat: a sodium dodecyl sulfate-polyacrylamide gel electrophoretic study. *Biochem. Biophys. Res. Commun.* 73, 577–583. doi: 10.1016/0006-291X(76)90849-4
- Ricquier, D., Nechad, M., and Mory, G. (1982). Ultrastructural and biochemical characterization of human brown adipose tissue in pheochromocytoma. *J. Clin. Endocrinol. Metab.* 54, 803–807.
- Rothwell, N. J., and Stock, M. J. (1979). A role for brown adipose tissue in diet-induced thermogenesis. *Nature* 281, 31–35. doi: 10.1038/281031a0
- Rothwell, N. J., and Stock, M. J. (1981). Regulation of energy balance. *Ann. Rev. Nutr.* 1, 235–256. doi: 10.1146/annurev.nu.01.070181.001315
- Sacks, H. S., Fain, J. N., Bahouth, S. W., Ojha, S., Frontini, A., Budge, H., et al. (2013). Adult epicardial fat exhibits beige features. *J. Clin. Endocrinol. Metab.* 98, E1448–E1455. doi: 10.1210/jc.2013-1265
- Smith, R. E., and Horwitz, B. A. (1969). Brown fat and thermogenesis. *Physiol. Rev.* 49, 330–425. doi: 10.1152/physrev.1969.49.2.330
- Stanford, K. I., Middelbeek, R. J., Townsend, K. L., An, D., Nygaard, E. B., Hitchcox, K. M., et al. (2013). Brown adipose tissue regulates glucose homeostasis and insulin sensitivity. *J. Clin. Invest.* 123, 215–223. doi: 10.1172/JCI62308
- Trayhurn, P. (1979). Thermoregulation in the diabetic-obese (*db/db*) mouse. The role of non-shivering thermogenesis in energy balance. *Pflügers Arch.* 380, 227–232.
- Trayhurn, P. (1981). Fatty acid synthesis in mouse brown adipose tissue: the influence of environmental temperature on the proportion of whole-body synthesis in brown adipose tissue and the liver. *Biochim. Biophys. Acta.* 664, 549–560. doi: 10.1016/0005-2760(81)90132-6
- Trayhurn, P. (1989). “Brown adipose tissue and energy balance,” in *Brown Adipose Tissue*, ed P. Trayhurn and D. G. Nicholls (London: Edward Arnold), 299–388.
- Trayhurn, P. (2013). Hypoxia and adipose tissue function and dysfunction in obesity. *Physiol. Rev.* 93, 1–21. doi: 10.1152/physrev.00017.2012
- Trayhurn, P. (2017). Origins and early development of the concept that brown adipose tissue thermogenesis is linked to energy balance and obesity. *Biochimie* 134, 62–70. doi: 10.1016/j.biochi.2016.09.007
- Trayhurn, P., and James, W. P. (1978). Thermoregulation and non-shivering thermogenesis in the genetically obese (*ob/ob*) mouse. *Pflügers Arch.* 373, 189–193.
- Trayhurn, P., Thomas, M. E., and Keith, J. S. (1993). Postnatal development of uncoupling protein, uncoupling protein mRNA, and GLUT4 in adipose tissues of goats. *Am. J. Physiol. Reg. Integr. Comp. Physiol.* 265, R676–R682. doi: 10.1152/ajpregu.1993.265.3.R676
- van der Lans, A. A., Hoeks, J., Brans, B., Vijgen, G. H., Visser, M. G., Vosselman, M. J., et al. (2013). Cold acclimation recruits human brown fat and increases nonshivering thermogenesis. *J. Clin. Invest.* 123, 3395–3403. doi: 10.1172/JCI68993
- van Marken Lichtenbelt, W. D., and Schrauwen, P. (2011). Implications of nonshivering thermogenesis for energy balance regulation in humans. *Am. J. Physiol. Reg. Integr. Comp. Physiol.* 301, R285–R296. doi: 10.1152/ajpregu.00652.2010
- van Marken Lichtenbelt, W. D., Vanhomerig, J. W., Smulders, N. M., Drossaerts, J. M., Kemerink, G. J., Bouvy, N. D., et al. (2009). Cold-activated brown adipose tissue in healthy men. *N. Engl. J. Med.* 360, 1500–1508. doi: 10.1056/NEJMoa0808718
- Villarroya, F., Gavalda-Navarro, A., Peyrou, M., Villarroya, J., and Giralt, M. (2017). The lives and times of brown adipokines. *Trends Endocrinol. Metab.* 28, 855–867. doi: 10.1016/j.tem.2017.10.005
- Villarroya, J., Cereijo, R., and Villarroya, F. (2013). An endocrine role for brown adipose tissue? *Am. J. Physiol. Endocrinol. Metab.* 305, E567–E572. doi: 10.1152/ajpendo.00250.2013
- Virtanen, K. A., Lidell, M. E., Orava, J., Heglind, M., Westergren, R., Niemi, T., et al. (2009). Functional brown adipose tissue in healthy adults. *N. Engl. J. Med.* 360, 1518–1525. doi: 10.1056/NEJMoa0808949
- Wijers, S. L., Saris, W. H., and van Marken Lichtenbelt, W. D. (2007). Individual thermogenic responses to mild cold and overfeeding are closely related. *J. Clin. Endocrinol. Metab.* 92, 4299–4305. doi: 10.1210/jc.2007-1065
- Wu, J., Boström, P., Sparks Lauren, M., Ye, L., Choi Jang, H., Giang, A.-H., et al. (2012). Beige Adipocytes are a distinct type of thermogenic fat cell in mouse and human. *Cell* 150, 366–376. doi: 10.1016/j.cell.2012.05.016

**Conflict of Interest Statement:** The author declares that the research was conducted in the absence of any commercial or financial relationships that could be construed as a potential conflict of interest.

Copyright © 2018 Trayhurn. This is an open-access article distributed under the terms of the Creative Commons Attribution License (CC BY). The use, distribution or reproduction in other forums is permitted, provided the original author(s) and the copyright owner(s) are credited and that the original publication in this journal is cited, in accordance with accepted academic practice. No use, distribution or reproduction is permitted which does not comply with these terms.



# Dietary Proteins, Brown Fat, and Adiposity

Lise Madsen<sup>1,2\*</sup>, Lene Secher Myrmet<sup>1</sup>, Even Fjære<sup>1</sup>, Jannike Øyen<sup>1</sup> and Karsten Kristiansen<sup>2</sup>

<sup>1</sup> Institute of Marine Research, Bergen, Norway, <sup>2</sup> Laboratory of Genomics and Molecular Biomedicine, Department of Biology, University of Copenhagen, Copenhagen, Denmark

## OPEN ACCESS

### Edited by:

Paula Oliver,  
Universidad de les Illes Balears, Spain

### Reviewed by:

Patrick Christian Even,  
Physiologie de la nutrition et du  
comportement alimentaire (PNCA),  
France  
Abdul G. Dulloo,  
Université de Fribourg, Switzerland

### \*Correspondence:

Lise Madsen  
lise.madsen@hi.no

### Specialty section:

This article was submitted to  
Integrative Physiology,  
a section of the journal  
Frontiers in Physiology

**Received:** 03 September 2018

**Accepted:** 28 November 2018

**Published:** 12 December 2018

### Citation:

Madsen L, Myrmet LS, Fjære E,  
Øyen J and Kristiansen K (2018)  
Dietary Proteins, Brown Fat, and  
Adiposity. *Front. Physiol.* 9:1792.  
doi: 10.3389/fphys.2018.01792

High protein diets have become popular for body weight maintenance and weight loss despite controversies regarding efficacy and safety. Although both weight gain and weight loss are determined by energy consumption and expenditure, data from rodent trials consistently demonstrate that the protein:carbohydrate ratio in high fat diets strongly influences body and fat mass gain per calorie eaten. Here, we review data from rodent trials examining how high protein diets may modulate energy metabolism and the mechanisms by which energy may be dissipated. We discuss the possible role of activating brown and so-called beige/BRITE adipocytes including non-canonical UCP1-independent thermogenesis and futile cycles, where two opposing metabolic pathways are operating simultaneously. We further review data on how the gut microbiota may affect energy expenditure. Results from human and rodent trials demonstrate that human trials are less consistent than rodent trials, where casein is used almost exclusively as the protein source. The lack of consistency in results from human trials may relate to the specific design of human trials, the possible distinct impact of different protein sources, and/or the differences in the efficiency of high protein diets to attenuate obesity development in lean subjects vs. promoting weight loss in obese subjects.

**Keywords:** brown adipose tissue (BAT), diet, futile cycles, high protein diets, human, obesity, mouse, weight loss

## INTRODUCTION

It has for long been known that dietary protein content influences energy efficiency and thereby the energy cost for weight gain (Stock, 1999). High protein diets represent a popular alternative to energy restriction for body weight maintenance and weight loss. For instance, the Atkins diet books have sold more than 45 million copies. The Atkins diet and similar diets such as the Stone-age diet claim to be effective despite *ad libitum* consumption of high energy food items, such as fatty meat, oils, and butter, as long as the intake of carbohydrates remains lower than 50 g per day. This has in part been explained by the high satiating effect of high protein meals (Veldhorst et al., 2008; Cuenca-Sánchez et al., 2015). However, pair-feeding experiments in mice strongly suggest that increased satiety and reduced energy-intake cannot fully explain why a high protein:carbohydrate ratio in high fat diets attenuates obesity development in mice (Madsen et al., 2008, 2017; Ma et al., 2011; Qin et al., 2012). Moreover, additional effects related to increased energy expenditure of diets with high protein and low carbohydrate content have been claimed in humans (Buchholz and Schoeller, 2004; Westerterp-Plantenga, 2008; Pesta and Samuel, 2014), and based on measurements



in metabolic chambers it was recently demonstrated that excess energy in the form of protein stimulated 24 h energy expenditure in men and women (Bray et al., 2015).

Taking the physical laws of energy into account, both weight gain and loss are inevitably related to consumption and use of energy. Considering the proposed positive effect of high protein diets, however, it is important to note that energy from different macronutrients may be lost to a different extent by heat generated by processing. Whereas, the thermic effects of lipids and carbohydrates are reported to be within the range of 2–3 and 6–8%, respectively, the thermic effect of proteins is reported to be 25–30% (Jequier, 2002). In addition to physical activity, energy in form of ATP may furthermore be lost in so-called “futile cycles” where two opposing metabolic pathways, such as synthesis and degradation of proteins and esterification of fatty acids and lipolysis of triacylglycerols are operating simultaneously. Energy may also be lost to the environment in form of heat via the action of uncoupling protein 1 (UCP1), present in brown and brown-like adipocytes termed BRITE (Petrovic et al., 2010) or beige adipocytes (Ishibashi and Seale, 2010; Wu et al., 2012), which uncouples oxidative phosphorylation by dissipating the proton gradient across the inner mitochondrial membrane. Historically, UCP1 was identified as the protein responsible for uncoupled respiration and heat generation in interscapular brown adipose tissue (iBAT), and cold exposure or administration of  $\beta$ -adrenergic agonists was subsequently reported to induce expression of UCP1 in formally white adipose tissue (WAT), especially in subcutaneous inguinal white adipose tissue (iWAT), a process termed browning, and UCP1 was considered essential for non-shivering thermogenesis and increased energy expenditure in response to cold (for a review see Cannon and Nedergaard, 2004).

Further, recent research has demonstrated additional UCP1-independent mechanisms increasing thermogenesis and energy expenditure via creatine-driven substrate cycling (Kazak et al., 2015, 2017; Bertholet et al., 2017) or  $\text{Ca}^{2+}$  cycling via the sarco/endoplasmic reticulum  $\text{Ca}^{2+}$ -ATPase 2b (SERCA2b) and the ryanodine receptor (Ikeda et al., 2017). Hence, by activation of these mechanisms it is possible to consume more energy without an accompanying weight gain. Remaining questions in this context are how such increased energy expenditure escapes the normal regulatory mechanisms aiming at maintaining energy balance, and how intake of high protein diets possibly affects this normally finely tuned homeostatic balance. So far, no comprehensive answers to these important questions have been presented, but clearly approaches to provide such answers are warranted.

Here we review mechanisms by which high protein diets may modulate energy metabolism including the possible role of activating brown and BRITE adipocytes, futile cycles, and UCP1-independent mechanisms. We also review recent data showing how the gut microbiota may impact on energy expenditure. We further discuss the lack of consistency in human trials in relation to the rodent trials demonstrating a huge difference in the potential of different protein sources to attenuate obesity development.

## RODENT TRIALS

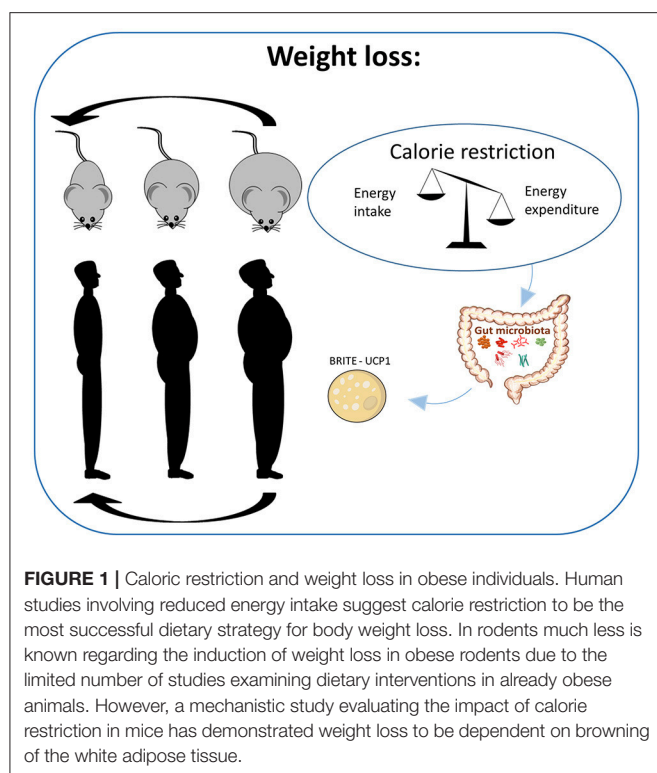
### High Protein Diets, Attenuation of Obesity, and Weight Loss in Rodents

A number of rodent studies by us and others has demonstrated that a high protein:carbohydrate ratio prevents high fat diet induced obesity with an accompanied reduced feed efficiency (Marsset-Baglieri et al., 2004; Morens et al., 2005; Pichon et al., 2006; Madsen et al., 2008; Ma et al., 2011; Freudenberg et al., 2012, 2013; McAllan et al., 2014). For instance, whereas mice fed a high fat diet with low protein:carbohydrate ratio gained 14.7 g body weight per Mcal eaten, mice fed an isocaloric high fat diet with a high protein:carbohydrate ratio gained only 2.2 g body weight per Mcal eaten (Madsen et al., 2008).

The vast majority of obesity-related rodent trials have investigated attenuation of and protection against obesity development and the efficiency of different diets to reverse obesity is far less studied (Figure 1). Inevitably, caloric restriction (Gao et al., 2015), exercise, and low fat diets promote weight loss (Jung et al., 2013), and it was suggested that weight loss is accompanied by browning of the WAT (Figure 1) (Pérez-Martí et al., 2017). Information on the efficiency of high protein diets to reverse or attenuate further obesity development is very limited. One article reported that increasing the protein content using whey, soy, red meat, or milk as the protein source to 30% at the expense of carbohydrate maintaining fat content at 40% did not reduce adipose tissue mass in already obese mice, but attenuated weight gain in a protein-dependent manner (Huang et al., 2008). Thus, when obese mice were fed whey as the protein source they gained less weight than when soy or red meat was used as protein source. The authors did not measure *Ucp1* expression or energy expenditure, and they suggested that increased adiponectin and decreased appetite may explain the stabilized adiposity in whey fed mice. Using low fat diets, we have demonstrated that the protein source may be of importance in reducing obesity, as intake of a low fat diet with casein, but not pork, reduced diet-induced obesity (Liisberg et al., 2016b). Hence, although diets with a high content of casein efficiently attenuate high fat diet induced obesity, no evidence of an obesity reversing effect of high protein diets has been published.

### Anti-obesogenic Properties of Different Protein Sources in Rodents

There is little knowledge as to how the protein source may modulate the response to high protein intake. In experiments using obesogenic diets with regular protein amounts, it has been demonstrated that protein from vegetable sources, milk protein, and proteins from seafood are less obesogenic than proteins from terrestrial animals, and this is associated with reduced energy efficiency (Figure 2) (Tastesen et al., 2014a,b; Holm et al., 2016; Liisberg et al., 2016a). However, rodent experiments, where the protein:carbohydrate ratio is increased, are in general performed using casein or whey as protein sources, and recent experiments indicate that casein and whey may not be representative. We have demonstrated that feeding obesity-prone C57BL/6J mice a high fat high protein diet using casein, soy, or filets of



cod, beef, chicken or pork as protein sources led to striking differences in obesity development at thermoneutral conditions (Liisberg et al., 2016b). Casein was the most efficient protein source preventing weight gain and accretion of adipose mass, whereas mice fed high protein diets based on “white meat” (lean pork or chicken filets) gained the largest quantities of adipose tissue. Of note, iBAT in pork fed mice was composed of large unilocular “white-like” adipocytes. In casein fed mice, the classic brown adipose tissue phenotype/appearance of the iBAT was preserved with multilocular adipocytes and high UCP1 expression even at thermoneutrality. Further, the casein-induced reduction in adiposity is associated with a reversal of the obesity-induced whitening of adipocytes in iBAT and induction of UCP1 expression. Similarly, intake of high protein diets based on beef, casein and soy protein was also shown to elicit markedly different responses in relation to lipid metabolism and composition of the gut microbiota (Ijaz et al., 2018). Compared to other protein sources, casein seems to stand out either by maintaining a  $\beta$ -adrenergic tone or by eliciting effects via  $\beta$ -adrenergic independent pathways still to be identified accompanied with high expression of genes involved in a futile recycling of fatty acids, including GYK (Liisberg et al., 2016b). The GYK-dependent futile cycle may be activated without a concomitant upregulation of *Ucp1* expression and may play a key role in regulation of the metabolic flexibility, not only in adipocytes, but in the entire organism. Furthermore, it is not known if different protein sources differentially activate creatine and/or SERCA2b-dependent  $\text{Ca}^{2+}$  cycling.

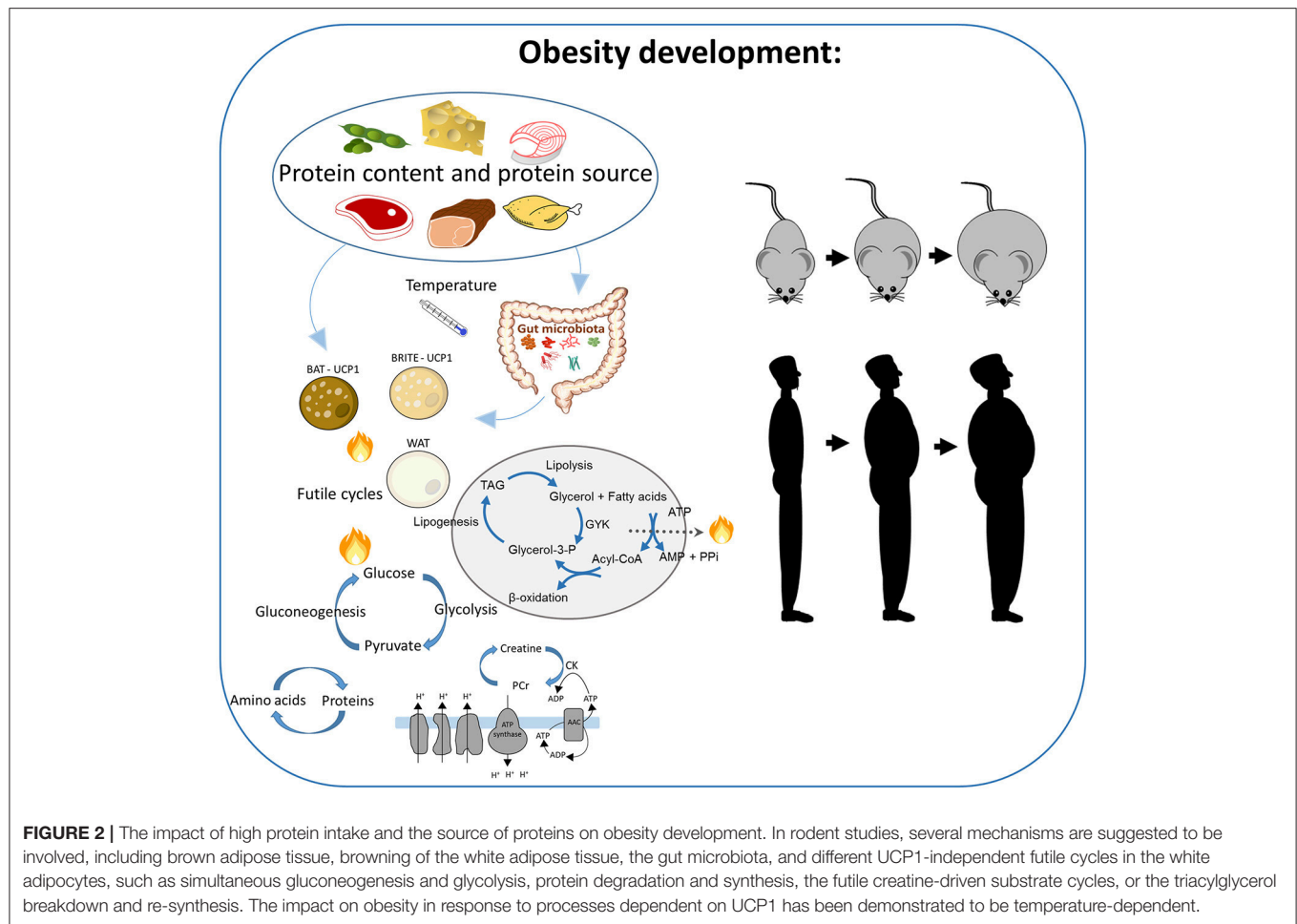
## Potential Mechanisms by Which High Protein Diets May Attenuate Obesity in Rodents

High protein diets may modulate energy efficiency and thermogenesis by several mechanisms. UCP1-dependent generation of heat in BAT through non-shivering thermogenesis unquestionable plays an important role in enabling rodents to defend their body temperature (Cannon and Nedergaard, 2004) and thereby also affecting energy efficiency. Thus, several different genetically modified animal models with increased capacity for non-shivering thermogenesis are protected against diet-induced obesity (Harms and Seale, 2013). A link between UCP1 and dietary composition of macronutrients has been demonstrated in a number of studies, where rodents fed high protein diets exhibited attenuated obesity development accompanied by increased UCP1 expression and energy expenditure. Using casein-based diets with five different protein:carbohydrate ratios, it was demonstrated in mice that the body surface temperature and expression of UCP1 as well as PGC1 $\alpha$  and DIO2, both key regulators of thermogenesis, increased in iBAT with increasing protein content in the feed. Mice fed the highest protein content gained less weight, whereas mice fed a so-called “balanced” protein to carbohydrate ratio had the highest weight gain and most pronounced adiposity (Huang et al., 2013).

In a short term experiment with rats given high protein diets, Petzke et al., demonstrated lower weight gain accompanied with higher overnight energy expenditure and oxygen consumption (Petzke et al., 2007). The expression of UCP1 was not significantly elevated in the high protein fed rats after 4 days of feeding compared with rats fed feed with lower protein content. Still, *Ucp1* mRNA levels correlated with night-time oxygen consumption, energy expenditure, and nitrogen intake. In long term experiments, the same group demonstrated increased *Ucp1* mRNA expression in iBAT by high protein feeding (Petzke et al., 2005). Also in these rats, *Ucp1* expression levels positively correlated with energy expenditure and oxygen consumption in the dark period. However, even though intake of a high dietary protein:carbohydrate ratio also attenuates obesity development during an entire life-span in mice, no increase of UCP1 expression in iBAT or iWAT was reported in these experiments (Keipert et al., 2011; Kiilerich et al., 2016).

A considerable number of experiments has failed to detect an increased level of *Ucp1* mRNA expression in iBAT despite attenuated obesity and reduced energy efficiency (Madsen et al., 2008; Ma et al., 2011; Freudenberg et al., 2012; Hao et al., 2012; Liisberg et al., 2016b). However, expression levels of *Ucp1* do not necessarily follow the thermogenic capacity (Nedergaard and Cannon, 2013), and we have in some experiments, despite no detectable induction of *Ucp1* mRNA expression, observed increased levels of UCP1 protein using immunohistochemistry and western-blotting in high protein fed mice (Liisberg et al., 2016b).

In male C57BL/6 mice, Klaus reported that development of high fat diet-induced obesity was delayed, but not prevented by increasing the protein:carbohydrate ratio (Klaus, 2005). In



this experiment, a lower respiratory quotient indicated higher oxidation of fat in protein fed mice, but no differences in energy expenditure were detected. It should be noted that the findings of many studies reporting that high protein diets do not result in a significant increase in UCP1 expression or activity in iBAT are consistent with early demonstrations that unlike the activation of the central nervous system (CNS) observed with dietary carbohydrate and fat, the CNS response to dietary protein in iBAT is absent or minimal (Kaufman et al., 1986). Whether this is due to the higher protein *per se* or to lower contents of carbohydrate or fat in these diets is unknown. However, reducing the carbohydrate content, without a concomitantly increased protein content did not appear to be sufficient for increased thermogenic capacity in rats (Betz et al., 2012).

A number of studies has reported on increased expression of *Ucp1* and other markers of a brown-like phenotype in iWAT in response to increased intake of dietary protein (Madsen et al., 2008; Ma et al., 2011; Hao et al., 2012). This browning of WAT together with induction of UCP1 was associated with a reduced propensity to develop obesity accompanied with improved metabolic health (Harms and Seale, 2013). However, it has been argued that at least after cold exposure all mitochondria of iWAT only correspond to approximately 30% of the total

number of mitochondria in iBAT (Shabalina et al., 2013). Still, high emergence of BRITE cells is a feature of mouse strains resistant to diet-induced obesity (Collins et al., 1997; Guerra et al., 1998). Further, the lean phenotype associated with aP2-driven expression of UCP1 is linked to increased energy dissipation in WAT (Kopecký et al., 1996b). Endogenous UCP1 expression as well as the respiration rate is actually reduced in iBAT from these mice (Kopecký et al., 1996a).

Resistance against high fat diet-induced obesity is demonstrated in several genetically modified mice associated with an increased occurrence of BRITE adipocytes in former WAT, such as mice deficient in RIP140 (Leonardsson et al., 2004), Caveolin (Razani et al., 2002), FSP27 (Toh et al., 2008), HSL (Ström et al., 2008), RB (Hansen et al., 2004; Dali-Youcef et al., 2007; Mercader et al., 2009), and p53 (Hallenborg et al., 2016). Interestingly, the thermogenic activity in iBAT of these modified strains was unchanged or reduced. It may also be noted that depletion of BRITE adipocytes by PRDM16 ablation in mice leads to moderate obesity (Cohen et al., 2014). For an extensive list of genes affecting formation of BRITE adipocytes, see (Harms and Seale, 2013). However, it is a distinct possibility that the blunted development of obesity in these studies with no detectable induction of UCP1 expression in BRITE or brown



adipocytes may be caused by UCP1-independent mechanisms including creatine-driven cycles and/or SERCA2b-dependent  $\text{Ca}^{2+}$  cycling, and future studies on the possible involvement of such mechanisms in response to intake of high protein diets would clearly be of interest.

Assessing the obesogenic capacity of different diets at different housing temperatures may also contribute to an understanding of the mechanisms by which diets influence obesity development. The importance of UCP1 and diet-induced thermogenesis during high protein feeding may only be clearly manifested in mice kept at thermoneutrality (28–30°C). Cold-sensitive mice lacking UCP1 are not more obesity prone than wild type mice when fed a high fat diet and kept at 21°C (Enerback et al., 1997). However, at 30°C, the *Ucp1*-KO mice are more susceptible to obesity than their wild type littermates and become by far more obese, demonstrating the importance of UCP1 for diet-induced thermogenesis and prevention of obesity development (Feldmann et al., 2009). Compared with thermoneutrality, housing at standard vivarium temperatures, 20–22°C, leads to higher food intake required to meet the increased energy demand for thermogenesis (Cannon and Nedergaard, 2004; Fischer et al., 2018). Increasing the protein:carbohydrate ratio in high fat diets attenuate obesity development and increase UCP1 expression in mice kept at both 22°C (Madsen et al., 2008) and at thermoneutrality (Ma et al., 2011), but obesity development and feed-efficiency in mice kept at the two different temperatures have not yet been directly compared. Such comparison may be useful in determining the mechanisms by which high protein diets mediate their anti-obesogenic effects.

Whereas UCP1-dependent uncoupled respiration in iBAT is crucial during cold exposure, recent results has convincingly demonstrated that UCP1-independent thermogenesis and increased energy expenditure are associated with BRITE adipocytes (for recent reviews see Ikeda et al., 2018; Sponton and Kajimura, 2018). Thus, it is possible that such UCP1-independent processes may also contribute to the decreased energy efficiency in response to intake of high-protein diets. This notion also extends to loss of fat mass in response to caloric restriction, which has been shown to be dependent on browning (Fabbiano et al., 2016). Still, although it is evident that feeding mice high protein diets reduces energy efficiency, further investigations are required to determine the importance of energy dissipation in form of heat by activation of UCP1 or UCP1-independent processes in BRITE adipocyte, but evidence from studies on the SERCA2b-dependent  $\text{Ca}^{2+}$  cycling would suggest that the contribution of this process may account for much of the diet-induced thermogenesis in BRITE adipocytes (Ikeda et al., 2018; Sponton and Kajimura, 2018).

Temperature may also affect the process of browning by changing the composition and function of the gut microbiota. It was initially observed that germ-free mice were resistant to high fat diet-induced obesity (Bäckhed et al., 2004). Interestingly, it has been shown that antibiotics-mediated depletion of the gut microbiota promoted browning of iWAT and perigonadal WAT (pWAT) in lean and obese mice, and increased browning was also observed in germ-free mice by the Trajkovski group (Suarez-Zamorano et al., 2015). Surprisingly, the same group also

reported that exposure to cold resulted in major changes in the composition and function of the gut microbiota in mice and that transplantation of the gut microbiota from cold-adapted mice to germ-free mice by co-housing increased browning of iWAT and pWAT (Chevalier et al., 2015). Similarly, the Bäckhed group reported that cold exposure drastically altered the composition of the gut microbiota accompanied by an attenuated propensity for diet-induced obesity, and the obesity-resistant phenotype could be transferred to germ-free mice by fecal transplantation (Zietak et al., 2016). However, in this case the most pronounced effect in terms of inducing UCP1 expression was observed in iBAT, and in addition, increased fatty acid oxidation was observed in the liver (Zietak et al., 2016).

Although commonly used in commercial available rodent feed, casein and whey protein, appear to possess anti-obesogenic properties (Lillefosse et al., 2014; Tastesen et al., 2014b; Pezeshki et al., 2015; Liisberg et al., 2016b; Singh et al., 2016). This may be related to the high content of the branched-chain amino acids (BCAA). BCAA is reported to increase the abundance of *Akkermansia* and *Bifidobacterium* in the gut (Yang et al., 2016). High levels of both *A. muciniphilia* (Everard et al., 2013; Shin et al., 2014) and some strains of *Bifidobacteria* (An et al., 2011; Wang et al., 2015; Li et al., 2016) have been reported to protect against diet-induced obesity.

BCAAs may also directly affect metabolism, as inclusion of BCAAs attenuates high fat diet induced obesity in rats (Newgard et al., 2009) and mice with a disrupted mitochondrial branched chain amino transferase gene exhibit chronic elevated levels of BCAAs in blood and have increased energy expenditure (She et al., 2007). The importance of BCAA is further supported by studies from Freudenberg et al. demonstrating that adding leucine to a high fat diet with regular protein content to a level matching a diet with high content of whey attenuated obesity development (Freudenberg et al., 2012, 2013). However, equimolar supplementation with alanine decreased body fat mass gain to the same extent (Freudenberg et al., 2013; Petzke et al., 2014). Hence, at least some of the observed effects are not specifically related to BCAA, but rather increased amino nitrogen consumption. Together, animal studies indicate that casein and whey have anti-obesogenic properties compared with other protein sources. Hence, studies investigating the effect of high protein diets using casein or whey may not be representative. In fact, high fat high protein diets with meat appear to promote obesity development (Pezeshki et al., 2015; Liisberg et al., 2016b; Madsen et al., 2017; Ijaz et al., 2018).

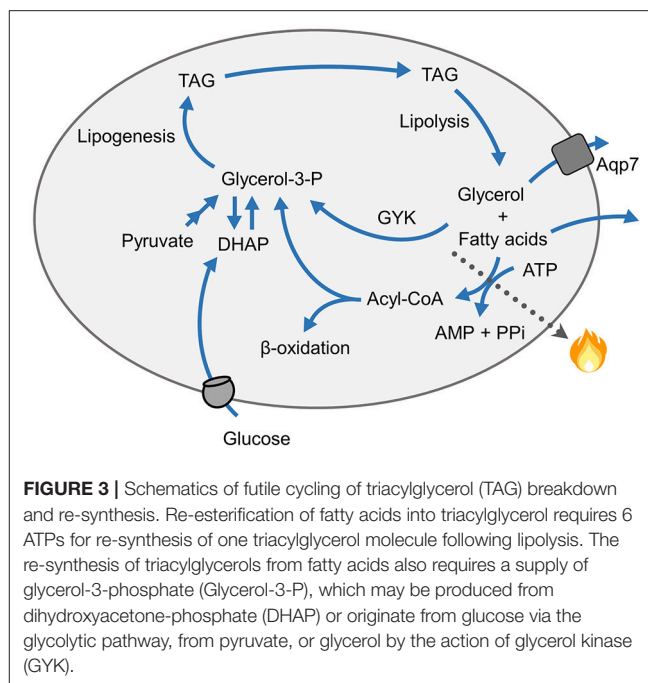
In mice fed either standard low fat diets, or high fat diets with high or low protein:sucrose ratio, the dietary fat content is a stronger driver of the composition of the gut microbiota than the protein:sucrose ratio (Kiilerich et al., 2016). However, still certain phylotypes within the *Clostridiaceae* family (*Anaerovorax*, *Bryantella*, *C. herbivorans*, *C. spheonoides*, *C. leptum*, and *C. symbiosum*) were found to characterize the gut in high protein fed mice (Kiilerich et al., 2016). Whether the accompanied high protein induced changes in energy expenditure and/or UCP1 expression are linked to the observed changes in gut microbiota composition requires further investigations. It should be mentioned, however,



that a high dietary protein content in diets with regular fat content led to decreased abundances of *Akkermansia muciniphila*, *Bifidobacterium*, *Prevotella*, *Ruminococcus bromii*, and *Roseburia/Eubacterium rectale*, and thereby a decreased number and activity of propionate- and butyrate-producing bacteria in rats (Mu et al., 2017). This would be counteractive in terms of obesity, as *Akkermansia muciniphila* (Everard et al., 2013; Shin et al., 2014), and short chain fatty acids are reported to attenuate diet induced obesity in mice (Lin et al., 2012; Lu et al., 2016) and have been associated with protection against diet-induced obesity and associated metabolic disorders in part by increased energy expenditure and thermogenesis (Gao et al., 2009). Thus, as high protein feeding modulates the composition of the gut microbiota, it is possible that such changes contribute to the reduced accumulation of fat, but it also remains to be investigated to what extent creatine-driven cycling or SERCA2b-dependent processes following browning contributes to these observed physiological phenotypes.

Apart from creatine and  $\text{Ca}^{2+}$  cycling discussed above, energy may also be lost in an UCP1-independent manner by futile cycling of fatty acids. Re-esterification of fatty acids into triacylglycerol following lipolysis occurs in both humans and rodents (Figure 3). This process of triacylglycerol/fatty acid cycling is a futile cycle as 6 ATPs are required for re-synthesis of one triacylglycerol molecule. Work from Kopecky's laboratory has demonstrated that the ATP required for both triacylglycerol/fatty acid cycling as well as the associated *de novo* synthesis of fatty acids is produced by oxidative phosphorylation in white adipocytes (Kuda et al., 2018). Their work suggested that the UCP1-independent energy dissipation linked to futile triacylglycerol/fatty acid cycling may contribute to non-shivering thermogenesis as well as the observed amelioration of obesity induced by calorie restriction combined with the intake of omega-3 fatty acids. Of note, cold exposure leads to induction of genes involved in both triacylglycerol synthesis as well as *de novo* lipogenesis in WAT (Hao et al., 2010; Kiskinis et al., 2014; Gao et al., 2015; Flachs et al., 2017).

Intake of diets with high protein:carbohydrate ratio is accompanied by increased expression of genes involved in futile recycling of glycerol and fatty acids in iBAT (Lisberg et al., 2016b). Re-esterification of fatty acids into triacylglycerols within adipocytes also requires a continuous supply of glycerol-3-phosphate (Figure 3). Possibly, to avoid re-esterification of glycerol, and thereby futile cycling of triacylglycerol in adipose tissue, glycerol kinase (GYK) expression and activity is absent or low in adipose tissue. However, PPAR $\gamma$  activating drugs, such as thiazolidinediones, induce the expression of GYK in adipocytes (Guan et al., 2002), and more studies have demonstrated that GYK expression in adipocytes is controlled by PGC-1 $\alpha$  and PPAR $\alpha$  (Mazzucotelli et al., 2007). In addition to increased *Ucp1* expression in eWAT, energy loss due to increased expression of GYK and other genes involved in the futile cycling of triacylglycerol breakdown and synthesis was suggested to explain the lean phenotype of mice lacking RIP140 (Leonardsson et al., 2004). Using casein as the protein source, we have observed that a high protein:carbohydrate ratio in a high fat diet is accompanied by increased expression levels of GYK and other



genes involved in a futile recycling of glycerol and fatty acids in iBAT (Lisberg et al., 2016b). We have suggested that futile cycling of triacylglycerol breakdown and re-synthesis supports the enhanced uncoupled respiration and thereby plays a part in mediating the anti-obesogenic effect of certain high protein diets. Of note, the diets used by us were not carbohydrate free, and GYK-expression may be related to a more brown phenotype and possibly higher sympathetic flow.

When the intake of carbohydrates is low, the ratio of circulating insulin:glucagon is low and glucose may be provided by hepatic gluconeogenesis via activation of hepatic PGC-1 $\alpha$  (Herzig et al., 2001; Yoon et al., 2001; Puigserver et al., 2003). Hence, when intake of carbohydrates is sufficiently low, gluconeogenesis and glycolysis may occur simultaneously. Gluconeogenesis requires a higher number of ATP molecules than provided by glycolysis. Further, a concomitant conversion of protein to metabolites that may enter gluconeogenesis may occur. Protein is converted to glucose at a cost of 4–5 kcal/g protein (Fine and Feinman, 2004), and this may contribute to reduced feed efficiency. We have earlier demonstrated that a reduced circulating insulin:glucagon ratio was accompanied by increased expression of PGC-1 $\alpha$  and gluconeogenesis in the liver of high protein fed mice and suggested that this may contribute to the lean phenotype in these mice (Madsen et al., 2008). The increased glucagon:insulin ratio observed in mice fed a high proportion of casein may further lead to reduced insulin signaling in adipose tissue. This may be of particular importance, as studies in mice with fat-specific disruption of the insulin receptor gene have demonstrated that insulin signaling in adipocytes is crucial for development of obesity (Blüher et al., 2002). Furthermore, prevention of hyperinsulinemia is demonstrated to protect against diet-induced obesity in *Ins1*<sup>+/-</sup>:*Ins2*<sup>-/-</sup>

mice (Mehran et al., 2012). Concomitantly, enhanced cAMP-dependent signaling and PKA activation in adipose tissues may occur as we have observed increased phosphorylation of CREB and enhanced expression of the canonical cAMP-responsive genes, cAMP-responsive element modulator and cAMP-specific phosphodiesterase 4c, in both white and brown adipose tissue (Madsen et al., 2008). Hence, processes required to efficiently store fat may be inhibited.

Feed efficiency may also be reduced by simultaneous increased protein degradation and synthesis as observed in mice with disrupted branched-chain amino acid metabolism (She et al., 2007). In addition, both protein synthesis and proteolysis are energy demanding processes (Reeds et al., 1985). In men, it has been reported that repeated intake of a high protein meals after fasting led to a higher thermic response and nitrogen turnover compared to what was observed after repeated intake of carbohydrate rich meals (Robinson et al., 1990). Using theoretical

estimates of ATP requirements, the authors suggested that increased protein synthesis accounted for more than 65% of the thermic response after high protein meals. An increased catabolism of amino acids requires ATP to dispose of nitrogen as urea at an energy cost of 1.33 kcal/g urea. In mice, increased intake of water and accompanied increased production of urea have been observed in high protein fed mice (Madsen et al., 2008). Interestingly, increased water intake has been associated with reduced obesity (Thornton, 2016). It is proposed that increased water intake, in addition to reducing food intake, can activate thermogenesis via release of atrial natriuretic peptide (Thornton, 2016).

Together, published results from rodent studies suggest that high protein diets can lead to increased energy expenditure by several mechanisms, including activation of brown and so-called BRITE adipocytes. As discussed above, recent findings would indicate that BRITE adipocytes seem to play a greater role than

**TABLE 1** | A selection of Randomized Controlled Trials investigating the long-term effects of high-protein diets on body weight.

References	Population	Design	Intervention groups (protein, carbohydrate, fat)	Energy restricted (kcal day)	Duration (months)	Drop out	Body weight reduction pre-post (kg)	P-between groups
Skov et al., 1999	N = 65 (15 M, 50 F) 18–56 y BMI: 25–34 kg/m <sup>2</sup>	RCT, parallel	1) HP/LF (25, 45, 30 E%) 2) LP/LF (12, 58, 30 E%)	No	6	8%	1) –8.9 2) –5.1	<0.001
Due et al., 2004	N = 50 19–55 y BMI: 26–34 kg/m <sup>2</sup>	RCT, parallel	1) HP/LF (25, 45, 30 E%) 2) LP/LF (12, 58, 30 E%)	No	24	66%	1) –6.4 2) –3.2	NS
Brinkworth et al., 2004b	N = 66 >60 y BMI: 27–40 kg/m <sup>2</sup>	RCT, parallel	1) HP/LF (30, 40, 30 E%) 2) LP/LF (15, 55, 30 E%)	1600 (8 weeks), energy balance (4 weeks), no restriction (follow-up)	15	42%	1) –3.7 2) –2.2	NS
Brinkworth et al., 2004a	N = 58 (13 M, 45 F) 20–65 y BMI: 27–43 kg/m <sup>2</sup>	RCT, parallel	1) HP/LF (30, 40, 30 E%) 2) LP/LF (15, 55, 30 E%)	1,555 (12 weeks), energy balance (4 weeks), no restriction (follow-up)	16	26%	1) –4.1 2) –2.9	NS
Layman et al., 2009	N = 130 (59 M, 71 F) 45 ± 1 y BMI: 32.6 ± 0.8 kg/m <sup>2</sup>	RCT, parallel	1) HP/LF (30, 40, 30 E%) 2) LP/LF (15, 55, 30 E%)	1,900 M, 1,700 F	12	55%	1) –10.4 2) –8.4	NS
Sacks et al., 2009	N = 811 51 ± 9 y BMI: 33 ± 4 kg/m <sup>2</sup>	RCT, parallel	1) AP/LF (15, 65, 20 E%) 2) HP/LF (25, 55, 20 E%) 3) AP/HF (15, 45, 40 E%) 4) HP/HF (25, 35, 40 E%)	–750	24	79%	1) –3.6 2) –4.5 3) –3.6 4) –4.5	NS
Larsen et al., 2011	N = 99 (48 M, 51 F) 58–62 y BMI: 27–40 kg/m <sup>2</sup>	RCT, parallel	1) HP/LF (30, 40, 30 E%) 2) LP/LF (15, 55, 30 E%)	1,530 (12 weeks), energy balance (follow-up)	12	20%	1) –2.23 2) –2.17	NS
Krebs et al., 2012	N = 419 (168 M, 251 F) 30–75 y BMI: 36.6 ± 6.5 kg/m <sup>2</sup>	RCT, parallel	1) HP/LF (30, 40, 30 E%) 2) LP/LF (15, 55, 30 E%)	–500	24	30%	1) –3.9 2) –6.0	NS
Wycherley et al., 2012a	N = 120 51 ± 9 y BMI: 33.0 ± 3.9 kg/m <sup>2</sup>	RCT, parallel	1) HP/LF (35, 40, 25 E%) 2) LP/LF (17, 58, 25 E%)	1,700	12	44%	1) –12 2) –10.9	NS

canonical iBAT and that creatine cycling, SERCA2b-dependent  $\text{Ca}^{2+}$  cycling, and/or futile cycling of fatty acids may play pivotal roles. In addition, energy loss via increased production of urea may also contribute. Furthermore, a number of secreted factors, batokines, from brown and BRITE adipocyte has been shown to positively or negative modulate brown/BRITE adipocyte differentiation and thermogenesis (Sponton and Kajimura, 2018), and also here is an interesting question whether intake of high protein diets and/or different types of protein will affect these processes as well.

## HUMAN TRIALS

### High Protein Diets and Weight Loss in Humans

The effects of high protein diets in rodents have mostly been investigated in relation to prevention of obesity development. By contrast, human trials have to a larger extent examined the ability of high protein diets to induce weight loss in obese subjects, and knowledge on how increased intake of protein prevents weight gain in humans is limited. Systematic reviews and meta-analyses examining the efficiency of high protein diets to promote weight loss in humans are not consistent. A systematic review and meta-analyses of 74 randomized controlled trials

(RCTs) from 2012, where diets low and high in protein content were compared, concluded that high protein diets led to a greater weight reduction after 3 months than low protein diet (Santesso et al., 2012). Wycherley et al. examining 24 trials concluded that increasing the protein content elicited modest weight loss (Wycherley et al., 2012b), whereas a systematic review by Lepe et al. concluded that the long-term effects of high-protein diets were neither consistent nor conclusive (Lepe et al., 2011). A selection of RCTs investigating the long-term effects of high-protein diets on body composition is presented in **Table 1**. In a number of these trials, no marked differences between the two dietary groups were observed, whereas a modest effect was observed in others. Of note, in these trials the interventions combined high protein diets with energy restriction.

### Effects of Different Dietary Protein Sources on Body Composition

Epidemiological studies indicate that whereas diets with dairy and vegetarian protein sources protect against obesity, diets with a high proportion of meat, in particular red meat, are associated with higher weight gain (Fogelholm et al., 2012; Smith et al., 2015; Mozaffarian, 2016). A number of RCTs examining the influence of diets based on different protein

**TABLE 2 |** A selection of Randomized Controlled Trials investigating the effects of diets based on different protein sources on body weight.

References	Population	Design	Intervention groups (protein, carbohydrate, fat)	Energy restricted (kcal day)	Duration (weeks)	Body weight reduction pre-post	P-between groups
Yamashita et al., 1998	N = 36 (F) 40 ± 9 y BMI: 32.4 ± 5.2 kg/m <sup>2</sup>	Non-randomized, parallel	1) Plant (25, 50, 23 E%) 2) Red meat (25, 51, 22 E%)	1,500	16	1) -7.6 kg 2) -7.8 kg	NS
Mori et al., 1999	N = 63 (42 M, 21 F) 54 ± 2 y BMI: 31.6 ± 1.1 kg/m <sup>2</sup>	RCT, parallel	1) Fish 2) Weight-loss 3) Fish + weight loss 4) Control	-478 to 1,554 (groups 2-3)	16	1) 0.5 2) -5.2 kg 3) -5.9 kg 4) 0.1 kg	P < 0.05 for groups 2 and 3 vs. 1 and 4
Melanson et al., 2003	N = 61 (F) 43 ± 8 y BMI: 32.1 ± 3.4 kg/m <sup>2</sup>	RCT, parallel	1) Chicken (21, 57, 22 E%) 2) Beef (20, 55, 25 E%)	-500	12	1) -6.0 ± 0.5 kg 2) -5.6 ± 0.6 kg	NS
Mahon et al., 2007	N = 54 (F) 58 ± 2 y BMI: 29.6 ± 0.8 kg/m <sup>2</sup>	RCT, parallel	1) Beef (26, 48, 26 E%) 2) Chicken (26, 48, 26 E%) 3) Carbohydrate (16, 58, 26 E%) 4) Control (habitual diet)	-1000 (groups 1-4)	9	1) -6.6 ± 2.7 kg 2) -7.9 ± 2.6 kg 3) -5.6 ± 1.8 kg 4) -1.2 ± 1.2 kg	P < 0.05 for groups 1-3 vs. 4, and 2 vs. 3
Thorsdottir et al., 2007	N = 324 (138 M, 186 F) 39 ± 5 y 30.1 ± 1.4 kg/m <sup>2</sup>	RCT, parallel	1) Control 2) Lean Fish 3) Fatty fish 4) Fish oil	-30% 2,694 M 2,022 F	8	M: 1) -5.3 ± 3.0 kg 2) -6.5 ± 2.8 kg 3) -7.0 ± 3.5 kg 4) -6.7 ± 3.2 kg	M: p < 0.05 for groups 2-4 vs. 1. All + F: NS
Liu et al., 2010	N = 180 (F) 56 ± 4 y BMI: 24.5 ± 3.7 kg/m <sup>2</sup>	Double blinded, RCT, parallel	1) Placebo (15 g milk protein) 2) Iso (15 g milk protein + 100 mg isoflavones) 3) Soy (15 g soy protein + 100 mg isoflavones)	≈2,140	26	1) -0.3 ± 2.6% 2) -0.3 ± 2.5% 3) -1.2 ± 3.0%	P < 0.05 for group 3 vs. 1 and 2
Aadland et al., 2015	N = 20 (7 M, 13 F) 50.6 ± 3.4 y BMI: 25.6 ± 0.7 kg/m <sup>2</sup>	RCT, cross-over	1) Lean seafood (20, 52, 28 E%) 2) Beef (20, 52, 28 E%)	717 M 538 F	2 × 4	1) -1.4 ± 0.2 kg 2) -1.5 ± 0.2 kg	NS

sources on weight loss has been carried out (Table 2). In several of these, where the dietary intervention was combined with energy restriction (Melanson et al., 2003; Mahon et al., 2007), the protein source did not affect weight loss, and differences in design and population groups make it difficult to draw clear and firm conclusions. However, a recent position paper from MyNewGut concluded that intake of a high protein diet generally decreased body weight development, but the effects varied according to the type of dietary intervention and protein source, and that intake of a high protein diet was accompanied with changes in the gut microbiota (Blachier et al., 2018).

Inclusion of fatty fish, lean fish, or fish oil as part of an energy-restricted diet significantly increased weight loss in young overweight men (Thorsdottir et al., 2007). From these RCTs comparing the impact of different protein sources on body weight when combined with energy restriction, there is no clear evidence that one protein source is to be preferred relative to another (Figure 1). Hence, it may be speculated if the protein sources are of more importance in the habitual diets to prevent weight gain than in energy restricted diets used to achieve weight loss.

## SUMMARY AND CONCLUSION

The ability of high protein diets using casein or whey as the protein source to prevent weight gain is well-documented in mouse studies. The accompanying reduced feed-efficiency may be related to an increased glucagon:insulin ratio, increased uncoupled respiration and/or ATP loss by futile cycling. To what extent the reduced feed-efficiency and increased energy expenditure are mediated via the gut microbiome is not yet known. Further, intake of high protein diets may lead to reduced

insulin signaling in adipose tissue. Of note, these effects appear to be restricted to diets where casein or whey are used as protein sources and evidence that high fat high protein diets are able to induce weight loss in rodents is lacking.

The effect of high protein diets on weight loss in humans is not conclusive. However, in line with the importance of the protein source in rodent studies, where obesity development is examined, epidemiological studies indicate that diets with dairy and vegetarian protein sources protect against, whereas diets with meat may promote obesity. However, when diets containing different protein sources are examined in combination with energy restriction, the protein source appears to be of little or no importance. Together, these data indicate that the dietary protein source is of greater importance in preventing weight gain than during weight reduction. It may be considered if dietary means for obesity prevention in lean persons may be different from dietary advices to obese subjects to achieve effective weight loss. Based on the different approaches in human and animal studies investigating dietary protein sources, we encourage to performing more studies in humans and animals focusing on weight gain, weight maintenance and weight loss with different dietary protein sources in order to determine the possible impact of protein source on obesity development and reversal. To what extent high protein intake in humans modulates energy expenditure via the gut microbiome, uncoupled respiration or other energy consuming futile cycles remains to be established.

## AUTHOR CONTRIBUTIONS

LM researched data and wrote the first draft. LSM, EF, JØ, and KK contributed with text, discussion of the content, illustrations, revised, and/or edited the manuscript before submission.

## REFERENCES

- Aadland, E. K., Lavigne, C., Graff, I. E., Eng, O., Paquette, M., Holthe, A., et al. (2015). Lean-seafood intake reduces cardiovascular lipid risk factors in healthy subjects: results from a randomized controlled trial with a crossover design. *Am. J. Clin. Nutr.* 102, 582–592. doi: 10.3945/ajcn.115.112086
- An, H. M., Park, S. Y., Lee, D. K., Kim, J. R., Cha, M. K., Lee, S. W., et al. (2011). Antiobesity and lipid-lowering effects of *Bifidobacterium* spp. in high fat diet-induced obese rats. *Lipids Health Dis.* 10:116. doi: 10.1186/1476-511X-10-116
- Bäckhed, F., Ding, H., Wang, T., Hooper, L. V., Koh, G. Y., Nagy, A., et al. (2004). The gut microbiota as an environmental factor that regulates fat storage. *Proc. Natl. Acad. Sci. U. S. A.* 101, 15718–15723. doi: 10.1073/pnas.0407076101
- Bertholet, A. M., Kazak, L., Chouchani, E. T., Bogaczynska, M. G., Paranjpe, I., Wainwright, G. L., et al. (2017). Mitochondrial patch clamp of beige adipocytes reveals UCP1-positive and UCP1-negative cells both exhibiting futile creatine cycling. *Cell Metab.* 25, 811–822 e814. doi: 10.1016/j.cmet.2017.03.002
- Betz, M. J., Bielohuby, M., Mauracher, B., Abplanalp, W., Muller, H. H., Pieper, K., et al. (2012). Isoenergetic feeding of low carbohydrate-high fat diets does not increase brown adipose tissue thermogenic capacity in rats. *PLoS ONE* 7:e38997. doi: 10.1371/journal.pone.0038997
- Blachier, F., Beaumont, M., Portune, K. J., Steuer, N., Lan, A., Audebert, M., et al. (2018). High-protein diets for weight management: interactions with the intestinal microbiota and consequences for gut health. A position paper by the my new gut study group. *Clin. Nutr.* doi: 10.1016/j.clnu.2018.09.016. [Epub ahead of print].
- Blüher, M., Michael, M. D., Peroni, O. D., Ueki, K., Carter, N., Kahn, B. B., et al. (2002). Adipose tissue selective insulin receptor knockout protects against obesity and obesity-related glucose intolerance. *Dev. Cell* 3, 25–38. doi: 10.1016/S1534-5807(02)00199-5
- Bray, G. A., Redman, L. M., de Jonge, L., Covington, J., Rood, J., Brock, C., et al. (2015). Effect of protein overfeeding on energy expenditure measured in a metabolic chamber. *Am. J. Clin. Nutr.* 101, 496–505. doi: 10.3945/ajcn.114.091769
- Brinkworth, G. D., Noakes, M., Keogh, J. B., Luscombe, N. D., Wittert, G. A., and Clifton, P. M. (2004a). Long-term effects of a high-protein, low-carbohydrate diet on weight control and cardiovascular risk markers in obese hyperinsulinemic subjects. *Int. J. Obes. Relat. Metab. Disord.* 28, 661–670. doi: 10.1038/sj.ijo.0802617
- Brinkworth, G. D., Noakes, M., Parker, B., Foster, P., and Clifton, P. M. (2004b). Long-term effects of advice to consume a high-protein, low-fat diet, rather than a conventional weight-loss diet, in obese adults with type 2 diabetes: one-year follow-up of a randomised trial. *Diabetologia* 47, 1677–1686. doi: 10.1007/s00125-004-1511-7
- Buchholz, A. C., and Schoeller, D. A. (2004). Is a calorie a calorie? *Am. J. Clin. Nutr.* 79, 899S–906S. doi: 10.1093/ajcn/79.5.899S
- Cannon, B., and Nedergaard, J. (2004). Brown adipose tissue: function and physiological significance. *Physiol. Rev.* 84, 277–359. doi: 10.1152/physrev.00015.2003



- Chevalier, C., Stojanovic, O., Colin, D. J., Suarez-Zamorano, N., Tarallo, V., Veyrat-Durebex, C., et al. (2015). Gut microbiota orchestrates energy homeostasis during cold. *Cell* 163, 1360–1374. doi: 10.1016/j.cell.2015.11.004
- Cohen, P., Levy, J. D., Zhang, Y., Frontini, A., Kolodin, D. P., Svensson, K. J., et al. (2014). Ablation of PRDM16 and beige adipose causes metabolic dysfunction and a subcutaneous to visceral fat switch. *Cell* 156, 304–316. doi: 10.1016/j.cell.2013.12.021
- Collins, S., Daniel, K. W., Petro, A. E., and Surwit, R. S., (1997). Strain-specific response to beta 3-adrenergic receptor agonist treatment of diet-induced obesity in mice. *Endocrinology* 138, 405–413. doi: 10.1210/endo.138.1.4829
- Cuenca-Sánchez, M., Navas-Carrillo, D., and Orenes-Pinero, E. (2015). Controversies surrounding high-protein diet intake: satiating effect and kidney and bone health. *Adv. Nutr.* 6, 260–266. doi: 10.3945/an.114.007716
- Dali-Youcef, N., Matak, C., Coste, A., Messaddeq, N., Giroud, S., Blanc, S., et al. (2007). Adipose tissue-specific inactivation of the retinoblastoma protein protects against diabetes because of increased energy expenditure. *Proc. Natl. Acad. Sci. U. S. A.* 104, 10703–10708. doi: 10.1073/pnas.0611568104
- Due, A., Toubro, S., Skov, A. R., and Astrup, A. (2004). Effect of normal-fat diets, either medium or high in protein, on body weight in overweight subjects: a randomised 1-year trial. *Int. J. Obes. Relat. Metab. Disord.* 28, 1283–1290. doi: 10.1038/sj.ijo.0802767
- Enerback, S., Jacobsson, A., Simpson, E. M., Guerra, C., Yamashita, H., Harper, M. E., et al. (1997). Mice lacking mitochondrial uncoupling protein are cold-sensitive but not obese. *Nature* 387, 90–94. doi: 10.1038/387090a0
- Everard, A., Belzer, C., Geurts, L., Ouwerkerk, J. P., Druart, C., Bindels, L. B., et al. (2013). Cross-talk between Akkermansia muciniphila and intestinal epithelium controls diet-induced obesity. *Proc. Natl. Acad. Sci. U. S. A.* 110, 9066–9071. doi: 10.1073/pnas.1219451110
- Fabbiano, S., Suarez-Zamorano, N., Rigo, D., Veyrat-Durebex, C., Stevanovic Dokic, A., Colin, D. J., et al. (2016). Caloric restriction leads to browning of white adipose tissue through type 2 immune signaling. *Cell Metab.* 24, 434–446. doi: 10.1016/j.cmet.2016.07.023
- Feldmann, H. M., Golozoubova, V., Cannon, B., and Nedergaard, J. (2009). UCP1 ablation induces obesity and abolishes diet-induced thermogenesis in mice exempt from thermal stress by living at thermoneutrality. *Cell Metab.* 9, 203–209. doi: 10.1016/j.cmet.2008.12.014
- Fine, E. J., and Feinman, R. D. (2004). Thermodynamics of weight loss diets. *Nutr. Metab.* 1:15. doi: 10.1186/1743-7075-1-15
- Fischer, A. W., Cannon, B., and Nedergaard, J. (2018). Optimal housing temperatures for mice to mimic the thermal environment of humans: an experimental study. *Mol. Metab.* 7, 161–170. doi: 10.1016/j.molmet.2017.10.009
- Flachs, P., Adamcova, K., Zouhar, P., Marques, C., Janovska, P., Viegas, I., et al. (2017). Induction of lipogenesis in white fat during cold exposure in mice: link to lean phenotype. *Int. J. Obes.* 41, 372–380. doi: 10.1038/ijo.2016.228
- Fogelholm, M., Anderssen, S., Gunnarsdottir, I., and Lahti-Koski, M. (2012). Dietary macronutrients and food consumption as determinants of long-term weight change in adult populations: a systematic literature review. *Food Nutr. Res.* 56. doi: 10.3402/fnr.v56i0.19103
- Freudenberg, A., Petzke, K. J., and Klaus, S. (2012). Comparison of high-protein diets and leucine supplementation in the prevention of metabolic syndrome and related disorders in mice. *J. Nutr. Biochem.* 23, 1524–1530. doi: 10.1016/j.jnutbio.2011.10.005
- Freudenberg, A., Petzke, K. J., and Klaus, S. (2013). Dietary L-leucine and L-alanine supplementation have similar acute effects in the prevention of high-fat diet-induced obesity. *Amino Acids* 44, 519–528. doi: 10.1007/s00726-012-1363-2
- Gao, X., Yan, D., Zhao, Y., Tao, H., and Zhou, Y. (2015). Moderate calorie restriction to achieve normal weight reverses beta-cell dysfunction in diet-induced obese mice: involvement of autophagy. *Nutr. Metab.* 12:34. doi: 10.1186/s12986-015-0028-z
- Gao, Z., Yin, J., Zhang, J., Ward, R. E., Martin, R. J., Lefevre, M., et al. (2009). Butyrate improves insulin sensitivity and increases energy expenditure in mice. *Diabetes* 58, 1509–1517. doi: 10.2337/db08-1637
- Guan, H. P., Li, Y., Jensen, M. V., Newgard, C. B., Steppan, C. M., and Lazar, M. A. (2002). A futile metabolic cycle activated in adipocytes by antidiabetic agents. *Nat. Med.* 8, 1122–1128. doi: 10.1038/nm780
- Guerra, C., Koza, R. A., Yamashita, H., Walsh, K., and Kozak, L. P. (1998). Emergence of brown adipocytes in white fat in mice is under genetic control. Effects on body weight and adiposity. *J. Clin. Invest.* 102, 412–420. doi: 10.1172/JCI3155
- Hallenborg, P., Fjaere, E., Liaset, B., Petersen, R. K., Murano, I., Sonne, S. B., et al. (2016). p53 regulates expression of uncoupling protein 1 through binding and repression of PPARgamma coactivator-1alpha. *Am. J. Physiol. Endocrinol. Metab.* 310, E116–E128. doi: 10.1152/ajpendo.00119.2015
- Hansen, J. B., Jorgensen, C., Petersen, R. K., Hallenborg, P., De Matteis, R., Boye, H. A., et al. (2004). Retinoblastoma protein functions as a molecular switch determining white versus brown adipocyte differentiation. *Proc. Natl. Acad. Sci. U. S. A.* 101, 4112–4117. doi: 10.1073/pnas.0301964101
- Hao, Q., Hansen, J. B., Petersen, R. K., Hallenborg, P., Jorgensen, C., Cinti, S., et al. (2010). ADD1/SREBP1c activates the PGC1-alpha promoter in brown adipocytes. *Biochim. Biophys. Acta* 1801, 421–429. doi: 10.1016/j.bbali.2009.11.008
- Hao, Q., Lillefosse, H. H., Fjaere, E., Myrmet, L. S., Midtbo, L. K., Jarlsby, R. H., et al. (2012). High-glycemic index carbohydrates abrogate the antiobesity effect of fish oil in mice. *Am. J. Physiol. Endocrinol. Metab.* 302, E1097–E1112. doi: 10.1152/ajpendo.00524.2011
- Harms, M., and Seale, P. (2013). Brown and beige fat: development, function and therapeutic potential. *Nat. Med.* 19, 1252–1263. doi: 10.1038/nm.3361
- Herzig, S., Long, F., Jhala, U. S., Hedrick, S., Quinn, R., Bauer, A., et al. (2001). CREB regulates hepatic gluconeogenesis through the coactivator PGC-1. *Nature* 413, 179–183. doi: 10.1038/35093131
- Holm, J. B., Ronnevik, A., Tastesen, H. S., Fjaere, E., Fauske, K. R., Liisberg, U., et al. (2016). Diet-induced obesity, energy metabolism and gut microbiota in C57BL/6J mice fed Western diets based on lean seafood or lean meat mixtures. *J. Nutr. Biochem.* 31, 127–136. doi: 10.1016/j.jnutbio.2015.12.017
- Huang, X., Hancock, D. P., Gosby, A. K., McMahon, A. C., Solon, S. M., Le Couteur, D. G., et al. (2013). Effects of dietary protein to carbohydrate balance on energy intake, fat storage, and heat production in mice. *Obesity* 21, 85–92. doi: 10.1002/oby.20007
- Huang, X. F., Liu, Y., Rahardjo, G. L., McLennan, P. L., Tapsell, L. C., and Buttemer, W. A. (2008). Effects of diets high in whey, soy, red meat and milk protein on body weight maintenance in diet-induced obesity in mice. *Nutr. Diet.* 65, 53–59. doi: 10.1111/j.1747-0080.2008.00262.x
- Ijaz, M. U., Ahmed, M. I., Zou, X., Hussain, M., Zhang, M., Zhao, F., et al. (2018). Beef, casein, and soy proteins differentially affect lipid metabolism, triglycerides accumulation and gut microbiota of high-fat diet-fed C57BL/6J mice. *Front. Microbiol.* 9:2200. doi: 10.3389/fmicb.2018.02200
- Ikeda, K., Kang, Q., Yoneshiro, T., Camporez, J. P., Maki, H., Homma, M., et al. (2017). UCP1-independent signaling involving SERCA2b-mediated calcium cycling regulates beige fat thermogenesis and systemic glucose homeostasis. *Nat. Med.* 23, 1454–1465. doi: 10.1038/nm.4429
- Ikeda, K., Maretich, P., and Kajimura, S. (2018). The common and distinct features of brown and beige adipocytes. *Trends Endocrinol. Metab.* 29, 191–200. doi: 10.1016/j.tem.2018.01.001
- Ishibashi, J., and Seale, P. (2010). Medicine. Beige can be slimming. *Science* 328, 1113–1114. doi: 10.1126/science.1190816
- Jequier, E. (2002). Pathways to obesity. *Int. J. Obes. Relat. Metab. Disord.* 26 (Suppl 2), S12–S17. doi: 10.1038/sj.ijo.0802123
- Jung, D. Y., Ko, H. J., Lichtman, E. I., Lee, E., Lawton, E., Ong, H., et al. (2013). Short-term weight loss attenuates local tissue inflammation and improves insulin sensitivity without affecting adipose inflammation in obese mice. *Am. J. Physiol. Endocrinol. Metab.* 304, E964–E976. doi: 10.1152/ajpendo.00462.2012
- Kaufman, L. N., Young, J. B., and Landsberg, L. (1986). Effect of protein on sympathetic nervous system activity in the rat. Evidence for nutrient-specific responses. *J. Clin. Invest.* 77, 551–558
- Kazak, L., Chouchani, E. T., Jedrychowski, M. P., Erickson, B. K., Shinoda, K., Cohen, P., et al. (2015). A creatine-driven substrate cycle enhances energy expenditure and thermogenesis in beige fat. *Cell* 163, 643–655. doi: 10.1016/j.cell.2015.09.035
- Kazak, L., Chouchani, E. T., Lu, G. Z., Jedrychowski, M. P., Bare, C. J., Mina, A. I., et al. (2017). Genetic depletion of adipocyte creatine metabolism inhibits diet-induced thermogenesis and drives obesity. *Cell Metab.* 26, 660–671 e663. doi: 10.1016/j.cmet.2017.09.007
- Keipert, S., Voigt, A., and Klaus, S. (2011). Dietary effects on body composition, glucose metabolism, and longevity are modulated by

- skeletal muscle mitochondrial uncoupling in mice. *Aging Cell* 10, 122–136. doi: 10.1111/j.1474-9726.2010.00648.x
- Kiilerich, P., Myrmet, L. S., Fjaere, E., Hao, Q., Hugenholtz, F., Sonne, S. B., et al. (2016). Effect of a long-term high-protein diet on survival, obesity development, and gut microbiota in mice. *Am. J. Physiol. Endocrinol. Metab.* 310, E886–E899. doi: 10.1152/ajpendo.00363.2015
- Kiskinis, E., Chatzeli, L., Curry, E., Kaforou, M., Frontini, A., Cinti, S., et al. (2014). RIP140 represses the “brown-in-white” adipocyte program including a futile cycle of triacylglycerol breakdown and synthesis. *Mol. Endocrinol.* 28, 344–356. doi: 10.1210/me.2013-1254
- Klaus, S. (2005). Increasing the protein:carbohydrate ratio in a high-fat diet delays the development of adiposity and improves glucose homeostasis in mice. *J. Nutr.* 135, 1854–1858. doi: 10.1093/jn/135.8.1854
- Kopecký, J., Hodny, Z., Rossmeisl, M., Syrový, I., and Kozak, L. P. (1996a). Reduction of dietary obesity in aP2-Ucp transgenic mice: physiology and adipose tissue distribution. *Am. J. Physiol.* 270, E768–E775.
- Kopecký, J., Rossmeisl, M., Hodny, Z., Syrový, I., Horakova, M., and Kolarova, P. (1996b). Reduction of dietary obesity in aP2-Ucp transgenic mice: mechanism and adipose tissue morphology. *Am. J. Physiol.* 270, E776–E786.
- Krebs, J. D., Elley, C. R., Parry-Strong, A., Lunt, H., Drury, P. L., Bell, D. A., et al. (2012). The Diabetes Excess Weight Loss (DEWL) trial: a randomised controlled trial of high-protein versus high-carbohydrate diets over 2 years in type 2 diabetes. *Diabetologia* 55, 905–914. doi: 10.1007/s00125-012-2461-0
- Kuda, O., Rossmeisl, M., and Kopecký, J. (2018). Omega-3 fatty acids and adipose tissue biology. *Mol. Aspects Med.* 64, 147–160. doi: 10.1016/j.mam.2018.01.004
- Larsen, R. N., Mann, N. J., Maclean, E., and Shaw, J. E. (2011). The effect of high-protein, low-carbohydrate diets in the treatment of type 2 diabetes: a 12 month randomised controlled trial. *Diabetologia* 54, 731–740. doi: 10.1007/s00125-010-2027-y
- Layman, D. K., Evans, E. M., Erickson, D., Seyler, J., Weber, J., Bagshaw, D., et al. (2009). A moderate-protein diet produces sustained weight loss and long-term changes in body composition and blood lipids in obese adults. *J. Nutr.* 139, 514–521. doi: 10.3945/jn.108.099440
- Leonardsson, G., Steel, J. H., Christian, M., Pocock, V., Milligan, S., Bell, J., et al. (2004). Nuclear receptor corepressor RIP140 regulates fat accumulation. *Proc. Natl. Acad. Sci. U. S. A.* 101, 8437–8442. doi: 10.1073/pnas.0401013101
- Lepe, M., Bacardi Gascon, M., and Jimenez Cruz, A. (2011). Long-term efficacy of high-protein diets: a systematic review. *Nutr. Hosp.* 26, 1256–1259. doi: 10.1590/S00212-16112011000600010
- Li, Z., Jin, H., Oh, S. Y., and Ji, G. E. (2016). Anti-obese effects of two lactobacilli and two *Bifidobacteria* on ICR mice fed on a high fat diet. *Biochem. Biophys. Res. Commun.* 480, 222–227. doi: 10.1016/j.bbrc.2016.10.031
- Liisberg, U., Fauske, K. R., Kuda, O., Fjaere, E., Myrmet, L. S., Norberg, N., et al. (2016a). Intake of a Western diet containing cod instead of pork alters fatty acid composition in tissue phospholipids and attenuates obesity and hepatic lipid accumulation in mice. *J. Nutr. Biochem.* 33, 119–127. doi: 10.1016/j.jnutbio.2016.03.014
- Liisberg, U., Myrmet, L. S., Fjaere, E., Ronnevik, A. K., Bjelland, S., Fauske, K. R., et al. (2016b). The protein source determines the potential of high protein diets to attenuate obesity development in C57BL/6J mice. *Adipocyte* 5, 196–211. doi: 10.1080/21623945.2015.1122855
- Lillefosse, H. H., Clausen, M. R., Yde, C. C., Ditlev, D. B., Zhang, X., Du, Z. Y., et al. (2014). Urinary loss of tricarboxylic acid cycle intermediates as revealed by metabolomics studies: an underlying mechanism to reduce lipid accretion by whey protein ingestion? *J. Proteome Res.* 13, 2560–2570. doi: 10.1021/pr500039t
- Lin, H. V., Frassetto, A., Kowalik, E. J. Jr., Nawrocki, A. R., Lu, M. M., Kosinski, J. R., et al. (2012). Butyrate and propionate protect against diet-induced obesity and regulate gut hormones via free fatty acid receptor 3-independent mechanisms. *PLoS ONE* 7:e35240. doi: 10.1371/journal.pone.0035240
- Liu, Z. M., Ho, S. C., Chen, Y. M., and Ho, Y. P. (2010). A mild favorable effect of soy protein with isoflavones on body composition—a 6-month double-blind randomized placebo-controlled trial among Chinese postmenopausal women. *Int. J. Obes.* 34, 309–318. doi: 10.1038/ijo.2009.236
- Lu, Y., Fan, C., Li, P., Chang, X., and Qi, K. (2016). Short chain fatty acids prevent high-fat-diet-induced obesity in mice by regulating G protein-coupled receptors and gut microbiota. *Sci. Rep.* 6:37589. doi: 10.1038/srep37589
- Ma, T., Liaset, B., Hao, Q., Petersen, R. K., Fjaere, E., Ngo, H. T., et al. (2011). Sucrose counteracts the anti-inflammatory effect of fish oil in adipose tissue and increases obesity development in mice. *PLoS ONE* 6:e21647. doi: 10.1371/journal.pone.0021647
- Madsen, L., Myrmet, L. S., Fjaere, E., Liaset, B., and Kristiansen, K. (2017). Links between dietary protein sources, the gut microbiota, and obesity. *Front. Physiol.* 8:1047. doi: 10.3389/fphys.2017.01047
- Madsen, L., Pedersen, L. M., Liaset, B., Ma, T., Petersen, R. K., van den Berg, S., et al. (2008). cAMP-dependent signaling regulates the adipogenic effect of n-6 polyunsaturated fatty acids. *J. Biol. Chem.* 283, 7196–7205. doi: 10.1074/jbc.M707775200
- Mahon, A. K., Flynn, M. G., Stewart, L. K., McFarlin, B. K., Iglay, H. B., Mattes, R. D., et al. (2007). Protein intake during energy restriction: effects on body composition and markers of metabolic and cardiovascular health in postmenopausal women. *J. Am. Coll. Nutr.* 26, 182–189. doi: 10.1080/07315724.2007.10719600
- Marsset-Baglieri, A., Fromentin, G., Tome, D., Bensaid, A., Makkarios, L., and Even, P. C. (2004). Increasing the protein content in a carbohydrate-free diet enhances fat loss during 35% but not 75% energy restriction in rats. *J. Nutr.* 134, 2646–2652. doi: 10.1093/jn/134.10.2646
- Mazzucotelli, A., Viguerie, N., Tirabby, C., Annicotte, J. S., Mairal, A., Klimcakova, E., et al. (2007). The transcriptional coactivator peroxisome proliferator activated receptor (PPAR)gamma coactivator-1 alpha and the nuclear receptor PPAR alpha control the expression of glycerol kinase and metabolism genes independently of PPAR gamma activation in human white adipocytes. *Diabetes* 56, 2467–2475. doi: 10.2337/db06-1465
- McAllan, L., Skuse, P., Cotter, P. D., O'Connor, P., Cryan, J. F., Ross, R. P., et al. (2014). Protein quality and the protein to carbohydrate ratio within a high fat diet influences energy balance and the gut microbiota in C57BL/6J mice. *PLoS ONE* 9:e88904. doi: 10.1371/journal.pone.0088904
- Mehran, A. E., Templeman, N. M., Brigidi, G. S., Lim, G. E., Chu, K. Y., Hu, X., et al. (2012). Hyperinsulinemia drives diet-induced obesity independently of brain insulin production. *Cell Metab.* 16, 723–737. doi: 10.1016/j.cmet.2012.10.019
- Melanson, K., Gootman, J., Myrdal, A., Kline, G., and Rippe, J. M. (2003). Weight loss and total lipid profile changes in overweight women consuming beef or chicken as the primary protein source. *Nutrition* 19, 409–414. doi: 10.1016/S0899-9007(02)01080-8
- Mercader, J., Ribot, J., Murano, I., Feddersen, S., Cinti, S., Madsen, L., et al. (2009). Haploinsufficiency of the retinoblastoma protein gene reduces diet-induced obesity, insulin resistance, and hepatosteatosis in mice. *Am. J. Physiol. Endocrinol. Metab.* 297, E184–E193. doi: 10.1152/ajpendo.00163.2009
- Morens, C., Keijzer, M., de Vries, K., Scheurink, A., and van Dijk, G. (2005). Effects of high-fat diets with different carbohydrate-to-protein ratios on energy homeostasis in rats with impaired brain melanocortin receptor activity. *Am. J. Physiol. Regul. Integr. Comp. Physiol.* 289, R156–R163. doi: 10.1152/ajpregu.00774.2004
- Mori, T. A., Bao, D. Q., Burke, V., Puddey, I. B., Watts, G. F., and Beilin, L. J. (1999). Dietary fish as a major component of a weight-loss diet: effect on serum lipids, glucose, and insulin metabolism in overweight hypertensive subjects. *Am. J. Clin. Nutr.* 70, 817–825. doi: 10.1093/ajcn/70.5.817
- Mozaffarian, D. (2016). Dietary and policy priorities for cardiovascular disease, diabetes, and obesity: a comprehensive review. *Circulation* 133, 187–225. doi: 10.1161/CIRCULATIONAHA.115.018585
- Mu, C., Yang, Y., Luo, Z., and Zhu, W. (2017). Temporal microbiota changes of high-protein diet intake in a rat model. *Anaerobe* 47, 218–225. doi: 10.1016/j.anaerobe.2017.06.003
- Nedergaard, J., and Cannon, B. (2013). UCP1 mRNA does not produce heat. *Biochim. Biophys. Acta* 1831, 943–949. doi: 10.1016/j.bbalip.2013.01.009
- Newgard, C. B., An, J., Bain, J. R., Muehlbauer, M. J., Stevens, R. D., Lien, L. F., et al. (2009). A branched-chain amino acid-related metabolic signature that differentiates obese and lean humans and contributes to insulin resistance. *Cell Metab.* 9, 311–326. doi: 10.1016/j.cmet.2009.02.002
- Pérez-Martí, A., García-Guasch, M., Tresserra-Rimbau, A., Carrilho-Do-Rosário, A., Estruch, R., Salas-Salvadó, J., et al. (2017). A low-protein diet induces body weight loss and browning of subcutaneous white adipose tissue through enhanced expression of hepatic fibroblast growth factor 21 (FGF21). *Mol. Nutr. Food Res.* 61. doi: 10.1002/mnfr.201600725
- Pesta, D. H., and Samuel, V. T. (2014). A high-protein diet for reducing body fat: mechanisms and possible caveats. *Nutr. Metab.* 11:53. doi: 10.1186/1743-7075-11-53

- Petrovic, N., Walden, T. B., Shabalina, I. G., Timmons, J. A., Cannon, B., and Nedergaard, J. (2010). Chronic peroxisome proliferator-activated receptor gamma (PPARgamma) activation of epididymally derived white adipocyte cultures reveals a population of thermogenically competent, UCP1-containing adipocytes molecularly distinct from classic brown adipocytes. *J. Biol. Chem.* 285, 7153–7164. doi: 10.1074/jbc.M109.053942
- Petzke, K. J., Freudenberg, A., and Klaus, S. (2014). Beyond the role of dietary protein and amino acids in the prevention of diet-induced obesity. *Int. J. Mol. Sci.* 15, 1374–1391. doi: 10.3390/ijms15011374
- Petzke, K. J., Friedrich, M., Metges, C. C., and Klaus, S. (2005). Long-term dietary high protein intake up-regulates tissue specific gene expression of uncoupling proteins 1 and 2 in rats. *Eur. J. Nutr.* 44, 414–421. doi: 10.1007/s00394-004-0545-4
- Petzke, K. J., Riese, C., and Klaus, S. (2007). Short-term, increasing dietary protein and fat moderately affect energy expenditure, substrate oxidation and uncoupling protein gene expression in rats. *J. Nutr. Biochem.* 18, 400–407. doi: 10.1016/j.jnutbio.2006.07.005
- Pezeshki, A., Fahim, A., and Chelikani, P. K. (2015). Dietary whey and casein differentially affect energy balance, gut hormones, glucose metabolism, and taste preference in diet-induced obese rats. *J. Nutr.* 145, 2236–2244. doi: 10.3945/jn.115.213843
- Pichon, L., Huneau, J. F., Fromentin, G., and Tome, D. (2006). A high-protein, high-fat, carbohydrate-free diet reduces energy intake, hepatic lipogenesis, and adiposity in rats. *J. Nutr.* 136, 1256–1260. doi: 10.1093/jn/136.5.1256
- Puigserver, P., Rhee, J., Donovan, J., Walkey, C. J., Yoon, J. C., Oriente, F., et al. (2003). Insulin-regulated hepatic gluconeogenesis through FOXO1-PGC-1alpha interaction. *Nature* 423, 550–555. doi: 10.1038/nature01667
- Qin, J., Li, Y., Cai, Z., Li, S., Zhu, J., Zhang, F., et al. (2012). A metagenome-wide association study of gut microbiota in type 2 diabetes. *Nature* 490, 55–60. doi: 10.1038/nature11450
- Razani, B., Combs, T. P., Wang, X. B., Frank, P. G., Park, D. S., Russell, R. G., et al. (2002). Caveolin-1-deficient mice are lean, resistant to diet-induced obesity, and show hypertriglyceridemia with adipocyte abnormalities. *J. Biol. Chem.* 277, 8635–8647. doi: 10.1074/jbc.M110970200
- Reeds, P. J., Fuller, M. F., and Nicholson, A. (1985). *Metabolic Basis of Energy Expenditure With Particular Reference to Protein*. London: John Libbey.
- Robinson, S. M., Jaccard, C., Persaud, C., Jackson, A. A., Jequier, E., and Schutz, Y. (1990). Protein turnover and thermogenesis in response to high-protein and high-carbohydrate feeding in men. *Am. J. Clin. Nutr.* 52, 72–80. doi: 10.1093/ajcn/52.1.72
- Sacks, F. M., Bray, G. A., Carey, V. J., Smith, S. R., Ryan, D. H., Anton, S. D., et al. (2009). Comparison of weight-loss diets with different compositions of fat, protein, and carbohydrates. *N. Engl. J. Med.* 360, 859–873. doi: 10.1056/NEJMoa0804748
- Santesso, N., Akl, E. A., Bianchi, M., Mente, A., Mustafa, R., Heels-Ansdell, D., et al. (2012). Effects of higher- versus lower-protein diets on health outcomes: a systematic review and meta-analysis. *Eur. J. Clin. Nutr.* 66, 780–788. doi: 10.1038/ejcn.2012.37
- Shabalina, I. G., Petrovic, N., de Jong, J. M., Kalinovich, A. V., Cannon, B., and Nedergaard, J. (2013). UCP1 in brite/beige adipose tissue mitochondria is functionally thermogenic. *Cell Rep.* 5, 1196–1203. doi: 10.1016/j.celrep.2013.10.044
- She, P., Reid, T. M., Bronson, S. K., Vary, T. C., Hajnal, A., Lynch, C. J., et al. (2007). Disruption of BCATm in mice leads to increased energy expenditure associated with the activation of a futile protein turnover cycle. *Cell Metab.* 6, 181–194. doi: 10.1016/j.cmet.2007.08.003
- Shin, N. R., Lee, J. C., Lee, H. Y., Kim, M. S., Whon, T. W., Lee, M. S., et al. (2014). An increase in the *Akkermansia* spp. population induced by metformin treatment improves glucose homeostasis in diet-induced obese mice. *Gut* 63, 727–735. doi: 10.1136/gutjnl-2012-303839
- Singh, A., Pezeshki, A., Zapata, R. C., Yee, N. J., Knight, C. G., Tuor, U. I., et al. (2016). Diets enriched in whey or casein improve energy balance and prevent morbidity and renal damage in salt-loaded and high-fat-fed spontaneously hypertensive stroke-prone rats. *J. Nutr. Biochem.* 37, 47–59. doi: 10.1016/j.jnutbio.2016.07.011
- Skov, A. R., Toubro, S., Ronn, B., Holm, L., and Astrup, A. (1999). Randomized trial on protein vs carbohydrate in ad libitum fat reduced diet for the treatment of obesity. *Int. J. Obes. Relat. Metab. Disord.* 23, 528–536. doi: 10.1038/sj.ijo.0800867
- Smith, J. D., Hou, T., Ludwig, D. S., Rimm, E. B., Willett, W., Hu, F. B., et al. (2015). Changes in intake of protein foods, carbohydrate amount and quality, and long-term weight change: results from 3 prospective cohorts. *Am. J. Clin. Nutr.* 101, 1216–1224. doi: 10.3945/ajcn.114.100867
- Sponton, C. H., and Kajimura, S. (2018). Multifaceted roles of Beige fat in energy homeostasis beyond UCP1. *Endocrinology* 159, 2545–2553. doi: 10.1210/en.2018-00371
- Stock, M. J. (1999). Gluttony and thermogenesis revisited. *Int. J. Obes. Relat. Metab. Disord.* 23, 1105–1117. doi: 10.1038/sj.ijo.0801108
- Ström, K., Hansson, O., Lucas, S., Nevsten, P., Fernandez, C., Klint, C., et al. (2008). Attainment of brown adipocyte features in white adipocytes of hormone-sensitive lipase null mice. *PLoS ONE* 3:e1793. doi: 10.1371/journal.pone.0001793
- Suarez-Zamorano, N., Fabbiano, S., Chevalier, C., Stojanovic, O., Colin, D. J., Stevanovic, A., et al. (2015). Microbiota depletion promotes browning of white adipose tissue and reduces obesity. *Nat. Med.* 21, 1497–1501. doi: 10.1038/nm.3994
- Tastesen, H. S., Keenan, A. H., Madsen, L., Kristiansen, K., and Liaset, B. (2014a). Scallop protein with endogenous high taurine and glycine content prevents high-fat, high-sucrose-induced obesity and improves plasma lipid profile in male C57BL/6J mice. *Amino Acids* 46, 1659–1671. doi: 10.1007/s00726-014-1715-1
- Tastesen, H. S., Ronnevik, A. K., Borkowski, K., Madsen, L., Kristiansen, K., and Liaset, B. (2014b). A mixture of cod and scallop protein reduces adiposity and improves glucose tolerance in high-fat fed male C57BL/6J mice. *PLoS ONE* 9:e112859. doi: 10.1371/journal.pone.0112859
- Thornton, S. N. (2016). Increased hydration can be associated with weight loss. *Front. Nutr.* 3:18. doi: 10.3389/fnut.2016.00018
- Thorsdottir, I., Tomasson, H., Gunnarsdottir, I., Gisladdottir, E., Kiely, M., Parra, M. D., et al. (2007). Randomized trial of weight-loss-diets for young adults varying in fish and fish oil content. *Int. J. Obes.* 31, 1560–1566. doi: 10.1038/sj.ijo.0803643
- Toh, S. Y., Gong, J., Du, G., Li, J. Z., Yang, S., Ye, J., et al. (2008). Up-regulation of mitochondrial activity and acquirement of brown adipose tissue-like property in the white adipose tissue of fsp27 deficient mice. *PLoS ONE* 3:e2890. doi: 10.1371/journal.pone.0002890
- Veldhorst, M., Smeets, A., Soenen, S., Hochstenbach-Waelen, A., Hursel, R., Diepvens, K., et al. (2008). Protein-induced satiety: effects and mechanisms of different proteins. *Physiol. Behav.* 94, 300–307. doi: 10.1016/j.physbeh.2008.01.003
- Wang, J., Tang, H., Zhang, C., Zhao, Y., Derrien, M., Rocher, E., et al. (2015). Modulation of gut microbiota during probiotic-mediated attenuation of metabolic syndrome in high fat diet-fed mice. *ISME J.* 9, 1–15. doi: 10.1038/ismej.2014.99
- Westerterp-Plantenga, M. S. (2008). Protein intake and energy balance. *Regul. Pept.* 149, 67–69. doi: 10.1016/j.regpep.2007.08.026
- Wu, J., Bostrom, P., Sparks, L. M., Ye, L., Choi, J. H., Giang, A. H., et al. (2012). Beige adipocytes are a distinct type of thermogenic fat cell in mouse and human. *Cell* 150, 366–376. doi: 10.1016/j.cell.2012.05.016
- Wycherley, T. P., Brinkworth, G. D., Clifton, P. M., and Noakes, M. (2012a). Comparison of the effects of 52 weeks weight loss with either a high-protein or high-carbohydrate diet on body composition and cardiometabolic risk factors in overweight and obese males. *Nutr Diabetes* 2:e40. doi: 10.1038/nutd.2012.11
- Wycherley, T. P., Moran, L. J., Clifton, P. M., Noakes, M., and Brinkworth, G. D. (2012b). Effects of energy-restricted high-protein, low-fat compared with standard-protein, low-fat diets: a meta-analysis of randomized controlled trials. *Am. J. Clin. Nutr.* 96, 1281–1298. doi: 10.3945/ajcn.112.044321
- Yamashita, T., Sasahara, T., Pomeroy, S. E., Collier, G., and Nestel, P. J. (1998). Arterial compliance, blood pressure, plasma leptin, and plasma lipids in women are improved with weight reduction equally with a meat-based diet and a plant-based diet. *Metab. Clin. Exp.* 47, 1308–1314. doi: 10.1016/S0026-0495(98)90297-9
- Yang, Z., Huang, S., Zou, D., Dong, D., He, X., Liu, N., et al. (2016). Metabolic shifts and structural changes in the gut microbiota upon branched-chain

- amino acid supplementation in middle-aged mice. *Amino Acids* 48, 2731–2745. doi: 10.1007/s00726-016-2308-y
- Yoon, J. C., Puigserver, P., Chen, G., Donovan, J., Wu, Z., Rhee, J., et al. (2001). Control of hepatic gluconeogenesis through the transcriptional coactivator PGC-1. *Nature* 413, 131–138. doi: 10.1038/35093050
- Zietak, M., Kovatcheva-Datchary, P., Markiewicz, L. H., Stahlman, M., Kozak, L. P., and Backhed, F. (2016). Altered microbiota contributes to reduced diet-induced obesity upon cold exposure. *Cell Metab.* 23, 1216–1223. doi: 10.1016/j.cmet.2016.05.001

**Conflict of Interest Statement:** The authors declare that the research was conducted in the absence of any commercial or financial relationships that could be construed as a potential conflict of interest.

Copyright © 2018 Madsen, Myrmet, Fjære, Øyen and Kristiansen. This is an open-access article distributed under the terms of the Creative Commons Attribution License (CC BY). The use, distribution or reproduction in other forums is permitted, provided the original author(s) and the copyright owner(s) are credited and that the original publication in this journal is cited, in accordance with accepted academic practice. No use, distribution or reproduction is permitted which does not comply with these terms.





# Environmental Pollutants Effect on Brown Adipose Tissue

Ilaria Di Gregorio<sup>†</sup>, Rosa Anna Busiello<sup>†</sup>, Mario Alberto Burgos Aceves, Marilena Lepretti, Gaetana Paoletta and Lillà Lionetti\*

Department of Chemistry and Biology "A. Zambelli", University of Salerno, Fisciano, Italy

## OPEN ACCESS

### Edited by:

Rita De Matteis,  
Università degli Studi di Urbino Carlo  
Bo, Italy

### Reviewed by:

Bruce Alan Bunnell,  
Tulane University School of Medicine,  
United States  
Pascal Imbeault,  
University of Ottawa, Canada

### \*Correspondence:

Lillà Lionetti  
llionetti@unisa.it

<sup>†</sup>These authors have contributed  
equally to this work

### Specialty section:

This article was submitted to  
Integrative Physiology,  
a section of the journal  
Frontiers in Physiology

**Received:** 01 September 2018

**Accepted:** 14 December 2018

**Published:** 09 January 2019

### Citation:

Di Gregorio I, Busiello RA,  
Burgos Aceves MA, Lepretti M,  
Paoletta G and Lionetti L (2019)  
Environmental Pollutants Effect on  
Brown Adipose Tissue.  
Front. Physiol. 9:1891.  
doi: 10.3389/fphys.2018.01891

Brown adipose tissue (BAT) with its thermogenic function due to the presence of the mitochondrial uncoupling protein 1 (UCP1), has been positively associated with improved resistance to obesity and metabolic diseases. During recent years, the potential influence of environmental pollutants on energetic homeostasis and obesity development has drawn increased attention. The purpose of this review is to discuss how regulation of BAT function could be involved in the environmental pollutant effect on body energy metabolism. We mainly focused in reviewing studies on animal models, which provide a better insight into the cellular mechanisms involved in this effect on body energy metabolism. The current literature supports the hypothesis that some environmental pollutants, acting as endocrine disruptors (EDCs), such as dichlorodiphenyltrichloroethane (DDT) and its metabolite dichlorodiphenylethylene (DDE) as well as some, traffic pollutants, are associated with increased obesity risk, whereas some other chemicals, such as perfluorooctane sulfonate (PFOS) and perfluorooctanoic acid (PFOA), had a reverse association with obesity. Noteworthy, the EDCs associated with obesity and metabolic disorders impaired BAT mass and function. Perinatal exposure to DDT impaired BAT thermogenesis and substrate utilization, increasing susceptibility to metabolic syndrome. Ambient particulate air pollutions induced insulin resistance associated with BAT mitochondrial dysfunction. On the other hand, the environmental pollutants (PFOS/PFOA) elicited a reduction in body weight and adipose mass associated with upregulation of UCP1 and increased oxidative capacity in brown-fat mitochondria. Further research is needed to better understand the physiological role of BAT in response to exposure to both obesogenic and anti-obesogenic pollutants and to confirm the same role in humans.

**Keywords:** brown adipocytes, air pollutants, dichlorodiphenyltrichloroethane (DDT), dichlorodiphenylethylene (DDE), perfluorooctane sulfonate (PFOS), perfluorooctanoic acid (PFOA), obesity, metabolic disorders

## INTRODUCTION

The potential influence of environmental pollutants on energetic homeostasis and obesity development by altering brown adipose tissue (BAT) thermogenic activity has recently drawn increased attention (reviewed in Zhang et al., 2016). Obesity is a condition that develops when energy intake is greater than energy expenditure and energy surplus is accumulated in

white adipose tissue (WAT). Indeed, WAT, characterized by the presence of white unilocular adipocytes, is typically considered an energy storage site in condition of chronic positive energy balance, but it also contributes to energy balance regulation by releasing special adipokines (Trayhurn and Beattie, 2001; Vázquez-Vela et al., 2008). The role of adipose tissue as a potential site of toxicant accumulation has been recently reviewed (Jackson et al., 2017). On the other, BAT is characterized by brown multilocular adipocytes and is involved in the activation of thermogenesis due to the presence of the uncoupling protein 1 (UCP1), that may be useful for increasing energy expenditure (Ricquier, 2005; Richard, 2007; Marcelin and Chua, 2010; Busiello et al., 2015) and avoiding excessive lipid accumulation in WAT, counteracting obesity and metabolic diseases development (Cannon and Nedergaard, 2004; Nedergaard et al., 2007; Saito et al., 2009; Ouellet et al., 2011; Lombardi et al., 2015). Indeed, recent literature suggested BAT as a prime target for the treatment of obesity and metabolic diseases by regulating energy expenditure (Blondin and Carpentier, 2016; Scheele and Nielsen, 2017; Trayhurn, 2017; Carpentier et al., 2018). However, although the role of BAT on thermogenesis and energy metabolism, is well-established in rodents, the contribution of BAT to energy balance in humans is more controversial. A detailed discussion on this topic is beyond the role of this review and has been well-analyzed in recent reviews (please see Trayhurn, 2017; Carpentier et al., 2018). We briefly summarized the main findings that provide the rationale for BAT thermogenesis involvement in energy metabolism regulation and obesity in rodents as well as in humans. Brown adipose tissue (BAT) was first identified as the major site of non-shivering thermogenesis in rats acclimated to cold and this finding had impact also in the research area of nutritional energetic where thermogenesis was starting to be considered a significant factor in obesity onset (Trayhurn, 2017). The first demonstrations of a link between obesity and BAT were obtained in genetic obese mice (ob/ob mice), where a reduction in BAT thermogenic activities was found, as well as in cafeteria-fed rats where an activation of BAT was evident (Rothwell and Stock, 1979, 1981; Thurlby and Trayhurn, 1979). These initial observations were followed by several studies in other genetic and non-genetic models of obesity, confirming a link between BAT thermogenesis and obesity in rodents (see Trayhurn, 2017). A critical point is whether the data showing the link between BAT and obesity in animal experimental models, may suggest a similar correlation in humans. Studies in the 1980s provided a clear evidence that BAT not only is present in the newborns, but also in adult humans, showing the presence of UCP1 in particular adipose depots, and its activation in patients with pheochromocytoma (Lean et al., 1986a,b). Two key discoveries in the late 2000s elicited a renaissance interest in BAT: (1) brown adipocytes, differently from white fat cells, are derived from myogenic precursors (Timmons et al., 2007) and (2) there is a third type of adipocyte (beige or brite fat cell) which express UCP1 together with other molecular markers of brown adipocyte (Petrovic et al., 2010; Wu et al., 2012). Moreover, fludeoxyglucose positron emission tomography (FDG-PET)

and UCP1 immunostaining studies showed that BAT activity is also present in adult humans (Cypess et al., 2009; Virtanen et al., 2009). Further FDG-PET studies showed that: (1) BAT in adults is stimulated by cold and insulin (van Marken Lichtenbelt et al., 2009; Orava et al., 2011), (2) it is less active in older subjects (Pfannenberger et al., 2010); (3) its activity inversely correlate with BMI (body mass index) and therefore lower in obese than in lean individuals (van Marken Lichtenbelt et al., 2009; Pfannenberger et al., 2010; Yoneshiro et al., 2011). Moreover, genetic variants of UCP1 are associated with fat metabolism, obesity, and diabetes (Jia et al., 2010). The finding that brown-fat like adipocytes are also present in WAT has opened new opportunities in targeting the adipose tissue to fight obesity-induced diseases (Cereijo et al., 2015; Bargut et al., 2017). Indeed, alteration in adipose tissue thermogenic gene expression has been found in response to obesity and diabetes (Keller and Attie, 2010; Marcelin and Chua, 2010; Ruschke et al., 2010). Moreover, it has been also suggested that WAT and BAT, in spite of their opposite functions, share the ability for reciprocal reversible transdifferentiation in response to physiologic needs. Thus, chronic positive energy balance has been suggested to induce whitening, whereas chronic need for thermogenesis has been suggested to induce browning (Cinti, 2011, 2018). Although there are some concerns on whether BAT facultative thermogenesis can be more than a very minor component of energy expenditure in adult humans, these last discoveries lead to a renewed interest in the activation and/or recruitment of BAT in the etiology and therapy of obesity and related metabolic diseases in humans.

Given the possible role played by BAT in the etiology of obesity, the purpose of this review is to summarize the current knowledge on the involvement of BAT in the effect of environmental pollutants on body energy metabolism by considering the opposite effect of obesogenic and anti-obesogenic pollutants. We focused in reviewing mainly rodent studies, either *in vitro* or *in vivo*, where the used methodologies allow to clarify cellular mechanisms involved in pollutants effect on BAT activity and obesity development. As regard obesogenic pollutants, we reviewed the literature on endocrine disruptors (EDCs), such as dichlorodiphenyltrichloroethane (DDT), and its primary metabolite dichlorodiphenyldichloroethylene (DDE) (Lee et al., 2011; Taylor et al., 2013; La Merrill et al., 2014) as well as on airborne fine particulate matter (traffic pollutants) (Xu et al., 2010, 2011a,b), which have been shown to impair BAT mass and function in association with the development of obesity and/or metabolic related diseases. Concerning anti-obesogenic pollutants, we discussed the effect of perfluorooctane sulfonate (PFOS) and perfluorooctanoic acid (PFOA), which have a reverse association with obesity and are associated with UCP1 upregulation and increased oxidative capacity in brown-fat mitochondria (Shabalina et al., 2015, 2016). The opposite effects of these different environmental pollutants suggest that further studies are needed to clarify the metabolic response to xenobiotic agents. Moreover, targeting brown adipocyte and mitochondria could be useful in the prevention and therapy of obesity and metabolic related diseases.

## ENVIRONMENTAL POLLUTANTS INDUCING OBESITY AND METABOLIC DISORDERS: THE ROLE OF BAT

### Dichlorodiphenyltrichloroethane (DDT) and Dichlorodiphenylethylene (DDE) Impact on BAT Function

Exposure to DDT and its primary metabolite DDE has been associated with increased prevalence of obesity and metabolic disease (Lee et al., 2011; Taylor et al., 2013).

Perinatal exposure to DDT in mice has been proved to decrease energy expenditure leading to increased body weight and insulin resistance, associated with BAT activity impairment in female adult offspring (La Merrill et al., 2014). In fact, reductions in the expression of numerous RNA involved in thermogenesis and substrate transport and utilization were found in BAT of female adult offspring fed high fat diet (see **Figure 1A**). Noteworthy, the authors also showed a reduction in iodothyronine type II deiodinase (*Dio2*). *Dio2* encodes the enzyme that locally activates thyroid hormones through the deiodination of T4 to T3, therefore stimulating BAT thermogenesis. La Merrill et al. (2014) also established a link between developmental exposure to DDT and increased risk of insulin resistance in adult offspring. It should be noted that peroxisome proliferative activated receptor gamma coactivator 1 alpha (*PGC1α*) has been suggested to play a role in linking thermogenesis to the risk of T2D. Indeed, thermogenesis impairment and HFD-induced insulin resistance susceptibility were observed in *Ppargc1a* genetic ablation studies in mice (Kleiner et al., 2012). La Merrill et al. (2014) therefore suggested a role for *PGC1α* reduction in thermogenesis and insulin resistance in DDT exposure adult offspring (**Figure 1A**).

The effect of DDT/DDE and other obesogenic xenobiotics on BAT may be mediated by the aryl hydrocarbon receptor (AhR) (Xu et al., 2015). AhR, initially characterized as a xenobiotic sensor to mediate toxicological response, has been also shown to act as a physiological regulator of energy metabolism. Therefore, AhR activation by environmental pollutants has been suggested to promote obesity and related diseases (Arsenescu et al., 2008; He et al., 2013). Indeed, AhR deficiency in mice protected against diet-induced obesity and metabolic disorders by stimulating energy expenditure through increased BAT activity (**Figure 1A**) (Xu et al., 2015). UCP1 and the key upstream regulators of Ucp1, PPARγ coactivator 1 α (*PGC1α*) and PR domain containing 16 (*PRDM16*), were increased in the BAT of AhR<sup>+/-</sup> mice compared to control mice (Xu et al., 2015). Taking into account the role of inflammatory pathways in obesity and related diseases, it is important to underline that AhR activation has been shown to be enhanced by pro-inflammatory cytokines (Champion et al., 2013; Drozdzik et al., 2014) and to play a key role in inflammatory pathways. Considering that DDT and its metabolite DDE have been shown to induce NF-κB activation and pro-inflammatory cytokines production (Kim et al., 2004; Alegría-Torres et al., 2009), which in turn may mediate the upregulation of AhR expression, the role of AhR over-expression induced by xenobiotics in BAT

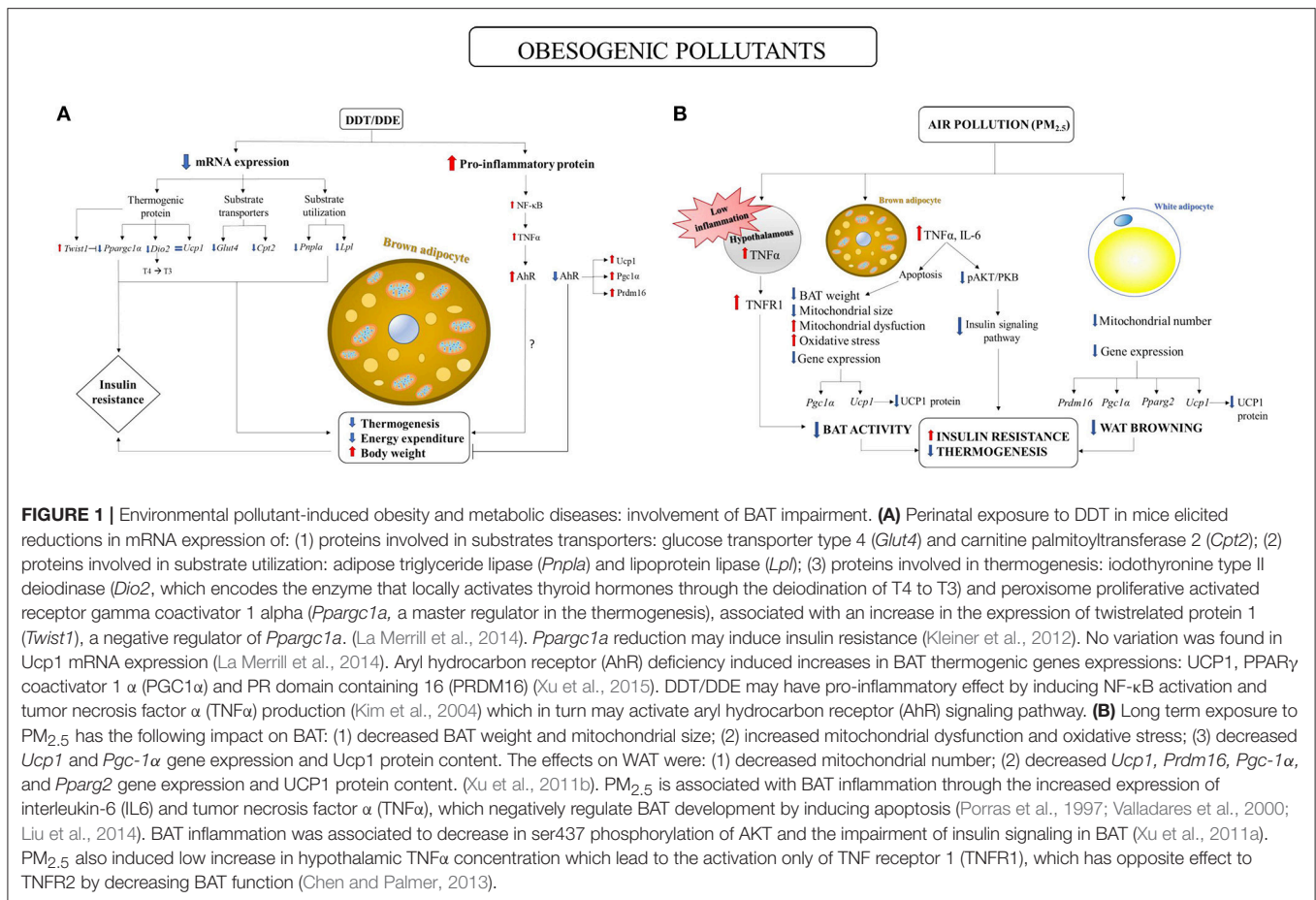
as well as its link with the inflammation, deserve further investigation.

### Air Pollutants Impact on BAT Function

Several studies showed a link between air pollution and obesity and metabolic disorders development (Araujo et al., 2008; Sun et al., 2009; Xu et al., 2010). Xu et al. (2011a) showed that long term exposure to airborne fine particulate matter (PM <2.5 μm in aerodynamic diameter, PM<sub>2.5</sub>) induced insulin resistance and inflammation, associated with a reduction in BAT weight, a significant decreased mitochondrial size in BAT and in mitochondrial number in WAT. Moreover, brown adipocyte-specific gene profiles and UCP1 content were impaired in both BAT and WAT, suggesting that long-term PM<sub>2.5</sub> exposure induces alterations in BAT activity and in browning of WAT (**Figure 1B**). These findings were associated with impaired glucose tolerance, insulin resistance and inflammation.

Evidence of significant changes in BAT activity in response to PM<sub>2.5</sub> was also found in male APOE knockout mice (Xu et al., 2011b). PM<sub>2.5</sub> exposure elicited a significant downregulation of brown adipocyte-specific gene profiles as well as a decrease in UCP1 content and in mitochondrial size and number in BAT. Noteworthy, homeobox C9 (*Hoxc9*) and insulin-like growth factor binding protein 3 (*Igfbp3*) genes, which are characteristic of WAT, were upregulated in BAT, suggesting that brown adipocyte may potentially transform to white adipose phenotype. This suggestion opens an interesting perspective in the studies on BAT involvement in toxicant-induced obesity and in the potential shift of BAT in WAT, in accordance with the hypothesis that brown to white conversion can be useful to meet the need of storing excess energy in response to obesogenic stimuli, as previously discussed (Cinti, 2011, 2018).

The effects of PM<sub>2.5</sub> exposure on BAT activity was also confirmed by the finding of the induction of BAT mitochondrial dysfunction and oxidative stress in both PM<sub>2.5</sub> long term-exposed mice and PM<sub>2.5</sub> exposed APOE knockout mice (Xu et al., 2011a,b). Zhang et al. (2016) also reviewed the hypothesis that exposure to PM<sub>2.5</sub> may impact BAT development through TNFα mediated apoptosis (Porrás et al., 1997; Valladares et al., 2000), inflammation (Liu et al., 2014) and insulin signaling pathway impairment (**Figure 1A**). PM<sub>2.5</sub> is associated with systemic proinflammatory response in animals and humans (Calderon-Garciduenas et al., 2008; Xu et al., 2010), as well as with BAT inflammation through the increased expression of interleukin-6 (IL6) and TNFα (Liu et al., 2014). It has been shown that TNFα negatively regulates BAT development by inducing apoptosis (Porrás et al., 1997; Valladares et al., 2000). Therefore, it has been suggested that exposure to PM<sub>2.5</sub> may impact BAT development through TNFα mediated apoptosis and inflammation (Zhang et al., 2016). Brown adipose tissue (BAT) inflammation was associated to the impairment of insulin signaling pathway as demonstrated by the decrease in ser437 phosphorylation of AKT in BAT (Xu et al., 2011a). Moreover, PM<sub>2.5</sub> exposure induced hypothalamic inflammation (Ying et al., 2014), which in turn may have a dual effect on BAT function. High concentration of hypothalamic TNFα increased BAT function by increasing UCP1 expression through sympathetic tonus activation (Arruda et al.,



2010). On the other hand, low concentration of hypothalamic TNFα only activated tumor necrosis factor-α receptor 1 (TNFR1), which has an opposite effect to TNFR2 (Chen and Palmer, 2013) and decreased BAT thermogenic activity by downregulating UCP1 expression (Romanatto et al., 2009; Arruda et al., 2011). Exposure to PM<sub>2.5</sub> has been suggested to induce low-grade inflammation in the hypothalamus, which in turn may induce BAT dysfunction (Zhang et al., 2016); **Figure 1B**.

PM<sub>2.5</sub> exposure also induced increased expression of TNFα gene expression associated with decreased expression of BAT specific gene expression (*UCP1* and *PGC1α*) in epicardial adipose tissue (EAT) (Sun et al., 2013). These findings suggested that further investigations are needed in clarifying EAT function and air pollution effect on it.

## Phthalates and Bisphenol a Impact on BAT Function

The impact of other obesogenic environmental pollutants on BAT activity also needs to be further investigated. The endocrine disruptor mono-(2-ethylhexyl) phthalate (MEHP), a metabolite of the widespread plasticizer DEHP [di-(2-ethylhexyl) phthalate], promotes adipocyte differentiation and induces obesity in mice

(Feige et al., 2010). In recent years, it has been shown that phthalates may promote childhood obesity (Kim and Park, 2014). However, BAT activity does not seem to be altered by phthalates, given that BAT UCP1 and PGC-1α expressions were not affected in DEHP-treated mice (Feige et al., 2010).

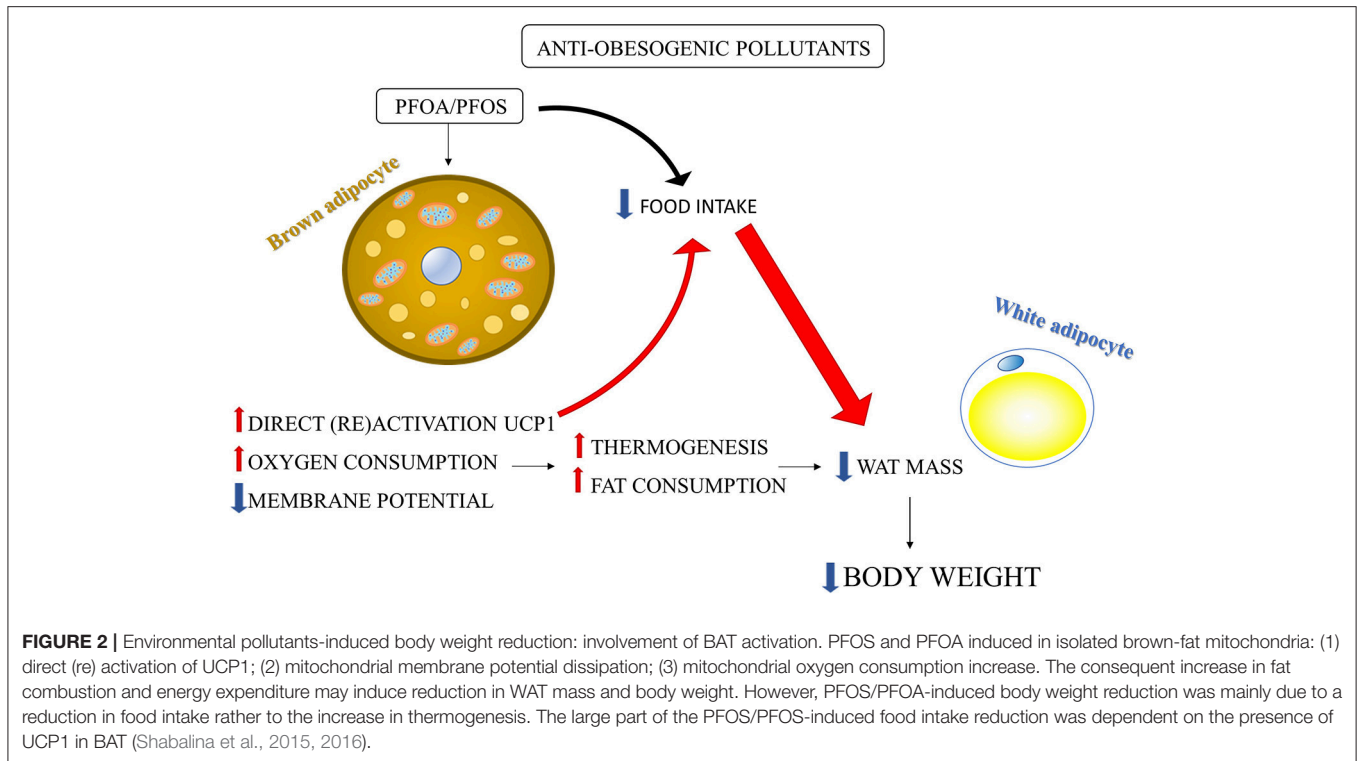
Epidemiologic evidence on the correlation between bisphenol A (BPA) exposure and obesity, diabetes, and other metabolic diseases has been reviewed by Bertoli et al. (2015). Nunez et al. (2001), showed that there was a preferential concentration of BPA in BAT in ovariectomized adult female rat. The authors therefore suggested that BAT may be a primary tissue into which BPA accumulates in mammals and, therefore, BPA can affect BAT thermogenesis and energy balance.

Further studies are needed to clarify the effect of phthalates and BPA on BAT and energy balance.

## BAT ROLE IN ANTI-OBESOGENIC EFFECT OF ENVIRONMENTAL POLLUTANTS

The anti-obesogenic effect of PFOA and PFOS associated with increased BAT activity has been well-studied by the group





of Nedergaard (Shabalina et al., 2015, 2016). PFOA/PFOS supplementation to the food elicited a marked decrease in body weight and WAT depots in mice (Xie et al., 2002, 2003), which has been shown to be due to the increased oxidative capacity in brown-fat mitochondria by UCP1 upregulation (Shabalina et al., 2015, 2016).

PFOA and PFOS, with their fatty acid octanoic acid structure, are structurally similar to a fatty acid and may exhibit properties akin to those of natural fatty acids, such as their ability to (re)activate UCP1 (Cannon and Nedergaard, 2004). The activation of UCP1 leads to increased fat combustion and may explain, at least in part, the body fat loss induced by PFOA and PFOS (Figure 2), which may be also explained by an UCP1-dependent decrease in food intake (Shabalina et al., 2015, 2016). Shabalina et al. (2016) showed that PFOS and PFOA induced oxygen consumption and dissipated membrane potential by directly activating UCP1 in isolated brown-fat mitochondria. The direct activation of UCP1 was confirmed by the absence of these effects in brown-fat mitochondria from UCP1-ablated mice (Shabalina et al., 2016). Considering that BAT has been recently found also in adult human and its (re)activation may be useful to counteract obesity (Nedergaard et al., 2007; Cereijo et al., 2015), the finding that PFCs directly activates BAT can be useful to enable the development of substances that selectively activate UCP1 allowing recruitment of BAT to ameliorate obesity problem (Shabalina et al., 2016). Shabalina et al. (2015) also demonstrated that the PFOA/PFOS-induced body weight reduction was only in part directly related to the presence of UCP1. Indeed, it was mainly due to a decrease in food intake which in turn was dependent

on the presence of UCP1 in BAT (Figure 2). Therefore, the reduction in body weight induced by PFOA/PFOS may be ascribed to a UCP1-dependent decrease in food intake (not due to food aversion), rather than to elevated BAT thermogenesis (Shabalina et al., 2015). A regulatory component of food intake depending upon BAT thermogenic activity can be suggested and further studies are needed to clarify this mechanism considering its possible key role in counteracting obesity.

## CONCLUSIONS

Diverse type of environmental pollutants differently affects body energy metabolism and BAT function. Among obesogenic pollutants, DDT/DDE impaired BAT activity by reducing the expression of protein involved in thermogenesis, substrate transport and utilization as well as by reducing the deiodination of T4 to T3 and inducing insulin resistance and inflammatory pathways in BAT. Air pollutants also induced inflammatory pathway and insulin resistance in BAT. Noteworthy, obesogenic effect of air pollutants was associated with downregulation of brown adipocyte-specific gene profiles as well as with a decrease in UCP1 content and mitochondrial size/number in both BAT and WAT, suggesting some common effects of environmental pollutants on adipose tissue in general. On the other hand, anti-obesogenic effect of PFOA/PFOS has been shown to be due to increased mitochondrial oxidative capacity and UCP1 activation in BAT, which in turn induced a decrease in food intake and body weight.

The different effects of diverse type of environmental pollutant may be due to the diverse chemical structure and proprieties as well as to the different dose and time of exposure utilized in the diverse experimental designs. Understanding the mechanisms by which obesogenic environmental pollutants impact BAT thermogenesis activity and body energy metabolism may be useful to shade light on the etiopathogenesis of obesity whereas the studies on the environmental pollutants acting impairing BAT function and reducing body weight may be useful in discovering new molecules to counteract obesity by directly targeting thermogenic adipocyte. Given that mitochondria play a key role in BAT and browned WAT thermogenesis, studies on mitochondrial bioenergetics are confirmed to be of great importance in understanding the etiopathogenesis of diet-induced (Putti et al., 2015a,b; Lepretti et al., 2018), and toxicant-induced (Llobet et al., 2015; Burgos-Aceves et al., 2018) obesity as well as in discovering new therapy for obesity related diseases.

## REFERENCES

- Alegría-Torres, J. A., Díaz-Barriga, F., Gandolfi, A. J., and Pérez-Maldonado, I. N. (2009). Mechanisms of p,p'-DDE-induced apoptosis in human peripheral blood mononuclear cells. *Toxicol. Vitro*. 23, 1000–1006. doi: 10.1016/j.tiv.2009.06.021
- Araujo, J. A., Barajas, B., Kleinman, M., Wang, X., Bennett, B. J., Gong, K. W., et al. (2008). Ambient particulate pollutants in the ultrafine range promote early atherosclerosis and systemic oxidative stress. *Circ. Res.* 102, 589–596. doi: 10.1161/CIRCRESAHA.107.164970
- Arruda, A. P., Milanski, M., Coope, A., Torsoni, A. S., Ropelle, E., Carvalho, D. P., et al. (2011). Low-grade hypothalamic inflammation leads to defective thermogenesis, insulin resistance, and impaired insulin secretion. *Endocrinology*. 152, 1314–1326. doi: 10.1210/en.2010-0659
- Arruda, A. P., Milanski, M., Romanatto, T., Solon, C., Coope, A., Alberici, L. C., et al. (2010). Hypothalamic actions of tumor necrosis factor alpha provide the thermogenic core for the wastage syndrome in cachexia. *Endocrinology* 151, 683–694. doi: 10.1210/en.2009-0865
- Arsenescu, V., Arsenescu, R. I., King, V., Swanson, H., and Cassis, L. A. (2008). Polychlorinated biphenyl-77 induces adipocyte differentiation and proinflammatory adipokines and promotes obesity and atherosclerosis. *Environ. Health Perspect.* 116, 761–768. doi: 10.1289/ehp.10554
- Bargut, T., Souza-Mello, V., Aguila, M. B., and Mandarin-de-Lacerda, C. A. (2017). Browning of white adipose tissue: lessons from experimental models. *Horm. Mol. Biol. Clin. Invest.* 18:31. doi: 10.1515/hmbci-2016-0051
- Bertoli, S., Leone, A., and Battezzati, A. (2015). Human Bisphenol A exposure and the "Diabesity Phenotype". *Dose Response* 13:1559325815599173. doi: 10.1177/1559325815599173
- Blondin, D. P., and Carpentier, A. C. (2016). The role of BAT in cardiometabolic disorders and aging. *Best Pract. Res. Clin. Endocrinol. Metab.* 30, 497–513. doi: 10.1016/j.beem.2016.09.002
- Burgos-Aceves, M. A., Cohen, A., Paolella, G., Lepretti, M., Smith, Y., Faggio, C., et al. (2018). Modulation of mitochondrial functions by xenobiotic-induced microRNA: from environmental sentinel organisms to mammals. *Sci. Total. Environ.* 645, 79–88. doi: 10.1016/j.scitotenv.2018.07.109
- Busiello, R. A., Savarese, S., and Lombardi, A. (2015). Mitochondrial uncoupling proteins and energy metabolism. *Front. Physiol.* 6:36. doi: 10.3389/fphys.2015.00036
- Calderón-Garcidueñas, L., Villarreal-Calderon, R., Valencia-Salazar, G., Henríquez-Roldán, C., Gutiérrez-Castrellón, P., Torres-Jardón, R., et al. (2008). Systemic inflammation, endothelial dysfunction, and activation in clinically healthy children exposed to air pollutants. *Inhal. Toxicol.* 20, 499–506. doi: 10.1080/08958370701864797
- Cannon, B., and Nedergaard, J. (2004). Brown adipose tissue: function and physiological significance. *Physiol. Rev.* 84, 277–359. doi: 10.1152/physrev.00015.2003

## AUTHOR CONTRIBUTIONS

ID and RAB equally contributed to the work, conducted bibliographic research, and wrote the initial draft. MABA conducted bibliographic research and revised the manuscript. ML and GP actively discussed and revised the manuscript. LL conceived the idea and wrote the final manuscript. All authors read and approved the final manuscript.

## FUNDING

The present work has been funded by University of Salerno, project FARB (Fondo di Ateneo per la Ricerca di Base) 2016, codes 300389FRB16LIONE (for LL), and GRI [GRI - Giovani ricercatori], 2016, codes 300389GRI16LIONE (for LL). The funder have no role in the design of the study and collection, analysis, and interpretation of data and in writing the manuscript.

- Carpentier, A. C., Blondin, D. P., Virtanen, K. A., Richard, D., Haman, F., and Turcotte, É. E. (2018). Brown adipose tissue energy metabolism in humans. *Front. Endocrinol.* 7:447. doi: 10.3389/fendo.2018.00447
- Cereijo, R., Giral, M., and Villarroja, F. (2015). Thermogenic brown and beige/brite adipogenesis in humans. *Ann. Med.* 47, 169–177. doi: 10.3109/07853890.2014.952328
- Champion, S., Sauzet, C., Bremond, P., Benbrahim, K., Abbrades, J., Seree, E., et al. (2013). Activation of the NF-κB pathway enhances AhR expression in intestinal Caco-2 cells. *ISRN Toxicol.* 2013:792452. doi: 10.1155/2013/792452
- Chen, Z., and Palmer, T. D. (2013). Differential roles of TNFR1 and TNFR2 signaling in adult hippocampal neurogenesis. *Brain Behav. Immun.* 30, 45–53. doi: 10.1016/j.bbi.2013.01.083
- Cinti, S. (2011). Between brown and white: novel aspects of adipocyte differentiation. *Ann. Med.* 43, 104–115. doi: 10.3109/07853890.2010.535557
- Cinti, S. (2018). Adipose organ development and remodeling. *Compr. Physiol.* 14, 1357–1431. doi: 10.1002/cphy.c170042
- Cypess, A. M., Lehman, S., Williams, G., Tal, I., and Rodman, D., Goldfine, et al. (2009). Identification and importance of brown adipose tissue in adult humans. *N. Engl. J. Med.* 360, 1509–1517. doi: 10.1056/NEJMoa0810780
- Drozdziak, A., Dziedzic, V., and Kurzawski, M. (2014). IL-1 and TNFα regulation of aryl hydrocarbon receptor (AhR) expression in HSY human salivary cells. *Arch. Oral Biol.* 59, 434–439. doi: 10.1016/j.archoralbio.2014.02.003
- Feige, J. N., Gerber, A., Casals-Casas, C., Yang, Q., Winkler, C., Bedu, E., et al. (2010). The pollutant Diethylhexyl Phthalate regulates hepatic energy metabolism via species-specific PPARα-dependent mechanisms. *Environ. Health Perspect.* 118, 234–241. doi: 10.1289/ehp.09.01217
- He, J., Hu, B., Shi, X., Weidert, E. R., Lu, P., Xu, M., et al. (2013). Activation of the aryl hydrocarbon receptor sensitizes mice to nonalcoholic steatohepatitis by deactivating mitochondrial sirtuin deacetylase Sirt3. *Mol. Cell. Biol.* 33, 2047–2055. doi: 10.1128/MCB.01658-12
- Jackson, E., Shoemaker, R., Larian, N., and Cassis, L. (2017). Adipose tissue as a site of toxin accumulation. *Compr. Physiol.* 7, 1085–1135. doi: 10.1002/cphy.c160038
- Jia, J. J., Tian, Y. B., Cao, Z. H., Tao, L. L., Zhang, X., Gao, S. Z., et al. (2010). The polymorphisms of UCP1 genes associated with fat metabolism, obesity and diabetes. *Mol. Biol. Rep.* 37, 1513–1522. doi: 10.1007/s11033-009-9550-2
- Keller, M. P., and Attie, A. D. (2010). Physiological insights gained from gene expression analysis in obesity and diabetes. *Annu. Rev. Nutr.* 30, 341–364. doi: 10.1146/annurev.nutr.012809.104747
- Kim, J. Y., Choi, C. Y., Lee, K. J., Shin, D. W., Jung, K. S., Chung, Y. C., et al. (2004). Induction of inducible nitric oxide synthase and proinflammatory cytokines expression by o,p'-DDT in macrophages. *Toxicol. Lett.* 147, 261–269. doi: 10.1016/j.toxlet.2003.12.001

- Kim, S. H., and Park, M. J. (2014). Phthalate exposure and childhood obesity. *Ann. Pediatr. Endocrinol. Metab.* 19, 69–75. doi: 10.6065/apem.2014.19.2.69
- Kleiner, S., Mepani, R. J., Laznik, D., Ye, L., Jurczak, M. J., Jornayvaz, F. R., et al. (2012). Development of insulin resistance in mice lacking PGC-1 $\alpha$  in adipose tissues. *Proc. Natl. Acad. Sci. U.S.A.* 109, 9635–9640. doi: 10.1073/pnas.1207287109
- La Merrill, M., Karey, E., Moshier, E., Lindtner, C., La Frano, M. R., Newman, J. W., et al. (2014). Perinatal exposure of mice to the pesticide DDT impairs energy expenditure and metabolism in adult female offspring. *PLoS ONE* 9:e103337. doi: 10.1371/journal.pone.0103337
- Lean, M. E., James, W. P., Jennings, G., and Trayhurn, P. (1986a). Brown adipose tissue uncoupling protein content in human infants, children and adults. *Clin. Sci.* 71, 291–297. doi: 10.1042/cs0710291
- Lean, M. E., James, W. P., Jennings, G., and Trayhurn, P. (1986b). Brown adipose tissue in patients with pheochromocytoma. *Int. J. Obes.* 10, 219–227.
- Lee, D. H., Steffes, M. W., Sjödin, A., Jones, R. S., Needham, L. L., and Jacobs, D. R. (2011). Low dose organochlorine pesticides and polychlorinated biphenyls predict obesity, dyslipidemia, and insulin resistance among people free of diabetes. *PLoS ONE* 6:e15977. doi: 10.1371/journal.pone.0015977
- Lepretti, M., Martucciello, S., Burgos Aceves, M. A., Putti, R., and Lionetti, L. (2018). Omega-3 fatty acids and insulin resistance: focus on the regulation of mitochondria and endoplasmic reticulum stress. *Nutrients* 10: 350. doi: 10.3390/nu10030350
- Liu, C., Bai, Y., Xu, X., Sun, L., Wang, A., Wang, T. Y., et al. (2014). Exaggerated effects of particulate matter air pollution in genetic type II diabetes mellitus. *Part. Fibre Toxicol.* 11:27. doi: 10.1186/1743-8977-11-27
- Llobet, L., Toivonen, J. M., Montoya, J., Ruiz-Pesini, E., and López-Gallardo, E. (2015). Xenobiotics that affect oxidative phosphorylation alter differentiation of human adipose-derived stem cells at concentrations that are found in human blood. *Dis. Models Mech.* 8, 1441–1455. doi: 10.1242/dmm.021774
- Lombardi, A., Senese, R., De Matteis, R., Busiello, R. A., Cioffi, F., Goglia, F., et al. (2015). 3,5-Diiodo-L-thyronine activates brown adipose tissue thermogenesis in hypothyroid rats. *PLoS ONE* 10:e0116498. doi: 10.1371/journal.pone.0116498
- Marcelin, G., and Chua, S. (2010). Contributions of adipocyte lipid metabolism to body fat content and implications for the treatment of obesity. *Curr. Opin. Pharmacol.* 10, 588–593. doi: 10.1016/j.coph.2010.05.008
- Nedergaard, J., Bengtsson, T., and Cannon, B. (2007). Unexpected evidence for active brown adipose tissue in adult humans. *Am. J. Physiol. Endocrinol. Metab.* 293, E444–E452. doi: 10.1152/ajpendo.00691.2006
- Nunez, A. A., Kannan, K., Giesy, J. P., Fang, J., and Clemens, L. G. (2001). Effects of bisphenol A on energy balance and accumulation in brown adipose tissue in rats. *Chemosphere* 42, 917–922. doi: 10.1016/S0045-6535(00)00196-X
- Orava, J., Nuutila, P., Lidell, M. E., Oikonen, V., Noponen, T., Viljanen, T., et al. (2011). Different metabolic responses of human brown adipose tissue to activation by cold and insulin. *Cell. Metab.* 14, 272–279. doi: 10.1016/j.cmet.2011.06.012
- Ouellet, V., Routhier-Labadie, A., Bellemare, W., Lakhal-Chaieb, L., Turcotte, E., Carpentier, A. C., et al. (2011). Outdoor temperature, age, sex, body mass index, and diabetic status determine the prevalence, mass, and glucose-uptake activity of 18F-FDG-detected BAT in humans. *J. Clin. Endocrinol. Metab.* 96, 192–199. doi: 10.1210/jc.2010-0989
- Petrovic, N., Walden, T. B., Shabalina, I. G., Timmons, J. A., Cannon, B., and Nedergaard, J. (2010). Chronic peroxisome proliferator-activated receptor gamma (PPARgamma) activation of epididymally derived white adipocyte cultures reveals a population of thermogenically competent, UCP1-containing adipocytes molecularly distinct from classic brown adipocytes. *J. Biol. Chem.* 285, 7153–7164. doi: 10.1074/jbc.M109.053942
- Pfannenberger, C., Werner, M. K., Ripkens, S., Stef, I., Deckert, A., Schmadl, M., et al. (2010). Impact of age on the relationships of brown adipose tissue with sex and adiposity in humans. *Diabetes* 59, 1789–1793. doi: 10.2337/db10-0004
- Porras, A., Alvarez, A. M., Valladares, A., and Benito, M. (1997). TNF- $\alpha$  induces apoptosis in rat fetal brown adipocytes in primary culture. *FEBS Lett.* 416, 324–328. doi: 10.1016/S0014-5793(97)01204-0
- Putti, R., Migliaccio, V., Sica, R., and Lionetti, L. (2015b). Skeletal muscle mitochondrial bioenergetics and morphology in high fat diet induced obesity and insulin resistance: focus on dietary fat source. *Front. Physiol.* 6:426. doi: 10.3389/fphys.2015.00426
- Putti, R., Sica, R., Migliaccio, V., and Lionetti, L. (2015a). Diet impact on mitochondrial bioenergetics and dynamics. *Front. Physiol.* 6:109. doi: 10.3389/fphys.2015.00109
- Richard, D. (2007). Energy expenditure: a critical determinant of energy balance with key hypothalamic controls. *Minerva Endocrinol.* 32, 173–183.
- Ricquier, D. (2005). Respiration uncoupling and metabolism in the control of energy expenditure. *Proc. Nutr. Soc.* 64, 47–52. doi: 10.1079/PNS20040408
- Romanatto, T., Roman, E. A., Arruda, A. P., Denis, R. G., Solon, C., Milanski, M., et al. (2009). Deletion of tumor necrosis factor- $\alpha$  receptor 1 (TNFR1) protects against diet-induced obesity by means of increased thermogenesis. *J. Biol. Chem.* 284, 36213–36222. doi: 10.1074/jbc.M109.030874
- Rothwell, N. J., and Stock, M. J. (1979). A role for brown adipose tissue in diet-induced thermogenesis. *Nature* 281, 31e35. doi: 10.1038/281031a0
- Rothwell, N. J., and Stock, M. J. (1981). Regulation of energy balance. *Ann. Rev. Nutr.* 1, 235–256. doi: 10.1146/annurev.nu.01.070181.001315
- Ruschke, K., Fishbein, L., Dietrich, A., Klötting, N., Tönjes, A., Oberbach, A., et al. (2010). Gene expression of PPAR $\gamma$  and PGC-1 $\alpha$  in human omental and subcutaneous adipose tissue is related to insulin resistance markers and mediates beneficial effects of physical training. *Eur. J. Endocrinol.* 162, 515–523. doi: 10.1530/EJE-09-0767
- Saito, M., Okamatsu-Ogura, Y., Matsushita, M., Watanabe, K., Yoneshiro, T., Nio-Kobayashi, J., et al. (2009). High incidence of metabolically active brown adipose tissue in healthy adult humans: effects of cold exposure and adiposity. *Diabetes* 58, 1526–1531. doi: 10.2337/db09-0530
- Scheele, C., and Nielsen, S. (2017). Metabolic regulation and the anti-obesity perspectives of human brown fat. *Redox Biol.* 12, 770–775. doi: 10.1016/j.redox.2017.04.011
- Shabalina, I. G., Kalinovich, A. V., Cannon, B., and Nedergaard, J. (2016). Metabolically inert perfluorinated fatty acids directly activate uncoupling protein 1 in brown-fat mitochondria. *Arch. Toxicol.* 90, 1117–1128. doi: 10.1007/s00204-015-1535-4
- Shabalina, I. G., Kramarova, T. V., Mattsson, C. L., Petrovic, N., Rahman Qazi, M., Csikasz, R. I., et al. (2015). The Environmental pollutants Perfluorooctane Sulfonate and Perfluorooctanoic Acid upregulate uncoupling Protein 1 (UCP1) in brown-fat mitochondria through a UCP1-dependent reduction in food intake. *Toxicol. Sci.* 146, 334–343. doi: 10.1093/toxsci/kfv098
- Sun, L., Liu, C., Xu, X., Ying, Z., Maisseyeu, A., Wang, A., et al. (2013). Ambient fine particulate matter and ozone exposures induce inflammation in epicardial and perirenal adipose tissues in rats fed a high fructose diet. *Part. Fibre Toxicol.* 10:43. doi: 10.1186/1743-8977-10-43
- Sun, Q., Yue, P., Deulilias, J. A., Lumeng, C. N., Kampfrath, T., Mikolaj, M. B., et al. (2009). Ambient air pollution exaggerates adipose inflammation and insulin resistance in a mouse model of diet-induced obesity. *Circulation* 119, 538–546. doi: 10.1161/CIRCULATIONAHA.108.799015
- Taylor, K. W., Novak, R. F., Anderson, H. A., Birnbaum, L. S., Blystone, C., Devito, M., et al. (2013). Evaluation of the association between persistent organic pollutants (POPs) and diabetes in epidemiological studies: a national toxicology program workshop review. *Environ. Health Perspect.* 121, 774–783. doi: 10.1289/ehp.1205502
- Thurlby, P. L., and Trayhurn, P. (1979). The role of thermoregulatory thermogenesis in the development of obesity in genetically obese (ob/ob) mice pair-fed with lean siblings. *Br. J. Nutr.* 42, 377–385. doi: 10.1079/BJN19790127
- Timmons, J. A., Wennmalm, K., Larsson, O., Walden, T. B., and Lassmann, T., Petrovic, et al. (2007). Myogenic gene expression signature establishes that brown and white adipocytes originate from distinct cell lineages. *Proc. Natl. Acad. Sci. U.S.A.* 104, 4401–4406. doi: 10.1073/pnas.0610615104
- Trayhurn, P. (2017). Origins and early development of the concept that brown adipose tissue thermogenesis is linked to energy balance and obesity. *Biochimie* 134, 62–70. doi: 10.1016/j.biochi.2016.09.007
- Trayhurn, P., and Beattie, J. H. (2001). Physiological role of adipose tissue: white adipose tissue as an endocrine and secretory organ. *Proc. Nutr. Soc.* 60, 329–339. doi: 10.1079/PNS2001194
- Valladares, A., Alvarez, A. M., Ventura, J. J., Roncero, C., and Benito, M., Porras, A. (2000). p38 mitogen-activated protein kinase mediates tumor necrosis factor- $\alpha$ -induced apoptosis in rat fetal brown adipocytes. *Endocrinology* 141, 4383–4395. doi: 10.1210/endo.141.12.7843

- van Marken Lichtenbelt, W. D., Vanhommerig, J. W., Smulders, N. M., Drossaerts, J. M., Kemerink, G. J., Bouvy, N. D., et al. (2009). Cold-activated brown adipose tissue in healthy men. *N. Engl. J. Med.* 360, 1500–1508. doi: 10.1056/NEJMoa0808718
- Vázquez-Vela, M. E., Torres, N., and Tovar, A. R. (2008). White adipose tissue as endocrine organ and its role in obesity. *Arch. Med. Res.* 39, 715–28. doi: 10.1016/j.arcmed.2008.09.005.
- Virtanen, K. A., Lidell, M. E., Orava, J., Heglind, M., Westergren, R., Niemi, T., et al. (2009). Functional brown adipose tissue in healthy adults. *N Engl J Med.* 360, 1518–1525. doi: 10.1056/NEJMoa0808949
- Wu, J., Boström, P., Sparks, L. M., Ye, L., Choi, J. H., Giang, A. H., Khandekar, M., et al. (2012). Beige adipocytes are a distinct type of thermogenic fat cell in mouse and human. *Cell* 150, 366–376. doi: 10.1016/j.cell.2012.05.016
- Xie, Y., Yang, Q., Nelson, B. D., and De Pierre, J. W. (2002). Characterization of the adipose tissue atrophy induced by peroxisome proliferators in mice. *Lipids* 37, 139–146. doi: 10.1007/s11745-002-0873-7
- Xie, Y., Yang, Q., Nelson, B. D., and De Pierre, J. W. (2003). The relationship between liver peroxisome proliferation and adipose tissue atrophy induced by peroxisome proliferator exposure and withdrawal in mice. *Biochem. Pharmacol.* 66, 749–756. doi: 10.1016/S0006-2952(03)00386-1
- Xu, C. X., Wang, C., Zhang, Z. M., Jaeger, C. D., Krager, S. L., Bottum, K. M., et al. (2015). Aryl hydrocarbon receptor deficiency protects mice from diet-induced adiposity and metabolic disorders through increased energy expenditure. *Int. J. Obes.* 39, 1300–1309. doi: 10.1038/ijo.2015.63
- Xu, X., Liu, C., Xu, Z., Tzan, K., Zhong, M., Wang, A., et al. (2011a). Long-term exposure to ambient fine particulate pollution induces insulin resistance and mitochondrial alteration in adipose tissue. *Toxicol. Sci.* 124, 88–98. doi: 10.1093/toxsci/kfr211
- Xu, X., Yavar, Z., Verdin, M., Ying, Z., Mihai, G., Kampfrath, T., et al. (2010). Effect of early particulate air pollution exposure on obesity in mice: role of p47phox. *Arterioscler. Thromb. Vasc. Biol.* 30, 2518–2527. doi: 10.1161/ATVBAHA.110.215350
- Xu, Z., Xu, X., Zhong, M., Hotchkiss, I. P., Lewandowski, R. P., Wagner, J. G., et al. (2011b). Ambient particulate air pollution induces oxidative stress and alterations of mitochondria and gene expression in brown and white adipose tissues. *Part. Fibre Toxicol.* 8:20. doi: 10.1186/1743-8977-8-20
- Ying, Z. K., Xu, X. H., Bai, Y. T., Zhong, J. X., Chen, M. J., Liang, Y. J., et al. (2014). Long-term exposure to concentrated ambient PM2.5 increases mouse blood pressure through abnormal activation of the sympathetic nervous system: a role for hypothalamic inflammation. *Environ. Health Perspect.* 122, 79–86. doi: 10.1289/ehp.1307151
- Yoneshiro, T., Aita, S., Matsushita, M., Kameya, T., Nakada, K., Kawai, Y., et al. (2011). Brown adipose tissue, whole-body energy expenditure, and thermogenesis in healthy adult men. *Obesity* 19, 13–6. doi: 10.1038/oby.2010.105
- Zhang, G., Sun, Q., Liu, C., (2016). Influencing factors of thermogenic adipose tissue activity. *Front. Physiol.* 7:29. doi: 10.3389/fphys.2016.00029

**Conflict of Interest Statement:** The authors declare that the research was conducted in the absence of any commercial or financial relationships that could be construed as a potential conflict of interest.

Copyright © 2019 Di Gregorio, Busiello, Burgos Aceves, Lepretti, Paoletta and Lionetti. This is an open-access article distributed under the terms of the Creative Commons Attribution License (CC BY). The use, distribution or reproduction in other forums is permitted, provided the original author(s) and the copyright owner(s) are credited and that the original publication in this journal is cited, in accordance with accepted academic practice. No use, distribution or reproduction is permitted which does not comply with these terms.





# High Fat Diet Increases Circulating Endocannabinoids Accompanied by Increased Synthesis Enzymes in Adipose Tissue

Elaine N. Kuipers<sup>1,2†</sup>, Vasudev Kantae<sup>3†</sup>, Boukje C. Eveleens Maarse<sup>1,2</sup>, Susan M. van den Berg<sup>4</sup>, Robin van Eenige<sup>1,2</sup>, Kimberly J. Nahon<sup>1,2</sup>, Anne Reifel-Miller<sup>5</sup>, Tamer Coskun<sup>5</sup>, Menno P. J. de Winther<sup>4</sup>, Esther Lutgens<sup>4,6</sup>, Sander Kooijman<sup>1,2,7</sup>, Amy C. Harms<sup>3</sup>, Thomas Hankemeier<sup>3</sup>, Mario van der Stelt<sup>8</sup>, Patrick C. N. Rensen<sup>1,2</sup> and Mariëtte R. Boon<sup>1,2\*</sup>

<sup>1</sup> Department of Medicine, Division of Endocrinology, Leiden University Medical Center, Leiden, Netherlands, <sup>2</sup> Einthoven Laboratory for Experimental Vascular Medicine, Leiden University Medical Center, Leiden, Netherlands, <sup>3</sup> Division of Systems Biomedicine and Pharmacology, Leiden Academic Centre for Drug Research, Leiden University, Leiden, Netherlands, <sup>4</sup> Department of Medical Biochemistry, Academic Medical Center, Amsterdam, Netherlands, <sup>5</sup> Department of Diabetes/Endocrine, Lilly Research Laboratories, Lilly Corporate Center, Indianapolis, IN, United States, <sup>6</sup> Institute for Cardiovascular Prevention (IPEK), Ludwig Maximilian University of Munich, Munich, Germany, <sup>7</sup> Oxford Centre for Diabetes, Endocrinology and Metabolism, University of Oxford, Oxford, United Kingdom, <sup>8</sup> Department of Molecular Physiology, Leiden Institute of Chemistry, Leiden University, Leiden, Netherlands

## OPEN ACCESS

### Edited by:

Paula Oliver,  
Universidad de les Illes Balears, Spain

### Reviewed by:

Emmanuel Modesto Awumey,  
North Carolina Central University,  
United States  
Cristoforo Silvetri,  
Laval University, Canada

### \*Correspondence:

Mariëtte R. Boon  
m.r.boon@lumc.nl

<sup>†</sup> These authors have contributed  
equally to this work

### Specialty section:

This article was submitted to  
Integrative Physiology,  
a section of the journal  
Frontiers in Physiology

Received: 03 August 2018

Accepted: 18 December 2018

Published: 10 January 2019

### Citation:

Kuipers EN, Kantae V, Maarse BCE, van den Berg SM, van Eenige R, Nahon KJ, Reifel-Miller A, Coskun T, de Winther MPJ, Lutgens E, Kooijman S, Harms AC, Hankemeier T, van der Stelt M, Rensen PCN and Boon MR (2019) High Fat Diet Increases Circulating Endocannabinoids Accompanied by Increased Synthesis Enzymes in Adipose Tissue. *Front. Physiol.* 9:1913. doi: 10.3389/fphys.2018.01913

The endocannabinoid system (ECS) controls energy balance by regulating both energy intake and energy expenditure. Endocannabinoid levels are elevated in obesity suggesting a potential causal relationship. This study aimed to elucidate the rate of dysregulation of the ECS, and the metabolic organs involved, in diet-induced obesity. Eight groups of age-matched male C57Bl/6J mice were randomized to receive a chow diet (control) or receive a high fat diet (HFD, 45% of calories derived from fat) ranging from 1 day up to 18 weeks before euthanasia. Plasma levels of the endocannabinoids 2-arachidonoylglycerol (2-AG) and anandamide (*N*-arachidonylethanolamine, AEA), and related *N*-acylethanolamines, were quantified by UPLC-MS/MS and gene expression of components of the ECS was determined in liver, muscle, white adipose tissue (WAT) and brown adipose tissue (BAT) during the course of diet-induced obesity development. HFD feeding gradually increased 2-AG (+132% within 4 weeks,  $P < 0.05$ ), accompanied by upregulated expression of its synthesizing enzymes *Dagl* $\alpha$  and  $\beta$  in WAT and BAT. HFD also rapidly increased AEA (+81% within 1 week,  $P < 0.01$ ), accompanied by increased expression of its synthesizing enzyme *Nape-pld*, specifically in BAT. Interestingly, *Nape-pld* expression in BAT correlated with plasma AEA levels ( $R^2 = 0.171$ ,  $\beta = 0.276$ ,  $P < 0.001$ ). We conclude that a HFD rapidly activates adipose tissue depots to increase the synthesis pathways of endocannabinoids that may aggravate the development of HFD-induced obesity.

**Keywords:** brown adipose tissue, white adipose tissue, diet-induced obesity, endocannabinoids, NAPE-PLD

**Abbreviations:** 2-AG, 2-arachidonoylglycerol; AA, arachidonic acid; ABHD4, *Abhd4* Alpha/beta hydrolase domain containing-4; AEA, anandamide (*N*-arachidonylethanolamine); BAT, brown adipose tissue; CB1R, cannabinoid receptor type 1; CB2R, cannabinoid receptor type 2; DAGL- $\alpha/\beta$ , *Dagl*- $\alpha/\beta$  diacylglycerol lipase- $\alpha/\beta$ ; DEA, *N*-docosahexaenoylethanolamine; DIO, diet-induced obesity; ECS, endocannabinoid system; FAAH, *Faah* fatty acid amide hydrolase; GDE1, *Gde1* glycerophosphodiesterase-1; gWAT, gonadal white adipose tissue; HFD, high fat diet; LC-MS/MS, liquid chromatography coupled tandem mass spectrometry; MAGL, *Mgl1* monoacylglycerol lipase; NAE, *N*-acylethanolamine; NAPE, *N*-acylphosphatidylethanolamine; NAPE-PLD, *Nape-pld* *N*-acylphosphatidylethanolamine phospholipase D; OEA, *N*-oleylethanolamine; PEA, *N*-palmitoylethanolamine; SEA, *N*-stearoylethanolamine.

## INTRODUCTION

Obesity is becoming a global epidemic and the need for development of novel therapeutic interventions is high. The endocannabinoid system (ECS) is regarded as a potential therapeutic target since it regulates energy balance by influencing appetite (Foltin et al., 1988; Jamshidi and Taylor, 2001), intracellular lipolysis and energy expenditure [reviewed in (Cota, 2007; Mazier et al., 2015)]. The ECS consists of cannabinoid receptors, their endogenous ligands, the endocannabinoids, and the enzymes that synthesize and degrade the endocannabinoids. The cannabinoid receptors are G-protein-coupled receptors, comprising the CB1R and CB2R. The CB1R is expressed centrally and in peripheral metabolic tissues including white adipose tissue (WAT), brown adipose tissue (BAT), liver, skeletal muscle and the pancreas. In contrast, the CB2R is mainly expressed in immune cells (Howlett et al., 2002).

The two main circulating endocannabinoids are anandamide (*N*-arachidonylethanolamine, AEA) and 2-arachidonoylglycerol (2-AG). Although they are both derived from cell membrane arachidonic acid (AA) derivatives, the levels of these endocannabinoids are differentially regulated. AEA can be generated via hydrolysis of *N*-acyl-phosphatidylethanolamines (NAPE) by a NAPE-specific phospholipase D (NAPE-PLD) and its degradation is primarily regulated by fatty acid amide hydrolase (FAAH). 2-AG levels are regulated by the biosynthesis enzymes diacylglycerol lipase  $\alpha$  and  $\beta$  (DAGL- $\alpha$  and  $\beta$ ) and the degradation enzyme mono-acylglycerol lipase (MAGL) (Muccioli, 2010; Bisogno and Maccarrone, 2014; Baggelaar et al., 2018).

Activation of the CB1R in peripheral tissues inhibits fatty acid oxidation resulting in a positive energy balance and thus development of obesity in mice (Ravinet Trillou et al., 2003; Osei-Hyiaman et al., 2005; Arrabal et al., 2015). In addition, an increased tone of the ECS is associated with obesity in humans (Engeli et al., 2005; Bluher et al., 2006). Efforts have been made to reverse obesity by blocking the CB1R by small molecules such as the inverse agonist rimonabant (Sam et al., 2011). Albeit that rimonabant was effective in humans as evident from sustained weight loss and reduction of dyslipidaemia, centrally mediated side effects resulted in removal from the market (Despres et al., 2005; Pi-Sunyer et al., 2006). Nevertheless, blocking the actions of the ECS is still regarded a potent therapeutic strategy [reviewed in (O'Keefe et al., 2014; Simon and Cota, 2017)].

To develop novel therapeutics that target specific aspects of the ECS, it is crucial to obtain more insight in how fast and in which organs the dysregulation of the ECS sets off. In this study, we aimed at elucidating these questions by exposing mice to a high fat diet (HFD) ranging from 1 day up to 18 weeks, which finally causes diet-induced obesity (DIO). We analyzed endocannabinoid levels in plasma as well as the expression of enzymes involved in endocannabinoid synthesis and breakdown in several metabolic organs.

## MATERIALS AND METHODS

### Animals and Diet

Eighty-six 7-week old male C57Bl/6J mice (Charles River Laboratories, United States) were obtained. All mice were group housed (3–4 mice per cage) under a 12 h:12 h light-dark cycle with *ad libitum* access to food and water. During the course of the experiment 7 out of 8 groups of mice were switched from a regular chow diet (Special Diets Services, United Kingdom) to a HFD (45% kcal fat, 35% kcal carbohydrate, 20% kcal protein, Special Diets Services, United Kingdom) in such a way that all mice were 25 weeks of age at the time of euthanasia. In total, the study consisted of eight groups receiving HFD for 0 day (control group, remaining on a regular chow diet), 1 day, 3 days, 1, 2, 4, 10, and 18 weeks ( $n = 10$ –11 per group). At the end of the study, mice were fasted overnight and subsequently euthanized by an injection with 0.25 mg ketamine and 0.05 mg xylazine per gram body weight. Blood was collected via a cardiac puncture with EDTA filled syringes and several organs (liver, quadriceps muscle, gonadal WAT and interscapular BAT) were isolated. The organs were immediately snap frozen in liquid nitrogen and stored at  $-80^{\circ}\text{C}$  until further analysis. For BAT, a small piece was fixated for histological analysis. A second experiment was performed in which 14-week old male C57Bl/6J mice (Charles River Laboratories, United States) were fed 0 day or 1 week HFD ( $n = 8$  per group) prior to euthanasia. Mice were fasted for 4 h and euthanized by  $\text{CO}_2$  suffocation. Blood was collected via cardiac puncture with EDTA filled syringes as described above. These studies were carried out in accordance with the recommendations of the animal experimentation guidelines of Amsterdam Medical Center ( $n = 86$  experiment) and Leiden University Medical Center ( $n = 16$  experiment) and approved by the local ethical review boards on animal experimentation.

### Endocannabinoid Plasma Levels

A liquid-liquid extraction using methyl tert-butyl ether as an organic solvent was used to extract endocannabinoids from plasma. Levels of endocannabinoids (AEA, 2-AG), *N*-acylethanolamines (NAEs), and AA were measured by UPLC-MS/MS (AB Sciex 6500 QTRAP) in 25  $\mu\text{L}$  plasma samples. From the pool of individual study samples, quality controls (QCs) were used to generate calibration curves. Additionally, all samples were randomized and each batch of study samples included calibration samples, an even distribution of QC samples and blanks. The sample extraction procedure and method has been described in detail previously (Kantae et al., 2017).

### RNA Isolation and RT-PCR Analysis

RNA of liver and muscle was isolated using TriPure Isolation reagent (Roche, Netherlands) and 1  $\mu\text{g}$  of RNA was reverse transcribed using Moloney Murine Leukemia Virus Reverse Transcriptase (Promega, Netherlands). For WAT and BAT, RNA was isolated using Trizol (Invitrogen, United States) and cDNA was synthesized using an iScript cDNA synthesis kit (Bio-Rad, Netherlands). RT-PCR was carried out on a CFX96 PCR machine

(Bio-Rad) using IQ SYBR-Green Supermix (Promega). mRNA expression was normalized to *Hprt* and *36b4* as household genes for liver, BAT and WAT; for muscle mRNA expression was normalized to the expression of *36b4* only. Changes in gene expression relative to basal expression levels were only calculated if the average expression of at least the control group were  $Ct < 32$ . Primer sequences are listed in **Table 1**.

## Histology and Determination of Lipid Droplet Content in BAT

After dissection, a small piece of interscapular BAT was immediately fixated in 4% paraformaldehyde, subsequently dehydrated and embedded in paraffin. A Haematoxylin and Eosin staining was performed on paraffin sections using standard protocols. Intracellular lipid content was quantified with ImageJ (version 1.49).

## Statistical Analysis

All data are expressed as mean  $\pm$  SEM. Data analysis was performed with an IBM SPSS Statistics 23 software package. Analysis between multiple groups was done by a one-way ANOVA with Dunnett's *post hoc* test. For the analysis of plasma 2-AG in the second experiment we used an unpaired two-sided *t*-test. Furthermore, linear regression analysis computed by Pearson's correlation was used to determine correlations. Significant differences are expressed relative to the chow-fed (0 week HFD) control group.

## RESULTS

### HFD Feeding Rapidly Increases Plasma 2-AG and AEA Levels in Mice

To investigate the time course of the dysregulation of the ECS in the development of DIO, C57B1/6J mice were fed a HFD for 1 day up to 18 weeks. As expected, dietary intervention increased body weight (up to +51% after 18 weeks,  $P < 0.001$ , **Table 2**). Blood glucose levels rapidly increased in response to the HFD (+88% after 1 day of HFD,  $P < 0.001$ ), whereas plasma TG

levels increased more gradually (+155% after 2 weeks of HFD,  $P < 0.01$ ) (**Table 2**).

First, we assessed plasma levels of the two main endocannabinoids in the course of DIO development (**Figure 1**). HFD feeding gradually increased 2-AG levels, which reached significance after 4 weeks (+132%,  $P < 0.05$ ) and further increased up to 18 weeks (+201%;  $P < 0.001$ ) (**Figure 1A**). Of note, in a few samples of the control group we observed extremely high 2-AG levels ( $>100$  pmol/mL) that masked an initial increase in 2-AG levels upon HFD. To determine whether these high levels would represent (biological) outliers, we determined plasma 2-AG levels in a separate cohort of mice fed a HFD for 0 or 7 days. Indeed these values lie more than six standard deviations away from the average of the repeated control animals and could therefore be regarded as biological outliers. Importantly, we observed a trend toward elevated 2-AG plasma levels in the 7 days HFD fed group (+34%,  $P = 0.055$ , not shown) compared to the 0 day group in the repeated experiment. Therefore, we excluded the mice of the control group with extremely high plasma 2-AG levels from calculation of the means of all endocannabinoids and related metabolites, and instead indicated these data in gray (**Figures 1A–I**). HFD feeding also rapidly increased levels of AEA, the other main endocannabinoid, which reached significance after 1 week (+81%,  $P < 0.01$ ) and further increased up to 18 weeks (+165%,  $P < 0.001$ ) (**Figure 1B**). Next, we determined whether plasma endocannabinoid levels were related to body weight. Linear regression analysis on all data combined showed that body weight correlated weakly but positively with 2-AG levels ( $R^2 = 0.073$ ,  $\beta = 1.447$ ,  $P = 0.017$ , **Figure 1C**) and much more strongly with AEA levels ( $R^2 = 0.654$ ,  $\beta = 0.041$ ,  $P < 0.001$ , **Figure 1D**).

NAPE-PLD does not only produce AEA, but generates a whole family of *N*-acylethanolamines (NAEs), including *N*-oleoylethanolamine (OEA), *N*-palmitoylethanolamine (PEA), *N*-stearoylethanolamine (SEA), and *N*-docosatetraenoylethanolamine (DEA). Similar to AEA, plasma concentrations of these non-cannabinoid fatty acid amides were raised in response to HFD feeding, albeit with different kinetics (**Figures 1E–H**). Plasma levels of AA, the precursor and degradation product of 2-AG and AEA (Piomelli, 2003), also rapidly increased in the first 2 weeks of HFD after which a plateau was reached (+89% after 18 weeks,  $P < 0.001$ , **Figure 1I**). Of note, the samples of the control group with extremely high 2-AG levels (**Figure 1A**) also showed elevated AA levels (**Figure 1I**).

### HFD Feeding Increases Expression of 2-AG Synthesis and Degradation Enzymes in WAT and BAT

Next, we assessed gene expression of the enzymes responsible for the synthesis (*Dagla* and *Daglb*) and degradation (*Mgll*) of 2-AG in liver, muscle, WAT and BAT (**Figure 2**; an overview of all relative gene expressions of the enzymes involved in synthesis and degradation is shown in **Supplementary Table S1**). HFD feeding transiently increased *Dagla* expression in WAT after

**TABLE 1** | List of primer sequences for RT-PCR.

Gene	Forward primer	Reverse primer
<i>Abhd4</i>	ATCCTCCAGTGTCTCCAGAACA	GGGTCCCTTGGGAATGTTGG
<i>Cd68</i>	ATCCACACCTGTCTCTCTCA	TTGCATTTCACAGCAGAAG
<i>Dagla</i>	TATCTTCTCTTCTGCT	CCATTTCGGCAATCATAC
<i>Daglb</i>	GGGTCTTTTGAGCTGTTT	AAGGAGGACTATCAGGTA
<i>Faah</i>	CAGCTACAAGGGCCATGCT	TTCCACGGGTTCTGGTCTG
<i>Gde1</i>	AAGGATTTGTCTCCCGGAC	ATGTAGCTGGACCCAAGGTG
<i>Hprt</i>	TTGCTCGAGATGTCATGAAGGA	AGCAGGTCAGCAAAGAACTATAG
<i>Mgll</i>	CAGAGAGGCCAACCTACTTT	ATGCGCCCCAAGGTCATATTT
<i>Nape-pld</i>	AAAACATCTCCATCCCGAA	CGTCCATTTCACCATCA
<i>Pla/at1</i>	CGGTAATGATTGCTTCAGT	CCACAACATCCTTCAAAGC
<i>Pla/at5</i>	CCTGGAGACCTGATTGAGA	GGTTGCTGAAGATAGAGGTG
<i>36b4</i>	GGACCCGAGAAGACCTCCTT	GCACATCACTCAGAATTTCAATGG

**TABLE 2 |** General characteristics of the mice during diet-induced obesity development.

	Duration of HFD (weeks), mean $\pm$ SEM							
	0	1/7	3/7	1	2	4	10	18
N=	11	11	10	10	11	11	11	11
Body weight (g)	27.3 $\pm$ 0.6	29.5 $\pm$ 0.6	31.1 $\pm$ 0.8~	31.5 $\pm$ 0.5*	34.4 $\pm$ 0.9***	36.5 $\pm$ 1.2***	38.1 $\pm$ 0.9***	41.3 $\pm$ 2.0***
Glucose (mg/dL)	69 $\pm$ 3	130 $\pm$ 15***	118 $\pm$ 7***	123 $\pm$ 4***	104 $\pm$ 5*	91 $\pm$ 4	112 $\pm$ 9**	124 $\pm$ 7***
Triglycerides (mM)	0.20 $\pm$ 0.02	0.25 $\pm$ 0.05	0.41 $\pm$ 0.09~	0.34 $\pm$ 0.06	0.51 $\pm$ 0.07**	0.81 $\pm$ 0.08***	0.54 $\pm$ 0.03**	0.60 $\pm$ 0.05***

Values are indicated in mean  $\pm$  SEM. ~ $P < 0.1$ , \* $P < 0.05$ , \*\* $P < 0.01$ , \*\*\* $P < 0.001$  compared to the control group. These data were previously published elsewhere (van den Berg et al., 2016).

3 days (+57%,  $P < 0.05$ , **Figure 2A**) and increased *Dagl $\alpha$*  expression in BAT after 1 and 4 weeks of HFD (**Figure 2B**). HFD feeding also induced *Dagl $\beta$*  expression in WAT (**Figure 2C**) and BAT (**Figure 2D**), especially toward the end of the intervention (i.e., +246% in WAT and +38% in BAT after 18 weeks). Linear regression analyses between the expression levels of DAG lipases in adipose tissues and plasma 2-AG levels showed inconclusive data (**Supplementary Figure S1**). HFD feeding also transiently increased *Mgll* expression in WAT reaching a peak after 1 week of HFD (+75%,  $P < 0.001$ ), which normalized toward the end of HFD intervention (**Figure 2E**). In contrast, HFD induced a sustained increase in *Mgll* expression levels in BAT from 1 day on (+28%,  $P < 0.05$ , **Figure 2F**). HFD feeding did not persistently affect gene expression of synthesis and degradation enzymes in liver and muscle. It only temporarily increased *Dagl $\alpha$*  expression in muscle (at 2 weeks), increased *Dagl $\beta$*  expression (at 3 days) and decreased *Mgll* expression (at 1 day) in liver (data in **Supplementary Table S1**). Collectively, these data show that the rise in 2-AG levels during DIO development coincided with enhanced expression of synthesis and degradation enzymes specifically in WAT and BAT.

## HFD Feeding Increases *Nape-pld* Expression in WAT and BAT

We next assessed gene expression of the enzyme responsible for AEA and NAEs synthesis (*Nape-pld*) in the various metabolic organs. HFD feeding tended to increase *Nape-pld* expression in WAT after 3 days, although expression levels normalized thereafter and were decreased after 18 weeks (−41%,  $P < 0.01$ , **Figure 3A**). Surprisingly, linear regression analysis showed a small, but significant, negative correlation between *Nape-pld* expression in WAT and plasma AEA levels ( $R^2 = 0.124$ ,  $\beta = -0.235$ ,  $P = 0.002$ , **Figure 3B**). Interestingly, HFD feeding increased *Nape-pld* expression in BAT starting at 3 days (+102%,  $P < 0.001$ , **Figure 3C**), after which levels reached a plateau. Moreover, *Nape-pld* expression in BAT positively correlated with plasma AEA levels ( $R^2 = 0.171$ ,  $\beta = 0.276$ ,  $P < 0.001$ , **Figure 3D**), supporting a contribution of BAT *Nape-pld* expression to circulating AEA levels. HFD feeding decreased the expression of *Nape-pld* in muscle reaching significance from 4 weeks onwards and did not affect *Nape-pld* expression in the liver (data in **Supplementary Table S1**). We also determined the potential contribution of the expression of genes involved in

the phospholipase A/acyltransferase (PLA/AT) family, which can produce NAPE in a  $Ca^{2+}$ -independent manner, in the increase in AEA levels in DIO (Hussain et al., 2017). However, expression of the PLA/AT (HRAS-like suppressor) gene family was either too low to detect (*Pla/at1* in liver, WAT, BAT and *Pla/at5* in liver) or did not show a clear or persistent rise in expression levels that could explain the rise in AEA levels (not shown). Alpha/beta hydrolase domain containing-4 (ABHD4) and glycerophosphodiesterase-1 (GDE1) have been suggested to be involved in AEA synthesis by BAT (Krott et al., 2016). However, time-dependent expression levels of *Abhd4* and *Gde1* in BAT did not coincide with the HFD-induced rise in AEA and NAEs (not shown).

Next, we determined gene expression levels of *Faah*, the enzyme involved in AEA and NAEs degradation. HFD feeding decreased *Faah* expression levels in the liver after 18 weeks (−41%,  $P < 0.01$ , **Supplementary Table S1**). Expression levels of *Faah* in muscle, WAT and BAT were too low to be detected. Altogether, these data show that HFD robustly increased the expression of *Nape-pld* in BAT, suggesting that this tissue may contribute to the increased plasma AEA and NAE levels during DIO development.

## Plasma AEA Levels Positively Correlate With Lipid Content of BAT

Next, we aimed to gain more insight into the cell types within BAT that may have contributed to the robust increased *Nape-pld* expression and plasma AEA levels in DIO development. Because macrophages have been shown to produce AEA (Di Marzo et al., 1996), we first determined gene expression levels of the macrophage marker *Cd68* in BAT. Linear regression analysis showed a weak positive correlation between *Cd68* expression and *Nape-pld* expression in BAT ( $R^2 = 0.113$ ,  $\beta = 0.170$ ,  $P = 0.002$ , **Figure 4A**) and plasma AEA levels ( $R^2 = 0.088$ ,  $\beta = 0.088$ ,  $P = 0.009$ , **Figure 4B**). Besides macrophages, brown adipocytes might also be involved. Since intracellular lipid droplets have been shown to co-localize with intracellular AEA (Oddi et al., 2008), we quantified BAT lipid droplet content in H&E stained BAT sections (**Supplementary Figure S2**). Compared to *Cd68*, BAT lipid droplet content showed a more pronounced positive correlation with *Nape-pld* expression levels in BAT ( $R^2 = 0.385$ ,  $\beta = 0.021$ ,  $P < 0.001$ , **Figure 4C**) as well as plasma AEA levels ( $R^2 = 0.172$ ,  $\beta = 0.010$ ,  $P < 0.001$ , **Figure 4D**).



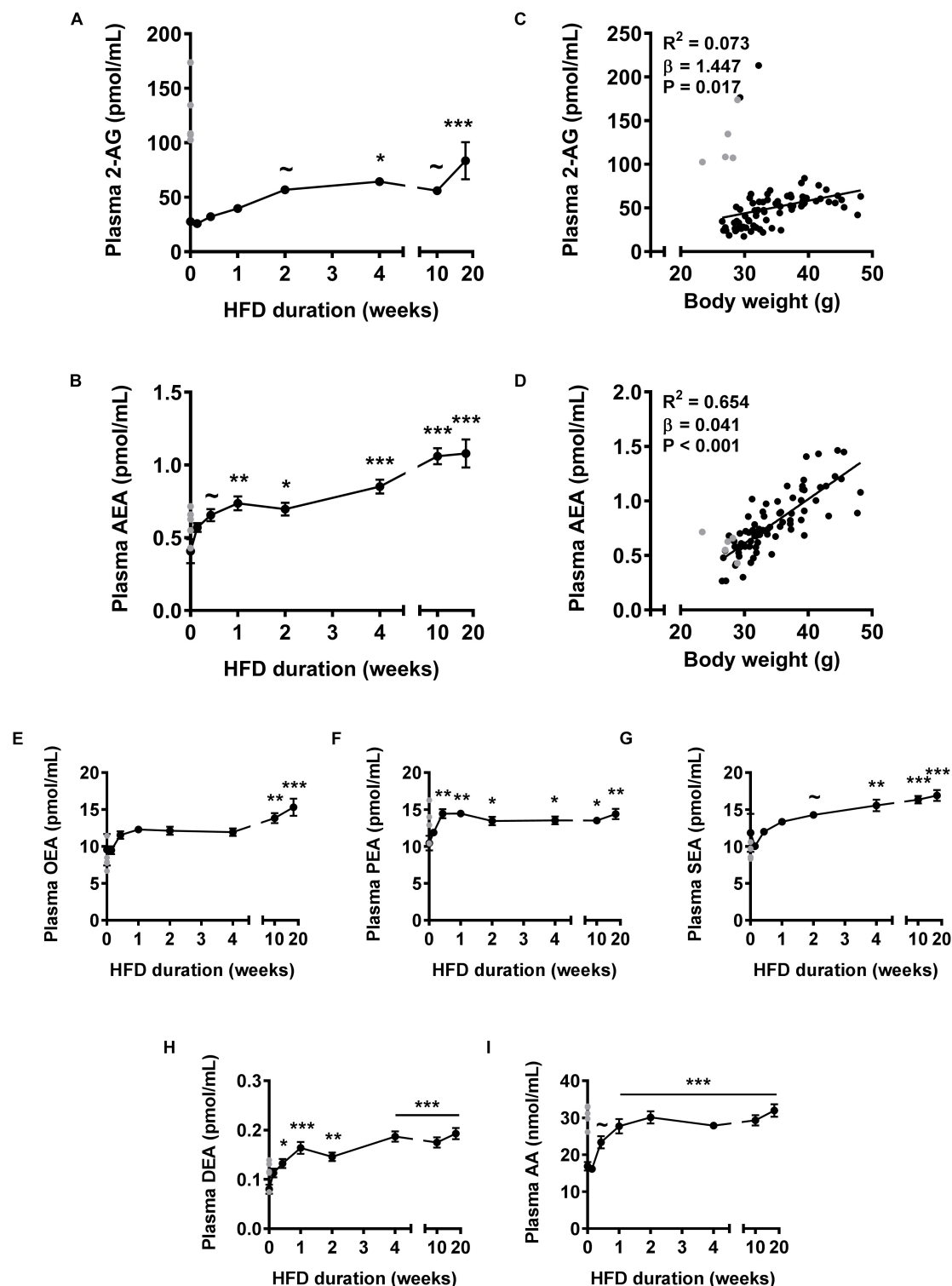
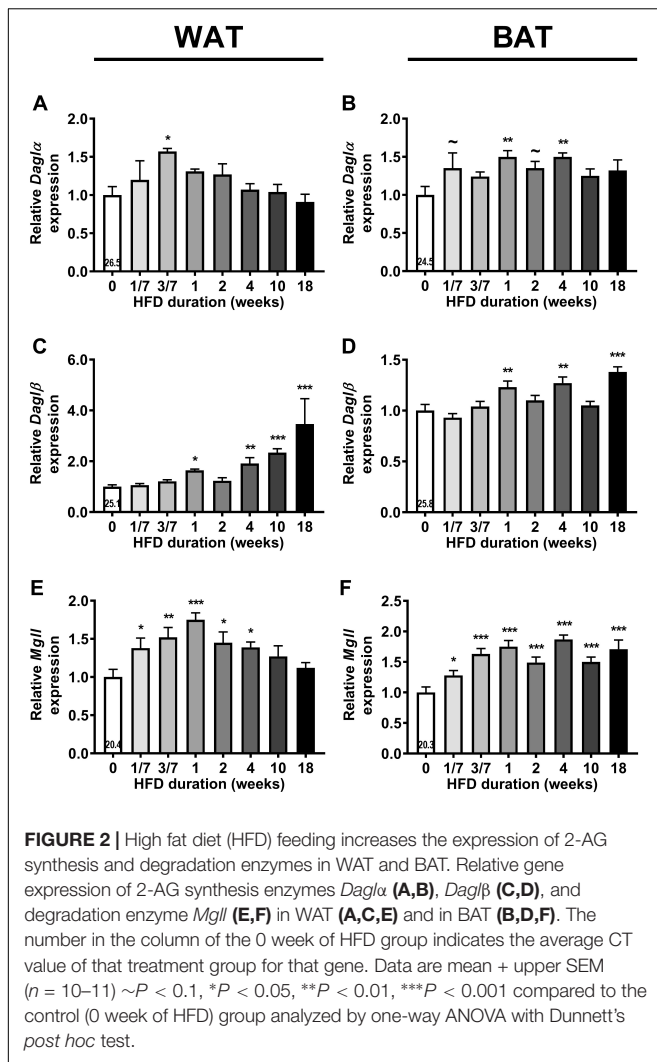


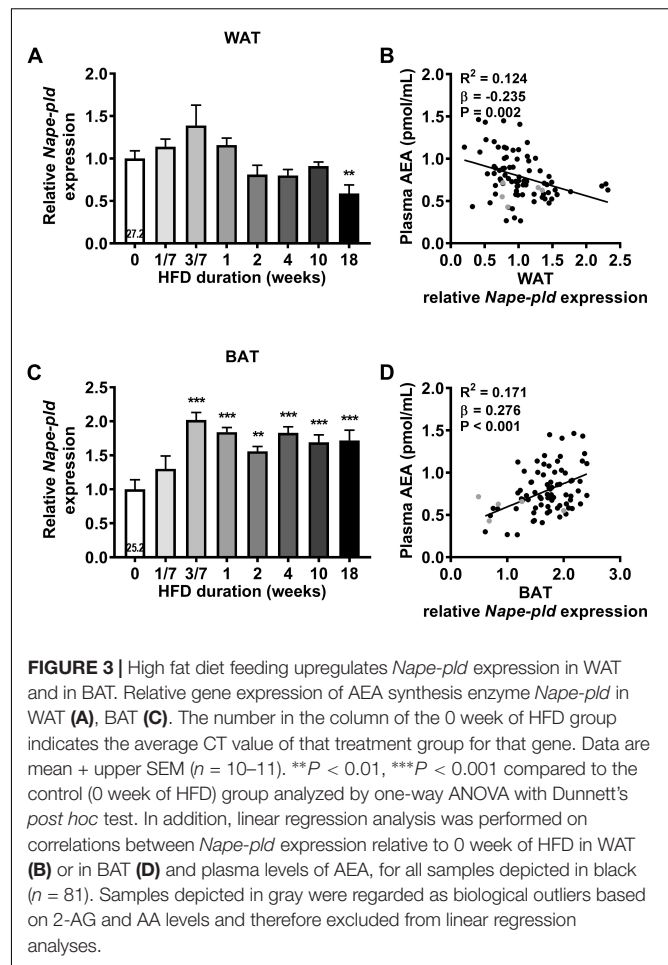
**FIGURE 1 |** High fat diet feeding time-dependently increases plasma levels of 2-AG and AEA in mice. Liquid chromatography coupled with tandem mass spectrometry (LC-MS/MS) was used to determine plasma levels of 2-AG (A), AEA (B), OEA (E), PEA (F), SEA (G), DEA (H), and AA (I). Data are mean  $\pm$  SEM ( $n = 10$ –11). Error bars were too small to be visible for several data points (in A, E–G, I).  $\sim P < 0.1$ ,  $*P < 0.05$ ,  $**P < 0.01$ ,  $***P < 0.001$  compared to the control (0 week of HFD) group analyzed by one-way ANOVA with Dunnett's *post hoc* test. In addition, linear regression analysis was performed on correlations between body weight and plasma levels of 2-AG (C) or AEA (D), for all samples depicted in black ( $n = 81$ ). Samples depicted in gray were regarded as biological outliers based on 2-AG and AA levels and therefore excluded from plasma data analyses.



## DISCUSSION

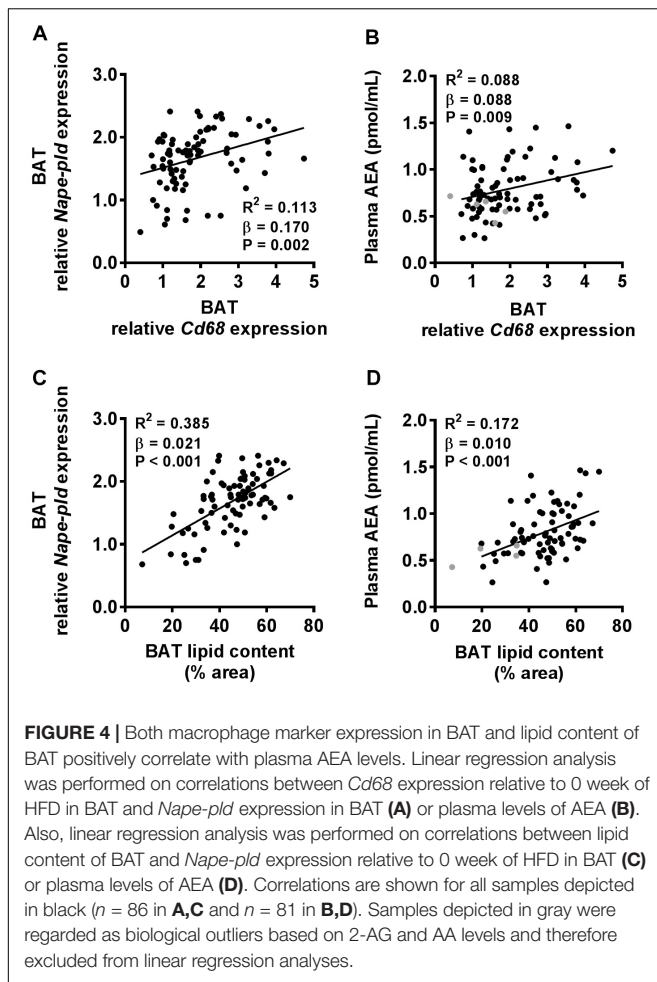
In this study, we demonstrated that HFD feeding increases circulating levels of endocannabinoids, with a rapid initial increase in AEA and a more gradual increase in 2-AG, in the course of DIO development. These changes were accompanied by increased gene expression of the synthesis and degradation enzymes of 2-AG in both WAT and BAT, and with increased expression of the AEA synthesis enzyme *Nape-pld* in BAT. Taken together, these data indicate that the dysregulation of the ECS in the development of obesity occurs rapidly and that WAT and BAT might contribute to these effects.

The observed increases in endocannabinoids in the development of DIO are in agreement with previous studies in mice that showed increased plasma 2-AG and AEA levels after 9 weeks (D'Eon et al., 2008) and 36 weeks (Pati et al., 2018) of HFD feeding and increased plasma AEA levels in a model for glucocorticoid induced obesity (Bowles et al., 2015). These data also are concordant with data in humans, since obese individuals have higher 2-AG levels compared to lean



individuals (Engeli et al., 2005; Bluher et al., 2006; Cote et al., 2007). It was somewhat surprising that a subset of the control group that were not fed a HFD showed very high 2-AG levels in addition to AA levels, the reason of which is currently unclear to us. By performing a second study in mice we confirmed that HFD feeding induced an initial rise rather than decrease in 2-AG levels. Thus, although the reason for the very high 2-AG levels in a subgroup is intriguing, we regarded those mice as biological outliers. Besides 2-AG and AEA, HFD feeding also increased the plasma levels of AA. Since AA is constituent and degradation product of 2-AG and AEA, elevated AA levels may either be a cause or consequence of the increased levels. HFD feeding also increased plasma levels of other *N*-acylethanolamines, including OEA, PEA, SEA and DEA. These NAEs have other biological targets involved in controlling the energy balance, such as peroxisome proliferator-activated receptors- $\alpha$  (PPAR $\alpha$ ), PPAR $\gamma$  and G protein-coupled receptor 119 (Fezza et al., 2014).

Currently, it is unknown which organs contribute to the increased plasma endocannabinoid levels in HFD-induced obesity (Hillard, 2018). We showed that body weight positively correlates with plasma endocannabinoid levels, albeit that the correlation with AEA ( $R^2 = 0.654$ ) is stronger than with 2-AG



( $R^2 = 0.073$ ). Since body weight differences in the range of approximately 30–50 g, as observed in this study, are mainly caused by differences in body fat (van Beek et al., 2015), it was considered likely that engulfment of lipids by adipocytes and/or expansion of the adipocyte pool would contribute to the increase in endocannabinoids. Insulin resistance, which is closely linked to increased intracellular lipid deposition (Tchernof and Despres, 2013) is also associated with a dysregulated ECS (Gruden et al., 2016). By performing gene expression analysis in metabolically active organs, we could demonstrate that expression of enzymes involved in endocannabinoid synthesis increased in WAT as well as BAT. This is in full agreement with a previous study in which 3 and 8 weeks of HFD feeding, with a diet closely resembling the HFD used in our experiments, resulted in increased local levels of endocannabinoids (AEA and 2-AG) in BAT (Matias et al., 2008). The increase in plasma 2-AG coincided with increased gene expression of DAGL $\alpha$  and DAGL $\beta$  in both WAT and BAT. Given the different time-course of expression, where the increase in *Dagla* seems to precede the increase in *Daglb*, we postulate that DAGL $\alpha$  may be responsible for the initial rise in 2-AG, while DAGL $\beta$  may mediate the late increase in 2-AG. Similarly, the increase in plasma AEA coincided with increased gene expression of its synthesizing

enzyme NAPE-PLD in BAT. Moreover, plasma AEA correlated positively with *Nape-pld* expression in BAT but not in WAT. It is therefore likely that BAT rather than WAT contributes to the rise in AEA levels. In this respect, it is interesting that expression of *Nape-pld* is higher in BAT than in WAT, as evident from lower Ct values. The expression levels of most of the enzymes showed a sharp increase in the first week of HFD feeding, which coincided with the timing of the largest increase in lipid deposition in BAT. In BAT, ABHD4, and GDE1 were shown to also be involved in AEA synthesis and their expression respond to BAT activating agents (Krott et al., 2016), although we did not find the expression levels of these enzymes to coincide with the increase in circulating AEA and NAEs levels with prolonged HFD feeding. Of note, expression of the endocannabinoid degradation enzymes *Faah* and *Mgl1* in the adipose tissues were either undetectable or increased. Although we have not been able to measure actual enzyme activities due to technical reasons, it is tempting to speculate that net whole body endocannabinoid synthesis exceeds degradation since circulating levels increase in the course of DIO. Synthesis enzymes of 2-AG in liver and skeletal muscle were only transiently increased, and the synthesis enzyme of AEA was decreased in skeletal muscle. Thus, although we cannot exclude the contribution of other organs as source for plasma endocannabinoid levels (e.g., brain and intestine), our data suggest that WAT and BAT are likely important organs that release 2-AG and AEA levels in HFD-induced obesity.

It is interesting to speculate on the cellular source within the adipose tissue depots that is involved in endocannabinoid synthesis. HFD-induced development of DIO causes accumulation of macrophages in WAT (van Beek et al., 2015) as well as BAT (Van den Berg S. M., unpublished). Macrophages are able to produce AEA (Di Marzo et al., 1996), and we found a positive correlation between macrophage marker *Cd68* and *Nape-pld* expression in BAT as well as with AEA levels in plasma. However, the concentration of macrophages in adipose tissue is relatively low, even in obesity, and stronger positive correlations were found between the lipid content in BAT and both *Nape-pld* expression and plasma AEA levels. Therefore, adipocytes likely contribute substantially more to the circulating endocannabinoid pool than macrophages. This hypothesis is corroborated by previous findings that AEA co-localizes with adiposomes or lipid droplets *in vitro* (Oddi et al., 2008) and that specific deletion of NAPE-PLD in adipocytes of mice decreased levels of PEA, OEA and SEA in WAT, despite increased inflammation and influx of macrophages (Geurts et al., 2015). In our study, HFD feeding increases the cellular mRNA levels of the synthesizing enzymes in adipose tissue. In addition, expansion of the total number of adipocytes in the time course of DIO further increases whole body expression of these enzymes. The rapid increases in gene expression in BAT may be explained by the rapid whitening of BAT as induced by HFD feeding (Shimizu et al., 2014). Indeed, BAT lipid droplet content positively correlated with *Nape-pld* expression and AEA plasma levels. Furthermore, these data are in line with the recent observation that acute activation of BAT decreases *Nape-pld* expression (Krott et al., 2016). Interestingly, the concentration

of 2-AG and AEA is higher in BAT than WAT (Krott et al., 2016), suggesting at least a role of BAT in determining circulating endocannabinoid levels. Collectively, it is likely that lipid-filled adipocytes rather than macrophages within the adipose tissues contribute to circulating plasma endocannabinoid levels.

In our study, we found no evidence for a contribution of decreased degradation pathways of 2-AG and AEA in adipose tissues determining plasma levels of endocannabinoids. Specifically, we were unable to detect any expression of AEA degradation enzyme *Faah* in WAT, BAT and muscle, and found decreased liver *Faah* expression after 18 weeks of HFD feeding. This is in line with the fact that FAAH was reported to play an important role in obesity. Notably, a missense polymorphism in the FAAH gene is associated with obesity in humans (Sipe et al., 2005) and FAAH deficient mice have increased AEA levels in, e.g., the liver and show increased fat mass and body weight (Tourino et al., 2010). On the other hand, Bartelt et al. (2011) found that HFD feeding for 16 weeks in mice caused a decrease in *Faah* expression and FAAH enzymatic activity in WAT which was accompanied by increased AEA in this tissue. To what extent catabolism of AEA and 2-AG by adipose tissue determines circulating levels of these endocannabinoids warrants further study.

It is tempting to speculate on the biological role of the increases of 2-AG and AEA in the time course of HFD-induced obesity. Endocannabinoids are known to decrease insulin sensitivity (Gruden et al., 2016) and to reduce sympathetic responses by inhibiting noradrenergic signaling (Quarta et al., 2011; Krott et al., 2016), and thereby decrease lipolysis in WAT and thermogenesis in BAT. Possibly, in case of acute lipid overload, as mimicked by a switch from regular chow to a HFD, initial accumulation of lipids in WAT and BAT drives the synthesis pathways of endocannabinoids that can have autocrine and even paracrine effects on these organs to inhibit sympathetic signaling. This sequence of events reduces intracellular lipolysis in BAT and WAT, thereby resulting in reduced thermogenesis in BAT and increased triglyceride storage in WAT. Such as a feed-forward mechanism may thus allow the body to store excess lipids effectively in adipose tissues. Interestingly, we have shown that inhibition of endocannabinoid signaling by strictly peripheral CB1R antagonism activates BAT and reduces adiposity in HFD-fed mice (Boon et al., 2014). In theory, HFD induced lipid accumulation can lead to increased endocannabinoid synthesis which attenuates BAT and WAT activity and results in a positive energy balance.

## CONCLUSION

The time course of HFD-induced obesity plasma endocannabinoid levels rapidly rise as most probably explained by increased synthesis pathways in adipose tissue depots. We speculate that this sequence of events may attenuate sympathetic signaling in these tissues by CB1R agonism, which would result

in reduced thermogenesis and increased storage of excess lipids in WAT. Given the fact that strictly peripheral CB1R antagonism activates BAT and reduces adiposity in mice, we anticipate that strategies inhibiting CB1R selectively on (brown) adipocytes or reducing endocannabinoid synthesis by adipocytes may be a worthwhile strategy to pursue in combating obesity and associated disorders.

## AUTHOR CONTRIBUTIONS

EK and VK performed the experiments, analyzed the data, wrote the manuscript, and contributed to the discussion. VK developed and validated the UPLC-MS/MS method to quantify endocannabinoids, NAEs and AA in murine plasma. BM and RvE analyzed the data, contributed to the discussion, and reviewed/edited the manuscript. SvdB designed the study, performed the *in vivo* experiment and kindly provided the samples for analysis, and reviewed and edited the manuscript. MdW and EL designed the study and reviewed and edited the manuscript. KN, SK, AH, and TH contributed to the discussion and reviewed and edited the manuscript. AR-M and TC reviewed and edited the manuscript. MvdS, PR, and MB designed and supervised the project, contributed to the discussion and reviewed and edited the manuscript.

## FUNDING

This project received support from the Faculty of Science ("Profiling programme: Endocannabinoids"), Leiden University (VK, MvdS, and TH). PR was an Established Investigator of the Dutch Heart Foundation (Grant 2009T038), and was supported a Lilly Research Award Program (LRAP) Award. MB was supported by a research grant from the Rembrandt Institute of Cardiovascular Science and by a grant from the Dutch Diabetes Foundation (2015.81.1808). Furthermore, we acknowledge the support from the Netherlands Cardiovascular Research Initiative: an initiative with support of the Dutch Heart Foundation (CVON2014-02 ENERGISE).

## ACKNOWLEDGMENTS

The authors thank T. C. M. Streefland (Department of Medicine, Division of Endocrinology, LUMC, Leiden), A. C. M. van Esbroeck-Weevers and E. D. Mock (Department of Molecular Physiology, Leiden Institute of Chemistry, Leiden) for their valuable technical support.

## SUPPLEMENTARY MATERIAL

The Supplementary Material for this article can be found online at: <https://www.frontiersin.org/articles/10.3389/fphys.2018.01913/full#supplementary-material>



## REFERENCES

- Arrabal, S., Lucena, M. A., Canduela, M. J., Ramos-Urriarte, A., Rivera, P., Serrano, A., et al. (2015). Pharmacological blockade of cannabinoid CB1 receptors in diet-induced obesity regulates mitochondrial dihydrolipoamide dehydrogenase in muscle. *PLoS One* 10:e0145244. doi: 10.1371/journal.pone.0145244
- Baggelaar, M. P., Maccarrone, M., and van der Stelt, M. (2018). 2-Arachidonoylglycerol: a signaling lipid with manifold actions in the brain. *Prog. Lipid Res.* 71, 1–17. doi: 10.1016/j.plipres.2018.05.002
- Bartelt, A., Orlando, P., Mele, C., Ligresti, A., Toedter, K., Scheja, L., et al. (2011). Altered endocannabinoid signaling after a high-fat diet in Apoe(-/-) mice: relevance to adipose tissue inflammation, hepatic steatosis and insulin resistance. *Diabetologia* 54, 2900–2910. doi: 10.1007/s00125-011-2274-6
- Bisogno, T., and Maccarrone, M. (2014). Endocannabinoid signaling and its regulation by nutrients. *Biofactors* 40, 373–380. doi: 10.1002/biof.1167
- Blüher, M., Engeli, S., Kloting, N., Berndt, J., Fasshauer, M., Batkai, S., et al. (2006). Dysregulation of the peripheral and adipose tissue endocannabinoid system in human abdominal obesity. *Diabetes Metab. Res. Rev.* 55, 3053–3060. doi: 10.2337/db06-0812
- Boon, M. R., Kooijman, S., van Dam, A. D., Pelgrom, L. R., Berbee, J. F., Visseren, C. A., et al. (2014). Peripheral cannabinoid 1 receptor blockade activates brown adipose tissue and diminishes dyslipidemia and obesity. *FASEB J.* 28, 5361–5375. doi: 10.1096/fj.13-247643
- Bowles, N. P., Karatsoreos, I. N., Li, X., Vemuri, V. K., Wood, J. A., Li, Z., et al. (2015). A peripheral endocannabinoid mechanism contributes to glucocorticoid-mediated metabolic syndrome. *Proc. Natl. Acad. Sci. U.S.A.* 112, 285–290. doi: 10.1073/pnas.1421420112
- Cota, D. (2007). CB1 receptors: emerging evidence for central and peripheral mechanisms that regulate energy balance, metabolism, and cardiovascular health. *Diabetes Metab. Res. Rev.* 23, 507–517. doi: 10.1002/dmrr.764
- Cote, M., Matias, I., Lemieux, I., Petrosino, S., Almeras, N., Despres, J. P., et al. (2007). Circulating endocannabinoid levels, abdominal adiposity and related cardiometabolic risk factors in obese men. *Int. J. Obes.* 31, 692–699. doi: 10.1038/sj.ijo.0803539
- D'Eon, T. M., Pierce, K. A., Roix, J. J., Tyler, A., Chen, H., and Teixeira, S. R. (2008). The role of adipocyte insulin resistance in the pathogenesis of obesity-related elevations in endocannabinoids. *Diabetes Metab. Res. Rev.* 57, 1262–1268. doi: 10.2337/db07-1186
- Despres, J. P., Golay, A., and Sjostrom, L. (2005). Effects of rimonabant on metabolic risk factors in overweight patients with dyslipidemia. *N. Engl. J. Med.* 353, 2121–2134. doi: 10.1056/NEJMoa044537
- Di Marzo, V., De Petrocellis, L., Sepe, N., and Buono, A. (1996). Biosynthesis of anandamide and related acylethanolamides in mouse J774 macrophages and N18 neuroblastoma cells. *Biochem. J.* 316(Pt 3), 977–984.
- Engeli, S., Bohnke, J., Feldpausch, M., Gorzelniak, K., Janke, J., Batkai, S., et al. (2005). Activation of the peripheral endocannabinoid system in human obesity. *Diabetes Metab. Res. Rev.* 54, 2838–2843.
- Fezza, F., Bari, M., Florio, R., Talamonti, E., Feole, M., and Maccarrone, M. (2014). Endocannabinoids, related compounds and their metabolic routes. *Molecules* 19, 17078–17106. doi: 10.3390/molecules19117078
- Foltin, R. W., Fischman, M. W., and Byrne, M. F. (1988). Effects of smoked marijuana on food intake and body weight of humans living in a residential laboratory. *Appetite* 11, 1–14.
- Geurts, L., Everard, A., Van Hul, M., Essaghir, A., Duparc, T., Matamoros, S., et al. (2015). Adipose tissue NAPE-PLD controls fat mass development by altering the browning process and gut microbiota. *Nat. Commun.* 6:6495. doi: 10.1038/ncomms7495
- Gruden, G., Barutta, F., Kunos, G., and Pacher, P. (2016). Role of the endocannabinoid system in diabetes and diabetic complications. *Br. J. Pharmacol.* 173, 1116–1127. doi: 10.1111/bph.13226
- Hillard, C. J. (2018). Circulating endocannabinoids: from whence do they come and where are they going? *Neuropsychopharmacology* 43, 155–172. doi: 10.1038/npp.2017.130
- Howlett, A. C., Barth, F., Bonner, T. I., Cabral, G., Casellas, P., Devane, W. A., et al. (2002). International Union of Pharmacology. XXVII. Classification of cannabinoid receptors. *Pharmacol. Rev.* 54, 161–202.
- Hussain, Z., Uyama, T., Tsuboi, K., and Ueda, N. (2017). Mammalian enzymes responsible for the biosynthesis of N-acyl ethanolamines. *Biochim. Biophys. Acta Mol. Cell Biol. Lipids* 1862, 1546–1561. doi: 10.1016/j.bbalip.2017.08.006
- Jamshidi, N., and Taylor, D. A. (2001). Anandamide administration into the ventromedial hypothalamus stimulates appetite in rats. *Br. J. Pharmacol.* 134, 1151–1154. doi: 10.1038/sj.bjp.0704379
- Kantae, V., Nahon, K. J., Straat, M. E., Bakker, L. E. H., Harms, A. C., van der Stelt, M., et al. (2017). Endocannabinoid tone is higher in healthy lean South Asian than white Caucasian men. *Sci. Rep.* 7:7558. doi: 10.1038/s41598-017-07980-5
- Krott, L. M., Piscitelli, F., Heine, M., Borrino, S., Scheja, L., Silvestri, C., et al. (2016). Endocannabinoid regulation in white and brown adipose tissue following thermogenic activation. *J. Lipid Res.* 57, 464–473. doi: 10.1194/jlr.M065227
- Matias, I., Petrosino, S., Racioppi, A., Capasso, R., Izzo, A. A., and Di Marzo, V. (2008). Dysregulation of peripheral endocannabinoid levels in hyperglycemia and obesity: effect of high fat diets. *Mol. Cell. Endocrinol.* 286, S66–S78. doi: 10.1016/j.mce.2008.01.026
- Mazier, W., Saucisse, N., Gatta-Cherifi, B., and Cota, D. (2015). The Endocannabinoid system: pivotal orchestrator of obesity and metabolic disease. *Trends Endocrinol. Metab.* 26, 524–537. doi: 10.1016/j.tem.2015.07.007
- Muccioli, G. G. (2010). Endocannabinoid biosynthesis and inactivation, from simple to complex. *Drug Discov. Today* 15, 474–483. doi: 10.1016/j.drudis.2010.03.007
- Oddi, S., Fezza, F., Pasquariello, N., De Simone, C., Rapino, C., Dainese, E., et al. (2008). Evidence for the intracellular accumulation of anandamide in adiposomes. *Cell. Mol. Life Sci.* 65, 840–850. doi: 10.1007/s00018-008-7494-7
- O'Keefe, L., Simcocks, A. C., Hryciw, D. H., Mathai, M. L., and McAinch, A. J. (2014). The cannabinoid receptor 1 and its role in influencing peripheral metabolism. *Diabetes Obes. Metab.* 16, 294–304. doi: 10.1111/dom.12144
- Osei-Hyiaman, D., DePetrillo, M., Pacher, P., Liu, J., Radaeva, S., Batkai, S., et al. (2005). Endocannabinoid activation at hepatic CB1 receptors stimulates fatty acid synthesis and contributes to diet-induced obesity. *J. Clin. Invest.* 115, 1298–1305. doi: 10.1172/jci23057
- Pati, S., Krishna, S., Lee, J. H., Ross, M. K., de La Serre, C. B., Harn, D. A. Jr., et al. (2018). Effects of high-fat diet and age on the blood lipidome and circulating endocannabinoids of female C57BL/6 mice. *Biochim. Biophys. Acta* 1863, 26–39. doi: 10.1016/j.bbalip.2017.09.011
- Piomelli, D. (2003). The molecular logic of endocannabinoid signalling. *Nat. Rev. Neurosci.* 4, 873–884. doi: 10.1038/nrn1247
- Pi-Sunyer, F. X., Aronne, L. J., Heshmati, H. M., Devin, J., and Rosenstock, J. (2006). Effect of rimonabant, a cannabinoid-1 receptor blocker, on weight and cardiometabolic risk factors in overweight or obese patients: RIO-North America: a randomized controlled trial. *JAMA* 295, 761–775. doi: 10.1001/jama.295.7.761
- Quarta, C., Mazza, R., Obici, S., Pasquali, R., and Pagotto, U. (2011). Energy balance regulation by endocannabinoids at central and peripheral levels. *Trends Mol. Med.* 17, 518–526. doi: 10.1016/j.molmed.2011.05.002
- Ravinet Trillou, C., Arnone, M., Delgorge, C., Gonalons, N., Keane, P., Maffrand, J. P., et al. (2003). Anti-obesity effect of SR141716, a CB1 receptor antagonist, in diet-induced obese mice. *Am. J. Physiol. Regul. Integr. Comp. Physiol.* 284, R345–R353. doi: 10.1152/ajpregu.00545.2002
- Sam, A. H., Salem, V., and Ghatei, M. A. (2011). Rimobant: from RIO to Ban. *J. Obes.* 2011:432607. doi: 10.1155/2011/432607
- Shimizu, I., Aprahamian, T., Kikuchi, R., Shimizu, A., Papanicolaou, K. N., MacLauchlan, S., et al. (2014). Vascular rarefaction mediates whitening of brown fat in obesity. *J. Clin. Invest.* 124, 2099–2112. doi: 10.1172/JCI71643
- Simon, V., and Cota, D. (2017). MECHANISMS IN ENDOCRINOLOGY: endocannabinoids and metabolism: past, present and future. *Eur. J. Endocrinol.* 176, R309–R324. doi: 10.1530/eje-16-1044
- Sipe, J. C., Waalen, J., Gerber, A., and Beutler, E. (2005). Overweight and obesity associated with a missense polymorphism in fatty acid amide hydrolase (FAAH). *Int. J. Obes.* 29, 755–759. doi: 10.1038/sj.ijo.0802954

- Tchernof, A., and Despres, J. P. (2013). Pathophysiology of human visceral obesity: an update. *Physiol. Rev.* 93, 359–404. doi: 10.1152/physrev.00033.2011
- Tourino, C., Oveisi, F., Lockney, J., Piomelli, D., and Maldonado, R. (2010). FAAH deficiency promotes energy storage and enhances the motivation for food. *Int. J. Obes.* 34, 557–568. doi: 10.1038/ijo.2009.262
- van Beek, L., van Klinken, J. B., Pronk, A. C., van Dam, A. D., Dirven, E., Rensen, P. C., et al. (2015). The limited storage capacity of gonadal adipose tissue directs the development of metabolic disorders in male C57Bl/6J mice. *Diabetologia* 58, 1601–1609. doi: 10.1007/s00125-015-3594-8
- van den Berg, S. M., Seijkens, T. T., Kusters, P. J., Beckers, L., den Toom, M., Smeets, E., et al. (2016). Diet-induced obesity in mice diminishes hematopoietic stem and progenitor cells in the bone marrow. *FASEB J.* 30, 1779–1788. doi: 10.1096/fj.201500175

**Conflict of Interest Statement:** AR-M and TC are employees of Lilly.

The remaining authors declare that the research was conducted in the absence of any commercial or financial relationships that could be construed as a potential conflict of interest.

Copyright © 2019 Kuipers, Kantae, Maarse, van den Berg, van Eenige, Nahon, Reifel-Miller, Coskun, de Winther, Lutgens, Kooijman, Harms, Hankemeier, van der Stelt, Rensen and Boon. This is an open-access article distributed under the terms of the Creative Commons Attribution License (CC BY). The use, distribution or reproduction in other forums is permitted, provided the original author(s) and the copyright owner(s) are credited and that the original publication in this journal is cited, in accordance with accepted academic practice. No use, distribution or reproduction is permitted which does not comply with these terms.



# Regulation of Adaptive Thermogenesis and Browning by Prebiotics and Postbiotics

Bàrbara Reynés<sup>1,2,3</sup>, Mariona Palou<sup>1,3</sup>, Ana M. Rodríguez<sup>1,2,3\*</sup> and Andreu Palou<sup>1,2,3</sup>

<sup>1</sup> CIBER Fisiopatología de la Obesidad y Nutrición (CIBERObn), Madrid, Spain, <sup>2</sup> Institut d'Investigació Sanitària Illes Balears (IdISBa), Palma de Mallorca, Spain, <sup>3</sup> Laboratory of Molecular Biology, Nutrition and Biotechnology, University of the Balearic Islands, Palma de Mallorca, Spain

## OPEN ACCESS

### Edited by:

Rita De Matteis,  
Università degli Studi di Urbino Carlo  
Bo, Italy

### Reviewed by:

Denis Richard,  
Laval University, Canada  
Vicente Lahera,  
Complutense University of Madrid,  
Spain

### \*Correspondence:

Ana M. Rodríguez  
amrodriguez@uib.es

### Specialty section:

This article was submitted to  
Integrative Physiology,  
a section of the journal  
Frontiers in Physiology

**Received:** 09 November 2018

**Accepted:** 18 December 2018

**Published:** 10 January 2019

### Citation:

Reynés B, Palou M, Rodríguez AM  
and Palou A (2019) Regulation of  
Adaptive Thermogenesis and  
Browning by Prebiotics and  
Postbiotics. *Front. Physiol.* 9:1908.  
doi: 10.3389/fphys.2018.01908

Prebiotics are non-digestible food components able to modify host microbiota toward a healthy profile, concomitantly conferring general beneficial health effects. Numerous research works have provided wide evidence regarding the effects of prebiotics on the protection against different detrimental phenotypes related to cancer, immunity, and features of the metabolic syndrome, among others. Nonetheless, one topic less studied so far, but relevant, relates to the connection between prebiotics and energy metabolism regulation (and the prevention or treatment of obesity), especially by means of their impact on adaptive (non-shivering) thermogenesis in brown adipose tissue (BAT) and in the browning of white adipose tissue (WAT). In the present review, a key link between prebiotics and the regulation of adaptive thermogenesis and lipid metabolism (in both BAT and WAT) is proposed, thus connecting prebiotic consumption, microbiota selection (especially gut microbiota), production of microbiota metabolites, and the regulation of energy metabolism in adipose tissue, particularly regarding the effects on browning promotion, or on BAT recruitment. In this sense, various types of prebiotics, from complex carbohydrates to phenolic compounds, have been studied regarding their microbiota-modulating role and their effects on crucial tissues for energy metabolism, including adipose tissue. Other studies have analyzed the effects of the main metabolites produced by selected microbiota on the improvement of metabolism, such as short chain fatty acids and secondary bile acids. Here, we focus on state-of-the-art evidence to demonstrate that different prebiotics can have an impact on energy metabolism and the prevention or treatment of obesity (and its associated disorders) by inducing or regulating adaptive thermogenic capacity in WAT and/or BAT, through modulation of microbiota and their derived metabolites.

**Keywords:** beige adipocytes, brite adipocytes, brown adipose tissue, microbiota, obesity, prebiotics, postbiotics, UCP1

## INTRODUCTION

Obesity is one of the major health problems throughout the world (Bray et al., 2017). Current obesity treatment strategies, mainly based on food intake control, seem not to be enough to address this multifactorial disorder of pandemic prevalence. In this sense, studies to counteract obesity development based on energy expenditure are recently booming (Marlatt and Ravussin, 2017). In rodents, browning of white adipose tissue (WAT), and especially adaptive thermogenesis

of brown adipose tissue (BAT), are relevant contributors to energy expenditure, being critical for energy balance and body weight maintenance. Uncoupling Protein 1 (UCP1) is the main effector of adaptive (non-shivering) thermogenesis in brown adipocytes, by uncoupling oxidative phosphorylation (Palou et al., 1998; Rodriguez and Palou, 2004). Although UCP1 is mainly expressed in BAT, browning is defined as “any significantly increased UCP1 expression at the mRNA level occurring in what are normally considered as WAT depots” (Nedergaard and Cannon, 2014). In the literature, cells expressing UCP1 in WAT can be referred to as beige or brite (brown-in-white), among other denominations (Nedergaard and Cannon, 2014). In contrast to rodents, adult humans do not exhibit well-defined BAT. However, the presence of discrete areas of active BAT—mainly in the cervical, supraclavicular, axillary, and paravertebral regions, activated in response to certain adrenergic stimuli—has been described in adult humans (Nedergaard et al., 2007). It must be noted that, unlike BAT thermogenesis, the role of beige WAT significantly influencing energy metabolism has been questioned, at least in response to chronic cold and adrenergic agonist treatment, even in the absence of functional interscapular BAT (Labbe et al., 2016, 2018). Nevertheless, although the real relevance of WAT browning to treat metabolic disorders in humans is still unclear (Bartelt and Heeren, 2014), all these findings have opened a new window to study novel treatment strategies of obesity based on enhancing energy expenditure capacity by induction of BAT recruitment and browning of WAT. Cold exposure is the main physiological thermogenic activator, although other physiological situations such as overfeeding can also physiologically activate adaptive thermogenesis (diet-induced thermogenesis) (Rothwell and Stock, 1979; Landsberg et al., 1984). In this sense, the role of the sympathetic nervous system (SNS) is crucial; SNS activation by cold exposure, as well as other thermogenic inductors which promote the release of norepinephrine, stimulates the expression and function of UCP1 in BAT and browning in WAT (Landsberg et al., 1984; Palou et al., 1998; Wu et al., 2012).

Although numerous stimuli, bioactive compounds, and physiological situations have been studied regarding the activation of adaptive thermogenesis, here we will focus on a less explored field, concerning the possible role of prebiotics and microbiota in thermogenic capacity modulation. Microbiota has emerged over the last few years as a key factor modulating different aspects of host health (Villanueva-Millan et al., 2015), and these aspects seem to include adaptive thermogenesis regulation. For instance, a study in mice showed that depletion of gut microbiota of genetically or diet induced obese mice increases browning induction in WAT (Suárez-Zamorano et al., 2015). Moreover, the main physiological activator of adaptive thermogenesis commented above, i.e., cold exposure, has been shown to induce adaptations in gut microbiota profile, which have been related to thermogenic and browning activation. Further, microbiota transplantation of cold exposed mice to germ free mice enhances cold tolerance, related to beige/brown fat formation in WAT (both inguinal and perigonadal) and, to a lesser extent, to BAT recruitment

(Chevalier et al., 2015), as we will discuss more extensively below.

Therefore, the relationship between the host microbiota and BAT thermogenesis or WAT browning becomes a focus of interest, even more so when taking into account the fact that the microbiota is physiologically and nutritionally mouldable. One effective physiological way to modulate microbiota, especially gut microbiota, is by the use of pro and prebiotics, especially prebiotics, which can potentially affect to large number of gut microbial species. A prebiotic is defined, at present, as “a substrate that is selectively utilized by host microorganisms conferring a health benefit,” and this modern definition is broad enough to expand the concept from classical carbohydrate molecules to non-carbohydrate compounds, as well as to different applications and sites of action beyond the gastrointestinal tract (Gibson et al., 2017). Sometimes the prebiotic concept has been confused, due to partial overlap in the type of molecules involved, with the concept of “dietary fiber.” Nevertheless, there are significant functional, health-related and structural differences. Dietary fiber has been defined as “non-digestible carbohydrates and lignin that are intrinsic and intact in plants” with “functional fiber” defined as “isolated, non-digestible carbohydrates that have beneficial physiological effects in humans” (Slavin, 2013). Therefore, the definition of fiber is vague in terms of functional/physiological effects and does not include other bioactive compounds distinct to carbohydrates and lignin. The prebiotic concept goes far beyond the fiber concept to include non-carbohydrate substances, applications in different body sites, and compounds from other categories apart from food (Gibson et al., 2017). Importantly, the prebiotic definition includes the requirement of microbiota involvement and selective mechanisms mediated by microbiota, also considering that the health beneficial effects must be documented in order to classify a substance as prebiotic (Gibson et al., 2017). Different mechanisms have emerged to explain the relationship of gut microbiota with health, and these include the modulation of metabolic endotoxemia (referring to lipopolysaccharide—LPS—circulating levels, related to inflammation), gut-endocrine barrier, gut hormones, and peripheral tissue metabolism, among others (Cani and Delzenne, 2010; Geurts et al., 2014; Cani and Everard, 2016). Among the mechanisms involved, the metabolic effects of the products released by the microbiota after their processing, i.e., postbiotics, are gaining a lot of interest and are the focus of specific research. Postbiotics can be defined as “those molecules released by bacteria and other microorganisms that when administered in adequate amount confer health benefits to the host” (Maguire and Maguire, 2018). For instance, short chain fatty acids (SCFA) and different bile acid species are postbiotics that have gained an important focus of attention, as will be discussed below.

Taking into consideration all these antecedents, this review explores the potential link between prebiotics and the regulation of thermogenic capacity and browning, through the modulation of microbiota and postbiotics, as a tool to prevent or combat obesity and its related metabolic disorders. We propose that there is an important impact of microbiota modulation by prebiotics on the regulation of adaptive thermogenic capacity; and that



the management of host microbiota by prebiotics might have a prominent role in the thermogenic process, with therapeutic potential.

## MICROBIOTA, EUBIOSIS, AND DYSBIOSIS

The microbiota is a complex ecosystem of microorganisms, including bacteria, viruses, protozoa and fungi, which live in the human body; about 70% of the microbiota is found in the gastrointestinal tract, where 100 trillion microorganisms coexist, which amounts to more than 10 times the total human cells (Pascale et al., 2018). The most important bacteria populations are in the colon, where a certain symbiosis with the host exists, key for health maintenance (Pascale et al., 2018). Most of the gut microbiota is composed of bacteria, with some predominant phyla such as *Firmicutes*, *Bacteroidetes*, *Actinobacteria*, *Verrucomicrobia*, and *Proteobacteria*, and *Methanobacteriales* of the phylum *Euryarchaeota* (Diamant et al., 2011; Chakraborti, 2015). Notably, gut microbiota could be used as a microbiological “fingerprint” since, at the taxonomic level, it exhibits important differences between individuals. In this sense, host genotype, environment and diet influence gut microbiota, responsible for these individual differences (Iebba et al., 2016).

A correct symbiosis between the intestinal microbiota and the host is required for the right production of substances and metabolites necessary for host health maintenance (Boulangé et al., 2016). This correct symbiosis, and the qualitative and quantitative equilibrium between the different species present in the gut microbiota is defined as eubiosis (Iebba et al., 2016), also known as normobiosis, and is key for well-being and health (Petschow et al., 2013). On the other hand, dysbiosis is the term that defines an ecosystem where the microbiota species do not live in harmony, which negatively affects host health; it is usually associated to reduced microbial diversity and the predominance of harmful species, creating a disease-prone situation (Petschow et al., 2013; Zhang et al., 2015).

## MICROBIOTA AND OBESITY, AND ITS METABOLIC DISORDERS

As suggested above, a healthy gut microbiota profile contributes to improve host metabolism, through dynamic changes in metabolites, nutrients, and vitamins, and to maintain energy homeostasis (Althani et al., 2016). Meanwhile, alterations in the microbiota profile have been related to the development of some diseases, including obesity and the metabolic disorders that accompany it. In this sense, obese people have been described to present significant differences in the composition of gut microbiota compared to lean people and, concretely, bacteria from the phylum *Bacteroidetes* decrease, whereas bacteria from the phylum *Firmicutes*, such as *Bacillaceae* and *Clostridiaceae*, increase in the obese state, especially related to prolonged exposure to a high-fat (HF) diet (Pascale et al., 2018). The detrimental change in microbiota composition may result in an augmented energy production from undigested materials, leading to a dysregulation in energy homeostasis (Pascale et al.,

2018). Moreover, it is also related to other numerous metabolic disturbances, associated with and/or contributing to obesity, such as changes in lipogenesis, triglyceride storage, hepatic steatosis, insulin sensitivity, control of food intake, etc., and the promotion of meta-inflammation (or low grade inflammation) (Cani and Delzenne, 2009). Thus, beyond microbiota involvement in energy utilization from diet, the microbiota seems to play a very relevant role in energy homeostasis, metabolism, and obesity development, thus explaining the increasing interest in analyzing the “obesity-microbiota” link in the last few years (Davis, 2016). Interestingly, differences in intestinal microbiota may even precede overweight development, a conclusion reached for the first time by Kalliomäki et al. (2008). They compared children who remained normal weight with children developing overweight/obesity at the age of 7 years, reporting that the genus *Bifidobacterium* was higher in number at an early age (6–12 months) (when no BMI differences were yet evident) in the posterior normal weight group compared to the overweight group (Kalliomäki et al., 2008). In addition, fecal numbers of *S. aureus* were lower in children remaining normal weight than in children developing overweight (Kalliomäki et al., 2008). These findings strongly reinforce the importance of microbiota in body weight control. In the same line, germ free C57BL/6J male mice fed a HF/high-sucrose diet are protected against diet-induced obesity in contrast to mice with normal gut microbiota (Bäckhed et al., 2007). This resistance to overweight in germ free mice was related to an increase, in liver and skeletal muscle, in the activity of AMP activated protein kinase (AMPK) and key downstream targets (related to the oxidation of fatty acids), together with the induction of the transcriptional co-activator peroxisome proliferator activated receptor gamma co-activator 1 $\alpha$  (PGC1 $\alpha$ ) (another key molecular regulator of energy metabolism) (Bäckhed et al., 2007). Therefore, these findings also support the idea of a marked role of microbiota in energy balance, and provide a clue for the key molecular mechanisms involved.

Bearing in mind this connection between gut microbiota and health, it is clear that prebiotic agents, or other types of gut microbiota modulators, might be considered as agents able to prevent or improve gut dysbiosis and obesity-related metabolic disorders. For instance, *Ganoderma lucidum*, a traditional anti-diabetic medical mushroom, reduces dysbiosis in diet-induced obese mice, related to the decrease in the *Firmicutes/Bacteroidetes* ratio and endotoxin (LPS) levels (Chang et al., 2015). These results were associated with decreased body weight, reduced inflammation, and improved insulin sensitivity in these animals (Chang et al., 2015). Interestingly, the beneficial effects of this prebiotic are transmissible to other diet-induced obese mice through feces transplantation. This suggests that the replacement of a microbial population by a new one, associated with the amelioration of dysbiosis, might confer beneficial health effects to the host (Chang et al., 2015). Recent results with transgenic mice with constitutive production of  $\omega$ 3 polyunsaturated fatty acids (PUFA) also point to the same idea. In this model, the microbiota modulation by  $\omega$ 3 PUFA improves the metabolic profile of high fat (HF) diet fed mice which are protected against obesity, also maintaining a normal gut barrier function and with reduced metabolic endotoxemia (Bidu et al., 2018).

Microbiota (fecal) transplantation from the transgenic animals to metabolically altered (by an obesogenic diet) wild type animals is able to improve metabolic profile of the latter and reverse weight gain (Bidu et al., 2018); therefore, these results also suggest an important relationship between gut microbiota and protection against obesity and the related altered metabolism.

## IMPACT OF GUT MICROBIOTA ON BAT THERMOGENESIS AND WAT BROWNING

Different aspects could be important to explain the relationship between gut microbiota and protection against obesity and its metabolic disorders, but when considering the main elements involved in overweight development, one outstanding factor is energy expenditure, where adaptive thermogenesis can play a crucial role. Different research works show an association between modulation of gut microbiota and thermogenic capacity in both BAT and WAT (browning). As far as we know, a link between gut microbiota and BAT metabolism was first shown by Mestdagh et al. (2012). Particularly when comparing conventional and germ-free mice, the authors showed that the absence of gut microbiota activates BAT and hepatic lipid catabolism and inhibits lipogenesis (Mestdagh et al., 2012). Following these lines, other authors have revealed relevant effects of microbiota on BAT thermogenesis and WAT browning, through cold microbiota transplantation experiments. Specifically, Chevalier et al. (2015) showed that cold exposure induces several changes in the microbiota composition and that cold microbiota transplantation (from 6°C exposed C57Bl/6 male mice, for 25 days) to germ free mice induces the expression of the gene coding for UCP1 in BAT, together with increased resting energy expenditure. Likewise, they also revealed that this microbiota transplantation induces browning (with the appearance of UCP1 positive adipocytes) in the inguinal and perigonadal WAT depots. Further supporting the browning phenotype, the expression of some brown/brite markers (*Ucp1*, *Cidea*, and *Ppargc1a*) (the genes coding for UCP1, cell death-inducing DFFA-Like effector A –CIDEA– and PGC1 $\alpha$ ) was also induced (Chevalier et al., 2015). Therefore, these studies suggest that cold microbiota transplantation induces browning in WAT and, to a lesser extent, BAT recruitment, possibly related to increased energy dissipation (Chevalier et al., 2015). Similarly, Zietak et al. showed a marked change in microbiota composition in mice exposed to 12°C for 4 weeks, characterized by the increase and decrease in bacterial genera associated to leanness and obesity, respectively, accompanied by an increase in *Ucp1* expression in BAT and WAT (Zietak et al., 2016). Moreover, they also demonstrated that fecal transplantation from cold exposed mice to germ free mice protected the latter from HF-associated disturbances after 6 weeks, increasing protein expression of UCP1 in BAT, reducing body adiposity increase, and improving insulin sensitivity, when compared to germ free mice transplanted with microbiota from 29°C exposed mice. In this case, in the germ free cold microbiota transplanted mice, no *Ucp1* gene expression in inguinal WAT was observed compared to the mice recipient from 29°C

microbiota, and the brown phenotype in inguinal WAT was considered minor compared to the marked interscapular BAT thermogenic phenotype observed (Zietak et al., 2016). This was unlike the study of Chevalier et al. discussed above, where browning was considered very relevant (Chevalier et al., 2015). Another interesting question raised by the study of Zietak et al. was the possible role of the modulation of bile acid metabolism by gut microbiota (Zietak et al., 2016), thus connecting with postbiotics (bile acids can act as metabolic regulators derived from microbiota, as will be discussed below). Moreover, Zietak et al. (2017) have pointed out that the functional link between cold and gut microbiota leading to BAT increased thermogenesis is not elucidated yet. As we have previously explained, SNS is crucial for the regulation of thermogenic capacity under cold, diet and other thermogenic inductors (Landsberg et al., 1984; Palou et al., 1998; Wu et al., 2012). Nonetheless, thermogenic capacity (by BAT recruitment or WAT browning) induced by pre- or post-biotics has not necessary been linked to SNS stimulation and adrenergic signaling. In some cases (as we will see for some specific examples below), this link has been suggested, at least as part of the possible mechanistic explanation, but in other cases important evidence supports mechanisms acting by alternative pathways independent of adrenergic signaling (e.g., microbiota derived bile acids) (Zietak et al., 2017). Another condition that correlates changes in gut microbiota with WAT browning, and ameliorates insulin resistance, hepatic steatosis and obesity, is intermittent fasting (in mice), also related to the production of specific postbiotics (acetate and lactate in this case) (Li et al., 2017).

In a model of mice resistant to diet-induced obesity due to enhanced energy expenditure and BAT activity, such as is the  $\beta$ -Klotho KO mouse model, the relationship between microbiota and thermogenic capacity is also suggested. In this model, the usual alteration in gut microbiota profile induced by HF diet feeding is reduced, since  $\beta$ -Klotho KO mice fed a HF diet show a *Bacteroidetes/Firmicutes* ratio similar to wild-type mice fed a chow diet (Somm et al., 2017). The results reported in this work suggest that changes in secondary bile acid production are related to host thermogenesis stimulation (Somm et al., 2017), thus pointing again toward the involvement of bile acids metabolized by bacteria in the thermogenic phenotype, as will be discussed further in the section on postbiotics.

Based on the evidence given so far, it is difficult to establish how much of the energy expenditure increase observed in different models of pre and/or postbiotic supplementation can be attributed specifically to increased adaptive thermogenesis. Nevertheless, all in all, the relationship between gut microbiota and thermogenic capacity (both by BAT recruitment or WAT browning) is evident. Hence, the possibility of modulating microbiota composition by nutritional factors, in this case prebiotics, arises as an interesting physiological way of influencing energy metabolism, concretely adaptive thermogenesis, and prevent or even treat overweight/obesity and the associated metabolic disturbances, as is discussed in the next section.

## IMPACT OF PREBIOTICS ON BAT THERMOGENESIS AND WAT BROWNING

The concept of prebiotics and the importance of their health promoting effects have already been defined. There are multiple natural sources of prebiotics, such as beans/legumes, starchy fruits, cereals, onions, soybean, etc., and generally multiple kinds of vegetables, as well as other food products such as milk and fungi (Geurts et al., 2014; George Kerry et al., 2018). Moreover, many substances could be considered possible prebiotics, such as galactooligosaccharides, inulin-type fructans, arabinoxylan, and arabinoxylan oligosaccharides, chitin-glucans from fungi or even several phenolic compounds, given that they favor the growth of some intestinal microorganisms and show potential health effects (Geurts et al., 2014; Markowiak and Slizewska, 2018).

There is extensive literature relating the consumption of diets rich in prebiotics to the improvement of food intake control, and the reduction of body fat content and body weight gain, even in overweight and obese subjects (Roberfroid et al., 2010; Requena et al., 2018). Now, with the present knowledge concerning multiple prebiotics and their effects on gut microbiota, we are able to connect prebiotics with the proposed health effects by the modulation of microbiota, postbiotics, and even deciphering the main mechanisms involved, including the induction of an increased thermogenic phenotype. Therefore, some representative prebiotics able to impact thermogenic capacity will be discussed in this section.

### Phenolic Compounds, Energy Metabolism, and Thermogenesis

Phenolic compounds, or polyphenols, are secondary metabolites naturally produced by plants, which can be classified into two main groups: flavonoids and non-flavonoids. Phenolic compounds are generally characterized by the presence of at least one aromatic ring with one or more hydroxyl groups attached (Crozier et al., 2009). Polyphenols or polyphenol-rich foods have been described to impact the relative abundance of different bacteria within the gut microbiota in various *in vitro* studies and animal models, by decreasing potential pathogens, such as *C. perfringens* and *C. histolyticum*, and certain Gram-negative *Bacteroides* spp., and inducing beneficial Clostridia, Bifidobacteria and Lactobacilli (Dueñas et al., 2015).

The impact of dietary polyphenols on obesity has also been a topic of interest. Over the years, human and animal studies have revealed that resveratrol, a polyphenol with prebiotic properties, exerts anti-obesity effects (Wang et al., 2015). There are several biological processes involved in the fat-lowering effects of resveratrol, even though the molecular mechanisms implicated have not been fully elucidated (Wang et al., 2015). An important number of studies puts the focus on *in vitro* effects (in cell culture models) of resveratrol, but these types of studies are not the focus of our review. Regarding *in vivo*

studies, Alberdi et al. described that resveratrol supplementation induces the expression of some genes involved in BAT activation (*cytochrome-C-oxidase subunit-2—Mtco2—*, *Pparg1a*, *sirtuin 1—Sirt1—*, and *mitochondrial transcription factor A—Tfam*), together with protein expression of UCP1, in Sprague-Dawley rats fed with an obesogenic diet for 6 weeks (Alberdi et al., 2013). Besides, the combination of resveratrol with another polyphenol, quercetin, also induces UCP1 in BAT (Arias et al., 2017). One possible molecular mechanism involved in BAT activation by resveratrol supplementation is based on AMPK activation (Wang et al., 2017). Nevertheless, part of these conclusions come from the combination of *in vivo* and *in vitro* studies and it is difficult to separate the possible direct effects of resveratrol from its putative effects as a prebiotic agent. In the same line, related to the activation of thermogenesis in BAT, dietary supplementation with resveratrol and quercetin also resulted in the stimulation of browning in WAT (Arias et al., 2017). Namely, the authors showed that resveratrol and quercetin supplementation for 6 weeks in Wistar rats fed with an obesogenic diet induced the appearance of brown-like adipocytes in perirenal WAT (Arias et al., 2017). These studies highlight the link between resveratrol, with its fat lowering effects, and browning and thermogenesis activation. Other interesting study with resveratrol supplementation and WAT browning was performed with oral supplementation of newborn mice throughout lactation, which is a critical period for metabolic programming and the shaping of gut microbiota (Pico and Palou, 2013; Milani et al., 2017). In such study, Serrano et al. (2018) supplemented mice with resveratrol (or vehicle) from day 2 to 20 of life and, in the adulthood (day 90) half of the animals were subjected to an HF diet for 10 weeks. The neonatally male treated animals did not show induction of thermogenic markers in BAT (where expression of *Ucp1* was decreased), but they showed resistance to weight gain and a metabolic programming toward browning in subcutaneous WAT (Serrano et al., 2018). Regarding the issue of the possible effects of resveratrol acting as a prebiotic, it must be highlighted that the direct action of resveratrol modulating gut microbiota has been demonstrated. For example, resveratrol supplementation has been associated with the attenuation of the *Firmicutes/Bacteroidetes* ratio and the selective growth of potential beneficial genera such as *Lactobacillus* and *Bifidobacterium*, either alone or in combination with quercetin (Larrosa et al., 2009; Etxeberria et al., 2015). It has also been reported to increase hepatic bile acid neosynthesis via gut microbiota remodeling, associated to the reduction of trimethylamine-N-oxide (TMAO) levels and atherosclerosis (Chen et al., 2016).

Other interesting polyphenols with prebiotic properties are anthocyanins. Positive effects against obesity and related alterations have been attributed to anthocyanin intake (from blueberries) (Meydani and Hasan, 2010). Anthocyanins are a major type of polyphenols, and have prebiotic properties since their low bioavailability make them likely to be metabolized by gut microbiota, and anthocyanins and their metabolites may exert a positive modulation on the intestinal bacterial population (Hidalgo et al., 2012). Relevant to this review is the described association between anthocyanins and BAT



activation. In this sense, animal studies on supplementation with anthocyanins, or anthocyanin metabolites, have shown a relationship with thermogenic capacity of BAT and browning of WAT. More specifically, supplementation with cyanidin-3-glucoside (C3G) of genetically obese mice (C57BLKS/J-Leprdb/Leprdb) for 16 weeks resulted in reduction of weight gain, ameliorated glucose homeostasis impairment and hepatic steatosis, improved tolerance to cold exposure, and stimulated BAT activity and browning in subcutaneous WAT (You et al., 2017). Similarly, wild type C57BL/6J mice supplemented with C3G for 15 weeks were resistant to HF/high fructose diet induced obesity, associated with increased thermogenic capacity of BAT and browning of inguinal WAT, by increasing mitochondrial biogenesis and function (You et al., 2018). Altogether, these data reveal that C3G intake may be considered as a novel approach to prevent and treat obesity.

Other polyphenols are also gaining significance in relation to their anti-obesity effects due to their thermogenic effect. For instance, supplementation with dietary green tea extract (GTE) from leaves for 8 weeks to mice fed a HF diet significantly reduces HF-induced adiposity in both WAT and BAT, by reducing both adipocyte size in WAT and lipid droplet size in BAT. It is noteworthy that markers of browning were induced in WAT in GTE treated mice, whereas markers of whitening were reduced in the BAT of these animals, suggesting a role of browning and thermogenesis induction in the anti-obesity beneficial effects of GTE intake (Neyrinck et al., 2017). Another extract rich in polyphenols used in research is camu camu (*Myrciaria dubia*) (an Amazonian fruit) crude extract (CC). Daily treatment with CC in mice fed a HF diet for 8 weeks markedly reshapes gut microbiota and confers protection against obesity development by increasing energy expenditure, accompanied by *Ucp1* induction in BAT and WAT, together with other markers of browning (Anhê et al., 2018). Moreover, CC-treated mice showed altered levels and composition of circulating bile acids and changes in bile acid composition (with higher unconjugated secondary bile acids) (Anhê et al., 2018). Finally, transplantation of microbiota from CC treated mice to germ-free mice partially reproduced the beneficial effects of CC supplementation (Anhê et al., 2018). One more example is capsaicin, which has also shown prebiotic properties (Kang et al., 2017). Capsaicin supplementation to male Wistar rats results in the appearance of multilocular adipocytes positive for UCP1 and CIDEA in retroperitoneal WAT, and increased expression of browning markers in inguinal WAT (Mosqueda-Solis et al., 2018).

## Prebiotics of Carbohydrate Nature and Thermogenesis

Different types of carbohydrates are classified as prebiotics, and we focus on different examples with experimental data supporting their role in the regulation of adaptive thermogenesis.

In the group of non-digestible complex carbohydrates with prebiotic properties, pectins are an interesting example and, concretely, high-esterified pectin (HEP). Regarding structure, pectin is a complex heteropolysaccharide, made up of a series of covalently linked polymers, and the degree of methylation

determines its usage by bacteria (Hamaker and Tuncil, 2014; Fak et al., 2015), with HEP importantly being fermented by gut bacteria. HEP is a main component of soluble dietary fiber in vegetables and fruits, and is recognized as a prebiotic (Lattimer and Haub, 2010; Hamaker and Tuncil, 2014), whose intake is associated with health-promoting effects on body weight, lipid metabolism, glucose homeostasis, etc. (Sanchez et al., 2008; Adam et al., 2015; Palou et al., 2015). Concerning the effect of HEP supplementation on BAT thermogenesis and WAT browning, we have developed studies in rats showing that chronic HEP supplementation (from apples) decreases energy efficiency and protects from fat accumulation and metabolic disturbances caused by maternal malnutrition, in part associated to increased thermogenic capacity in BAT and WAT, including the induction of UCP1 (unpublished manuscript in preparation). Therefore, HEP is a cheap, easy-to-get prebiotic with important effects on metabolic health, influencing thermogenic capacity. There are more examples of fermentable polysaccharides that have been related to adaptive thermogenesis modulation. Weitkunat et al. investigated how inulin and guar gum supplementation for 30 weeks affects the metabolic syndrome-related disorders associated to HF diet feeding in mice. The results showed that both inulin and guar gum affect gut microbiota composition but only inulin, and not guar gum supplementation, attenuates the HF diet induced body weight and fat gain, and significantly induces brown/brite markers in subcutaneous WAT (Weitkunat et al., 2017). In the same work, the authors also investigated the effect of SCFA, as will be discussed below (see section on postbiotics).

Another example of non-digestible, but in this case not complex, carbohydrate with beneficial physiological effects on metabolic health is epilactose (Murakami et al., 2015). Epilactose is a rare disaccharide proposed to prevent diet-induced obesity from studies in mice. Murakami et al. showed how HF fed mice supplemented with epilactose were protected against body and fat gain, and revealed greater *Ucp1* gene expression in BAT and, surprisingly, also in muscle; they also reported decreased gene expression of macrophage infiltration markers in epididymal WAT. Moreover, supplemented mice showed a different caecum SCFA profile, with increased acetate and propionate levels (Murakami et al., 2015).

Given the above evidence, it seems clear that different types of prebiotics can affect adaptive thermogenic capacity, although this is a relative by new field where more studies are needed. Furthermore, the underlying mechanisms explaining the relationship between prebiotic supplementation and the induction of thermogenesis and browning is still not fully clear, although some works are starting to focus on unraveling such mechanisms. Although not the only one, an important point of connection between thermogenic capacity and prebiotics, as we have already suggested here, is the production of secondary metabolites by resident bacteria after fermentation of prebiotics. For instance, as already pointed out, SCFA profile and secondary bile acids might be important metabolites derived from bacteria metabolism able to connect prebiotic supplementation to thermogenic capacity regulation in BAT and WAT. Although the importance of postbiotics has been



relatively overlooked, scientific evidence of their beneficial health effects by BAT thermogenic activation and WAT browning is progressively increasing, as will be discussed in the next section.

## IMPACT OF POSTBIOTICS ON BAT THERMOGENESIS AND WAT BROWNING

Postbiotics (also known as metabiotics, biogenics, or metabolite/cell-free supernatants) are “soluble factors (products or metabolic byproducts) secreted by live bacteria or released after bacterial lysis” and they provide physiological benefits to the host (Aguilar-Toalá et al., 2018). There are multiple types of postbiotics with varied structures, such as SCFA, peptides, enzymes, teichoic acids, exo- and endo-polysaccharides, vitamins, etc. (Aguilar-Toalá et al., 2018). As key examples, here we discuss the scientific evidence of the link between BAT activation and WAT browning with bile acids and SCFA.

### Bile Acids and BAT Thermogenesis

Bile acids (BA) are synthesized in liver from cholesterol, as primary bile acids, which are cholic acid ( $3\alpha,7\alpha,12\alpha$ -trihydroxy- $5\beta$ -cholanoic acid, CA) and chenodeoxycholic acid ( $3\alpha,7\alpha$ -dihydroxy- $5\beta$ -cholanoic acid, CDCA) in humans, while in rodents CDCA is metabolized to muricholic acids (less toxic) (Martinot et al., 2017). The synthesized primary BA are conjugated with the aminoacids glycine or taurine (forming bile salts), prior to their secretion, which is fundamental to their role of emulsification of lipids during digestion (Martinot et al., 2017). There are also secondary BA, which are produced by the metabolism of primary BA by gut microbiota; the most common secondary BA species are deoxycholic acid (DCA) and lithocholic acid (LCA), coming from CA and CDCA, respectively, although dozens of secondary BA are produced by the gut flora, increasing the diversity of possible secondary BA (Martinot et al., 2017). It should be taken into account that the profile of secondary bile acids might be modulated by environmental conditions which can affect gut microbiota composition. In this sense, in the work already commented above by Zietak et al. (2016), it is reported that cold exposure and diet are able to modify BA metabolism. For instance, cold acclimation at  $12^{\circ}\text{C}$  of C57BL/6J mice, after only 1 day, increases conjugated BA levels, related to reduced abundance of *Lactobacillus*, which possesses greater bile acid deconjugation capacity than other species (Zietak et al., 2016). Moreover, in this work, cold acclimation increased both the production of BA species and the expression of genes related to BA synthesis (Zietak et al., 2016).

BA regulate numerous metabolic pathways in the host via the nuclear receptor farnesoid X receptor (FXR) and the G-coupled receptor TGR5 (Martinot et al., 2017). Among these metabolic pathways, the regulation of thermogenesis is included. Watanabe et al. showed that TGR5 activation by BA promotes intracellular thyroid hormone activity and increases thermogenesis in BAT (Watanabe et al., 2006). Diet supplementation with CA to HF diet fed C57BL/6J mice prevents,

and even reverts, diet induced obesity, related to increased energy expenditure and the induction of TGR5 receptor, which increases cAMP production, involved in increased expression of genes coding for proteins related to BAT activation (PGC1 $\alpha$  and  $\beta$ , UCP1 and 3, 2 iodothyronine deiodinase—D2—, straight-chain acyl-CoA oxidase 1—ACO—and muscle-type carnitine palmitoyltransferase 1—mCPT1), therefore showing activation of thermogenesis in BAT (Watanabe et al., 2006). In this work, apart from primary BA, the authors showed, *in vitro*, the capacity of secondary BA (DCA) and taurine conjugates (of CA and DCA) to induce cAMP production in cells (related to TGR5 activation) (Watanabe et al., 2006). Therefore, this work demonstrates the capacity of both primary and bacteria-metabolized BA to potentially induce thermogenic activity. In another related paper, it was suggested that UCP1 expression is required for weight-reducing action of bile acids (Zietak and Kozak, 2016). Other studies relate BA to BAT activation (even in humans) (e.g., Teodoro et al., 2014; Broeders et al., 2015) although focused on primary BA. Since we are focusing on postbiotics, another interesting study, which we have formerly discussed, is the work by Somm et al. with  $\beta$ -Klotho KO mice. Here, the authors show that  $\beta$ -Klotho KO mice have a high production of CA in liver, resulting in an important excess of DCA (secondary BA) production by microbiota, suggesting that resistance of these KO mice to diet-induced obesity is mainly caused by the high production of DCA and its signaling through the receptor TGR5 (Somm et al., 2017). It is important to note that DCA is suggested to be especially responsible of the activation of TGR5 to stimulate BAT thermogenesis (Somm et al., 2017), related to its greater potency (compared with other BA) to activate TGR5 *in vitro* (Maruyama et al., 2002) and that, in fact, TGR5 is mainly considered as a receptor for secondary BA (Kawamata et al., 2003).

### Role of SCFA in BAT Thermogenesis and WAT Browning

SCFA are important metabolites produced by gut microbiota by the fermentation of non-digestible carbohydrates. SCFAs are monocarboxylic acids of 2–6 carbons and the main SCFA for their abundance in plasma and caecum are (in order from more to less abundant) acetate, propionate, and butyrate, as measured in humans and rats (Topping and Clifton, 2001; Jakobsdottir et al., 2013; Schonfeld and Wojtczak, 2016). It should be taken into account that the microbiota profile conditions the relative proportions of individual SCFA produced; namely this, *Bacteroidetes* mainly produce acetate and propionate, and *Firmicutes* mainly butyrate (Pascale et al., 2018). However, the relationship may not be that simple and different phyla or genera are not exclusively associated to the production of a specific SCFA, e.g., a positive correlation between relative abundance of *Firmicutes* and plasma acetate levels in humans has been shown (Moreno-Navarrete et al., 2018).

SCFA affect a variety of biological processes in multiple organs and tissues and have been described to play a role in different aspects of energy metabolism and body weight control. For instance, diet supplementation for 4 weeks with salts of

**TABLE 1** | Studies evaluated in this review of effects of prebiotics on adaptive thermogenesis by BAT recruitment and/or WAT browning.

Type of Prebiotic	Prebiotic	Experimental design	Main results on BAT thermogenesis and WAT browning	References
Phenolic compounds	Resveratrol	HF/high sucrose fed rats treated with resveratrol (15 mg/kg body/day), quercetin (30 mg/kg body/day) or both, for 6 weeks	Resveratrol and quercetin treatment: Appearance UCP1+multilocular cells in perirenal WAT ↑Expression of browning markers in perirenal WAT ↑Expression thermogenic markers <i>Cox-2</i> and UCP1 in BAT Resveratrol treatment: ↑Expression thermogenic markers <i>Cidea</i> and UCP1 in BAT	Arias et al., 2017
		HF/high sucrose fed Sprague-Daley rats treated with resveratrol (30 mg/kg body/day), for 6 weeks	↑Expression thermogenic markers in BAT, including <i>Ucp1</i>	Alberdi et al., 2013
		NMRI mice supplemented with resveratrol (2 mg/Kg body/day) during lactation (day 2–20 of life). HF diet from day 90 of life (for 10 weeks) vs. normal fat diet	↑Expression of browning markers in inguinal WAT in males ↑Multilocular UCP1+ adipocytes in inguinal WAT under normal fat diet ↓ <i>Ucp1</i> expression in BAT	Serrano et al., 2018
	Anthocyanins	Obese male C57BLKS/J-Leprdb/Leprdb mice treated with Cyanidin 3-glucoside (1mg/ml) for 16 weeks	↑Energy expenditure ↑Expression of browning markers in subcutaneous WAT ↑Expression of BAT thermogenic markers and BAT activity	You et al., 2017
		HF/high fructose fed male C57BL/6J mice treated with Cyanidin 3-glucoside (1mg/ml) for 15 weeks	↑Energy expenditure Better performance maintaining body temperature compared with diet induced obese mice ↑Mitochondrial biogenesis and function ↑Expression of browning markers in inguinal WAT ↑Expression thermogenic markers in BAT	You et al., 2018
	Green Tea extracts	Male C57BL/6J mice fed with HF diet supplemented with green tea extract (0.5% green tea leaf extract) for 8 weeks	↑Expression of browning markers in subcutaneous WAT ↓Whitening in BAT ↑Appearance of UCP1+ adipocytes in subcutaneous WAT depot	Neyrinck et al., 2017
	Camu Camu ( <i>Myrciaria dubia</i> )	Male C57BL/6J mice fed with HF/high sucrose diet supplemented with Camu Camu crude extract (200 mg/Kg) compared to Vitamin C (6.6 mg/Kg) for 8 weeks	↑Energy expenditure ↑Interscapular temperature (tendency) ↑Expression of browning markers in inguinal WAT ↑Expression thermogenic markers in BAT	Anhê et al., 2018
	Capsaicin	Male Wistar rats fed with HF/high sucrose and supplemented with Capsaicin (4 mg/kg body/day) for 8 weeks	↑Appearance of UCP1+ and CIDEA+ adipocytes in retroperitoneal WAT ↑Expression of browning markers in inguinal WAT	Mosqueda-Solis et al., 2018
	Carbohydrates	Male C57/BL6 mice fed with HF diet, supplemented with Epilactose (10% by weight) for 8 weeks	↑UCP1 expression in BAT and muscle	Murakami et al., 2015
		Male C57BL/6JRj mice fed with HF diet supplemented with inulin or guar gum (7%) for 30 weeks	Inulin but not guar gum: ↑Body temperature ↑Expression of browning markers in subcutaneous WAT	Weitkunat et al., 2017

The ability to induce or inhibit the assessed effects is indicated with ↑ or ↓, respectively. BAT, Brown adipose tissue; Cidea, Cell death-inducing DFFA-Like effector A; Cox-2, Cytochrome c oxidase subunit II; HF, High fat; UCP1, Uncoupling Protein 1; WAT, White adipose tissue.

butyrate (5%), propionate (4.3%), or acetate (3.7%) has been described to protect against diet-induced obesity and insulin resistance in mice fed a HF diet (Lin et al., 2012). Butyrate and propionate, but not acetate, were able to stimulate gut

hormones and reduce food intake (Lin et al., 2012). Propionate has also been described to inhibit lipogenesis via fatty acid synthase down-regulation in the liver, while acetate can act as a lipogenic substrate, therefore the acetate/propionate ratio

**TABLE 2 |** Studies evaluated in this review of effects of postbiotics on adaptive thermogenesis by BAT recruitment and/or WAT browning.

Type of postbiotic	Postbiotic	Experimental design	Main results on BAT thermogenesis and WAT browning	References
Secondary BA	DCA	Male Klb <sup>-/-</sup> mice fed with HF diet for 8 weeks	Effects associated to DCA: Thermogenesis and BAT stimulation	Somm et al., 2017
	DCA	Treatment with BAs to BAT cells <i>in vitro</i> from chow and HF fed C57BL/6J mice	Effects associated to DCA: ↑cAMP levels in BAT cells	Watanabe et al., 2006
SCFA	Acetate	Immortalized brown adipocytes cell line treated during differentiation with acetate (10 mM) or acute treatment 6 h (10 mM)	↑Expression of thermogenic markers both treatments (during differentiation and acute) ↑Mitochondriogenesis (during differentiation)	Hu et al., 2016
	Acetate	Male C57BL/6J mice supplemented with sodium acetate (150 mM) in drinking water for 6 weeks	↑Expression of thermogenic markers in BAT	Hu et al., 2016
	Acetate	Male C57BL/6JRj mice fed with HF diet supplemented with 5% of SCFA (10:1 Acetate/Propionate or 1:2.5 Acetate/Propionate) for 30 weeks	Effects attributed to acetate: ↑Body temperature ↑Expression browning markers in subcutaneous WAT	Weitkunat et al., 2017
	Acetate	Male C57BL/6 mice fed with HF diet treated with nanoparticle-delivered acetate (intraperitoneal injection three times per week) for 6 weeks	↑Expression browning markers in subcutaneous WAT No BAT recruitment	Sahuri-Arisoylu et al., 2016
	Acetate	34 morbidly obese humans (28 women and 6 men)	Relative abundance of <i>Firmicutes</i> is positively associated with browning markers in subcutaneous fat. Plasma acetate levels are positively associated with <i>Firmicutes</i> relative abundance, also linked to the brown marker PRDM16 mRNA in subcutaneous fat	Moreno-Navarrete et al., 2018
	Acetate	<i>In vitro</i> : 3T3L1 treated with sodium acetate (1 mM) during differentiation (day 0 to harvesting) <i>In vivo</i> : Obese diabetic male kk-Ay mice treated with acetate (0.6%) in drinking water for 16 weeks	<i>In vitro</i> : ↑Expression of browning markers <i>In vivo</i> : =Expression of thermogenic markers in BAT ↑Expression of browning markers in gonadal WAT =Expression of browning markers in subcutaneous WAT	Hanatani et al., 2016
	Butyrate	Male C57BL/6J mice fed with HF diet supplemented with sodium butyrate (5%) for 12 weeks	↑Cold tolerance ↑Energy expenditure ↑Expression of thermogenic markers in BAT ↑Mitochondrial function and biogenesis in BAT	Gao et al., 2009
	Butyrate	Male APOE*3-Leiden. CETP mice fed with HF diet supplemented with sodium butyrate (5%) for 9 weeks	↑Fat oxidation rate during day ↑Expression of UCP1 in BAT in BAT =Expression of browning markers in subcutaneous and gonadal WAT	Li et al., 2018
Anthocyanin metabolites	Vanillic acid	Male C57BL/6J mice fed with HF/high sucrose diet supplemented with vanillic acid (0.5%) for 16 weeks	↑Cold tolerance ↑Expression of thermogenic markers in BAT ↑Expression of browning markers in inguinal WAT ↑Mitochondriogenesis in BAT and WAT	Han et al., 2018
Linoleic acid metabolites	KetoA	Male C57BL/6 and TRPV1-deficient C57BL/6 mice fed with HF diet supplemented with KetoA (0.1%) for 10 weeks	↑Ucp1 gene and protein expression in BAT ↑Ucp1 gene and protein expression in inguinal WAT ↑Expression of thermogenic markers in BAT ↑Expression of browning markers in inguinal WAT These results depends on TRPV1 SNS dependent activation	Kim et al., 2017

The ability to induce the assessed effects is indicated with ↑ while = indicates no significant changes. BA, Bile acids; BAT, Brown adipose tissue; DCA, Deoxycholic acid; HF, High fat; KetoA, 10-oxo-12(Z)-octadecenoic acid; PRDM16, PR domain containing 16; SCFA, Short chain fatty acids; SNS, sympathetic nervous system; TRPV1, Transient receptor potential vanilloid 1; UCP1, Uncoupling Protein 1; WAT, White adipose tissue.

seems important for *de novo* lipogenesis (Conterno et al., 2011). Moreover, De Vadder et al. showed that propionate and butyrate induce the expression of gluconeogenesis related

genes and activate intestinal gluconeogenesis through different mechanisms, and this has metabolic benefits such as reduced body weight and adiposity, and improvement in glucose

homeostasis, as studied in rodents (De Vadder et al., 2014). *In vitro* experiments revealed that butyrate can directly activate the expression of intestinal gluconeogenesis related genes (coding for glucose-6-phosphatase—G6PC—and the cytosolic form of phosphoenolpyruvate carboxykinase—PCK1), while propionate requires the gut-brain circuit involving the free fatty acid receptor 3 (FFAR3) in mice to induce intestinal gluconeogenesis (De Vadder et al., 2014). Regarding acetate, the literature points toward a complex role. As has already been commented, acetate can act as a substrate for lipogenesis, but it has also been described to activate AMPK *in vitro* and to reduce the expression of key genes for gluconeogenesis and lipogenesis in liver of KK-A(y) diabetic mice supplemented with acetic acid, associated to reduced hyperglycaemia (Sakakibara et al., 2006). Strikingly, in the literature, there are both studies suggesting that acetate treatment induces an increase in lipogenic and adipogenic capacity (Hong et al., 2005; Ge et al., 2008; Aberdein et al., 2014) or the promotion of obesity through a gut-brain- $\beta$ -cell axis (Perry et al., 2016; Trent and Blaser, 2016), and studies that suggest beneficial and protection-against-obesity effects, such as the one commented above and some others (e.g., see Kondo et al., 2009; Aoki et al., 2017, and see below). Therefore, the role of acetate is somewhat controversial. Regarding BAT thermogenesis and WAT browning, recent literature points to a role of some SCFA, as discussed below.

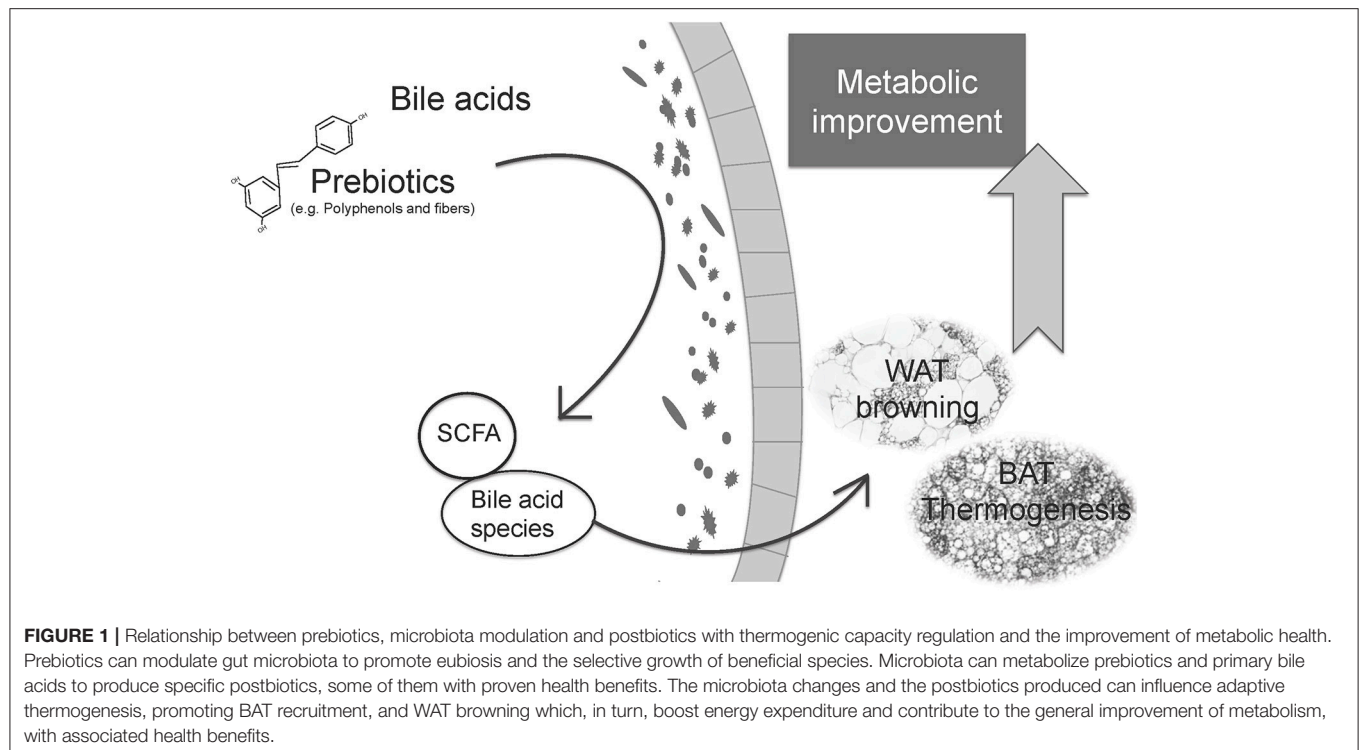
Concerning acetate and thermogenesis, new findings agree with the potential capacity of acetate to increase the activity of BAT or WAT browning in different models. In this sense, Hu et al. (2016) studied BAT of mice treated with sodium acetate (150 mM) in drinking water for 6 weeks, reporting an induction of the expression of genes coding for PGC1 $\alpha$  and UCP1 as compared to controls, accompanied by morphological changes, including mitochondrial biogenesis. Moreover, treatment with acetate of immortalized brown adipocyte cells (IM-BAT), obtained by primary cell culture of BAT from C57BL/6 mice, induced adipogenesis and mitochondriogenesis, together with up-regulation of gene expression of key thermogenic markers, such as adipocyte protein 2 (AP2), PGC1 $\alpha$ , and UCP1, depending on the activation of the free fatty acid receptor G protein-coupled receptor 43 (GPCR43) (FFAR2) (Hu et al., 2016). Moreover, the work of Weitkunat et al. (2017) has already been commented in the section on prebiotics of carbohydrate nature and thermogenesis; herein, the authors suggest an induction of beige markers (browning) in WAT driven by acetate. Other studies also suggest an involvement of acetate in WAT browning (Sahuri-Arisoylu et al., 2016; Moreno-Navarrete et al., 2018). Intraperitoneal injection of nanoparticles of acetate increases gene expression of brown adipocyte markers (UCP1 and PR domain containing 16—PRDM16) in subcutaneous WAT of HF diet fed mice, which might be partly responsible for the reduced obesogenic phenotype of these treated animals (Sahuri-Arisoylu et al., 2016). However, no BAT recruitment due to acetate treatment was found in this work (Sahuri-Arisoylu et al., 2016). On the other hand, a recent study in obese humans has shown a positive significant association between brown markers PRDM16, UCP1 and thyroxine deiodinase 2—DIO2—in subcutaneous WAT and the *Firmicutes* relative

abundance, which seems to contribute significantly to the variance of these markers in this adipose depot (Moreno-Navarrete et al., 2018). Moreover, *Firmicutes* relative abundance associates positively with circulating acetate levels (Moreno-Navarrete et al., 2018). Therefore, the authors conclude that microbiota composition influences WAT browning in these obese subjects, probably through plasma acetate (Moreno-Navarrete et al., 2018). There is also *in vitro* evidence linking acetate with browning. For instance, 3T3-L1 adipocytes have been described to increase the expression levels of several browning markers after acetate treatment (UCP1, PRDM16, DIO2, CIDEA, and transmembrane protein 26—TMEM26—, among others) (Hanatani et al., 2016). The authors also provide *in vivo* evidence in mice and conclude that acetate might exert its anti-obesity effects through the dissipation of energy excess, at least in part (Hanatani et al., 2016). We have also performed *in vitro* experiments with murine primary cultures of adipocytes treated with acetate, showing that it induces thermogenic capacity in brown adipocytes and in recruited beige/brite adipocytes form subcutaneous WAT (unpublished manuscript in preparation). Therefore, different studies suggest that acetate might have an anti-obesity effect partly related to the induction of WAT browning, together with the recruitment of BAT, thus increasing energy expenditure capacity.

There is less evidence regarding adaptive thermogenesis capacity and other SCFA. Nevertheless, there is some evidence for butyrate as a thermogenic molecule. For instance, Gao et al. showed, among other effects, that dietary butyrate treatment in HF diet fed mice for 12 weeks induces the expression of UCP1 and PGC1 $\alpha$  in BAT and mitochondrial function and biogenesis in BAT and muscle, accompanied by an improvement in insulin sensitivity (Gao et al., 2009). Besides, Li and collaborators demonstrated in mice that chronic butyrate supplementation prevents diet-induced obesity, hypertriglyceridemia, hepatic steatosis, and hyperinsulinemia, although mainly attributed to reduction of food intake (Li et al., 2018). Nevertheless, the authors also showed an activation of BAT, associated to increased fatty acid utilization from plasma triglycerides (Li et al., 2018). Moreover, it must be highlighted that butyrate treatment in mice has also been shown to promote BAT thermogenic capacity by activating UCP1 protein expression (and PGC1 $\alpha$ ) (Gao et al., 2009). In the work of Li et al., no evidence of browning in subcutaneous fat was found, suggesting the butyrate is not involved in browning induction (Li et al., 2018). Regarding propionate, indirect evidence for its involvement on adaptive thermogenic capacity is given by the fact that it can directly induce SNS activity via GPR41 (FFAR3) at sympathetic ganglia, correlated with energy consumption (Kimura et al., 2011). Moreover, in this work, GPR41 ablation (*Gpr41*<sup>-/-</sup> mice) was associated with lower *Ucp1* expression in BAT. The authors suggest an important role of SCFA-GPR41 interactions regulating SNS as a mechanism accounting for the effects of diet and pre/probiotics on body homeostasis (Kimura et al., 2011).

Overall, despite some controversial results, SCFA, particularly acetate, seem to be proper candidates to continue to be tested





as inducers of thermogenesis in BAT and browning in WAT, in order to reduce the detrimental health effects associated to diet-induced obesity. In this sense, human studies are essential to establish a strong association between SCFA and their beneficial effects at different levels.

### Role of Other Postbiotics on BAT Thermogenesis and WAT Browning

Apart from the postbiotics shown here, there are other various possibilities. For instance, we commented above that anthocyanins may have positive beneficial effects as anti-obesity factors and as thermogenesis and browning inducers (You et al., 2015, 2017) yet, interestingly, the metabolites produced by the utilization of anthocyanins by gut microbiota may also develop a role in host thermogenesis induction, similar to other postbiotics. In this sense, vanillic acid has been recently described to exhibit thermogenesis induction capacity (Han et al., 2018). Vanillic acid is one of the metabolites produced through the metabolization of anthocyanins by intestinal microbes (Keppler and Humpf, 2005). It has been reported that supplementation with vanillic acid for 16 weeks protects mice from HF/high sucrose diet induced obesity, by activating thermogenesis in BAT and browning in WAT (Han et al., 2018). These results, again, point out the capacity of postbiotics as BAT activators, and browning agents, in the treatment or prevention of diet-induced obesity. Another interesting postbiotic is 10-oxo-12(Z)-octadecenoic acid (KetoA). KetoA is a metabolite of linoleic acid produced by lactic acid bacteria in the gut able to stimulate SNS through activation of the ion channel transient receptor potential vanilloid 1 (TRPV1) in the gastrointestinal

tract, concomitantly enhancing energy expenditure, related to activation of BAT function and inguinal WAT browning (Kim et al., 2017).

## SUMMARY AND PERSPECTIVES

The main bibliography and evidence of the different results shown in this review, supporting the role of prebiotics and postbiotics in adaptive thermogenesis regulation, is summarized in **Tables 1, 2**. Additionally, **Figure 1** summarizes the central idea shown in this review, linking prebiotics, microbiota modulation, and postbiotics with BAT thermogenesis and WAT browning and the improvement of metabolism.

The incipient growth of studies suggesting a connection between microbiota and energy expenditure brings to light the potential of establishing new strategies against the pandemic of obesity. It is important to highlight the opportunity of the present review, since in the last 2–3 years numerous articles have been published studying the role of microbiota and the effects of prebiotics and postbiotics on the development of obesity and, more specifically, relating them to the activation of thermogenesis in BAT and browning in WAT. Microbiota suffers adaptations to the conditions of the host and responds to feeding, in such a way that it can be modulated by prebiotics conferring health benefits, which include the increase in thermogenic capacity, in both BAT and WAT (especially subcutaneous WAT). Therefore, boosting thermogenic capacity, and therefore energy expenditure, can be added to the list of the described beneficial health effects of prebiotics.

Moreover, the products of microbiota metabolism, so-called postbiotics, are involved in the mechanisms that connect prebiotics and microbiota modulation with thermogenesis and protection against obesity and its associated metabolic disorders. Interestingly, the direct use of postbiotics, through dietary supplementation, can also be considered as an interesting strategy to combat obesity and improve host metabolism.

In conclusion, the use of both prebiotics and postbiotics, in order to induce adaptive thermogenesis in the treatment or prevention of obesity and metabolic disorders emerges as an interesting strategy which deserves further research. Taking into account the fact that an important part of this research has been carried out in animal models, more studies are needed in humans. Moreover, the use of prebiotics represents a physiological, and even easy and affordable, way to improve health and energy metabolism. Overall, it is worthwhile to continue investigating this connection, given its therapeutic potential.

## REFERENCES

- Aberdein, N., Schweizer, M., and Ball, D. (2014). Sodium acetate decreases phosphorylation of hormone sensitive lipase in isoproterenol-stimulated 3T3-L1 mature adipocytes. *Adipocyte* 3, 121–125. doi: 10.4161/adip.27936
- Adam, C. L., Thomson, L. M., Williams, P. A., and Ross, A. W. (2015). Soluble fermentable dietary fibre (pectin) decreases caloric intake, adiposity and lipidaemia in high-fat diet-induced obese rats. *PLoS ONE* 10:e0140392. doi: 10.1371/journal.pone.0140392
- Aguilar-Toalá, J. E., García-Varela, R., García, H. S., Mata-Haro, V., González-Córdova, A. F., Vallejo-Cordoba, B., et al. (2018). Postbiotics: an evolving term within the functional foods field. *Trends Food Sci. Technol.* 75, 105–114. doi: 10.1016/j.tifs.2018.03.009
- Alberdi, G., Rodríguez, V. M., Miranda, J., Macarulla, M. T., Churruga, I., and Portillo, M. P. (2013). Thermogenesis is involved in the body-fat lowering effects of resveratrol in rats. *Food Chem.* 141, 1530–1535. doi: 10.1016/j.foodchem.2013.03.085
- Althani, A. A., Marei, H. E., Hamdi, W. S., Nasrallah, G. K., El Zowalaty, M. E., Al Khodor, S., et al. (2016). Human microbiome and its association with health and diseases. *J. Cell. Physiol.* 231, 1688–1694. doi: 10.1002/jcp.25284
- Anhê, F. F., Nachbar, R. T., Varin, T. V., Trottier, J., Dudonné, S., Le Barz, M., et al. (2018). Treatment with camu camu. *Gut*. doi: 10.1136/gutjnl-2017-315565. [Epub ahead of print].
- Aoki, R., Kamikado, K., Suda, W., Takii, H., Mikami, Y., Suganuma, N., et al. (2017). A proliferative probiotic *Bifidobacterium* strain in the gut ameliorates progression of metabolic disorders via microbiota modulation and acetate elevation. *Sci. Rep.* 7:43522. doi: 10.1038/srep43522
- Arias, N., Picó, C., Teresa Macarulla, M., Oliver, P., Miranda, J., Palou, A., et al. (2017). A combination of resveratrol and quercetin induces browning in white adipose tissue of rats fed an obesogenic diet. *Obesity* 25, 111–121. doi: 10.1002/oby.21706
- Bäckhed, F., Manchester, J. K., Semenkovich, C. F., and Gordon, J. I. (2007). Mechanisms underlying the resistance to diet-induced obesity in germ-free mice. *Proc. Natl. Acad. Sci. U.S.A.* 104, 979–984. doi: 10.1073/pnas.0605374104
- Bartelt, A., and Heeren, J. (2014). Adipose tissue browning and metabolic health. *Nat. Rev. Endocrinol.* 10, 24–36. doi: 10.1038/nrendo.2013.204
- Bidu, C., Escoula, Q., Bellenger, S., Spor, A., Galan, M., Geissler, A., et al. (2018). The Transplantation of  $\omega$ 3 PUFA-altered gut microbiota of fat-1 mice to wild-type littermates prevents obesity and associated metabolic disorders. *Diabetes* 67, 1512–1523. doi: 10.2337/db17-1488
- Boulangé, C. L., Neves, A. L., Chilloux, J., Nicholson, J. K., and Dumas, M. E. (2016). Impact of the gut microbiota on inflammation, obesity, and metabolic disease. *Genome Med.* 8:42. doi: 10.1186/s13073-016-0303-2
- Bray, G. A., Kim, K. K., Wilding, J. P. H., and Federation, W. O. (2017). Obesity: a chronic relapsing progressive disease process. A position statement of the world obesity federation. *Obes. Rev.* 18, 715–723. doi: 10.1111/ob.12551
- Broeders, E. P., Nascimento, E. B., Havekes, B., Brans, B., Roumans, K. H., Tailleux, A., et al. (2015). The bile acid chenodeoxycholic acid increases human brown adipose tissue activity. *Cell Metab.* 22, 418–426. doi: 10.1016/j.cmet.2015.07.002
- Cani, P. D., and Delzenne, N. M. (2009). The role of the gut microbiota in energy metabolism and metabolic disease. *Curr. Pharm. Des.* 15, 1546–1558. doi: 10.2174/138161209788168164
- Cani, P. D., and Delzenne, N. M. (2010). Involvement of the gut microbiota in the development of low grade inflammation associated with obesity: focus on this neglected partner. *Acta Gastroenterol. Belg.* 73, 267–269.
- Cani, P. D., and Everard, A. (2016). Talking microbes: when gut bacteria interact with diet and host organs. *Mol. Nutr. Food Res.* 60, 58–66. doi: 10.1002/mnfr.201500406
- Chakraborti, C. K. (2015). New-found link between microbiota and obesity. *World J. Gastrointest. Pathophysiol.* 6, 110–119. doi: 10.4291/wjgp.v6.i4.110
- Chang, C. J., Lin, C. S., Lu, C. C., Martel, J., Ko, Y. F., Ojcius, D. M., et al. (2015). *Ganoderma lucidum* reduces obesity in mice by modulating the composition of the gut microbiota. *Nat. Commun.* 6:7489. doi: 10.1038/ncomms8489
- Chen, M. L., Yi, L., Zhang, Y., Zhou, X., Ran, L., Yang, J., et al. (2016). Resveratrol attenuates trimethylamine-N-oxide (TMAO)-induced atherosclerosis by regulating TMAO synthesis and bile acid metabolism via remodeling of the gut microbiota. *MBio* 7, e02210–02215. doi: 10.1128/mBio.02210-15
- Chevalier, C., Stojanović, O., Colin, D. J., Suarez-Zamorano, N., Tarallo, V., Veyrat-Durebex, C., et al. (2015). Gut microbiota orchestrates energy homeostasis during cold. *Cell* 163, 1360–1374. doi: 10.1016/j.cell.2015.11.004
- Conterno, L., Fava, F., Viola, R., and Tuohy, K. M. (2011). Obesity and the gut microbiota: does up-regulating colonic fermentation protect against obesity and metabolic disease? *Genes Nutr.* 6, 241–260. doi: 10.1007/s12263-011-0230-1
- Crozier, A., Jaganath, I. B., and Clifford, M. N. (2009). Dietary phenolics: chemistry, bioavailability and effects on health. *Nat. Prod. Rep.* 26, 1001–1043. doi: 10.1039/b802662a
- Davis, C. D. (2016). The gut microbiome and its role in obesity. *Nutr. Today* 51, 167–174. doi: 10.1097/NT.0000000000000167
- De Vadder, F., Kovatcheva-Datchary, P., Goncalves, D., Vinera, J., Zitoun, C., Duchamp, A., et al. (2014). Microbiota-generated metabolites promote metabolic benefits via gut-brain neural circuits. *Cell* 156, 84–96. doi: 10.1016/j.cell.2013.12.016

## AUTHOR CONTRIBUTIONS

All authors designed the review. BR, MP, and AMR wrote the manuscript. AP and AMR revised the definitive version. All authors read and approved the final manuscript.

## FUNDING

This work was supported by the Spanish Government: INTERBIOBES-AGL2015-67019-P (MINECO/FEDER, EU).

## ACKNOWLEDGMENTS

CIBER de Fisiopatología de la Obesidad y Nutrición is an initiative of the Instituto de Salud Carlos III. The Laboratory of Molecular Biology, Nutrition and Biotechnology is a member of the European Network of Excellence NuGO (European Nutrigenomics Organization).

- Diamant, M., Blaak, E. E., and de Vos, W. M. (2011). Do nutrient-gut-microbiota interactions play a role in human obesity, insulin resistance and type 2 diabetes? *Obes. Rev.* 12, 272–281. doi: 10.1111/j.1467-789X.2010.00797.x
- Dueñas, M., Muñoz-González, I., Cueva, C., Jiménez-Girón, A., Sánchez-Patán, F., Santos-Buelga, C., et al. (2015). A survey of modulation of gut microbiota by dietary polyphenols. *Biomed Res. Int.* 2015:850902. doi: 10.1155/2015/850902
- Ettxeberria, U., Arias, N., Boque, N., Macarulla, M. T., Portillo, M. P., Martinez, J. A., et al. (2015). Reshaping faecal gut microbiota composition by the intake of trans-resveratrol and quercetin in high-fat sucrose diet-fed rats. *J. Nutr. Biochem.* 26, 651–660. doi: 10.1016/j.jnutbio.2015.01.002
- Fak, F., Jakobsdottir, G., Kulcinskaja, E., Marunguung, N., Matziouridou, C., Nilsson, U., et al. (2015). The physico-chemical properties of dietary fibre determine metabolic responses, short-chain Fatty Acid profiles and gut microbiota composition in rats fed low- and high-fat diets. *PLoS ONE* 10:e0127252. doi: 10.1371/journal.pone.0127252
- Gao, Z., Yin, J., Zhang, J., Ward, R. E., Martin, R. J., Lefevre, M., et al. (2009). Butyrate improves insulin sensitivity and increases energy expenditure in mice. *Diabetes* 58, 1509–1517. doi: 10.2337/db08-1637
- Ge, H., Li, X., Weizmann, J., Wang, P., Baribault, H., Chen, J. L., et al. (2008). Activation of G protein-coupled receptor 43 in adipocytes leads to inhibition of lipolysis and suppression of plasma free fatty acids. *Endocrinology* 149, 4519–4526. doi: 10.1210/en.2008-0059
- George Kerry, R., Patra, J. K., Gouda, S., Park, Y., Shin, H. S., and Das, G. (2018). Benefaction of probiotics for human health: a review. *J. Food Drug Anal.* 26, 927–939. doi: 10.1016/j.jfda.2018.01.002
- Geurts, L., Neyrinck, A. M., Delzenne, N. M., Knauf, C., and Cani, P. D. (2014). Gut microbiota controls adipose tissue expansion, gut barrier and glucose metabolism: novel insights into molecular targets and interventions using prebiotics. *Benef. Microbes* 5, 3–17. doi: 10.3920/BM2012.0065
- Gibson, G. R., Hutkins, R., Sanders, M. E., Prescott, S. L., Reimer, R. A., Salminen, S. J., et al. (2017). Expert consensus document: The International Scientific Association for Probiotics and Prebiotics (ISAPP) consensus statement on the definition and scope of prebiotics. *Nat. Rev. Gastroenterol. Hepatol.* 14, 491–502. doi: 10.1038/nrgastro.2017.75
- Hamaker, B. R., and Tuncil, Y. E. (2014). A perspective on the complexity of dietary fiber structures and their potential effect on the gut microbiota. *J. Mol. Biol.* 426, 3838–3850. doi: 10.1016/j.jmb.2014.07.028
- Han, X., Guo, J., You, Y., Yin, M., Liang, J., Ren, C., et al. (2018). Vanillic acid activates thermogenesis in brown and white adipose tissue. *Food Funct.* 9, 4366–4375. doi: 10.1039/C8FO00978C
- Hanatani, S., Motoshima, H., Takaki, Y., Kawasaki, S., Igata, M., Matsumura, T., et al. (2016). Acetate alters expression of genes involved in beige adipogenesis in 3T3-L1 cells and obese KK-Ay mice. *J. Clin. Biochem. Nutr.* 59, 207–214. doi: 10.3164/jcnn.16-23
- Hidalgo, M., Oruna-Concha, M. J., Kolida, S., Walton, G. E., Kallithraka, S., Spencer, J. P., et al. (2012). Metabolism of anthocyanins by human gut microflora and their influence on gut bacterial growth. *J. Agric. Food Chem.* 60, 3882–3890. doi: 10.1021/jf3002153
- Hong, Y. H., Nishimura, Y., Hishikawa, D., Tsuzuki, H., Miyahara, H., Gotoh, C., et al. (2005). Acetate and propionate short chain fatty acids stimulate adipogenesis via GPCR43. *Endocrinology* 146, 5092–5099. doi: 10.1210/en.2005-0545
- Hu, J., Kyrou, I., Tan, B. K., Dimitriadis, G. K., Ramanjaneya, M., Tripathi, G., et al. (2016). Short-chain fatty acid acetate stimulates adipogenesis and mitochondrial biogenesis via GPR43 in brown adipocytes. *Endocrinology* 157, 1881–1894. doi: 10.1210/en.2015-1944
- Iebba, V., Totino, V., Gagliardi, A., Santangelo, F., Cacciotti, F., Trancassini, M., et al. (2016). Eubiosis and dysbiosis: the two sides of the microbiota. *New Microbiol.* 39, 1–12.
- Jakobsdottir, G., Jadert, C., Holm, L., and Nyman, M. E. (2013). Propionic and butyric acids, formed in the caecum of rats fed highly fermentable dietary fibre, are reflected in portal and aortic serum. *Br. J. Nutr.* 110, 1565–1572. doi: 10.1017/S0007114513000809
- Kalliomäki, M., Collado, M. C., Salminen, S., and Isolauri, E. (2008). Early differences in fecal microbiota composition in children may predict overweight. *Am. J. Clin. Nutr.* 87, 534–538. doi: 10.1093/ajcn/87.3.534
- Kang, C., Wang, B., Kaliannan, K., Wang, X., Lang, H., Hui, S., et al. (2017). Gut microbiota mediates the protective effects of dietary capsaicin against chronic low-grade inflammation and associated obesity induced by high-fat diet. *MBio* 8:e00470-17. doi: 10.1128/mBio.00470-17
- Kawamata, Y., Fujii, R., Hosoya, M., Harada, M., Yoshida, H., Miwa, M., et al. (2003). A G protein-coupled receptor responsive to bile acids. *J. Biol. Chem.* 278, 9435–9440. doi: 10.1074/jbc.M209706200
- Keppler, K., and Humpf, H. U. (2005). Metabolism of anthocyanins and their phenolic degradation products by the intestinal microflora. *Bioorg. Med. Chem.* 13, 5195–5205. doi: 10.1016/j.bmc.2005.05.003
- Kim, M., Furuzono, T., Yamakuni, K., Li, Y., Kim, Y. I., Takahashi, H., et al. (2017). 10-oxo-12(Z)-octadecenoic acid, a linoleic acid metabolite produced by gut lactic acid bacteria, enhances energy metabolism by activation of TRPV1. *FASEB J.* 31, 5036–5048. doi: 10.1096/fj.201700151R
- Kimura, I., Inoue, D., Maeda, T., Hara, T., Ichimura, A., Miyauchi, S., et al. (2011). Short-chain fatty acids and ketones directly regulate sympathetic nervous system via G protein-coupled receptor 41 (GPR41). *Proc. Natl. Acad. Sci. U.S.A.* 108, 8030–8035. doi: 10.1073/pnas.1016088108
- Kondo, T., Kishi, M., Fushimi, T., and Kaga, T. (2009). Acetic acid upregulates the expression of genes for fatty acid oxidation enzymes in liver to suppress body fat accumulation. *J. Agric. Food Chem.* 57, 5982–5986. doi: 10.1021/jf900470c
- Labbe, S. M., Caron, A., Chechi, K., Laplante, M., Lecomte, R., and Richard, D. (2016). Metabolic activity of brown, “beige,” and white adipose tissues in response to chronic adrenergic stimulation in male mice. *Am. J. Physiol. Endocrinol. Metab.* 311, E260–E268. doi: 10.1152/ajpendo.00545.2015
- Labbe, S. M., Caron, A., Festuccia, W. T., Lecomte, R., and Richard, D. (2018). Interscapular brown adipose tissue denervation does not promote the oxidative activity of inguinal white adipose tissue in male mice. *Am. J. Physiol. Endocrinol. Metab.* doi: 10.1152/ajpendo.00210.2018. [Epub ahead of print].
- Landsberg, L., Saville, M. E., and Young, J. B. (1984). Sympathoadrenal system and regulation of thermogenesis. *Am. J. Physiol.* 247(2 Pt 1), E181–E189. doi: 10.1152/ajpendo.1984.247.2.E181
- Larrosa, M., Yanez-Gascon, M. J., Selma, M. V., Gonzalez-Sarrias, A., Toti, S., Ceron, J. J., et al. (2009). Effect of a low dose of dietary resveratrol on colon microbiota, inflammation and tissue damage in a DSS-induced colitis rat model. *J. Agric. Food Chem.* 57, 2211–2220. doi: 10.1021/jf803638d
- Lattimer, J. M., and Haub, M. D. (2010). Effects of dietary fiber and its components on metabolic health. *Nutrients* 2, 1266–1289. doi: 10.3390/nu2121266
- Li, G., Xie, C., Lu, S., Nichols, R. G., Tian, Y., Li, L., et al. (2017). Intermittent fasting promotes white adipose browning and decreases obesity by shaping the gut microbiota. *Cell Metab.* 26, 672–685.e4. doi: 10.1016/j.cmet.2017.08.019
- Li, Z., Yi, C. X., Katiraei, S., Kooijman, S., Zhou, E., Chung, C. K., et al. (2018). Butyrate reduces appetite and activates brown adipose tissue via the gut-brain neural circuit. *Gut* 67, 1269–1279. doi: 10.1136/gutjnl-2017-314050
- Lin, H. V., Frassetto, A., Kowalik, E. J., Nawrocki, A. R., Lu, M. M., Kosinski, J. R., et al. (2012). Butyrate and propionate protect against diet-induced obesity and regulate gut hormones via free fatty acid receptor 3-independent mechanisms. *PLoS ONE* 7:e35240. doi: 10.1371/journal.pone.0035240
- Maguire, M., and Maguire, G. (2018). Gut dysbiosis, leaky gut, and intestinal epithelial proliferation in neurological disorders: towards the development of a new therapeutic using amino acids, prebiotics, probiotics, and postbiotics. *Rev. Neurosci.* doi: 10.1515/revneuro-2018-0024. [Epub ahead of print].
- Markowiak, P., and Slizewska, K. (2018). The role of probiotics, prebiotics and synbiotics in animal nutrition. *Gut Pathog.* 10:21. doi: 10.1186/s13099-018-0250-0
- Marlatt, K. L., and Ravussin, E. (2017). Brown adipose tissue: an update on recent findings. *Curr. Obes. Rep.* 6, 389–396. doi: 10.1007/s13679-017-0283-6
- Martinot, E., Sedes, L., Baptissart, M., Lobaccaro, J. M., Caira, F., Beaudoin, C., et al. (2017). Bile acids and their receptors. *Mol. Aspects Med.* 56, 2–9. doi: 10.1016/j.mam.2017.01.006
- Maruyama, T., Miyamoto, Y., Nakamura, T., Tamai, Y., Okada, H., Sugiyama, E., et al. (2002). Identification of membrane-type receptor for bile acids (M-BAR). *Biochem. Biophys. Res. Commun.* 298, 714–719. doi: 10.1016/S0006-291X(02)02550-0
- Mestdagh, R., Dumas, M. E., Rezzi, S., Kochhar, S., Holmes, E., Claus, S. P., et al. (2012). Gut microbiota modulate the metabolism of brown adipose tissue in mice. *J. Proteome Res.* 11, 620–630. doi: 10.1021/pr200938v

- Meydani, M., and Hasan, S. T. (2010). Dietary polyphenols and obesity. *Nutrients* 2, 737–751. doi: 10.3390/nu2070737
- Milani, C., Duranti, S., Bottacini, F., Casey, E., Turroni, F., Mahony, J., et al. (2017). The first microbial colonizers of the human gut: composition, activities, and health implications of the infant gut microbiota. *Microbiol. Mol. Biol. Rev.* 81, e00036–17. doi: 10.1128/MMBR.00036-17
- Moreno-Navarrete, J. M., Serino, M., Blasco-Baque, V., Azalbert, V., Barton, R. H., Cardellini, M., et al. (2018). Gut microbiota interacts with markers of adipose tissue browning, insulin action and plasma acetate in morbid obesity. *Mol. Nutr. Food Res.* 62:1700721. doi: 10.1002/mnfr.201700721
- Mosqueda-Solis, A., Sanchez, J., Portillo, M. P., Palou, A., and Pico, C. (2018). Combination of capsaicin and hesperidin reduces the effectiveness of each compound to decrease the adipocyte size and to induce browning features in adipose tissue of western diet fed rats. *J. Agric. Food Chem.* 66, 9679–9689. doi: 10.1021/acs.jafc.8b02611
- Murakami, Y., Ojima-Kato, T., Saburi, W., Mori, H., Matsui, H., Tanabe, S., et al. (2015). Supplemental epilactose prevents metabolic disorders through uncoupling protein-1 induction in the skeletal muscle of mice fed high-fat diets. *Br. J. Nutr.* 114, 1774–1783. doi: 10.1017/S0007114515003505
- Nedergaard, J., Bengtsson, T., and Cannon, B. (2007). Unexpected evidence for active brown adipose tissue in adult humans. *Am. J. Physiol. Endocrinol. Metab.* 293, E444–E452. doi: 10.1152/ajpendo.00691.2006
- Nedergaard, J., and Cannon, B. (2014). The browning of white adipose tissue: some burning issues. *Cell Metab.* 20, 396–407. doi: 10.1016/j.cmet.2014.07.005
- Neyrinck, A. M., Bindels, L. B., Geurts, L., Van Hul, M., Cani, P. D., and Delzenne, N. M. (2017). A polyphenolic extract from green tea leaves activates fat browning in high-fat-diet-induced obese mice. *J. Nutr. Biochem.* 49, 15–21. doi: 10.1016/j.jnutbio.2017.07.008
- Palou, A., Picó, C., Bonet, M. L., and Oliver, P. (1998). The uncoupling protein, thermogenin. *Int. J. Biochem. Cell Biol.* 30, 7–11. doi: 10.1016/S1357-2725(97)00065-4
- Palou, M., Sánchez, J., García-Carrizo, F., Palou, A., and Picó, C. (2015). Pectin supplementation in rats mitigates age-related impairment in insulin and leptin sensitivity independently of reducing food intake. *Mol. Nutr. Food Res.* 59, 2022–2033. doi: 10.1002/mnfr.201500292
- Pascale, A., Marchesi, N., Marelli, C., Coppola, A., Luzi, L., Govoni, S., et al. (2018). Microbiota and metabolic diseases. *Endocrine* 61, 357–371. doi: 10.1007/s12020-018-1605-5
- Perry, R. J., Peng, L., Barry, N. A., Cline, G. W., Zhang, D., Cardone, R. L., et al. (2016). Acetate mediates a microbiome-brain-beta-cell axis to promote metabolic syndrome. *Nature* 534, 213–217. doi: 10.1038/nature18309
- Petschow, B., Dore, J., Hibberd, P., Dinan, T., Reid, G., Blaser, M., et al. (2013). Probiotics, prebiotics, and the host microbiome: the science of translation. *Ann. N.Y. Acad. Sci.* 1306, 1–17. doi: 10.1111/nyas.12303
- Pico, C., and Palou, A. (2013). Perinatal programming of obesity: an introduction to the topic. *Front. Physiol.* 4:255. doi: 10.3389/fphys.2013.00255
- Requena, T., Martínez-Cuesta, M. C., and Pelaez, C. (2018). Diet and microbiota linked in health and disease. *Food Funct.* 9, 688–704. doi: 10.1039/C7FO01820G
- Roberfroid, M., Gibson, G. R., Hoyle, L., McCartney, A. L., Rastall, R., Rowland, I., et al. (2010). Prebiotic effects: metabolic and health benefits. *Br. J. Nutr.* 104(Suppl. 2), S1–S63. doi: 10.1017/S0007114510003363
- Rodríguez, A. M., and Palou, A. (2004). Uncoupling proteins: gender-dependence and their relation to body weight control. *Int. J. Obes. Relat. Metab. Disord.* 28, 327–329. doi: 10.1038/sj.ijo.0802579
- Rothwell, N. J., and Stock, M. J. (1979). A role for brown adipose tissue in diet-induced thermogenesis. *Nature* 281, 31–35. doi: 10.1038/281031a0
- Sahuri-Arisoylu, M., Brody, L. P., Parkinson, J. R., Parkes, H., Navaratnam, N., Miller, A. D., et al. (2016). Reprogramming of hepatic fat accumulation and “browning” of adipose tissue by the short-chain fatty acid acetate. *Int. J. Obes.* 40, 955–963. doi: 10.1038/ijo.2016.23
- Sakakibara, S., Yamauchi, T., Oshima, Y., Tsukamoto, Y., and Kadowaki, T. (2006). Acetic acid activates hepatic AMPK and reduces hyperglycemia in diabetic KK-A(y) mice. *Biochem. Biophys. Res. Commun.* 344, 597–604. doi: 10.1016/j.bbrc.2006.03.176
- Sanchez, D., Muguera, B., Moulay, L., Hernandez, R., Miguel, M., and Aleixandre, A. (2008). Highly methoxylated pectin improves insulin resistance and other cardiometabolic risk factors in Zucker fatty rats. *J. Agric. Food Chem.* 56, 3574–3581. doi: 10.1021/jf703598j
- Schonfeld, P., and Wojtczak, L. (2016). Short- and medium-chain fatty acids in energy metabolism: the cellular perspective. *J. Lipid Res.* 57, 943–954. doi: 10.1194/jlr.R067629
- Serrano, A., Asnani-Kishnani, M., Rodríguez, A. M., Palou, A., Ribot, J., and Bonet, M. L. (2018). Programming of the beige phenotype in white adipose tissue of adult mice by mild resveratrol and nicotinamide riboside supplementations in early postnatal life. *Mol. Nutr. Food Res.* 62:e1800463. doi: 10.1002/mnfr.201800463
- Slavin, J. (2013). Fiber and prebiotics: mechanisms and health benefits. *Nutrients* 5, 1417–1435. doi: 10.3390/nu5041417
- Somm, E., Henry, H., Bruce, S. J., Aeby, S., Rosikiewicz, M., Sykietis, G. P., et al. (2017).  $\beta$ -Klotho deficiency protects against obesity through a crosstalk between liver, microbiota, and brown adipose tissue. *JCI Insight* 2:91809. doi: 10.1172/jci.insight.91809
- Suárez-Zamorano, N., Fabbiano, S., Chevalier, C., Stojanović, O., Colin, D. J., Stevanović, A., et al. (2015). Microbiota depletion promotes browning of white adipose tissue and reduces obesity. *Nat. Med.* 21, 1497–1501. doi: 10.1038/nm.3994
- Teodoro, J. S., Zouhar, P., Flachs, P., Bardova, K., Janovska, P., Gomes, A. P., et al. (2014). Enhancement of brown fat thermogenesis using chenodeoxycholic acid in mice. *Int. J. Obes.* 38, 1027–1034. doi: 10.1038/ijo.2013.230
- Topping, D. L., and Clifton, P. M. (2001). Short-chain fatty acids and human colonic function: roles of resistant starch and nonstarch polysaccharides. *Physiol. Rev.* 81, 1031–1064. doi: 10.1152/physrev.2001.81.3.1031
- Trent, C. M., and Blaser, M. J. (2016). Microbially produced acetate: a “missing link” in understanding obesity? *Cell Metab.* 24, 9–10. doi: 10.1016/j.cmet.2016.06.023
- Villanueva-Millan, M. J., Perez-Matute, P., and Oteo, J. A. (2015). Gut microbiota: a key player in health and disease. A review focused on obesity. *J. Physiol. Biochem.* 71, 509–525. doi: 10.1007/s13105-015-0390-3
- Wang, S., Liang, X., Yang, Q., Fu, X., Zhu, M., Rodgers, B. D., et al. (2017). Resveratrol enhances brown adipocyte formation and function by activating AMP-activated protein kinase (AMPK)  $\alpha$ 1 in mice fed high-fat diet. *Mol. Nutr. Food Res.* 61. doi: 10.1002/mnfr.2016.00746
- Wang, S., Zhu, M. J., and Du, M. (2015). Prevention of obesity by dietary resveratrol: how strong is the evidence? *Expert Rev. Endocrinol. Metab.* 10, 561–564. doi: 10.1586/17446651.2015.1096771
- Watanabe, M., Houten, S. M., Matak, C., Christoffolete, M. A., Kim, B. W., Sato, H., et al. (2006). Bile acids induce energy expenditure by promoting intracellular thyroid hormone activation. *Nature* 439, 484–489. doi: 10.1038/nature04330
- Weitkunat, K., Stuhlmann, C., Postel, A., Rumberger, S., Fankhänel, M., Woting, A., et al. (2017). Short-chain fatty acids and inulin, but not guar gum, prevent diet-induced obesity and insulin resistance through differential mechanisms in mice. *Sci. Rep.* 7:6109. doi: 10.1038/s41598-017-06447-x
- Wu, J., Boström, P., Sparks, L. M., Ye, L., Choi, J. H., Giang, A. H., et al. (2012). Beige adipocytes are a distinct type of thermogenic fat cell in mouse and human. *Cell* 150, 366–376. doi: 10.1016/j.cell.2012.05.016
- You, Y., Han, X., Guo, J., Guo, Y., Yin, M., Liu, G., et al. (2018). Cyanidin-3-glucoside attenuates high-fat and high-fructose diet-induced obesity by promoting the thermogenic capacity of brown adipose tissue. *J. Funct. Foods* 41:10. doi: 10.1016/j.jff.2017.12.025
- You, Y., Yuan, X., Lee, H. J., Huang, W., Jin, W., and Zhan, J. (2015). Mulberry and mulberry wine extract increase the number of mitochondria during brown adipogenesis. *Food Funct.* 6, 401–408. doi: 10.1039/C4FO00719K



- You, Y., Yuan, X., Liu, X., Liang, C., Meng, M., Huang, Y., et al. (2017). Cyanidin-3-glucoside increases whole body energy metabolism by upregulating brown adipose tissue mitochondrial function. *Mol. Nutr. Food Res.* 61. doi: 10.1002/mnfr.201700261
- Zhang, Y. J., Li, S., Gan, R. Y., Zhou, T., Xu, D. P., and Li, H. B. (2015). Impacts of gut bacteria on human health and diseases. *Int. J. Mol. Sci.* 16, 7493–7519. doi: 10.3390/ijms16047493
- Zietak, M., Chabowska-Kita, A., and Kozak, L. P. (2017). Brown fat thermogenesis: stability of developmental programming and transient effects of temperature and gut microbiota in adults. *Biochimie* 134, 93–98. doi: 10.1016/j.biochi.2016.12.006
- Zietak, M., Kovatcheva-Datchary, P., Markiewicz, L. H., Ståhlman, M., Kozak, L. P., and Bäckhed, F. (2016). Altered microbiota contributes to reduced diet-induced obesity upon cold exposure. *Cell Metab.* 23, 1216–1223. doi: 10.1016/j.cmet.2016.05.001
- Zietak, M., and Kozak, L. P. (2016). Bile acids induce uncoupling protein 1-dependent thermogenesis and stimulate energy expenditure at thermoneutrality in mice. *Am. J. Physiol. Endocrinol. Metab.* 310, E346–E354. doi: 10.1152/ajpendo.00485.2015

**Conflict of Interest Statement:** The authors declare that the research was conducted in the absence of any commercial or financial relationships that could be construed as a potential conflict of interest.

Copyright © 2019 Reynés, Palou, Rodríguez and Palou. This is an open-access article distributed under the terms of the Creative Commons Attribution License (CC BY). The use, distribution or reproduction in other forums is permitted, provided the original author(s) and the copyright owner(s) are credited and that the original publication in this journal is cited, in accordance with accepted academic practice. No use, distribution or reproduction is permitted which does not comply with these terms.



# Opposing Actions of Adrenocorticotrophic Hormone and Glucocorticoids on UCP1-Mediated Respiration in Brown Adipocytes

Katharina Schnabl<sup>1,2,3</sup>, Julia Westermeier<sup>1,2</sup>, Yongguo Li<sup>1,2</sup> and Martin Klingenspor<sup>1,2,3\*</sup>

<sup>1</sup> Chair for Molecular Nutritional Medicine, TUM School of Life Sciences Weihenstephan, Technical University of Munich, Freising, Germany, <sup>2</sup> EKFZ – Else Kröner-Fresenius Zentrum for Nutritional Medicine, Technical University of Munich, Freising, Germany, <sup>3</sup> ZIEL – Institute for Food & Health, Technical University of Munich, Freising, Germany

## OPEN ACCESS

### Edited by:

Rita De Matteis,  
Università degli Studi di Urbino  
Carlo Bo, Italy

### Reviewed by:

Alessandro Bartolomucci,  
University of Minnesota Twin Cities,  
United States  
Vicente Lahera,  
Complutense University of Madrid,  
Spain

### \*Correspondence:

Martin Klingenspor  
mk@tum.de

### Specialty section:

This article was submitted to  
Integrative Physiology,  
a section of the journal  
Frontiers in Physiology

**Received:** 08 October 2018

**Accepted:** 21 December 2018

**Published:** 17 January 2019

### Citation:

Schnabl K, Westermeier J, Li Y  
and Klingenspor M (2019) Opposing  
Actions of Adrenocorticotrophic  
Hormone and Glucocorticoids on  
UCP1-Mediated Respiration in Brown  
Adipocytes. *Front. Physiol.* 9:1931.  
doi: 10.3389/fphys.2018.01931

Brown fat is a potential target in the treatment of metabolic disorders as recruitment and activation of this thermogenic organ increases energy expenditure and promotes satiation. A large variety of G-protein coupled receptors, known as classical drug targets in pharmacotherapy, is expressed in brown adipocytes. In the present study, we analyzed transcriptome data for the expression of these receptors to identify potential pathways for the recruitment and activation of thermogenic capacity in brown fat. Our analysis revealed 12 G<sub>s</sub>-coupled receptors abundantly expressed in murine brown fat. We screened ligands for these receptors in brown adipocytes for their ability to stimulate UCP1-mediated respiration and *Ucp1* gene expression. Adrenocorticotrophic hormone (ACTH), a ligand for the melanocortin 2 receptor (MC2R), turned out to be the most potent activator of UCP1 whereas its capability to stimulate *Ucp1* gene expression was comparably low. Adrenocorticotrophic hormone is the glandotropic hormone of the endocrine hypothalamus–pituitary–adrenal-axis stimulating the release of glucocorticoids in response to stress. In primary brown adipocytes ACTH acutely increased the cellular respiration rate similar to isoproterenol, a  $\beta$ -adrenergic receptor agonist. The effect of ACTH on brown adipocyte respiration was mediated via the MC2R as confirmed by using an antagonist. Inhibitor-based studies revealed that ACTH-induced respiration was dependent on protein kinase A and lipolysis, compatible with a rise of intracellular cAMP in response to ACTH. Furthermore, it is dependent on UCP1, as cells from UCP1-knockout mice did not respond. Taken together, ACTH is a non-adrenergic activator of murine brown adipocytes, initiating the canonical adenylyl cyclase–cAMP–protein kinase A–lipolysis–UCP1 pathway, and thus a potential target for the recruitment and activation of thermogenic capacity. Based on these findings in primary cell culture, the physiological significance might be that cold-induced ACTH in concert with norepinephrine released from sympathetic

nerves contributes to BAT thermogenesis. Notably, dexamethasone attenuated isoproterenol-induced respiration. This effect increased gradually with the duration of pretreatment. *In vivo*, glucocorticoid release triggered by ACTH might oppose beta-adrenergic stimulation of metabolic fuel combustion in BAT and limit stress-induced hyperthermia.

**Keywords: glucocorticoids (GC), brown adipose tissue, non-adrenergic activation, non-shivering thermogenesis, uncoupling protein 1, adrenocorticotrophic hormone, obesity**

## INTRODUCTION

We are facing a worldwide epidemic of obesity, a major risk factor in the development of non-communicable diseases such as diabetes mellitus and arteriosclerosis. In 2016, 1.9 billion adults aged 18 and over were overweight, of which 650 million were obese, representing an almost threefold increase in obesity prevalence since 1975 (WHO, 2018). Obesity is the state of excessive white adipose tissue (WAT) accumulation caused by prolonged positive energy balance. In mammals there is a second type of adipose tissue, brown adipose tissue (BAT), which in contrast to WAT generates heat in response to cold exposure and food consumption (Rosen and Spiegelman, 2006; Vosselman et al., 2013; U Din et al., 2018). It dissipates the chemical energy of macro-nutrients by uncoupling oxygen consumption from ATP synthesis in mitochondria (Klingenspor, 2003). This mechanism, known as non-shivering thermogenesis, is dependent on the presence of mitochondrial uncoupling protein 1 (UCP1), which is a unique feature of brown adipocytes. The activation of BAT increases energy expenditure and opposes positive energy balance. In addition to the activation of UCP1, it is worth noting that cold exposure also induces the thermogenic gene expression program and thereby recruits thermogenic capacity in brown fat (Cannon and Nedergaard, 2004). Furthermore, brown-like adipocytes, also known as inducible brown fat cells, beige (Ishibashi and Seale, 2010) or “brite” (brown-in-white) (Petrovic et al., 2010) adipocytes, can be found interspersed in WAT (Li et al., 2014a). Similar to brown adipocytes in classical brown fat depots brite adipocyte abundance can be increased by adrenergic stimulation (Galmozzi et al., 2014) and cold exposure (Maurer et al., 2015) in a process coined browning of WAT. Besides activation and recruitment of BAT, the browning of WAT displays therapeutic potential with regard to the development of new obesity treatment strategies.

For a long time, the occurrence of metabolically active BAT was believed to be restricted to hibernators, small mammals and human newborns. Adult humans, however, also have metabolically active BAT, as demonstrated by the detection of cold-induced uptake of tracers for glucose, fatty acids and acetate with positron emission tomography (Cypess et al., 2009, 2015; van Marken Lichtenbelt et al., 2009; Virtanen et al., 2009; Ouellet et al., 2011). Furthermore, cold-induced BAT activity is strongly reduced in obese (Saito et al., 2009) and diabetic patients and can be recovered by cold acclimation (van Marken Lichtenbelt et al., 2009).

On this background BAT displays a focal point of current research as it harbors a remarkable capacity to evoke energy

expenditure through UCP1 dependent energy dissipation. The recruitment and activation of BAT and appears as an attractive and potentially effective strategy for the prevention and treatment of obesity (Tseng et al., 2010). Importantly, in the attempt to increase energy expenditure, the recruitment of more brown adipocytes with higher UCP1 expression and higher respiration capacity is required, but not sufficient. UCP1 is not constitutively active, but rather must be activated to dissipate mitochondrial proton-motive force as heat. This activation of UCP1 is inevitable to increase carbohydrate and lipid oxidation. Beyond boosting energy expenditure, we recently demonstrated that meal-induced activation of BAT thermogenesis also induces satiation which might also be applicable to promote negative energy balance (Li et al., 2018).

As sympathomimetic drugs exhibit unwanted detrimental cardiovascular effects, their application as BAT-stimulating agents is considered problematic (Cypess et al., 2015). Thus, the identification of druggable non-adrenergic regulators of BAT is one step toward the modulation of the heating organ as a regulator of energy expenditure and body fat in humans.

Besides the  $\beta$ -adrenergic receptors mature brown adipocytes express a variety of around 230 other G protein-coupled receptors (GPCRs) (Klepac et al., 2016) which are responsible for transferring extracellular signals to the cytosol. GPCRs group in a large family of seven transmembrane proteins (Lefkowitz, 2007; Kobilka, 2011) that regulate important biological processes in diverse tissues including adipose tissues (Wettschurek and Offermanns, 2005; Latek et al., 2012). Approximately 30% of all approved drugs target GPCRs, illustrating their importance in disease and therapeutics (Hauser et al., 2017; Santos et al., 2017). These receptors are coupled to heterotrimeric G proteins which are composed of  $\alpha$ ,  $\beta$ , and  $\gamma$  subunits. Ligand binding and thus activation of GPCRs leads to the dissociation of  $G\alpha$  from the  $G\beta\gamma$  dimer, allowing the binding and regulation of signaling effectors. The downstream signaling of GPCRs is in part determined by their G protein coupling (Neves et al., 2002). There are four main sub-classes of  $G\alpha$  proteins:  $G_s$ ,  $G_i$ ,  $G_q$  and  $G_{12/13}$ . Activation of  $G_s$  and  $G_i$  leads to the stimulation or inhibition the second messenger cyclic adenosine monophosphate (cAMP), respectively, while  $G_q$  activates phospholipase C and thus, to an increase of inositol triphosphate.  $G_{12/13}$  activates the small GTPase Rho, a pathway also known to be modulated by  $G_q$  family proteins (Buhl et al., 1995; Wang et al., 2013). Due to cAMP-PKA activating properties the analysis of BAT GPCRs has mainly focused on  $G_s$ -coupled receptors [for example,  $\beta$ -adrenergic (Cannon and Nedergaard, 2004) and adenosine receptors (Gnad et al., 2014)] as they have the potency to activate

UCP1-dependent thermogenesis. Cold-exposure induced release of norepinephrine from sympathetic nerves in BAT activates canonical adenylyl cyclase – cAMP – protein kinase A (PKA) signaling via  $\beta$ -adrenergic receptors. This pathway stimulates lipolysis and activation of UCP1 and therefore induces non-shivering thermogenesis (Klingenspor et al., 2017). Lipolysis plays a crucial role and is an essential requirement for UCP1 activation. Indeed, pharmacological inhibition of ATGL and HSL, the two lipases which catalyze the first two steps in the hydrolysis of triglycerides, completely diminishes adrenergic stimulation of thermogenesis (Li et al., 2014b).

The aim of the present study was to investigate a selection of non-adrenergic  $G_s$ -coupled GPCRs in the light of their ability to activate and recruit UCP1-mediated thermogenesis in brown adipocytes.

## MATERIALS AND METHODS

### Materials

Murine ACTH<sub>(1–39)</sub> trifluoroacetate salt was purchased from Bachem (H-4998), ACTH<sub>(4–10)</sub> was ordered from Abcam (ab142255), and the synthetic ACTH<sub>(4–10)</sub> analog was synthesized and obtained from JPT Peptide Technologies GmbH. H89 was purchased from Tocris. Atglistatin and Hi 76-0079 were a kind gift from Prof. Robert Zimmermann. All other chemicals were ordered from Sigma unless otherwise specified. MC2R antagonist GPS1573 was purchased from Abbiotech (Bouw et al., 2014).

### Animals and Primary Cell Culture

All mice were bred at the specific-pathogen free animal facility of the Technical University of Munich registered at the local authorities according to §11 of the German Animal Welfare Act (Az32-568, 01/22/2015). In the present study, mice were killed for the dissection of tissues in deep CO<sub>2</sub> anesthesia as approved by the ethics committee of the state supervisory authority (Government of Upper Bavaria). They had *ad libitum* access to food and water and were maintained at 22 ± 1°C and 50–60% relative humidity in a 12 h:12 h light:dark cycle. Male 129S6/SvEvTac, 129S1/SvEvTac mice (UCP1<sup>−/−</sup> mice and wild-type littermates UCP1<sup>+/+</sup>) and heterozygous C57BL/6N Ucp1 dual-reporter gene mice (C57BL/6NTac-Ucp1tm3588<sup>(Luciferase-T2A-iRFP-T2A-Ucp1)</sup>Arte named here as Ucp1<sup>+/ki</sup>) aged 5–6 weeks, were used to prepare primary cultures of brown and white adipocytes. Latter simultaneously express firefly luciferase and near-infrared fluorescent protein 713 (iRFP713). The *Luciferase-T2A-iRFP713-T2A* sequence was introduced into the 5′-untranslated region of the endogenous *Ucp1* gene (Wang et al., 2018). Interscapular brown and inguinal WATs were dissected and digested with collagenase as described previously (Li et al., 2014a). Stromal vascular fraction cells were seeded, grown to confluency and differentiated into mature adipocytes following a standard protocol. Adipocyte differentiation was induced for 48 h with 5 µg/ml insulin, 1 nM 3,3′,5-triiodo-L-thyronine (T3), 125 µM indomethacin, 500 µM isobutylmethylxanthine (IBMX) and 1 µM dexamethasone

in adipocyte culture media (DMEM supplemented with 10% heat-inactivated FBS, penicillin/streptomycin). Cells were then maintained in adipocyte culture media supplemented with 5 µg/ml insulin and 1 nM T3 for 6 days with media changes every 2 days. Assays were performed on day 7 of differentiation.

### Luciferase Assay

After overnight stimulation of primary brown adipocytes of Ucp1<sup>ki/ki</sup> mice luciferase activity was assayed using a commercial kit system (Luciferase Assay System Freezer Pack E4030, Promega GmbH). Primary cells were lysed in 1x reporter lysis buffer by shaking for 20 min at room temperature. 10 µl lysate was mixed with 50 µl luciferase assay substrate solution, and the mixture was measured by FB12 in a luminometer (Single Tube Luminometer, Titertek-Berthold GmbH). Bioluminescence readouts were normalized to total protein content.

### Respiration Assays

Oxygen consumption of primary brown adipocytes was measured at 37°C using microplate-based respirometry (XF96 extracellular flux analyzer, Seahorse Bioscience) as described previously (Li et al., 2014b) following the subsequent protocol at day 7 of differentiation. Prior to the respiration measurement, primary cells were washed with warmed, unbuffered assay medium (DMEM basal medium supplemented with 25 mM glucose, 31 mM NaCl, 2 mM GlutaMax and 15 mg/l phenol red, pH 7.4) (basal assay medium). Subsequent to the medium replacement with basal assay medium containing 1–2% essentially fatty acid free bovine serum albumin (BSA), cells were incubated at 37°C in a CO<sub>2</sub>-free incubator for 1 h. Assay reagents were loaded into the drug injections ports of the sensor cartridges at 10X in basal assay medium (no BSA). After assessment of basal oxygen consumption in untreated cells oligomycin (5 µM) was injected to inhibit coupled respiration and to determine basal leak respiration. Next, effector was added to investigate UCP1-dependant uncoupled respiration. By the addition of FCCP (1 µM) maximal respiratory capacity was determined. Lastly, non-mitochondrial oxygen consumption was assessed by blocking mitochondrial respiration with antimycin A (5 µM). For some experiments, cells were pretreated for 1 h with 50 µM H89 (PKA inhibitor), 1–100 µM propranolol ( $\beta$ -adrenergic receptor antagonist), 40 µM Atglistatin (ATGL inhibitor) and 40 µM Hi76-0079 (HSL inhibitor) 1 h prior to the measurement. Oxygen consumption rates were automatically calculated by the Seahorse XF-96 software. Each experiment was repeated at least three times with similar results and five to eight replicate wells for every condition in each independent experiment. Results are predominately expressed as stimulated respiration which is calculated as fold increase of basal leak.

### Gene Expression Analysis (qRT-PCR)

Total RNA was isolated using Trisure (Bioline) and purified with SV total RNA Isolation System (Promega). Reverse transcriptase reactions were performed using SensiFAST cDNA Synthesis Kit (Bioline). Quantitative real-time PCR (qRT-PCR) was performed with SYBR green fluorescent dye in 384-well format using LightCycler 480 (Roche). General Transcription Factor IIB



(Gtf2b) served as an internal control. To be able to calculate relative gene expression levels of samples, standard reactions containing serial diluted pooled cDNA of all samples (Pure, 1:2, 1:4, 1:8, 1:16, 1:32 and 1:64) as a template were used to establish a standard curve. The RNA abundance of *Ucp1* gene was normalized to the housekeeping gene *Gtf2b*. The following primers were used:

Ucp1	F: 5'-GTACACCAAGGAAGGACCGA-3',
	R: 5'-TTTATTCGTGGTCTCCCAGC-3';
Gtf2b	F: 5'-TGGAGATTTGTCCACCATGA-3',
	R: 5'-GAATTGCCAACTCATCAAACT-3'.

## Western Blot Analysis

Primary brown adipocytes were lysed in RIPA buffer for western blot analysis. 30 µg of total lysates were separated by SDS-PAGE (12.5% gels), transferred to Odyssey® nitrocellulose membrane (Millipore), and probed with anti-UCP1 (1:10,000; ab10983, Abcam), and anti-Actin (1:10,000; MAB1501, Millipore). Secondary antibodies conjugated to IRDye™ 680 or IRDye™ 800 (Licor Biosciences) were incubated at a dilution of 1:20,000. Fluorescent images were captured by Odyssey infrared imaging system (Licor Biosciences).

## Quantification of Cellular cAMP

Changes in cytosolic cAMP concentrations were determined in primary brown adipocytes in response to ACTH- or isoproterenol stimulation using cAMP-Glo Assay (Promega) following the manufacturer's instructions.

## Statistical Analysis

Significant differences for single comparisons were assessed by two-tailed Student's *t*-test. Analysis of variance (ANOVA) with Tukey's *post hoc* tests were used for multiple comparisons (GraphPad Prism 6.0 software). *P*-values < 0.05 were considered a statistically significant difference. All data are presented as mean ± SD.

# RESULTS

## G<sub>s</sub>-Coupled GPCRs Abundantly Expressed in Brown Adipose Tissue

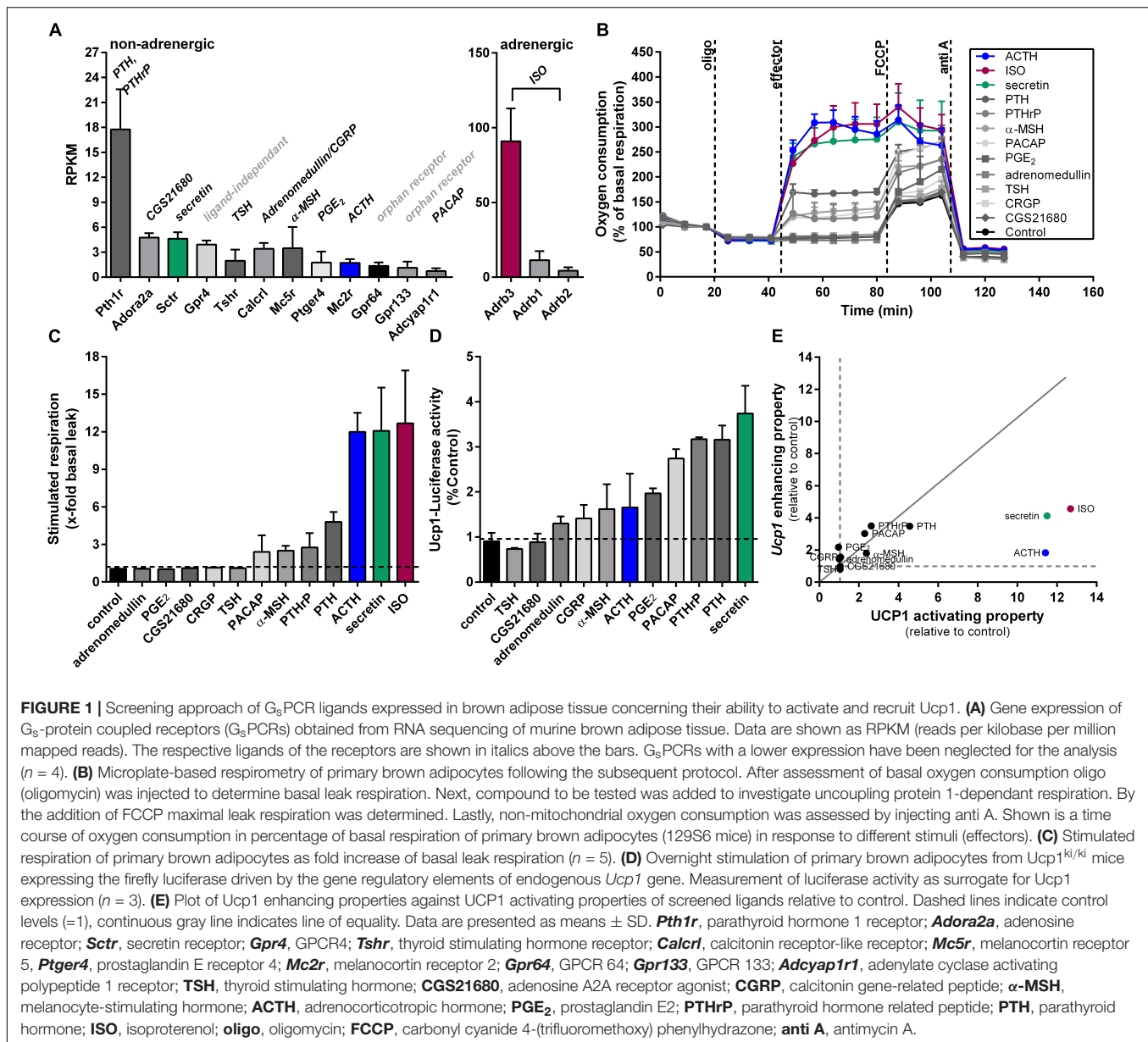
In our search for non-adrenergic targets to activate and recruit UCP1 in BAT, we identified 12 G<sub>s</sub>-protein coupled receptors (GPCRs) expressed in the interscapular BAT of mice (C57BL/6J, 12 weeks old, room temperature, chow diet) at different abundances (threshold was set at RPKM > 1) based on our recently published RNA-seq data (GEO: GSE119452). Among these G<sub>s</sub>PCRs, parathyroid hormone receptor (*Pthr*) showed the highest abundance, whereas adenylyl cyclase activating polypeptide 1 receptor concluded with the lowest expression (Figure 1A). GPCR64 and GPCR133 turned out to be adhesion receptors and GPCR4 is reported to carry out ligand independent signaling mediated through proton-sensing mechanisms (Ludwig et al., 2003; Bohnekamp and Schoneberg, 2011). We therefore excluded these three receptors for further investigations. In

comparison to non-adrenergic receptors, the genes encoding for the β-adrenergic receptors ADRB1/2/3 showed most abundant expression in murine BAT, with *Adrb3* standing out with the highest expression. We used Isoproterenol, a non-selective β-adrenoreceptor agonist, to activate β-adrenergic signaling in brown adipocytes. For all other non-adrenergic receptors, the corresponding ligands were selected to test their capability to activate and recruit UCP1. In case of PTHR and calcitonin gene-related peptide receptor (CALCRL), two established ligands were chosen (Chang et al., 2004; Dean et al., 2006).

## Reporter-Assays and Cellular Respirometry Screening of G<sub>s</sub>-Coupled GPCR Ligands for UCP1 Activity and Regulation

In our first screen, we tested whether these G<sub>s</sub>PCR ligands can activate oxygen consumption acutely in brown adipocytes. UCP1-mediated uncoupled respiration was quantified in cultured adherent intact primary brown adipocytes, according to a protocol established in our lab (Li et al., 2014b). After recording basal respiration and the fraction of coupled and uncoupled respiration, UCP1-dependent respiration was measured. Finally, maximal respiratory capacity and non-mitochondrial oxygen consumption were assessed by adding the uncoupling agent carbonyl cyanide 4-(trifluoromethoxy) phenylhydrazone (FCCP) and antimycin A was added to block the electron transport chain, respectively. All respiration assays were performed in the presence of BSA to buffer free fatty acid (FFA) levels in the respiration medium. For ACTH and secretin, we observed the most prominent induction of UCP1-dependant uncoupled respiration. The potency of these two peptides was comparable to ISO, the β-adrenergic receptor agonist. Both PTH and its related peptide both stimulated UCP1-dependant respiration, although the effect was modest compared to ISO. The weakest effects on cellular respiration were observed for PACAP and α-MSH. All other ligands failed to increase basal leak respiration (Figures 1B,C).

We then measured FLUC activity in primary brown adipocytes from *Ucp1<sup>ki/ki</sup>* reporter gene mice to determine the effect of the G<sub>s</sub>PCR ligands on *Ucp1* gene expression in response to overnight stimulation. As the expression of *Fluc* in these cells is driven by *Ucp1* promoter, FLUC activity served as a surrogate for *Ucp1* expression. We found highest FLUC activities in response to secretin, parathyroid hormone (PTH), parathyroid hormone related peptide (PTHrP), and pituitary adenylyl cyclase-activating peptide (PACAP) (Figure 1D). Prostaglandin E2 (PGE2), adrenocorticotrophic hormone (ACTH) and α-melanocyte-stimulating hormone (α-MSH) showed a moderate rise in FLUC activity. The two ligands for calcitonin receptor-like receptor (CALCRL), calcitonin gene-related peptide (CGRP), and adrenomedullin only had minor effects, whereas thyroid hormone and the adenosine 2A receptor agonist CGS21680 had no effect on FLUC (Figure 1D). Comparing the effect sizes for all ligands on the ability to activate respiration and to recruit *Ucp1* expression, ACTH and secretin were most potent to acutely activate respiration. Notably, although secretin,



PTH and PTHrP showed comparable strong induction of FLUC activity, PTH and PTHrP were much less potent as secretin in the acute activation assay. Moreover, ACTH matched secretin in the acute activation assay, but was much less potent to induce FLUC (Figure 1E). Based on the pronounced and relatively preferential stimulatory effect of ACTH on UCP1-mediated respiration we chose the ACTH to further investigate its thermogenic properties.

## ACTH Activates Respiration via the Canonical cAMP-PKA-Lipolysis Pathway

The hypothalamic–pituitary–adrenal (HPA) axis plays a critical role in maintaining homeostasis and in mounting appropriate responses to stress. Key components of the stress response are aimed at providing adequate amounts of glucocorticoids which

exert pleiotropic effects on energy supply, fuel metabolism, immunity and cardiovascular function. The melanocortin ACTH is the glandotropic hormone of the HPA which stimulates synthesis and release of glucocorticoids by the cortex of the adrenal gland. The 39 amino acid peptide hormone is synthesized within the anterior pituitary by corticotrophic cells as a much larger, 241-amino-acid precursor known as proopiomelanocortin (POMC) in response to tonic control from the hypothalamus by corticotrophin-releasing hormone (CRH). ACTH is able to activate all five  $G_s$ -protein coupled melanocortin receptors, but at physiological circulating plasma levels, the sensitivity of all receptors, except MC2R, is so low that they are not activated. In rodent adipocytes, ACTH binds to the MC2R, which stimulates lipolysis via  $G_s$ -coupled cAMP-PKA mediated phosphorylation of HSL (Cho et al., 2005).

Since ACTH was previously reported to stimulate uncoupled respiration in the immortalized murine white fat cell line T37i (van den Beukel et al., 2014), we next investigated UCP1-mediated respiration and its respective signaling pathway in primary brown adipocytes. In a dose-response experiment we found that 200 nM ACTH stimulated respiration, defined as fold increase of respiration over basal leak respiration, with the most robust effect at 1  $\mu$ M ACTH (Figure 2A). This effect of ACTH on brown adipocyte respiration was independent of adrenergic receptors, since pre-treatment of the cells with propranolol, a non-selective  $\beta$ -adrenergic receptor antagonist, did not attenuate ACTH stimulated respiration while blocking the effect of ISO in a dose-dependent manner (Figure 2B). The effect of ACTH, however, depends on MC2R, as pretreatment with the MC2R antagonist GPS1573 (100 nM and 750 nM) blunted the effects of ACTH on oxygen consumption (Figure 2C). ACTH stimulation of primary

brown adipocytes resulted in a dose-dependent increase of cytosolic cAMP levels. Compared to ISO, however,  $EC_{50}$  of ACTH was approximately 165-fold higher (9.415 nM vs. 1.493  $\mu$ M) (Figure 2D). Pre-treatment of cells with H89, a selective inhibitor of PKA (Figure 2E), or inhibitors targeting the two essential lipases involved in lipolysis (ATGL, adipose triglyceride lipase; HSL, hormone-sensitive lipase), completely blocked the effect on respiration of ACTH (Figure 2F). The stimulating effect of ACTH depended on UCP1 as it was attenuated in primary brown adipocytes of UCP1<sup>-/-</sup> compared to UCP1<sup>+/+</sup> (Figure 2G). As the ACTH-induced stimulated respiration was dependent on UCP1, we consider the effect of the ACTH on brown adipocytes as thermogenic.

Taken together, ACTH activates UCP1-dependent respiration in primary brown adipocytes via the canonical cAMP-PKA-lipolysis pathway.

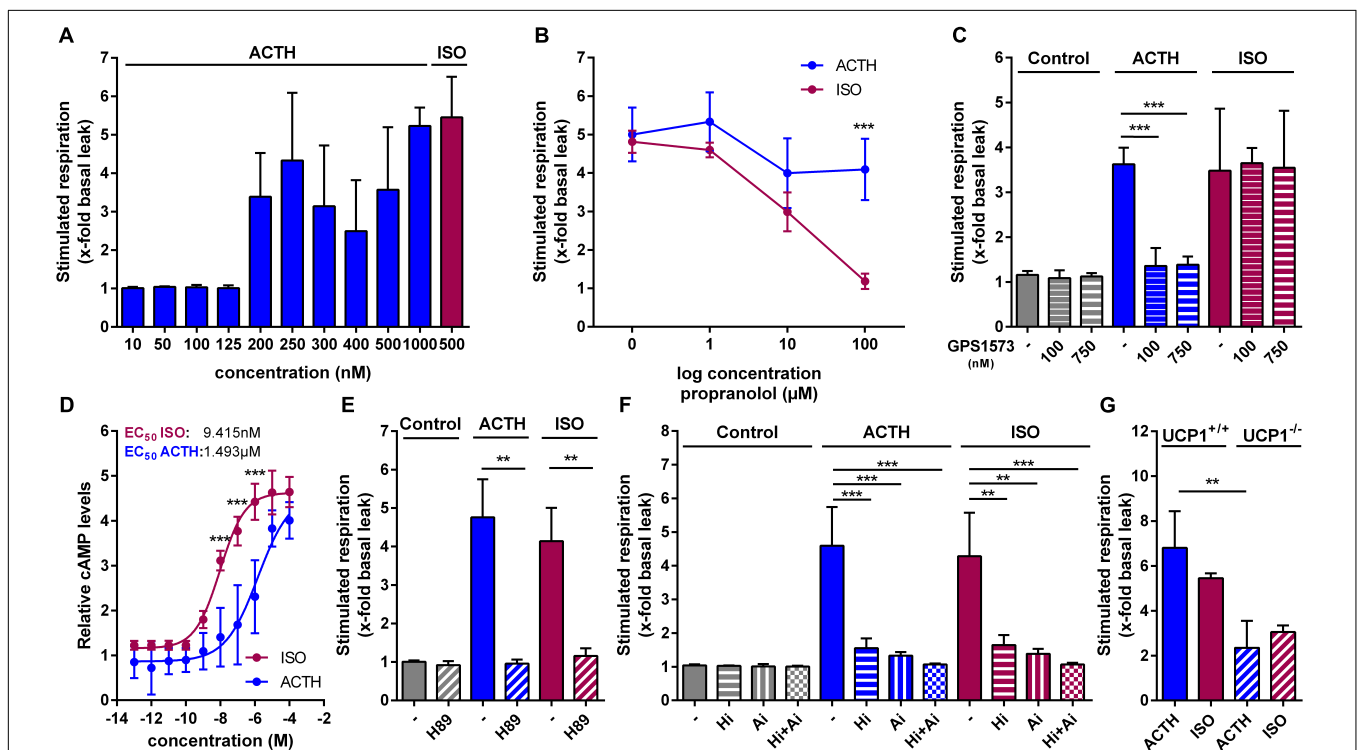


**FIGURE 2 |** ACTH activates UCP1 via the canonical cAMP-PKA-lipolysis pathway. Oxygen consumption of primary brown adipocytes was assessed using microplate-based respirometry. First, basal respiration was determined and then, oligomycin (oligo) was added, which inhibits adenosine triphosphate (ATP) synthase resulting in basal leak respiration. UCP1 mediated uncoupled respiration was determined after injection of isoproterenol (ISO, 0.5  $\mu$ M) as a positive control or adrenocorticotrophic hormone (ACTH, 1  $\mu$ M). Next, carbonyl cyanide 4-(trifluoromethoxy) phenylhydrazone (FCCP), an uncoupler that allows assessment of maximal respiratory capacity, was added. Finally, antimycin A (anti A) was added in order to determine non-mitochondrial respiration. (A) Dose-response experiment revealing most robust effects at a ACTH concentration of 1  $\mu$ M assessed as stimulated respiration as fold increase of basal leak respiration. (B) ACTH- and ISO-stimulated respiration after 1 h pretreatment with different concentrations of propranolol, a non-selective blocker of adrenergic  $\beta$ -receptors ( $n = 4$ ). (C) Effects of different concentrations of GPS1573 (100 nM and 750 nM), a MC2R antagonist, on ACTH- and ISO-stimulated UCP1-mediated uncoupled respiration. (D) Cytosolic cAMP abundance after stimulation with increasing ACTH and ISO concentrations for 30 min ( $n = 3$ ). (E) Fold increase of basal leak respiration after stimulation with ISO, ACTH and vehicle (control, assay medium) with or without protein kinase A inhibitor H89 (50  $\mu$ M). Inhibitor was injected together with oligo prior to addition of stimulators ( $n = 4$ ). (F) Respiration stimulated by ISO, ACTH or vehicle as fold increase of basal leak after 1 h pre-treatment with lipolysis inhibitors Ai (Atglstatin, ATGL-inhibitor, 40  $\mu$ M) and Hi (Hi76-0079, HSL-inhibitor, 40  $\mu$ M) ( $n = 4$ ). (G) Stimulated respiration of primary brown adipocytes from UCP1<sup>+/+</sup> and UCP1<sup>-/-</sup> mice ( $n = 3$ ). Data are presented as means  $\pm$  SD. (B,D,E,F) were analyzed by two-way ANOVA (Tukey's test). (C,E,F) were analyzed by unpaired  $t$ -test. (D)  $EC_{50}$  was determined by non-linear regression analysis. \* $p < 0.05$ , \*\* $p < 0.01$ , \*\*\* $p < 0.001$ .

## ACTH Increases *Ucp1* Expression in Primary Brown and White Adipocytes

Next, we aimed to investigate the effect of ACTH on *Ucp1* gene expression in primary brown and white adipocytes. Indeed, treatment of differentiated brown and white adipocytes with two different doses of ACTH caused a dose-dependent increase in *Ucp1* mRNA levels (Figures 3A,B). The maximal induction of *Ucp1* mRNA achieved by 1  $\mu$ M ACTH was comparable to the effect of ISO treatment (500 nM). Concomitant, UCP1 protein was also induced either by ACTH or ISO in primary brown adipocytes. This effect on gene expression was more pronounced after 12 h of stimulation compared to 8 h, and was dose-dependent. At a concentration of 1  $\mu$ M, ACTH and ISO were equipotent in recruiting UCP1 protein in primary brown adipocytes (Figures 3C–E).

## A Synthetic ACTH Fragment Slightly Stimulates Respiration and Increases *Ucp1* mRNA Level in Primary Brown Adipocytes

We showed that both ACTH and  $\alpha$ -MSH are capable in stimulating uncoupled respiration (Figures 1B,C). The heptapeptide sequence, Met-Glu-His-Phe-Arg-Trp-Gly, is common to all the adrenocorticotrophic (ACTH), melanotropic (MSH), and lipotropic (LPH) hormones. Structure function studies on melanocortin peptides from the early 1970s using stimulation of lipolysis as a criterion for biological potency revealed that the heptapeptide core sequence exerts biological activity. An amino acid exchange from Glu to Arg in the ACTH core sequence resulted in a fourfold increased activity on the release of FFAs compared to the natural ACTH core sequence (Draper et al., 1973). As lipolysis is an essential prerequisite for the activation of UCP1, we included both the natural and the synthetic version of the ACTH fragment in our study. In primary brown adipocytes, the natural core sequence of ACTH [ACTH<sub>(4–10)</sub>] had no impact on respiration (Figures 4A,B), but significantly increased *Ucp1* mRNA expression, although not to the extent as seen for ISO (Figure 4C). The mutant ACTH fragment [synACTH<sub>(4–10)</sub>] showed limited potential to activate UCP1 as it mildly increased respiration (Figures 4D,E). The induction of *Ucp1* mRNA expression was comparable to that of the natural heptapeptide (Figure 4F). As it turned out, the synthetic ACTH fragment has potential to stimulate both thermogenic capacity and activity, and therefore is a potential non-adrenergic activator of BAT thermogenesis.

## Acute Glucocorticoid Treatment Attenuates $\beta$ 3-Adrenergic Signaling but Does Not Affect Thermogenic Effects of ACTH

To address the physiological role of ACTH in brown fat thermogenesis we analyzed the expression of its receptor in BAT of mice in response to cold exposure. Indeed, *Mc2r* is down-regulated in response to cold (Figure 5A) indicating that its contribution to cold-induced BAT thermogenesis might be

rather minor. Nevertheless, subsequent to cold exposure plasma ACTH levels are significantly increased (van den Beukel et al., 2014). Basically, ACTH triggers the release of glucocorticoids from the cortex of the adrenal gland. Circulating glucocorticoids exert negative feedback control on the secretion of CRH and ACTH from the hypothalamus and the anterior pituitary. In addition, it is known that corticosterone reduces *Ucp1* mRNA and UCP1 protein in response to both adrenergic stimulation and ACTH treatment (Soumano et al., 2000; van den Beukel et al., 2014). Furthermore, glucocorticoids may exert rapid non-genomic effects mediated by a putative membrane-bound receptor as reported for the murine brain (Nahar et al., 2016; Shaqura et al., 2016). Therefore, we finally investigated the acute effect of treatment with the glucocorticoid dexamethasone (Dexa) on  $\beta$ -adrenergic and ACTH signaling. Therefore we pretreated primary brown adipocytes with 5  $\mu$ M Dexa for 0–4 h and analyzed UCP1-dependent uncoupled respiration. One-hour pre-treatment as well as acute stimulation with Dexa had no effect on respiration (Figure 5B). With increasing exposure time Dexa attenuated ISO-stimulated respiration whereas ACTH-induced respiration was unaffected (Figure 5C). This was not a consequence of reduced or increased expression of the  $\beta$ 3-adrenergic or the melanocortin 2 receptor (Figures 5D,E). Of note, although there was trend toward a decrease in *Ucp1* mRNA, a 4-h treatment with Dexa had no significant effect on *Ucp1* expression (Figure 5F). Our further analysis revealed that Dexa attenuated the ISO induced rise in cellular cAMP levels, whereas no such effect was observed for ACTH (Figure 5G). This implies that the inhibitory action of DEXA must occur upstream of cAMP.

## DISCUSSION

Targeting brown fat to increase energy expenditure and promote negative energy balance has been a long sought strategy to prevent overweight and treat obesity (Tseng et al., 2010). In line with the hypothesis of thermoregulatory feeding (Himms-Hagen, 1995), our recent identification of an endocrine gut – secretin – brown fat – brain axis inhibiting food intake demonstrates that brown fat can also attenuate energy intake (Li et al., 2018). In addition to positive effects on energy balance, chronic activation of BAT leads to improved glucose tolerance and the release of batokines that beneficially regulate metabolism in rodent models (Bartelt et al., 2011; Hondares et al., 2011). Several novel molecular mediators for the recruitment of BAT and/or the browning of WAT have been found (Bartelt and Heeren, 2014), but only few direct activators of respiration in brown adipocytes were reported, so far (Braun et al., 2018). The latter mostly are adrenergic receptor agonists which exhibit unwanted systemic side effects (Cypess et al., 2012, 2015; Vosselman et al., 2012; Carey and Kingwell, 2013). Therefore, the present study was designed to reveal novel non-adrenergic activators of brown adipocytes. As the activation of the G<sub>s</sub>-coupled  $\beta$ 3-adrenergic receptor leads to increased lipolytic activity by the canonical cAMP-PKA pathway providing FFAs essential for the activation of UCP1-mediated respiration, we screened for



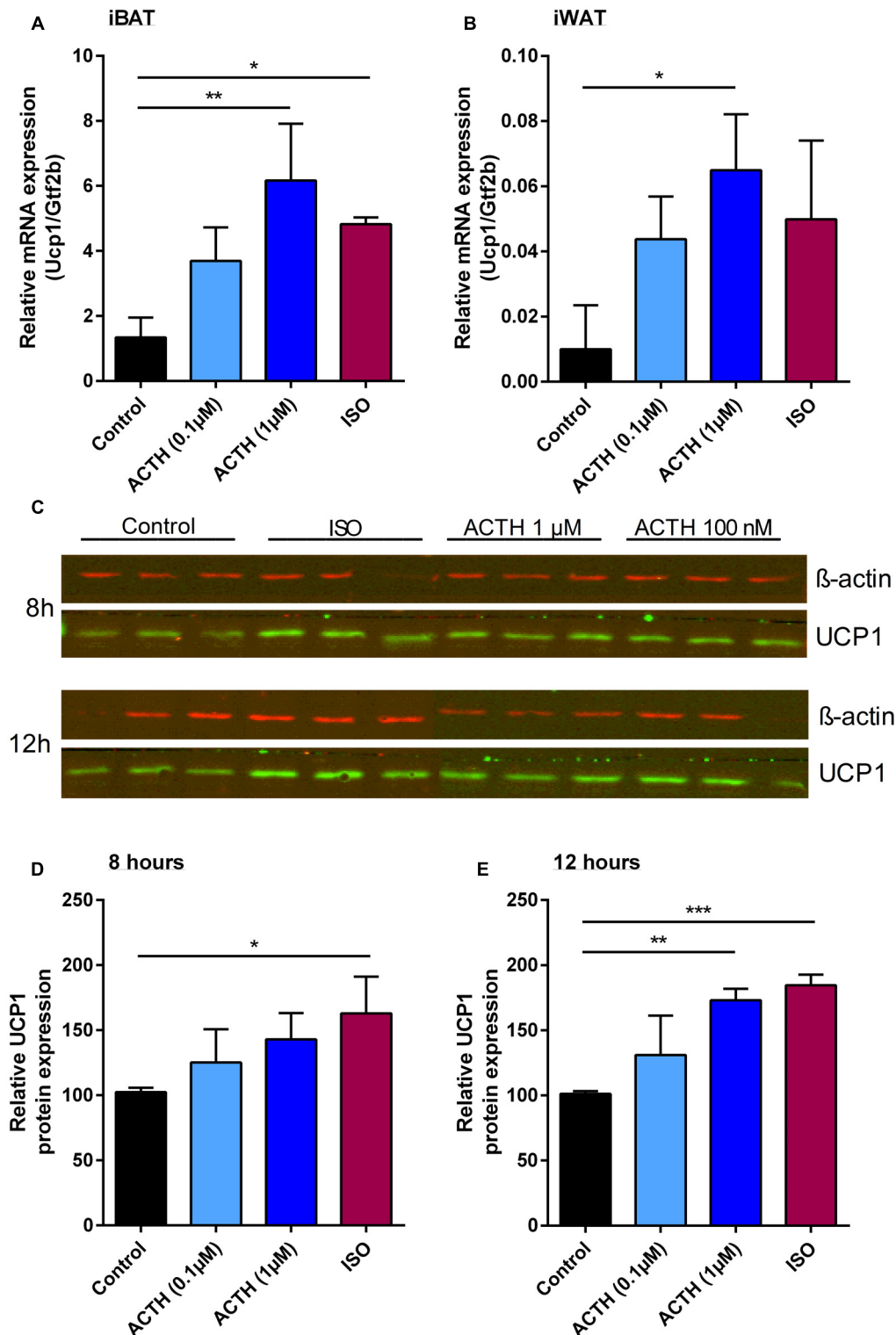
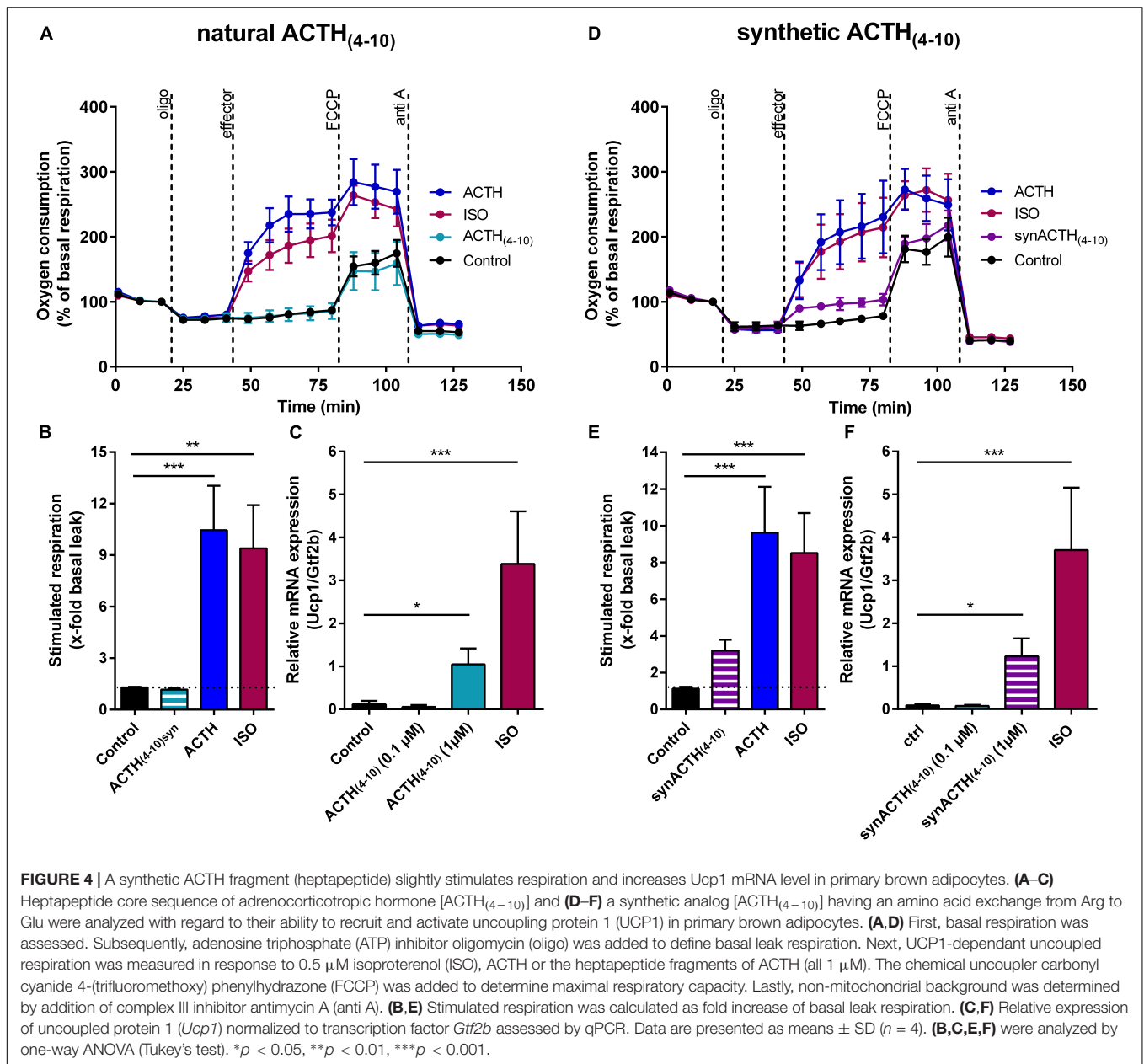


**FIGURE 3 |** ACTH increases Ucp1 expression in primary brown and white adipocytes. Relative expression of uncoupling protein 1 (*Ucp1*) normalized to transcription factor *Gtf2b* in primary adipocytes from both (A) interscapular brown (iBAT) and (B) inguinal white adipose tissue (iWAT) in response to isoproterenol (ISO) or adrenocorticotrophic hormone (ACTH). (C) Western blot analysis of UCP1 and β-actin in primary inguinal adipocytes after stimulation with ISO or ACTH for 8 and 12 h. Relative UCP1 protein expression normalized to β-actin in primary inguinal white adipocytes after treatment with differentiation medium (control), ACTH (0.1 μM), ACTH (1 μM) or ISO (0.5 μM) for (D) 8 or (E) 12 h. Data are presented as means ± SD ( $n = 4$ ). (A,B,D,E) were analyzed by one-way ANOVA (Tukey's test). \* $p < 0.05$ , \*\* $p < 0.01$ , \*\*\* $p < 0.001$ .



G<sub>s</sub>PCR expressed in mature murine adipocytes and assessed their capability to trigger the same signaling cascade. In our screen, we identified six peptidergic ligands of non-adrenergic G<sub>s</sub>PCR expressed in brown fat which acutely activated UCP1-mediated respiration in cultured brown adipocytes. Among these ligands, the glandotropic peptide hormone ACTH was one of the most potent activators of brown adipocyte respiration.

Some technical premises were of particular importance in our search for activators of UCP1-mediated respiration. Firstly, we tested the selected ligands for their acute effect on respiration. Secondly, by adding essentially fatty acid-free bovine serum into the respiration medium we prevented unspecific UCP1-independent uncoupling activity induced by uncontrolled high FFA levels (Li et al., 2014b). Thirdly, for

ACTH we compared the effects in primary brown adipocytes from *wild-type* and *Ucp1* knockout mice. In previous studies identifying potential activators of brown adipocyte uncoupled respiration, either UCP1 specificity was uncertain due to the applied assay conditions, or the effects on respiration were due to mitochondrial biogenesis induced by long term stimulation with the putative activator.

Consistent with our recent report (Li et al., 2018), secretin was the strongest activator of UCP1-mediated uncoupled respiration, closely followed by ACTH. In comparison, the effects of PTH and PTHrP on respiration were rather minor, demonstrating some potential of these peptides to activate brown adipocytes, in addition to their demonstrated role in WAT browning (Kir et al., 2014). Furthermore, in line with the known pro-lipolytic activity

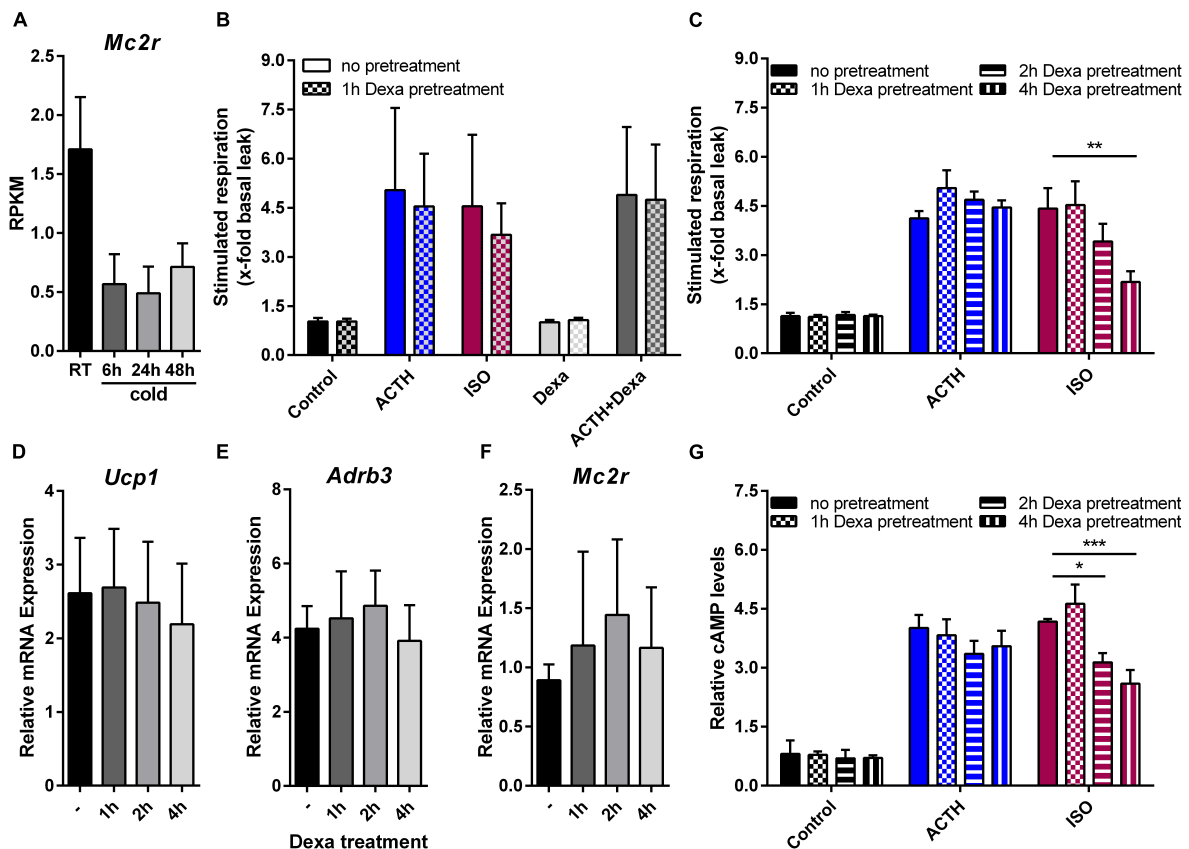


**FIGURE 5 |** Acute glucocorticoid treatment attenuates  $\beta 3$  adrenergic signaling but does not affect non-adrenergic ACTH-signaling. **(A)** Gene expression of melanocortin 2 receptor (*Mc2r*) in response to varying ambient temperatures obtained from RNA sequencing of murine brown adipose tissue. Data are shown as RPKM (reads per kilobase per million mapped reads) **(B)** Primary brown adipocytes were either not pretreated or with dexamethasone (Dexa) for 1 h prior to microplate-based respirometry. Subsequently, stimulated respiration as fold increase of basal respiration was determined in response to adrenocorticotrophic hormone (ACTH), isoproterenol (ISO), Dexa or a combination of ACTH and Dexa. After either no or 1, 2 or 4 h of pretreatment with Dexa **(C)** ACTH- and ISO-stimulated respiration, relative expression of **(D)** uncoupling protein 1 (*Ucp1*), **(E)**  $\beta 3$ -adrenergic receptor (*Adrb3*) and **(F)** *Mc2r* or **(G)** relative cellular cyclic adenosine monophosphate (cAMP) was assessed in primary brown adipocytes. Data are presented as means  $\pm$  SD ( $n = 4$ ). **(B, C, G)** were analyzed by two-way ANOVA (Tukey's test). **(D–F)** were analyzed by one-way ANOVA. \* $p < 0.05$ , \*\* $p < 0.01$ , \*\*\* $p < 0.001$ .

of  $\alpha$ -MSH and PACAP (Akesson et al., 2003; Lafontan, 2012), these peptides also showed low stimulation of brown adipocyte respiration.

Most peptides were about equipotent in stimulating respiration and gene expression, whereas secretin and ACTH showed a bias toward acute activation, thus resembling ISO (Figure 1E). Other than ACTH, the ACTH<sub>(4–10)</sub> fragment stimulated *Ucp1* gene expression but failed to activate UCP1-dependant respiration (Figures 4B,C). This discrepancy is unexpected as activation and recruitment of BAT share a common signaling pathway that furcates at the level of PKA. Upon cAMP binding, activated PKA phosphorylates the lipid droplet coating proteins perilipin and HSL which are essential for lipolysis and acute activation of thermogenesis (Li et al., 2014b), as well as the transcription factor cAMP response element binding protein (CREB). In concert with activating transcription factor 2 (ATF-2) and PPAR coactivator 1 $\alpha$  (PGC1 $\alpha$ ), both downstream of PKA, CREB induces *Ucp1* expression (Klingenspor et al., 2017). On this background, one

would assume a fixed ratio for the increase in *Ucp1* expression and UCP1 activity in response to the  $G_s$ -coupled activation of the canonical cAMP-PKA pathway. Alike isoproterenol, however, ACTH and secretin both prioritize acute activation of respiration over gene expression. This phenomenon, known as signaling bias, is due to a receptor's ability to selectively engage specific subsets of downstream signaling modules. Bias may have multiple causes, including variation of ligand concentration and selective G-protein activation. Depending on concentration, one ligand can trigger variable activation of multiple cellular pathways (Kenakin, 1995), and GPCRs can interact with different G-proteins, arrestins and accessory proteins (Wooten et al., 2018). The secretin receptor for example couples to both  $G_s$ - and  $G_q$ -protein with opposing downstream signaling effects (Siu et al., 2006), and ACTH stimulates arrestin-dependent internalization of MC2R and MC2R accessory protein 1 (MRAP1) in a concentration dependent manner (Roy et al., 2011). The molecular mechanisms responsible for biased signaling of ACTH and secretin in brown adipocytes merit

further investigation to identify signaling events that prioritize activation of UCP1.

In mice, ACTH increases thermogenic gene expression, hallmarked by *Ucp1*, in immortalized brown adipocytes (T37i) and in primary brown adipocytes, respectively (van den Beukel et al., 2014; Biswas, 2017). We here demonstrate acute activation of UCP1-dependent respiration in primary brown adipocytes by ACTH, as proven by the exclusion of unspecific uncoupling by fatty acids, the dose-dependent thermogenic response, and the knockout of UCP1. In combination, the pronounced acute stimulating effect on respiration and the induction of *Ucp1* gene expression qualify ACTH as a non-adrenergic effector candidate to boost activation of BAT thermogenesis *in vivo*. The discrepancy in the magnitude of ACTH effects on *Ucp1* expression assessed by either luciferase activity in our screening assay or *Ucp1* mRNA levels is probably due to strain differences of primary brown adipocytes, methodological differences and/or different duration of stimulation.

The melanocortins ACTH and  $\alpha$ -MSH are known for their lipolytic action in rodent adipocytes, as first reported in 1958 (Lafontan, 2012; Braun et al., 2018). Cold exposure increased the plasma level of ACTH and in adipocytes it also progressively increased the responsiveness to this hormone (Rochon and Bukowiecki, 1990; van den Beukel et al., 2014). ACTH enhanced BAT function in obese rats (York and Al-Baker, 1984), and increased glucose transport and respiration in isolated brown adipocytes (Marette and Bukowiecki, 1990) via fatty acid activation of mitochondrial uncoupled respiration. In mouse strains with different stress reactivity, the physiological serum ACTH concentrations are variable, ranging from 12 to 27 pM at basal level (Ochedalski et al., 2001; Touma et al., 2008) and 133–246 pM after 15-min restraint stress (Heinzmann et al., 2010). In response to cold exposure (4°C for 24 h), serum ACTH levels rise up to 260 pM (van den Beukel et al., 2014). In cell culture, adipocytes respond to ACTH at concentrations ranging from 50 nM (T37i cells) to 100 nM (immortalized murine adipocytes) (Iwen et al., 2008; van den Beukel et al., 2014). We observed increased respiration rates at 200 nM, with most robust effects at 1  $\mu$ M, with effective concentrations on *Ucp1* gene expression in a comparable range reported by others (Biswas, 2017). Thus, effective concentrations in cell culture are approximately 1,000-fold higher than the maximal physiological ACTH levels in response to restraint stress or cold exposure. To the best of our knowledge, no published studies are available that tested the effect of ACTH on brown adipocyte respiration at physiological doses. Treatment with a supraphysiological dose (15  $\mu$ M ACTH, ~50,000-fold above physiological levels), however, increased glucose uptake into BAT (van den Beukel et al., 2014). Pathophysiological chronic exposure to excessive concentrations of ACTH results in elevated glucocorticoid levels, as known for Cushing's syndrome, with symptoms like visceral obesity, growth retardation, hirsutism, acne and hypertension (Bista and Beck, 2014; Lacroix et al., 2015), but no evidence for increased BAT activity. Further analysis is necessary to evaluate the thermogenic effect of physiological concentrations of ACTH *in vivo*. In a physiological context, it has to be taken into account that the sensitivity and affinity of the receptor

*in vivo* might be different, or increased by certain stimuli such as cold.

In the attempt to reduce side effects as well as to improve efficacy, alternative MC2R ligands could be of advantage to develop strategies for tissue-specific MC2R activation or selective intracellular signaling. We therefore compared an ACTH heptapeptide representing the core sequence of melanocortins (Draper et al., 1975) with an synthetic analog of this ACTH fragment carrying a mutation in position 5 (Arg > Glu). Despite the high lipolytic activity reported for the synthetic analog ACTH<sub>(4–10)</sub><sub>syn</sub>, it had only minor effects on brown adipocyte respiration, whereas the heptapeptide fragment was inactive. Thus, these alternative ligands are unsuitable to efficiently activate brown fat.

The glandotropic hormone ACTH induces the production and secretion of glucocorticoids (GCs) in the adrenal glands. The interplay between the murine GC corticosterone and ACTH has been previously studied (van den Beukel et al., 2014). Higher GC doses, and more chronic elevation of GC inhibit BAT activity, as concluded from cell culture data and clinical observations reporting a lower <sup>18</sup>FDG uptake by BAT in patients during chronic glucocorticoid therapy (Ramage et al., 2016). In rodents, GC exert inhibitory effects on BAT development and activity, most likely mediated via the glucocorticoid receptor (Soumano et al., 2000; Viengchareun et al., 2001; Armengol et al., 2012). Furthermore, in animal studies, adrenalectomy led to an increased BAT activity (Strack et al., 1995; Scarpace et al., 2000), while GC replacement normalized BAT activity (Scarpace et al., 1988, 2000). As these studies did not investigate a direct effect of ACTH on BAT activity, it remains elusive whether increased BAT activity can be attributed to the absence of GC or to increased ACTH levels as GC are strong negative regulators of ACTH secretion. Thus, the physiological relevance of ACTH in regulating BAT function may rather be indirect, depending on glucocorticoids. Notably, in obese rats the thermogenic effect of ACTH was attenuated by chronic increases in corticosterone (York and Al-Baker, 1984). However, no study so far addressed the immediate impact of GC on respiration in brown adipocytes. Therefore, we tested the thermogenic effects of ACTH and ISO after pretreatment of brown adipocytes with DEXA for up to 4 h. We found that DEXA had no effect on ACTH mediated respiration but attenuated the effect of ISO. We therefore conclude that the inhibitory action of DEXA occurs upstream of cAMP, as we observed an attenuation of the adrenergic signaling already at this level. For example, there might be an inhibition of G<sub>s</sub>-mediated activation of adenylyl cyclase which is selective for ADRB3 signaling. Such selectivity would require that ADRB3 and MC2R couple to different isoforms of G-proteins and/or adenylyl cyclases expressed in brown adipocytes. Two hours of DEXA treatment was sufficient to obtain a significant downregulation of the thermogenic response to ISO. This effect was more pronounced after extended DEXA treatment for 4 h. This temporal increase of inhibitory action is compatible with the activation or repression of gene transcription mediated by DEXA via the glucocorticoid receptor. DEXA treatment for 1 h had no effect, thus excluding the involvement of rapid non-genomic effects of GC.



Pertaining to systemic demands and BAT functionality, cold exposure and restraint stress, both elevating circulating ACTH levels, fundamentally differ. In the cold, metabolic fuels need to be mobilized and delivered to BAT, whereas in a fight-or-flight situation, metabolic fuels must be channeled to brain, heart and skeletal muscle. Cold exposure (24 h) led to a strong rise in ACTH plasma levels (van den Beukel et al., 2014). It remains to be clarified whether this physiological rise in ACTH levels is sufficient to transiently activate BAT thermogenesis and contribute to the initial defense of body temperature in the cold. The lipolytic activity of ACTH in WAT may also indirectly support fuel supply to BAT in the cold by augmenting the release of fatty acids into circulation. As the ACTH receptor MC2R in BAT is down-regulated in chronic cold exposure, it seems less likely, that ACTH is involved in long term stimulation and maintenance of cold-induced thermogenesis. In restraint stress, extended activation of BAT thermogenesis by ACTH and the sympathetic neurotransmitter norepinephrine would be rather counterproductive. In this context, the observed attenuation of beta-adrenergic stimulation of thermogenesis by GC avoids excessive fuel wasting in BAT and limits stress-induced hyperthermia. However, pertaining to cold stress glucocorticoid levels rise as well as norepinephrine levels (Young et al., 1982; Sesti-Costa et al., 2010). Maximal activation of BAT thermogenesis can lead to a rapid depletion of lipid stores in brown adipocytes. Acute GC-mediated downregulation of beta-adrenergic signaling might transiently hinder the sequestration of lipid stores in brown adipocytes and promote the import of metabolic fuel from circulation, for example fatty acids from lipolysis in WAT depots or triglyceride-rich lipoproteins originating from intestine and liver.

Regarding long-term effects of the HPA-axis the bidirectional effect of stress on body weight might be explained by eating behavior and BAT recruitment and thermogenesis (Razzoli et al., 2016). Obesity is associated with chronic stress and low socio-economic status and stress induced thermogenesis has been repeatedly reported in mice and humans (Lkhagvasuren et al., 2011; Kataoka et al., 2014; Robinson et al., 2016). Thus, BAT function is a determinant of the vulnerability to stress-induced obesity (Razzoli et al., 2016). An attenuation of the beta-adrenergic stimulation of BAT thermogenesis by glucocorticoids could contribute to an amplification of the obese phenotype.

## REFERENCES

- Akesson, L., Ahren, B., Manganiello, V. C., Holst, L. S., Edgren, G., and Degerman, E. (2003). Dual effects of pituitary adenylate cyclase-activating polypeptide and isoproterenol on lipid metabolism and signaling in primary rat adipocytes. *Endocrinology* 144, 5293–5299. doi: 10.1210/en.2003-0364
- Armengol, J., Villena, J. A., Hondares, E., Carmona, M. C., Sul, H. S., Iglesias, R., et al. (2012). Pref-1 in brown adipose tissue: specific involvement in brown adipocyte differentiation and regulatory role of C/EBPdelta. *Biochem. J.* 443, 799–810. doi: 10.1042/BJ20111714
- Bartelt, A., Bruns, O. T., Reimer, R., Hohenberg, H., Itrich, H., Peldschus, K., et al. (2011). Brown adipose tissue activity controls triglyceride clearance. *Nat. Med.* 17, 200–205. doi: 10.1038/nm.2297
- Bartelt, A., and Heeren, J. (2014). Adipose tissue browning and metabolic health. *Nat. Rev. Endocrinol.* 10, 24–36. doi: 10.1038/nrendo.2013.204
- Bista, B., and Beck, N. (2014). Cushing syndrome. *Indian J. Pediatr.* 81, 158–164. doi: 10.1007/s12098-013-1203-8
- Biswas, H. M. (2017). Effect of adrenocorticotrophic hormone on UCP1 gene expression in brown adipocytes. *J. Basic Clin. Physiol. Pharmacol.* 28, 267–274. doi: 10.1515/jbcp-2016-0017
- Bohnekamp, J., and Schoneberg, T. (2011). Cell adhesion receptor GPR133 couples to Gs protein. *J. Biol. Chem.* 286, 41912–41916. doi: 10.1074/jbc.C111.265934
- Bouw, E., Huisman, M., Neggers, S. J., Themmen, A. P., van der Lely, A. J., and Delhanty, P. J. (2014). Development of potent selective competitive-antagonists of the melanocortin type 2 receptor. *Mol. Cell. Endocrinol.* 394, 99–104. doi: 10.1016/j.mce.2014.07.003
- In summary, we identified several activators in cell culture which can serve as potential candidates to induce BAT thermogenesis *in vivo*. As a showcase, we demonstrated that ACTH activates the canonical pathway also targeted by  $\beta$ -adrenergic receptor signaling for activation of BAT thermogenesis. Furthermore, we add a synthetic ACTH peptide fragment to the expanding list of thermogenic compounds. As the ACTH receptor MC2R is down-regulated in response to cold, we hypothesize that its impact on cold-induced thermogenesis is rather transient. ACTH triggers the synthesis and release of GCs from the adrenal glands which have been reported to inhibit *Ucp1* expression in brown adipocytes. Additionally, in the present study we demonstrate that the GC dexamethasone attenuates  $\beta$ -adrenergic receptor signaling. We conclude that stress induced GC levels *in vivo* may limit extended energy dissipation in brown adipocytes and stress-induced hyperthermia, probably in a rather transient manner. Further studies *in vivo* are required to elucidate the effects of physiological cold- and stress-induced ACTH and glucocorticoid levels on BAT thermogenesis.

## DATA AVAILABILITY STATEMENT

Publicly available datasets were analyzed in this study. This data can be found here: <https://www.ncbi.nlm.nih.gov/geo/query/acc.cgi?acc=GSE119452>.

## AUTHOR CONTRIBUTIONS

KS and MK conceived and designed the study. KS and JW performed the experiments. YL helped with the luciferase assay. KS analyzed the data. KS and MK wrote the manuscript. All authors read and approved the manuscript.

## FUNDING

This work was supported by grants to MK from the German Research Foundation (Deutsche Forschungsgemeinschaft, DFG KL973/12 and RTG1482) and the Else Kröner-Fresenius-Stiftung. KS was a fellow in the DFG Research Training Group RTG1482.

- Braun, K., Oeckl, J., Westermeier, J., Li, Y., and Klingenspor, M. (2018). Non-adrenergic control of lipolysis and thermogenesis in adipose tissues. *J. Exp. Biol.* 221(Pt Suppl. 1):jeb165381. doi: 10.1242/jeb.165381
- Buhl, A. M., Johnson, N. L., Dhanasekaran, N., and Johnson, G. L. (1995). G alpha 12 and G alpha 13 stimulate Rho-dependent stress fiber formation and focal adhesion assembly. *J. Biol. Chem.* 270, 24631–24634. doi: 10.1074/jbc.270.42.24631
- Cannon, B., and Nedergaard, J. (2004). Brown adipose tissue: function and physiological significance. *Physiol. Rev.* 84, 277–359. doi: 10.1152/physrev.00015.2003
- Carey, A. L., and Kingwell, B. A. (2013). Brown adipose tissue in humans: therapeutic potential to combat obesity. *Pharmacol. Ther.* 140, 26–33. doi: 10.1016/j.pharmthera.2013.05.009
- Chang, C. L., Roh, J., and Hsu, S. Y. (2004). Intermedin, a novel calcitonin family peptide that exists in teleosts as well as in mammals: a comparison with other calcitonin/intermedin family peptides in vertebrates. *Peptides* 25, 1633–1642. doi: 10.1016/j.peptides.2004.05.021
- Cho, K. J., Shim, J. H., Cho, M. C., Choe, Y. K., Hong, J. T., Moon, D. C., et al. (2005). Signaling pathways implicated in alpha-melanocyte stimulating hormone-induced lipolysis in 3T3-L1 adipocytes. *J. Cell Biochem.* 96, 869–878. doi: 10.1002/jcb.20561
- Cypess, A. M., Chen, Y. C., Sze, C., Wang, K., English, J., Chan, O., et al. (2012). Cold but not sympathomimetics activates human brown adipose tissue *in vivo*. *Proc. Natl. Acad. Sci. U.S.A.* 109, 10001–10005. doi: 10.1073/pnas.1207911109
- Cypess, A. M., Lehman, S., Williams, G., Tal, I., Rodman, D., Goldfine, A. B., et al. (2009). Identification and importance of brown adipose tissue in adult humans. *N. Engl. J. Med.* 360, 1509–1517. doi: 10.1056/NEJMoa0810780
- Cypess, A. M., Weiner, L. S., Roberts-Toler, C., Franquet Elia, E., Kessler, S. H., Kahn, P. A., et al. (2015). Activation of human brown adipose tissue by a beta3-adrenergic receptor agonist. *Cell Metab.* 21, 33–38. doi: 10.1016/j.cmet.2014.12.009
- Dean, T., Linglart, A., Mahon, M. J., Bastepe, M., Juppner, H., Potts, J. T., et al. (2006). Mechanisms of ligand binding to the parathyroid hormone (PTH)/PTH-related protein receptor: selectivity of a modified PTH(1-15) radioligand for GalphaS-coupled receptor conformations. *Mol. Endocrinol.* 20, 931–943. doi: 10.1210/me.2005-0349
- Draper, M. W., Merrifield, R. B., and Rizack, M. A. (1973). Lipolytic activity of Met-Arg-His-Phe-Arg-Trp-Gly, a synthetic analog of the ACTH (4-10) core sequence. *J. Med. Chem.* 16, 1326–1330. doi: 10.1021/jm00270a003
- Draper, M. W., Rizack, M. A., and Merrifield, R. B. (1975). Synthetic position 5 analogs of adrenocorticotropin fragments and their *in vitro* lipolytic activity. *Biochemistry* 14, 2933–2938. doi: 10.1021/bi00684a022
- Galmozzi, A., Sonne, S. B., Altshuler-Keylin, S., Hasegawa, Y., Shinoda, K., Luijten, I. H. N., et al. (2014). ThermoMouse: an *in vivo* model to identify modulators of UCP1 expression in brown adipose tissue. *Cell Rep.* 9, 1584–1593. doi: 10.1016/j.celrep.2014.10.066
- Gnad, T., Scheibler, S., von Kugelgen, I., Scheele, C., Kilic, A., Glode, A., et al. (2014). Adenosine activates brown adipose tissue and recruits beige adipocytes via A2A receptors. *Nature* 516, 395–399. doi: 10.1038/nature13816
- Hauser, A. S., Attwood, M. M., Rask-Andersen, M., Schioth, H. B., and Gloriam, D. E. (2017). Trends in GPCR drug discovery: new agents, targets and indications. *Nat. Rev. Drug Discov.* 16, 829–842. doi: 10.1038/nrd.2017.178
- Heinzmann, J. M., Thoeringer, C. K., Knapman, A., Palme, R., Holsboer, F., Uhr, M., et al. (2010). Intrahippocampal corticosterone response in mice selectively bred for extremes in stress reactivity: a microdialysis study. *J. Neuroendocrinol.* 22, 1187–1197. doi: 10.1111/j.1365-2826.2010.02062.x
- Himmels-Hagen, J. (1995). Role of brown adipose tissue thermogenesis in control of thermoregulatory feeding in rats: a new hypothesis that links homeostatic and glucostatic hypotheses for control of food intake. *Proc. Soc. Exp. Biol. Med.* 208, 159–169. doi: 10.3181/00379727-208-43847A
- Hondares, E., Iglesias, R., Giral, A., Gonzalez, F. J., Giral, M., Mampel, T., et al. (2011). Thermogenic activation induces FGF21 expression and release in brown adipose tissue. *J. Biol. Chem.* 286, 12983–12990. doi: 10.1074/jbc.M110.215889
- Ishibashi, J., and Seale, P. (2010). Medicine. Beige can be slimming. *Science* 328, 1113–1114. doi: 10.1126/science.1190816
- Iwen, K. A., Senyaman, O., Schwartz, A., Drenckhan, M., Meier, B., Hadaschik, D., et al. (2008). Melanocortin cross-talk with adipose functions: ACTH directly induces insulin resistance, promotes a pro-inflammatory adipokine profile and stimulates UCP-1 in adipocytes. *J. Endocrinol.* 196, 465–472. doi: 10.1677/JOE-07-0299
- Kataoka, N., Hioki, H., Kaneko, T., and Nakamura, K. (2014). Psychological stress activates a dorsomedial hypothalamus-medullary raphe circuit driving brown adipose tissue thermogenesis and hyperthermia. *Cell Metab.* 20, 346–358. doi: 10.1016/j.cmet.2014.05.018
- Kenakin, T. (1995). Agonist-receptor efficacy. II. Agonist trafficking of receptor signals. *Trends Pharmacol. Sci.* 16, 232–238. doi: 10.1016/S0165-6147(00)89032-X
- Kir, S., White, J. P., Kleiner, S., Kazak, L., Cohen, P., Baracos, V. E., et al. (2014). Tumour-derived PTH-related protein triggers adipose tissue browning and cancer cachexia. *Nature* 513, 100–104. doi: 10.1038/nature13528
- Klepac, K., Kilic, A., Gnad, T., Brown, L. M., Herrmann, B., Wilderman, A., et al. (2016). The Gq signalling pathway inhibits brown and beige adipose tissue. *Nat. Commun.* 7:10895. doi: 10.1038/ncomms10895
- Klingenspor, M. (2003). Cold-induced recruitment of brown adipose tissue thermogenesis. *Exp. Physiol.* 88, 141–148. doi: 10.1113/eph802508
- Klingenspor, M., Bast, A., Bolze, F., Li, Y., Maurer, S. F., Schweizer, S., et al. (2017). “Brown adipose tissue,” in *Adipose Tissue Biology*, ed. M. E. Symonds (Cham: Springer), 91–147. doi: 10.1007/978-3-319-52031-5\_4
- Kobilka, B. K. (2011). Structural insights into adrenergic receptor function and pharmacology. *Trends Pharmacol. Sci.* 32, 213–218. doi: 10.1016/j.tips.2011.02.005
- Lacroix, A., Feelders, R. A., Stratakis, C. A., and Nieman, L. K. (2015). Cushing's syndrome. *Lancet* 386, 913–927. doi: 10.1016/S0140-6736(14)61375-1
- Lafontan, M. (2012). Historical perspectives in fat cell biology: the fat cell as a model for the investigation of hormonal and metabolic pathways. *Am. J. Physiol. Cell Physiol.* 302, C327–C359. doi: 10.1152/ajpcell.00168.2011
- Latek, D., Modzelewska, A., Trzaskowski, B., Palczewski, K., and Filipek, S. (2012). G protein-coupled receptors—recent advances. *Acta Biochim. Pol.* 59, 515–529.
- Lefkowitz, R. J. (2007). Seven transmembrane receptors: something old, something new. *Acta Physiol.* 190, 9–19. doi: 10.1111/j.1365-201X.2007.01693.x
- Li, Y., Bolze, F., Fromme, T., and Klingenspor, M. (2014a). Intrinsic differences in BRITe adipogenesis of primary adipocytes from two different mouse strains. *Biochim. Biophys. Acta* 1841, 1345–1352. doi: 10.1016/j.bbalip.2014.06.003
- Li, Y., Fromme, T., Schweizer, S., Schottl, T., and Klingenspor, M. (2014b). Taking control over intracellular fatty acid levels is essential for the analysis of thermogenic function in cultured primary brown and brite/beige adipocytes. *EMBO Rep.* 15, 1069–1076. doi: 10.15252/embr.201438775
- Li, Y., Schnabl, K., Gabler, S. M., Willershauser, M., Reber, J., Karlas, A., et al. (2018). Secretin-activated brown fat mediates prandial thermogenesis to induce satiation. *Cell* 175, 1561.e–1574.e. doi: 10.1016/j.cell.2018.10.016
- Lkhagvasuren, B., Nakamura, Y., Oka, T., Sudo, N., and Nakamura, K. (2011). Social defeat stress induces hyperthermia through activation of thermoregulatory sympathetic premotor neurons in the medullary raphe region. *Eur. J. Neurosci.* 34, 1442–1452. doi: 10.1111/j.1460-9568.2011.07863.x
- Ludwig, M. G., Vanek, M., Guerini, D., Gasser, J. A., Jones, C. E., Junker, U., et al. (2003). Proton-sensing G-protein-coupled receptors. *Nature* 425, 93–98. doi: 10.1038/nature01905
- Marette, A., and Bukowiecki, L. J. (1990). Mechanism of norepinephrine stimulation of glucose transport in isolated rat brown adipocytes. *Int. J. Obes.* 14, 857–867.
- Maurer, S. F., Fromme, T., Grossman, L. I., Huttemann, M., and Klingenspor, M. (2015). The brown and brite adipocyte marker Cox7a1 is not required for non-shivering thermogenesis in mice. *Sci. Rep.* 5:17704. doi: 10.1038/srep17704
- Nahar, J., Rainville, J. R., Dohanich, G. P., and Tasker, J. G. (2016). Further evidence for a membrane receptor that binds glucocorticoids in the rodent hypothalamus. *Steroids* 114, 33–40. doi: 10.1016/j.steroids.2016.05.013
- Neves, S. R., Ram, P. T., and Iyengar, R. (2002). G protein pathways. *Science* 296, 1636–1639. doi: 10.1126/science.1071550
- Ochedalski, T., Zylinska, K., Laudanski, T., and Lachowicz, A. (2001). Corticotrophin-releasing hormone and ACTH levels in maternal and fetal blood during spontaneous and oxytocin-induced labour. *Eur. J. Endocrinol.* 144, 117–121. doi: 10.1530/eje.0.1440117
- Ouellet, V., Routhier-Labadie, A., Bellemare, W., Lakhal-Chaieb, L., Turcotte, E., Carpentier, A. C., et al. (2011). Outdoor temperature, age, sex, body mass index, and diabetic status determine the prevalence, mass, and glucose-uptake activity

- of 18F-FDG-detected BAT in humans. *J. Clin. Endocrinol. Metab.* 96, 192–199. doi: 10.1210/jc.2010-0989
- Petrovic, N., Walden, T. B., Shabalina, I. G., Timmons, J. A., Cannon, B., and Nedergaard, J. (2010). Chronic peroxisome proliferator-activated receptor gamma (PPARgamma) activation of epididymally derived white adipocyte cultures reveals a population of thermogenically competent, UCP1-containing adipocytes molecularly distinct from classic brown adipocytes. *J. Biol. Chem.* 285, 7153–7164. doi: 10.1074/jbc.M109.053942
- Ramage, L. E., Akyol, M., Fletcher, A. M., Forsythe, J., Nixon, M., Carter, R. N., et al. (2016). Glucocorticoids acutely increase brown adipose tissue activity in humans, revealing species-specific differences in UCP-1 regulation. *Cell Metab.* 24, 130–141. doi: 10.1016/j.cmet.2016.06.011
- Razzoli, M., Frontini, A., Gurney, A., Mondini, E., Cubuk, C., Katz, L. S., et al. (2016). Stress-induced activation of brown adipose tissue prevents obesity in conditions of low adaptive thermogenesis. *Mol. Metab.* 5, 19–33. doi: 10.1016/j.molmet.2015.10.005
- Robinson, L. J., Law, J. M., Symonds, M. E., and Budge, H. (2016). Brown adipose tissue activation as measured by infrared thermography by mild anticipatory psychological stress in lean healthy females. *Exp. Physiol.* 101, 549–557. doi: 10.1113/EP085642
- Rochon, L., and Bukowiecki, L. J. (1990). Alterations in adipocyte response to lipolytic hormones during cold acclimation. *Am. J. Physiol.* 258, C835–C840. doi: 10.1152/ajpcell.1990.258.5.C835
- Rosen, E. D., and Spiegelman, B. M. (2006). Adipocytes as regulators of energy balance and glucose homeostasis. *Nature* 444, 847–853. doi: 10.1038/nature05483
- Roy, S., Roy, S. J., Pinard, S., Taillefer, L. D., Rached, M., Parent, J. L., et al. (2011). Mechanisms of melanocortin-2 receptor (MC2R) internalization and recycling in human embryonic kidney (hek) cells: identification of Key Ser/Thr (S/T) amino acids. *Mol. Endocrinol.* 25, 1961–1977. doi: 10.1210/me.2011-0018
- Saito, M., Okamatsu-Ogura, Y., Matsushita, M., Watanabe, K., Yoneshiro, T., Nio-Kobayashi, J., et al. (2009). High incidence of metabolically active brown adipose tissue in healthy adult humans: effects of cold exposure and adiposity. *Diabetes* 58, 1526–1531. doi: 10.2337/db09-0530
- Santos, R., Ursu, O., Gaulton, A., Bento, A. P., Donadi, R. S., Bologa, C. G., et al. (2017). A comprehensive map of molecular drug targets. *Nat. Rev. Drug Discov.* 16, 19–34. doi: 10.1038/nrd.2016.230
- Scarpace, P. J., Baresi, L. A., and Morley, J. E. (1988). Glucocorticoids modulate beta-adrenoceptor subtypes and adenylate cyclase in brown fat. *Am. J. Physiol.* 255, E153–E158. doi: 10.1152/ajpendo.1988.255.2.E153
- Scarpace, P. J., Kumar, M. V., Li, H., and Tumer, N. (2000). Uncoupling proteins 2 and 3 with age: regulation by fasting and beta3-adrenergic agonist treatment. *J. Gerontol. A Biol. Sci. Med. Sci.* 55, B588–B592. doi: 10.1093/gerona/55.12.B588
- Sesti-Costa, R., Baccan, G. C., Chedraoui-Silva, S., and Mantovani, B. (2010). Effects of acute cold stress on phagocytosis of apoptotic cells: the role of corticosterone. *Neuroimmunomodulation* 17, 79–87. doi: 10.1159/000258690
- Shaqura, M., Li, X., Al-Khrasani, M., Shakibaei, M., Tafelski, S., Furst, S., et al. (2016). Membrane-bound glucocorticoid receptors on distinct nociceptive neurons as potential targets for pain control through rapid non-genomic effects. *Neuropharmacology* 111, 1–13. doi: 10.1016/j.neuropharm.2016.08.019
- Siu, F. K., Lam, I. P., Chu, J. Y., and Chow, B. K. (2006). Signaling mechanisms of secretin receptor. *Regul. Pept.* 137, 95–104. doi: 10.1016/j.regpep.2006.02.011
- Soumano, K., Desbiens, S., Rabelo, R., Bakopanos, E., Camirand, A., and Silva, J. E. (2000). Glucocorticoids inhibit the transcriptional response of the uncoupling protein-1 gene to adrenergic stimulation in a brown adipose cell line. *Mol. Cell. Endocrinol.* 165, 7–15. doi: 10.1016/S0303-7207(00)00276-8
- Strack, A. M., Horsley, C. J., Sebastian, R. J., Akana, S. F., and Dallman, M. F. (1995). Glucocorticoids and insulin: complex interaction on brown adipose tissue. *Am. J. Physiol.* 268, R1209–R1216. doi: 10.1152/ajpregu.1995.268.5.R1209
- Touma, C., Bunck, M., Glas, L., Nussbaumer, M., Palme, R., Stein, H., et al. (2008). Mice selected for high versus low stress reactivity: a new animal model for affective disorders. *Psychoneuroendocrinology* 33, 839–862. doi: 10.1016/j.psychneu.2008.03.013
- Tseng, Y. H., Cypess, A. M., and Kahn, C. R. (2010). Cellular bioenergetics as a target for obesity therapy. *Nat. Rev. Drug Discov.* 9, 465–482. doi: 10.1038/nrd3138
- U Din, M., Saari, T., Raiko, J., Kudomi, N., Maurer, S. F., Laheesmaa, M., et al. (2018). Postprandial oxidative metabolism of human brown fat indicates thermogenesis. *Cell Metab.* 28, 207.e3–216.e3. doi: 10.1016/j.cmet.2018.05.020
- van den Beukel, J. C., Grefhorst, A., Quarta, C., Steenbergen, J., Mastroberardino, P. G., Lombes, M., et al. (2014). Direct activating effects of adrenocorticotrophic hormone (ACTH) on brown adipose tissue are attenuated by corticosterone. *FASEB J.* 28, 4857–4867. doi: 10.1096/fj.14-254839
- van Marken Lichtenbelt, W. D., Vanhommerig, J. W., Smulders, N. M., Drossaerts, J. M., Kemerink, G. J., Bouvy, N. D., et al. (2009). Cold-activated brown adipose tissue in healthy men. *N. Engl. J. Med.* 360, 1500–1508. doi: 10.1056/NEJMoa0808718
- Viangchareun, S., Penforis, P., Zennaro, M. C., and Lombes, M. (2001). Mineralocorticoid and glucocorticoid receptors inhibit UCP expression and function in brown adipocytes. *Am. J. Physiol. Endocrinol. Metab.* 280, E640–E649. doi: 10.1152/ajpendo.2001.280.4.E640
- Virtanen, K. A., Lidell, M. E., Orava, J., Heglind, M., Westergren, R., Niemi, T., et al. (2009). Functional brown adipose tissue in healthy adults. *N. Engl. J. Med.* 360, 1518–1525. doi: 10.1056/NEJMoa0808949
- Vosselman, M. J., Brans, B., van der Lans, A. A., Wierds, R., van Baak, M. A., Mottaghy, F. M., et al. (2013). Brown adipose tissue activity after a high-calorie meal in humans. *Am. J. Clin. Nutr.* 98, 57–64. doi: 10.3945/ajcn.113.059022
- Vosselman, M. J., van der Lans, A. A., Brans, B., Wierds, R., van Baak, M. A., Schrauwen, P., et al. (2012). Systemic beta-adrenergic stimulation of thermogenesis is not accompanied by brown adipose tissue activity in humans. *Diabetes* 61, 3106–3113. doi: 10.2337/db12-0288
- Wang, H., Willershäuser, M., Karlas, A., Gorpas, D., Reber, J., et al. (2018). A dual *Ucp1* reporter mouse model for imaging and quantitation of brown and brite fat recruitment. *Mol. Metab.* doi: 10.1016/j.molmet.2018.11.009. [Epub ahead of print].
- Wang, Y., Falting, J. M., Mattsson, C. L., Holmstrom, T. E., and Nedergaard, J. (2013). In brown adipocytes, adrenergically induced beta(1)-/beta(3)-(Gs)-, alpha(2)-(Gi)- and alpha(1)-(Gq)-signalling to Erk1/2 activation is not mediated via EGF receptor transactivation. *Exp. Cell Res.* 319, 2718–2727. doi: 10.1016/j.yexcr.2013.08.007
- Wettschreck, N., and Offermanns, S. (2005). Mammalian G proteins and their cell type specific functions. *Physiol. Rev.* 85, 1159–1204. doi: 10.1152/physrev.00003.2005
- WHO (2018). *Obesity and Overweight*. Available at: <http://www.who.int/en/news-room/fact-sheets/detail/obesity-and-overweight>
- Wootton, D., Christopoulos, A., Marti-Solano, M., Babu, M. M., and Sexton, P. M. (2018). Mechanisms of signalling and biased agonism in G protein-coupled receptors. *Nat. Rev. Mol. Cell. Biol.* 19, 638–653. doi: 10.1038/s41580-018-0049-3
- York, D. A., and Al-Baker, I. (1984). Effect of corticotropin on brown adipose tissue mitochondrial GDP binding in obese rats. *Biochem. J.* 223, 263–266. doi: 10.1042/bj2230263
- Young, J. B., Saville, E., Rothwell, N. J., Stock, M. J., and Landsberg, L. (1982). Effect of diet and cold exposure on norepinephrine turnover in brown adipose tissue of the rat. *J. Clin. Invest.* 69, 1061–1071. doi: 10.1172/JCI110541

**Conflict of Interest Statement:** The authors declare that the research was conducted in the absence of any commercial or financial relationships that could be construed as a potential conflict of interest.

Copyright © 2019 Schnabl, Westermeier, Li and Klingenspor. This is an open-access article distributed under the terms of the Creative Commons Attribution License (CC BY). The use, distribution or reproduction in other forums is permitted, provided the original author(s) and the copyright owner(s) are credited and that the original publication in this journal is cited, in accordance with accepted academic practice. No use, distribution or reproduction is permitted which does not comply with these terms.



# Autophagy in Adipocyte Browning: Emerging Drug Target for Intervention in Obesity

Seung-Hyun Ro<sup>1\*</sup>, Yura Jang<sup>1,2</sup>, Jiyoung Bae<sup>1,3</sup>, Isaac M. Kim<sup>1</sup>, Cameron Schaecher<sup>1,4</sup> and Zachery D. Shomo<sup>1</sup>

<sup>1</sup> Department of Biochemistry, University of Nebraska–Lincoln, Lincoln, NE, United States, <sup>2</sup> Department of Neurology, Johns Hopkins University School of Medicine, Baltimore, MD, United States, <sup>3</sup> Department of Cell and Regenerative Biology, University of Wisconsin School of Medicine and Public Health, Madison, WI, United States, <sup>4</sup> College of Medicine, University of Nebraska Medical Center, Omaha, NE, United States

## OPEN ACCESS

### Edited by:

Rita De Matteis,  
University of Urbino Carlo Bo, Italy

### Reviewed by:

Xiaohu Huang,  
Children's National Health System,  
United States  
Pablo Nicolas Fernandez Larrosa,  
Consejo Nacional de Investigaciones  
Científicas y Técnicas (CONICET),  
Argentina  
Paul Michael Yen,  
Duke-NUS Medical School,  
Singapore

### \*Correspondence:

Seung-Hyun Ro  
shro@unl.edu

### Specialty section:

This article was submitted to  
Integrative Physiology,  
a section of the journal  
Frontiers in Physiology

**Received:** 06 October 2018

**Accepted:** 10 January 2019

**Published:** 28 January 2019

### Citation:

Ro S-H, Jang Y, Bae J, Kim IM,  
Schaecher C and Shomo ZD (2019)  
Autophagy in Adipocyte Browning:  
Emerging Drug Target for Intervention  
in Obesity. *Front. Physiol.* 10:22.  
doi: 10.3389/fphys.2019.00022

Autophagy, lipophagy, and mitophagy are considered to be the major recycling processes for protein aggregates, excess fat, and damaged mitochondria in adipose tissues in response to nutrient status-associated stress, oxidative stress, and genotoxic stress in the human body. Obesity with increased body weight is often associated with white adipose tissue (WAT) hypertrophy and hyperplasia and/or beige/brown adipose tissue atrophy and aplasia, which significantly contribute to the imbalance in lipid metabolism, adipocytokine secretion, free fatty acid release, and mitochondria function. In recent studies, hyperactive autophagy in WAT was observed in obese and diabetic patients, and inhibition of adipose autophagy through targeted deletion of autophagy genes in mice improved anti-obesity phenotypes. In addition, active mitochondria clearance through activation of autophagy was required for beige/brown fat whitening – that is, conversion to white fat. However, inhibition of autophagy seemed detrimental in hypermetabolic conditions such as hepatic steatosis, atherosclerosis, thermal injury, sepsis, and cachexia through an increase in free fatty acid and glycerol release from WAT. The emerging concept of white fat browning–conversion to beige/brown fat–has been controversial in its anti-obesity effect through facilitation of weight loss and improving metabolic health. Thus, proper regulation of autophagy activity fit to an individual metabolic profile is necessary to ensure balance in adipose tissue metabolism and function, and to further prevent metabolic disorders such as obesity and diabetes. In this review, we summarize the effect of autophagy in adipose tissue browning in the context of obesity prevention and its potential as a promising target for the development of anti-obesity drugs.

**Keywords:** autophagy, lipophagy, mitophagy, beige/brown adipose tissue, browning, white adipose tissue, whitening, obesity

## INTRODUCTION: AUTOPHAGY IN ADIPOCYTES

### Autophagy

Macroautophagy, generally referred to as autophagy, is a cytosolic degradation and recycling process of damaged organelles and unwanted components in the cell (Singh et al., 2009b; Zhang et al., 2012; Cairo et al., 2016). When the cells or tissues are limited in their nutrient supply or exposed to a substantial amount of environmental, oxidative, or genotoxic stresses, autophagy



as a cellular survival and defense mechanism can be activated (Zhang et al., 2012; Bluher, 2013; Choi et al., 2013; Cairo et al., 2016). Autophagy can be induced in the cell through inhibition of either the nutrient-sensing kinase, mechanistic target of rapamycin complex 1 (mTORC1), or the activating-stress-sensing kinase, 5'-AMP activated protein kinase (AMPK) (Jung et al., 2010; Kim et al., 2011; Stienstra et al., 2014). On the other hand, when cells or tissues are supplied with excessive nutrients, the autophagy process is not necessary and is attenuated through mTORC1 activation and AMPK inhibition (Jung et al., 2010; Kim et al., 2011; Stienstra et al., 2014). When autophagy is suppressed for an extended period of time from continuous overnutrition, as with a high fat and/or fructose diet, the accumulation of unwanted proteins and organelles in the major metabolic tissues – such as adipose, liver, muscle, and pancreas – can become detrimental and eventually induce metabolic dysfunction and diseases such as obesity and diabetes (Zhang et al., 2012; Bluher, 2013; Rocchi and He, 2015). However, contradictory to findings of previous studies, autophagy seems hyperactivated in an effort to generate more fats from recycled energy in adipose tissues of obese patients (Kovsan et al., 2011; Jansen et al., 2012). A few reports suggest that autophagy inhibition can be a protective mechanism against high-fat diet-induced metabolic dysfunction by converting white adipose tissue (WAT) to brown adipose tissue (BAT) (Armani et al., 2014; Parray and Yun, 2017). Throughout the last decade, the therapeutics of modulating autophagy activity have drawn much attention; however, their clinical effectiveness in improving the metabolic profiles of humans with adipocyte metabolic dysfunctions linked to overweight, obesity, and diabetes has not been ascertained (Shoji-Kawata et al., 2013; Galluzzi et al., 2017).

## Adipogenesis

Adipogenesis is a unique adipocyte differentiation process that generates lipid droplets with triglycerides and fatty acids inside the lipid vacuoles (Rosen and Spiegelman, 2006; Ro et al., 2013; Ahmed et al., 2018). Autophagy for non-selective bulk degradation of proteins and lipids through the fusion of autophagosomes and lysosomes is suggested as one of the major types of autophagy in adipocytes (Singh et al., 2009b; Singh and Cuervo, 2012; Ro et al., 2013). The relationship between adipogenesis and autophagy has drawn much attention over the past decade regarding the potential link to metabolic diseases such as obesity. Autophagy is necessary and activated when white adipocyte undergoes differentiation (Singh et al., 2009b; Singh and Cuervo, 2012; Zhang et al., 2012; Ahmed et al., 2018). Chloroquine treatment and autophagy-related protein (ATG) 5 knockdown decreases adipogenesis of mouse embryonic fibroblast (MEF) cells. Targeted deletion of ATG5 in mice leads to a dramatically reduced mass of Perilipin A-positive white adipocytes in late-stage embryos and neonatal pups (Baerga et al., 2009; Singh et al., 2009b). Singh et al. and other research groups also observed decreased levels of microtubule-associated protein 1A/1B-light chain 3 (LC3), peroxisome proliferator-activated receptor (PPAR)- $\gamma$ , and triglyceride. This finding indicates that adipocyte differentiation and lipid accumulation are blocked by inhibition of autophagy when ATG7 is knocked down in

adipocytes or in adipose-specific deletion in mice (Singh et al., 2009b; Zhang et al., 2009; Singh and Cuervo, 2012). When ULK1, the mammalian homolog of ATG1 and the downstream autophagy kinase target of mTORC1, is knocked down in 3T3-L1 white adipocytes, adipogenesis increases, although autophagy is inhibited. However, the ULK2 knockdown in white adipocytes blocks both autophagy and adipogenesis (Ro et al., 2013). An increase in autophagy has been reported in adipose tissues derived from obese humans and mice, supporting adipogenesis in forming and storing more fat depots in the face of overnutrition (Kovsan et al., 2011; Cummins et al., 2014; Kosacka et al., 2015). Both an increased level of the lipidated form of LC3 (LC3-II) as an autophagosome marker and a decreased level of ubiquitin-binding scaffold protein p62, also called sequestosome 1 (SQSTM1), were observed in obese humans and mice, the combination of which would appear to be consistent with an increase in autophagy activity during adipogenesis (Klionsky et al., 2016; Yoshii and Mizushima, 2017). The level of autophagy activity seems to differ or at least to fluctuate depending on the adipose tissue type, external stimuli, and tissue age (Bluher, 2013; Kosacka et al., 2015; Li and Ding, 2017). Autophagy is activated when white adipocyte is undergoing differentiation to form lipid droplets. However, in an opposite way, autophagy also can be inhibited when brown adipocyte is activated with UCP1 and PPAR- $\gamma$ , increasing thermogenesis and browning, respectively, under cold exposure (Singh and Cuervo, 2012; Cairo et al., 2016; Ferhat et al., 2018). Based on previous studies on autophagy in different types of adipocytes, the inhibition of autophagy seems to be better for obesity prevention by reducing the formation of lipid droplets in white adipocytes and promoting energy expenditure in beige or brown adipocytes (Singh et al., 2009b; Kovsan et al., 2011; Ro et al., 2013; Cairo et al., 2016).

## Adipocytes

Adipocytes are the main type of cells found in both white and brown adipose tissues (Lo and Sun, 2013). White adipocytes contain a single lipid droplet and a small number of mitochondria. Brown adipocytes contain multiple small lipid droplets, enriched amounts of mitochondria, and exhibit a unique thermogenesis function through uncoupling protein 1 (UCP1). Beige adipocytes are the brown-like cells located within WAT, and they have a higher expression level of UCP1 than white adipocytes (Wu et al., 2012; Lo and Sun, 2013; Armani et al., 2014; Cummins et al., 2014). Browning is a process of dynamic conversion or modification of white adipocytes into beige/brown adipocytes upon activation by exposure to physiological, pharmacological, or hormonal stimuli (Wu et al., 2013; Abdullahi and Jeschke, 2016). Browning of white adipocytes is generally induced under cold exposure and exercise (Wu et al., 2012; Lo and Sun, 2013; Aldiss et al., 2018). However, this process does not completely transform or transdifferentiate white adipocytes into brown adipocytes. The white adipocytes become only a brown adipocyte-like phenotype, which is also called beige, inducible brown, brown-in-white, or brite adipocyte (Bartelt and Heeren, 2014; Scheele and Nielsen, 2017). In mouse studies, more beige cells have been detected in WAT of lean, compared to obese mice (Rachid et al., 2015). However in

human studies, they only observed higher native BAT activity but not active beige cells in lean subjects (Vijgen et al., 2011). Conventional methods to increase UCP1 in beige/brown fat cells, such as cold acclimation in humans, have not revealed any inducible browning fat depots in addition to the constitutively present depots and have not also proven enough to mediate browning of white fat depots (Scheele and Nielsen, 2017). There indeed are a few reports on cold-induced browning of human perirenal fat, but whether this fat depot is a good representation of visceral fat still remains controversial (Betz et al., 2013). In the study of human patients with pheochromocytoma disease who had performed both  $^{18}\text{F}$ -fluorodeoxyglucose positron emission tomography/computed tomography ( $^{18}\text{F}$ -FDG PET/CT) and plasma total metanephrine (TMN) measurements in China, browning of human visceral fat has been observed and reduces whole body fat mass by burning more fats through increased UCP1 in beige cells or BAT (Wang et al., 2011). Additionally, recent studies suggest that browning can increase the basal metabolism by burning fat through UCP1 and has been proposed as a potential approach for reducing body fat or treating obesity (Wu et al., 2012; Cummins et al., 2014).

## Autophagy Types in Adipocytes

Adipocytes undergo three major types of autophagy: macroautophagy, macrolipophagy (generally referred as lipophagy), and mitophagy. These occur dynamically depending on browning status (Baerga et al., 2009; Singh et al., 2009b; Zhang et al., 2009; Singh and Cuervo, 2012; Li and Ding, 2017; Ghosh et al., 2018). Both autophagy malfunction and adipocyte dysfunction are clearly connected with the causes of metabolic disorders such as obesity and diabetes (Baerga et al., 2009; Singh et al., 2009b; Zhang et al., 2009; Bjorndal et al., 2011; Singh and Cuervo, 2012; Bluher, 2013; Scheele and Nielsen, 2017; Ghosh et al., 2018). To examine this, both mechanistic and clinical studies have investigated the significant relationship between autophagy and browning (Armani et al., 2014; Stienstra et al., 2014). Here, we summarize the following: 1) the three major types of autophagy and their significance in regulating adipose lipid and energy metabolism; and 2) autophagy manipulations through direct autophagy gene knockdown or chemical/drug administration affecting the browning process in humans and mice from previous publications.

## LIPHAGY IN ADIPOCYTE LIPID METABOLISM

Lipophagy is the selective removal of lipid droplets in cytosolic organelles by lysosomes, which are derived from stimulated autophagy markers such as LC3 and p62 (Singh and Cuervo, 2012; Ward et al., 2016). Lipogenesis, often considered identical to adipogenesis, is focused on the formation of lipid droplets during white adipocyte differentiation with autophagy activation; lipolysis, on the other hand, is the secretion of glycerol and fatty acid partially resulting from the degradation of lipid droplets by autophagy (Cingolani and Czaja, 2016; Ahmed et al., 2018). The balance between lipogenesis and lipolysis plays a vital role in

regulating the lipid metabolism in white and brown adipocytes (Singh and Cuervo, 2012; Martinez-Lopez et al., 2016; Zechner et al., 2017). ULK1 activates lipolysis by activating autophagy in 3T3-L1 adipocytes. However, ULK1 inhibits fatty acid synthesis and uptake and activates fatty acid oxidation in the mitochondria independent of autophagy in adipocytes (Ro et al., 2013). In an *in vivo* study of POMC neurons using C57BL/6 WT mice, lipophagy in BAT and liver was activated by both cold exposure and rapamycin administration via the specific surface protein of lipid droplets, adipose triglyceride lipase (ATGL), and LC3 association (Martinez-Lopez et al., 2016). Although both liver and adipose tissue are important tissues in regulating lipid metabolism (Martinez-Lopez et al., 2016), when lipophagy was blocked in liver-specific ATG7 knockout mice, the lipid droplets accumulated in the liver and showed a steatosis-like phenotype (Singh and Cuervo, 2012; Liu and Czaja, 2013). However, in the case of adipose-specific ATG7 knockout mice, white adipocytes showed more brown adipocyte phenotypes with decreased lipids, increased number of mitochondria and beta oxidation (Singh et al., 2009b; Zhang et al., 2009).

The mechanism underlying different tissue specificity is still unclear (Singh and Cuervo, 2012; Martinez-Lopez et al., 2016). When basal lipophagy is inhibited by hyperactivation of mTORC1 due to overnutrition in the human body, lipid droplets are rapidly accumulated in BAT and liver (Singh et al., 2009a). By contrast, when inducible lipophagy is enhanced by inhibition of mTORC1 and activation of AMPK under starvation, lipophagy actively degrades lipid droplets in WAT and releases them as free fatty acids so that other metabolic tissues such as liver and muscle can utilize them as an energy source (Rosen and Spiegelman, 2006; Liu and Czaja, 2013; Ward et al., 2016). Thus, the balance between basal lipophagy and inducible lipophagy, as well as the balance between lipogenesis and lipolysis, is important and seems to be a possible mechanism explaining tissue specificity. BAT and liver tissue would be more prone to the balance between the basal and inducible status of lipophagy, whereas WAT would be more prone to the balance between lipogenesis and lipolysis. These different sensitivities and availability of lipophagy according to the type of tissues and stimuli may create advantages by allowing it to quickly adapt to the different levels of nutrient status in the human body (Martinez-Lopez et al., 2016; Ward et al., 2016). In future studies, transgenic mice with an inducible lipophagy system may serve as a very plausible model for identifying lipophagy specificity and its effect on lipid contents depending on nutrient availability (Singh and Cuervo, 2012).

## MITOPHAGY IN ADIPOCYTE MITOCHONDRIA FUNCTION

Mitophagy is the process of actively removing excess mitochondria through selective autophagy when mitochondria have accumulated during differentiation or have been damaged by oxidative stress such as ROS (Zhang et al., 2012; Ashrafi and Schwarz, 2013; Li et al., 2015; Taylor and Gottlieb, 2017). Mitophagy can be induced by ULK1 upon AMPK activation or mTORC1 inhibition under cellular maturation or nutrient

deprivation (Kundu et al., 2008; Egan et al., 2011; Kim et al., 2011). The main mitophagy process, the association between mitochondria and autophagolysosomes, is mediated by the ubiquitin-dependent PINK1-Parkin pathway (Narendra et al., 2010; Vincow et al., 2013; Bingol and Sheng, 2016). Alternatively, mitochondria can be degraded by selective autophagy via LC3 and p62 protein independent of ubiquitin in adipose tissue (Altshuler-Keylin and Kajimura, 2017; Taylor and Gottlieb, 2017; Lu et al., 2018). Mitochondria can also be degraded and decreased in number through mitophagy to form more lipid droplets in white adipocyte tissue during differentiation by limiting fatty acid oxidation (Gospodarska et al., 2015; Altshuler-Keylin and Kajimura, 2017). Mitophagy at least in part contributes to whitening of beige adipocytes, turning them into white adipocytes by removing mitochondria after the withdrawal of cold exposure (Altshuler-Keylin et al., 2016; Altshuler-Keylin and Kajimura, 2017; Lu et al., 2018). Therefore, when mitophagy is blocked in white adipocytes, mitochondria cannot be degraded and accumulated while inhibiting adipogenesis, which results in a beige/brown adipocyte phenotype (Altshuler-Keylin and Kajimura, 2017). Consistent with cell culture studies, when mitophagy is inhibited in mice either by autophagy gene deficiency or chemical administration, WAT shows accumulation of mitochondria with decreased fat mass and changes into a phenotype like the beige or brown adipocytes (Singh and Cuervo, 2012; Altshuler-Keylin et al., 2016; Taylor and Gottlieb, 2017; Lu et al., 2018). Clinical researchers have observed more accumulation of dysfunctional or metabolically impaired mitochondria in obese people compared to a lean control group (Kraunsoe et al., 2010; Chattopadhyay et al., 2015). These observations possibly suggest that mitophagy would be negatively regulated by excessive fat accumulation or in obese condition. In conditions of overnutrition, mTORC1 activation and mitophagy inhibition resulted in greater accumulation of impaired mitochondria (Altshuler-Keylin and Kajimura, 2017). Studies using autophagy-related gene knockout mice fed with a high-fat diet suggest that when autophagy and mitophagy in adipocytes are impaired by overnutrition, inhibition of lipogenesis and activation of lipophagy can occur as a compensatory mechanism (Zhang et al., 2009; Altshuler-Keylin and Kajimura, 2017). To our surprise, the browning of WAT was observed in skeletal muscle-specific Atg7 knockout mice that were resistant to obesity induced by a high-fat diet (Kim et al., 2013). This ambivalence of mitophagy in adipocyte turnover and the existence of compensation mechanisms with other selective autophagy may be for purposes of more effectively maintaining mitochondrial integrity and mass in adipocytes (Lu et al., 2018). Although mitophagy is suggested as a positive regulator of white adipogenesis and a negative regulator of beige and brown adipogenesis, the level of mitophagy necessary for browning seems controversial due to the complicated regulation of activity dependent on nutrition status (Altshuler-Keylin and Kajimura, 2017). Therefore, the proper modulation of mitophagy in adipocytes in humans and mice seems necessary for the timely turnover between white, beige, and brown adipocytes, dependent on nutrition level.

## AUTOPHAGY MANIPULATIONS IN ADIPOCYTE BROWNING

Although the distribution of adipose tissue is distinct in humans and mice, both share common characteristics (Seale et al., 2009; Zhang et al., 2018). Anatomically in male mice, interscapular brown adipose tissue (iBAT) contains classic brown adipocytes, whereas epididymal white adipose tissue (eWAT) and subcutaneous white adipose tissue (sWAT) contain classic white adipocytes (Sanchez-Gurmaches and Guertin, 2014; Gospodarska et al., 2015). In humans, most classic brown adipocytes develop mainly around the neck and supraclavicular area through infancy, but gradually decrease until adulthood (Wu et al., 2012; Zhang et al., 2018). Several studies using positron emission tomography (PET)-CT have demonstrated that, in addition to size reduction in aging, BAT activity is reduced in obese and diabetic patients (Lee et al., 2010; Leitner et al., 2017). A few other clinical research groups have suggested that stimulating browning in WAT would be beneficial in slowing obesity, diabetes, and even the aging process (Scheele and Nielsen, 2017). Therefore, the existence of active turnover from WAT to beige fat to BAT in humans and mice has been recognized as a potential therapeutic target for prevention and treatment of obesity and related metabolic diseases (Kajimura et al., 2015; Schrauwen et al., 2015; Giordano et al., 2016). Even whole tissue switching of WAT to BAT through surgical transplantation or implantation of mesenchymal stem cells, brown adipocytes, or BAT into WAT areas in humans and mice is gaining a new spotlight as a novel method to prevent or treat obesity and diabetes (Liu et al., 2013; Soler-Vazquez et al., 2018). However, the activity and selectivity of autophagy after the transplantation or implantation still needs further investigation.

Indeed, autophagy plays an important role in the browning of WAT and beige adipocytes. A recent study has reported that autophagy is needed to convert beige adipocytes to WAT upon removal of  $\beta$ 3-AR agonists or recovery from cold exposure (Altshuler-Keylin et al., 2016). Cairo et al. (2016) reported that thermogenic activation through cold exposure inhibits autophagy, which leads to increased UCP1 level in BAT. Although we have selected only a few significant factors to discuss in our review, numerous factors are involved in the manipulation of the autophagy pathway, which regulate the browning of WAT and beige adipocyte (Table 1).

### Parkin-Mediated Mitophagy in Browning

Parkin (gene name: Park2) is a E3 ubiquitin ligase that plays a critical role in ubiquitination as a mitophagy-associated degradation signal (Geisler et al., 2010; Jin and Youle, 2012; Pickrell and Youle, 2015). The role of Parkin in browning of WAT has been studied in 3T3-L1 adipocytes and the Parkin-deficient C57BL/6 mice model. Parkin expression increases during 3T3-L1 adipocyte differentiation, while its expression decreases in rosiglitazone-treated 3T3-L1 adipocytes, which have phenotypes of beige adipocytes due to enhanced UCP1 expression. Inhibition of the Parkin gene does not affect browning, but

**TABLE 1 |** Summary of recent studies about the effect of direct autophagy gene manipulation or autophagy-related regulators on adipocyte browning.

Study	Target Gene Intervention	Application	Results	Clinical/Physiological Function
Baerga et al., 2009; Singh et al., 2009b	ATG5	<i>In vitro</i> Chloroquine (autophagy inhibitor) treatment in MEF cells (Baerga et al., 2009) siAtg5 (knockdown) in MEF cells (Singh et al., 2009b) <i>In vivo</i> Histological analysis of Atg5 <sup>-/-</sup> late-stage embryos and neonatal pups (Baerga et al., 2009)	Chloroquine treatment and Atg5 knockdown decreased adipogenesis of MEF cells (Singh et al., 2009b). Perilipin A positive adipocytes in sWAT as dramatically reduced in Atg5 <sup>-/-</sup> late-stage embryos and neonatal pups (Baerga et al., 2009). Chloroquine's or Atg5's effect on browning is not observed.	Chloroquine increased success in an autophagy-inhibitor based treatment therapy for a variety of cancer types in humans, when compared to chemotherapy or radiation alone (Xu et al., 2018).
Singh et al., 2009b; Zhang et al., 2009	ATG7	<i>In vitro</i> siAtg7 in 3T3-L1 adipocytes (Singh et al., 2009b) <i>In vivo</i> Adipose-specific Atg7 <sup>-/-</sup> and WT mice (both groups)	White adipocyte differentiation is blocked upon Atg7 loss, and mice showed brown adipocyte phenotypes with decreased lipids, increased number of mitochondria and beta oxidation.	N/A
Ro et al., 2013	ATG1	<i>In vitro</i> Rapamycin treatment, siULK1 or siULK2 in 3T3-L1 adipocytes	ULK1 or ULK2 is necessary for autophagy induction in adipocytes. ULK1 negatively regulates lipogenesis independent of autophagy in adipocytes. ULK1's or ULK2's effect on browning is not investigated.	Rapamycin, a potent ATG1 activator through mTORC1 inhibition, has been shown to increase the rate of autophagy in ischemic adipose derived stem cells used during transplantation in humans, promoting overall success of the surgical implantation (Li et al., 2017).
Martinez-Lopez et al., 2016	ATGL	<i>In vivo</i> Cold or rapamycin administration on C57BL/6 WT mice	Both cold and rapamycin administration in POMC neuron activates lipophagy in BAT via ATGL-LC3 association.	See above
Cairo et al., 2016; Altshuler-Keylin et al., 2016	UCP1	<i>In vivo</i> Cold administration on C57BL/6 WT mice (Cairo et al., 2016) Cold or $\beta$ 3-AR agonist administration on [UCP1(+)]-adipocyte-specific Atg5 or Atg12 knockout mice (Altshuler-Keylin et al., 2016)	Activation of UCP1 suppresses autophagy in BAT (Cairo et al., 2016). Atg5 or Atg12 knockout in beige/brown adipose tissue prevents white-like characteristics through inhibiting autophagic clearance of mitochondria (Altshuler-Keylin et al., 2016).	N/A
Taylor and Gottlieb, 2017; Lu et al., 2018	PARKIN or PARK2	<i>In vitro</i> Rosiglitazone (browning stimulant), siParkin, or mCherry-Parkin (overexpression) in 3T3-L1 adipocytes (Taylor and Gottlieb, 2017) <i>In vivo</i> Parkin <sup>-/-</sup> and WT mice with rosiglitazone or CL316243 injection (Taylor and Gottlieb, 2017) <i>In vivo</i> Park2 knockout mice administered with $\beta$ 3-AR agonist, CL316243 (Lu et al., 2018)	Rosiglitazone induces browning in 3T3-L1 white adipocytes; Parkin knockdown does not affect browning, but Parkin overexpression inhibits browning in adipocytes (Taylor and Gottlieb, 2017). When browning stimulus CL316243 was removed, UCP1 was reduced in WAT of WT, but was maintained in Park2 knockout mice and BAT of both groups (Lu et al., 2018).	Rosiglitazone, a PPAR- $\gamma$ agonist, has been shown to increase overall body fat content in humans, but does not affect heart rate variability (Grenier et al., 2016). CL 316,243 has been shown to increase the effectiveness of insulin, and fat oxidation in lean male subjects, by acting as an agonist for $\beta$ 3-adrenergic receptor (Weyer et al., 1998).
Armani et al., 2014	Mineralocorticoid receptor antagonist: spironolactone (spiro) or drospirenone (DRSP)	<i>In vitro</i> 3T3-L1 was differentiated with $10^{-8}$ M aldosterone, $10^{-5}$ M DRSP or $10^{-5}$ M spiro treatment <i>In vivo</i> High-fat diet-fed mice with	white adipocytes, revealed by increase of brown adipose-specific markers such as UCP1 and PRDM16.	Serum aldosterone reduction through diet change and increase in physical activity has been shown to decrease obesity-related health factors in young adults only diagnosed with excess body fat (Cooper et al., 2013).

(Continued)



TABLE 1 | Continued

Study	Target Gene Intervention	Application	Results	Clinical/Physiological Function
		6 mg/kg/day DRSP or 20 mg/kg/day spiro for 90 days	Mineralocorticoid receptor antagonists reduced body weight gain and WAT mass gain via autophagy activation, but significantly increased browning of WAT and primary	DRSP, an autophagy activator, currently has no human clinical trials available. Spiro was shown to rescue insulin resistance in humans with chronic kidney disease, and reversed glucose intolerance in mice possibly by activating autophagy (Hosoya et al., 2015).
Ghosh et al., 2018	PIK3C3	<i>In vivo</i> Aged C57BL/6 male mice with mutant PIK3C3 gene	PIK3C3 mutation led to enhanced browning of gWAT when autophagy is impaired.	N/A
Parray and Yun, 2017	Thiodigalactoside (TDG)	<i>In vitro</i> 500 $\mu$ M during 3T3-L1 and HIB1B adipocyte differentiation <i>In vivo</i> 5-week-old rats peritoneal injected 5 mg/kg/week for 5 weeks	TDG, an inhibitor of autophagy, increases browning markers, thermogenic protein UCP1, and mitochondrial functions and activities.	TDG currently has no clinical data available in humans.
Leu et al., 2018	Raspberry ketone	<i>In vitro</i> 100 $\mu$ M for 48 hrs after fully differentiated 3T3-L1 adipocytes <i>In vivo</i> 8-week-old rats administered 160 mg/kg/day for 8 weeks	Raspberry ketone-fed rats had less adipose tissue, more browning-related markers through inhibition of autophagy.	Currently, clinical data is not available in humans for Raspberry ketone.

overexpression of Parkin significantly reduces browning in adipocytes (Taylor and Gottlieb, 2017). Furthermore, Parkin is highly expressed during beige adipocyte differentiation (Lu et al., 2018). The Kajimura group has shown that Parkin is required to maintain beige adipocytes in WAT. When CL316243, a  $\beta$ 3-AR agonist, is removed, UCP1 expression is significantly reduced in WAT of wild type (WT) mice, but still expressed in WAT of Park2 knockout mice. In contrast, UCP1 expression in BAT is not changed in both WT and Park2 knockout mice after CL316243 is removed (Lu et al., 2018).

## Mineralocorticoid Receptor Antagonism in Browning

The Yan group has shown that autophagy is regulated by mineralocorticoid receptor (MR) antagonism (Li et al., 2016). Spironolactone induces LC3 and ATG5 expression and reduces PI3K/AKT/mTOR pathways in injured human podocytes (Li et al., 2016). Previous research has reported the role of MR in adipocyte differentiation. Drospirenone (DRSP) significantly reduces 3T3-L1 and 3T3-F442A adipocyte differentiation without cell cytotoxicity (Caprio et al., 2011). MR also regulates browning of WAT through autophagy. Additionally, it has been determined that MR antagonists fully prevent aldosterone-induced autophagy in white adipocytes along with an increase of UCP1 expression. MR antagonists significantly enhance browning of WAT in diet-induced obese mice as well as brown adipose-specific markers in primary adipocytes isolated from WAT (Armani et al., 2014).

## PIK3C3 in Browning

PIK3C3 is a subunit of class III phosphoinositide 3-kinase (PI3K) that phosphorylates phosphatidylinositol to generate

phosphatidylinositol 3-phosphate. The PIK3C3-ATG14 complex induces autophagy especially in nutrient-stress conditions such as starvation (Yuan et al., 2013). Recently, it has been shown that in aged mice with a PIK3C3 mutation, compared to fl/fl control mice, adipogenesis markers, such as AP2 and C/EBP- $\alpha$ , are reduced, but brown adipose-specific markers, such as UCP1 and PPAR- $\gamma$  coactivator (PGC)1 $\alpha$ , are enhanced in both mRNA and protein levels in the gonadal WAT (gWAT), possibly through blocking of autophagy (Ghosh et al., 2018).

## Thiodigalactoside in Browning

Thiodigalactoside (TDG), an inhibitor of galectin 1 and autophagy, has recently been studied in obesity research by the Yun group (Mukherjee et al., 2015; Parray and Yun, 2015; 2017). They have reported that TDG-treated adipocytes significantly inhibit lipid accumulation, and TDG also reduces body weight in high-fat diet-fed rats (Mukherjee et al., 2015). Their second study has shown proteomic identification of TDG in WAT of rats with high-fat diet-induced obesity. Specifically, proteins involved in carbohydrate metabolism and the tricarboxylic acid cycle remarkably increased in WAT of TDG-injected obese rats (Parray and Yun, 2015). A most recent study has reported that TDG plays an important role in browning of white adipocytes and WAT in obese rats (Parray and Yun, 2017). Dose-dependent TDG treatment reduces galectin 1 and ATG 5 gene expression, but enhances brown-specific markers, UCP1 and PGC1 $\alpha$ , in 3T3-L1 adipocytes. Moreover, UCP1 and PGC1 $\alpha$  gene and protein expressions are upregulated by PDG injection in iWAT, eWAT, and BAT of diet-induced obese rats, possibly through inhibition of ATG5/LC3-II and increase of p62 expression (Parray and Yun, 2017).

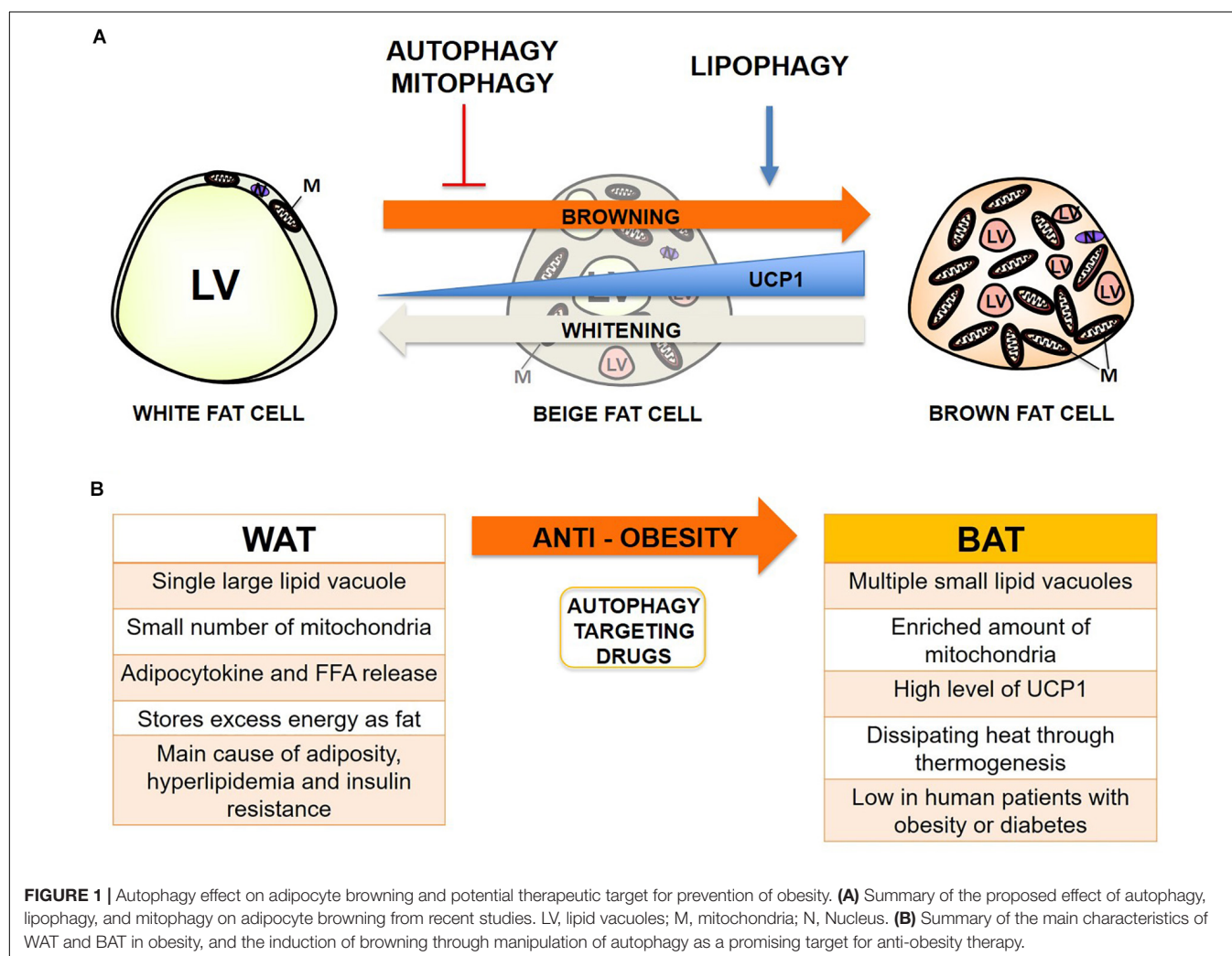
## Raspberry Ketone in Browning

Raspberry ketone, 4-(4-hydroxyphenyl) butan-2-one, a phenolic compound found in red raspberry, has emerged as a dietary bioactive compound with beneficial effects on obesity (Cotten et al., 2017; Tsai et al., 2017). Evidence suggests that raspberry ketone reduces body weight and food intake in high-fat diet-fed mice (Cotten et al., 2017) and ovariectomy-induced obese rats (Leu et al., 2017). In addition, raspberry ketone inhibits 3T3-L1 adipogenesis, revealed by inhibition of expression of adipogenesis markers such as PPAR- $\gamma$ , C/EBP- $\alpha$ , FAS, and AP2, possibly via inhibition of autophagy, confirmed by decrease of ATG12 and LC3B levels, as well as increase of p62 and mTORC1 levels (Leu et al., 2017; Tsai et al., 2017). It has been recently reported that high concentration of raspberry ketone (100  $\mu$ M) significantly increases browning of 3T3-L1 adipocytes, revealed by an increase of browning-specific markers, including UCP1 and PGC1 $\alpha$ , and lipolysis markers such as hormone-sensitive lipase and triglyceride lipase (Leu et al., 2018). Moreover, expression of brown adipose markers is increased in ovariectomy-induced obese rats that have been administered raspberry, compared to control groups mediated by inhibition

of ATG12 and an increase of p62 expression (Leu et al., 2018).

## CONCLUSION: AUTOPHAGY- AND BROWNING-TARGETING THERAPEUTICS FOR THE PREVENTION OF OBESITY

Adipose metabolism is closely linked with metabolic dysfunctions such as obesity and diabetes when fat distribution and energy balance through mitochondria are not strictly maintained (Bjorndal et al., 2011; Bluher, 2013; Stienstra et al., 2014; Scheele and Nielsen, 2017). The relationship between adipose metabolism and autophagy has become an increasingly intriguing topic since the dawn of the discovery of selective autophagy, including lipophagy and mitophagy, which can also actively occur in adipose tissue (Rocchi and He, 2015). Autophagy has previously been shown to be increased in adipocytes from obese humans and mice (Ost et al., 2010; Kovsan et al., 2011; Jansen et al., 2012). Previous reports indicate that excess free



fatty acid (FFA) – particularly saturated FFA like palmitic acid (PA), but not unsaturated FFA such as oleic acid (OA) – formed by a high-fat diet can activate autophagy through JNK2 or PKC activation (Tan et al., 2012; Tu et al., 2014). Conversely, lipophagy seems beneficial for degrading excess fats from WAT and generating more intracellular space for the expansion of the mitochondrial contents from BAT when mitophagy is inhibited or mitochondrial biogenesis is activated, thus protecting the human body from nutrient oversupply which, can occur in obesity conditions (Singh and Cuervo, 2012; Cummins et al., 2014). Mitophagy seems much more controversial because basal activity can be beneficial through elimination of damaged mitochondria from accumulated ROS in obesity; however, hyperactive inducible mitophagy can convert BAT or beige fat to white during differentiation, which is called “reverse browning or whitening,” and subsequently cause systemic change in adipocytokine release and lipid metabolism (Hill et al., 2012; Gospodarska et al., 2015). Overall, inhibition or deficiency of autophagy, activation of lipophagy rather than lipolysis, and a basal or moderate level of mitophagy seems the most optimal combination for the prevention of obesity so far (Figure 1).

However, we have also encountered a few exceptional cases from previous reports noting that hyperactive autophagy can be beneficial during hypermetabolic conditions such as hepatic steatosis, atherosclerosis, injuries from burning, sepsis, and cachexia (Volzke et al., 2005; Penna et al., 2014; Pravda, 2014; Song et al., 2014; Abdullahi and Jeschke, 2016). Normally, hyperactivation of autophagy leads to apoptotic cell death (Lum et al., 2005), but highly autophagic cells under hypermetabolic conditions such as post-thermal injury may survive better by efficiently regulating energy metabolism (Auger et al., 2017). Paradoxically, autophagy activation in WAT can be beneficial for obese or diabetic patients with a hypermetabolic profile or complications, because it decreases FFA and glycerol release from hypertrophic and hyperplastic WAT by actively degrading lipid vacuoles (LV) as an energy source. We have summarized previously

reported autophagy and selective autophagy manipulations and their effect on adipocyte browning (Table 1). Since the combined delicate manipulation of autophagy, lipophagy, and mitophagy seems necessary for the timely turnover between white, beige, and brown adipocytes dependent on nutrition levels in humans and mice, the direct manipulation of autophagy and selective autophagy or the administration of autophagy-targeting drugs should be cautiously performed. Finally, summarizing autophagy regulation and its implications in browning could help give insights for the development of autophagy-targeting drugs in the prevention of obesity.

## AUTHOR CONTRIBUTIONS

All authors listed have made a substantial, direct and intellectual contribution to the work, and approved it for publication.

## FUNDING

This work was supported by NSF-REU site: Training in Redox Biology (DBI-1757951) to ZS, Undergraduate Creative Activities and Research Experience (UCARE) program-scholarship from the Pepsi Quasi Endowment and Union Bank & Trust to CS, University of Nebraska-Lincoln ARD/ORED/BIOC grants, Layman award, Nebraska Tobacco Settlement-Biomedical research enhancement funds, and Nebraska Center for the Prevention of Obesity Diseases (NPOD) seed grant from NIH (P20GM104320) to S-HR.

## ACKNOWLEDGMENTS

We thank every present and past Ro lab member for helpful discussion and comments. We apologize that we could not include many original publications due to limited space.

## REFERENCES

- Abdullahi, A., and Jeschke, M. G. (2016). White adipose tissue browning: a double-edged sword. *Trends Endocrinol. Metab.* 27, 542–552. doi: 10.1016/j.tem.2016.06.006
- Ahmed, M., Nguyen, H. Q., Hwang, J. S., Zada, S., Lai, T. H., Kang, S. S., et al. (2018). Systematic characterization of autophagy-related genes during the adipocyte differentiation using public-access data. *Oncotarget* 9, 15526–15541. doi: 10.18632/oncotarget.24506
- Aldiss, P., Betts, J., Sale, C., Pope, M., Budge, H., and Symonds, M. E. (2018). Exercise-induced ‘browning’ of adipose tissues. *Metabolism* 81, 63–70. doi: 10.1016/j.metabol.2017.11.009
- Altshuler-Keylin, S., and Kajimura, S. (2017). Mitochondrial homeostasis in adipose tissue remodeling. *Sci. Signal.* 10:eaa19248. doi: 10.1126/scisignal.aai9248
- Altshuler-Keylin, S., Shinoda, K., Hasegawa, Y., Ikeda, K., Hong, H., Kang, Q., et al. (2016). Beige adipocyte maintenance is regulated by autophagy-induced mitochondrial clearance. *Cell Metab.* 24, 402–419. doi: 10.1016/j.cmet.2016.08.002
- Armani, A., Cinti, F., Marzolla, V., Morgan, J., Cranston, G. A., Antelmi, A., et al. (2014). Mineralocorticoid receptor antagonism induces browning of white adipose tissue through impairment of autophagy and prevents adipocyte dysfunction in high-fat-diet-fed mice. *FASEB J.* 28, 3745–3757. doi: 10.1096/fj.13-245415
- Ashrafi, G., and Schwarz, T. L. (2013). The pathways of mitophagy for quality control and clearance of mitochondria. *Cell Death Differ.* 20, 31–42. doi: 10.1038/cdd.2012.81
- Auger, C., Samadi, O., and Jeschke, M. G. (2017). The biochemical alterations underlying post-burn hypermetabolism. *Biochim. Biophys. Acta* 1863(10 Pt B), 2633–2644. doi: 10.1016/j.bbdis.2017.02.019
- Baerga, R., Zhang, Y., Chen, P. H., Goldman, S., and Jin, S. (2009). Targeted deletion of autophagy-related 5 (atg5) impairs adipogenesis in a cellular model and in mice. *Autophagy* 5, 1118–1130. doi: 10.4161/auto.5.8.9991
- Bartelt, A., and Heeren, J. (2014). Adipose tissue browning and metabolic health. *Nat. Rev. Endocrinol.* 10, 24–36. doi: 10.1038/nrendo.2013.204
- Betz, M. J., Slawik, M., Lidell, M. E., Osswald, A., Heglind, M., Nilsson, D., et al. (2013). Presence of brown adipocytes in retroperitoneal fat from patients with benign adrenal tumors: relationship with outdoor temperature. *J. Clin. Endocrinol. Metab.* 98, 4097–4104. doi: 10.1210/jc.2012-3535
- Bingol, B., and Sheng, M. (2016). Mechanisms of mitophagy: PINK1, Parkin, USP30 and beyond. *Free Radic. Biol. Med.* 100, 210–222. doi: 10.1016/j.freeradbiomed.2016.04.015

- Bjorndal, B., Burri, L., Staalesen, V., Skorve, J., and Berge, R. K. (2011). Different adipose depots: their role in the development of metabolic syndrome and mitochondrial response to hypolipidemic agents. *J. Obes.* 2011, 490650. doi: 10.1155/2011/490650
- Bluher, M. (2013). Adipose tissue dysfunction contributes to obesity related metabolic diseases. *Best Pract. Res. Clin. Endocrinol. Metab.* 27, 163–177. doi: 10.1016/j.beem.2013.02.005
- Cairo, M., Villarroya, J., Cereijo, R., Campderros, L., Giralt, M., and Villarroya, F. (2016). Thermogenic activation represses autophagy in brown adipose tissue. *Int. J. Obes. (Lond.)* 40, 1591–1599. doi: 10.1038/ijo.2016.115
- Caprio, M., Antelmi, A., Chetrite, G., Muscat, A., Mammi, C., Marzolla, V., et al. (2011). Antiadipogenic effects of the mineralocorticoid receptor antagonist drospirenone: potential implications for the treatment of metabolic syndrome. *Endocrinology* 152, 113–125. doi: 10.1210/en.2010-0674
- Chattopadhyay, M., Khemka, V. K., Chatterjee, G., Ganguly, A., Mukhopadhyay, S., and Chakrabarti, S. (2015). Enhanced ROS production and oxidative damage in subcutaneous white adipose tissue mitochondria in obese and type 2 diabetes subjects. *Mol. Cell Biochem.* 399, 95–103. doi: 10.1007/s11010-014-2236-7
- Choi, A. M., Ryter, S. W., and Levine, B. (2013). Autophagy in human health and disease. *N. Engl. J. Med.* 368, 651–662. doi: 10.1056/NEJMr1205406
- Cingolani, F., and Czaja, M. J. (2016). Regulation and functions of autophagic lipolysis. *Trends Endocrinol. Metab.* 27, 696–705. doi: 10.1016/j.tem.2016.06.003
- Cooper, J. N., Fried, L., Tepper, P., Barinas-Mitchell, E., Conroy, M. B., Evans, R. W., et al. (2013). Changes in serum aldosterone are associated with changes in obesity-related factors in normotensive overweight and obese young adults. *Hypertens. Res.* 36, 895–901. doi: 10.1038/hr.2013.45
- Cotten, B. M., Diamond, S. A., Banh, T., Hsiao, Y. H., Cole, R. M., Li, J., et al. (2017). Raspberry ketone fails to reduce adiposity beyond decreasing food intake in C57BL/6 mice fed a high-fat diet. *Food Funct.* 8, 1512–1518. doi: 10.1039/c6fo01831a
- Cummins, T. D., Holden, C. R., Sansbury, B. E., Gibb, A. A., Shah, J., Zafar, N., et al. (2014). Metabolic remodeling of white adipose tissue in obesity. *Am. J. Physiol. Endocrinol. Metab.* 307, E262–E277. doi: 10.1152/ajpendo.00271.2013
- Egan, D. F., Shackelford, D. B., Mihaylova, M. M., Gelino, S., Kohnz, R. A., Mair, W., et al. (2011). Phosphorylation of ULK1 (hATG1) by AMP-activated protein kinase connects energy sensing to mitophagy. *Science* 331, 456–461. doi: 10.1126/science.1196371
- Ferhat, M., Funai, K., and Boudina, S. (2018). Autophagy in adipose tissue physiology and pathophysiology. *Antioxid. Redox Signal.* doi: 10.1089/ars.2018.7626 [Epub ahead of print].
- Galluzzi, L., Bravo-San Pedro, J. M., Levine, B., Green, D. R., and Kroemer, G. (2017). Pharmacological modulation of autophagy: therapeutic potential and persisting obstacles. *Nat. Rev. Drug Discov.* 16, 487–511. doi: 10.1038/nrd.2017.22
- Geisler, S., Holmstrom, K. M., Skujat, D., Fiesel, F. C., Rothfuss, O. C., Kahle, P. J., et al. (2010). PINK1/Parkin-mediated mitophagy is dependent on VDAC1 and p62/SQSTM1. *Nat. Cell Biol.* 12, 119–131. doi: 10.1038/ncb2012
- Ghosh, A. K., Mau, T., O'Brien, M., and Yung, R. (2018). Novel role of autophagy-associated Pik3c3 gene in gonadal white adipose tissue browning in aged C57/BL6 male mice. *Aging (Albany NY)* 10, 764–774. doi: 10.18632/aging.101426
- Giordano, A., Frontini, A., and Cinti, S. (2016). Convertible visceral fat as a therapeutic target to curb obesity. *Nat. Rev. Drug Discov.* 15, 405–424. doi: 10.1038/nrd.2016.31
- Gospodarska, E., Nowialis, P., and Kozak, L. P. (2015). Mitochondrial turnover: a phenotype distinguishing brown adipocytes from interscapular brown adipose tissue and white adipose tissue. *J. Biol. Chem.* 290, 8243–8255. doi: 10.1074/jbc.M115.637785
- Grenier, A., Brassard, P., Bertrand, O. F., Despres, J. P., Costerousse, O., Almeras, N., et al. (2016). Rosiglitazone influences adipose tissue distribution without deleterious impact on heart rate variability in coronary heart disease patients with type 2 diabetes. *Clin. Auton. Res.* 26, 407–414. doi: 10.1007/s10286-016-0373-7
- Hill, B. G., Benavides, G. A., Lancaster, J. R., Ballinger, S., Dell'Italia, L., Jianhua, Z., et al. (2012). Integration of cellular bioenergetics with mitochondrial quality control and autophagy. *Biol. Chem.* 393, 1485–1512. doi: 10.1515/hsz-2012-0198
- Hosoya, K., Minakuchi, H., Wakino, S., Fujimura, K., Hasegawa, K., Komatsu, M., et al. (2015). Insulin resistance in chronic kidney disease is ameliorated by spironolactone in rats and humans. *Kidney Int.* 87, 749–760. doi: 10.1038/ki.2014.348
- Jansen, H. J., van Essen, P., Koenen, T., Joosten, L. A., Netea, M. G., Tack, C. J., et al. (2012). Autophagy activity is up-regulated in adipose tissue of obese individuals and modulates proinflammatory cytokine expression. *Endocrinology* 153, 5866–5874. doi: 10.1210/en.2012-1625
- Jin, S. M., and Youle, R. J. (2012). PINK1- and Parkin-mediated mitophagy at a glance. *J. Cell Sci.* 125(Pt 4), 795–799. doi: 10.1242/jcs.093849
- Jung, C. H., Ro, S. H., Cao, J., Otto, N. M., and Kim, D. H. (2010). mTOR regulation of autophagy. *FEBS Lett.* 584, 1287–1295. doi: 10.1016/j.febslet.2010.01.017
- Kajimura, S., Spiegelman, B. M., and Seale, P. (2015). Brown and beige fat: physiological roles beyond heat generation. *Cell Metab.* 22, 546–559. doi: 10.1016/j.cmet.2015.09.007
- Kim, J., Kundu, M., Viollet, B., and Guan, K. L. (2011). AMPK and mTOR regulate autophagy through direct phosphorylation of Ulk1. *Nat. Cell Biol.* 13, 132–141. doi: 10.1038/ncb2152
- Kim, K. H., Jeong, Y. T., Oh, H., Kim, S. H., Cho, J. M., Kim, Y. N., et al. (2013). Autophagy deficiency leads to protection from obesity and insulin resistance by inducing Fgf21 as a mitokine. *Nat. Med.* 19, 83–92. doi: 10.1038/nm.3014
- Klionsky, D. J., Abdelmohsen, K., Abe, A., Abedin, M. J., Abeliovich, H., Acevedo Arozana, A., et al. (2016). Guidelines for the use and interpretation of assays for monitoring autophagy (3rd edition). *Autophagy* 12, 1–222. doi: 10.1080/15548627.2015.1100356
- Kosacka, J., Kern, M., Kloting, N., Paeschke, S., Rudich, A., Haim, Y., et al. (2015). Autophagy in adipose tissue of patients with obesity and type 2 diabetes. *Mol. Cell. Endocrinol.* 409, 21–32. doi: 10.1016/j.mce.2015.03.015
- Kovsan, J., Bluher, M., Tarnowski, T., Kloting, N., Kirshtein, B., Madar, L., et al. (2011). Altered autophagy in human adipose tissues in obesity. *J. Clin. Endocrinol. Metab.* 96, E268–E277. doi: 10.1210/jc.2010-1681
- Kraunsoe, R., Boushel, R., Hansen, C. N., Schjerling, P., Qvortrup, K., Stockel, M., et al. (2010). Mitochondrial respiration in subcutaneous and visceral adipose tissue from patients with morbid obesity. *J. Physiol.* 588(Pt 12), 2023–2032. doi: 10.1113/jphysiol.2009.184754
- Kundu, M., Lindsten, T., Yang, C. Y., Wu, J., Zhao, F., Zhang, J., et al. (2008). Ulk1 plays a critical role in the autophagic clearance of mitochondria and ribosomes during reticulocyte maturation. *Blood* 112, 1493–1502. doi: 10.1182/blood-2008-02-137398
- Lee, P., Greenfield, J. R., Ho, K. K., and Fulham, M. J. (2010). A critical appraisal of the prevalence and metabolic significance of brown adipose tissue in adult humans. *Am. J. Physiol. Endocrinol. Metab.* 299, E601–E606. doi: 10.1152/ajpendo.00298.2010
- Leitner, B. P., Huang, S., Brychta, R. J., Duckworth, C. J., Baskin, A. S., McGehee, S., et al. (2017). Mapping of human brown adipose tissue in lean and obese young men. *Proc. Natl. Acad. Sci. U.S.A.* 114, 8649–8654. doi: 10.1073/pnas.1705287114
- Leu, S. Y., Chen, Y. C., Tsai, Y. C., Hung, Y. W., Hsu, C. H., Lee, Y. M., et al. (2017). Raspberry ketone reduced lipid accumulation in 3T3-L1 cells and ovariectomy-induced obesity in wistar rats by regulating autophagy mechanisms. *J. Agric. Food Chem.* 65, 10907–10914. doi: 10.1021/acs.jafc.7b03831
- Leu, S. Y., Tsai, Y. C., Chen, W. C., Hsu, C. H., Lee, Y. M., and Cheng, P. Y. (2018). Raspberry ketone induces brown-like adipocyte formation through suppression of autophagy in adipocytes and adipose tissue. *J. Nutr. Biochem.* 56, 116–125. doi: 10.1016/j.jnutbio.2018.01.017
- Li, C., Ye, L., Yang, L., Yu, X., He, Y., Chen, Z., et al. (2017). Rapamycin promotes the survival and adipogenesis of ischemia-challenged adipose derived stem cells by improving autophagy. *Cell Physiol. Biochem.* 44, 1762–1774. doi: 10.1159/000485783
- Li, D., Lu, Z., Xu, Z., Ji, J., Zheng, Z., Lin, S., et al. (2016). Spironolactone promotes autophagy via inhibiting PI3K/AKT/mTOR signalling pathway and reduce adhesive capacity damage in podocytes under mechanical stress. *Biosci. Rep.* 36:e00355. doi: 10.1042/BSR20160086
- Li, L., Tan, J., Miao, Y., Lei, P., and Zhang, Q. (2015). ROS and autophagy: interactions and molecular regulatory mechanisms. *Cell. Mol. Neurobiol.* 35, 615–621. doi: 10.1007/s10571-015-0166-x



- Li, Y., and Ding, W. X. (2017). Adipose tissue autophagy and homeostasis in alcohol-induced liver injury. *Liver Res.* 1, 54–62. doi: 10.1016/j.livres.2017.03.004
- Liu, K., and Czaja, M. J. (2013). Regulation of lipid stores and metabolism by lipophagy. *Cell Death Differ.* 20, 3–11. doi: 10.1038/cdd.2012.63
- Liu, X., Zheng, Z., Zhu, X., Meng, M., Li, L., Shen, Y., et al. (2013). Brown adipose tissue transplantation improves whole-body energy metabolism. *Cell Res.* 23, 851–854. doi: 10.1038/cr.2013.64
- Lo, K. A., and Sun, L. (2013). Turning WAT into BAT: a review on regulators controlling the browning of white adipocytes. *Biosci. Rep.* 33:e00065. doi: 10.1042/bsr20130046
- Lu, X., Altshuler-Keylin, S., Wang, Q., Chen, Y., Henrique Sponton, C., Ikeda, K., et al. (2018). Mitophagy controls beige adipocyte maintenance through a Parkin-dependent and UCP1-independent mechanism. *Sci. Signal.* 11:eap8526. doi: 10.1126/scisignal.aap8526
- Lum, J. J., Bauer, D. E., Kong, M., Harris, M. H., Li, C., Lindsten, T., et al. (2005). Growth factor regulation of autophagy and cell survival in the absence of apoptosis. *Cell* 120, 237–248. doi: 10.1016/j.cell.2004.11.046
- Martinez-Lopez, N., Garcia-Macia, M., Sahu, S., Athonvarangkul, D., Liebling, E., Merlo, P., et al. (2016). Autophagy in the CNS and periphery coordinate lipophagy and lipolysis in the brown adipose tissue and liver. *Cell Metab.* 23, 113–127. doi: 10.1016/j.cmet.2015.10.008
- Mukherjee, R., Kim, S. W., Park, T., Choi, M. S., and Yun, J. W. (2015). Targeted inhibition of parkin-1 by thiodigalactoside dramatically reduces body weight gain in diet-induced obese rats. *Int. J. Obes. (Lond.)* 39, 1349–1358. doi: 10.1038/ijo.2015.74
- Narendra, D. P., Jin, S. M., Tanaka, A., Suen, D. F., Gautier, C. A., Shen, J., et al. (2010). PINK1 is selectively stabilized on impaired mitochondria to activate Parkin. *PLoS Biol.* 8:e1000298. doi: 10.1371/journal.pbio.1000298
- Ost, A., Svensson, K., Ruishalme, I., Brannmark, C., Franck, N., Krook, H., et al. (2010). Attenuated mTOR signaling and enhanced autophagy in adipocytes from obese patients with type 2 diabetes. *Mol. Med.* 16, 235–246. doi: 10.2119/molmed.2010.00023
- Parry, H. A., and Yun, J. W. (2015). Proteomic identification of target proteins of thiodigalactoside in white adipose tissue from diet-induced obese rats. *Int. J. Mol. Sci.* 16, 14441–14463. doi: 10.3390/ijms160714441
- Parry, H. A., and Yun, J. W. (2017). Combined inhibition of autophagy protein 5 and galectin-1 by thiodigalactoside reduces diet-induced obesity through induction of white fat browning. *IUBMB Life* 69, 510–521. doi: 10.1002/iub.1634
- Penna, F., Baccino, F. M., and Costelli, P. (2014). Coming back: autophagy in cachexia. *Curr. Opin. Nutr. Metab. Care* 17, 241–246. doi: 10.1097/MCO.0000000000000048
- Pickrell, A. M., and Youle, R. J. (2015). The roles of PINK1, parkin, and mitochondrial fidelity in Parkinson's disease. *Neuron* 85, 257–273. doi: 10.1016/j.neuron.2014.12.007
- Pravda, J. (2014). Metabolic theory of septic shock. *World J. Crit. Care Med.* 3, 45–54. doi: 10.5492/wjccm.v3.i2.45
- Rachid, T. L., Penna-de-Carvalho, A., Bringhenti, I., Aguilu, M. B., Mandarim-de-Lacerda, C. A., and Souza-Mello, V. (2015). Fenofibrate (PPAR $\alpha$  agonist) induces beige cell formation in subcutaneous white adipose tissue from diet-induced male obese mice. *Mol. Cell Endocrinol.* 402, 86–94. doi: 10.1016/j.mce.2014.12.027
- Ro, S. H., Jung, C. H., Hahn, W. S., Xu, X., Kim, Y. M., Yun, Y. S., et al. (2013). Distinct functions of Ulk1 and Ulk2 in the regulation of lipid metabolism in adipocytes. *Autophagy* 9, 2103–2114. doi: 10.4161/auto.26563
- Rocchi, A., and He, C. (2015). Emerging roles of autophagy in metabolism and metabolic disorders. *Front. Biol. (Beijing)* 10:154–164. doi: 10.1007/s11515-015-1354-2
- Rosen, E. D., and Spiegelman, B. M. (2006). Adipocytes as regulators of energy balance and glucose homeostasis. *Nature* 444, 847–853. doi: 10.1038/nature05483
- Sanchez-Gurmaches, J., and Guertin, D. A. (2014). Adipocyte lineages: tracing back the origins of fat. *Biochim. Biophys. Acta* 1842, 340–351. doi: 10.1016/j.bbdis.2013.05.027
- Scheele, C., and Nielsen, S. (2017). Metabolic regulation and the anti-obesity perspectives of human brown fat. *Redox. Biol.* 12, 770–775. doi: 10.1016/j.redox.2017.04.011
- Schrauwen, P., van Marken Lichtenbelt, W. D., and Spiegelman, B. M. (2015). The future of brown adipose tissues in the treatment of type 2 diabetes. *Diabetologia* 58, 1704–1707. doi: 10.1007/s00125-015-3611-y
- Seale, P., Kajimura, S., and Spiegelman, B. M. (2009). Transcriptional control of brown adipocyte development and physiological function-of mice and men. *Genes Dev.* 23, 788–797. doi: 10.1101/gad.1779209
- Shoji-Kawata, S., Sumpter, R., Leveno, M., Campbell, G. R., Zou, Z., Kinch, L., et al. (2013). Identification of a candidate therapeutic autophagy-inducing peptide. *Nature* 494, 201–206. doi: 10.1038/nature11866
- Singh, R., and Cuervo, A. M. (2012). Lipophagy: connecting autophagy and lipid metabolism. *Int. J. Cell. Biol.* 2012:282041. doi: 10.1155/2012/282041
- Singh, R., Kaushik, S., Wang, Y., Xiang, Y., Novak, I., Komatsu, M., et al. (2009a). Autophagy regulates lipid metabolism. *Nature* 458, 1131–1135. doi: 10.1038/nature07976
- Singh, R., Xiang, Y., Wang, Y., Baikati, K., Cuervo, A. M., Luu, Y. K., et al. (2009b). Autophagy regulates adipose mass and differentiation in mice. *J. Clin. Invest.* 119, 3329–3339. doi: 10.1172/jci39228
- Soler-Vazquez, M. C., Mera, P., Zagmutt, S., Serra, D., and Herrero, L. (2018). New approaches targeting brown adipose tissue transplantation as a therapy in obesity. *Biochem. Pharmacol.* 155, 346–355. doi: 10.1016/j.bcp.2018.07.022
- Song, J., de Libero, J., and Wolf, S. E. (2014). Hepatic autophagy after severe burn in response to endoplasmic reticulum stress. *J. Surg. Res.* 187, 128–133. doi: 10.1016/j.jss.2013.09.042
- Stienstra, R., Haim, Y., Riahi, Y., Netea, M., Rudich, A., and Leibowitz, G. (2014). Autophagy in adipose tissue and the beta cell: implications for obesity and diabetes. *Diabetologia* 57, 1505–1516. doi: 10.1007/s00125-014-3255-3
- Tan, S. H., Shui, G., Zhou, J., Li, J. J., Bay, B. H., Wenk, M. R., et al. (2012). Induction of autophagy by palmitic acid via protein kinase C-mediated signaling pathway independent of mTOR (mammalian target of rapamycin). *J. Biol. Chem.* 287, 14364–14376. doi: 10.1074/jbc.M111.294157
- Taylor, D., and Gottlieb, R. A. (2017). Parkin-mediated mitophagy is downregulated in browning of white adipose tissue. *Obesity (Silver Spring)* 25, 704–712. doi: 10.1002/oby.21786
- Tsai, Y. C., Yang, B. C., Peng, W. H., Lee, Y. M., Yen, M. H., and Cheng, P. Y. (2017). Heme oxygenase-1 mediates anti-adipogenesis effect of raspberry ketone in 3T3-L1 cells. *Phytomedicine* 31, 11–17. doi: 10.1016/j.phymed.2017.05.005
- Tu, Q. Q., Zheng, R. Y., Li, J., Hu, L., Chang, Y. X., Li, L., et al. (2014). Palmitic acid induces autophagy in hepatocytes via JNK2 activation. *Acta Pharmacol. Sin.* 35, 504–512. doi: 10.1038/aps.2013.170
- Vijgen, G. H., Bouvy, N. D., Teule, G. J., Brans, B., Schrauwen, P., and van Marken Lichtenbelt, W. D. (2011). Brown adipose tissue in morbidly obese subjects. *PLoS One* 6:e17247. doi: 10.1371/journal.pone.0017247
- Vincow, E. S., Merrihew, G., Thomas, R. E., Shulman, N. J., Beyer, R. P., MacCoss, M. J., et al. (2013). The PINK1-Parkin pathway promotes both mitophagy and selective respiratory chain turnover in vivo. *Proc. Natl. Acad. Sci. U.S.A.* 110, 6400–6405. doi: 10.1073/pnas.1221132110
- Volzke, H., Robinson, D. M., Kleine, V., Deutscher, R., Hoffmann, W., Ludemann, J., et al. (2005). Hepatic steatosis is associated with an increased risk of carotid atherosclerosis. *World J. Gastroenterol.* 11, 1848–1853. doi: 10.3748/wjg.v11.i12.1848
- Wang, Q., Zhang, M., Ning, G., Gu, W., Su, T., Xu, M., et al. (2011). Brown adipose tissue in humans is activated by elevated plasma catecholamines levels and is inversely related to central obesity. *PLoS One* 6:e21006. doi: 10.1371/journal.pone.0021006
- Ward, C., Martinez-Lopez, N., Otten, E. G., Carroll, B., Maetzel, D., Singh, R., et al. (2016). Autophagy, lipophagy and lysosomal lipid storage disorders. *Biochim. Biophys. Acta* 1861, 269–284. doi: 10.1016/j.bbailp.2016.01.006
- Weyer, C., Tataranni, P. A., Snitker, S., Danforth, E. Jr., and Ravussin, E. (1998). Increase in insulin action and fat oxidation after treatment with CL 316,243, a highly selective beta3-adrenoceptor agonist in humans. *Diabetes* 47, 1555–1561. doi: 10.2337/diabetes.47.10.1555
- Wu, J., Bostrom, P., Sparks, L. M., Ye, L., Choi, J. H., Giang, A. H., et al. (2012). Beige adipocytes are a distinct type of thermogenic fat cell in mouse and human. *Cell* 150, 366–376. doi: 10.1016/j.cell.2012.05.016
- Wu, J., Cohen, P., and Spiegelman, B. M. (2013). Adaptive thermogenesis in adipocytes: is beige the new brown? *Genes Dev.* 27, 234–250. doi: 10.1101/gad.211649.112

- Xu, R., Ji, Z., Xu, C., and Zhu, J. (2018). The clinical value of using chloroquine or hydroxychloroquine as autophagy inhibitors in the treatment of cancers: a systematic review and meta-analysis. *Medicine (Baltimore)* 97:e12912. doi: 10.1097/MD.00000000000012912
- Yoshii, S. R., and Mizushima, N. (2017). Monitoring and measuring autophagy. *Int. J. Mol. Sci.* 18:E1865. doi: 10.3390/ijms18091865
- Yuan, H. X., Russell, R. C., and Guan, K. L. (2013). Regulation of PIK3C3/VPS34 complexes by MTOR in nutrient stress-induced autophagy. *Autophagy* 9, 1983–1995. doi: 10.4161/auto.26058
- Zechner, R., Madeo, F., and Kratky, D. (2017). Cytosolic lipolysis and lipophagy: two sides of the same coin. *Nat. Rev. Mol. Cell. Biol.* 18, 671–684. doi: 10.1038/nrm.2017.76
- Zhang, F., Hao, G., Shao, M., Nham, K., An, Y., Wang, Q., et al. (2018). An adipose tissue Atlas: an image-guided identification of human-like BAT and beige depots in rodents. *Cell Metab.* 252.e3–262.e3. doi: 10.1016/j.cmet.2017.12.004
- Zhang, Y., Goldman, S., Baerga, R., Zhao, Y., Komatsu, M., and Jin, S. (2009). Adipose-specific deletion of autophagy-related gene 7 (atg7) in mice reveals a role in adipogenesis. *Proc. Natl. Acad. Sci. U.S.A.* 106, 19860–19865. doi: 10.1073/pnas.0906048106
- Zhang, Y., Zeng, X., and Jin, S. (2012). Autophagy in adipose tissue biology. *Pharmacol. Res.* 66, 505–512. doi: 10.1016/j.phrs.2012.09.004
- Conflict of Interest Statement:** The authors declare that the research was conducted in the absence of any commercial or financial relationships that could be construed as a potential conflict of interest.

Copyright © 2019 Ro, Jang, Bae, Kim, Schaecher and Shomo. This is an open-access article distributed under the terms of the Creative Commons Attribution License (CC BY). The use, distribution or reproduction in other forums is permitted, provided the original author(s) and the copyright owner(s) are credited and that the original publication in this journal is cited, in accordance with accepted academic practice. No use, distribution or reproduction is permitted which does not comply with these terms.



# Brown and Brite: The Fat Soldiers in the Anti-obesity Fight

Shireesh Srivastava<sup>1</sup> and Richard L. Veech<sup>2\*</sup>

<sup>1</sup> Systems Biology for Biofuels Group, International Centre for Genetic Engineering and Biotechnology (ICGEB), New Delhi, India, <sup>2</sup> Laboratory of Metabolic Control, National Institute on Alcohol Abuse and Alcoholism (NIAAA), National Institutes of Health (NIH), Bethesda, MD, United States

## OPEN ACCESS

### Edited by:

Rita De Matteis,  
University of Urbino Carlo Bo, Italy

### Reviewed by:

Marta Letizia Hribal,  
Università degli studi Magna Graecia  
di Catanzaro, Italy  
Petros Dinas,  
University of Thessaly, Greece

### \*Correspondence:

Richard L. Veech  
rveech@mail.nih.gov

### Specialty section:

This article was submitted to  
Integrative Physiology,  
a section of the journal  
Frontiers in Physiology

**Received:** 03 September 2018

**Accepted:** 14 January 2019

**Published:** 30 January 2019

### Citation:

Srivastava S and Veech RL (2019)  
Brown and Brite: The Fat Soldiers  
in the Anti-obesity Fight.  
Front. Physiol. 10:38.  
doi: 10.3389/fphys.2019.00038

Brown adipose tissue (BAT) is proposed to maintain thermal homeostasis through dissipation of chemical energy as heat by the uncoupling proteins (UCPs) present in their mitochondria. The recent demonstration of the presence of BAT in humans has invigorated research in this area. The research has provided many new insights into the biology and functioning of this tissue and the biological implications of its altered activities. Another finding of interest is browning of white adipose tissue (WAT) resulting in what is known as beige/brite cells, which have increased mitochondrial proteins and UCPs. In general, it has been observed that the activation of BAT is associated with various physiological improvements such as a reduction in blood glucose levels increased resting energy expenditure and reduced weight. Given the similar physiological functions of BAT and beige/ brite cells and the higher mass of WAT compared to BAT, it is likely that increasing the brite/beige cells in WATs may also lead to greater metabolic benefits. However, development of treatments targeting brown fat or WAT browning would require not only a substantial understanding of the biology of these tissues but also the effect of altering their activity levels on whole body metabolism and physiology. In this review, we present evidence from *recent* literature on the substrates utilized by BAT, regulation of BAT activity and browning by circulating molecules. We also present dietary and pharmacological activators of brown and beige/brite adipose tissue and the effect of physical exercise on BAT activity and browning.

**Keywords:** brown fat, dietary additive, exercise, metabolism, hormones

## INTRODUCTION

Given the widespread prevalence of obesity and associated diseases, efforts are underway to reduce the body weight gain through modulating the energy intake and/or expenditure. A large portion of the resting energy expenditure is spent on thermoregulation (Lee and Greenfield, 2015). Uncoupled respiration – a process where the oxidative phosphorylation is uncoupled from ATP generation, shivering thermogenesis, and diet-induced thermogenesis play an important part in thermal homeostasis. Overall, thermogenesis accounts for about 15% of the daily energy expenditure (van Marken Lichtenbelt and Schrauwen, 2011) or about 20% of the oxygen consumed (Rolfe and Brown, 1997). Thus, activation of uncoupled respiration could be a useful strategy to counter body weight gain. In mammals, brown adipose tissue (BAT) plays an important role in uncoupled respiration. While some previous studies had shown the existence of BAT in adult humans (Heaton, 1972; Huttunen et al., 1981; Bouillaud et al., 1983), it was the (re)demonstration of active BAT in

adult humans about 10 years ago (Nedergaard et al., 2007; Cypess et al., 2009; Virtanen et al., 2009; Zingaretti et al., 2009) that has greatly increased the research efforts to understand and modulate this tissue. In humans, BAT is often seen in the cervical, upper supraclavicular area, mediastinal and perirenal regions. Due to its intense PET signal in the upper supraclavicular area (abbreviated “USA”), it became popularly known as “USA” fat (Cohade et al., 2003).

Brown adipose tissue plays an active role in thermoregulation in adult humans (Chondronikola et al., 2016). Biochemical and ultrastructural analyses identified that this tissue is rich in mitochondria and possesses a unique protein called the uncoupling protein 1 (UCP1). Other pathways, such as the glycerol-3-phosphate shuttle (Anunciado-Koza et al., 2008) and creatinine cycling (Kazak et al., 2015) may also contribute to heat generation along with UCP1 mediated uncoupling. These molecules provide the tissue with a thermogenic capacity which helps in maintaining body temperature without the need to shiver constantly. The heat thus generated is termed as non-shivering thermogenesis (NST). Some recent review articles have looked into the effect of various biochemical mediators on UCP1 activity and molecular tools used to study UCP1 functioning (Klingenberg, 2017; Ricquier, 2017). Given the potential of regulated uncoupling to dissipate energy, novel chemical uncouplers are being investigated (Ost et al., 2017) in other tissues such as WAT and skeletal muscle.

A lot of our understanding of BAT functioning comes from rodent studies. In mice, the interscapular BAT (IBAT) is the primary BAT depot, while brown adipocytes are also present in the supraclavicular region (scBAT). Several mice depots with topological similarities to human BAT-like and beige depots were identified recently (Zhang et al., 2018). Another study has shown that the gene expression pattern of mice scBAT was similar to that of human scBAT (Mo et al., 2017).

Under prolonged cold conditions, the brown fat size and activity increases, a term called BAT “recruitment.” BAT recruitment is associated with increased proliferation and differentiation of BAT precursor cells. Exposure to cold also increases BAT volume and activity in humans (Blondin et al., 2014) and also in individuals with obesity and type 2 diabetes (Hanssen et al., 2016). Increased sympathetic nervous system (SNS) activity, including on cold exposure, is a primary mechanism of BAT activation. Activated SNS releases norepinephrine which acts on the beta-adrenergic receptors on the BAT. In addition to epinephrine and norepinephrine, dopamine stimulation of brown adipocytes was also associated with increased oxygen consumption, UCP1 protein and mitochondrial mass (Kohlmeier et al., 2017). Prolonged exposure of mice to cold not only leads to brown fat recruitment but also to appearance of white adipocytes containing multilocular fat droplets and UCP1-expressing mitochondria – a process called “browning” of the white adipose tissue (WAT) depots. Brown-like adipocytes in WAT can arise from several origins – through the development of distinct subpopulations or through the trans-differentiation of differentiated white adipocytes (Okamatsu-Ogura et al., 2018). Additionally, the “brite” cells may also develop through the

bi-directional interconversion of some cells between brite and white adipocyte phenotypes (Rosenwald et al., 2013). In spite of many molecular similarities between the BAT and brite cells, there is a differential expression of certain genes between BAT and brite cell. These include metabolic proteins (e.g., Slc27a1), inflammatory proteins (e.g., CD40 and CD137) and transcription factors (Tbx15 and Zic1) (Waldén et al., 2012; Wu et al., 2012). The gene expression profile of BAT in human infants resembles that of the classical BAT (Lidell et al., 2013), though they also express typical brite marker proteins TBX1 and CD137 (Sharp et al., 2012). The BAT in the neck of adult humans contains a mixture of classical brown and brite cells (Jespersen et al., 2013; Lidell et al., 2013). While the expression of browning genes in mice is greater in subcutaneous WAT (scWAT) compared to visceral WAT (vWAT), an opposite pattern of browning gene expression with vWAT having higher expression than scWAT was observed in humans (Zuriaga et al., 2017).

Brown adipose tissue and UCP1 levels have been shown to be involved in body weight regulation, glucose, and lipid homeostasis in mice (Kontani et al., 2005; Feldmann et al., 2009; Stanford et al., 2013). Mice strains which have a tendency to be obese have comparable BAT levels and activity but diminished browning of WAT depots (Guerra et al., 1998; Xue et al., 2007). Interestingly, transplantation of BAT from healthy mice into the visceral cavity of apoE<sup>-/-</sup> mice led to a 20% reduction in atherosclerotic lesions (Kikai et al., 2017). Similarly, transplantation of human beige tissue in mice significantly improved their metabolic parameters (Min et al., 2016). Obese humans have reduced BAT compared to those with normal weight (Orava et al., 2013) and the amount of detectable BAT correlated inversely with total, subcutaneous and visceral adiposity (Saito et al., 2009). Individuals who are BAT-positive have a reduced probability of type 2 diabetes and obesity (Cypess et al., 2009). Another study employing retrospective analysis of FDG-PET/CT scans of 4852 patients showed that BAT-positive patients had lower visceral, subcutaneous and liver fat content (Brendle et al., 2018). BAT-positive individuals have better insulin-stimulated glucose disposal compared to BAT-negative individuals (Chondronikola et al., 2014). Among patients with cardiovascular comorbidities, those with higher BAT fraction had better metabolic profiles (Franssens et al., 2017). The activated BAT was shown to be associated with reduced arterial inflammation and fatty liver (Nam and Jun, 2017). Even in newborns, those with the higher BAT at birth were shown to have lesser fat-gain over the period of 6 months (Entringer et al., 2017). Activation of BAT by cold-exposure was shown to be associated with improved glucose uptake, insulin sensitivity and reduced plasma FFA levels (Iwen et al., 2017), and lesser central adiposity (Green et al., 2017). Activated BAT is also associated with other physiological benefits such as amelioration of obesity-associated reduction in male fertility (Liu H. et al., 2017) and improved menstrual regularity in rat model of Polycystic ovary syndrome (PCOS) (Yuan et al., 2016). Thus, BAT recruitment has been suggested as an anti-obesity agent in humans (Yoneshiro et al., 2013). Individuals with active BAT weighed on an average 4 kg less than BAT negative individuals (Lee et al., 2010). Leaner individuals had about 50% higher UCP1 mRNA levels.



Interestingly, the UCP1 levels accounted for about 50% of BMI variance (Lee et al., 2011).

Given the strong correlation between active BAT and positive metabolic and physiological responses, there is an intense interest in understanding the biology and regulation of this tissue. The level of interest can be gleaned from the fact that the search for the term “brown adipose tissue” in Pubmed produced a list of over 10000 articles, most of which were published in the past decade. While there are many reviews that cover specific aspects of brown and brite adipocyte biology and some of the recent ones are referenced in this review, our aim is to provide an integrative overview of the recent literature and current understanding of brown/brite adipocyte biology and functioning.

## SUBSTRATES UTILIZED BY BROWN FAT FOR HEAT PRODUCTION

Brown fat is a metabolically active tissue that can metabolize a variety of substrates for the production of heat. A major source for short-term activity is the intracellular lipid that is stored in the form of multi-locular droplets. However, knockout of essential enzymes of lipolysis (Schreiber et al., 2017; Shin et al., 2017) indicate that lipolysis is not essential for cold-induced thermogenesis in mice. However, inhibition of intracellular lipolysis by feeding nicotinic acid was associated with a diminished increase in cold-induced BAT activity in men (Blondin et al., 2017a).

Brown fat can also metabolize a variety of extracellular substrates, primary among which is glucose. The rapid uptake of glucose by this tissue is the reason for its prominent display during the FDG-PET imaging. It has been suggested that the glucose can be used for *de novo* fatty acid synthesis which is then channeled to a pool of triacylglycerol (TAG) which is rapidly hydrolyzed to yield fatty acids that can serve as substrates for increased thermogenesis (Irshad et al., 2017). Circulating lipids and lipoproteins are also utilized by BAT (Bartelt et al., 2011; Berbée et al., 2015; Khedoe et al., 2015; Blondin et al., 2017b). The clearance of glucose and triglycerides by cold-activated BAT can account for about two-thirds of total increase in substrate clearance (Bartelt et al., 2011). Circulating acylcarnitines (Simcox et al., 2017), as well as lipoproteins (Hoeke et al., 2016) can also be utilized by activated BAT as substrates. Lipid oxidation was shown to be important for BAT thermogenic function (Gonzalez-Hurtado et al., 2018). A correlation between BAT activity and serum HDL cholesterol levels has been reported (Bartelt et al., 2017). Thus, the BAT, when activated, could be an important organ for clearance of glucose and lipid species.

## CIRCULATING MODULATORS OF BROWN ADIPOSE ACTIVITY AND BROWNING

Several previous and recent studies have shown that BAT activation and WAT browning are regulated by the actions of

various hormones. The regulation of BAT activity and browning by hormonal mediators was the subject of some recent review articles (Hu and Christian, 2017; Rodríguez et al., 2017; Ludwig et al., 2018). In this section, we present some of the recent literature reports on BAT regulation, linking those to the overall understanding of BAT physiology and function. **Figure 1** provides an overall picture of the regulation of brown fat activity and browning by hormones and circulating factors.

Hyperinsulinemia, induced by daily injection of insulin, was associated with a reduction in IWAT and IBAT respiratory activity (Dallon et al., 2018). Leptin, a hormone released by WAT and known for its appetite suppressing effects, was shown to increase SNS activity to BAT (Enriori et al., 2011). However, the IBAT SNS activity was shown to be not necessary for leptin-induced weight loss (Côté et al., 2018). Proopiomelanocortin (POMC) and Agouti-related protein (AgRP) neurons play a role in leptin-mediated increased SNS activity to BAT, while the AgRP are the major regulators of increased SNS activity to the inguinal fat in response to leptin in mice (Bell et al., 2018). Significantly reduced levels of the  $\beta$ 3-adrenergic receptor, PGC-1 $\alpha$ , and UCP1, were found in the leptin-deficient ob/ob (–/–) mice (Martins et al., 2017) which were improved by injection of capsules containing poly-L-lysine-embedded engineered 3T3-L1 adipocytes constitutively expressing leptin (DiSilvestro et al., 2016).

Increased thyroid hormone activity is known to promote energy expenditure. One study showed that both hypothyroidism, as well as hyperthyroidism, led to increased WAT browning in mice (Weiner et al., 2016). The study showed that hyperthyroid mice had higher BAT mass and activity than the hypothyroid mice. The thyroid hormone T3 can increase SNS activity to BAT, increasing BAT activity (López et al., 2010). Treatment with T4 or administration of T3 to VMH was shown to be associated with the browning of WAT (Martínez-Sánchez et al., 2017a). In humans too, the cold-induced increase in energy expenditure was shown to be associated with circulating T3 levels (Gavrila et al., 2017). The action of T3 on BAT activity was shown to be mediated by a reduction of endoplasmic reticulum stress in the VMH (Martínez-Sánchez et al., 2017b). Angiotensin type 2 receptor (AT2R) was shown to play a role in T3-induced upregulation of browning genes in WAT (Than et al., 2017) and an AT2R agonist was shown to increase WAT browning. On the other hand, deleting the AT1aR was shown to be associated with IWAT browning (Tsukuda et al., 2016). Injection of angiotensin 1–7 peptide through a micro-osmotic pump was shown to increase in BAT size and UCP1 levels as well as increase thermogenesis in subcutaneous WAT without affecting UCP1 levels there (Morimoto et al., 2018). A thyroid receptor beta (TR- $\beta$ ) specific agonist GC-1 was shown to increase energy expenditure and prevent weight gain in rats (Villicev et al., 2007). The molecular mechanisms involved in the TH-induced increase in thermogenesis was reviewed in Weiner et al. (2017) and involves both direct activation of thyroid hormone receptors in the adipose tissues as well as indirectly through the activation of hypothalamic neurons. A recent study has identified the carbohydrate response element binding protein (ChREBP) as one of the targets of T3 which regulates the UCP1 expression in brown adipocytes (Katz et al., 2018).

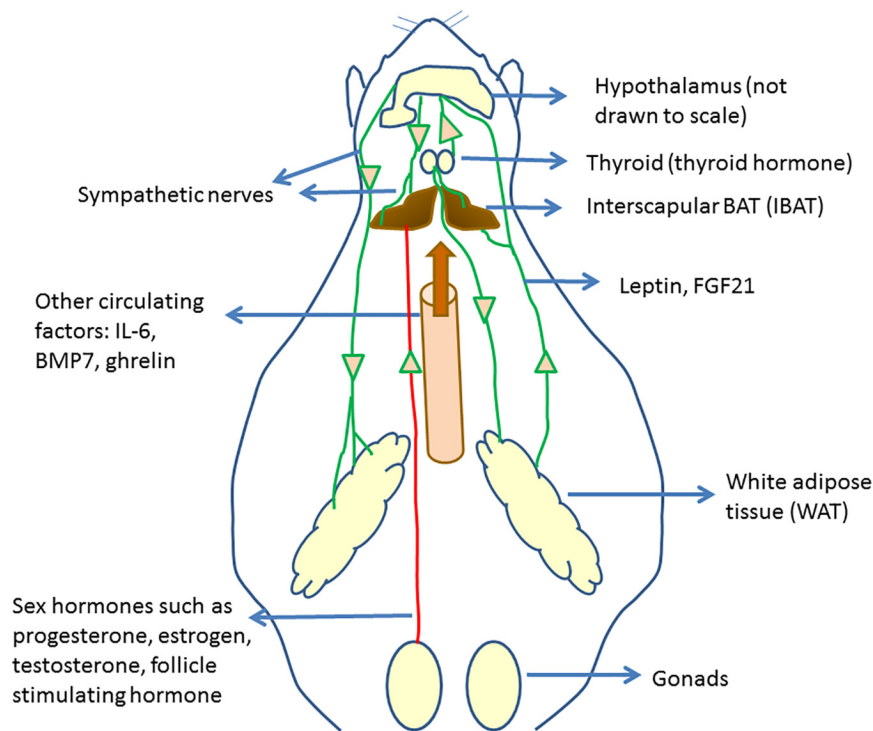


**FIGURE 1 |** Circulating regulators of BAT and their origin. Hypothalamus plays an important role in regulating brown fat activity through regulating the sympathetic nervous system activity. Several circulating regulators impact BAT functioning and browning. Many of these act through increasing the sympathetic nervous activity to BAT and WAT, increasing UCP1 expression.

Sex hormones play an important role in regulating brown fat function. As several studies have shown that females have higher BAT activity than males, it is likely that estrogen levels impact BAT activity (Frank et al., 2018). Reduced levels of estradiol (E2), an ovary-derived hormone, are associated with reduced BAT activity (López and Tena-Sempere, 2016) and E2 treatment can increase BAT activity by activating hypothalamic AMPK (López and Tena-Sempere, 2017). The roles of E2 in regulating thermogenesis were recently reviewed (González-García et al., 2017). Pharmacological activation of estrogen receptor  $\beta$  (ER- $\beta$ ) was shown to increase BAT volume and energy expenditure (Ponnusamy et al., 2017). Progesterone, a hormone associated with gestation, was shown to cause a brown-to-white conversion of BAT in mice (McIlvrde et al., 2017). Removal of BAT prior to conception led to maternal and fetal hyperlipidemia and larger fetuses. Inhibiting follicle stimulating hormone (FSH) through a polyclonal antibody was shown to induce beiging, activate BAT and thermogenesis and reduce WAT (Liu P. et al., 2017). BAT was shown to have the highest expression of Follistatin (Fst), previously known as FSH-suppressing protein. Overexpression of Fst was shown to increase BAT mass as well of browning of WAT (Singh et al., 2017). These results suggest that FSH has an inhibitory effect on BAT activity and browning. Castration was shown to increase browning of IWAT in mice (Hashimoto et al., 2016).

Some other hormones or peptides have been reported to affect BAT functioning. These include ghrelin, which negatively

correlated with BAT activity (Chondronikola et al., 2017) and erythropoietin (EPO), which was shown to promote thermogenic activity (Kodo et al., 2017).

Small molecule circulating regulators of BAT physiology include hydrogen sulfide (H<sub>2</sub>S) (Soriano et al., 2018), pyruvate (Soto et al., 2018) and abscisic acid (Sturla et al., 2017).

Brown fat is also a source of various BATokines which can impact other organs. FGF21 is a well-studied batokine, though it can also be released by liver and WAT. FGF21 can act on BAT and WAT through the central nervous system and increase the SNS activity, leading to weight loss and increased energy expenditure (Bookout et al., 2013; Owen et al., 2014; Douris et al., 2015). FGF21 can also act in an autocrine manner on the tissue. FGF21 can also lead to browning of WAT through increased PPAR- $\gamma$  (Dutchak et al., 2012) and PGC1- $\alpha$  activity (Fisher et al., 2012). A clinical trial showed a reduction in body weight and improvements in lipid metabolism in obese patients on treatment with LY2405319, analog of FGF-21 (Gaich et al., 2013). Batokines and their effects have been reviewed in Villarroya et al. (2017).

## DIETARY AND PLANT-DERIVED MOLECULES

Alterations in diets and major dietary components have been shown to be associated with variation in the activity of BAT. **Figure 2** depicts some of the food items whose derived

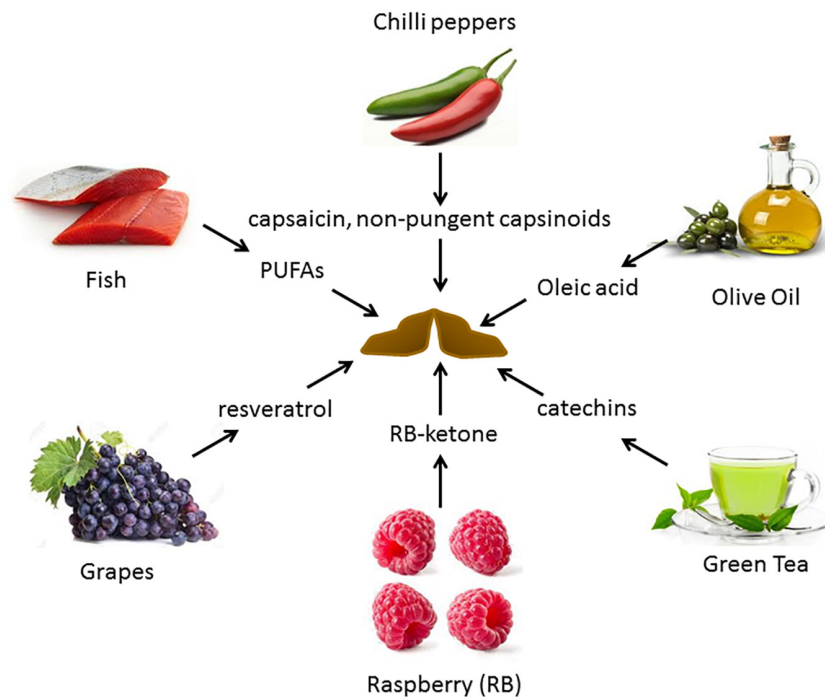


**FIGURE 2 |** Food-derived molecules shown to be involved in BAT activation and browning, and their sources. Several diet-derived molecules have been shown to activate brown fat and browning. These are obtained from both plant and animal products.

compounds have been shown to increase BAT activity and browning of WAT.

## Macromolecular Composition of Diets

The macromolecular composition of diets can affect BAT activity and browning. A comparison of several diets showed that a high protein diet was associated with higher amounts of BAT (de Macêdo et al., 2017). However, other studies have shown that diets low in protein diet were associated with increased BAT activity and browning (Pereira et al., 2017; Kitada et al., 2018). Some studies have observed that the source of protein affects diet-induced thermogenesis (DIT) and BAT UCP1 levels (Ezoe et al., 2016; Li T. et al., 2018). The BAT response on a high fat diet was time-dependent – shorter (2–4 week) high-fat diet increase UCP1 levels in BAT, while longer feeding with HFD (20 weeks) bringing them back to normal levels (Ohtomo et al., 2017).

Surprisingly, sucrose intake was shown to increase BAT activity (Maekawa et al., 2017; Velickovic et al., 2018). Addition of dietary fiber to a high-fat diet (HFD) increased lipolysis and the levels of various thermogenic proteins in WAT (Han S.-F. et al., 2017).

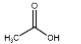
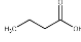
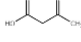
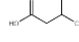
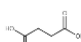
## Dietary Components Known to Increase BAT Activity

Long-term feeding of specific diets may cause alterations in the BAT composition and activity. Our work has shown that a high fat, low carbohydrate ketogenic (KG) diet (Srivastava et al., 2013) increased BAT volume and the expression of

mitochondrial proteins in BAT in mice. A novel dietary additive, which can be given along with a normal carbohydrate-level diet and yet can increase blood ketone levels, was developed in the lab of R.L. Veech. This ketone ester, when given to mice in liquid diets, produced blood ketone ( $\beta$ -hydroxybutyrate) levels much greater than that achieved with the KG diets without the need to restrict carbohydrate intake (Srivastava et al., 2012). The increased ketone levels were associated with several positive metabolic effects. These include a significant activation of BAT and mitochondrial biogenesis in this tissue, increased UCP1 levels in WAT. Dietary administration of medium chain triglycerides (MCTs) (Zhang et al., 2015) as well as MCT-enriched diacylglycerol oil (MCE-DAG) (Kim et al., 2017), which also increase blood ketone levels, was shown to activate BAT. Azelaic acid, a pharmacological activator of Olfr544, was shown to induce ketogenesis in the liver and increased UCP1 expression in the BAT (Wu et al., 2017). All these results indicate that increased blood ketone levels can modulate brown fat activity. Other diet-derived small molecule BAT activators have also been identified. These include butyrate (Li Z. et al., 2018), acetate (Sahuri-Arisoylu et al., 2016) and succinate (Mills et al., 2018). These studies suggest that elevation of TCA cycle metabolites can trigger changes in BAT activity. **Table 1** lists some of the diet-derived small molecules shown to increase BAT activity and browning of WAT.

There is a significant interest in identifying dietary additives that can improve BAT activity. Several dietary BAT modulators have been identified. **Figure 2** provides a summary of reported dietary molecules that increase BAT activity and browning.

**TABLE 1 |** Some diet-derived small molecules known to activate brown fat and/or browning.

Molecule	Structure	Reference
Acetic acid		Sahuri-Arisoylu et al., 2016
Butyric acid		Khan and Jena, 2016; Li Z. et al., 2018
Ketone bodies	 	Srivastava et al., 2012, 2013
Succinic acid		Mills et al., 2018

Feeding mice a diet rich in fish oil (Bargut et al., 2016), olive oil (Shin and Ajuwon, 2018) or PUFAs (Crescenzo et al., 2017; Pahlavani et al., 2017; Ghandour et al., 2018) or conjugated linoleic acid (Shen and McIntosh, 2016) was shown to activate BAT and browning in rodents.

Chronic cold exposure was associated with increased bile acid production by the liver and modulation of the bile acid production modulated the thermogenic response (Worthmann et al., 2017). Studies have shown activating effect of bile acids on BAT activity in rodents (Watanabe et al., 2006; Eggink et al., 2018) and humans (Broeders et al., 2015).

Supplementation with non-pungent capsinoids (compounds associated with the hotness of peppers) (Yoneshiro et al., 2012) as well as grains of paradise (Sugita et al., 2013) was associated with increased thermogenesis. Activation of the transient receptor potential cation channel subfamily V member 1 (TRPV1) by these compounds (Baskaran et al., 2016) leads to increased SNS activity to induce BAT (Saito and Yoneshiro, 2013). Selective ablation of inguinal WAT (IWAT) sensory neurons by capsaicin treatment was shown to reduce the norepinephrine turnover not only in the IWAT but also in the IBAT, and reduce UCP1 expression in IBAT (Nguyen et al., 2018). Similarly, loss of TRPV2 was associated with impaired thermogenic response to  $\beta$ -adrenergic stimulation and poor cold tolerance (Sun et al., 2016a, 2). Expression of TRPV2 is significantly increased during brown fat differentiation, and TRPV2-agonists inhibited the brown adipocyte differentiation (Sun et al., 2016b). Human studies have shown that increased energy expenditure following capsaicin treatment was observed only in individuals with the active BAT (Sun et al., 2018). Supplementation of vanillic acid also increases BAT activity (Jung et al., 2018). These studies have shown that BAT plays a role in the increased energy expenditure following intake of “hot” foods and have elucidated the underlying mechanisms, providing new targets to modulate BAT activity.

Several studies have shown that intake of tea-derived compounds is associated with increased thermogenic capacity in mice (Neyrinck et al., 2017) and humans (Nirengi et al., 2016; Yoneshiro et al., 2017).

Resveratrol (RSV), a flavonoid found on the skin of grapes, and related compounds have been shown to activate BAT and increase thermogenesis (Andrade et al., 2014; Ku et al., 2016; Li et al., 2017) likely through AMPK $\alpha$  activation (Wang et al., 2017). A combination of RSV with Quercetin, active compound

from onion peels (Arias et al., 2017), and pentamethyl quercetin (PMQ) (Han Y. et al., 2017) was shown to induce BAT activation and browning.

Dietary supplementation of raspberry to mice on a high-fat diet (Xing et al., 2018) or oral treatment with raspberry ketone (Leu et al., 2018) was recently shown to increase beiging through AMPK activation (Zou et al., 2018).

While the list given in this section is not exhaustive, it is clear that BAT and WAT are responsive to diet composition, type of lipid and to several natural compounds. This also calls for an appropriate control diet as well as a careful comparison of the macro and micronutrient composition of diets while designing dietary studies involving BAT activators.

## PHARMACOLOGICAL ACTIVATORS OF BROWN AND BEIGE FAT

Several pharmacological activators of brown fat and browning have been reported. These include  $\beta$ 3-adrenergic receptor agonist (Cypess et al., 2015), PPAR- $\gamma$  activators (Xie et al., 2017; Loh et al., 2018; Merlin et al., 2018), PGC-1 $\alpha$  stabilizers (Pettersson-Klein et al., 2018), PPAR- $\alpha$  agonist (Rachid et al., 2018), AMPK activators (Kim et al., 2016, 2018; Tokubuchi et al., 2017) and PDE5 inhibitors Sildenafil and Tadalafil (Maneschi et al., 2016; Li S. et al., 2018). Several other pharmacological modulators of BAT activity and browning have been reported. While some of them are expected from our understanding of brown fat biology, the other modulators identified could be used to gain further insights into the mechanisms of regulation of brown fat activation and browning.

## EFFECT OF PHYSICAL EXERCISE ON BAT AND BROWNING

Physical exercise can have beneficial effects on general metabolism and physiology. Several rodent studies showed increased BAT activity and browning of WAT in rodents on exercise (De Matteis et al., 2013; Aldiss et al., 2017; Peppler et al., 2018). However, a systematic review concluded that regular exercise is not a major stimulus for increased BAT activity even though an increase may be observed in animals consuming high-fat diets or with low endogenous UCP1 levels (Flouris et al., 2017). Most human studies have shown a negative correlation of BAT activity with exercise (Motiani et al., 2017; Trexler et al., 2017). Endurance-trained athletes have reduced BAT activity compared to sedentary controls (Trexler et al., 2017). Endurance training was also not associated with beiging of abdominal or subcutaneous WAT (Tsiloulis et al., 2018). Two weeks of exercise training decreased insulin-mediated glucose uptake by BAT in healthy middle-aged men (Motiani et al., 2017). Thus, human studies have generally shown that metabolic benefits of exercise are not mediated by increased BAT activity and browning.

Several exercise-induced mediators have been suggested to play a role in browning of WAT in rodents. These include myokines such as Irisin, a hormone released by skeletal muscles



whose levels increase following exercise (Boström et al., 2012), IL-6 (Knudsen et al., 2014) and  $\beta$ -amino isobutyric acid (BAIBA) (Roberts et al., 2014), etc. While the initial findings of existence of irisin were questioned due to non-specificity of the antibodies (Atherton and Phillips, 2013; Albrecht et al., 2015), a mass spectrometry-based analysis confirmed the presence of irisin in human plasmas and its increase following exercise (Jedrychowski et al., 2015). In humans, habitual physical activity was shown to be positively correlated with serum irisin levels (Buscemi et al., 2018) but a lower active BAT (Singhal et al., 2016). A systematic review of the literature has concluded that it may not be possible to conclude an association between physical activity and Irisin or PGC-1 $\alpha$  because of lack of precision of available methods (Dinas et al., 2017). Thus, further research is needed to evaluate the effects of myokines on brown fat physiology and browning process, taking into consideration that trained individual may show a divergent response than untrained/sedentary individuals (Vosselman et al., 2015).

## CONCLUSION AND FUTURE DIRECTIONS

It is now clear that BAT is a metabolically active tissue and when activated, can clear very high levels of glucose and lipids on a per weight tissue basis. Increased BAT activity is associated with several metabolic benefits such as reduced body weight and improved glucose control. The beiging of WAT holds promise to further increase the metabolic benefits.

An important, less-emphasized factor regulating the activity of this tissue is the ambient temperature. Most of our knowledge has come from studies conducted under cold conditions which lead to chronic BAT activation. Housing at or near thermoneutral temperature is associated with significantly reduced basal metabolic rate and UCP1 levels and higher body fat (Shi et al., 2017). Chronic exposure to thermoneutral and warm conditions significantly reduce the levels and activity of this tissue in rodents (Cui et al., 2016) and humans (Turner et al., 2016). Warmer temperatures are also associated with higher incidences of diabetes and glucose intolerance in humans (Blauw et al., 2017). As most humans live at or near thermoneutrality, only a small fraction of the total BAT may be active in humans under normal living conditions. Similarly, ambient temperature may also affect the response to “inducers” of BAT activity. For BAT research to be applicable to humans, a careful choice of ambient temperature is needed.

## REFERENCES

- Albrecht, E., Norheim, F., Thiede, B., Holen, T., Ohashi, T., Schering, L., et al. (2015). Irisin – A myth rather than an exercise-inducible myokine. *Sci. Rep.* 5:8889. doi: 10.1038/srep08889
- Aldiss, P., Betts, J., Sale, C., Pope, M., and Symonds, M. E. (2017). Exercise-induced “browning” of adipose tissues. *Metab. Clin. Exp.* 81, 63–70. doi: 10.1016/j.metabol.2017.11.009

While physical exercises of different modalities are generally associated with improved metabolic parameters, studies generally suggest a divergent response of WAT browning to exercise in rodents vs. humans. Human studies have generally shown a reduced BAT activity and no significant effect on browning, while rodent studies have generally shown browning of WAT by exercising. It is plausible that this divergent response may be related to the different ambient temperatures, along with other factors such as greater genetic and dietary diversity of humans compared to the mice studied. Nonetheless, the tantalizing possibility exists of further improving the benefits of exercise in humans through a parallel activation of browning by environmental, dietary or pharmacological treatments. Various exercise-induced factors have also been identified, with the goal to extend the metabolic benefits of exercising to sedentary individuals.

Given our increased understanding of the metabolic effects of the activated BAT, novel approaches to increase its activity are being explored. Using optical and electrical genetic stimulation of specific neurons in the sympathetic nervous offers an interesting option (François et al., 2017) to modulate the activity of BAT or to induce browning in specific depots. Oral genetic therapy to manipulate BAT has been reported in mice (Huang et al., 2016) and was able to increase BAT mass and activity. Similarly, stem cells derived from rat and human WAT were successfully differentiated into a three dimensional BAT using hydrogels (Yang et al., 2017). The effect of gut microbiota on BAT activity and browning is increasingly being recognized (Moreno-Navarrete et al., 2018) and would likely be a fertile area of research.

Novel small molecule activators of BAT and brite cells are being developed, along with novel delivery systems such as functionalized nanoparticles (Xue et al., 2016) and lipid nanocarriers (Zu et al., 2017). Such delivery systems hold promise for precise and efficient delivery of bioactives to their target site(s). Similarly, several dietary additives that activate BAT and browning have been reported. However, long-term studies with pharmacological and dietary treatments are needed. Future studies can also investigate the combined dietary and pharmacological treatments. Further research is likely to generate more information on BAT and brite biology and its interaction with various other physiological processes.

## AUTHOR CONTRIBUTIONS

SS and RV wrote the manuscript.

- Andrade, J. M. O., Frade, A. C. M., Guimarães, J. B., Freitas, K. M., Lopes, M. T. P., Guimarães, A. L. S., et al. (2014). Resveratrol increases brown adipose tissue thermogenesis markers by increasing SIRT1 and energy expenditure and decreasing fat accumulation in adipose tissue of mice fed a standard diet. *Eur. J. Nutr.* 53, 1503–1510. doi: 10.1007/s00394-014-0655-6
- Anunciado-Koza, R., Ukropec, J., Koza, R. A., and Kozak, L. P. (2008). Inactivation of UCP1 and the glycerol phosphate cycle synergistically increases energy expenditure to resist diet-induced obesity. *J. Biol. Chem.* 283, 27688–27697. doi: 10.1074/jbc.M804268200

- Arias, N., Picó, C., Teresa Macarulla, M., Oliver, P., Miranda, J., Palou, A., et al. (2017). A combination of resveratrol and quercetin induces browning in white adipose tissue of rats fed an obesogenic diet. *Obesity (Silver Spring)* 25, 111–121. doi: 10.1002/oby.21706
- Atherton, P. J., and Phillips, B. E. (2013). Greek goddess or Greek myth: the effects of exercise on irisin/FNDC5 in humans. *J. Physiol. (Lond.)* 591, 5267–5268. doi: 10.1113/jphysiol.2013.265371
- Bargut, T. C. L., Silva-e-Silva, A. C. A. G., Souza-Mello, V., Mandarin-de-Lacerda, C. A., and Aguilu, M. B. (2016). Mice fed fish oil diet and upregulation of brown adipose tissue thermogenic markers. *Eur. J. Nutr.* 55, 159–169. doi: 10.1007/s00394-015-0834-0
- Bartelt, A., Bruns, O. T., Reimer, R., Hohenberg, H., Itrich, H., Peldschus, K., et al. (2011). Brown adipose tissue activity controls triglyceride clearance. *Nat. Med.* 17, 200–205. doi: 10.1038/nm.2297
- Bartelt, A., John, C., Schaltenberg, N., Berbée, J. F. P., Worthmann, A., Cherradi, M. L., et al. (2017). Thermogenic adipocytes promote HDL turnover and reverse cholesterol transport. *Nat. Commun.* 8:15010. doi: 10.1038/ncomms15010
- Baskaran, P., Krishnan, V., Ren, J., and Thyagarajan, B. (2016). Capsaicin induces browning of white adipose tissue and counters obesity by activating TRPV1 channel-dependent mechanisms. *Br. J. Pharmacol.* 173, 2369–2389. doi: 10.1111/bph.13514
- Bell, B. B., Harlan, S. M., Morgan, D. A., Guo, D.-F., and Rahmouni, K. (2018). Differential contribution of POMC and AgRP neurons to the regulation of regional autonomic nerve activity by leptin. *Mol. Metab.* 8, 1–12. doi: 10.1016/j.molmet.2017.12.006
- Berbée, J. F. P., Boon, M. R., Khedoe, P. P. S. J., Bartelt, A., Schlein, C., Worthmann, A., et al. (2015). Brown fat activation reduces hypercholesterolaemia and protects from atherosclerosis development. *Nat. Commun.* 6:6356. doi: 10.1038/ncomms7356
- Blauw, L. L., Aziz, N. A., Tannemaat, M. R., Blauw, C. A., de Craen, A. J., Pijl, H., et al. (2017). Diabetes incidence and glucose intolerance prevalence increase with higher outdoor temperature. *BMJ Open Diabetes Res. Care* 5:e000317. doi: 10.1136/bmjdr-2016-000317
- Blondin, D. P., Frisch, F., Phoenix, S., Guérin, B., Turcotte, É. E., Haman, F., et al. (2017a). Inhibition of intracellular triglyceride lipolysis suppresses cold-induced brown adipose tissue metabolism and increases shivering in humans. *Cell Metab.* 25, 438–447. doi: 10.1016/j.cmet.2016.12.005
- Blondin, D. P., Tingelstad, H. C., Noll, C., Frisch, F., Phoenix, S., Guérin, B., et al. (2017b). Dietary fatty acid metabolism of brown adipose tissue in cold-acclimated men. *Nat. Commun.* 8:14146. doi: 10.1038/ncomms14146
- Blondin, D. P., Labbé, S. M., Tingelstad, H. C., Noll, C., Kunach, M., Phoenix, S., et al. (2014). Increased brown adipose tissue oxidative capacity in cold-acclimated humans. *J. Clin. Endocrinol. Metab.* 99, E438–E446. doi: 10.1210/jc.2013-3901
- Bookout, A. L., de Groot, M. H. M., Owen, B. M., Lee, S., Gautron, L., Lawrence, H. L., et al. (2013). FGF21 regulates metabolism and circadian behavior by acting on the nervous system. *Nat. Med.* 19, 1147–1152. doi: 10.1038/nm.3249
- Boström, P., Wu, J., Jedrychowski, M. P., Korde, A., Ye, L., Lo, J. C., et al. (2012). A PGC1- $\alpha$ -dependent myokine that drives brown-fat-like development of white fat and thermogenesis. *Nature* 481, 463–468. doi: 10.1038/nature10777
- Bouillaud, F., Combes-George, M., and Ricquier, D. (1983). Mitochondria of adult human brown adipose tissue contain a 32 000-Mr uncoupling protein. *Biosci. Rep.* 3, 775–780. doi: 10.1007/BF01120989
- Brendle, C., Werner, M. K., Schmadl, M., la Fougère, C., Nikolaou, K., Stefan, N., et al. (2018). Correlation of brown adipose tissue with other body fat compartments and patient characteristics: a retrospective analysis in a large patient cohort using PET/CT. *Acad. Radiol.* 25, 102–110. doi: 10.1016/j.acra.2017.09.007
- Broeders, E. P. M., Nascimento, E. B. M., Havekes, B., Brans, B., Roumans, K. H. M., Tailleux, A., et al. (2015). The bile acid chenodeoxycholic acid increases human brown adipose tissue activity. *Cell Metab.* 22, 418–426. doi: 10.1016/j.cmet.2015.07.002
- Buscemi, S., Corleo, D., Vasto, S., Buscemi, C., Massenti, M. F., Nuzzo, D., et al. (2018). Factors associated with circulating concentrations of irisin in the general population cohort of the ABCD study. *Int. J. Obes (Lond.)* 42, 398–404. doi: 10.1038/ijo.2017.255
- Chondronikola, M., Porter, C., Malagaris, I., Nella, A. A., and Sidossis, L. S. (2017). Brown adipose tissue is associated with systemic concentrations of peptides secreted from the gastrointestinal system and involved in appetite regulation. *Eur. J. Endocrinol.* 177, 33–40. doi: 10.1530/EJE-16-0958
- Chondronikola, M., Volpi, E., Børsheim, E., Chao, T., Porter, C., Annamalai, P., et al. (2016). Brown adipose tissue is linked to a distinct thermoregulatory response to mild cold in people. *Front. Physiol.* 7:129. doi: 10.3389/fphys.2016.00129
- Chondronikola, M., Volpi, E., Børsheim, E., Porter, C., Annamalai, P., Enerbäck, S., et al. (2014). Brown adipose tissue improves whole-body glucose homeostasis and insulin sensitivity in humans. *Diabetes Metab. Res. Rev.* 63, 4089–4099. doi: 10.2337/db14-0746
- Cohade, C., Osman, M., Pannu, H. K., and Wahl, R. L. (2003). Uptake in supraclavicular area fat (“USA-Fat”): description on 18F-FDG PET/CT. *J. Nucl. Med.* 44, 170–176.
- Côté, I., Sakarya, Y., Green, S. M., Morgan, D., Carter, C. S., Tümer, N., et al. (2018). iBAT sympathetic innervation is not required for body weight loss induced by central leptin delivery. *Am. J. Physiol. Endocrinol. Metab.* 314, E224–E231. doi: 10.1152/ajpendo.00219.2017
- Crescenzo, R., Mazzoli, A., Cancelliere, R., Bianco, F., Giacco, A., Liverini, G., et al. (2017). Polyunsaturated fatty acids stimulated novolipogenesis and improve glucose homeostasis during refeeding with high fat diet. *Front. Physiol.* 8:178. doi: 10.3389/fphys.2017.00178
- Cui, X., Nguyen, N. L. T., Zarebidaki, E., Cao, Q., Li, F., Zha, L., et al. (2016). Thermoneutrality decreases thermogenic program and promotes adiposity in high-fat diet-fed mice. *Physiol. Rep.* 4:e12799. doi: 10.14814/phy2.12799
- Cypess, A. M., Lehman, S., Williams, G., Tal, I., Rodman, D., Goldfine, A. B., et al. (2009). Identification and importance of brown adipose tissue in adult humans. *N. Engl. J. Med.* 360, 1509–1517. doi: 10.1056/NEJMoa0810780
- Cypess, A. M., Weiner, L. S., Roberts-Toler, C., Franquet Elia, E., Kessler, S. H., Kahn, P. A., et al. (2015). Activation of human brown adipose tissue by a  $\beta$ -adrenergic receptor agonist. *Cell Metab.* 21, 33–38. doi: 10.1016/j.cmet.2014.12.009
- Dallon, B. W., Parker, B. A., Hodson, A. E., Tippetts, T. S., Harrison, M. E., Appiah, M. M. A., et al. (2018). Insulin selectively reduces mitochondrial uncoupling in brown adipose tissue in mice. *Biochem. J.* 475, 561–569. doi: 10.1042/BCJ20170736
- de Macêdo, S. M., Lelis, D., de, F., Mendes, K. L., Fraga, C. A., de, C., et al. (2017). Effects of dietary macronutrient composition on FNDC5 and irisin in mice skeletal muscle. *Metab. Syndr. Relat. Disord.* 15, 161–169. doi: 10.1089/met.2016.0109
- De Matteis, R., Lucertini, F., Guescini, M., Polidori, E., Zeppa, S., Stocchi, V., et al. (2013). Exercise as a new physiological stimulus for brown adipose tissue activity. *Nutr. Metab. Cardiovasc. Dis.* 23, 582–590. doi: 10.1016/j.numecd.2012.01.013
- Dinas, P. C., Lahart, I. M., Timmons, J. A., Svensson, P.-A., Koutedakis, Y., Flouris, A. D., et al. (2017). Effects of physical activity on the link between PGC-1 $\alpha$  and FNDC5 in muscle, circulating irisin and UCP1 of white adipocytes in humans: a systematic review. *F1000Res* 6:286. doi: 10.12688/f1000research.11107.2
- DiSilvestro, D. J., Melgar-Bermudez, E., Yasmeen, R., Fadda, P., Lee, L. J., Kalyanasundaram, A., et al. (2016). Leptin production by encapsulated adipocytes increases brown fat, decreases resistin, and improves glucose intolerance in obese mice. *PLoS One* 11:e0153198. doi: 10.1371/journal.pone.0153198
- Douris, N., Stevanovic, D. M., Fisher, F. M., Cisu, T. I., Chee, M. J., Nguyen, N. L., et al. (2015). Central fibroblast growth factor 21 browns white fat via sympathetic action in male mice. *Endocrinology* 156, 2470–2481. doi: 10.1210/en.2014-2001
- Dutthak, P. A., Katafuchi, T., Bookout, A. L., Choi, J. H., Yu, R. T., Mangelsdorf, D. J., et al. (2012). Fibroblast growth factor-21 regulates PPAR $\gamma$  activity and the antidiabetic actions of thiazolidinediones. *Cell* 148, 556–567. doi: 10.1016/j.cell.2011.11.062
- Eggink, H. M., Tambyrajah, L. L., van den Berg, R., Mol, I. M., van den Heuvel, J. K., Koehorst, M., et al. (2018). Chronic infusion of taurochenodeoxycholate into the brain increases fat oxidation in mice. *J. Endocrinol.* 236, 85–97. doi: 10.1530/JOE-17-0503
- Enriori, P. J., Sinnayah, P., Simonds, S. E., Garcia Rudaz, C., and Cowley, M. A. (2011). Leptin action in the dorsomedial hypothalamus increases sympathetic tone to brown adipose tissue in spite of systemic leptin resistance. *J. Neurosci.* 31, 12189–12197. doi: 10.1523/JNEUROSCI.2336-11.2011

- Entringer, S., Rasmussen, J., Cooper, D. M., Ikenoue, S., Waffarn, F., Wadhwa, P. D., et al. (2017). Association between supraclavicular brown adipose tissue composition at birth and adiposity gain from birth to 6 months of age. *Pediatr. Res.* 82, 1017–1021. doi: 10.1038/pr.2017.159
- Ezoe, M., Wakamatsu, J.-I., Takahata, Y., Hasegawa, T., Morimatsu, F., and Nishimura, T. (2016). Diet-induced thermogenesis and expression levels of thyroid hormone target genes and their products in rats differ between meat proteins. *J. Nutr. Sci. Vitaminol.* 62, 93–100. doi: 10.3177/jnsv.62.93
- Feldmann, H. M., Golozoubova, V., Cannon, B., and Nedergaard, J. (2009). UCP1 ablation induces obesity and abolishes diet-induced thermogenesis in mice exempt from thermal stress by living at thermoneutrality. *Cell Metab.* 9, 203–209. doi: 10.1016/j.cmet.2008.12.014
- Fisher, F. M., Kleiner, S., Douris, N., Fox, E. C., Mepani, R. J., Verdegue, F., et al. (2012). FGF21 regulates PGC-1 $\alpha$  and browning of white adipose tissues in adaptive thermogenesis. *Genes Dev.* 26, 271–281. doi: 10.1101/gad.177857.111
- Flouris, A. D., Dinas, P. C., Valente, A., Andrade, C. M. B., Kawashita, N. H., and Sakellariou, P. (2017). Exercise-induced effects on UCP1 expression in classical brown adipose tissue: a systematic review. *Horm. Mol. Biol. Clin. Investig.* 31, 1–13. doi: 10.1515/hmbci-2016-0048
- François, M., Qualls-Creekmore, E., Berthoud, H.-R., Münzberg, H., and Yu, S. (2017). Genetics-based manipulation of adipose tissue sympathetic innervation. *Physiol. Behav.* 190, 21–27. doi: 10.1016/j.physbeh.2017.08.024
- Frank, A. P., Palmer, B. F., and Clegg, D. J. (2018). Do estrogens enhance activation of brown and beige of adipose tissues? *Physiol. Behav.* 187, 24–31. doi: 10.1016/j.physbeh.2017.09.026
- Franssens, B. T., Hoogduin, H., Leiner, T., van der Graaf, Y., and Visseren, F. L. J. (2017). Relation between brown adipose tissue and measures of obesity and metabolic dysfunction in patients with cardiovascular disease. *J. Magn. Reson. Imaging* 46, 497–504. doi: 10.1002/jmri.25594
- Gaich, G., Chien, J. Y., Fu, H., Glass, L. C., Deeg, M. A., Holland, W. L., et al. (2013). The effects of LY2405319, an FGF21 analog, in obese human subjects with type 2 diabetes. *Cell Metab.* 18, 333–340. doi: 10.1016/j.cmet.2013.08.005
- Gavrilu, A., Hasselgren, P.-O., Glasgow, A., Doyle, A. N., Lee, A. J., Fox, P., et al. (2017). Variable cold-induced brown adipose tissue response to thyroid hormone status. *Thyroid* 27, 1–10. doi: 10.1089/thy.2015.0646
- Ghandour, R. A., Colson, C., Giroud, M., Maurer, S., Rekima, S., Ailhaud, G., et al. (2018). Impact of dietary  $\omega$ 3 polyunsaturated fatty acid supplementation on brown and brite adipocyte function. *J. Lipid Res.* 59, 452–461. doi: 10.1194/jlr.M081091
- González-García, I., Tena-Sempere, M., and López, M. (2017). Estradiol regulation of brown adipose tissue thermogenesis. *Adv. Exp. Med. Biol.* 1043, 315–335. doi: 10.1007/978-3-319-70178-3\_15
- Gonzalez-Hurtado, E., Lee, J., Choi, J., and Wolfgang, M. J. (2018). Fatty acid oxidation is required for active and quiescent brown adipose tissue maintenance and thermogenic programming. *Mol. Metab.* 7, 45–56. doi: 10.1016/j.molmet.2017.11.004
- Green, A. L., Bagci, U., Hussein, S., Kelly, P. V., Muzaffar, R., Neuschwander-Tetri, B. A., et al. (2017). Brown adipose tissue detected by PET/CT imaging is associated with less central obesity. *Nucl. Med. Commun.* 38, 629–635. doi: 10.1097/MNM.0000000000000691
- Guerra, C., Koza, R. A., Yamashita, H., Walsh, K., and Kozak, L. P. (1998). Emergence of brown adipocytes in white fat in mice is under genetic control. Effects on body weight and adiposity. *J. Clin. Invest.* 102, 412–420. doi: 10.1172/JCI3155
- Han, S.-F., Jiao, J., Zhang, W., Xu, J.-Y., Zhang, W., Fu, C.-L., et al. (2017). Lipolysis and thermogenesis in adipose tissues as new potential mechanisms for metabolic benefits of dietary fiber. *Nutrition* 33, 118–124. doi: 10.1016/j.nut.2016.05.006
- Han, Y., Wu, J.-Z., Shen, J.-Z., Chen, L., He, T., Jin, M.-W., et al. (2017). Pentamethylquercetin induces adipose browning and exerts beneficial effects in 3T3-L1 adipocytes and high-fat diet-fed mice. *Sci. Rep.* 7:1123. doi: 10.1038/s41598-017-01206-4
- Hanssen, M. J. W., van der Lans, A. A. J. J., Brans, B., Hoeks, J., Jardon, K. M. C., Schaart, G., et al. (2016). Short-term cold acclimation recruits brown adipose tissue in obese humans. *Diabetes Metab. Res. Rev.* 65, 1179–1189. doi: 10.2337/db15-1372
- Hashimoto, O., Noda, T., Morita, A., Morita, M., Ohtsuki, H., Sugiyama, M., et al. (2016). Castration induced browning in subcutaneous white adipose tissue in male mice. *Biochem. Biophys. Res. Commun.* 478, 1746–1750. doi: 10.1016/j.bbrc.2016.09.017
- Heaton, J. M. (1972). The distribution of brown adipose tissue in the human. *J. Anat.* 112, 35–39.
- Hoeke, G., Kooijman, S., Boon, M. R., Rensen, P. C. N., and Berbée, J. F. P. (2016). Role of brown fat in lipoprotein metabolism and atherosclerosis. *Circ. Res.* 118, 173–182. doi: 10.1161/CIRCRESAHA.115.306647
- Hu, J., and Christian, M. (2017). Hormonal factors in the control of the browning of white adipose tissue. *Horm. Mol. Biol. Clin. Investig.* 31, 17–33. doi: 10.1515/hmbci-2017-0017
- Huang, W., McMurphy, T., Liu, X., Wang, C., and Cao, L. (2016). Genetic manipulation of brown fat via oral administration of an engineered recombinant adeno-associated viral serotype vector. *Mol. Ther.* 24, 1062–1069. doi: 10.1038/mt.2016.34
- Huttunen, P., Hirvonen, J., and Kinnula, V. (1981). The occurrence of brown adipose tissue in outdoor workers. *Eur. J. Appl. Physiol. Occup. Physiol.* 46, 339–345. doi: 10.1007/BF00422121
- Irshad, Z., Dimitri, F., Christian, M., and Zammit, V. A. (2017). Diacylglycerol acyltransferase 2 links glucose utilization to fatty acid oxidation in the brown adipocytes. *J. Lipid Res.* 58, 15–30. doi: 10.1194/jlr.M068197
- Iwen, K. A., Backhaus, J., Cassens, M., Waltl, M., Hedesan, O. C., Merkel, M., et al. (2017). Cold-induced brown adipose tissue activity alters plasma fatty acids and improves glucose metabolism in men. *J. Clin. Endocrinol. Metab.* 102, 4226–4234. doi: 10.1210/je.2017-01250
- Jedrychowski, M. P., Wrann, C. D., Paulo, J. A., Gerber, K. K., Szpyt, J., Robinson, M. M., et al. (2015). Detection and quantitation of circulating human irisin by tandem mass spectrometry. *Cell Metab.* 22, 734–740. doi: 10.1016/j.cmet.2015.08.001
- Jespersen, N. Z., Larsen, T. J., Peijs, L., Dagaard, S., Homøe, P., Loft, A., et al. (2013). A classical brown adipose tissue mRNA signature partly overlaps with brite in the supraclavicular region of adult humans. *Cell Metab.* 17, 798–805. doi: 10.1016/j.cmet.2013.04.011
- Jung, Y., Park, J., Kim, H.-L., Sim, J.-E., Youn, D.-H., Kang, J., et al. (2018). Vanillic acid attenuates obesity via activation of the AMPK pathway and thermogenic factors in vivo and in vitro. *FASEB J.* 32, 1388–1402. doi: 10.1096/fj.201700231RR
- Katz, L. S., Xu, S., Ge, K., Scott, D. K., and Gershengorn, M. C. (2018). T3 and glucose coordinately stimulate ChREBP-mediated Ucp1 expression in brown adipocytes from male mice. *Endocrinology* 159, 557–569. doi: 10.1210/en.2017-00579
- Kazak, L., Chouchani, E. T., Jedrychowski, M. P., Erickson, B. K., Shinoda, K., Cohen, P., et al. (2015). A creatine-driven substrate cycle enhances energy expenditure and thermogenesis in beige fat. *Cell* 163, 643–655. doi: 10.1016/j.cell.2015.09.035
- Khan, S., and Jena, G. (2016). Sodium butyrate reduces insulin-resistance, fat accumulation and dyslipidemia in type-2 diabetic rat: a comparative study with metformin. *Chem. Biol. Interact.* 254, 124–134. doi: 10.1016/j.cb.2016.06.007
- Khedoe, P. P. S. J., Hoeke, G., Kooijman, S., Dijk, W., Buijs, J. T., Kersten, S., et al. (2015). Brown adipose tissue takes up plasma triglycerides mostly after lipolysis. *J. Lipid Res.* 56, 51–59. doi: 10.1194/jlr.M052746
- Kikai, M., Yamada, H., Wakana, N., Terada, K., Yamamoto, K., Wada, N., et al. (2017). Transplantation of brown adipose tissue inhibits atherosclerosis in apoE $^{-/-}$  mice: contribution of the activated FGF-21-adiponectin axis. *Cardiovasc. Res.* 114, i1–i13. doi: 10.1093/cvr/cvx212
- Kim, E. K., Lee, S. H., Jhun, J. Y., Byun, J. K., Jeong, J. H., Lee, S.-Y., et al. (2016). Metformin prevents fatty liver and improves balance of white/brown adipose in an obesity mouse model by inducing FGF21. *Mediat. Inflamm.* 2016:5813030. doi: 10.1155/2016/5813030
- Kim, E.-K., Lee, S. H., Lee, S.-Y., Kim, J.-K., Jhun, J. Y., Na, H. S., et al. (2018). Metformin ameliorates experimental-obesity-associated autoimmune arthritis by inducing FGF21 expression and brown adipocyte differentiation. *Exp. Mol. Med.* 50:e432. doi: 10.1038/emmm.2017.245
- Kim, H., Choe, J.-H., Choi, J. H., Kim, H. J., Park, S. H., Lee, M. W., et al. (2017). Medium-chain enriched diacylglycerol (MCE-DAG) oil decreases body fat mass in mice by increasing lipolysis and thermogenesis in adipose tissue. *Lipids* 52, 665–673. doi: 10.1007/s11745-017-4277-7
- Kitada, M., Ogura, Y., Suzuki, T., Monno, I., Kanasaki, K., Watanabe, A., et al. (2018). A low-protein diet exerts a beneficial effect on diabetic status and



- presents diabetic nephropathy in Wistar fatty rats, an animal model of type 2 diabetes and obesity.
- Nutr. Metab. (Lond.)*
- 15, 20. doi: 10.1186/s12986-018-0255-1
- Klingenberg, M. (2017). UCP1 – A sophisticated energy valve. *Biochimie* 134, 19–27. doi: 10.1016/j.biochi.2016.10.012
- Knudsen, J. G., Murholm, M., Carey, A. L., Biesø, R. S., Basse, A. L., Allen, T. L., et al. (2014). Role of IL-6 in exercise training- and cold-induced UCP1 expression in subcutaneous white adipose tissue. *PLoS One* 9:e84910. doi: 10.1371/journal.pone.0084910
- Kodo, K., Sugimoto, S., Nakajima, H., Mori, J., Itoh, I., Fukuhara, S., et al. (2017). Erythropoietin (EPO) ameliorates obesity and glucose homeostasis by promoting thermogenesis and endocrine function of classical brown adipose tissue (BAT) in diet-induced obese mice. *PLoS One* 12:e0173661. doi: 10.1371/journal.pone.0173661
- Kohlme, R., Perwitz, N., Resch, J., Schmid, S. M., Lehnert, H., Klein, J., et al. (2017). Dopamine directly increases mitochondrial mass and thermogenesis in brown adipocytes. *J. Mol. Endocrinol.* 58, 57–66. doi: 10.1530/JME-16-0159
- Kontani, Y., Wang, Y., Kimura, K., Inokuma, K.-I., Saito, M., Suzuki-Miura, T., et al. (2005). UCP1 deficiency increases susceptibility to diet-induced obesity with age. *Aging Cell* 4, 147–155. doi: 10.1111/j.1474-9726.2005.00157.x
- Ku, C. R., Cho, Y. H., Hong, Z. Y., Lee, H., Lee, S. J., Hong, S. S., et al. (2016). The effects of high fat diet and resveratrol on mitochondrial activity of brown adipocytes. *Endocrinol. Metab. (Seoul.)* 31, 328–335. doi: 10.3803/EnM.2016.31.2328
- Lee, P., and Greenfield, J. R. (2015). Non-pharmacological and pharmacological strategies of brown adipose tissue recruitment in humans. *Mol. Cell. Endocrinol.* 418(Pt 2), 184–190. doi: 10.1016/j.mce.2015.05.025
- Lee, P., Greenfield, J. R., Ho, K. K. Y., and Fulham, M. J. (2010). A critical appraisal of the prevalence and metabolic significance of brown adipose tissue in adult humans. *Am. J. Physiol. Endocrinol. Metab.* 299, E601–E606. doi: 10.1152/ajpendo.00298.2010
- Lee, P., Zhao, J. T., Swarbrick, M. M., Gracie, G., Bova, R., Greenfield, J. R., et al. (2011). High prevalence of brown adipose tissue in adult humans. *J. Clin. Endocrinol. Metab.* 96, 2450–2455. doi: 10.1210/jc.2011-0487
- Leu, S.-Y., Tsai, Y.-C., Chen, W.-C., Hsu, C.-H., Lee, Y.-M., and Cheng, P.-Y. (2018). Raspberry ketone induces brown-like adipocyte formation through suppression of autophagy in adipocytes and adipose tissue. *J. Nutr. Biochem.* 56, 116–125. doi: 10.1016/j.jnutbio.2018.01.017
- Li, Q., Wang, K., Ma, Y., Qin, C., Dong, C., Jin, P., et al. (2017). Resveratrol derivative BTM-0512 mitigates obesity by promoting beige remodeling of subcutaneous preadipocytes. *Acta Biochim. Biophys. Sin. (Shanghai)* 49, 318–327. doi: 10.1093/abbs/gmx009
- Li, S., Li, Y., Xiang, L., Dong, J., Liu, M., and Xiang, G. (2018). Sildenafil induces browning of subcutaneous white adipose tissue in overweight adults. *Metab. Clin. Exp.* 78, 106–117. doi: 10.1016/j.metabol.2017.09.008
- Li, T., Gao, J., Du, M., Song, J., and Mao, X. (2018). Milk fat globule membrane attenuates high-fat diet-induced obesity by inhibiting adipogenesis and increasing uncoupling protein 1 expression in white adipose tissue of mice. *Nutrients* 10:E331. doi: 10.3390/nu10030331
- Li, Z., Yi, C.-X., Katiraei, S., Kooijman, S., Zhou, E., Chung, C. K., et al. (2018). Butyrate reduces appetite and activates brown adipose tissue via the gut-brain neural circuit. *Gut* 67, 1269–1279. doi: 10.1136/gutjnl-2017-314050
- Lidell, M. E., Betz, M. J., Dahlqvist Leinhard, O., Heglund, M., Elander, L., Slawik, M., et al. (2013). Evidence for two types of brown adipose tissue in humans. *Nat. Med.* 19, 631–634. doi: 10.1038/nm.3017
- Liu, H., Liu, X., Wang, L., and Sheng, N. (2017). Brown adipose tissue transplantation ameliorates male fertility impairment caused by diet-induced obesity. *Obes. Res. Clin. Pract.* 11, 198–205. doi: 10.1016/j.orcp.2016.06.001
- Liu, P., Ji, Y., Yuen, T., Rendina-Ruedy, E., DeMambro, V. E., Dhawan, S., et al. (2017). Blocking FSH induces thermogenic adipose tissue and reduces body fat. *Nature* 546, 107–112. doi: 10.1038/nature22342
- Loh, R. K. C., Formosa, M. F., Eikelis, N., Bertovic, D. A., Anderson, M. J., Barwood, S. A., et al. (2018). Pioglitazone reduces cold-induced brown fat glucose uptake despite induction of browning in cultured human adipocytes: a randomised, controlled trial in humans. *Diabetologia* 61, 220–230. doi: 10.1007/s00125-017-4479-9
- López, M., and Tena-Sempere, M. (2016). Estradiol and brown fat. *Best Pract. Res. Clin. Endocrinol. Metab.* 30, 527–536. doi: 10.1016/j.beem.2016.08.004
- López, M., and Tena-Sempere, M. (2017). Estradiol effects on hypothalamic AMPK and BAT thermogenesis: a gateway for obesity treatment? *Pharmacol. Ther.* 178, 109–122. doi: 10.1016/j.pharmthera.2017.03.014
- López, M., Varela, L., Vázquez, M. J., Rodríguez-Cuenca, S., González, C. R., Velagapudi, V. R., et al. (2010). Hypothalamic AMPK and fatty acid metabolism mediate thyroid regulation of energy balance. *Nat. Med.* 16, 1001–1008. doi: 10.1038/nm.2207
- Ludwig, R. G., Rocha, A. L., and Mori, M. A. (2018). Circulating molecules that control brown/beige adipocyte differentiation and thermogenic capacity. *Cell Biol. Int.* 42, 701–710. doi: 10.1002/cbin.10946
- Maekawa, R., Seino, Y., Ogata, H., Murase, M., Iida, A., Hosokawa, K., et al. (2017). Chronic high-sucrose diet increases fibroblast growth factor 21 production and energy expenditure in mice. *J. Nutr. Biochem.* 49, 71–79. doi: 10.1016/j.jnutbio.2017.07.010
- Maneschi, E., Cellai, I., Aversa, A., Mello, T., Filippi, S., Comeglio, P., et al. (2016). Tadalafil reduces visceral adipose tissue accumulation by promoting preadipocytes differentiation towards a metabolically healthy phenotype: studies in rabbits. *Mol. Cell. Endocrinol.* 424, 50–70. doi: 10.1016/j.mce.2016.01.015
- Martínez-Sánchez, N., Moreno-Navarrete, J. M., Contreras, C., Rial-Pensado, E., Fernø, J., Nogueiras, R., et al. (2017a). Thyroid hormones induce browning of white fat. *J. Endocrinol.* 232, 351–362. doi: 10.1530/JOE-16-0425
- Martínez-Sánchez, N., Seoane-Collazo, P., Contreras, C., Varela, L., Villarroja, J., Rial-Pensado, E., et al. (2017b). Hypothalamic AMPK-ER stress-JNK1 axis mediates the central actions of thyroid hormones on energy balance. *Cell Metab.* 26, 212.e12–229.e12. doi: 10.1016/j.cmet.2017.06.014
- Martins, F. F., Bargut, T. C. L., Aguila, M. B., and Mandarim-de-Lacerda, C. A. (2017). Thermogenesis, fatty acid synthesis with oxidation, and inflammation in the brown adipose tissue of ob/ob (–/–) mice. *Ann. Anat.* 210, 44–51. doi: 10.1016/j.aanat.2016.11.013
- McIlvride, S., Mushtaq, A., Papacleovoulou, G., Hurling, C., Steel, J., Jansen, E., et al. (2017). A progesterone-brown fat axis is involved in regulating fetal growth. *Sci. Rep.* 7:10671. doi: 10.1038/s41598-017-10979-7
- Merlin, J., Sato, M., Nowell, C., Pakzad, M., Fahey, R., Gao, J., et al. (2018). The PPAR $\gamma$  agonist rosiglitazone promotes the induction of brite adipocytes, increasing  $\beta$ -adrenoceptor-mediated mitochondrial function and glucose uptake. *Cell. Signal.* 42, 54–66. doi: 10.1016/j.cellsig.2017.09.023
- Mills, E. L., Pierce, K. A., Jedrychowski, M. P., Garrity, R., Winther, S., Vidoni, S., et al. (2018). Accumulation of succinate controls activation of adipose tissue thermogenesis. *Nature* 560, 102–106. doi: 10.1038/s41586-018-0353-2
- Min, S. Y., Kady, J., Nam, M., Rojas-Rodríguez, R., Berkenwald, A., Kim, J. H., et al. (2016). Human “brite/beige” adipocytes develop from capillary networks, and their implantation improves metabolic homeostasis in mice. *Nat. Med.* 22, 312–318. doi: 10.1038/nm.4031
- Mo, Q., Salley, J., Roshan, T., Baer, L. A., May, F. J., Jaehnig, E. J., et al. (2017). Identification and characterization of a supraclavicular brown adipose tissue in mice. *JCI Insight* 2 doi: 10.1172/jci.insight.93166 [Epub ahead of print].
- Moreno-Navarrete, J. M., Serino, M., Blasco-Baque, V., Azalbert, V., Barton, R. H., Cardellini, M., et al. (2018). Gut microbiota interacts with markers of adipose tissue browning, insulin action and plasma acetate in morbid obesity. *Mol. Nutr. Food Res.* 62. doi: 10.1002/mnfr.201700721
- Morimoto, H., Mori, J., Nakajima, H., Kawabe, Y., Tsuma, Y., Fukuhara, S., et al. (2018). Angiotensin 1–7 stimulates brown adipose tissue and reduces diet-induced obesity. *Am. J. Physiol. Endocrinol. Metab.* 314, E131–E138. doi: 10.1152/ajpendo.00192.2017
- Motiani, P., Virtanen, K. A., Motiani, K. K., Eskelinen, J. J., Middelbeek, R. J., Goodyear, L. J., et al. (2017). Decreased insulin-stimulated brown adipose tissue glucose uptake after short-term exercise training in healthy middle-aged men. *Diabetes. Obes. Metab.* 19, 1379–1388. doi: 10.1111/dom.12947
- Nam, H.-Y., and Jun, S. (2017). Association between active brown adipose tissue and coronary artery calcification in healthy men. *Nuklearmedizin* 56, 184–190. doi: 10.3413/Nukmed-0887-17-03
- Nedergaard, J., Bengtsson, T., and Cannon, B. (2007). Unexpected evidence for active brown adipose tissue in adult humans. *Am. J. Physiol. Endocrinol. Metab.* 293, E444–E452. doi: 10.1152/ajpendo.00691.2006
- Neyrinck, A. M., Bindels, L. B., Geurts, L., Van Hul, M., Cani, P. D., and Delzenne, N. M. (2017). A polyphenolic extract from green tea leaves activates



- fat browning in high-fat-diet-induced obese mice. *J. Nutr. Biochem.* 49, 15–21. doi: 10.1016/j.jnutbio.2017.07.008
- Nguyen, N. L. T., Xue, B., and Bartness, T. J. (2018). Sensory denervation of inguinal white fat modifies sympathetic outflow to white and brown fat in Siberian hamsters. *Physiol. Behav.* 190, 28–33. doi: 10.1016/j.physbeh.2018.02.019
- Nirengi, S., Amagasa, S., Homma, T., Yoneshiro, T., Matsumiya, S., Kurosawa, Y., et al. (2016). Daily ingestion of catechin-rich beverage increases brown adipose tissue density and decreases extramitochondrial lipids in healthy young women. *Springerplus* 5:1363. doi: 10.1186/s40064-016-3029-0
- Ohtomo, T., Ino, K., Miyashita, R., Chigira, M., Nakamura, M., Someya, K., et al. (2017). Chronic high-fat feeding impairs adaptive induction of mitochondrial fatty acid combustion-associated proteins in brown adipose tissue of mice. *Biochem. Biophys. Rep.* 10, 32–38. doi: 10.1016/j.bbrep.2017.02.002
- Okamatsu-Ogura, Y., Nio-Kobayashi, J., Nagaya, K., Tsubota, A., and Kimura, K. (2018). Brown adipocytes postnatally arise through both differentiation from progenitors and conversion from white adipocytes in Syrian hamster. *J. Appl. Physiol.* 124, 99–108. doi: 10.1152/japplphysiol.00622.2017
- Orava, J., Nuutila, P., Noponen, T., Parkkola, R., Viljanen, T., Enerbäck, S., et al. (2013). Blunted metabolic responses to cold and insulin stimulation in brown adipose tissue of obese humans. *Obesity (Silver Spring)* 21, 2279–2287. doi: 10.1002/oby.20456
- Ost, M., Keipert, S., and Klaus, S. (2017). Targeted mitochondrial uncoupling beyond UCP1 – The fine line between death and metabolic health. *Biochimie* 134, 77–85. doi: 10.1016/j.biochi.2016.11.013
- Owen, B. M., Ding, X., Morgan, D. A., Coate, K. C., Bookout, A. L., Rahmouni, K., et al. (2014). FGF21 acts centrally to induce sympathetic nerve activity, energy expenditure, and weight loss. *Cell Metab.* 20, 670–677. doi: 10.1016/j.cmet.2014.07.012
- Pahlavani, M., Razafimanjato, F., Ramalingam, L., Kalupahana, N. S., Moussa, H., Scoggins, S., et al. (2017). Eicosapentaenoic acid regulates brown adipose tissue metabolism in high-fat-fed mice and in clonal brown adipocytes. *J. Nutr. Biochem.* 39, 101–109. doi: 10.1016/j.jnutbio.2016.08.012
- Peppler, W. T., Townsend, L. K., Knuth, C. M., Foster, M. T., and Wright, D. C. (2018). Subcutaneous inguinal white adipose tissue is responsive to, but dispensable for, the metabolic health benefits of exercise. *Am. J. Physiol. Endocrinol. Metab.* 314, E66–E77. doi: 10.1152/ajpendo.00226.2017
- Pereira, M. P., Ferreira, L. A. A., da Silva, F. H. S., Christoffoleto, M. A., Metsios, G. S., Chaves, V. E., et al. (2017). A low-protein, high-carbohydrate diet increases browning in perirenal adipose tissue but not in inguinal adipose tissue. *Nutrition* 42, 37–45. doi: 10.1016/j.nut.2017.05.007
- Pettersson-Klein, A. T., Izadi, M., Ferreira, D. M. S., Cervenka, I., Correia, J. C., Martinez-Redondo, V., et al. (2018). Small molecule PGC-1 $\alpha$ 1 protein stabilizers induce adipocyte Ucp1 expression and uncoupled mitochondrial respiration. *Mol. Metab.* 9, 28–42. doi: 10.1016/j.molmet.2018.01.017
- Ponnusamy, S., Tran, Q. T., Harvey, I., Smallwood, H. S., Thiagarajan, T., Banerjee, S., et al. (2017). Pharmacologic activation of estrogen receptor  $\beta$  increases mitochondrial function, energy expenditure, and brown adipose tissue. *FASEB J.* 31, 266–281. doi: 10.1096/fj.201600787RR
- Rachid, T. L., Silva-Veiga, F. M., Graus-Nunes, F., Brighenti, I., Mandarim-de-Lacerda, C. A., and Souza-Mello, V. (2018). Differential actions of PPAR- $\alpha$  and PPAR- $\beta/\delta$  on beige adipocyte formation: a study in the subcutaneous white adipose tissue of obese male mice. *PLoS One* 13:e0191365. doi: 10.1371/journal.pone.0191365
- Ricquier, D. (2017). UCP1, the mitochondrial uncoupling protein of brown adipocyte: a personal contribution and a historical perspective. *Biochimie* 134, 3–8. doi: 10.1016/j.biochi.2016.10.018
- Roberts, L. D., Boström, P., O'Sullivan, J. F., Schinzel, R. T., Lewis, G. D., Dejam, A., et al. (2014).  $\beta$ -Aminoisobutyric acid induces browning of white fat and hepatic  $\beta$ -oxidation and is inversely correlated with cardiometabolic risk factors. *Cell Metab.* 19, 96–108. doi: 10.1016/j.cmet.2013.12.003
- Rodríguez, A., Becerril, S., Ezquerro, S., Méndez-Giménez, L., and Frühbeck, G. (2017). Crosstalk between adipokines and myokines in fat browning. *Acta Physiol. (Oxf.)* 219, 362–381. doi: 10.1111/apha.12686
- Rolfe, D. F., and Brown, G. C. (1997). Cellular energy utilization and molecular origin of standard metabolic rate in mammals. *Physiol. Rev.* 77, 731–758. doi: 10.1152/physrev.1997.77.3.731
- Rosenwald, M., Perdikari, A., Rülcke, T., and Wolfrum, C. (2013). Bi-directional interconversion of brite and white adipocytes. *Nat. Cell Biol.* 15, 659–667. doi: 10.1038/ncb2740
- Sahuri-Arisoylu, M., Brody, L. P., Parkinson, J. R., Parkes, H., Navaratnam, N., Miller, A. D., et al. (2016). Reprogramming of hepatic fat accumulation and “browning” of adipose tissue by the short-chain fatty acid acetate. *Int. J. Obes. (Lond.)* 40, 955–963. doi: 10.1038/ijo.2016.23
- Saito, M., Okamatsu-Ogura, Y., Matsushita, M., Watanabe, K., Yoneshiro, T., Nio-Kobayashi, J., et al. (2009). High incidence of metabolically active brown adipose tissue in healthy adult humans: effects of cold exposure and adiposity. *Diabetes Metab. Res. Rev.* 58, 1526–1531. doi: 10.2337/db09-0530
- Saito, M., and Yoneshiro, T. (2013). Capsinoids and related food ingredients activating brown fat thermogenesis and reducing body fat in humans. *Curr. Opin. Lipidol.* 24, 71–77. doi: 10.1097/MOL.0b013e32835a4f40
- Schreiber, R., Diwoky, C., Schoiswohl, G., Feiler, U., Wongsiriroj, N., Abdellatif, M., et al. (2017). Cold-induced thermogenesis depends on ATGL-mediated lipolysis in cardiac muscle, but not brown adipose tissue. *Cell Metab.* 26, 753.e7–763.e7. doi: 10.1016/j.cmet.2017.09.004
- Sharp, L. Z., Shinoda, K., Ohno, H., Scheel, D. W., Tomoda, E., Ruiz, L., et al. (2012). Human BAT possesses molecular signatures that resemble beige/brite cells. *PLoS One* 7:e49452. doi: 10.1371/journal.pone.0049452
- Shen, W., and McIntosh, M. K. (2016). Nutrient regulation: conjugated linoleic acid's inflammatory and browning properties in adipose tissue. *Annu. Rev. Nutr.* 36, 183–210. doi: 10.1146/annurev-nutr-071715-050924
- Shi, L.-L., Fan, W.-J., Zhang, J.-Y., Zhao, X.-Y., Tan, S., Wen, J., et al. (2017). The roles of metabolic thermogenesis in body fat regulation in striped hamsters fed high-fat diet at different temperatures. *Comp. Biochem. Physiol. Part A Mol. Integr. Physiol.* 212, 35–44. doi: 10.1016/j.cbpa.2017.07.002
- Shin, H., Ma, Y., Chanturiya, T., Cao, Q., Wang, Y., Kadegowda, A. K. G., et al. (2017). Lipolysis in brown adipocytes is not essential for cold-induced thermogenesis in mice. *Cell Metab.* 26, 764.e5–777.e5. doi: 10.1016/j.cmet.2017.09.002
- Shin, S., and Ajuwon, K. M. (2018). Effects of diets differing in composition of 18-C fatty acids on adipose tissue thermogenic gene expression in mice fed high-fat diets. *Nutrients* 10:E256. doi: 10.3390/nu10020256
- Simcox, J., Geoghegan, G., Maschek, J. A., Bensard, C. L., Pasquali, M., Miao, R., et al. (2017). Global analysis of plasma lipids identifies liver-derived acylcarnitines as a fuel source for brown fat thermogenesis. *Cell Metab.* 26, 509.e6–522.e6. doi: 10.1016/j.cmet.2017.08.006
- Singh, R., Braga, M., Reddy, S. T., Lee, S.-J., Parveen, M., Grijalva, V., et al. (2017). Follistatin targets distinct pathways to promote brown adipocyte characteristics in brown and white adipose tissues. *Endocrinology* 158, 1217–1230. doi: 10.1210/en.2016-1607
- Singhal, V., Maffaioli, G. D., Ackerman, K. E., Lee, H., Elia, E. F., Woolley, R., et al. (2016). Effect of chronic athletic activity on brown fat in young women. *PLoS One* 11:e0156353. doi: 10.1371/journal.pone.0156353
- Soriano, R. N., Braga, S. P., Breder, J. S. C., Batalhao, M. E., Oliveira-Pelegrin, G. R., Ferreira, L. F. R., et al. (2018). Endogenous peripheral hydrogen sulfide is prophyretic: its permissive role in brown adipose tissue thermogenesis in rats. *Exp. Physiol.* 103, 397–407. doi: 10.1113/EP086775
- Soto, M., Orliaguet, L., Reyzer, M. L., Manier, M. L., Caprioli, R. M., and Kahn, C. R. (2018). Pyruvate induces torpor in obese mice. *Proc. Natl. Acad. Sci. U.S.A.* 115, 810–815. doi: 10.1073/pnas.1717507115
- Srivastava, S., Baxa, U., Niu, G., Chen, X., and Veech, R. L. (2013). A ketogenic diet increases brown adipose tissue mitochondrial proteins and UCP1 levels in mice. *IUBMB Life* 65, 58–66. doi: 10.1002/iub.1102
- Srivastava, S., Kashiwaya, Y., King, M. T., Baxa, U., Tam, J., Niu, G., et al. (2012). Mitochondrial biogenesis and increased uncoupling protein 1 in brown adipose tissue of mice fed a ketone ester diet. *FASEB J.* 26, 2351–2362. doi: 10.1096/fj.11-200410
- Stanford, K. I., Middelbeek, R. J. W., Townsend, K. L., An, D., Nygaard, E. B., Hitchcox, K. M., et al. (2013). Brown adipose tissue regulates glucose homeostasis and insulin sensitivity. *J. Clin. Invest.* 123, 215–223. doi: 10.1172/JCI62308
- Sturla, L., Mannino, E., Scarfi, S., Bruzzone, S., Magnone, M., Sociali, G., et al. (2017). Abscisic acid enhances glucose disposal and induces brown fat activity

- in adipocytes in vitro and in vivo. *Biochim. Biophys. Acta* 1862, 131–144. doi: 10.1016/j.bbailip.2016.11.005
- Sugita, J., Yoneshiro, T., Hatano, T., Aita, S., Ikemoto, T., Uchiwa, H., et al. (2013). Grains of paradise (*Aframomum melegueta*) extract activates brown adipose tissue and increases whole-body energy expenditure in men. *Br. J. Nutr.* 110, 733–738. doi: 10.1017/S0007114512005715
- Sun, L., Camps, S. G., Goh, H. J., Govindharajulu, P., Schaefferkoetter, J. D., Townsend, D. W., et al. (2018). Capsinoids activate brown adipose tissue (BAT) with increased energy expenditure associated with subthreshold 18-fluorine fluorodeoxyglucose uptake in BAT-positive humans confirmed by positron emission tomography scan. *Am. J. Clin. Nutr.* 107, 62–70. doi: 10.1093/ajcn/nqx025
- Sun, W., Uchida, K., Suzuki, Y., Zhou, Y., Kim, M., Takayama, Y., et al. (2016a). Lack of TRPV2 impairs thermogenesis in mouse brown adipose tissue. *EMBO Rep.* 17, 383–399. doi: 10.15252/embr.201540819
- Sun, W., Uchida, K., Takahashi, N., Iwata, Y., Wakabayashi, S., Goto, T., et al. (2016b). Activation of TRPV2 negatively regulates the differentiation of mouse brown adipocytes. *Pflugers. Arch.* 468, 1527–1540. doi: 10.1007/s00424-016-1846-1
- Than, A., Xu, S., Li, R., Leow, M.-S., Sun, L., and Chen, P. (2017). Angiotensin type 2 receptor activation promotes browning of white adipose tissue and brown adipogenesis. *Signal. Transduct. Target. Ther.* 2, 17022. doi: 10.1038/sigtrans.2017.22
- Tokubuchi, I., Tajiri, Y., Iwata, S., Hara, K., Wada, N., Hashinaga, T., et al. (2017). Beneficial effects of metformin on energy metabolism and visceral fat volume through a possible mechanism of fatty acid oxidation in human subjects and rats. *PLoS One* 12:e0171293. doi: 10.1371/journal.pone.0171293
- Trexler, E. T., McCallister, D., Smith-Ryan, A. E., and Branca, R. T. (2017). Incidental finding of low brown adipose tissue activity in endurance-trained individuals: methodological considerations for positron emission tomography. *J. Nat. Sci.* 3:e335.
- Tsiloulis, T., Carey, A. L., Bayliss, J., Canny, B., Meex, R. C. R., and Watt, M. J. (2018). No evidence of white adipocyte browning after endurance exercise training in obese men. *Int. J. Obes. (Lond.)* 42, 721–727. doi: 10.1038/ijo.2017.295
- Tsukuda, K., Mogi, M., Iwanami, J., Kanno, H., Nakaoka, H., Wang, X.-L., et al. (2016). Enhancement of adipocyte browning by angiotensin II type 1 receptor blockade. *PLoS One* 11:e0167704. doi: 10.1371/journal.pone.0167704
- Turner, J. B., Kumar, A., and Koch, C. A. (2016). The effects of indoor and outdoor temperature on metabolic rate and adipose tissue – The Mississippi perspective on the obesity epidemic. *Rev. Endocr. Metab. Disord.* 17, 61–71. doi: 10.1007/s11154-016-9358-z
- van Marken Lichtenbelt, W. D., and Schrauwen, P. (2011). Implications of nonshivering thermogenesis for energy balance regulation in humans. *Am. J. Physiol. Regul. Integr. Comp. Physiol.* 301, R285–R296. doi: 10.1152/ajpregu.00652.2010
- Velickovic, K. D., Ukropina, M. M., Glisic, R. M., and Cakic-Milosevic, M. M. (2018). Effects of long-term sucrose overfeeding on rat brown adipose tissue: a structural and immunohistochemical study. *J. Exp. Biol.* 221:pii: jeb166538. doi: 10.1242/jeb.166538
- Villarroya, F., Gavalda-Navarro, A., Peyrou, M., Villarroya, J., and Giral, M. (2017). The lives and times of brown adipokines. *Trends Endocrinol. Metab.* 28, 855–867. doi: 10.1016/j.tem.2017.10.005
- Villicev, C. M., Freitas, F. R. S., Aoki, M. S., Taffarel, C., Scanlan, T. S., Moriscot, A. S., et al. (2007). Thyroid hormone receptor beta-specific agonist GC-1 increases energy expenditure and prevents fat-mass accumulation in rats. *J. Endocrinol.* 193, 21–29. doi: 10.1677/joe.1.07066
- Virtanen, K. A., Lidell, M. E., Orava, J., Heglund, M., Westergren, R., Niemi, T., et al. (2009). Functional brown adipose tissue in healthy adults. *N. Engl. J. Med.* 360, 1518–1525. doi: 10.1056/NEJMoa0808949
- Vosselman, M. J., Hoeks, J., Brans, B., Pallubinsky, H., Nascimento, E. B. M., van der Lans, A. A. J. J., et al. (2015). Low brown adipose tissue activity in endurance-trained compared with lean sedentary men. *Int. J. Obes.* 39, 1696–1702. doi: 10.1038/ijo.2015.130
- Waldén, T. B., Hansen, I. R., Timmons, J. A., Cannon, B., and Nedergaard, J. (2012). Recruited vs. nonrecruited molecular signatures of brown, “brite,” and white adipose tissues. *Am. J. Physiol. Endocrinol. Metab.* 302, E19–E31. doi: 10.1152/ajpendo.00249.2011
- Wang, S., Liang, X., Yang, Q., Fu, X., Zhu, M., Rodgers, B. D., et al. (2017). Resveratrol enhances brown adipocyte formation and function by activating AMP-activated protein kinase (AMPK)  $\alpha 1$  in mice fed high-fat diet. *Mol. Nutr. Food. Res.* 61, 746–765. doi: 10.1002/mnfr.201600746
- Watanabe, M., Houten, S. M., Matak, C., Christoffolete, M. A., Kim, B. W., Sato, H., et al. (2006). Bile acids induce energy expenditure by promoting intracellular thyroid hormone activation. *Nature* 439, 484–489. doi: 10.1038/nature04330
- Weiner, J., Hankir, M., Heiker, J. T., Fenske, W., and Krause, K. (2017). Thyroid hormones and browning of adipose tissue. *Mol. Cell. Endocrinol.* 458, 156–159. doi: 10.1016/j.mce.2017.01.011
- Weiner, J., Kranz, M., Klöting, N., Kunath, A., Steinhoff, K., Rijntjes, E., et al. (2016). Thyroid hormone status defines brown adipose tissue activity and browning of white adipose tissues in mice. *Sci. Rep.* 6:38124. doi: 10.1038/srep38124
- Worthmann, A., John, C., Rühlemann, M. C., Baguhl, M., Heinsen, F.-A., Schaltenberg, N., et al. (2017). Cold-induced conversion of cholesterol to bile acids in mice shapes the gut microbiome and promotes adaptive thermogenesis. *Nat. Med.* 23, 839–849. doi: 10.1038/nm.4357
- Wu, C., Hwang, S. H., Jia, Y., Choi, J., Kim, Y.-J., Choi, D., et al. (2017). Olfactory receptor 544 reduces adiposity by steering fuel preference toward fats. *J. Clin. Invest.* 127, 4118–4123. doi: 10.1172/JCI89344
- Wu, J., Boström, P., Sparks, L. M., Ye, L., Choi, J. H., Giang, A.-H., et al. (2012). Beige adipocytes are a distinct type of thermogenic fat cell in mouse and human. *Cell* 150, 366–376. doi: 10.1016/j.cell.2012.05.016
- Xie, X., Chen, W., Zhang, N., Yuan, M., Xu, C., Zheng, Z., et al. (2017). Selective tissue distribution mediates tissue-dependent PPAR $\gamma$  activation and insulin sensitization by INT131, a selective PPAR $\gamma$  modulator. *Front. Pharmacol.* 8:317. doi: 10.3389/fphar.2017.00317
- Xing, T., Kang, Y., Xu, X., Wang, B., Du, M., and Zhu, M.-J. (2018). Raspberry supplementation improves insulin signaling and promotes brown-like adipocyte development in white adipose tissue of obese mice. *Mol. Nutr. Food. Res.* 62. doi: 10.1002/mnfr.201701035
- Xue, B., Rim, J.-S., Hogan, J. C., Coulter, A. A., Koza, R. A., and Kozak, L. P. (2007). Genetic variability affects the development of brown adipocytes in white fat but not in interscapular brown fat. *J. Lipid Res.* 48, 41–51. doi: 10.1194/jlr.M600287-JLR200
- Xue, Y., Xu, X., Zhang, X.-Q., Farokhzad, O. C., and Langer, R. (2016). Preventing diet-induced obesity in mice by adipose tissue transformation and angiogenesis using targeted nanoparticles. *Proc. Natl. Acad. Sci. U.S.A.* 113, 5552–5557. doi: 10.1073/pnas.1603840113
- Yang, J. P., Anderson, A. E., McCartney, A., Ory, X., Ma, G., Pappalardo, E., et al. (2017). Metabolically active three-dimensional brown adipose tissue engineered from white adipose-derived stem cells. *Tissue Eng. Part A* 23, 253–262. doi: 10.1089/ten.TEA.2016.0399
- Yoneshiro, T., Aita, S., Kawai, Y., Iwanaga, T., and Saito, M. (2012). Nonpungent capsaicin analogs (capsinoids) increase energy expenditure through the activation of brown adipose tissue in humans. *Am. J. Clin. Nutr.* 95, 845–850. doi: 10.3945/ajcn.111.018606
- Yoneshiro, T., Aita, S., Matsushita, M., Kayahara, T., Kameya, T., Kawai, Y., et al. (2013). Recruited brown adipose tissue as an antiobesity agent in humans. *J. Clin. Invest.* 123, 3404–3408. doi: 10.1172/JCI67803
- Yoneshiro, T., Matsushita, M., Hibi, M., Tone, H., Takeshita, M., Yasunaga, K., et al. (2017). Tea catechin and caffeine activate brown adipose tissue and increase cold-induced thermogenic capacity in humans. *Am. J. Clin. Nutr.* 105, 873–881. doi: 10.3945/ajcn.116.144972
- Yuan, X., Hu, T., Zhao, H., Huang, Y., Ye, R., Lin, J., et al. (2016). Brown adipose tissue transplantation ameliorates polycystic ovary syndrome. *Proc. Natl. Acad. Sci. U.S.A.* 113, 2708–2713. doi: 10.1073/pnas.1523236113
- Zhang, F., Hao, G., Shao, M., Nham, K., An, Y., Wang, Q., et al. (2018). An adipose tissue atlas: an image-guided identification of human-like BAT and beige depots in rodents. *Cell Metab.* 27, 252.e3–262.e3. doi: 10.1016/j.cmet.2017.12.004
- Zhang, Y., Xu, Q., Liu, Y. H., Zhang, X. S., Wang, J., Yu, X. M., et al. (2015). Medium-chain triglyceride activated brown adipose tissue and induced

- reduction of fat mass in C57BL/6J mice fed high-fat diet. *Biomed. Environ. Sci.* 28, 97–104. doi: 10.3967/bes2015.012
- Zingaretti, M. C., Crosta, F., Vitali, A., Guerrieri, M., Frontini, A., Cannon, B., et al. (2009). The presence of UCP1 demonstrates that metabolically active adipose tissue in the neck of adult humans truly represents brown adipose tissue. *FASEB J.* 23, 3113–3120. doi: 10.1096/fj.09-133546
- Zou, T., Wang, B., Yang, Q., de Avila, J. M., Zhu, M.-J., You, J., et al. (2018). Raspberry promotes brown and beige adipocyte development in mice fed high-fat diet through activation of AMP-activated protein kinase (AMPK)  $\alpha 1$ . *J. Nutr. Biochem.* 55, 157–164. doi: 10.1016/j.jnutbio.2018.02.005
- Zu, Y., Overby, H., Ren, G., Fan, Z., Zhao, L., and Wang, S. (2017). Resveratrol liposomes and lipid nanocarriers: comparison of characteristics and inducing browning of white adipocytes. *Colloids Surf. B Biointerfaces* 164, 414–423. doi: 10.1016/j.colsurfb.2017.12.044
- Zuriaga, M. A., Fuster, J. J., Gokce, N., and Walsh, K. (2017). Humans and mice display opposing patterns of “browning” gene expression in visceral and subcutaneous white adipose tissue depots. *Front. Cardiovasc. Med.* 4:27. doi: 10.3389/fcvm.2017.00027

**Conflict of Interest Statement:** The authors declare that the research was conducted in the absence of any commercial or financial relationships that could be construed as a potential conflict of interest.

Copyright © 2019 Srivastava and Veech. This is an open-access article distributed under the terms of the Creative Commons Attribution License (CC BY). The use, distribution or reproduction in other forums is permitted, provided the original author(s) and the copyright owner(s) are credited and that the original publication in this journal is cited, in accordance with accepted academic practice. No use, distribution or reproduction is permitted which does not comply with these terms.



# Neuregulin 4 Is a Novel Marker of Beige Adipocyte Precursor Cells in Human Adipose Tissue

Ferran Comas<sup>1,2†</sup>, Cristina Martínez<sup>1†</sup>, Mònica Sabater<sup>1,2</sup>, Francisco Ortega<sup>1,2</sup>, Jessica Latorre<sup>1,2</sup>, Francisco Díaz-Sáez<sup>3,4</sup>, Julian Aragonés<sup>5,6</sup>, Marta Camps<sup>3,4</sup>, Anna Gumà<sup>3,4</sup>, Wifredo Ricart<sup>1,2,7</sup>, José Manuel Fernández-Real<sup>1,2,7</sup> and José María Moreno-Navarrete<sup>1,2,7\*</sup>

<sup>1</sup> Department of Diabetes, Endocrinology and Nutrition, Institut d'Investigació Biomèdica de Girona, Girona, Spain, <sup>2</sup> CIBEROBN (CB06/03/010), Instituto de Salud Carlos III, Madrid, Spain, <sup>3</sup> Department of Biochemistry and Molecular Biomedicine, Faculty of Biology, Institute of Biomedicine of the University of Barcelona, Barcelona, Spain, <sup>4</sup> CIBER de Diabetes y Enfermedades Metabólicas Asociadas, Instituto de Salud Carlos III, Madrid, Spain, <sup>5</sup> Research Unit, Hospital of Santa Cristina, Research Institute Princesa, Autonomous University of Madrid, Madrid, Spain, <sup>6</sup> CIBER de Enfermedades Cardiovasculares, Carlos III Health Institute, Madrid, Spain, <sup>7</sup> Department of Medicine, University of Girona, Girona, Spain

## OPEN ACCESS

### Edited by:

Paula Oliver,  
Universidad de les Illes Balears, Spain

### Reviewed by:

Rushita Bagchi,  
University of Colorado Denver,  
United States  
Yongguo Li,  
Technische Universität München,  
Germany

### \*Correspondence:

José María Moreno-Navarrete  
jmoreno@idibgi.org

<sup>†</sup>These authors have contributed  
equally to this work

### Specialty section:

This article was submitted to  
Integrative Physiology,  
a section of the journal  
Frontiers in Physiology

**Received:** 17 August 2018

**Accepted:** 14 January 2019

**Published:** 31 January 2019

### Citation:

Comas F, Martínez C, Sabater M, Ortega F, Latorre J, Díaz-Sáez F, Aragonés J, Camps M, Gumà A, Ricart W, Fernández-Real JM and Moreno-Navarrete JM (2019) Neuregulin 4 Is a Novel Marker of Beige Adipocyte Precursor Cells in Human Adipose Tissue. *Front. Physiol.* 10:39. doi: 10.3389/fphys.2019.00039

**Background:** Nrg4 expression has been linked to brown adipose tissue activity and browning of white adipocytes in mice. Here, we aimed to investigate whether these observations could be translated to humans by investigating *NRG4* mRNA and markers of brown/beige adipocytes in human visceral (VAT) and subcutaneous adipose tissue (SAT). We also studied the possible association of *NRG4* with insulin action.

**Methods:** SAT and VAT *NRG4* and markers of brown/beige (*UCP1*, *UCP3*, and *TMEM26*)-related gene expression were analyzed in two independent cohorts ( $n = 331$  and  $n = 59$ ). Insulin resistance/sensitivity was measured using HOMA<sub>IR</sub> and glucose infusion rate during euglycemic hyperinsulinemic clamp.

**Results:** In both cohort 1 and cohort 2, *NRG4* and thermogenic/beige-related gene expression were significantly increased in VAT compared to SAT. Adipogenic-related genes followed an opposite pattern. In cohort 1, VAT *NRG4* gene expression was positively correlated with BMI and expression of *UCP1*, *UCP3*, *TMEM26*, and negatively with adipogenic (*FASN*, *PPARG*, and *SLC2A4*)- and inflammatory (*IL6* and *IL8*)-related genes. In SAT, *NRG4* gene expression was negatively correlated with HOMA<sub>IR</sub> and positively with *UCP1* and *TMEM26* gene expression. Multiple linear regression analysis revealed that expression of *TMEM26* gene was the best predictor of *NRG4* gene expression in both VAT and SAT. Specifically, *NRG4* and *TMEM26* gene expression was significantly increased in VAT, but not in SAT stromal vascular fraction cells ( $p < 0.001$ ). In cohort 2, the significant association between *NRG4* and *TMEM26* gene expression in both VAT and SAT was confirmed, and SAT *NRG4* gene expression also was positively correlated with insulin action and the expression of *UCP1*.

**Conclusion:** Current findings suggest *NRG4* gene expression as a novel marker of beige adipocytes in human adipose tissue.

**Keywords:** obesity, neuregulin 4, browning, adipose tissue, insulin sensitivity



## INTRODUCTION

The modulation of brown adipose tissue activity and browning of white adipose tissue has been proposed as a promising therapeutic strategy in the treatment of obesity-associated metabolic disturbances (Wu et al., 2012; Bartelt and Heeren, 2014; Hepler et al., 2017; Rabhi et al., 2018; Zhang S. et al., 2018), with the intention of improving insulin sensitivity (Hepler et al., 2017; Rabhi et al., 2018) and hepatic steatosis (Huang et al., 2017), among others.

Several studies pointed to neuregulins as an important family of ligands that regulate diverse aspects of glucose and lipid metabolism and energy balance. In skeletal muscle cells, recombinant neuregulin administration stimulated glucose uptake in muscle cells (Suárez et al., 2001) in an alternative insulin-independent mechanism, activating PI3K, PDK1, and PKC $\zeta$  pathways (Cantó et al., 2004), and promoted glucose and palmitate oxidation, enhancing mitochondrial oxidative capacity (Cantó et al., 2007). In liver, neuregulin 1 (Nrg1) and neuregulin 4 (Nrg4) reduced gluconeogenesis and lipogenesis and increased fatty acid oxidation, improving systemic insulin sensitivity and glucose tolerance (Wang et al., 2014; Ennequin et al., 2015; Ma et al., 2016; Chen et al., 2017; Zhang P. et al., 2018). In fact, the Nrg4/ErbB4 signaling pathway protects hepatocytes from stress-induced cell death, preventing the steatosis to steatohepatitis progression (Guo et al., 2017). In human breast cancer cells, NRG1 binding to ERBB4 activates SREBP-2 and led to increased expression of LDL uptake- and cholesterol biosynthesis-related genes (Haskins et al., 2015). A recent study demonstrated that ErbB4 deletion accelerated the development of obesity, dyslipidemia, hepatic steatosis, hyperglycemia, hyperinsulinemia and insulin resistance after 24 week on a medium-fat diet (Zeng et al., 2018). Nrg4, a specific ligand for ErbB4 involved in neurite growth, administration in 3T3-L1 adipocytes inhibited lipogenesis and induced browning and glucose uptake, but did not exert any effects on adipogenesis and lipolysis (Zeng et al., 2018). In fact, Nrg4 has been proposed as a marker of brown adipose tissue (BAT) activity in mice, being highly expressed in cold-induced BAT activity and white adipose tissue (WAT) browning (Rosell et al., 2014; Wang et al., 2014). NRG4 was expressed in fully differentiated brown adipocytes, but not in preadipocytes, and increased during brown adipocyte differentiation (Rosell et al., 2014; Wang et al., 2014). *In vitro* experiments showed that brown adipocytes-derived NRG4 might promote the growth of neurites in adipose tissue, increasing sympathetic innervation, enhancing BAT activity and browning of WAT (Rosell et al., 2014). However, Wang et al. (2014) reported that despite the abundant expression of Nrg4 in BAT, it seems dispensable for cold-induced hypothermia response, being Ucp1 and Dio2 induced to similar extent by cold exposure in WT and NRG4KO mice. These findings indicated that Nrg4 did not directly participate in BAT thermogenesis.

Diet-induced obesity led to a significant decreased Nrg4 gene expression in WAT but not BAT (Wang et al., 2014; Ma et al., 2016; Chen et al., 2017) in mice. A recent study also showed that diet-induced non-alcoholic steatohepatitis (NASH) resulted in a significant reduced Nrg4 in both BAT and WAT

(Guo et al., 2017). These studies suggested that adipose tissue-derived Nrg4 could exert positive effects on obesity associated metabolic disturbances (Wang et al., 2014; Ma et al., 2016; Chen et al., 2017; Guo et al., 2017), improving glucose tolerance and insulin sensitivity and attenuating adipose tissue and liver inflammation (Wang et al., 2014; Ma et al., 2016; Chen et al., 2017; Guo et al., 2017).

In humans, only one study investigates *NRG4* mRNA levels in adipose tissue in association with body fat mass, liver lipid content and glucose tolerance (Wang et al., 2014), but no previous studies investigated the relationship between NRG4 and markers of adipose tissue browning in human adipose tissue. Since previous mice studies demonstrated that NRG4 was a marker of BAT activity and browning of WAT (Rosell et al., 2014; Wang et al., 2014; Ma et al., 2016; Chen et al., 2017), in the present study we aimed to investigate the potential relationship between human adipose tissue NRG4 and markers of brown/beige adipocytes. Furthermore, the impact of adipose tissue NRG4 on human obesity and insulin sensitivity was also evaluated.

## MATERIALS AND METHODS

### Human Adipose Tissue Samples

In cohort 1, a group of 331 [155 visceral (VAT) and 176 subcutaneous (SAT) adipose tissues] (Cohort 1) from participants with normal body weight and different degrees of obesity, with body mass index (BMI) within 20 and 68 kg/m<sup>2</sup>, were analyzed. In a second cohort of morbidly obese (BMI > 35 kg/m<sup>2</sup>) subjects with different degrees of insulin action [measured using hyperinsulinemic-euglycemic clamp (Moreno-Navarrete et al., 2013)], VAT ( $n = 34$ ) and SAT ( $n = 25$ ) samples (Cohort 2) were studied. Altogether these subjects were recruited at the Endocrinology Service of the Hospital of Girona “Dr Josep Trueta.” All subjects were of Caucasian origin and reported that their body weight had been stable for at least 3 months before the study. Subjects were studied in the post-absorptive state. BMI was calculated as weight (in kg) divided by height (in m) squared. They had no systemic disease other than obesity and all were free of any infections in the previous month before the study. Liver diseases (specifically tumoral disease and HCV infection) and thyroid dysfunction were specifically excluded by biochemical work-up. Samples and data from patients included in this study were partially provided by the *FATBANK* platform promoted by the *CIBEROBN* and coordinated by the *IDIBGI Biobank* (Biobank *IDIBGI*, B.0000872), integrated in the Spanish National Biobanks Network and they were processed following standard operating procedures with the appropriate approval of the Ethics, External Scientific and *FATBANK* Internal Scientific Committees.

### Ethics Statement

This study was carried out in accordance with the recommendations of the ethical committee of the Hospital of Girona “Dr Josep Trueta.” The protocol was approved by the ethical committee of the Hospital of Girona “Dr Josep Trueta.”

All subjects gave written informed consent in accordance with the Declaration of Helsinki, after the purpose of the study was explained to them.

AT samples were obtained from SAT and VAT depots during elective surgical procedures (cholecystectomy, surgery of abdominal hernia and gastric bypass surgery). Adipose tissue samples were washed, fragmented and immediately flash-frozen in liquid nitrogen before being stored at  $-80^{\circ}\text{C}$ .

The isolation of adipocyte and stromal vascular fraction cells (SVF) was performed from 17 SAT and 20 VAT non-frozen adipose tissue samples. These samples were washed three to four times with phosphate-buffered saline (PBS) and suspended in an equal volume of PBS supplemented with 1% penicillin-streptomycin and 0.1% collagenase type I prewarmed to  $37^{\circ}\text{C}$ . The tissue was placed in a shaking water bath at  $37^{\circ}\text{C}$  with continuous agitation for 60 min and centrifuged for 5 min at 400 g at room temperature. The supernatant, containing mature adipocytes, was recollected. The pellet was identified as the SVF. Isolated mature adipocytes and SVF stored at  $-80^{\circ}\text{C}$  for gene expression analysis.

## Analytical Methods

Serum glucose concentrations were measured in duplicate by the glucose oxidase method using a Beckman glucose analyser II (Beckman Instruments, Brea, CA, United States). Intraassay and interassay coefficients of variation were less than 4% for all these tests. HDL cholesterol was quantified by a homogeneous enzymatic colorimetric assay through the cholesterol esterase/cholesterol oxidase/peroxidase reaction (Cobas HDLC3). Total serum triglycerides were measured by an enzymatic, colorimetric method with glycerol phosphate oxidase and peroxidase (Cobas TRIGL). We used a Roche Hitachi Cobas c 711 instrument to perform the determinations.

## RNA Expression

RNA purification was performed using the RNeasy Lipid Tissue Mini Kit (QIAGEN, Izasa SA, Barcelona, Spain) and the integrity was checked by the Agilent Bioanalyzer (Agilent Technologies, Palo Alto, CA, United States). Gene expression was assessed by real time PCR using a LightCycler<sup>®</sup> 480 Real-Time PCR System (Roche Diagnostics SL, Barcelona, Spain), using TaqMan<sup>®</sup> and SYBR green technology suitable for relative genetic expression quantification. The RT-PCR reaction was performed in a final volume of 12  $\mu\text{l}$ . The cycle program consisted of an initial denaturing of 10 min at  $95^{\circ}\text{C}$  then 40 cycles of 15 s denaturing phase at  $95^{\circ}\text{C}$  and 1 min annealing and extension phase at  $60^{\circ}\text{C}$ . A threshold cycle (Ct value) was obtained for each amplification curve and a  $\Delta\text{Ct}$  value was first calculated by subtracting the Ct value for human cyclophilin A (*PPIA*) RNA from the Ct value for each sample. Fold changes compared with the endogenous control were then determined by calculating  $2^{-\Delta\text{Ct}}$ , so that gene expression results are expressed as expression ratio relative to *PPIA* gene expression according to the manufacturer's guidelines. *PPIA* Ct values in both SAT and VAT were comparable ( $23.48 \pm 0.81$  in SAT vs.  $23.49 \pm 1.28$  in VAT,  $p = 0.9$ ,  $n = 152$ ). Primer/probe sets used were: neuregulin 4 (*NRG4*, Hs00163592\_m1), fatty acid synthase (*FASN*, Hs00188012\_m1),

peroxisome proliferator-activated receptor gamma (*PPARG*, Hs00234592\_m1), solute carrier family 2 (facilitated glucose transporter), member 4 (*SLC2A4* or *GLUT4*, Hs00168966\_m1), perilipin 1 (*PLIN1*, Hs00160173\_m1), *PPARG* coactivator 1 alpha (*PPARGC1A*, Hs00173304\_m1), uncoupling protein 1 (*UCP1*, Hs01084772\_m1), uncoupling protein 3 (*UCP3*, Hs01106052\_m1), transmembrane protein 26 (*TMEM26*, Hs00415619\_m1), interleukin 6 (*IL6*, Hs00174131\_m1), C-X-C motif chemokine ligand 8 (*CXCL8* or also named *IL8*, Hs00174103\_m1), and peptidylprolyl isomerase A (cyclophilin A) (4333763, *PPIA* as endogenous control).

## Statistical Analyses

Statistical analyses were performed using the SPSS 12.0 software. Unless otherwise stated, descriptive results of continuous variables are expressed as mean and SD for Gaussian variables or median and interquartile range for non-Gaussian variables. Parameters that did not fulfill normal distribution criteria were log transformed to improve symmetry for subsequent analyses. The relation between variables was analyzed by simple correlation (using Spearman's and Pearson's tests) and multiple linear regression analyses. ANOVA and unpaired Student's *t*-tests were used to compare clinical variables and gene expression relative to obesity and type 2 diabetes (T2D).

## RESULTS

Representative Ct values of analyzed genes were shown in **Table 1**.

### Cohort 1

Anthropometric and clinical data from cohort 1 were detailed in **Table 2**. Similar to thermogenic/beige-related gene expression, *NRG4* was significantly increased in VAT compared to SAT, whereas adipogenesis-related genes followed an opposite gene expression pattern (**Figure 1A**). In cohort 1, VAT *NRG4* gene expression was significantly increased in participants with obesity (**Table 2**), but no significant differences were found between non-diabetic obese and obese participants with T2D (**Table 2**).

**TABLE 1** | Representative Ct values of analyzed genes.

	Mean $\pm$ SD
<i>PPIA</i>	23.22 $\pm$ 0.25
<i>FASN</i>	25.91 $\pm$ 1.83
<i>PPARG</i>	29.49 $\pm$ 0.85
<i>SLC2A4</i>	27.71 $\pm$ 0.53
<i>PLIN1</i>	22.78 $\pm$ 0.49
<i>PPARGC1A</i>	30.86 $\pm$ 0.71
<i>UCP1</i>	36.82 $\pm$ 0.91
<i>UCP3</i>	34.11 $\pm$ 0.65
<i>TMEM26</i>	34.16 $\pm$ 0.95
<i>IL6</i>	31.81 $\pm$ 2.28
<i>IL8</i>	30.89 $\pm$ 1.92
<i>NRG4</i>	35.57 $\pm$ 0.99

**TABLE 2 |** Anthropometric and clinical characteristics according to obesity and T2D in cohort 1.

	Non-obese	Obese	Obese + T2D	<i>p</i>
N	54	88	34	
Age (years)	47.4 ± 10.1	45.6 ± 10.5	47.2 ± 9.5	0.5
BMI (kg/m <sup>2</sup> )	25.4 ± 3.8	43.9 ± 7.4*	44.7 ± 4.1*	<b>&lt;0.0001</b>
Fasting glucose (mg/dl) <sup>a</sup>	86 (80–94)	93 (84–100.5)	126 (93.5–169.5)*#	<b>&lt;0.0001</b>
HOMA <sub>IR</sub> ( <i>n</i> = 56) <sup>a</sup>	1.18 (0.79–1.76)	2.06 (1.44–3.39)	5.59 (3.93–7.05)*#	<b>0.001</b>
Total-cholesterol (mg/dl) <sup>a</sup>	199 (174–219)	193 (167.5–218.7)	182 (166–214)	0.5
HDL-cholesterol (mg/dl) <sup>a</sup>	64.5 (50.7–77.5)	55 (45.5–62.6)	50.1 (42–62)*	<b>0.04</b>
LDL-cholesterol (mg/dl) <sup>a</sup>	114.5 (88.7–135.5)	116.8 (97.5–134.7)	101.5 (89.5–137.7)	0.5
Fasting triglycerides (mg/dl) <sup>a</sup>	79.5 (57.7–101.2)	98 (75–132)	136 (89.5–164.5)*#	<b>&lt;0.0001</b>
VAT <i>NRG4</i> (RU) × 10 <sup>−3a</sup>	1.26 (0.217–4.11)	3.59 (2.24–5.56)*	4.58 (2.54–6.52)*	<b>0.001</b>
SAT <i>NRG4</i> (RU) × 10 <sup>−3a</sup>	0.141 (0.061–0.239)	0.168 (0.095–0.381)	0.083 (0.057–0.155)	0.2

VAT, visceral adipose tissue; SAT, subcutaneous adipose tissue; T2D, type 2 diabetes; HOMA<sub>IR</sub>, homeostasis model assessment – insulin resistance index; RU, relative gene expression units.

<sup>a</sup>Median and interquartile range.

\**p* < 0.05 compared to non-obese participants after performing Bonferroni post hoc test.

#*p* < 0.05 compared to obese participants after performing Bonferroni post hoc test.

Bold values mean that *p*-value reached statistical significance.

No significant differences were observed on SAT *NRG4* gene expression according to obesity or T2D. In VAT, *NRG4* gene expression was positively correlated with BMI, and negatively correlated with adipogenic-related genes (*FASN*, *PPARG*, and *SLC2A4*) (**Table 3**). Interestingly, *NRG4* gene expression was significantly positively associated with expression of brown/beige adipocyte activity-related (*UCP1*, *UCP3*, and *TMEM26*) and negatively with inflammatory-related (*IL6* and *IL8*) genes (**Table 3** and **Figure 2A**). In SAT, *NRG4* gene expression was negatively correlated with HOMA<sub>IR</sub> and positively with *UCP1* and *TMEM26* gene expression (**Table 3** and **Figure 2B**).

In multiple linear regression analysis, *TMEM26* ( $\beta = 0.58$ ,  $p < 0.0001$ ; model adjusted  $R^2 = 0.37$ ,  $p < 0.0001$ ), *UCP3* ( $\beta = 0.24$ ,  $p = 0.03$ ; model adjusted  $R^2 = 0.13$ ,  $p = 0.001$ ), *IL6* ( $\beta = -0.32$ ,  $p = 0.01$ ; model adjusted  $R^2 = 0.16$ ,  $p = 0.001$ ), *IL8* ( $\beta = -0.36$ ,  $p = 0.008$ ; model adjusted  $R^2 = 0.17$ ,  $p < 0.0001$ ), *FASN* ( $\beta = -0.42$ ,  $p = 0.001$ , model adjusted  $R^2 = 0.12$ ,  $p = 0.001$ ) and *PPARG* ( $\beta = -0.38$ ,  $p = 0.005$ ; model adjusted  $R^2 = 0.11$ ,  $p = 0.008$ ) significantly contributed to the variance of *NRG4* gene expression in VAT after controlling for BMI. In SAT, *TMEM26* ( $\beta = 0.77$ ,  $p < 0.0001$ ; model adjusted  $R^2 = 0.61$ ,  $p < 0.0001$ ) significantly contributed to the variance of *NRG4* gene expression after controlling for BMI. Multiple linear regression analysis revealed that expression of *TMEM26* gene was the best predictor of *NRG4* gene expression in both VAT and SAT.

In addition, correlations between *UCP1*, a specific marker of brown adipocytes, and clinical and metabolic parameters were also explored. No significant correlation between SAT or VAT *UCP1* gene expression and BMI, fasting glucose, HOMA<sub>IR</sub>, total-, LDL- and HDL-cholesterol, and fasting triglycerides were observed. VAT, but not SAT, *UCP1* was positively correlated with *SLC2A4* ( $r = 0.43$ ,  $p < 0.0001$ ), *PPARGC1A* ( $r = 0.36$ ,  $p = 0.001$ ) and *UCP3* ( $r = 0.31$ ,  $p = 0.005$ ) gene expression.

In adipose tissue fractions, *NRG4* and *TMEM26*, but not *UCP1*, gene expression was significantly increased in visceral SVFs compared to visceral adipocytes, subcutaneous SVFs and subcutaneous adipocytes (**Figure 2C**).

## Cohort 2

To examine the findings replication of cohort 1 excluding the effects of obesity, an independent cohort (cohort 2) composed of morbidly subjects with different degrees of insulin action has been analyzed. Anthropometric and clinical data from cohort 2 were detailed in **Table 4**. Similar to cohort 1, *NRG4* and thermogenic/beige-related gene expression was increased in VAT (**Figure 1B**). No significant differences on SAT or VAT *NRG4* gene expression according to glucose tolerance or T2D were found. VAT *NRG4* gene expression were associated with expression of *TMEM26* gene (**Table 5**), and SAT *NRG4* with insulin sensitivity (M) and expression of *SLC2A4*, *UCP1* and *TMEM26* genes (**Table 5**).

## DISCUSSION

To the best of our knowledge, this is the first study showing a significant relationship between *NRG4* and *TMEM26* gene expression in human adipose tissue. Interestingly, this association was found in both VAT and SAT, and validated in a second independent cohort. *TMEM26* has been described as a specific marker of brite/beige adipocytes (Wu et al., 2012; Torriani et al., 2016; Finlin et al., 2017). We also found positive associations among *NRG4* and markers of thermogenic activity (characteristic of both brown and beige adipocytes) such as expression of *UCP1* and *UCP3* genes. In addition, VAT *NRG4* gene expression was negatively correlated with expression of white lipogenic/adipogenic (*FASN* and *PPARG*)- and inflammatory (*IL6* and *IL8*)-related genes, even after controlling for BMI. Since beige adipocytes have less lipogenic capacity compared to white adipocytes (Aziz et al., 2017; Zuriaga et al., 2017), and browning/beiging of adipose tissue protected against visceral adipose tissue inflammation (Wu et al., 2017; Gonzalez-Hurtado et al., 2018), the negative association between *NRG4* and white adipogenic/inflammatory genes reinforced *NRG4* as a marker of beige adipocytes. In fact, these correlations were only observed

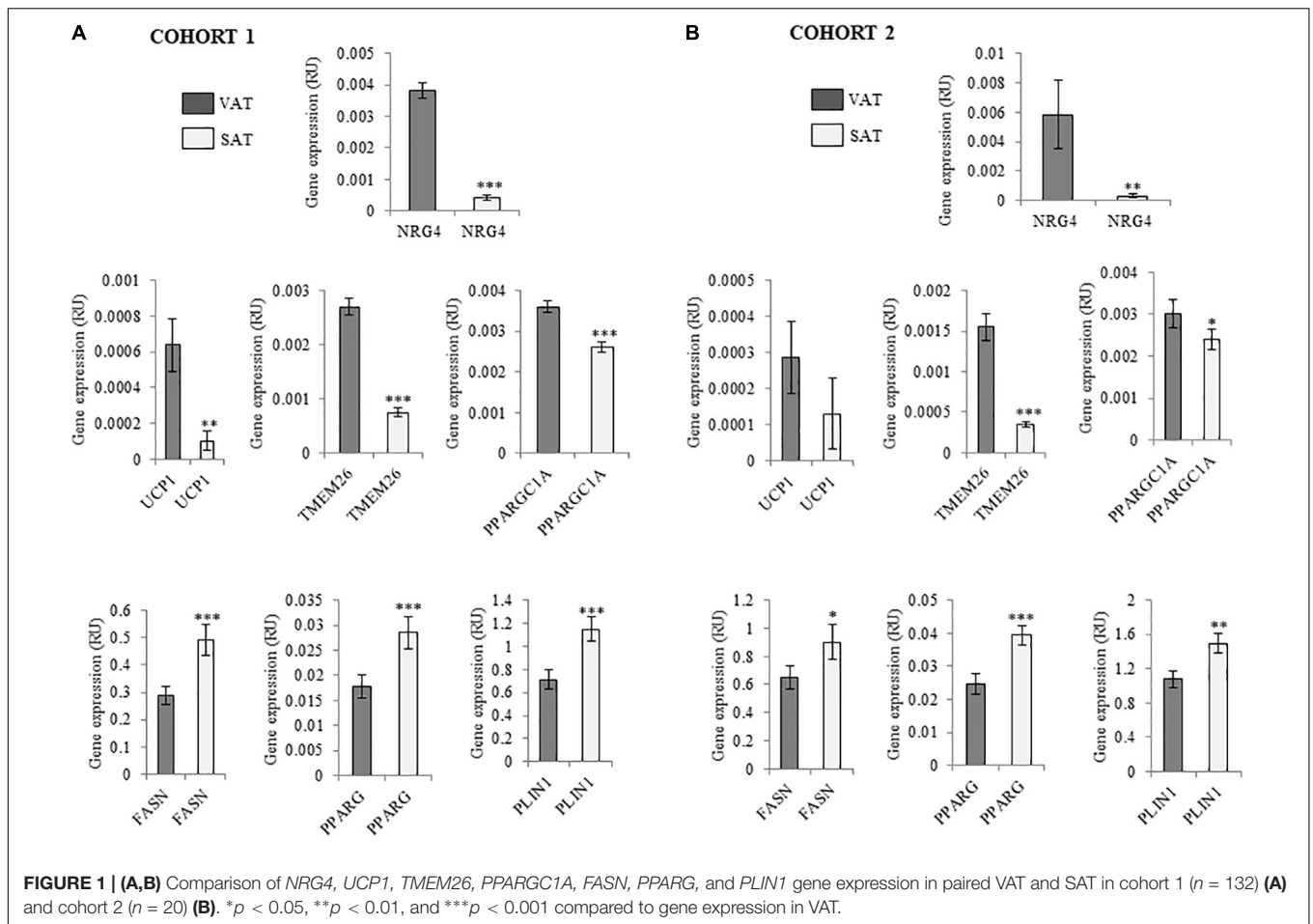


**TABLE 3 |** Correlation between *NRG4* gene expression and anthropometric and clinical characteristics and selected gene expression in SAT ( $n = 176$ ) and VAT ( $n = 155$ ) from cohort 1.

	VAT		SAT	
	<i>r</i>	<i>P</i>	<i>r</i>	<i>P</i>
Age (years)	-0.02	0.7	0.11	0.2
BMI (kg/m <sup>2</sup> )	0.28	<b>&lt;0.0001</b>	0.06	0.5
Fasting glucose (mg/dl)	0.17	<b>0.03</b>	0.01	0.8
HOMA <sub>IR</sub> ( $n = 56$ )	0.17	0.3	-0.32	<b>0.02</b>
Total cholesterol (mg/dl)	-0.10	0.2	0.11	0.2
HDL cholesterol (mg/dl)	-0.01	0.9	0.15	0.1
LDL cholesterol (mg/dl)	-0.09	0.3	0.08	0.4
Fasting triglycerides (mg/dl)	0.05	0.5	-0.09	0.3
<i>FASN</i> (RU)	-0.37	<b>&lt;0.0001</b>	-0.05	0.6
<i>PPARG</i> (RU)	-0.39	<b>&lt;0.0001</b>	0.05	0.6
<i>SLC2A4</i> (RU)	-0.33	<b>0.002</b>	0.12	0.2
<i>PLIN1</i> (RU)	-0.15	0.1	-0.10	0.4
<i>PPARGC1A</i> (RU)	0.06	0.5	0.18	0.05
<i>UCP1</i> (RU)	0.30	<b>0.005</b>	0.30	<b>0.001</b>
<i>UCP3</i> (RU)	0.29	<b>0.005</b>	0.13	0.1
<i>TMEM26</i> (RU)	0.77	<b>&lt;0.0001</b>	0.56	<b>&lt;0.0001</b>
<i>IL6</i> (RU)	-0.45	<b>&lt;0.0001</b>	0.06	0.5
<i>IL8</i> (RU)	-0.36	<b>0.001</b>	-0.05	0.6

Bold values mean that *p*-value reached statistical significance.



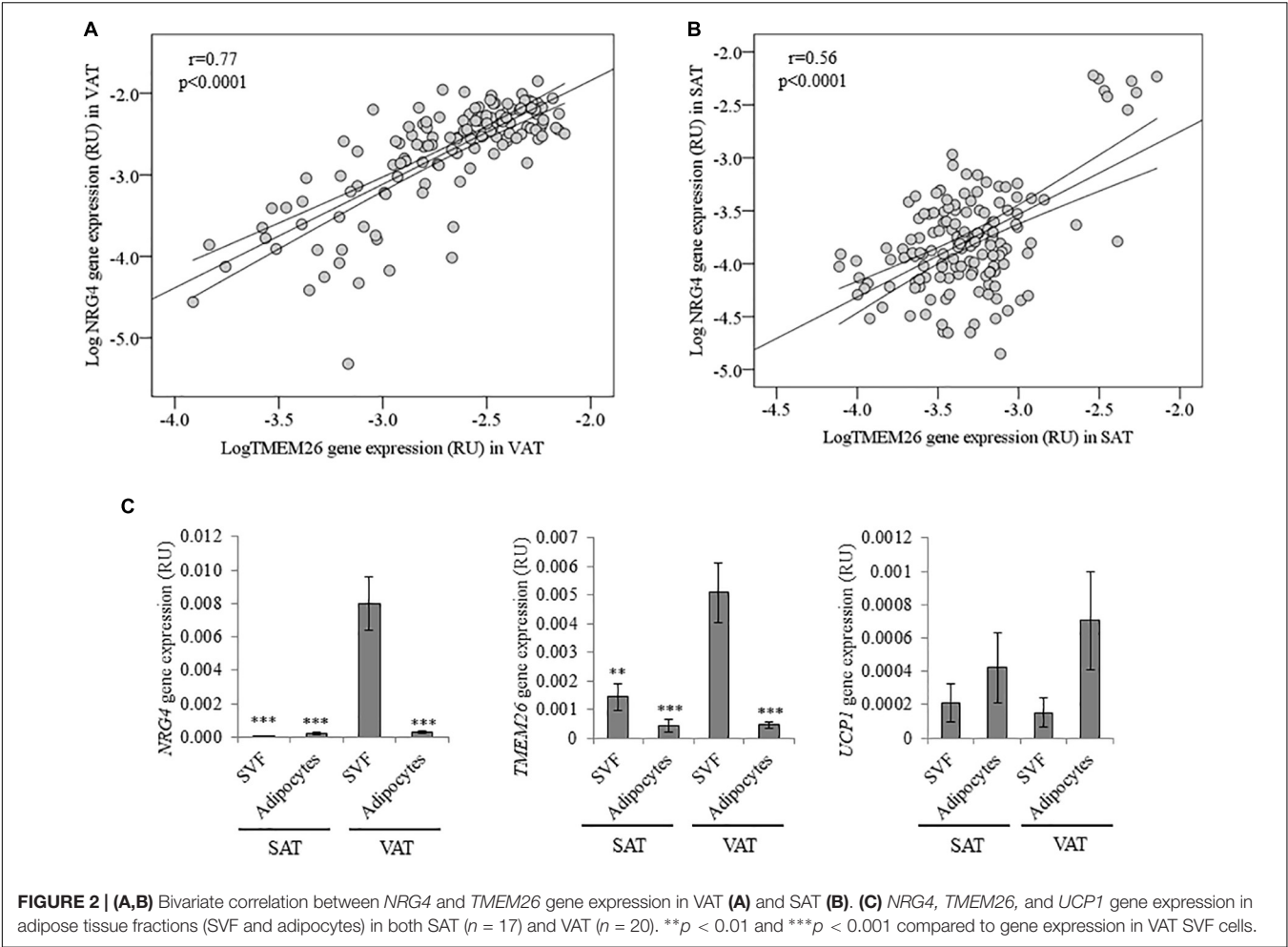


**TABLE 4 |** Anthropometric and clinical characteristics according to glucose tolerance in cohort 2.

	NGT	IGT	T2D	<i>p</i>
	11	10	13	
Age (years)	41.6 ± 4.1	50 ± 8.5*	51.5 ± 7.5*	<b>0.004</b>
BMI (kg/m <sup>2</sup> )	46.3 ± 8.7	47.8 ± 3.2	44.7 ± 8.1	0.6
Fasting glucose (mg/dl) <sup>a</sup>	90 (83–98)	102.5 (96–107)	121 (100.5–132)*	<b>0.003</b>
M [mg/(kg.min)] <sup>a</sup>	4.35 (2.21–6.28)	3.41 (1.92–5.21)	2.79 (1.68–4.31)	0.6
Total-cholesterol (mg/dl) <sup>a</sup>	182 (163–221)	207 (184.5–252)	179 (162–209)	0.07
HDL-cholesterol (mg/dl) <sup>a</sup>	49 (40–58)	45 (34.5–55.5)	46 (40.5–49.5)	0.5
LDL-cholesterol (mg/dl) <sup>a</sup>	105 (95–129)	147 (110.7–176.2)	108 (84.5–133)	<b>0.03</b>
Fasting triglycerides (mg/dl) <sup>a</sup>	99 (68–134)	141.5 (66.7–190.7)	139 (87.5–183)	0.4
VAT <i>NRG4</i> (RU) × 10 <sup>−3a</sup>	4.04 (1.11–6.08)	2.97 (0.141–5.92)	3.37 (2.14–6.17)	0.4
SAT <i>NRG4</i> (RU) × 10 <sup>−3a</sup>	0.172 (0.072–0.287)	0.099 (0.081–0.129)	0.131 (0.039–0.182)	0.4

VAT, visceral adipose tissue; SAT, subcutaneous adipose tissue; NGT, normal glucose tolerance; IGT, impaired glucose tolerance; T2D, type 2 diabetes; M, insulin sensitivity obtained from hyperinsulinemic-euglycemic clamp; RU, relative gene expression units.

<sup>a</sup>Median and interquartile range.

\* $p < 0.05$  compared to NGT participants after performing Bonferroni post hoc test.

Bold values mean that  $p$ -value reached statistical significance.

in the samples with the highest correlation between *NRG4* and *TMEM26* ( $r = 0.77$ ,  $p < 0.0001$ ). However, the correlations between VAT *NRG4* and *UCP1*, *UCP3*, lipogenic/adipogenic -

and inflammatory-related gene expression were not replicated in morbidly obese participants (cohort 2). Further studies in human adipose tissue should be required to validate these correlations.

**TABLE 5 |** Correlation between *NRG4* gene expression and anthropometric and clinical characteristics and selected gene expression in SAT (*n* = 25) and VAT (*n* = 34) from cohort 2.

	VAT		SAT	
	<i>r</i>	<i>p</i>	<i>r</i>	<i>p</i>
Age (years)	−0.07	0.7	−0.17	0.4
BMI (kg/m <sup>2</sup> )	0.06	0.7	−0.08	0.7
Fasting glucose (mg/dl)	0.13	0.4	−0.21	0.3
M [mg/(kg.min)]	−0.03	0.9	0.43	<b>0.04</b>
Total cholesterol (mg/dl)	−0.23	0.2	−0.22	0.3
HDL cholesterol (mg/dl)	0.07	0.7	0.11	0.5
LDL cholesterol (mg/dl)	−0.07	0.7	−0.27	0.2
Fasting triglycerides (mg/dl)	−0.14	0.4	−0.14	0.5
<i>FASN</i> (RU)	0.05	0.8	0.13	0.6
<i>PPARG</i> (RU)	−0.09	0.6	0.17	0.4
<i>SLC2A4</i> (RU)	−0.09	0.6	0.49	<b>0.01</b>
<i>PLIN1</i> (RU)	0.04	0.8	−0.15	0.5
<i>PPARGC1A</i> (RU)	0.37	0.1	0.04	0.8
<i>UCP1</i> (RU)	0.29	0.1	0.43	<b>0.04</b>
<i>UCP3</i> (RU)	0.13	0.6	0.03	0.8
<i>TMEM26</i> (RU)	0.56	<b>0.002</b>	0.51	<b>0.01</b>
<i>IL6</i> (RU)	0.03	0.9	−0.10	0.6

Bold values mean that *p*-value reached statistical significance.

Furthermore, in both cohort 1 and 2, similar to beige adipocytes-related genes (*TMEM26*), *NRG4* gene expression was significantly more expressed in VAT, whereas, as expected adipogenic-related genes were more expressed in SAT (Sauma et al., 2007; Moreno-Navarrete et al., 2016; Zuriaga et al., 2017). Contrary to mice, increased pattern of browning gene expression in human VAT compared to SAT has been reported (Zuriaga et al., 2017). Interestingly, *NRG4* and *TMEM26* gene expression was enriched in SVFs from VAT compared to SVFs from SAT or adipocytes from VAT or SAT. This finding points to a specific population of beige precursor cells in VAT, characterized by increased *NRG4* and *TMEM26* gene expression, and could explain the increased expression of beige/browning-related genes observed in this fat depot (current data and Zuriaga et al., 2017). Reinforcing this idea, previous studies demonstrated that *TMEM26* gene expression was also increased in SVF and decreased in the late stages of beige adipocyte differentiation, and indicated its abundance in the precursors of beige adipocytes (Lee et al., 2015; Garcia et al., 2016).

Altogether these findings indicated *NRG4* as an additional marker of beige adipocytes in human adipose tissue, and suggested a possible role of this factor in the development of beige adipocytes in human fat depots. Supporting this hypothesis, Rosell et al. (2014) suggested that *NRG4* might promote the growth of neurites in adipose tissue, increasing sympathetic innervation and in consequence, enhancing browning of WAT. Regarding the possible role of *NRG4* on thermogenic activity, Wang et al. (2014) demonstrated in *Nrg4* deficient mice that *Nrg4* did not directly participate in BAT thermogenesis, but Ma et al. (2016) showed that *Nrg4* overexpression enhanced BAT activity with an increase of ~1°C body temperature, and BAT and iWAT thermogenic gene expression. These studies supported a possible role of *NRG4* in beige of human adipose tissue, but

contradictory data in relation to its thermogenic activity. Further functional studies in human adipose tissue should be required to confirm the possible role of *NRG4* in this process.

Another interesting finding of current study was the positive association between SAT *NRG4* gene expression and insulin sensitivity. In a previous study, SAT and VAT *NRG4* was significantly decreased in patients with impaired glucose tolerance (IGT) and T2D (Wang et al., 2014), but this study did not evaluate insulin sensitivity. Even tough, no significant differences were found in relation to IGT or T2D, probably due to the relatively low number of adipose tissue samples compared to the previous study (*n* = 642) (Wang et al., 2014). The current study showed a positive association between SAT *NRG4* and insulin sensitivity in both cohort 1 and cohort 2, evaluated by two different methods (HOMA<sub>IR</sub> in cohort 1 and hyperinsulinemic-euglycemic clamp in cohort 2). In agreement with these findings, mice studies demonstrated that liver and adipose tissue *Nrg4* overexpression improved insulin sensitivity and glucose tolerance and prevented HFD-induced hyperinsulinemia (Ma et al., 2016). In fact, two recent studies (López-Soldado et al., 2016; Zhang P. et al., 2018) demonstrated that recombinant neuregulin administration improved glucose tolerance in both control and diabetic rats by enhancing hepatic glucose utilization (López-Soldado et al., 2016) and insulin sensitivity in high fat-fed mice (Zhang P. et al., 2018).

On the other hand, contrary to previous study that demonstrated that SAT *NRG4* was negatively correlated with body fat mass (Wang et al., 2014), in the current study no significant association was found between SAT *NRG4* and BMI. In cohort 1, VAT *NRG4* gene expression was increased in obese compared to non-obese participants, and positively correlated with BMI, but in cohort 2, VAT *NRG4* gene expression was not correlated with BMI. Of note, similar *NRG4* gene expression

values were observed comparing obese participants from cohort 1 vs. those from cohort 2. Strikingly, the positive effects of diet-induced weight loss reducing body fat mass were not associated with expression of brown/beige-related genes (Barquissau et al., 2018). However, additional studies will be necessary to clarify the relationship between human adipose tissue *NRG4* and obesity.

A significant limitation of current study was the absence of VAT or SAT *NRG4* protein analysis by scarce availability of adipose tissue lysates for protein in the same tissue samples used for RNA analysis. Similar to this, *NRG4* protein analysis was not evaluated in recent relevant studies that demonstrated the importance of *NRG4* in adipose tissue (Wang et al., 2014; Chen et al., 2017; Guo et al., 2017; Nugroho et al., 2018; Pellegrinelli et al., 2018). Thus, additional studies should be performed to investigate if *NRG4* protein follows the same pattern of mRNA expression in human adipose tissue. Interestingly and consistent with current findings, increased *NRG4* mRNA and protein release in human beige adipogenesis of mural-like mesenchymal stem cell was more recently reported (Su et al., 2018), indicating that *NRG4* gene expression were correlated with *NRG4* protein levels and supporting *NRG4* participation in beige adipocyte differentiation. However, it is important to note that expression of *NRG4* and brown/beige adipose tissue markers (*UCP1*, *UCP3*, and *TMEM26*) were extremely low, suggesting that browning of white adipose tissue in humans may have less relevance than in mice.

In conclusion, all these observations suggest *NRG4* gene expression as a novel marker of beige adipocytes in human adipose tissue.

## REFERENCES

- Aziz, S. A., Wakeling, L. A., Miwa, S., Alberdi, G., Hesketh, J. E., and Ford, D. (2017). Metabolic programming of a beige adipocyte phenotype by genistein. *Mol. Nutr. Food. Res.* 61:1600574. doi: 10.1002/mnfr.201600574
- Barquissau, V., Léger, B., Beuzelin, D., Martins, F., Amri, E. Z., Pisani, D. F., et al. (2018). Caloric restriction and diet-induced weight loss do not induce browning of human subcutaneous white adipose tissue in women and men with obesity. *Cell. Rep.* 22, 1079–1089. doi: 10.1016/j.celrep.2017.12.102
- Bartelt, A., and Heeren, J. (2014). Adipose tissue browning and metabolic health. *Nat. Rev. Endocrinol.* 10, 24–36. doi: 10.1038/nrendo.2013.204
- Cantó, C., Pich, S., Paz, J. C., Sanches, R., Martínez, V., Orpinell, M., et al. (2007). Neuregulins increase mitochondrial oxidative capacity and insulin sensitivity in skeletal muscle cells. *Diabetes Metab. Res. Rev.* 56, 2185–2193. doi: 10.2337/db06-1726
- Cantó, C., Suárez, E., Lizcano, J. M., Grifó, E., Shepherd, P. R., Fryer, L. G., et al. (2004). Neuregulin signaling on glucose transport in muscle cells. *J. Biol. Chem.* 279, 12260–12268. doi: 10.1074/jbc.M308554200
- Chen, Z., Wang, G. X., Ma, S. L., Jung, D. Y., Ha, H., Altamimi, T., et al. (2017). *Nrg4* promotes fat oxidation and a healthy adipokine profile to ameliorate diet-induced metabolic disorders. *Mol. Metab.* 6, 863–872. doi: 10.1016/j.molmet.2017.03.016
- Ennequin, G., Boisseau, N., Caillaud, K., Chavanelle, V., Etienne, M., Li, X., et al. (2015). Neuregulin 1 improves glucose tolerance in db/db mice. *PLoS One* 10:e0130568. doi: 10.1371/journal.pone.0130568
- Finlin, B. S., Zhu, B., Confides, A. L., Westgate, P. M., Harfmann, B. D., Dupont-Versteegden, E. E., et al. (2017). Mast cells promote seasonal white adipose beiging in humans. *Diabetes Metab. Res. Rev.* 66, 1237–1246. doi: 10.2337/db16-1057

## AUTHOR CONTRIBUTIONS

JF-R and JM-N participated in study design and analysis of data and wrote and edited the manuscript. FC, CM, MS, FO, JL, and FD-S participated in acquisition of data. JA, MC, AG, and WR participated in interpretation of data. FC, CM, MS, FO, JL, FD-S, JA, MC, AG, and WR revised the manuscript critically for important intellectual content. All authors participated in final approval of the version to be published.

## FUNDING

This work was partially supported by research grants PI16/01173 from the Instituto de Salud Carlos III from Spain, FEDER funds and by Fundació Marató de TV3 (201626-30). CIBEROBN Fisiopatología de la Obesidad y Nutrición is an initiative from the Instituto de Salud Carlos III and Fondo Europeo de Desarrollo Regional (FEDER) from Spain.

## ACKNOWLEDGMENTS

We acknowledge the technical assistance of Emili Loshuertos (IdIBGi) and Oscar Rovira (IdIBGi). We also want to particularly acknowledge the patients, the *FATBANK* platform promoted by the *CIBEROBN* and the *IDIBGI* Biobank (Biobanc *IDIBGI*, B.0000872), integrated in the Spanish National Biobanks Network, for their collaboration and coordination.

- Garcia, R. A., Roemmich, J. N., and Claycombe, K. J. (2016). Evaluation of markers of beige adipocytes in white adipose tissue of the mouse. *Nutr. Metab.* 13:24. doi: 10.1186/s12986-016-0081-2
- Gonzalez-Hurtado, E., Lee, J., Choi, J., and Wolfgang, M. J. (2018). Fatty acid oxidation is required for active and quiescent brown adipose tissue maintenance and thermogenic programming. *Mol. Metab.* 7, 45–56. doi: 10.1016/j.molmet.2017.11.004
- Guo, L., Zhang, P., Chen, Z., Xia, H., Li, S., Zhang, Y., et al. (2017). Hepatic neuregulin 4 signaling defines an endocrine checkpoint for steatosis-to-NASH progression. *J. Clin. Invest.* 127, 4449–4461. doi: 10.1172/JCI96324
- Haskins, J. W., Zhang, S., Means, R. E., Kelleher, J. K., Cline, G. W., Canfrán-Duque, A., et al. (2015). Neuregulin-activated ERBB4 induces the SREBP-2 cholesterol biosynthetic pathway and increases low-density lipoprotein uptake. *Sci. Signal.* 8:ra111. doi: 10.1126/scisignal.aac5124
- Hepler, C., Shao, M., Xia, J. Y., Ghaben, A. L., Pearson, M. J., Vishvanath, L., et al. (2017). Directing visceral white adipocyte precursors to a thermogenic adipocyte fate improves insulin sensitivity in obese mice. *eLife* 6:e27669. doi: 10.7554/eLife.27669
- Huang, L., Pan, D., Chen, Q., Zhu, L. J., Ou, J., Wabitsch, M., et al. (2017). Transcription factor Hlx controls a systematic switch from white to brown fat through Prdm16-mediated co-activation. *Nat. Commun.* 8:68. doi: 10.1038/s41467-017-00098-2
- Lee, M. W., Odegaard, J. I., Mukundan, L., Qiu, Y., Molofsky, A. B., Nussbaum, J. C., et al. (2015). Activated type 2 innate lymphoid cells regulate beige fat biogenesis. *Cell* 160, 74–87. doi: 10.1016/j.cell.2014.12.011
- López-Soldado, I., Niisuke, K., Veiga, C., Adrover, A., Manzano, A., Martínez-Redondo, V., et al. (2016). Neuregulin improves response to glucose tolerance test in control and diabetic rats. *Am. J. Physiol. Endocrinol. Metab.* 310, E440–E451. doi: 10.1152/ajpendo.00226.2015

- Ma, Y., Gao, M., and Liu, D. (2016). Preventing high fat diet-induced obesity and improving insulin sensitivity through neuregulin 4 gene transfer. *Sci. Rep.* 6:26242. doi: 10.1038/srep26242
- Moreno-Navarrete, J. M., Escoté, X., Ortega, F., Serino, M., Campbell, M., Michalski, M. C., et al. (2013). A role for adipocyte-derived lipopolysaccharide-binding protein in inflammation- and obesity-associated adipose tissue dysfunction. *Diabetologia* 56, 2524–2537. doi: 10.1007/s00125-013-3015-9
- Moreno-Navarrete, J. M., Jove, M., Ortega, F., Xifra, G., Ricart, W., Obis, È, et al. (2016). Metabolomics uncovers the role of adipose tissue PDXK in adipogenesis and systemic insulin sensitivity. *Diabetologia* 59, 822–832. doi: 10.1007/s00125-016-3863-1
- Nugroho, D. B., Ikeda, K., Barinda, A. J., Wardhana, D. A., Yagi, K., Miyata, K., et al. (2018). Neuregulin-4 is an angiogenic factor that is critically involved in the maintenance of adipose tissue vasculature. *Biochem. Biophys. Res. Commun.* 503, 378–384. doi: 10.1016/j.bbrc.2018.06.043
- Pellegrinelli, V., Peirce, V. J., Howard, L., Virtue, S., Türei, D., Senzacqua, M., et al. (2018). Adipocyte-secreted BMP8b mediates adrenergic-induced remodeling of the neuro-vascular network in adipose tissue. *Nat. Commun.* 9:4974. doi: 10.1038/s41467-018-07453-x
- Rabhi, N., Hannou, S. A., Gromada, X., Salas, E., Yao, X., Oger, F., et al. (2018). Cdkn2a deficiency promotes adipose tissue browning. *Mol. Metab.* 8, 65–76. doi: 10.1016/j.molmet.2017.11.012
- Rosell, M., Kaforou, M., Frontini, A., Okolo, A., Chan, Y. W., Nikolopoulou, E., et al. (2014). Brown and white adipose tissues: intrinsic differences in gene expression and response to cold exposure in mice. *Am. J. Physiol. Endocrinol. Metab.* 306, E945–E964. doi: 10.1152/ajpendo.00473.2013
- Sauma, L., Franck, N., Paulsson, J. F., Westermark, G. T., Kjölhede, P., Strålfors, P., et al. (2007). Peroxisome proliferator activated receptor gamma activity is low in mature primary human visceral adipocytes. *Diabetologia* 50, 195–201. doi: 10.1007/s00125-006-0515-x
- Su, S., Guntur, A. R., Nguyen, D. C., Fakory, S. S., Doucette, C. C., Leech, C., et al. (2018). A renewable source of human beige adipocytes for development of therapies to treat metabolic syndrome. *Cell Rep.* 25, 3215.e9–3228.e9. doi: 10.1016/j.celrep.2018.11.037
- Suárez, E., Bach, D., Cadefau, J., Palacin, M., Zorzano, A., and Gumá, A. (2001). A novel role of neuregulin in skeletal muscle. Neuregulin stimulates glucose uptake, glucose transporter translocation, and transporter expression in muscle cells. *J. Biol. Chem.* 276, 18257–18264. doi: 10.1074/jbc.M008100200
- Torriani, M., Srinivasa, S., Fitch, K. V., Thomou, T., Wong, K., Petrow, E., et al. (2016). Dysfunctional subcutaneous fat with reduced Dicer and brown adipose tissue gene expression in HIV-infected patients. *J. Clin. Endocrinol. Metab.* 101, 1225–1234. doi: 10.1210/jc.2015-3993
- Wang, G. X., Zhao, X. Y., Meng, Z. X., Kern, M., Dietrich, A., Chen, Z., et al. (2014). The brown fat-enriched secreted factor Nrg4 preserves metabolic homeostasis through attenuation of hepatic lipogenesis. *Nat. Med.* 20, 1436–1443. doi: 10.1038/nm.3713
- Wu, J., Boström, P., Sparks, L. M., Ye, L., Choi, J. H., Giang, A. H., et al. (2012). Beige adipocytes are a distinct type of thermogenic fat cell in mouse and human. *Cell* 150, 366–376. doi: 10.1016/j.cell.2012.05.016
- Wu, W., Shi, F., Liu, D., Ceddia, R. P., Gaffin, R., Wei, W., et al. (2017). Enhancing natriuretic peptide signaling in adipose tissue, but not in muscle, protects against diet-induced obesity and insulin resistance. *Sci. Signal.* 10:489. doi: 10.1126/scisignal.aam6870
- Zeng, F., Wang, Y., Kloepper, L. A., Wang, S., and Harris, R. C. (2018). ErbB4 deletion predisposes to development of metabolic syndrome in mice. *Am. J. Physiol. Endocrinol. Metab.* 315, E583–E593. doi: 10.1152/ajpendo.00166.2018
- Zhang, P., Kuang, H., He, Y., Idiga, S. O., Li, S., Chen, Z., et al. (2018). NRG1-Fc improves metabolic health via dual hepatic and central action. *JCI Insight* 3:98522. doi: 10.1172/jci.insight.98522
- Zhang, S., Cao, H., Li, Y., Jing, Y., Liu, S., Ye, C., et al. (2018). Metabolic benefits of inhibition of p38α in white adipose tissue in obesity. *PLoS Biol.* 16:e2004225. doi: 10.1371/journal.pbio.2004225
- Zuriaga, M. A., Fuster, J. J., Gokce, N., and Walsh, K. (2017). Humans and mice display opposing patterns of “Browning” gene expression in visceral and subcutaneous white adipose tissue depots. *Front. Cardiovasc. Med.* 4:27. doi: 10.3389/fcvm.2017.00027

**Conflict of Interest Statement:** The authors declare that the research was conducted in the absence of any commercial or financial relationships that could be construed as a potential conflict of interest.

Copyright © 2019 Comas, Martínez, Sabater, Ortega, Latorre, Díaz-Sáez, Aragonés, Camps, Gumà, Ricart, Fernández-Real and Moreno-Navarrete. This is an open-access article distributed under the terms of the Creative Commons Attribution License (CC BY). The use, distribution or reproduction in other forums is permitted, provided the original author(s) and the copyright owner(s) are credited and that the original publication in this journal is cited, in accordance with accepted academic practice. No use, distribution or reproduction is permitted which does not comply with these terms.





# Beta 3 Adrenergic Receptor Activation Rescues Metabolic Dysfunction in Female Estrogen Receptor Alpha-Null Mice

Stephanie L. Clookey<sup>1</sup>, Rebecca J. Welly<sup>1</sup>, Dusti Shay<sup>1</sup>, Makenzie L. Woodford<sup>1</sup>, Kevin L. Fritsche<sup>1</sup>, R. Scott Rector<sup>1,2,3</sup>, Jaume Padilla<sup>1,4,5</sup>, Dennis B. Lubahn<sup>6</sup> and Victoria J. Vieira-Potter<sup>1\*</sup>

<sup>1</sup> Department of Nutrition and Exercise Physiology, University of Missouri, Columbia, MO, United States, <sup>2</sup> Harry S. Truman Memorial Veterans' Hospital, Columbia, MO, United States, <sup>3</sup> Department of Medicine, University of Missouri, Columbia, MO, United States, <sup>4</sup> Dalton Cardiovascular Research Center, University of Missouri, Columbia, MO, United States, <sup>5</sup> Child Health, University of Missouri, Columbia, MO, United States, <sup>6</sup> Department of Biochemistry, University of Missouri, Columbia, MO, United States

## OPEN ACCESS

### Edited by:

Rita De Matteis,  
Università degli Studi di Urbino Carlo  
Bo, Italy

### Reviewed by:

Ismael González-García,  
Helmholtz Center Munich – German  
Research Center for Environmental  
Health, Germany  
Alexandre Caron,  
University of Texas Southwestern  
Medical Center, United States  
Bin Feng,  
Sichuan Agricultural University, China

### \*Correspondence:

Victoria J. Vieira-Potter  
vieirapotterv@missouri.edu

### Specialty section:

This article was submitted to  
Integrative Physiology,  
a section of the journal  
Frontiers in Physiology

**Received:** 04 October 2018

**Accepted:** 08 January 2019

**Published:** 05 February 2019

### Citation:

Clookey SL, Welly RJ, Shay D,  
Woodford ML, Fritsche KL,  
Rector RS, Padilla J, Lubahn DB and  
Vieira-Potter VJ (2019) Beta 3  
Adrenergic Receptor Activation  
Rescues Metabolic Dysfunction  
in Female Estrogen Receptor  
Alpha-Null Mice. *Front. Physiol.* 10:9.  
doi: 10.3389/fphys.2019.00009

Metabolic disease risk escalates following menopause. The mechanism is not fully known, but likely involves reduced signaling through estrogen receptor alpha (ER $\alpha$ ), which is highly expressed in brown and white adipose tissue (BAT and WAT).

**Objective:** Test the hypothesis that uncoupling protein (UCP1) activation mitigates metabolic dysfunction caused by loss of signaling through ER $\alpha$ .

**Methods:** At 8 weeks of age, female ER $\alpha$  knock out (KO) and wild-type mice were housed at 28°C and fed a Western-style high-fat, high sucrose diet (HFD) or a normal low-fat chow diet (NC) for 10 weeks. During the final 2 weeks, they received daily injections of CL 316,256 (CL), a selective  $\beta$ 3 adrenergic agonist, or vehicle control (CTRL), creating eight groups: WT-CTRL, WT-CL, KO-CTRL, and KO-CL on HFD or NC;  $n = 4$ –10/group.

**Results:** ER $\alpha$ KO demonstrated exacerbated HFD-induced adiposity gain ( $P < 0.001$ ) and insulin resistance ( $P = 0.006$ ). CL treatment improved insulin sensitivity ( $P < 0.05$ ) and normalized ER $\alpha$ KO-induced adiposity increase ( $P < 0.05$ ). In both genotypes, CL increased resting energy expenditure ( $P < 0.05$ ) and induced WAT browning indicated by increased UCP1 protein in both perigonadal (PGAT) and subcutaneous (SQAT) depots. These effects were attenuated under HFD conditions ( $P < 0.05$ ). In KO, CL reduced HFD energy consumption compared to CTRL ( $P < 0.05$ ). Remarkably, CL increased WAT ER $\beta$  protein levels of both WT and KO ( $P < 0.001$ ), revealing CL-mediated changes in estrogen signaling may have protective metabolic effects.

**Conclusion:** CL completely restored metabolic dysfunction in ER $\alpha$ KO mice. Thus, UCP1 may be a therapeutic target for treating metabolic dysfunction following loss of estrogen receptor signaling.

**Keywords:** adipose tissue, energy expenditure, browning, insulin resistance, high fat diet, CL 316,243, obesity, rodent

## INTRODUCTION

Compared to males, ovary-intact females are protected against obesity and its associated metabolic consequences, including insulin resistance, which precedes diabetes onset (Brand et al., 2012). However, postmenopausal women are more likely to be obese (Auro et al., 2014; Stefanska et al., 2015) and are twice as likely to develop type 2 diabetes compared to men and younger women (Klötting et al., 2010). Reducing metabolic disease risk in this vulnerable population is an urgent public health priority (Tchernof et al., 1998; Spritzer and Oppermann, 2013; Stefanska et al., 2015). While ovarian hormones (notably, estrogen) are known to be metabolically protective (Klötting et al., 2010), the mechanism(s) remain largely unknown.

Adipose tissue is heavily influenced by estrogen (Ogden et al., 2012; Davis et al., 2013) and is an important target tissue to improve metabolic health. Importantly, it is a vital glucose-regulator (Lomonaco et al., 2012) especially among women who generally have greater relative fat mass (Wade et al., 1985). In fact, insulin-mediated adipose tissue glucose uptake predicted systemic insulin sensitivity following ovariectomy (OVX) in a rodent model used to mimic the effects of menopause (Park Y.M. et al., 2015). Pinpointing what factors protect female adipose tissue prior to menopause could have tremendous implications for women's health. In this regard, the protection against adipose tissue dysfunction is likely due to adipocyte-specific estrogen signaling (D'Eon et al., 2005; Mauvais-Jarvis et al., 2013; Kim et al., 2014; Luglio, 2014) through estrogen receptor alpha (ER $\alpha$ ) (Davis et al., 2013). Signaling through this steroid receptor has been shown to increase mitochondrial function and biogenesis in adipose tissue (Klinge, 2008), consistent with a signature profile of healthy adipose tissue 'immunometabolism' (Zidon et al., 2018). On the other hand, directly decreasing adipocyte ER $\alpha$  signaling causes adipocyte dysfunction (Davis et al., 2013).

A specific kind of adipose tissue typified by its high mitochondrial content and activity, the brown adipose tissue (BAT), and the more recently appreciated "beige" adipose tissue, play important roles in improving whole body metabolic function (Bartelt and Heeren, 2014). Notably, ovary-intact females, who are more insulin sensitive and protected against metabolic dysfunction, also have more BAT relative to total adiposity (Cypess et al., 2009; Pfannenberger et al., 2010; Ouellet et al., 2011; Wang et al., 2011) and may be more responsive than males to white adipose tissue "beiging" (Himms-Hagen et al., 1994; Kim et al., 2016), a process by which WAT increases its mitochondrial content and expression of key signature BAT proteins [e.g., uncoupling protein 1 (UCP1)]. Thus, estrogen may mediate WAT beiging.

Via ER $\alpha$  signaling, estrogen has been shown to be protective against high fat diet (HFD)-induced insulin resistance (Riant et al., 2009), suggesting that the ER $\alpha$  pathway may be a viable strategy to mitigate diet-induced metabolic dysfunction. ER $\alpha$  is also protective against HFD-induced metabolic inflammation (Morselli et al., 2014), whereas HFD suppresses ER $\alpha$  in adipose tissues (Gorres et al., 2011) and the central nervous system (Scudiero and Verderame, 2017). Further, suppression of hepatic

ER $\alpha$  in mice exacerbates their response to HFD-induced hepatic insulin resistance (Zhu et al., 2014).

The chemical ligand, CL 316,243 (Bloom et al., 1992) (i.e., CL) is a highly selective systemic  $\beta_3$  adrenergic receptor agonist known to induce beiging of WAT. CL induces ectopic expression of UCP1 in WAT and improves insulin sensitivity (Borst and Hennessy, 2001; Poher et al., 2015). The mechanism by which CL reduces insulin resistance has not been fully elucidated. CL has also been shown to stimulate insulin secretion (Pang et al., 2010), which may contribute to its ability to increase glucose uptake; however, CL has been shown to reduce obesity-associated hyperinsulinemia (Ghorbani and Himms-Hagen, 1997). We and others have demonstrated that lack of UCP1 reduces insulin sensitivity (Winn et al., 2017). Thus, the insulin sensitizing effect of CL may involve its ability to increase UCP1. However, UCP1 is not required for all of the metabolic benefits of CL (Granneman et al., 2003). Whether or not CL's metabolic benefits require ER $\alpha$  is not known. To test this hypothesis, we determined the effectiveness of CL to reduce obesity and insulin resistance in the presence and absence of ER $\alpha$  expression. We used ER $\alpha$ KO mice because ER $\alpha$  is diminished following menopause in women (Park et al., 2017), and the phenotype of metabolic dysfunction in ER $\alpha$ KO mice mimics that of postmenopausal women and OVX rodents. We compared mice null (i.e., whole body knock-out [KO]) for ER $\alpha$  expression (ER $\alpha$ KO) to littermate wild-type controls for their responsiveness to HFD-induced metabolic dysfunction, and the possible protective role of CL. We confirm that young otherwise healthy ER $\alpha$ KO mice have an increased susceptibility to HFD-induced obesity compared to WT littermate controls (Heine et al., 2000; Ohlsson et al., 2000 #122) and further demonstrate that CL mitigates metabolic dysfunction caused by loss of ER $\alpha$  and HFD-induced obesity.

## MATERIALS AND METHODS

### Ethics Statement

All animal husbandry and experimental procedures were carried out in accordance with the AAALAC International and approved by the University of Missouri Institutional Animal Care and Use Committee.

### Animals and Experimental Design

Heterozygote ER $\alpha$ -/+ mice on a C57BL/6J background were bred at our facility to produce homozygote (ER $\alpha$ -/-) and littermate wild-type mice, as previously described (Lubahn et al., 1993; Eddy et al., 1996). Briefly, development of the ER $\alpha$ -/- (i.e., ER $\alpha$ KO) mouse was accomplished by homologous recombination and insertion of a neomycin sequence containing premature stop codons and polyadenylation sequences into a Not one site in exon 2 of the mouse estrogen receptor gene. At 8 weeks of age, mice were fed a high sucrose, HFD consisting of 46.4% kcal from fat, 36% carbohydrate, and 17.6% protein, with a density of 4.68 kcal per gram (Test Diet, St. Louis, MO, United States, #1814692), or a normal chow (NC) diet (3.3 kcal/g of food, 13% kcal fat, 57% kcal carbohydrate, and 30% kcal protein, LabDiet, St. Louis, MO, United States, #5001) for a total of 10 weeks.

Animals were housed two to three per cage (within group) at 28°C (i.e., thermoneutral conditions), in a light cycle from 0700 to 1900. At 16 weeks of age, animals began a regiment of daily intraperitoneal injections of CL 316,243 (#C5976, Sigma-Aldrich) or equal dose of saline control at 7 am during the final 2 weeks of the study. CL 316,243 compound (CL) was put in solution using deionized water, and was administered at a dose of 1 µg/g body weight. Thus, the study consisted of eight groups ( $n = 4$ – $5$ /group for NC-fed animals, 10/group for HFD-fed animals): WT/control (CTRL), WT/CL, ER $\alpha$ KO/CTRL, ER $\alpha$ KO/CL either on HFD or NC. After a total of 10 weeks on each respective diet, with CL administration during the last 2 weeks, the animals were euthanized at 18 weeks of age following a 5-h fast. Blood and tissues were collected. Tissues were harvested and either fixed in 10% formalin or snap-frozen in liquid nitrogen and stored at  $-80^{\circ}\text{C}$  until analyses. The basic study design including timeline is depicted in **Figure 1**.

## Body Composition and Tissue Weights

Body fat percentage (BF%) was measured by a nuclear magnetic resonance imaging whole-body composition analyzer (EchoMRI 4 in 1/1100; Echo Medical Systems, Houston, TX), 1 week prior to sacrifice. Upon sacrifice, interscapular BAT, subcutaneous (inguinal) WAT (SQAT), and visceral (perigonadal) WAT (PGAT) were extracted and tissue weights were collected.

## Energy Expenditure Assessments

Indirect calorimetry was utilized when mice were 17 weeks of age, after 1 week of CL treatment. HFD-fed animals ( $n = 10$ /group) were placed in indirect calorimetry chambers (Promethion; Sable Systems International, Las Vegas, Nevada) to assess metabolic activity parameters including total energy expenditure (TEE), resting energy expenditure (REE), respiratory quotient estimation (RQ), and spontaneous physical activity (SPA) by the summation of  $x$ -,  $y$ -, and  $z$ -axis beam breaks. Body weight and food intake were measured before and after each 48-h assessment. Each 48-h run captured at least two light and two dark cycles of REE.

## Insulin Tolerance Testing (ITT)

Insulin tolerance tests were performed on HFD-fed animals at 17 weeks of age, 5 days before sacrifice ( $n = 10$ /group). After a 5-h fast, blood glucose was measured from the tail vein (i.e., time 0), and blood was sampled by a glucometer (Alpha Trak, Abbott Labs). Insulin was administered at a dose of (0.7 U/kg body weight (BW)) via intraperitoneal injection, as previously described (Vieira Potter et al., 2012). Glucose measures were taken 30, 45, 60 and 120 min after the insulin injections, however, an abbreviated ITT curve is presented due to incidences of hypoglycemia during testing despite the reduced insulin dose. Glucose area under curve (AUC) from baseline was calculated.

## Fasting Blood Parameters

Plasma insulin, glucose, and non-esterified fatty acids (NEFA) assays were performed by a commercial laboratory (Comparative

Clinical Pathology Services, Columbia, MO, United States) on an Olympus AU680 automated chemistry analyzer (Beckman-Coulter, Brea, CA, United States) using assays as per manufacturer's guidelines. The homeostasis model assessment of insulin resistance (HOMA-IR) was used as a surrogate measure of systemic insulin resistance [(fasting insulin ( $\mu\text{U/l}$ )  $\times$  fasting glucose (mg/dl))/405.1] (Matthews et al., 1985)] and indices of adipose tissue insulin resistance (ADIPO-IR) were calculated as the product of fasting insulin ( $\mu\text{U/l}$ ) and fasting NEFAs (mmol/l) (Lomonaco et al., 2012). Fasting levels of circulating adiponectin were measured using colorimetric ELISA (Quantikine MRP300; R&D Systems, Minneapolis, MN, United States) and data are presented as ng/ml.

## Histological Assessments

Formalin-fixed samples were processed through paraffin embedment, sectioned at 5 µm (interscapular BAT, visceral (PGAT) and subcutaneous (SQAT) WAT) and stained in a 1:1200 dilution with UCP1 antibody (#U6382, 1:1000, Sigma-Aldrich; secondary antibody, #K400311-2, Envision Rabbit, Agilent) for 30 min with a heat-induced epitope retrieval (HIER) pretreatment, using DAKO brand citrate in a decloaking chamber. Sections were evaluated via an Olympus BX34 photomicroscope (Olympus, Melville, NY) and images were taken via an Olympus SC30 Optical Microscope Accessory CMOS color camera. Adipocyte size was calculated from three independent regions of the same 40 $\times$  objective fields for SQAT, PGAT, and interscapular BAT depots (50 adipocytes/animal). Cross-sectional areas of the adipocytes were obtained from perimeter tracings using Image J software as previously described (Wainright et al., 2015). An investigator blinded to the groups performed all procedures.

## RNA Extraction and Quantitative Real-Time RT-PCR

Interscapular BAT samples were homogenized in TRIzol solution using a tissue homogenizer (TissueLyser LT, Qiagen, Valencia, CA, United States). Total RNA was isolated according to the Qiagen's RNeasy lipid tissue protocol and assayed using a Nanodrop spectrophotometer (Thermo Scientific, Wilmington, DE, United States) to assess purity and concentration. First-strand cDNA was synthesized from total RNA using the High Capacity cDNA Reverse Transcription kit (Applied Biosystems, Carlsbad, CA, United States). Quantitative real-time PCR was performed as previously described using the ABI Step One Plus sequence detection system (Applied Biosystems) (Roseguini et al., 2010; Padilla et al., 2013). All primers were purchased from IDT (Coralville, IA, United States) and Sigma Aldrich (St. Louis, MO, United States). Housekeeping gene cycle threshold (CT) was not different among the groups of animals. mRNA expression was calculated by  $2^{-\Delta\text{CT}}$  where  $\Delta\text{CT} = \text{Housekeeping gene CT} - \text{gene of interest CT}$  and presented as fold-difference. mRNA levels were normalized to the WT/CTRL group, which was set at 1. All primer sequences are provided in **Table 1**.

## Western Blotting

Protein was measured as previously described (Winn et al., 2017). Briefly, protein samples (10  $\mu$ g/lane) were separated by SDS-PAGE, transferred to polyvinylidene difluoride membranes, and probed with primary antibodies, including UCP1 (#U6382, 1:1000; Sigma-Aldrich), UCP2 (#89326, 1:1000; Cell Signaling), ER $\alpha$  (#75635, 1:1000, Abcam), and ER $\beta$  (#AB3577, 1:2000, Abcam). Intensity of individual protein bands were quantified using FluoroChem HD2 (AlphaView, version 3.4.0.0), and expressed relative to the housekeeping protein, beta-tubulin. Amido Black was used as an additional control of total protein loading.

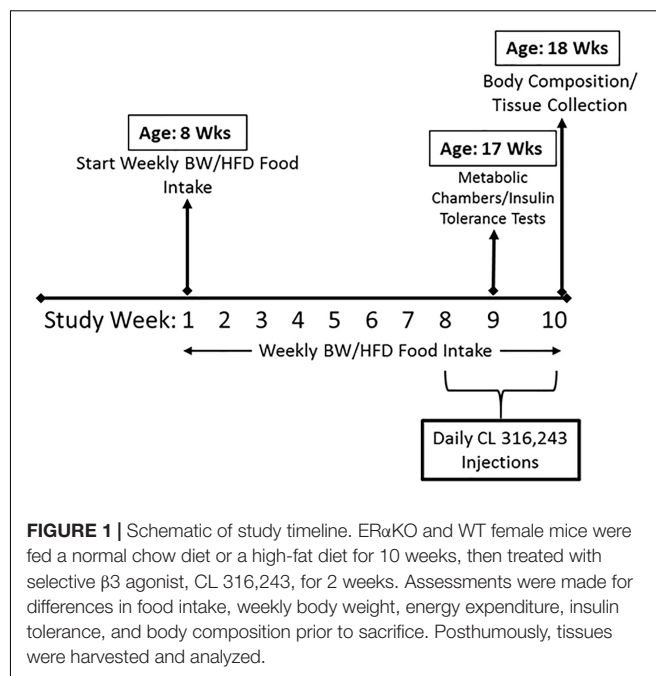
## Statistics

A 2 $\times$ 2 $\times$ 2 analysis of variance (ANOVA) was used to evaluate the effects of genotype (G, ER $\alpha$ KO vs. WT), treatment (T, CL vs. CTRL), and diet (D, NC vs. HFD), as well as treatment interactions. Where appropriate, Tukey's *post hoc* tests were used to indicate significant between-group differences with the following symbols: \* different from all other groups, # different from all other groups except NC WT/CL, \$ different from all other groups except HFD KO/CL, 2 different from NC WT/CL, 4 different from NC KO/CL, 5 different from HFD WT/CTRL, 6 different from HFD WT/CL, 7 different from HFD KO/CTRL, 8 different from HFD KO/CL. All data are presented as mean  $\pm$  standard error of the mean (SEM). For all statistical tests, significance was accepted at  $P < 0.05$ . All statistical analyses were performed with SPSS V25.0.

## RESULTS

### ER $\alpha$ Ablation Exacerbates HFD Induced Metabolic Dysfunction

Consistent with many previous studies (Ohlsson et al., 2000; Ribas et al., 2010; Gao and Dahlman-Wright, 2013), female ER $\alpha$ KO were heavier than WT (G,  $P < 0.001$ ) and both genotypes increased body weight under conditions of HFD feeding (D,  $P < 0.001$ ). However, ER $\alpha$ KOs experienced a greater increase in body weight in response to HFD than WT (G $\times$ D,  $P = 0.002$ ) (Figure 2A). Increases in adiposity coincided with differences in body weight such that ER $\alpha$ KOs had significantly greater perigonadal (i.e., PGAT, a visceral depot) adipose tissue and subcutaneous inguinal adipose tissue (SQAT)



following consumption of the HFD when compared to WT mice (G $\times$ D,  $P < 0.001$ ) (Figures 2B,C). BAT depot weight in the ER $\alpha$ KO was greater than that in the WT mice, possibly due to increased lipid accumulation or 'BAT whitening' (G,  $P < 0.001$ ) (Figure 2D) compared to BAT of WT mice both on either diet. Although they had increased body weight and adiposity, the ER $\alpha$ KOs did not consume more calories than WT when fed a NC diet; however, both genotypes increased caloric consumption under HFD conditions, as expected (D,  $P < 0.001$ ) (Figure 2E). Furthermore, unlike WT, ER $\alpha$ KOs exhibited evidence of insulin resistance via elevated HOMA-IR in response to HFD (G $\times$ D,  $P = 0.006$ ) (Figure 2F). The same trend was observed in ADIPO-IR, though not significant (Figure 2G). The increase in those surrogate markers of insulin resistance were primarily driven by hyperinsulinemia in the ER $\alpha$ KOs in response to HFD; ER $\alpha$ KOs fed HFD exhibited a fourfold increase in fasting insulin compared to NC (G $\times$ D,  $P = 0.036$ ) (Table 2). This coincided with HFD-associated reductions in non-esterified fatty acids (NEFAs) in circulation (D,  $P = 0.03$ ) likely due to insulin-mediated suppression of lipolysis. Similarly,

**TABLE 1** | Primer sequences.

Primer	Forward	Reverse	Company
UCP1	CACGGGGACCTACAATGCTT	ACAGTAAATGGCAGGGGACG	IDT
CD11c	ATGCCACTGTCTGCCTTCAT	GAGCCAGGTCAAAGGTGACA	IDT
TNF $\alpha$	CTATGTCTCAGCCTCTTCTC	CATTTGGGAACTTCTCATCC	Sigma
ER $\alpha$	CAAGGTAAATGTGTGGAAGG	GTGTACACTCCGGAATTAAG	Sigma
ER $\beta$	CTCAACTCCAGTATGTACCC	CATGAGAAAGAAGCATCAGG	Sigma
B actin	GATGTATGAAGGCTTTGGTC	TGTGCACTTTTATTGGTCTC	Sigma
18 s	TCAAGAACGAAAGTCGGAGG	GGACATCTAAGGGCATCAC	IDT
RPS13	TGCCGTTTCCTACCTCGTTT	CACGTCGTCAGACGTCAACT	IDT



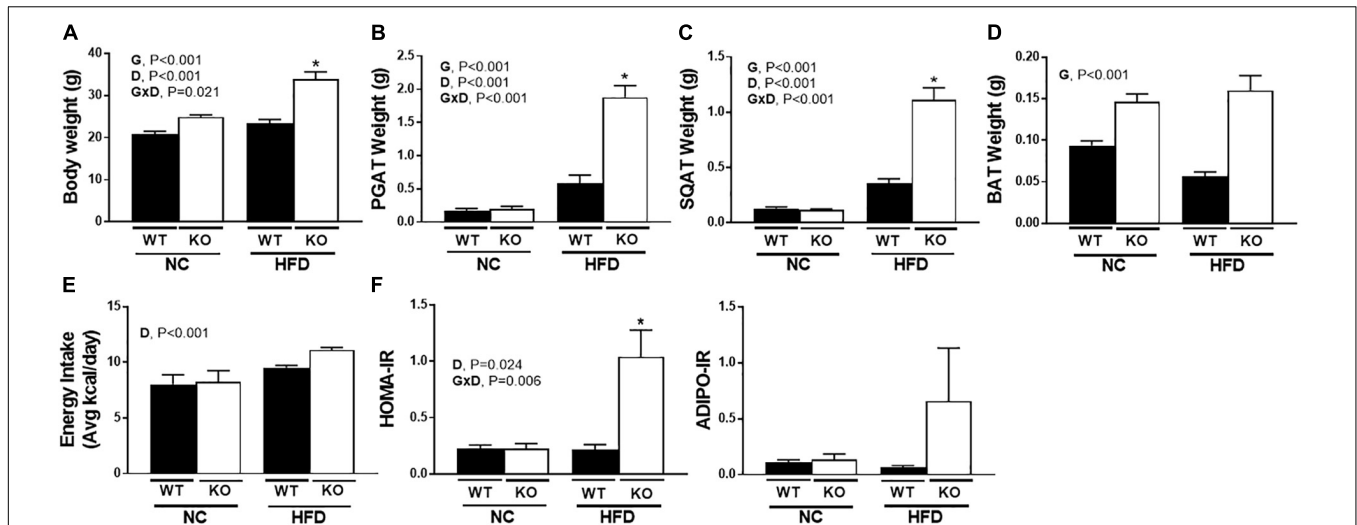


**FIGURE 2 |** ER $\alpha$  ablation exacerbates high-fat diet induced metabolic dysfunction. ER $\alpha$ KO and WT female mice were fed a normal chow diet or a high-fat diet. Assessments were made for differences in (A) body weight, (B) perigonadal adipose tissue (PGAT) weight, (C) subcutaneous adipose tissue (SQAT) weight, (D) brown adipose tissue (BAT) weight, (E) energy intake, (F) HOMA-IR, (G) ADIPO-IR. WT, wild-type; KO, ER $\alpha$  knock-out; NC, normal chow; HFD, high fat diet; data are expressed as means  $\pm$  standard error (SE);  $n = 4$ –10/group. G = significant main effect of genotype,  $P < 0.05$ . D = significant main effect of diet,  $P < 0.05$ . G $\times$ D = significant interaction between genotype and diet,  $P < 0.05$ . \* $P < 0.05$  compared to all other groups.

fasting glucose was significantly elevated in ER $\alpha$ KO (but not WT) under HFD conditions (G $\times$ D,  $P = 0.009$ ) (Table 2). Thus, ER $\alpha$  ablation increases susceptibility to HFD-induced metabolic dysfunction.

## CL Rescues HFD-Induced Metabolic Dysfunction in the ER $\alpha$ KO

As discussed above, ER $\alpha$ KO animals exhibited greater increases in body weight compared to WT under both dietary conditions (G,  $P < 0.001$ ); however, the CL treatment mitigated their HFD-induced weight gain (T,  $P = 0.009$ ) (Figures 3A,B). Whereas ER $\alpha$  ablation increased adiposity (G,  $P < 0.001$ ), CL induced a significant adiposity reduction (T,  $P < 0.001$ ) (Figure 3C). While ER $\alpha$ KO animals gained more weight on HFD, they were also more responsive to CL-induced decreases in adiposity than WT (G $\times$ T,  $P < 0.05$ ) (Figure 3C). Likewise, ER $\alpha$ KO had greater CL-induced reductions in SQAT and PGAT depot weights relative to WT (G $\times$ T,  $P < 0.001$  for both) (Figure 3D). ER $\alpha$  ablation also increased BAT weight in both interscapular and periaortic fat depots, possibly indicative of a “whitening” of BAT; however, this increase was normalized with CL (G $\times$ T,  $P < 0.001$ ) (Figure 3E).

ER $\alpha$ KO animals had impaired insulin tolerance compared to WT littermates (G,  $P = 0.011$ ), whereas CL treatment decreased glucose AUC during ITT (T,  $P = 0.018$ ) (Figure 3F), normalized HOMA-IR in the KO to those of WT CTRL (G $\times$ T,  $P < 0.05$ ) (Figure 3G), and tended to improve ADIPO-IR (Figure 3H). However, it is important to note that CL treatment caused hypoglycemia in a subset of animals (WT  $n = 8$ ; KO  $n = 5$ ) which prevented full ITT curves from being determined in those animals. No animals in the CTRL groups experienced hypoglycemia. Although this confirms the robust

insulin-sensitizing effect of CL, future studies should perform more precise measures of insulin sensitivity in order to validate our suggested findings. The CL-induced hypoglycemia during the ITT may have been attributed to the effect of CL to increase insulin secretion, but since insulin levels were not measured throughout the ITT, this is an important assessment that should be done in future studies. Thus, CL reduced weight gain and adiposity, and improved insulin sensitivity in both ER $\alpha$ KO and WT animals on HFD, effectively normalizing metabolic health.

## CL Increases Energy Expenditure and Attenuates Energy Consumption in HFD-fed ER $\alpha$ KO Mice

There was no influence of CL on energy intake in WT mice under either dietary condition (Supplementary Figure S1), yet CL attenuated HFD energy overconsumption in the ER $\alpha$ KO animals (G $\times$ T,  $P = 0.04$ ) (Figure 4A). CL also decreased metabolic efficiency in the ER $\alpha$ KOs (G $\times$ T,  $P = 0.019$ ) (Figure 4B), yet did not affect cage (i.e., spontaneous) physical activity (SPA) (Figure 4C). Similarly, CL increased total energy expenditure (TEE) (T,  $P < 0.05$ ) (Figure 4D) by increasing resting energy expenditure (REE) (T,  $P < 0.05$ ) (Figure 4E). The EE data were generated based on  $\text{VO}_2$  and  $\text{VCO}_2$  (Figure 4F) which indicate that KO reduced and CL increased these measures. CL treatment also increased RQ (Figure 4G), suggestive of a shift away from oxidative and toward glycolytic metabolism.

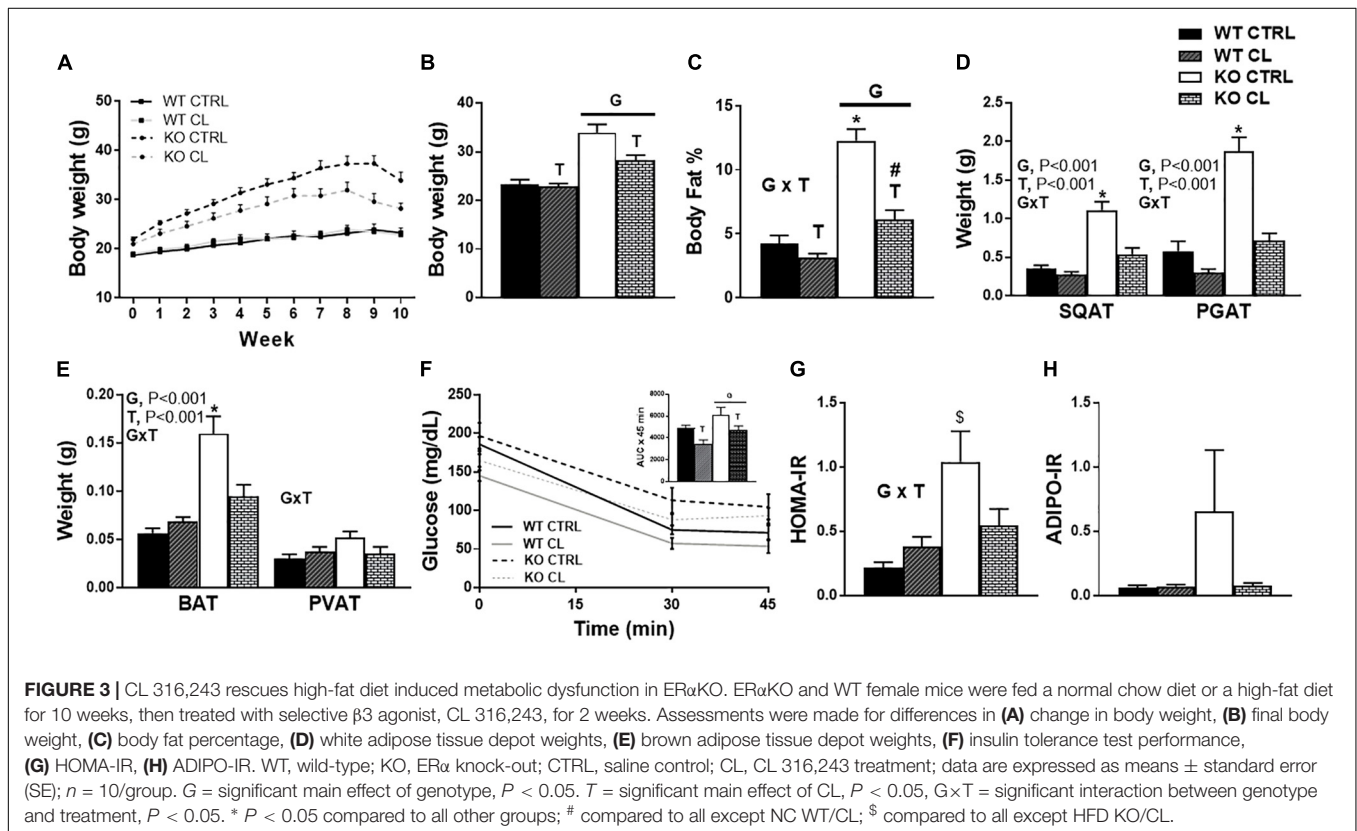
## CL Induced WAT Beiging Differs in WT and ER $\alpha$ KO Mice

Under NC dietary conditions, assessments of UCP1-stained SQAT [i.e., the WAT depot thought to be most susceptible

**TABLE 2** | Blood biochemistry.

Diet	Group	Adiponectin (ng/mL)	Insulin (ng/ml)	Glucose (mg/dl)	NEFA (mmol/L)
NC	WT Ctrl	12628.50 ± 1691.48	0.46 ± 0.09	211.25 ± 22.02	0.26 ± 0.06
	WT CL	11807.75 ± 446.48	0.79 ± 0.30	241.25 ± 16.12	0.13 ± 0.03
	KO Ctrl	7419 ± 857.18	0.51 ± 0.06	180.75 ± 35.32	0.26 ± 0.07
	KO CL	7809.25 ± 2147.32	0.46 ± 0.05	115.00 ± 24.09	0.13 ± 0.04
HFD	WT Ctrl	9903.60 ± 726.41	0.46 ± 0.07	179.90 ± 16.21	0.14 ± 0.04
	WT CL	12819.18 ± 1011.91	0.81 ± 0.13	178.27 ± 16.16	0.09 ± 0.02
	KO Ctrl	9513.50 ± 841.55	2.05 ± 0.58	222.00 ± 25.10	0.17 ± 0.06
	KO CL	13566.44 ± 1058.08	1.11 ± 0.14	180.60 ± 24.14	0.06 ± 0.01
P-value		G, $P = 0.013$ ; G×D, $P = 0.008$ ; T×D, $P = 0.037$	D, $P = 0.031$ ; G×D, $P = 0.036$	G×D, $P = 0.009$	T, $P = 0.004$ ; D, $P = 0.03$

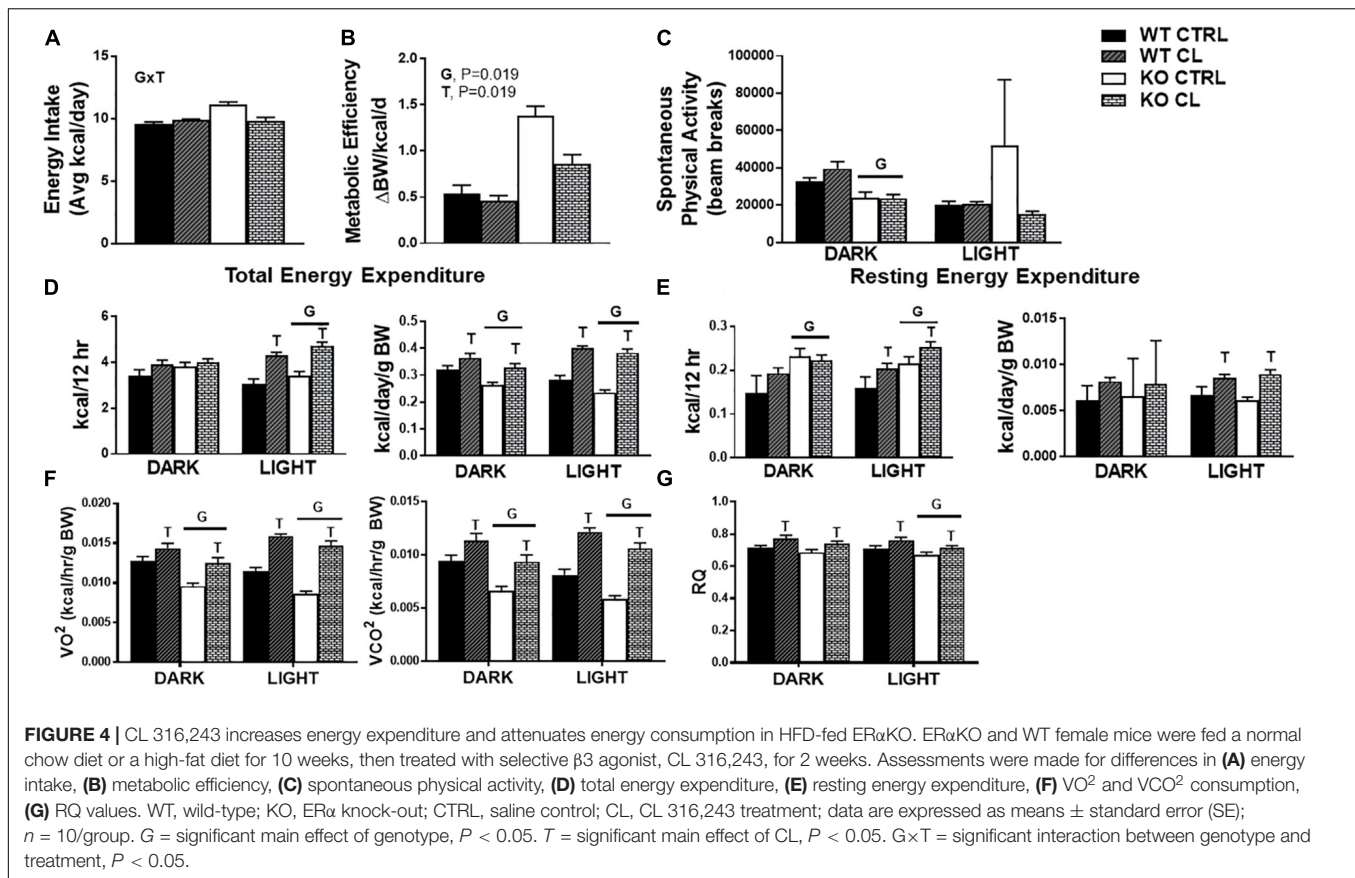
G,  $P < 0.05$  main effect of genotype; T,  $P < 0.05$  main effect of CL treatment; D,  $P < 0.05$  main effect of diet; G×T  $P < 0.05$  G, T interaction; G×D  $P < 0.05$  G, D interaction; T×D  $P < 0.05$  T, D interaction; G×T×D  $P < 0.05$  G, T, D interaction.



to being (Himms-Hagen et al., 1994)] revealed a CL-induced multi-locular phenotype in both WTs and KOs, which appeared more robust in the lean WT compared to the more insulin resistant ERαKO (Figure 5A). Under HFD conditions, histological analysis did not show differences in CL-induced UCP1+ staining between WT and KO (Figure 5B). Overall, there was a main effect of CL treatment ( $P < 0.001$ ) (Figure 5C), and HFD increased mean adipocyte size ( $P = 0.001$ ) (Figure 5D) and attenuated CL-induced being ( $T \times D$ ,  $P < 0.001$ ) (Figure 5E). Interestingly, assessments of UCP1 protein (Figure 5E) and mRNA (Figure 5F) indicated that the ERαKO were more responsive to CL ( $G \times T$ ,  $P < 0.01$  for both protein and mRNA) under NC conditions. An additional finding was that HFD

reduced basal (i.e., untreated) levels of SQAT UCP1 staining ( $P = 0.039$ , Figure 5C), protein ( $P < 0.001$ , Figure 5E) and mRNA ( $P = 0.002$ , Figure 5F) in both KO and WT mice.

Similar to SQAT, CL-induced being was also evident by visual assessment of PGAT UCP1-staining (Figures 6A,B), quantification of UCP1 staining (Figure 6C), reduced adipocyte size (Figure 6D) (T,  $P < 0.001$ ), increased UCP1 protein content (Figure 6E) (T,  $P = 0.005$ ), and increased UCP1 mRNA expression (Figure 6F) in both genotypes. Similar to SQAT, under NC dietary conditions, the lean WT appeared to be more susceptible to CL-induced being compared to fatter ERαKO based on the intensity of UCP1+ staining (Figures 6A,B), although this difference did not reach statistical significance,



possibly due to small sample size ( $n = 4\text{--}5/\text{group}$ ). Also similar to SQAT, HFD increased mean adipocyte size (D,  $P < 0.001$ ) and significantly blunted CL-induced beiging in PGAT. Interestingly, ER $\alpha$ KOs had greater “basal” PGAT UCP1 protein (G,  $P = 0.008$ ) than WT, but also experienced greater reductions in UCP1 protein in response to HFD (G $\times$ D $\times$ T,  $P = 0.011$ ) (Figure 6E). This was likely driven by the heightened CL-induced UCP1 increase in the ER $\alpha$ KO under NC conditions (T $\times$ D,  $P = 0.011$ ).

### HFD Increases BAT UCP1 Independently of ER $\alpha$

BAT UCP1+ staining (Figures 7A–C) revealed that the effects of CL were less robust in BAT compared to WAT, confirming what others have reported (Park J.W. et al., 2015). CL significantly reduced BAT mean adipocyte size (Figure 7D) and increased UCP1 levels (Figure 7E) (T,  $P = 0.008$ ). The effects were similar between WT and KO mice. ER $\alpha$ KOs had greater BAT mean adipocyte size than WTs (G,  $P = 0.007$ ) (Figure 7D) possibly suggestive of a “whiter” BAT phenotype. As was the case with the WAT depots, the effects of CL were less robust under HFD conditions (T $\times$ D,  $P = 0.002$ ) (Figure 7D). And, as previously reported by our group and others (Feldmann et al., 2009; Cannon and Nedergaard, 2010; Yao et al., 2014; Sakamoto et al., 2016; Winn et al., 2017), HFD significantly increased UCP1 protein (D,  $P < 0.001$ ) (Figure 7E). Here, we illustrate for the first time

that this HFD-induced increase in BAT UCP1 content occurs independently of ER $\alpha$  (T,  $P < 0.001$ ).

### Effects of CL and HFD on Blood Biochemistry

Adiponectin is an insulin-sensitizing adipokine (Berg et al., 2001; Fruebis et al., 2001; Yamauchi et al., 2001), and changes in adiponectin production and/or sensitivity has been proposed as a potential mechanism behind CLs insulin sensitizing effects. Others have observed increases in adiponectin (Fu et al., 2007) and adiponectin receptors (Fu et al., 2008) following CL administration. In our study, we observed CL-induced increases in circulating adiponectin only under HFD conditions (T $\times$ D,  $P = 0.037$ ) (Table 2). In fact, whereas ER $\alpha$ KOs had lower circulating adiponectin than WTs (G,  $P = 0.013$ ), that genotype difference was only present under NC diet conditions (G $\times$ D,  $P = 0.008$ ). CL did not affect fasting levels of insulin or glucose but reduced fasting NEFAs in both genotypes and dietary conditions (T,  $P = 0.004$ ) (Table 2).

### CL Increases ER $\beta$ Expression in WAT

To test the hypothesis that CL may improve adipocyte health by suppressing inflammation, we measured several inflammatory markers in various adipose tissue depots, but found no evidence of an anti-inflammatory effect of CL (SQAT inflammatory genes shown in Supplementary Figure S1). Next, we assessed how



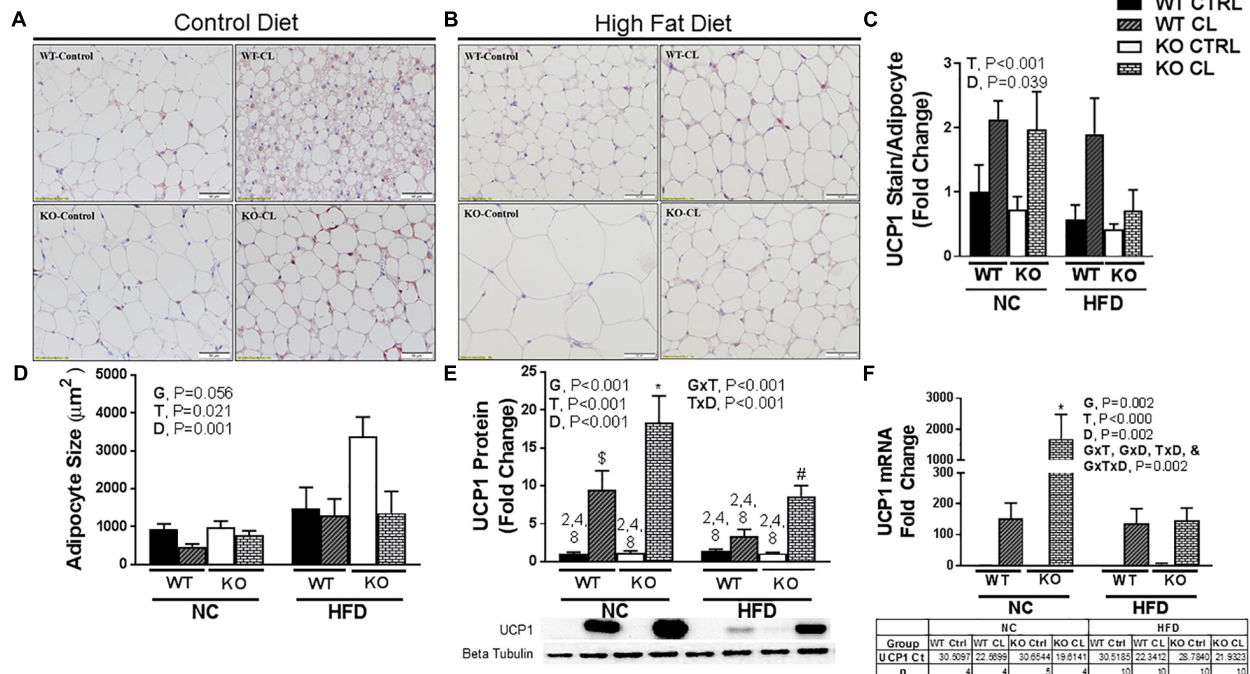


**FIGURE 5 |** CL 316,243 induces SQAT browning in WT and ER $\alpha$ KO mice. High-fat diet fed ER $\alpha$ KO and WT female mice were treated with selective  $\beta$ 3 agonist, CL 316,243, for 2 weeks. Assessments were made for differences in (A) NC, UCP1-positive stained subcutaneous adipose tissue (SQAT) histology, (B) HFD, UCP1-positive stained SQAT, (C) UCP1 stain per adipocyte, (D) adipocyte size ( $\mu$ m), (E) UCP1 protein expression, (F) UCP1 mRNA expression. WT, wild-type; KO, ER $\alpha$  knock-out; CTRL, saline control; CL, CL 316,243 treatment; NC, normal chow; HFD, high fat diet; data are expressed as means  $\pm$  standard error (SE);  $n = 4$ –10/group. G = significant main effect of genotype,  $P < 0.05$ . T = significant main effect of CL,  $P < 0.05$ . D = significant main effect of diet,  $P < 0.05$ . G  $\times$  T = significant interaction between genotype and treatment,  $P < 0.05$ . G  $\times$  D = significant interaction between genotype and diet,  $P < 0.05$ . G  $\times$  T  $\times$  D = significant interaction between genotype, treatment, and diet,  $P < 0.05$ . \*  $P < 0.05$  compared to all other groups; # compared to all except NC WT/CL; \$ compared to all except HFD KO/CL.

HFD and CL might affect ER $\alpha$  levels in the adipose tissues of WT mice (Figure 8). We confirmed previous findings (Gorres et al., 2011) that HFD significantly reduces ER $\alpha$  levels in WAT (Figures 8A,B). This was specific to WAT, as HFD did not affect BAT ER $\alpha$  levels (Figure 8C). Interestingly, CL treatment increased PGAT ER $\alpha$  levels and also increased in ER $\beta$  protein expression in both WAT depots (PGAT – T,  $P < 0.001$  and SQAT – T,  $P = 0.018$ ; Figures 8D,E) but not in BAT (Figure 8F). In line with what happened with UCP1 in PGAT, HFD mitigated the response of CL to increase ER $\beta$  (T  $\times$  D,  $P = 0.034$ ) and there was also a main effect of HFD to decrease ER $\beta$  expression in both WAT depots (both D,  $P < 0.001$ ), an effect that also occurred in both genotypes. Notably, ER $\alpha$ KOs were more susceptible to HFD-mediated reduction in PGAT ER $\beta$  expression compared to WTs (G  $\times$  D,  $P = 0.006$ ) which coincided with their overall higher susceptibility to HFD-induced metabolic dysfunction.

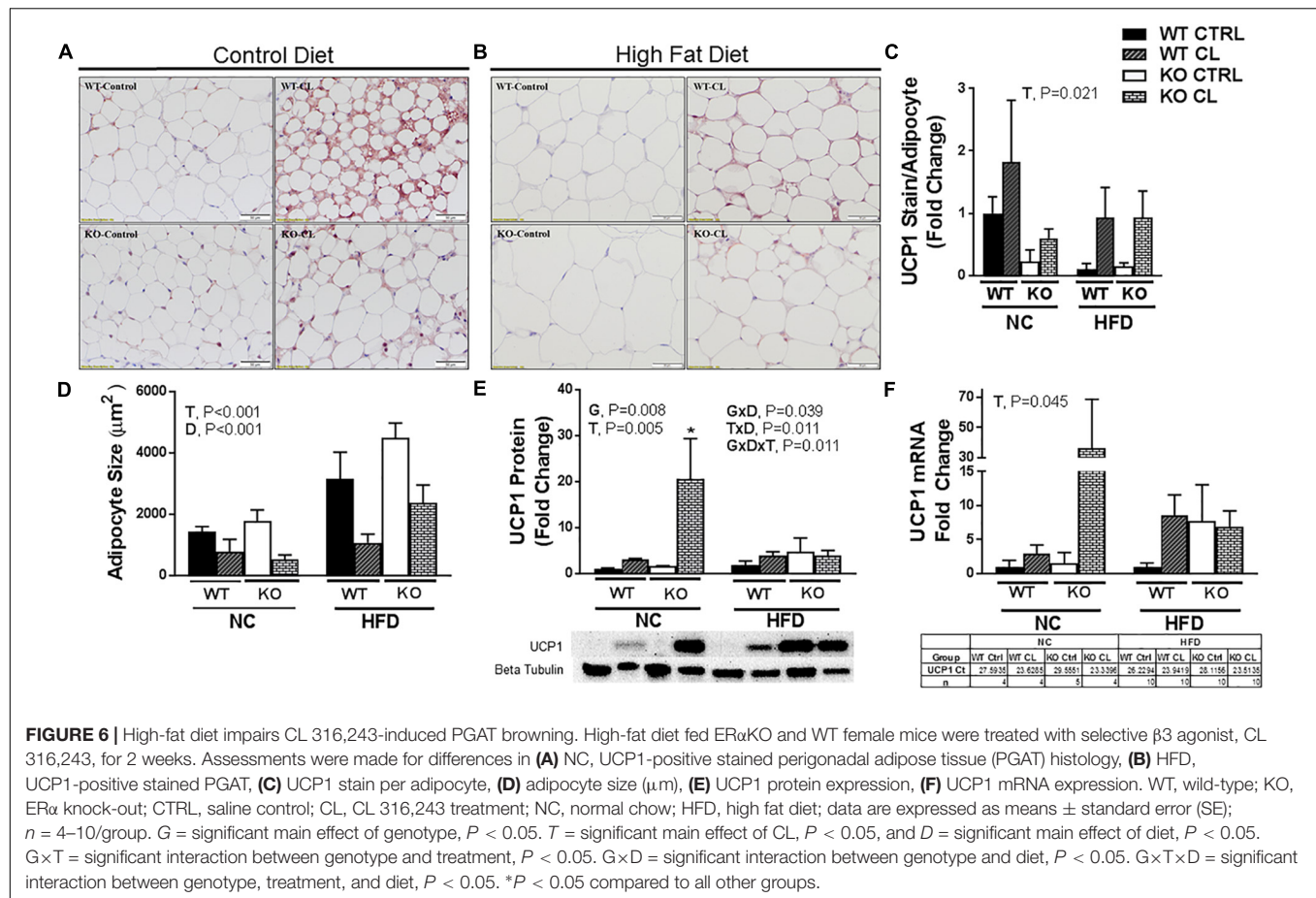
## DISCUSSION

$\beta$ 3 adrenergic activation via the compound, CL 314,243 (i.e., CL) restored metabolic health in a rodent model of menopause-associated metabolic dysfunction, the whole-body ER $\alpha$ KO mouse. CL caused WAT beiging, indicated by a CL-induced

increase in UCP1, and this correlated with systemic metabolic improvements such as reduced adiposity and improved insulin sensitivity, indicating that the ability of CL to induce adipocyte beiging and improve systemic metabolism does not require ER $\alpha$ . Another notable novel finding was that CL increased WAT ER $\beta$  expression, and this occurred similarly in both ER $\alpha$ KO and WT mice. Although the relationship between CL treatment and ER $\beta$  expression observed herein is only correlative, the possibility exists that this steroid receptor may play a role in mediating CL's beneficial effects. Future studies should further interrogate the mechanism driving the increase in ER $\beta$  as well as the potential role that ER $\beta$  plays in CL-mediated benefits. Taken together, our findings demonstrate that a short 2-week daily treatment with CL effectively restores metabolic health in a model of menopause-associated metabolic dysfunction, the ER $\alpha$ KO mouse.

Previous studies have shown that ER $\alpha$  ablation causes obesity and insulin resistance (Heine et al., 2000; Ohlsson et al., 2000; Davis et al., 2013). Furthermore, activation of ER $\alpha$  signaling protects female mice from diet-induced obesity (Yasrebi et al., 2016). And, studies investigating the role of brain ER signaling have demonstrated that central ER signaling protects against energy balance disturbances. Importantly, our previous studies show that weight gain following ovarian hormone loss is driven specifically by reduced energy expenditure. Here we confirm





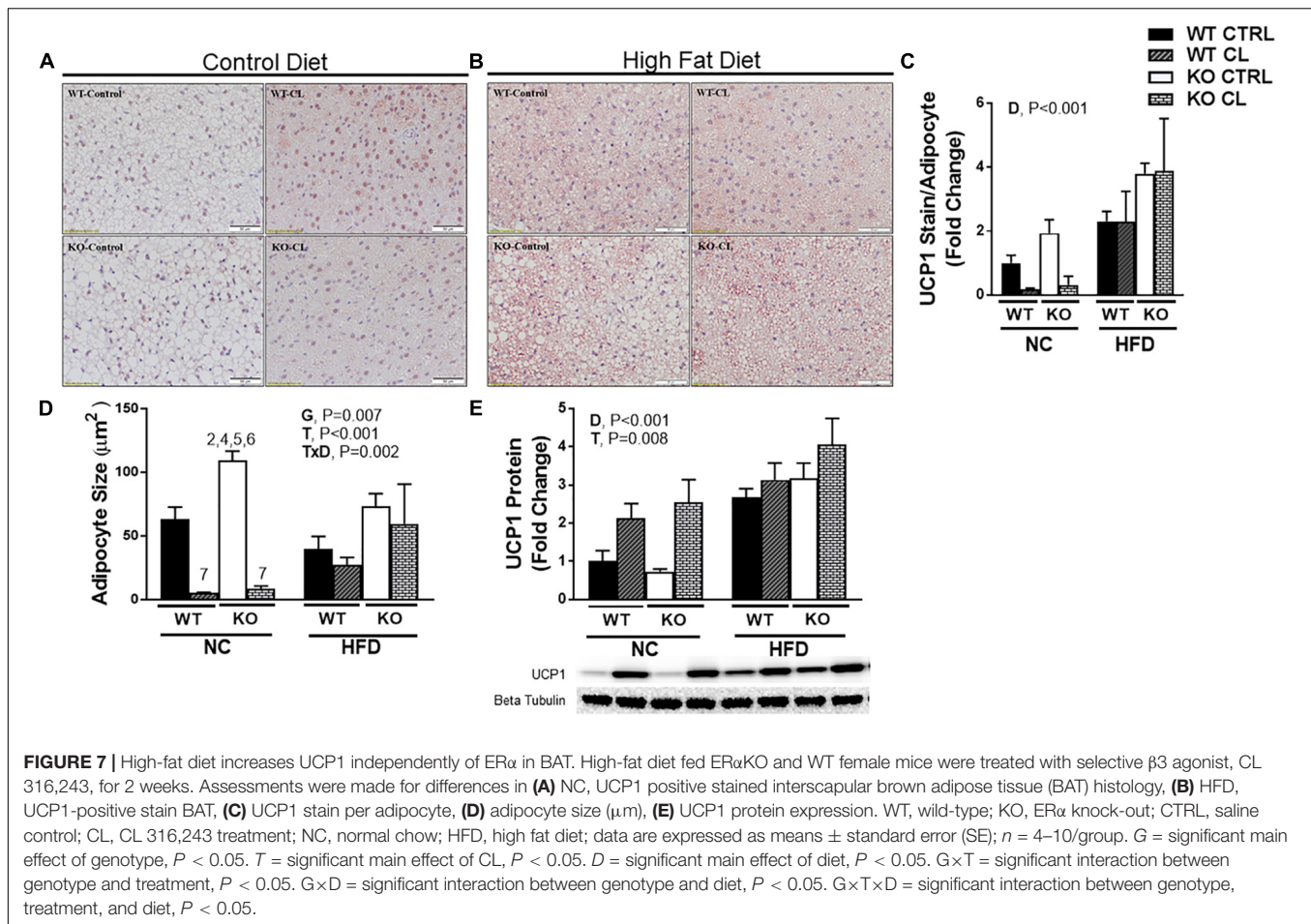
those findings, demonstrating while ERαKO do not consume more total energy when fed normal rodent chow (NC), they still experience significant weight gain due to suppressed energy expenditure. In addition, we found that the ERαKO overconsume energy when fed HFD and exemplify enhanced energy efficiency on HFD compared to WT, suggesting that the increased weight gain in ERαKO upon HFD feeding is twofold, due to increased energy intake and enhanced energy efficiency. Thus, we confirmed that female ERαKO mice are metabolically impaired compared to their WT counterparts under typically “healthy” NC feeding conditions (Ohlsson et al., 2000; Ribas et al., 2010; Gao and Dahlman-Wright, 2013), and this is exacerbated under HFD feeding, validating that ERα is protective against metabolic dysfunction. This is critical since levels of this steroid receptor diminish following menopause in humans, and this may be responsible for the significant increase in metabolic dysfunction, increasing risk for diabetes and cardiovascular disease among aging women.

ERαKO animals exhibited improvements in body weight, adiposity, and insulin sensitivity following CL, normalizing them to the WT/CTRL. In order to determine if the metabolic improvements attributed to CL treatment differ between WT and ERαKO mice, we fed WT (and ERαKO) HFD in order to induce weight gain and metabolic dysfunction in both genotypes. Confirming many other reports (Ogawa et al., 2003; Li and

Krashes, 2015; Park Y.M. et al., 2015), we observed reductions in SPA (G, *P* < 0.001) (Figure 4C) and TEE (G, *P* = 0.023) (Figure 4D) in the ERαKO animals in the rodent active period. Since energy intake was not affected, this reduction in SPA resulted in weight gain in those ERαKO mice (G, *P* < 0.001). However, CL-induced increase in TEE (T, *P* < 0.05) (Figure 4D) due to increased REE (T, *P* = 0.026) (Figure 4E) rescued that increase in body weight and reduced adiposity in the ERαKO.

Under HFD feeding conditions, both WT and ERαKO mice responded positively to CL treatment in terms of attenuation of weight gain and increase in insulin-stimulated glucose clearance. There was a genotype difference in dietary energy overconsumption on HFD, which contributed to the ERαKO gaining more weight on HFD, but CL normalized this in the ERαKO (Figure 4A). This may have contributed to the greater CL-induced weight loss in the ERαKO. Remarkably, CL's ability to both increase resting energy expenditure (Figure 4E) and reduce HFD energy intake were sufficient to prevent weight gain despite no changes in physical activity (Figure 4C).

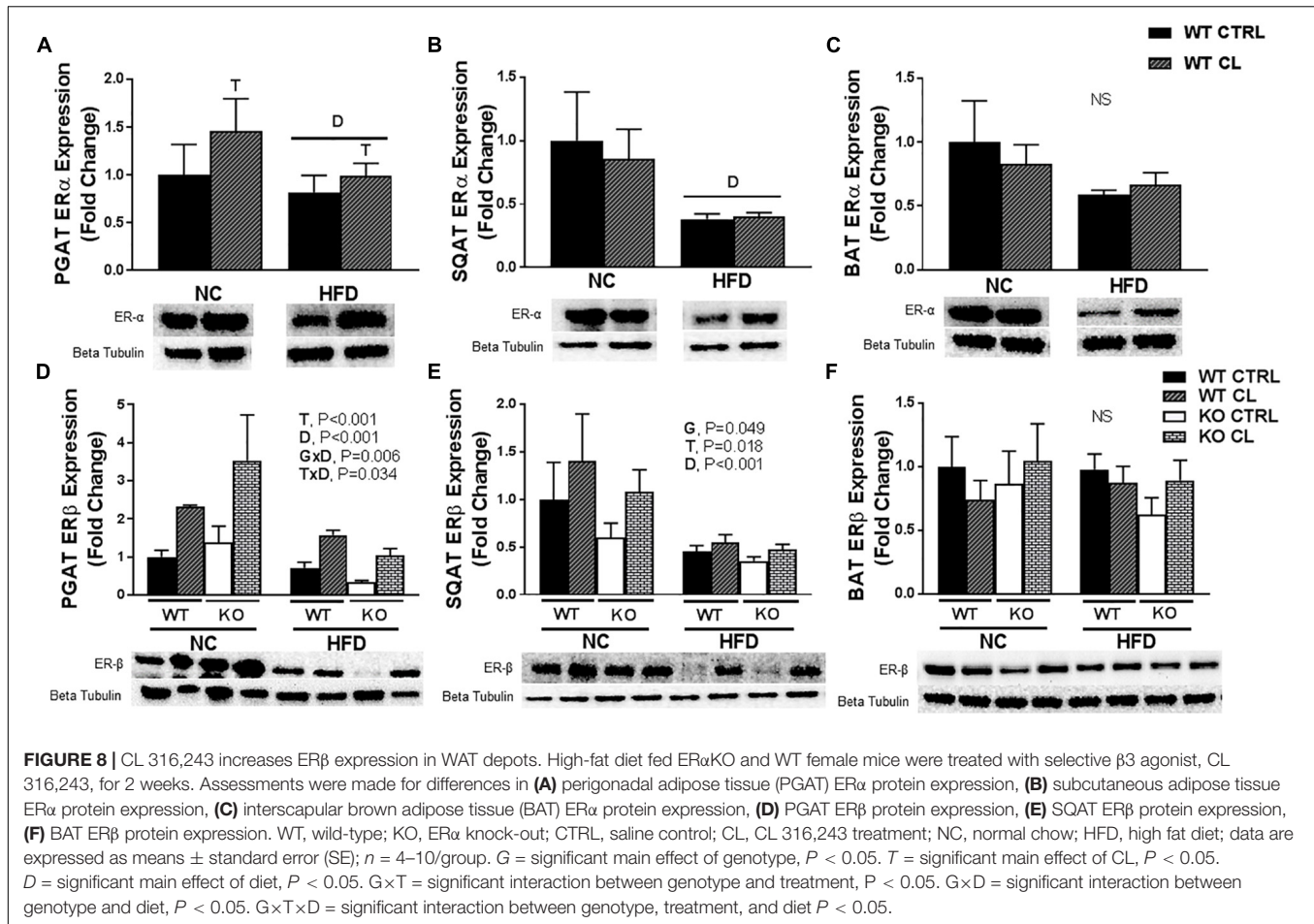
Similar to other studies performed in other models (Ghorbani et al., 2012; Poher et al., 2015), we found evidence that CL improved insulin sensitivity, although only surrogate measures of insulin sensitivity were used. A notable experimental problem was that CL induced hypoglycemia during the insulin tolerance testing procedure. While we consider this anecdotal evidence



of the insulin-sensitizing effect of CL (none of the vehicle-treated animals experienced hypoglycemia), future studies should perform the gold standard glucose clamp procedure in order to more accurately assess insulin sensitivity. Importantly, the insulin-mediated hypoglycemia occurred in both WT and KO mice (WT  $n = 8$ ; KO  $n = 5$ ), suggesting that both genotypes were sensitive to CL's effect. While the increase in energy expenditure was likely caused by activation of UCP1 (i.e., adipocyte beiging), the full mechanism responsible for CL-induced improvements remains elusive. In support of the hypothesis that CL-induced beiging of WAT was likely at least partially responsible, we demonstrated CL-induced WAT UCP1 increases in both WT and ER $\alpha$ KO mice. We also observed in both genotypes that animals fed HFD had an attenuated response to CL-induced increases in UCP1 in WAT (Figures 5, 6). Thus, HFD may lessen the therapeutic effectiveness of  $\beta$ 3 adrenergic agonists. It is possible that the CL-induced increase in UCP1 may contribute to the insulin-sensitizing effects of CL, although studies need to be conducted in UCP1-null animals in order to directly test this hypothesis. Importantly, we previously demonstrated in female mice that UCP1 has insulin-sensitizing effects that may be independent of adiposity changes (Winn et al., 2017) and respond more adversely to ovariectomy compared to WT controls (Clookey et al., 2018).

Some evidence suggests that ER $\alpha$  may facilitate WAT browning by increasing sensitivity to browning stimuli in progenitor cells (Lapid et al., 2014). This topic was reviewed recently (Frank et al., 2017). Here, we demonstrate that CL improves metabolic health in ER $\alpha$ KO mice, demonstrating that the metabolic benefits of CL do not require ER $\alpha$ . Further, CL-induced browning was indicated by both increased UCP1 content and adipocyte phenotypic changes in both genotypes. However, under NC dietary conditions, visual examination of the WT WAT following CL indicated smaller, more multilocular adipocytes compared to that of the ER $\alpha$ KO/CL suggesting that loss of ER $\alpha$  signaling may impair beiging. Because this genotype difference did not hold true under HFD feeding conditions, the differential response under NC conditions may have been attributed to the greater adiposity in ER $\alpha$ KOs, and not necessarily their lack of ER $\alpha$ . In fact, ER $\alpha$ KOs appeared more sensitive to CL when assessed for total UCP1 protein and RNA expression in response to CL compared to WT (Figures 5, 6). And, responses to CL in the HFD-fed WT and the NC-fed ER $\alpha$ KO (i.e., adjusting for adiposity difference between KO and WT) were strikingly similar.

While cold is the main stimulus for UCP1 increases in BAT, diet-induced obesity also increases BAT UCP1 (Feldmann et al., 2009; Cannon and Nedergaard, 2010; Yao et al., 2014; Sakamoto et al., 2016; Winn et al., 2017). Obesity-induced increases in



BAT UCP1 may serve as a means to restore energy balance during energy surplus. We previously observed that ovariectomy-induced obesity also increases BAT UCP1 (Vieira-Potter et al., 2015). However, that finding was surprising to us since other studies have shown that estrogen increases UCP1 gene expression and BAT activity in rodents (Pedersen et al., 2001; Martinez de Morentin et al., 2014) and humans (Valle et al., 2008; Velickovic et al., 2014). Clearly, the relationship between estrogen and UCP1 is complex and far from completely understood. Here, we show that obesity induced by ERα ablation does not significantly increase BAT UCP1, yet HFD-induced obesity did induce BAT UCP1 both in WT and ERαKO mice. CL did not further increase BAT UCP1 under HFD conditions (Figure 7E), perhaps due to a ceiling effect of BAT UCP1. Previous studies have also reported that CL more potently induces UCP1 in WAT (i.e., induces beige) than BAT and supports the hypothesis that the beneficial effects of CL are mediated more through WAT than BAT (Poher et al., 2015). This is of particular relevance and importance since we have far greater relative abundance of WAT than BAT.

A novel observation made in this present study was that ERβ protein expression also increased with CL, specifically in WAT depots, paralleling what was observed with UCP1. Again, strikingly similar to the effects on UCP1, the ability of CL to increase ERβ was attenuated under conditions of HFD (Figure 8).

Notably, ERβ ligands have been shown to reduce body weight and fat mass (Ponnusamy et al., 2016; Gonzalez-Granillo et al., 2019) and rescue ovariectomy-induced obesity (Yepuru et al., 2010). Moreover, ERβ ligands increase oxygen consumption and mitochondrial activity (Ponnusamy et al., 2016), and increase UCP1 protein in BAT (Yepuru et al., 2010; Ponnusamy et al., 2016 #124). Although we did not observe any changes in ERβ in BAT, we did observe increases in this protein in WAT, the depot where CL most strongly induces UCP1 expression. Thus, CL's effects may be mediated via interaction with ERβ. In thinking about potential mechanisms, this nuclear hormone receptor shares a similar cofactor pool to that of PPARγ, another nuclear hormone receptor (Foryst-Ludwig et al., 2008), which is known to enhance insulin sensitivity and induce adipocyte proliferation. In cell culture, ERβ inhibits PPARγ activity (i.e., adipogenic gene expression and adipogenesis) (Chu et al., 2014) while CL also has been shown to suppress PPARγ (Li et al., 2017), a finding that may explain CL's ability to suppress adiponectin production, which requires PPARγ. In support of that hypothesis, ERαKO (but not WT) were resistant to HFD-induced decrease in circulating adiponectin levels. It is noteworthy that adiponectin, besides increasing insulin sensitivity, activates central AMPK, which is known to activate feeding centers in the brain and suppress BAT UCP1 levels, thereby enhancing energy storage via hyperphagia



and increased energy efficiency (i.e., via reduced diet-induced thermogenesis) (Martinez de Morentin et al., 2014). Thus, in WT mice, HFD-induced reduction in adiponectin levels was consistent with their protection from excess HFD-induced energy intake and HFD-induced BAT UCP1 increase, both observed in the ER $\alpha$ KO. The effect of CL on ER $\beta$  and its crosstalk with PPAR $\gamma$  certainly requires further investigation.

The findings of this study should be considered in light of its potential limitations. First, we used the ER $\alpha$ KO model, which still produces ovarian estrogen yet does not have ER $\alpha$ —mediated estrogen signaling in any tissues. This is different from human menopause where women display reduced production of ovarian estrogen and thus reduced signaling, but still have functional ERs. Future studies should compare the efficacy of CL treatment in ovary-intact vs. ovariectomized rodents. Secondly, we chose to conduct our studies at thermoneutrality because cooler temperatures may affect metabolic parameters in rodents. That is, we wanted to isolate the effects of CL from those induced by cold. A recent study showed that C57BL/6J mice are not more susceptible to HFD-induced insulin resistance, but cooler temperatures do cause the rodents to increase energy expenditure (which is coupled with increased intake) (Small et al., 2018). Notwithstanding, future studies should test how environmental temperature affects responses to CL in this animal model. In addition, the studies performed herein were only done in whole body ER $\alpha$ KO and WT mice. Since ER $\alpha$  is expressed in many tissues, and has various developmental roles, it is also critical to perform these studies in conditional knock-out models, where ER can be experimentally suppressed after development, as well as in adipose tissue-specific ER knock out models. Finally, it is important to note that the diets used in this study were not free of soy phytoestrogens, which are weak ER ligands. Thus, interactions between soy phytoestrogens and CL treatment could not be determined in the current study; future studies should determine the role(s) played by endogenous, exogenous, and dietary estrogens.

## OVERALL CONCLUSION

Postmenopausal women are at heightened risk for obesity and its related metabolic disorders (Carr, 2003; Dubnov-Raz et al., 2007; Teede et al., 2010), whereas estrogen-sufficient females have superior metabolic health, more relative BAT, and may be more responsive to WAT beiging (Himms-Hagen, 1989; Cypess et al., 2009; Pfannenberger et al., 2010; Ouellet et al., 2011; Kim et al., 2016). Mechanisms are not fully understood, but suppressed estrogen signaling through ER $\alpha$  is thought to play a major role in the adipose tissue dysfunction that follows hormone loss (Heine et al., 2000; Ohlsson et al., 2000; Geary et al., 2001; Liang et al., 2002; Ribas et al., 2010; Davis et al., 2013). We sought to determine if the adipose tissue and systemic metabolic dysfunction caused by loss of estrogen signaling through ER $\alpha$  could be rescued by systemic  $\beta_3$  adrenergic receptor activation via CL 316,243, a known  $\beta_3$  adrenergic receptor agonist. Further, we determined if the effectiveness of this drug to induce WAT

beiging and improve metabolism varies in the presence and absence of systemic ER $\alpha$  and under normal chow and high-fat (i.e., Western style) dietary conditions. We discovered that CL effectively rescues HFD- and ER $\alpha$  ablation-induced metabolic dysfunction, and that ER $\alpha$ -null animals may be more sensitive to WAT UCP1 induction. Finally, HFD feeding may interfere with CL's effectiveness to activate UCP1, which may be an important consideration for utilizing  $\beta_3$  adrenergic agonists as a therapeutic for obesity.

## AUTHOR CONTRIBUTIONS

SC, RW, DS, and MW performed the experiments. SC, RW, and VV-P analyzed the data. SC and VV-P interpreted the results and prepared the manuscript. SC and RW prepared the figures. SC, RW, JP, DL, KF, RR, and VV-P revised and edited the manuscript. SC, RW, DS, MW, DL, JP, KF, RR, and VV-P approved final version of the manuscript. VV-P conceived and designed the research.

## FUNDING

This study was supported in parts by grants from the University of Missouri Research Council (VV-P), Flynn Faculty Scholar Award (VV-P), National Institutes of Health K01-HL-125503 (JP), and VA Merit Grant I01BX003271-01 (RR). DL provided all of the mice used in these studies. This work was partially supported with resources and the use of facilities at the Harry S. Truman Memorial Veterans' Hospital in Columbia, MO, United States.

## SUPPLEMENTARY MATERIAL

The Supplementary Material for this article can be found online at: <https://www.frontiersin.org/articles/10.3389/fphys.2019.00009/full#supplementary-material>

**FIGURE S1** | Normal chow and high-fat diet comparison of body weight, energy intake, depot weights, adipose tissue inflammatory gene expression, adipose tissue UCP2 protein content, liver triglycerides, and insulin resistance. Normal chow and high-fat diet fed ER $\alpha$ KO and WT female mice were treated with selective  $\beta_3$  agonist, CL 316,243, for 2 weeks. Assessments were made for differences in (A) body weight, (B) energy intake, (C) subcutaneous adipose tissue (SQAT) depot weight, (D) perigonadal adipose tissue (PGAT) depot weight, (E) brown adipose tissue (BAT) depot weight, (F) HOMA-IR, (G) ADIPO-IR, (H) subcutaneous adipose tissue integrin (CD11c) gene expression, (I) subcutaneous adipose tissue tumor necrosis factor alpha (TNF $\alpha$ ) gene expression, (J) perigonadal adipose tissue (PGAT) UCP2 expression, (K) subcutaneous adipose tissue (SQAT) UCP2 expression, (L) brown adipose tissue (BAT) UCP2 expression, (M) liver triglyceride content. WT, wild-type; KO, ER $\alpha$  knock-out; CTRL, saline control; CL, CL 316,243 treatment; NC, normal chow; HFD, high fat diet; data are expressed as means  $\pm$  standard error (SE);  $n = 4-10$ /group. G, significant main effect of genotype,  $P < 0.05$ . T, significant main effect of CL,  $P < 0.05$ . D, significant main effect of diet,  $P < 0.05$ . GxT, significant interaction between genotype and treatment,  $P < 0.05$ . GxD, significant interaction between genotype and diet,  $P < 0.05$ . GxTxD, significant interaction between genotype, treatment, and diet,  $P < 0.05$ .



## REFERENCES

- Auro, K., Joensuu, A., Fischer, K., Kettunen, J., Salo, P., Mattsson, H., et al. (2014). A metabolic view on menopause and ageing. *Nat. Commun.* 5:4708. doi: 10.1038/ncomms5708
- Bartelt, A., and Heeren, J. (2014). Adipose tissue browning and metabolic health. *Nat. Rev. Endocrinol.* 10, 24–36. doi: 10.1038/nrendo.2013.204
- Berg, A. H., Combs, T. P., Du, X., Brownlee, M., and Scherer, P. E. (2001). The adipocyte-secreted protein Acrp30 enhances hepatic insulin action. *Nat. Med.* 7, 947–953. doi: 10.1038/90992
- Bloom, J. D., Dutia, M. D., Johnson, B. D., Wissner, A., Burns, M. G., Largis, E. E., et al. (1992). Disodium (R, R)-5-[2-[[2-(3-chlorophenyl)-2-hydroxyethyl] amino] propyl]-1, 3-benzodioxole-2, 2-dicarboxylate (CL 316,243). A potent. beta-adrenergic agonist virtually specific for. beta. 3 receptors. A promising antidiabetic and antiobesity agent. *J. Med. Chem.* 35, 3081–3084. doi: 10.1021/jm00094a025
- Borst, S. E., and Hennessy, M. (2001).  $\beta$ -3 Adrenergic agonist restores skeletal muscle insulin responsiveness in sprague-dawley rats. *Biochem. Biophys. Res. Commun.* 289, 1188–1191. doi: 10.1006/bbrc.2001.6075
- Brand, J. S., van der Schouw, Y. T., Onland-Moret, N. C., Sharp, S. J., Ong, K. K., Khaw, K. T., et al. (2012). Age at menopause, reproductive life span, and type 2 diabetes risk: results from the EPIC-InterAct study. *Diabetes Care* 36, 1012–1019. doi: 10.2337/dc12-1020
- Cannon, B., and Nedergaard, J. (2010). Metabolic consequences of the presence or absence of the thermogenic capacity of brown adipose tissue in mice (and probably in humans). *Int. J. Obes.* 34:S7. doi: 10.1038/ijo.2010.177
- Carr, M. C. (2003). The emergence of the metabolic syndrome with menopause. *J. Clin. Endocrinol. Metab.* 88, 2404–2411. doi: 10.1210/jc.2003-030242
- Chu, R., van Hasselt, A., Vlantis, A. C., Ng, E. K., Liu, S. Y., Fan, M. D., et al. (2014). The cross-talk between estrogen receptor and peroxisome proliferator-activated receptor gamma in thyroid cancer. *Cancer* 120, 142–153. doi: 10.1002/cncr.28383
- Clookey, S. L., Welly, R. J., Zidon, T. M., Gastecki, M. L., Woodford, M. L., Grunewald, Z. I., et al. (2018). Increased susceptibility to OVX-associated metabolic dysfunction in UCP1-null mice. *J. Endocrinol.* 239, 107–120. doi: 10.1530/JOE-18-0139
- Cypess, A. M., Lehman, S., Williams, G., Tal, I., Rodman, D., Goldfine, A. B., et al. (2009). Identification and importance of brown adipose tissue in adult humans. *N. Engl. J. Med.* 360, 1509–1517. doi: 10.1056/NEJMoa0810780
- Davis, K. E., Neinast, D. M., Sun, K., Skiles, W. M., Bills, J. D., Zehr, J. A., et al. (2013). The sexually dimorphic role of adipose and adipocyte estrogen receptors in modulating adipose tissue expansion, inflammation, and fibrosis. *Mol. Metab.* 2, 227–242. doi: 10.1016/j.molmet.2013.05.006
- D'Eon, T. M., Souza, S. C., Aronovitz, M., Obin, M. S., Fried, S. K., and Greenberg, A. S. (2005). Estrogen regulation of adiposity and fuel partitioning. Evidence of genomic and non-genomic regulation of lipogenic and oxidative pathways. *J. Biol. Chem.* 280, 35983–35991. doi: 10.1074/jbc.M507339200
- Dubnov-Raz, G., Pines, A., and Berry, E. (2007). Diet and lifestyle in managing postmenopausal obesity. *Climacteric* 10, 38–41. doi: 10.1080/13697130701586428
- Eddy, E., Washburn, T. F., Bunch, D. O., Goulding, E. H., Gladen, B. C., Lubahn, D. B., et al. (1996). Targeted disruption of the estrogen receptor gene in male mice causes alteration of spermatogenesis and infertility. *Endocrinology* 137, 4796–4805. doi: 10.1210/endo.137.11.8895349
- Feldmann, H. M., Golozoubova, V., Cannon, B., and Nedergaard, J. (2009). UCP1 ablation induces obesity and abolishes diet-induced thermogenesis in mice exempt from thermal stress by living at thermoneutrality. *Cell Metab.* 9, 203–209. doi: 10.1016/j.cmet.2008.12.014
- Forst-Ludwig, A., Clemenz, M., Hohmann, S., Hartge, M., Sprang, C., Frost, N., et al. (2008). Metabolic actions of estrogen receptor beta (ERbeta) are mediated by a negative cross-talk with PPARgamma. *PLoS Genet* 4:e1000108. doi: 10.1371/journal.pgen.1000108
- Frank, A. P., Palmer, B. F., and Clegg, D. J. (2017). Do estrogens enhance activation of brown and beige of adipose tissues? *Physiol. Behav.* 187, 24–31. doi: 10.1016/j.physbeh.2017.09.026
- Fruebis, J., Tsao, T.-S., Javorschi, S., Ebbets-Reed, D., Erickson, M. R. S., Yen, F. T., et al. (2001). Proteolytic cleavage product of 30-kDa adipocyte complement-related protein increases fatty acid oxidation in muscle and causes weight loss in mice. *Proc. Natl. Acad. Sci. U.S.A.* 98, 2005–2010. doi: 10.1073/pnas.98.4.\break2005
- Fu, L., Isobe, K., Zeng, Q., Suzukawa, K., Takekoshi, K., and Kawakami, Y. (2007).  $\beta$ -adrenoceptor agonists downregulate adiponectin, but upregulate adiponectin receptor 2 and tumor necrosis factor- $\alpha$  expression in adipocytes. *Eur. J. Pharmacol.* 569, 155–162. doi: 10.1016/j.ejphar.2007.05.005
- Fu, L., Isobe, K., Zeng, Q., Suzukawa, K., Takekoshi, K., and Kawakami, Y. (2008). The effects of  $\beta$ 3-adrenoceptor agonist CL-316,243 on adiponectin, adiponectin receptors and tumor necrosis factor- $\alpha$  expressions in adipose tissues of obese diabetic KKAY mice. *Eur. J. Pharmacol.* 584, 202–206. doi: 10.1016/j.ejphar.2008.01.028
- Gao, H., and Dahlman-Wright, K. (2013). Implications of estrogen receptor alpha and estrogen receptor beta for adipose tissue functions and cardiometabolic complications. *Horm. Mol. Biol. Clin. Investig.* 15, 81–90. doi: 10.1515/hmbci-2013-0021
- Geary, N., Asarian, L., Korach, K. S., Pfaff, D. W., and Ogawa, S. (2001). Deficits in E2-dependent control of feeding, weight gain, and cholecystokinin satiation in ER- $\alpha$  null mice. *Endocrinology* 142, 4751–4757. doi: 10.1210/endo.142.11.8504
- Ghorbani, M., and Himms-Hagen, J. (1997). Appearance of brown adipocytes in white adipose tissue during CL 316,243-induced reversal of obesity and diabetes in Zucker fa/fa rats. *Int. J. Obes.* 21, 465–475. doi: 10.1038/sj.ijo.0800432
- Ghorbani, M., Shafiee Ardestani, M., Gigloo, S. H., Cohan, R. A., Inanlou, D. N., and Ghorbani, P. (2012). Anti diabetic effect of CL 316,243 (a beta3-adrenergic agonist) by down regulation of tumour necrosis factor (TNF- $\alpha$ ) expression. *PLoS One* 7:e45874. doi: 10.1371/journal.pone.0045874
- Gonzalez-Granillo, M., Savva, C., Li, X., Fitch, M., Pedrelli, M., Hellerstein, M., et al. (2019). ERbeta activation in obesity improves whole body metabolism via adipose tissue function and enhanced mitochondria biogenesis. *Mol. Cell. Endocrinol.* 479, 147–158. doi: 10.1016/j.mce.2018.10.007
- Gorres, B. K., Bomhoff, G. L., Gupte, A. A., and Geiger, P. C. (2011). Altered estrogen receptor expression in skeletal muscle and adipose tissue of female rats fed a high-fat diet. *J. Appl. Physiol.* 110, 1046–1053. doi: 10.1152/japplphysiol.00541.2010
- Granneman, J. G., Burnazi, M., Zhu, Z., and Schwamb, L. A. (2003). White adipose tissue contributes to UCP1-independent thermogenesis. *Am. J. Physiol. Endocrinol. Metab.* 285, E1230–E1236. doi: 10.1152/ajpendo.00197.2003
- Heine, P., Taylor, J., Iwamoto, G., Lubahn, D., and Cooke, P. (2000). Increased adipose tissue in male and female estrogen receptor- $\alpha$  knockout mice. *Proc. Natl. Acad. Sci. U.S.A.* 97, 12729–12734. doi: 10.1073/pnas.97.23.12729
- Himms-Hagen, J. (1989). Brown adipose tissue thermogenesis and obesity. *Prog. Lipid Res.* 28, 67–115. doi: 10.1016/0163-7827(89)90009-X
- Himms-Hagen, J., Cui, J., Danforth, E., Taatjes, D. J. Jr., Lang, S. S., Waters, B. L., et al. (1994). Effect of CL-316,243, a thermogenic beta 3-agonist, on energy balance and brown and white adipose tissues in rats. *Am. J. Physiol.* 266(4 Pt 2), R1371–R1382. doi: 10.1152/ajpregu.1994.266.4.R1371
- Kim, J. H., Cho, H. T., and Kim, Y. J. (2014). The role of estrogen in adipose tissue metabolism: insights into glucose homeostasis regulation. *Endocr. J.* 61, 1055–1067. doi: 10.1507/endocrj.EJ14-0262
- Kim, S.-N., Jung, Y.-S., Kwon, H.-J., Seong, J. K., Granneman, J. G., and Lee, Y.-H. (2016). Sex differences in sympathetic innervation and browning of white adipose tissue of mice. *Biol. Sex Differ.* 7:67. doi: 10.1186/s13293-016-0121-7
- Klinge, C. M. (2008). Estrogenic control of mitochondrial function and biogenesis. *J. Cell. Biochem.* 105, 1342–1351. doi: 10.1002/jcb.21936
- Klötting, N., Fasshauer, M., Dietrich, A., Kovacs, P., Schön, M. R., Kern, M., et al. (2010). Insulin-sensitive obesity. *Am. J. Physiol. Endocrinol. Metab.* 299, E506–E515. doi: 10.1152/ajpendo.00586.2009
- Lapid, K., Lim, A., Clegg, D. J., Zeve, D., and Graff, J. M. (2014). Oestrogen signalling in white adipose progenitor cells inhibits differentiation into brown adipose and smooth muscle cells. *Nat. Commun.* 5:5196. doi: 10.1038/ncomms6196
- Li, C., and Krashes, M. J. (2015). Hypoactivity following perturbed estrogen signaling in the medial amygdala. *J. Clin. Invest.* 125, 2576–2578. doi: 10.1172/JCI82578
- Li, Y. L., Li, X., Jiang, T. T., Fan, J. M., Zheng, X. L., Shi, X. E., et al. (2017). An additive effect of promoting thermogenic gene expression in mice adipose-derived stromal vascular cells by combination of rosiglitazone and CL316,243. *Int. J. Mol. Sci.* 18:E1002. doi: 10.3390/ijms18051002

- Liang, Y., Akishita, M., Kim, S., Ako, J., Hashimoto, M., Iijima, K., et al. (2002). Estrogen receptor beta is involved in the anorectic action of estrogen. *Int. J. Obes. Relat. Metab. Disord.* 26, 1103–1109. doi: 10.1038/sj.ijo.0802054
- Lomonaco, R., Ortiz-Lopez, C., Orsak, B., Webb, A., Hardies, J., Darland, C., et al. (2012). Effect of adipose tissue insulin resistance on metabolic parameters and liver histology in obese patients with nonalcoholic fatty liver disease. *Hepatology* 55, 1389–1397. doi: 10.1002/hep.25539
- Lubahn, D. B., Moyer, J. S., Golding, T. S., Couse, J. F., Korach, K. S., and Smithies, O. (1993). Alteration of reproductive function but not prenatal sexual development after insertional disruption of the mouse estrogen receptor gene. *Proc. Natl. Acad. Sci. U.S.A.* 90, 11162–11166. doi: 10.1073/pnas.90.23.11162
- Luglio, H. F. (2014). Estrogen and body weight regulation in women: the role of estrogen receptor alpha (ER- $\alpha$ ) on adipocyte lipolysis. *Acta Med Indones* 46, 333–338.
- Martinez de Morentin, P. B., Gonzalez-Garcia, I., Martins, L., Lage, R., Fernandez-Mallo, V., Martinez-Sanchez, N., et al. (2014). Estradiol regulates brown adipose tissue thermogenesis via hypothalamic AMPK. *Cell Metab.* 20, 41–53. doi: 10.1016/j.cmet.2014.03.031
- Matthews, D. R., Hosker, J. P., Rudenski, A. S., Naylor, B. A., Treacher, D. F., and Turner, R. C. (1985). Homeostasis model assessment: insulin resistance and beta-cell function from fasting plasma glucose and insulin concentrations in man. *Diabetologia* 28, 412–419. doi: 10.1007/BF00280883
- Mauvais-Jarvis, F., Clegg, D. J., and Hevener, A. L. (2013). The role of estrogens in control of energy balance and glucose homeostasis. *Endocr. Rev.* 34, 309–338. doi: 10.1210/er.2012-1055
- Morselli, E., Fuente-Martin, E., Finan, B., Kim, M., Frank, A., Garcia-Caceres, C., et al. (2014). Hypothalamic PGC-1 $\alpha$  protects against high-fat diet exposure by regulating ER $\alpha$ . *Cell Rep.* 9, 633–645. doi: 10.1016/j.celrep.2014.09.025
- Ogawa, S., Chan, J., Gustafsson, J. A., Korach, K. S., and Pfaff, D. W. (2003). Estrogen increases locomotor activity in mice through estrogen receptor alpha: specificity for the type of activity. *Endocrinology* 144, 230–239. doi: 10.1210/en.2002-220519
- Ogden, C. L., Carroll, M. D., Kit, B. K., and Flegal, K. M. (2012). Prevalence of obesity among adults: United States. *NCHS Data Brief* 1–8.
- Ohlsson, C., Hellberg, N., Parini, P., Vidal, O., Bohlooly, M., Rudling, M., et al. (2000). Obesity and disturbed lipoprotein profile in estrogen receptor- $\alpha$ -deficient male mice. *Biochem. Biophys. Res. Commun.* 278, 640–645. doi: 10.1006/bbrc.2000.3827
- Ouellet, V., Routhier-Labadie, A., Bellemare, W., Lakhal-Chaieb, L., Turcotte, E., Carpentier, A. C., et al. (2011). Outdoor temperature, age, sex, body mass index, and diabetic status determine the prevalence, mass, and glucose-uptake activity of 18F-FDG-detected BAT in humans. *J. Clin. Endocrinol. Metab.* 96, 192–199. doi: 10.1210/jc.2010-0989
- Padilla, J., Jenkins, N. T., Roberts, M. D., Arce-Esquivel, A. A., Martin, J. S., Laughlin, M. H., et al. (2013). Differential changes in vascular mRNA levels between rat iliac and renal arteries produced by cessation of voluntary running. *Exp. Physiol.* 98, 337–347. doi: 10.1113/expphysiol.2012.066076
- Pang, Z., Wu, N., Zhang, X., Avallone, R., Croci, T., Dressler, H., et al. (2010). GPR40 is partially required for insulin secretion following activation of beta3-adrenergic receptors. *Mol. Cell. Endocrinol.* 325, 18–25. doi: 10.1016/j.mce.2010.04.014
- Park, J. W., Jung, K.-H., Lee, J. H., Quach, C. S., Moon, H., Cho, Y. S., et al. (2015). 18F-FDG PET/CT monitoring of  $\beta$ 3 agonist-stimulated brown adipocyte recruitment in white adipose tissue. *J. Nucl. Med.* 56, 153–158. doi: 10.2967/jnumed.114.147603
- Park, Y. M., Rector, R. S., Thyfault, J. P., Zidon, T. M., Padilla, J., Welly, R. J., et al. (2015). Effects of ovariectomy and intrinsic aerobic capacity on tissue-specific insulin sensitivity. *Am. J. Physiol. Endocrinol. Metab.* 310, E190–E199. doi: 10.1152/ajpendo.00434.2015
- Park, Y. M., Pereira, R. I., Erickson, C. B., Swibas, T. A., Cox-York, K. A., and Van Pelt, R. E. (2017). Estradiol-mediated improvements in adipose tissue insulin sensitivity are related to the balance of adipose tissue estrogen receptor alpha and beta in postmenopausal women. *PLoS One* 12:e0176446. doi: 10.1371/journal.pone.0176446
- Pedersen, S. B., Bruun, J. M., Kristensen, K., and Richelsen, B. (2001). Regulation of UCP1, UCP2, and UCP3 mRNA expression in brown adipose tissue, white adipose tissue, and skeletal muscle in rats by estrogen. *Biochem. Biophys. Res. Commun.* 288, 191–197. doi: 10.1006/bbrc.2001.5763
- Pfannenberger, C., Werner, M. K., Ripkens, S., Stef, I., Deckert, A., Schmadl, M., et al. (2010). Impact of age on the relationships of brown adipose tissue with sex and adiposity in humans. *Diabetes Metab. Res. Rev.* 59, 1789–1793. doi: 10.2337/db10-0004
- Poher, A. L., Veyrat-Durebex, C., Altirriba, J., Montet, X., Colin, D. J., Caillon, A., et al. (2015). Ectopic UCP1 overexpression in white adipose tissue improves insulin sensitivity in Lou/C rats, a model of obesity resistance. *Diabetes Metab. Res. Rev.* 64, 3700–3712. doi: 10.2337/db15-0210
- Ponnusamy, S., Tran, Q. T., Harvey, I., Smallwood, H. S., Thiyagarajan, T., Banerjee, S., et al. (2016). Pharmacologic activation of estrogen receptor  $\beta$  increases mitochondrial function, energy expenditure, and brown adipose tissue. *FASEB J.* 31, 266–281. doi: 10.1096/fj.201600787RR
- Riant, E., Waget, A., Cogo, H. J., Arnal, F., Burcelin, R., and Gourdy, P. (2009). Estrogens protect against high-fat diet-induced insulin resistance and glucose intolerance in mice. *Endocrinology* 150, 2109–2117. doi: 10.1210/en.2008-0971
- Ribas, V., Nguyen, M. A., Henstridge, D. C., Nguyen, A.-K., Beaven, S. W., Watt, M. J., et al. (2010). Impaired oxidative metabolism and inflammation are associated with insulin resistance in ER $\alpha$ -deficient mice. *Am. J. Physiol. Endocrinol. Metab.* 298, E304–E319. doi: 10.1152/ajpendo.00504.2009
- Roseguini, B. T., Mehmet Soylu, S., Whyte, J. J., Yang, H. T., Newcomer, S., and Laughlin, M. H. (2010). Intermittent pneumatic leg compressions acutely upregulate VEGF and MCP-1 expression in skeletal muscle. *Am. J. Physiol. Heart Circ. Physiol.* 298, H1991–H2000. doi: 10.1152/ajpheart.00006.2010
- Sakamoto, T., Nitta, T., Maruno, K., Yeh, Y.-S., Kuwata, H., Tomita, K., et al. (2016). Macrophage infiltration into obese adipose tissues suppresses the induction of UCP1 level in mice. *Am. J. Physiol. Endocrinol. Metab.* 310, E676–E687. doi: 10.1152/ajpendo.00028.2015
- Scudiero, R., and Verderame, M. (2017). Gene expression profile of estrogen receptors alpha and beta in rat brain during aging and following high fat diet. *C. R. Biol.* 340, 372–378. doi: 10.1016/j.crv.2017.08.001
- Small, L., Gong, H., Yassmin, C., Cooney, G. J., and Brandon, A. E. (2018). Thermoneutral housing does not influence fat mass or glucose homeostasis in C57BL/6 mice. *J. Endocrinol.* 239, 313–324. doi: 10.1530/JOE-18-0279
- Spritzer, P. M., and Oppermann, K. (2013). Weight gain and abdominal obesity at menopause. *Climacteric* 16:292. doi: 10.3109/13697137.2012.753874
- Stefanska, A., Bergmann, K., and Sypniewska, G. (2015). Metabolic syndrome and menopause: pathophysiology, clinical and diagnostic significance. *Adv. Clin. Chem.* 72, 1–75. doi: 10.1016/bs.acc.2015.07.001
- Tchernof, A., Calles-Escandon, J., Sites, C. K., and Poehlman, E. T. (1998). Menopause, central body fatness, and insulin resistance: effects of hormone-replacement therapy. *Coron. Artery Dis.* 9, 503–511. doi: 10.1097/00019501-199809080-00006
- Teede, H., Lombard, C., and Deeks, A. (2010). Obesity, metabolic complications and the menopause: an opportunity for prevention. *Climacteric* 13, 203–209. doi: 10.3109/13697130903296909
- Valle, A., Santandreu, F. M., Garcia-Palmer, F. J., Roca, P., and Oliver, J. (2008). The serum levels of 17 $\beta$ -estradiol, progesterone and triiodothyronine correlate with brown adipose tissue thermogenic parameters during aging. *Cell Physiol. Biochem.* 22, 337–346. doi: 10.1159/000149812
- Velickovic, K., Cvorovic, A., Srdic, B., Stokic, E., Markelic, M., Golic, I., et al. (2014). Expression and subcellular localization of estrogen receptors alpha and beta in human fetal brown adipose tissue. *J. Clin. Endocrinol. Metab.* 99, 151–159. doi: 10.1210/jc.2013-2017
- Vieira Potter, V. J., Strissel, K. J., Xie, C., Chang, E., Bennett, G., Defuria, J., et al. (2012). Adipose tissue inflammation and reduced insulin sensitivity in ovariectomized mice occurs in the absence of increased adiposity. *Endocrinology* 153, 4266–4277. doi: 10.1210/en.2011-2006
- Vieira-Potter, V. J., Padilla, J., Park, Y. M., Welly, R. J., Scroggins, R. J., Britton, S. L., et al. (2015). Female rats selectively bred for high intrinsic aerobic fitness are protected from ovariectomy-associated metabolic dysfunction. *Am. J. Physiol. Regul. Integr. Comp. Physiol.* 308, R530–R542. doi: 10.1152/ajpregu.00401.2014
- Wade, G. N., Gray, J. M., and Bartness, T. J. (1985). Gonadal influences on adiposity. *Int J Obes* 9(Suppl. 1), 83–92.
- Wainwright, K. S., Fleming, N. J., Rowles, J. L., Welly, R. J., Zidon, T. M., Park, Y. M., et al. (2015). Retention of sedentary obese visceral white adipose tissue phenotype with intermittent physical activity despite reduced adiposity. *Am. J. Physiol. Regul. Integr. Comp. Physiol.* 309, R594–R602. doi: 10.1152/ajpregu.00042.2015

- Wang, Q., Zhang, M., Ning, G., Gu, W., Su, T., Xu, M., et al. (2011). Brown adipose tissue in humans is activated by elevated plasma catecholamines levels and is inversely related to central obesity. *PLoS One* 6:e21006. doi: 10.1371/journal.pone.0021006
- Winn, N. C., Vieira-Potter, V. J., Gastecki, M. L., Welly, R. J., Scroggins, R. J., Zidon, T. M., et al. (2017). Loss of UCP1 exacerbates Western diet-induced glycemic dysregulation independent of changes in body weight in female mice. *Am. J. Physiol. Regul. Integr. Comp. Physiol.* 312, R74–R84. doi: 10.1152/ajpregu.00425.2016
- Yamauchi, T., Kamon, J., Waki, H., Terauchi, Y., Kubota, N., Hara, K., et al. (2001). The fat-derived hormone adiponectin reverses insulin resistance associated with both lipoatrophy and obesity. *Nat. Med.* 7, 941–946. doi: 10.1038/90984
- Yao, L., Heuser-Baker, J., Herlea-Pana, O., Zhang, N., Szweda, L. I., Griffin, T. M., et al. (2014). Deficiency in adipocyte chemokine receptor CXCR4 exacerbates obesity and compromises thermoregulatory responses of brown adipose tissue in a mouse model of diet-induced obesity. *FASEB J.* 28, 4534–4550. doi: 10.1096/fj.14-249797
- Yasrebi, A., Rivera, J. A., Krumm, E. A., Yang, J. A., and Roepke, T. A. (2016). Activation of estrogen response element-independent  $\alpha$  signaling protects female mice from diet-induced obesity. *Endocrinology* 158, 319–334.
- Yepuru, M., Eswaraka, J., Kearbey, J. D., Barrett, C. M., Raghov, S., Veverka, K. A., et al. (2010). Estrogen receptor- $\beta$ -selective ligands alleviate high-fat diet- and ovariectomy-induced obesity in mice. *J. Biol. Chem.* 285, 31292–31303. doi: 10.1074/jbc.M110.147850
- Zhu, L., Martinez, M. N., Emfinger, C. H., Palmisano, B. T., and Stafford, J. M. (2014). Estrogen signaling prevents diet-induced hepatic insulin resistance in male mice with obesity. *Am. J. Physiol. Endocrinol. Metab.* 306, E1188–E1197. doi: 10.1152/ajpendo.00579.2013
- Zidon, T. M., Park, Y.-M., Welly, R. J., Woodford, M. L., Scroggins, R. J., Britton, S. L., et al. (2018). Voluntary wheel running improves adipose tissue immunometabolism in ovariectomized low-fit rats. *Adipocyte* 7, 20–34. doi: 10.1080/21623945.2017.1402991

**Conflict of Interest Statement:** The authors declare that the research was conducted in the absence of any commercial or financial relationships that could be construed as a potential conflict of interest.

Copyright © 2019 Clookey, Welly, Shay, Woodford, Fritsche, Rector, Padilla, Lubahn and Vieira-Potter. This is an open-access article distributed under the terms of the Creative Commons Attribution License (CC BY). The use, distribution or reproduction in other forums is permitted, provided the original author(s) and the copyright owner(s) are credited and that the original publication in this journal is cited, in accordance with accepted academic practice. No use, distribution or reproduction is permitted which does not comply with these terms.



# Fibroblast Growth Factor 21 and Browning of White Adipose Tissue

Daniel Cuevas-Ramos<sup>1</sup>, R. Mehta<sup>1,2</sup> and Carlos A. Aguilar-Salinas<sup>1,2,3\*</sup>

<sup>1</sup> Department of Endocrinology and Metabolism, Instituto Nacional de Ciencias Médicas y Nutrición Salvador Zubirán, Mexico City, Mexico, <sup>2</sup> Unidad de Investigación de Enfermedades Metabólicas, Instituto Nacional de Ciencias Médicas y Nutrición Salvador Zubirán, Mexico City, Mexico, <sup>3</sup> Instituto Tecnológico y de Estudios Superiores de Monterrey Tec Salud, Monterrey, Mexico

## OPEN ACCESS

### Edited by:

Rita De Matteis,  
University of Urbino Carlo Bo, Italy

### Reviewed by:

Neal Lee Weintraub,  
Augusta University, United States  
Gautham Yepuri,  
New York University, United States  
Patricia Vázquez,  
Institute of Biomedical Research  
Alberto Sols (IIBM), Spain

### \*Correspondence:

Carlos A. Aguilar-Salinas  
caguilar-salinas@yahoo.com;  
ceptamim@gmail.com

### Specialty section:

This article was submitted to  
Integrative Physiology,  
a section of the journal  
Frontiers in Physiology

**Received:** 10 October 2018

**Accepted:** 14 January 2019

**Published:** 05 February 2019

### Citation:

Cuevas-Ramos D, Mehta R and  
Aguilar-Salinas CA (2019) Fibroblast  
Growth Factor 21 and Browning  
of White Adipose Tissue.  
Front. Physiol. 10:37.  
doi: 10.3389/fphys.2019.00037

Interest has been focused on differentiating anatomical, molecular, and physiological characteristics of the types of mammalian adipose tissues. White adipose tissue (WAT) and brown adipose tissue (BAT) are the two main forms of adipose tissue in humans. WAT functions as an endocrine organ and serves as a reservoir of energy in the form of triglycerides. The hormones released by WAT are called adipokines. BAT consists of a group of specialized cells with abundant uncoupling protein 1 (UCP1) in the inner mitochondrial membrane and also fulfills endocrine functions. Following the identification of functional (BAT) in human adults, there has been a great deal of interest in finding out how it is induced, its localization, and the mechanisms by which it regulates thermogenesis. Fibroblast growth factor 21 (FGF21) is a key regulator of the differentiation to brown adipocytes. The main mechanisms occur through enhancing UCP1 expression. In addition, following exposure to cold or exercise, FGF21 induces upregulation of local peroxisome proliferator-activated receptor gamma co-activator (PGC)-1- $\alpha$  and thus promotes thermogenesis in adipose tissue and skeletal muscle. FGF21 integrates several pathways allowing the regulation of human energy balance, glucose levels, and lipid metabolism. Such mechanisms and their clinical relevance are summarized in this review.

**Keywords:** fibroblast growth factor 21, glucose, energy balance, insulin resistance, irisin, exercise, noradrenaline, free fatty acids

## INTRODUCTION

Fibroblast growth factor 21 (FGF21) has important effects on energy balance, glucose metabolism, and lipid metabolism (Kharitonov et al., 2005). Initial reports identified the liver as its main source (Nishimura et al., 2000). On secretion, its most important target is white adipose tissue (WAT), where FGF21 increases expression of GLUT1 and consequently glucose uptake (Kharitonov et al., 2005). During fasting or starvation, lipolysis is triggered, with a subsequent increment in circulating free fatty acids (FFAs). FFAs induce the activation of the peroxisome proliferator-activated receptor (PPAR)- $\alpha$  in the liver, resulting in the synthesis and release of FGF21. Since carbohydrate ingestion is absent during starvation, FGF21 induces ketone body formation in the liver as an additional energy source (Badman et al., 2007; Inagaki et al., 2008). FGF21 may also be considered an adipokine, since it is also synthesized and released from WAT. It shows complementary actions to adiponectin (Lin et al., 2013), increasing insulin sensitivity, improving the lipid profile, reducing glucose levels without causing hypoglycemia, and ensuring



energy availability during starvation (Badman et al., 2007; Inagaki et al., 2008). In human insulin resistance states, FGF21 levels have a positive correlation with the number of metabolic syndrome traits, the severity of oxidative stress, and the presence of type 2 diabetes (Zhang et al., 2008; Cuevas-Ramos et al., 2010; Gómez-Sámano et al., 2017). Other human stress-related conditions that increase circulating FGF21 levels are lactation (Schoenberg et al., 2011), exercise (Cuevas-Ramos et al., 2012b), growth hormone treatment (Chen et al., 2011), and anorexia nervosa (Dostálová, 2008). Interestingly, FGF21 is now considered an important mediator for decreasing oxidative stress, and possibly, preventing microvascular diseases such as diabetic nephropathy (Jian et al., 2012).

The role of FGF21 as a therapeutic option in human metabolic diseases is of increasing importance. Currently, there are multiple recombinant FGF21 analogs in phase 2 and phase 3 clinical trials (Mu et al., 2012; Gaich et al., 2013; Talukdar et al., 2016). Interest has increased even more so after the discovery of the crucial role of FGF21 in inducing the proliferation of brown adipose tissue (BAT) (Fisher et al., 2012). This review describes the mechanisms by which FGF21 induces “browning” of adipose tissue and how it may have a role in the treatment of human metabolic diseases, including obesity and type 2 diabetes.

## WHITE, BEIGE, AND BROWN SUBTYPES OF ADIPOSE TISSUES IN HUMANS

WAT and BAT are the two main subtypes of adipose tissue in humans. WAT has important endocrine functions in addition to its role as a reservoir of energy in the form of triglycerides. The hormones released from WAT, namely adipokines, are a well-recognized group of bioactive factors with endocrine actions that act through specific cell-membrane receptors. Adipokines trigger certain intracellular signaling pathways, which modulate human metabolism (Piya et al., 2013). The most important are leptin and adiponectin, but visfatin, chemerin, omentin, hepcidin, apelin, and vaspin have also been described (Piya et al., 2013).

BAT is also an important endocrine organ. It consists of a group of specialized cells with abundant expression of uncoupling protein 1 (UCP1) in the inner mitochondrial membrane (Aherne and Hull, 1966; Cannon and Nedergaard, 2004). The BAT hormones are named “batokines” (Baboota et al., 2015; Booth et al., 2016). The principle function of BAT is to dissipate stored energy in the form of heat by uncoupling energy oxidation from ATP synthesis (Fedorenko et al., 2012). Initially, BAT was only considered as an energy-producing organ in rodents and human infants (Bartness et al., 2010). However, after the development of 18F-fluorodeoxyglucose (FDG) positron emission tomography-computed tomography (PET-CT), BAT has also been identified in human adults (Nedergaard et al., 2007; Cypess et al., 2009). Nevertheless, the origin of BAT is still under debate, although originally it was thought to be derived from skeletal muscle-like lineage (Myf5+) (Seale et al., 2007). In human adults, a type of adipose tissue showing characteristics between that of white and brown adipocytes has been identified; this kind of

adipose tissue is known as beige adipose tissue (*brite*, brown-in-white) (Jespersen et al., 2013). It appears that beige and white adipocytes arise from both Myf5+ and Myf5- progenitor cells. These findings confirm that the skeletal muscle-like lineage is not the only source of BAT (Wu et al., 2012).

The location of the different types of adipose tissue varies. Beige and WAT have mainly visceral (mesenteric, perigonadal or omental adipose tissue surrounding organs) and subcutaneous (under skin) locations. BAT is located only in axillary, subscapular, interscapular, and periaortic regions in rodents; in cervical, supraclavicular, paravertebral, mediastinal regions in humans; and in perirenal regions in both (Park et al., 2014; Sanchez-Gurmaches and Guertin, 2014). *Brite* or beige adipocytes have basal metabolic actions similar to those seen in white adipocytes, and with the enough stimulus, they are able to transform into thermogenic adipocytes with higher UCP1 expression similar to BAT (Wu et al., 2012). This process is referred as “browning” and it describes the capacity of white adipocytes to acquire a phenotype similar to that of BAT, leading to increased thermogenesis. It is achieved when white adipocytes are exposed to cold or to beta 3-adrenoreceptor agonists (Young et al., 1984; Harms and Seale, 2013). Browning occurs mainly in subcutaneous white adipose fat depots. The underlying molecular mechanisms for this trans-differentiation are currently under intensive research (Luo and Liu, 2016). In addition, there are important structural differences among WAT, *brite*, and BAT. WAT is a large lipid droplet, with a peripheral nucleus and a small amount of cytoplasm, whereas BAT has a central nucleus with more cytoplasm but smaller lipid droplets. In between these is the *brite* or beige tissue; this has the mixed structural characteristics of both. Sometimes the different structures are found together; for example, the ectopic expression of UCP1 and the presence of the PR domain containing 16 (PRDM16) suggests that *brite* adipocytes are mixed with white adipocyte depots (Wu et al., 2013). The balance between WAT and BAT, and their endocrine regulation, are key elements to better understand the development of weight gain and human metabolic diseases.

## MOLECULAR PATHWAYS AND CLINICAL RELEVANCE OF BROWNING INDUCED BY FGF21

Since the discovery of FGF21, it has been appreciated that its synthesis is strongly related to cold exposure (Badman et al., 2007; Inagaki et al., 2008). In mice, during hypothermia, FGF21 induces torpor, a short-term hibernation state in which animals can save energy by reducing body temperature and physical activity (Badman et al., 2007). More recently, studies have shown a higher expression of FGF21 in inguinal WAT after cold exposure. The role of FGF21 produced in WAT includes both paracrine and autocrine actions; this results in the local upregulation of peroxisome proliferator-activated receptor gamma co-activator (PGC)-1- $\alpha$  and thus an increase in thermogenesis (Hondares et al., 2010; Fisher et al., 2012; Adams et al., 2013; Emanuelli et al., 2014). PGC1- $\alpha$  is a protein involved in modulating several effects in post-exercise skeletal muscle, including the

improvement of energy and glucose metabolism (Summermatter et al., 2013). Interestingly, PGC1- $\alpha$  is also induced after irisin or insulin exposure, both hormones showing a clear interaction with FGF21 post-exercise (Cuevas-Ramos et al., 2010, 2012b; Bostrom et al., 2012; Fisher et al., 2012; Hu and Christian, 2017). Irisin-induced phosphorylation of p38 mitogen-activated protein kinase (p38 MAPK) and extracellular signal-related kinase (ERK) show a positive correlation with shivering intensity (Bostrom et al., 2012; Zhang et al., 2014). FGF21 also shows a direct relationship with exercise intensity (Cuevas-Ramos et al.,

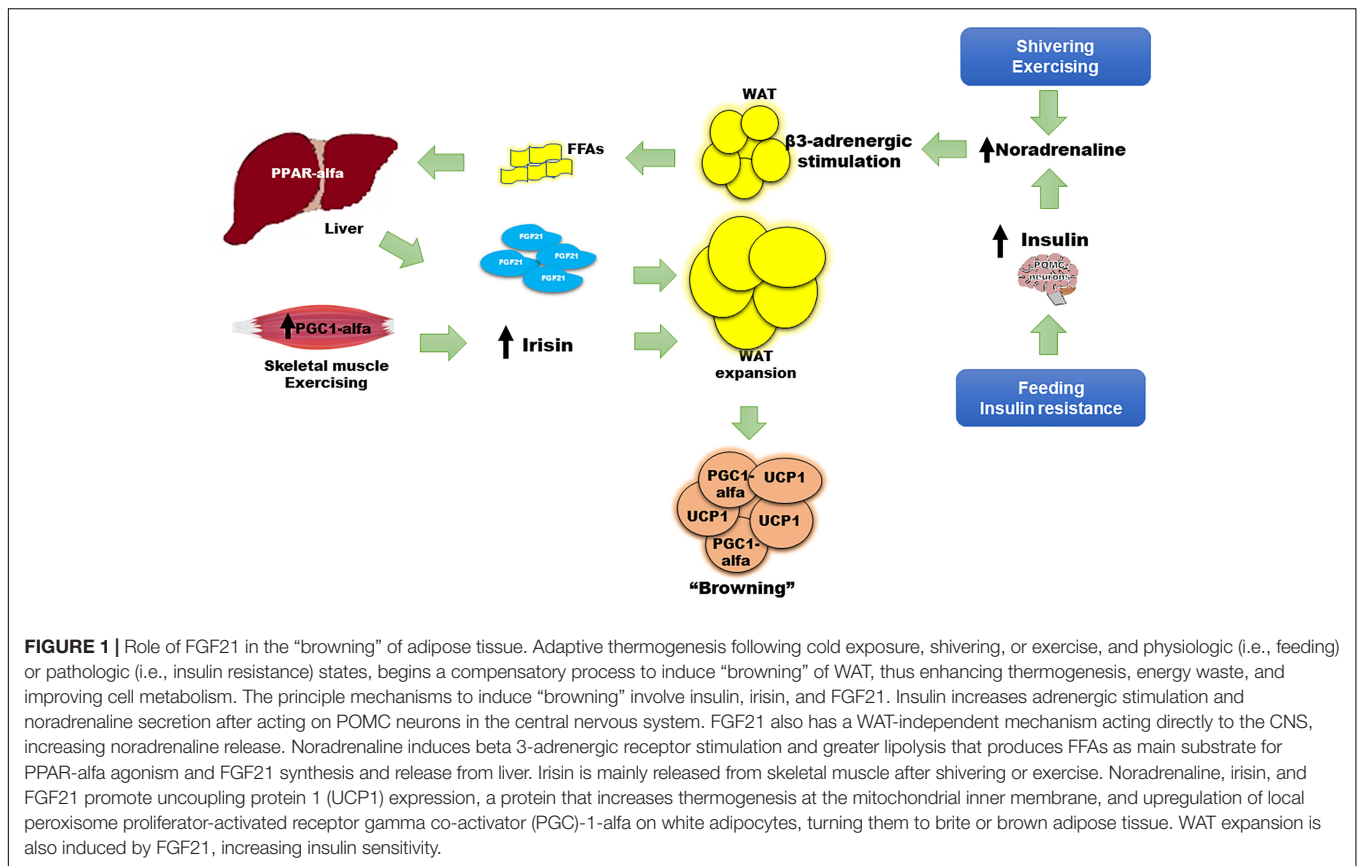
2010, 2012b). The consequence of these PGC1- $\alpha$  inducers is to promote adaptive thermogenesis with “browning” of WAT (Fisher et al., 2012). The main mechanism following FGF21 action is PPAR- $\gamma$  activation in WAT, together with the irisin effect inducing MAPK and ERK pathways. This results in differentiation of pre-adipocytes to mature white adipocytes, which are then available for “browning” (Hondares et al., 2011; Zhang Y. et al., 2016).

Some animal models have reported findings consistent with these actions. For example, FGF21 deficiency in mice

**TABLE 1 |** Most important hormones, drugs, and nutritional inducers of browning.

Effector	Effect and mechanism on WAT
AMPK activators	Higher thermogenesis, increase energy expenditure and mitochondrial biogenesis. Enhance PGC1- $\alpha$ and UCP1. Ej: with AICAR (Gaidhu et al., 2009)
BMPs	BMP7 and BMP 8 induce higher thermogenesis, increase energy expenditure and mitochondrial biogenesis. Enhance PGC1- $\alpha$ and UCP1. Increases lipid oxidation (Schulz et al., 2011; Whittle et al., 2012).
Beta-3-adrenergic stimulation	Higher thermogenesis, increase energy expenditure and mitochondrial biogenesis, enhance UCP1, and activation of c-AMP, PKA, p38 MAPK, PGC1- $\alpha$ , and PPAR- $\alpha$ (Jimenez et al., 2003; Li et al., 2005).
Fenofibrate	Effects are through PPAR- $\alpha$ agonism (Magliano et al., 2013; Rachid et al., 2015)
FGF21 recombinant analogs	After cold exposure or adrenergic stimulation induced higher thermogenesis, increase energy expenditure and mitochondrial biogenesis. Enhance PGC1- $\alpha$ and UCP1. After exercising, possible interaction with irisin reducing fat depots (Dostálová, 2008; Cuevas-Ramos et al., 2012b; Lee et al., 2014).
FGFR1/KLB antibodies	Higher thermogenesis but through UCP1-independent mechanism (Chen et al., 2017).
Insulin and leptin (adipoinular axis)	Acts in hypothalamic POMC neurons to induce browning (Dodd et al., 2015).
Irisin	Higher thermogenesis, increase energy expenditure and mitochondrial biogenesis, enhance UCP1, through PPAR- $\alpha$ agonism. Irisin also stimulated browning after exercising (Bostrom et al., 2012; Wu et al., 2012; Zhang Y. et al., 2016).
Thyroid hormones	Higher thermogenesis, increase energy expenditure and mitochondrial biogenesis (Lee et al., 2012).
Natriuretic peptides (ANP)	Synergism with beta-3-adrenergic receptor stimulation after exercising inducing higher thermogenesis, enhancing UCP1 expression, and lipolysis through PKA, c-GMP and PKG (Lafontan et al., 2008; Bordinchia et al., 2012).
Thiazolidinediones	Higher thermogenesis, enhancing UCP1 expression and inducing insulin sensitivity. Synergism after adrenergic stimulus (Petrovic et al., 2010).
Capsaicin	Adrenergic stimulation causing higher thermogenesis, through TRPV1 protein activating neurons (Teodoro et al., 2014; Baskaran et al., 2016).
Bile acids	Higher thermogenesis, enhancing UCP1 expression through TGR5 (Watanabe et al., 2006; Teodoro et al., 2014).
Citrulline	Higher thermogenesis, increase energy expenditure and mitochondrial biogenesis, enhance UCP1, and PPAR- $\alpha$ agonism (Joffin et al., 2015).
Fucoanthin	Higher thermogenesis, enhancing UCP1 expression (Maeda et al., 2005).
Luteolin	Higher thermogenesis, increase energy expenditure and mitochondrial biogenesis, enhance UCP1 (Zhang X. et al., 2016).
Methionine restriction	Higher thermogenesis, enhancing UCP1 expression (Hasek et al., 2010).
n-3 PUFAs	Higher thermogenesis, enhancing UCP1 expression (Zhao and Chen, 2014; Bargut et al., 2016).
Resveratrol	Higher thermogenesis, increase energy expenditure and mitochondrial biogenesis, enhancing PGC1- $\alpha$ and UCP1. Also increase PRDM16 expression, and increases lipid oxidation activating AMPK (Wang et al., 2015).
Retinoic acid	Higher thermogenesis, enhancing UCP1 expression. Also, PPAR- $\beta$ /delta expression (Murholm et al., 2013).
Beta-hydroxybutyrate	Higher thermogenesis, enhancing UCP1 expression (Carriere et al., 2014).

AICAR, Activator 5-aminoimidazole-4-carboxamide ribonucleoside; AMPK, adenosin monophosphate activated protein kinase; ANP, atrial natriuretic peptide; c-GMP, cyclic-guanosine monophosphate protein; FFA, free fatty acids; FGF21, fibroblast growth factor 21; MAPK, Mitogen-activated protein kinase; PGC1- $\alpha$ , peroxisome proliferator-activated receptor gamma coactivator (PGC) 1- $\alpha$ ; PKA, protein kinase A; PKG, protein kinase G; PPAR, peroxisome proliferator-activated receptor; PRDM16, PR domain containing 16; PUFA, polyunsaturated fatty acids; TRG5, G protein-coupled receptor 5; TRPV1, transient receptor potential V1; UCP1, uncoupled protein 1; WAT, white adipose tissue.



results in increased body weight with excessive adiposity, higher serum cholesterol, insulin resistance, and hyperglycemia (Kharitononkov et al., 2005). The finding of a 30–40% lower nuclear content of PGC1-alfa at the hepatic mitochondrial level in *Fgf21* KO mice compared with WT mice, is a potential explanation for these results (Fletcher et al., 2016). FGF21 induces palmitate oxidation and  $\beta$ -hydroxyacyl-CoA dehydrogenase ( $\beta$ -HAD) activity. In the *Fgf21* KO model, these enzymatic activities are decreased, indicating lower lipid oxidation, a reduction in glucose metabolism, and a lower degree of energy waste (Fletcher et al., 2016). In contrast, overexpression of FGF21 effectively decreases weight, adiposity, levels of FFAs, triglycerides, glucose, and insulin, all due to the normalization of mitochondrial oxidation (Fletcher et al., 2016) and the improvement in insulin sensitivity (Kharitononkov et al., 2005). Interestingly, exercise, irisin, and noradrenaline were necessary to restore PGC1-alfa content in the liver despite overexpression of FGF21, emphasizing the key interaction of such inducers with FGF21 (Fletcher et al., 2016). Insulin, the most important regulator of energy and glucose metabolism, enhanced differentiation of WAT to *brite* and brown adipocytes through pro-opiomelanocortin (POMC) neurons (Table 1 and Figure 1); (Dodd et al., 2015). Therefore, multiple mechanisms may be inter-connected to improve metabolism in humans, with FGF21 functioning as an important link between them.

The exogenous administration of an FGF21 analog in animal models has been associated with a thermogenic effect,

an improvement in glucose homeostasis, lipid profile, and a reduction in body weight (Wu et al., 2011; Veniant et al., 2012). However, in humans, recombinant FGF21 analogs have not shown these effects. FGF21 is paradoxically increased in insulin-resistant states such as obesity or type 2 diabetes; this suggests either a resistance to FGF21 effects or a compensatory response to these metabolic disarrangements (Zhang et al., 2008; Cuevas-Ramos et al., 2010). Nevertheless, the key metabolic role of FGF21 is clear. Firstly, WAT increases FGF21 expression in response to feeding, which has an autocrine action on PPAR-gamma activity; PPAR-gamma is an important inducer of insulin sensitivity pathways, adipocyte maturation, and function (Dutchak et al., 2012). Secondly, FGF21 is significantly induced after moderate to intensive physical activity (Cuevas-Ramos et al., 2010, 2012b), and interestingly, its release has been correlated with sympathetic nervous system activation and lipolysis markers, such as noradrenaline and serum free fatty acids, respectively (Cuevas-Ramos et al., 2012b). Thirdly, FGF21 regulates metabolism through increasing insulin sensitivity at WAT and BAT, but this may happen in an acute and a chronic manner. Acute and chronic exogenous administration of FGF21 induce insulin sensitivity independently of adiponectin action (BonDurant et al., 2017). However, the chronic effect of FGF21 is not necessarily via a direct effect on WAT since it also induces signaling in the central nervous system via POMC neurons, and on brown adipocytes, enhancing thermogenesis and insulin-sensitivity in mice (Figure 1). These effects require functional

insulin signaling in adipose tissue, otherwise the FGF21-benefit is lost. In addition, the action of FGF21 on the central nervous system is important to induce energy expenditure, mainly by increasing noradrenaline release (**Figure 1**) (Owen et al., 2014). Noradrenaline plays an important role in the regulation of “browning.” It is the most studied activator of thermogenesis, increasing UCP1 transcription, enhancing lipolysis and mitochondrial oxidation (**Figure 1**; Puigserver et al., 1996). After cold-induced shivering or physical activity stress, noradrenergic pathways increase thermogenic gene expression through c-AMP-mediated mechanisms (Hondares et al., 2011). Lipolysis and FFAs increase following noradrenaline release. With acute intensive exercise, the increase in beta 3-receptor activity also causes an increment in circulating FGF21 (Cuevas-Ramos et al., 2012b). Increased circulating FFAs induce PPAR- $\alpha$  expression in the liver, increasing FGF21 synthesis and release into circulation (Badman et al., 2007; Inagaki et al., 2008). FGF21 can also increase insulin sensitivity by promoting the expansion of subcutaneous WAT. *Fgf21* knockout mice show less subcutaneous WAT and a greater degree of insulin resistance. After treatment with recombinant FGF21, subcutaneous adipose tissue was restored with a subsequent improvement in insulin sensitivity (Li et al., 2018). The expression of co-factor beta klotho is necessary to accomplish the FGF21-related expansion of subcutaneous fat (Li et al., 2018). Finally, chronic pharmacologic administration of FGF21 in obese mice has been shown to suppress growth hormone (GH) and the insulin growth factor-1 (IGF1) signaling axis in the liver, increasing lifespan through an improvement in insulin sensitization, normalization of glycemia, and a reduction in body weight (Zhang Y. et al., 2012).

Under normal conditions, FGF21 is synthesized and released from the liver. However, in certain circumstances, such as adaptive thermogenesis induced by cold exposure or exercise, BAT expresses and releases FGF21 (Chartoumpekis et al., 2011; Hondares et al., 2011; Giralt et al., 2015; Lee et al., 2015). The production of FGF21 by BAT is not negligible; it significantly contributes to systemic FGF21 levels (Hondares et al., 2011). Following exposure to cold, the production of FGF21 by BAT is greater than that of the liver, enhancing thermogenesis, confirming the key roles of BAT in regulating FGF21 levels (Hondares et al., 2011). Moreover, a dramatic rise in *Fgf21* expression in BAT has also been reported in *Ucp1*-null mice or after genetic inactivation of UCP1 protein. In these situations, there is an increase in serum FGF21 levels without changes in FGF21 gene expression in the liver (Keipert et al., 2015; Samms et al., 2015). This suggests thermogenic regulation of FGF21 through both UCP1-dependent as well as UCP1-independent mechanisms (Keipert et al., 2015; Samms et al., 2015).

Taken together, adipose tissue, liver, and skeletal muscle respond to multiple stimuli in order to increase adaptive thermogenesis and induce the browning of WAT (**Figure 1**). Expression and release of FGF21 by the liver, BAT, and skeletal muscle is induced by shivering (Badman et al., 2007; Inagaki et al., 2008; Hondares et al., 2011), physical activity (Cuevas-Ramos et al., 2010, 2012b; Kim et al., 2013), protein synthesis after growth hormone treatment (Chen et al., 2011), and as a consequence of experimental or

clinical mitochondrial dysfunction following DNA mutations (Suomalainen et al., 2011; Keipert et al., 2014). FGF21, together with irisin, insulin, and noradrenaline, provokes metabolically healthy effects that are concomitantly associated with the browning of WAT (Moschen et al., 2014; Lee et al., 2015; Villarroja et al., 2017). The higher BAT activity and increased heat production may benefit human health, reducing weight, preventing hyperglycemia, and hyperlipidemia, and protecting against obesity through enhancement of energy waste (Cuevas-Ramos et al., 2012a). These effects explain the association of FGF21 and explain its key role in the “browning” of WAT. This was probably aimed to allow the adaptation of human metabolism to obesity, diabetes, dyslipidemia, metabolic syndrome, and other insulin resistance states (**Figure 1**).

## FGF21 AS POTENTIAL MEDICAL TREATMENT TO INDUCE BROWNING OF WAT

The beneficial metabolic consequences of “browning” may be useful to treat metabolic diseases in humans (Barquissau et al., 2016). There are multiple medical drugs or nutritional inducers that may help to stimulate browning (**Table 1**). Recently, the role of FGF21 in the browning of WAT has been evaluated with the development of recombinant FGF21-analogs. Initially, clinical trials with analogs LY2405319 and PF05231023 were focused on treating human metabolic diseases including obesity, metabolic syndrome and type 2 diabetes (Gaich et al., 2013; Talukdar et al., 2016). However, resistance to their actions, resulting in an inadequate clinical effect, has been a problem; in humans, only a slight glucose, weight or triglyceride reduction was achieved. The subcutaneous depots of WAT are small cells with greater potential to differentiate (Gustafson and Smith, 2015). Therefore, it is feasible to hypothesize a positive effect if “browning” can be induced, following a sufficient stimulus using FGF21-analogs. In addition, the FGF receptor type 1 together with beta klotho cofactor, called the FGFR1/KLB complex, is the functional target for FGF21 (Kolumam et al., 2015). The use of FGF21 agonist antibodies that specifically activate this complex largely mimic the action of recombinant FGF21 in mice (Kolumam et al., 2015). These include the agonist antibodies BFKB8488 and NGM313, which are currently under clinical research (ClinicalTrials.gov, NCT02593331, NCT02708576, and NCT03060538). Both FGF21 recombinant analogs (Gaich et al., 2013; Talukdar et al., 2016) and the FGFR1/KLB complex agonist antibodies induce higher thermogenesis and browning of BAT through UCP1-dependent pathways. Although UCP1 has traditionally been thought of as indispensable for browning and thermogenesis (Golozeubova et al., 2001; Feldmann et al., 2009), recent research suggests a role of a UCP1-independent pathway (Chen et al., 2017). In *Ucp1* KO mice, higher thermogenesis with weight loss and beneficial changes in cardiometabolic markers have been reported (Veniant et al., 2015; Chen et al., 2017). The origin of this UCP1-independent thermogenesis is still controversial, with different reports suggesting the opposite (Keipert et al., 2015). Further



investigation is warranted to clarify if higher thermogenesis can be obtained without overexpression of UCP1.

In addition to FGF21-recombinant analogs or the FGFR1-KLB complex agonist antibodies, other drugs have been used with similar aims; however, most have shown little clinical utility. For example, PPAR- $\alpha$  agonists (fibrates), adrenergic  $\beta$ -3-receptor stimulators, thyroid hormones, and more recently irisin have been tested (Table 1). There are also certain nutritional inducers of “browning” of WAT that may be considered as therapeutic options. The most important hormones, drugs and nutritional inducers of browning are summarized on Table 1. It is important to mention that although nicotine has been associated with body weight reduction, mainly due to the associated decreased appetite, greater lipolysis, and increased energy waste (Zoli and Picciotto, 2012), it has never been confirmed that smoking cigarettes can induce browning (Chen et al., 2005).

## CONCLUSION

FGF21 is a key regulator of the differentiation of WAT to brown adipocytes, resulting in enhanced thermogenesis and energy waste. The main action seems to be through UCP1-dependent and -independent mechanisms. In addition, after cold exposure or exercising, FGF21-induced upregulation of local peroxisome proliferator-activated receptor gamma co-activator (PGC)-1- $\alpha$

increases thermogenesis in adipose tissue and skeletal muscle. Potential mechanisms involve higher noradrenaline levels that act on the WAT- $\beta$ -3 adrenergic receptor, inducing lipolysis, and higher serum free fatty acids, which in turn increase PPAR- $\alpha$  agonism at liver, and higher FGF21 synthesis and then release into circulation. This effect contributes to other FGF21-related mechanisms that integrate metabolic pathways to regulate human energy balance, glucose and lipid levels. Therefore, the development of better recombinant FGF21 analogs as a potential treatment for metabolic diseases in humans is necessary.

## AUTHOR CONTRIBUTIONS

All authors made substantial contributions to the conception and/or design of the work; acquisition, analysis, and interpretation of data for the work; drafting the work or revising it critically for important intellectual content; and approved the final version of the article to be published.

## FUNDING

This review was supported by Department of Endocrinology and Metabolism at the Instituto Nacional de Ciencias Médicas y Nutrición Salvador Zubirán, Mexico City, Mexico.

## REFERENCES

- Adams, A. C., Coskun, T., Cheng, C. C., Ls, O. F., Dubois, S. L., and Kharitonov, A. (2013). Fibroblast growth factor 21 is not required for the antidiabetic actions of the thiazolidinediones. *Mol. Metab.* 2, 205–214. doi: 10.1016/j.molmet.2013.05.005
- Aherne, W., and Hull, D. (1966). Brown adipose tissue and heat production in the newborn infant. *J. Pathol. Bacteriol.* 91, 223–234. doi: 10.1002/path.1700910126
- Baboota, R. K., Sarma, S. M., Boparai, R. K., Kondepudi, K. K., Mantri, S., and Bishnoi, M. (2015). Microarray based gene expression analysis of murine brown and subcutaneous adipose tissue: significance with human. *PLoS One* 10:e0127701. doi: 10.1371/journal.pone.0127701
- Badman, M. K., Pissios, P., Kennedy, A. R., Koukos, G., Flier, J. S., and Maratos-Flier, E. (2007). Hepatic fibroblast growth factor 21 is regulated by PPAR- $\alpha$  and is a key mediator of hepatic lipid metabolism in ketotic states. *Cell Metab.* 5, 426–437. doi: 10.1016/j.cmet.2007.05.002
- Bargut, T. C., Souza-Mello, V., Mandarim-de-Lacerda, C. A., and Aguilu, M. B. (2016). Fish oil diet modulates epididymal and inguinal adipocyte metabolism in mice. *Food Funct.* 7, 1468–1476. doi: 10.1039/c5fo00909j
- Barquissau, V., Beuzelin, D., Pisani, D. F., Beranger, G. E., Mairal, A., Montagner, A., et al. (2016). White-to-brite conversion in human adipocytes promotes metabolic reprogramming towards fatty acid anabolic and catabolic pathways. *Mol. Metab.* 5, 352–365. doi: 10.1016/j.molmet.2016.03.002
- Bartness, T. J., Vaughan, C. H., and Song, C. K. (2010). Sympathetic and sensory innervation of brown adipose tissue. *Int. J. Obes.* 34(Suppl. 1), S36–S42. doi: 10.1038/ijo.2010.182
- Basarkan, P., Krishnan, V., Ren, J., and Thyagarajan, B. (2016). Capsaicin induces browning of white adipose tissue and counters obesity by activating TRPV1 channel-dependent mechanisms. *Br. J. Pharmacol.* 173, 2369–2389. doi: 10.1111/bph.13514
- BonDurant, L. D., Ameka, M., Naber, M. C., Markan, K. R., Idiga, S. O., Acevedo, M. R., et al. (2017). FGF21 regulates metabolism through adipose-dependent and independent-mechanisms. *Cell Metab.* 25, 935–944. doi: 10.1016/j.cmet.2017.03.005
- Booth, A., Magnuson, A., Fouts, J., and Foster, M. T. (2016). Adipose tissue: an endocrine organ playing a role in metabolic regulation. *Horm. Mol. Biol. Clin. Invest.* 26, 25–42. doi: 10.1515/hmbci-2015-0073
- Bordicchia, M., Liu, D., Amri, E. Z., Ailhaud, G., Dessi-Fulgheri, P., Zhang, C., et al. (2012). Cardiac natriuretic peptides act via p38 MAPK to induce the brown fat thermogenic program in mouse and human adipocytes. *J. Clin. Invest.* 122, 1022–1036. doi: 10.1172/JCI59701
- Bostrom, P., Wu, J., Jedrychowski, M. P., Korde, A., Ye, L., Lo, J. C., et al. (2012). A PGC1- $\alpha$ -dependent myokine that drives brown-fat-like development of white fat and thermogenesis. *Nature* 481, 463–468. doi: 10.1038/nature10777
- Cannon, B., and Nedergaard, J. (2004). Brown adipose tissue: function and physiological significance. *Physiol. Rev.* 84, 277–359. doi: 10.1152/physrev.00015.2003
- Carriere, A., Jeanson, Y., Berger-Muller, S., Andre, M., Chenouard, V., Arnaud, E., et al. (2014). Browning of white adipose cells by intermediate metabolites: an adaptive mechanism to alleviate redox pressure. *Diabetes* 63, 3253–3265. doi: 10.2337/db13-1885
- Chartoumpekis, D. V., Habeos, I. G., Ziros, P. G., Psyrogiannis, A. I., Kyriazopoulou, V. E., Papavassiliou, A. G., et al. (2011). Brown adipose tissue responds to cold and adrenergic stimulation by induction of FGF21. *Mol. Med.* 17, 736–740. doi: 10.2119/molmed.2011.00075
- Chen, H., Vlahos, R., Bozinovski, S., Jones, J., Anderson, G. P., and Morris, M. J. (2005). Effect of short-term cigarette smoke exposure on body weight, appetite and brain neuropeptide Y in mice. *Neuropsychopharmacology* 30, 713–719. doi: 10.1038/sj.npp.1300597
- Chen, M. Z., Chang, J. C., Zavala-Solorio, J., Kates, L., Thai, M., Ogasawara, A., et al. (2017). FGF21 mimetic antibody stimulates UCP1-independent brown fat thermogenesis via FGFR1/Beta Klotho complex in non-adipocytes. *Mol. Metab.* 6, 1454–1467. doi: 10.1016/j.molmet.2017.09.003
- Chen, W., Hoo, R. L., Konishi, M., Itoh, N., Lee, P. C., Ye, H. Y., et al. (2011). Growth hormone induces hepatic production of fibroblast growth factor 21 through a mechanism dependent on lipolysis in adipocytes. *J. Biol. Chem.* 286, 34559–34566. doi: 10.1074/jbc.M111.285965

- Cuevas-Ramos, D., Aguilar-Salinas, C. A., and Gomez-Perez, F. J. (2012a). Metabolic actions of fibroblast growth factor 21. *Curr. Opin. Pediatr.* 24, 523–529. doi: 10.1097/MOP.0b013e3283557d22
- Cuevas-Ramos, D., Almeda-Valdés, P., Meza-Arana, C. E., Brito-Córdova, G., Gómez-Pérez, F. J., Mehta, R., et al. (2012b). Exercise increases serum fibroblast growth factor 21 (FGF21) levels. *PLoS One* 7:e38022. doi: 10.1371/journal.pone.0038022
- Cuevas-Ramos, D., Almeda-Valdes, P., Gomez-Perez, F. J., Meza-Arana, C. E., Cruz-Bautista, I., Arellano-Campos, O., et al. (2010). Daily physical activity, fasting glucose, uric acid, and body mass index are independent factors associated with serum fibroblast growth factor 21 levels. *Eur. J. Endocrinol.* 163, 469–477. doi: 10.1530/EJE-10-0454
- Cypess, A. M., Lehman, S., Williams, G., Tal, I., Rodman, D., Goldfine, A. B., et al. (2009). Identification and importance of brown adipose tissue in adult humans. *N. Engl. J. Med.* 360, 1509–1517. doi: 10.1056/NEJMoa0810780
- Dodd, G. T., Decherf, S., Loh, K., Simonds, S. E., Wiede, F., Balland, E., et al. (2015). Leptin and insulin act on POMC neurons to promote the browning of white fat. *Cell* 160, 88–104. doi: 10.1016/j.cell.2014.12.022
- Dostálová, I., Kavalčíková, P., Haluzíková, D., Lacinová, Z., Mráz, M., Papezová, H., et al. (2008). Plasma concentrations of fibroblast growth factors 19 and 21 in patients with anorexia nervosa. *J. Clin. Endocrinol. Metab.* 93, 3627–3632. doi: 10.1210/jc.2008-0746
- Dutchak, P. A., Katafuchi, T., Bookout, A. L., Choi, J. H., Yu, R. T., Mangelsdorf, D. J., et al. (2012). Fibroblast growth factor-21 regulates PPAR $\gamma$  activity and the antidiabetic actions of thiazolidinediones. *Cell* 148, 556–567. doi: 10.1016/j.cell.2011.11.062
- Emanuelli, B., Vienberg, S. G., Smyth, G., Cheng, C., Stanford, K. I., Arumugam, M., et al. (2014). Interplay between FGF21 and insulin action in the liver regulates metabolism. *J. Clin. Invest.* 124, 515–527. doi: 10.1172/JCI67353
- Fedorenko, A., Lishko, P. V., and Kirichok, Y. (2012). Mechanism of fatty-acid-dependent UCP1 uncoupling in brown fat mitochondria. *Cell* 151, 400–413. doi: 10.1016/j.cell.2012.09.010
- Feldmann, H. M., Golozoubova, V., Cannon, B., and Nedergaard, J. (2009). UCP1 ablation induces obesity and abolishes diet-induced thermogenesis in mice exempt from thermal stress by living at thermoneutrality. *Cell Metab.* 9, 203–209. doi: 10.1016/j.cmet.2008.12.014
- Fisher, F. M., Kleiner, S., Douris, N., Fox, E. C., Mepani, R. J., Verdeguez, F., et al. (2012). FGF21 regulates PGC-1 $\alpha$  and browning of white adipose tissues in adaptive thermogenesis. *Genes Dev.* 26, 271–281. doi: 10.1101/gad.177857.111
- Fletcher, J. A., Linden, M. A., Sheldon, R. D., Meers, G. M., Morris, E. M., Butterfield, A., et al. (2016). Fibroblast growth factor 21 and exercise-induced hepatic mitochondrial adaptations. *Am. J. Physiol. Gastrointest. Liver Physiol.* 310, G832–G843. doi: 10.1152/ajpgi.00355.2015
- Gaich, G., Chien, J. Y., Fu, H., Glass, L. C., Deeg, M. A., Holland, W. L., et al. (2013). The effects of LY2405319, an FGF21 analog, in obese human subjects with type 2 diabetes. *Cell Metab.* 18, 333–340. doi: 10.1016/j.cmet.2013.08.005
- Gaidhu, M. P., Fediuc, S., Anthony, N. M., So, M., Mirpourian, M., Perry, R. L., et al. (2009). Prolonged AICAR-induced AMP-kinase activation promotes energy dissipation in white adipocytes: novel mechanisms integrating HSL and ATGL. *J. Lipid Res.* 50, 704–715. doi: 10.1194/jlr.M800480-JLR200
- Giralt, M., Gavalda-Navarro, A., and Villarroya, F. (2015). Fibroblast growth factor-21, energy balance and obesity. *Mol. Cell. Endocrinol.* 418, 66–73. doi: 10.1016/j.mce.2015.09.018
- Golozoubova, V., Hohtola, E., Matthias, A., Jacobsson, A., Cannon, B., and Nedergaard, J. (2001). Only UCP1 can mediate adaptive nonshivering thermogenesis in the cold. *FASEB J.* 15, 2048–2050. doi: 10.1096/fj.00-0536fje
- Gómez-Sámano, M. Á., Grajales-Gómez, M., Zuñiga-Vázquez, J. M., Navarro-Flores, M. F., Martínez-Saavedra, M., Juárez-León, Ó. A., et al. (2017). Fibroblast growth factor 21 and its novel association with oxidative stress. *Redox Biol.* 11, 335–341. doi: 10.1016/j.redox.2016.12.024
- Gustafson, B., and Smith, U. (2015). Regulation of white adipogenesis and its relation to ectopic fat accumulation and cardiovascular risk. *Atherosclerosis* 241, 27–35. doi: 10.1016/j.atherosclerosis.2015.04.812
- Harms, M., and Seale, P. (2013). Brown and beige fat: development, function and therapeutic potential. *Nat. Med.* 19, 1252–1263. doi: 10.1038/nm.3361
- Hasek, B. E., Stewart, L. K., Henagan, T. M., Boudreau, A., Lenard, N. R., Black, C., et al. (2010). Dietary methionine restriction enhances metabolic flexibility and increases uncoupled respiration in both fed and fasted states. *Am. J. Physiol. Regul. Integr. Comp. Physiol.* 299, R728–R739. doi: 10.1152/ajpregu.00837.2009
- Hondares, E., Iglesias, R., Giralt, A., Gonzalez, F. J., Giralt, M., Mampel, T., et al. (2011). Thermogenic activation induces FGF21 expression and release in brown adipose tissue. *J. Biol. Chem.* 286, 12983–12990. doi: 10.1074/jbc.M110.215889
- Hondares, E., Rosell, M., Gonzalez, F. J., Giralt, M., Iglesias, R., and Villarroya, F. (2010). Hepatic FGF21 expression is induced at birth via PPAR  $\alpha$  in response to milk intake and contributes to thermogenic activation of neonatal brown fat. *Cell Metab.* 11, 206–212. doi: 10.1016/j.cmet.2010.02.001
- Hu, J., and Christian, M. (2017). Hormonal factors in the control of the browning of white adipose tissue. *Horm. Mol. Biol. Clin. Invest.* 31, 1868–1891. doi: 10.1515/hmbci-2017-0017
- Inagaki, T., Lin, V. Y., Goetz, R., Mohammadi, M., Mangelsdorf, D. J., and Kliewer, S. A. (2008). Inhibition of growth hormone signaling by the fasting-induced hormone FGF21. *Cell Metab.* 8, 77–83. doi: 10.1016/j.cmet.2008.05.006
- Jespersen, N. Z., Larsen, T. J., Peijs, L., Dagaard, S., Homoe, P., Loft, A., et al. (2013). A classical brown adipose tissue mRNA signature partly overlaps with brite in the supraclavicular region of adult humans. *Cell Metab.* 17, 798–805. doi: 10.1016/j.cmet.2013.04.011
- Jian, W.-X., Peng, W.-H., Jin, J., Chen, X.-R., Fang, W.-J., Wang, W.-X., et al. (2012). Association between serum fibroblast growth factor 21 and diabetic nephropathy. *Metabolism* 61, 853–859. doi: 10.1016/j.metabol.2011.10.012
- Jimenez, M., Barbatelli, G., Allevi, R., Cinti, S., Seydoux, J., Giacobino, J. P., et al. (2003). Beta 3-adrenoceptor knockout in C57BL/6J mice depresses the occurrence of brown adipocytes in white fat. *Eur. J. Biochem.* 270, 699–705. doi: 10.1046/j.1432-1033.2003.03422.x
- Joffin, N., Jaubert, A. M., Bamba, J., Barouki, R., Noirez, P., and Forest, C. (2015). Acute induction of uncoupling protein 1 by citrulline in cultured explants of white adipose tissue from lean and high-fat-diet-fed rats. *Adipocyte* 4, 129–134. doi: 10.4161/21623945.2014.989748
- Keipert, S., Kutschke, M., Lamp, D., Brachthäuser, L., Neff, F., Meyer, C. W., et al. (2015). Genetic disruption of uncoupling protein 1 in mice renders brown adipose tissue a significant source of FGF21 secretion. *Mol. Metab.* 4, 537–542. doi: 10.1016/j.molmet.2015.04.006
- Keipert, S., Ost, M., Johann, K., Imber, F., Jastroch, M., van Schothorst, E. M., et al. (2014). Skeletal muscle mitochondrial uncoupling drives endocrine cross-talk through the induction of FGF21 as a myokine. *Am. J. Physiol. Endocrinol. Metab.* 306, E469–E482. doi: 10.1152/ajpendo.00330.2013
- Kharitonov, A., Shiyanova, T. L., Koester, A., Ford, A. M., Micanovic, R., Galbreath, E. J., et al. (2005). FGF-21 as a novel metabolic regulator. *J. Clin. Invest.* 115, 1627–1635. doi: 10.1172/JCI23606
- Kim, K. H., Kim, S. H., Yang, H. M., Lee, J. B., and Lee, M. S. (2013). Acute exercise induces FGF21 expression in mice and healthy humans. *PLoS One* 8:e63517. doi: 10.1371/journal.pone.0063517
- Kolumam, G., Chen, M. Z., Tong, R., Zavala-Solorio, J., Kates, L., van Bruggen, N., et al. (2015). Sustained brown fat stimulation and insulin sensitization by a humanized bispecific antibody agonist for fibroblast growth factor receptor 1/ $\beta$ KLTHO complex. *EBioMedicine* 2, 730–743. doi: 10.1016/j.ebiom.2015.05.028
- Lafontan, M., Moro, C., Berlan, M., Crampes, F., Sengenès, C., and Galitzky, J. (2008). Control of lipolysis by natriuretic peptides and cyclic GMP. *Trends Endocrinol. Metab.* 19, 130–137. doi: 10.1016/j.tem.2007.11.006
- Lee, H. J., Lee, J. O., Kim, N., Kim, J. K., Kim, H. I., Lee, Y. W., et al. (2015). Irisin, a novel myokine, regulates glucose uptake in skeletal muscle cells via AMPK. *Mol. Endocrinol.* 29, 873–881. doi: 10.1210/me.2014-1353
- Lee, J. Y., Takahashi, N., Yasubuchi, M., Kim, Y. I., Hashizaki, H., Kim, M. J., et al. (2012). Triiodothyronine induces UCP-1 expression and mitochondrial biogenesis in human adipocytes. *Am. J. Physiol. Cell Physiol.* 302, C463–C472. doi: 10.1152/ajpcell.00010.2011

- Lee, P., Linderman, J. D., Smith, S., Brychta, R. J., Wang, J., Idelson, C., et al. (2014). Irisin and FGF21 are cold-induced endocrine activators of brown fat function in humans. *Cell Metab.* 19, 302–309. doi: 10.1016/j.cmet.2013.12.017
- Li, H., Wu, G., Fang, Q., Zhang, M., Hui, X., Sheng, B., et al. (2018). Fibroblast growth factor 21 increases insulin sensitivity through specific expansion of subcutaneous fat. *Nat. Commun.* 2:272. doi: 10.1038/s41467-017-02677-9
- Li, P., Zhu, Z., Lu, Y., and Granneman, J. G. (2005). Metabolic and cellular plasticity in white adipose tissue II: role of peroxisome proliferator-activated receptor- $\alpha$ . *Am. J. Physiol. Endocrinol. Metab.* 289, E617–E626. doi: 10.1152/ajpendo.00010.2005
- Lin, Z., Tian, H., Lam, K. S., Lin, S., Hoo, R. C., Konishi, M., et al. (2013). Adiponectin mediates the metabolic effects of FGF21 on glucose homeostasis and insulin sensitivity in mice. *Cell Metab.* 17, 779–789. doi: 10.1016/j.cmet.2013.04.005
- Luo, L., and Liu, M. (2016). Adipose tissue in control of metabolism. *J. Endocrinol.* 231, R77–R99. doi: 10.1530/JOE-16-0211
- Maeda, H., Hosokawa, M., Sashima, T., Funayama, K., and Miyashita, K. (2005). Fucoxanthin from edible seaweed, *Undaria pinnatifida*, shows antiobesity effect through UCP1 expression in white adipose tissues. *Biochem. Biophys. Res. Commun.* 332, 392–397. doi: 10.1016/j.bbrc.2005.05.002
- Magliano, D. C., Bargut, T. C., de Carvalho, S. N., Aguila, M. B., Mandarim-de-Lacerda, C. A., and Souza-Mello, V. (2013). Peroxisome proliferator-activated receptors- $\alpha$  and gamma are targets to treat offspring from maternal diet-induced obesity in mice. *PLoS One* 8:e64258. doi: 10.1371/journal.pone.0064258
- Mossenbock, K., Vegiopoulos, A., Rose, A. J., Sijmonsma, T. P., Herzig, S., and Schafmeier, T. (2014). Browning of white adipose tissue uncouples glucose uptake from insulin signaling. *PLoS One* 9:e110428. doi: 10.1371/journal.pone.0110428
- Mu, J., Pinkstaff, J., Li, Z., Skidmore, L., Li, N., Myler, H., et al. (2012). FGF21 analogs of sustained action enabled by orthogonal biosynthesis demonstrate enhanced antidiabetic pharmacology in rodents. *Diabetes* 61, 505–512. doi: 10.2337/db11-0838
- Murholm, M., Isidor, M. S., Basse, A. L., Winther, S., Sorensen, C., Skovgaard-Petersen, J., et al. (2013). Retinoic acid has different effects on UCP1 expression in mouse and human adipocytes. *BMC Cell Biol.* 14:41. doi: 10.1186/1471-2121-14-41
- Nedergaard, J., Bengtsson, T., and Cannon, B. (2007). Unexpected evidence for active brown adipose tissue in adult humans. *Ame. J. Physiol. Endocrinol. Metabol.* 293, E444–E452. doi: 10.1152/ajpendo.00691.2006
- Nishimura, T., Nakatake, Y., Konishi, M., and Itoh, N. (2000). Identification of a novel FGF, FGF-21, preferentially expressed in the liver. *Biochem. Biophys. Acta* 1492, 203–206. doi: 10.1016/S0167-4781(00)00067-1
- Owen, B. M., Ding, X., Morgan, D. A., Coate, K. C., Bookout, A. L., Rahmouni, K., et al. (2014). FGF21 acts centrally to induce sympathetic nerve activity, energy expenditure, and weight loss. *Cell Metab.* 20, 670–677. doi: 10.1016/j.cmet.2014.07.012
- Park, A., Kim, W. K., and Bae, K. H. (2014). Distinction of white, beige and brown adipocytes derived from mesenchymal stem cells. *World J. Stem Cells* 6, 33–42. doi: 10.4252/wjsc.v6.i1.33
- Petrovic, N., Walden, T. B., Shabalina, I. G., Timmons, J. A., Cannon, B., and Nedergaard, J. (2010). Chronic peroxisome proliferator-activated receptor gamma (PPARgamma) activation of epididymally derived white adipocyte cultures reveals a population of thermogenically competent, UCP1-containing adipocytes molecularly distinct from classic brown adipocytes. *J. Biol. Chem.* 285, 7153–7164. doi: 10.1074/jbc.M109.053942
- Piya, M. K., McTernan, P. G., and Kumar, S. (2013). Adipokine inflammation and insulin resistance: the role of glucose, lipids, and endotoxin. *J. Endocrinol.* 216, T1–T15. doi: 10.1530/JOE-12-0498
- Puigserver, P., Pico, C., Stock, M. J., and Palou, A. (1996). Effect of selective beta-adrenoceptor stimulation on UCP synthesis in primary cultures of brown adipocytes. *Mol. Cell. Endocrinol.* 117, 7–16. doi: 10.1016/0303-7207(95)03727-6
- Rachid, T. L., Penna-de-Carvalho, A., Brighenti, I., Aguila, M. B., Mandarim-de-Lacerda, C. A., and Souza-Mello, V. (2015). Fenofibrate (PPARalpha agonist) induces beige cell formation in subcutaneous white adipose tissue from diet-induced male obese mice. *Mol. Cell. Endocrinol.* 402, 86–94. doi: 10.1016/j.mce.2014.12.027
- Samms, R. J., Smith, D. P., Cheng, C. C., Antonellis, P. P., Perfield, J. W. II, Kharitononkov, A., et al. (2015). Discrete aspects of FGF21 in vivo pharmacology do not require UCP1. *Cell Rep.* 11, 991–999. doi: 10.1016/j.celrep.2015.04.046
- Sanchez-Gurmaches, J., and Guertin, D. A. (2014). Adipocytes arise from multiple lineages that are heterogeneously and dynamically distributed. *Nat. Commun.* 5:4099. doi: 10.1038/ncomms5099
- Schoenberg, K. M., Giesy, S. L., Harvatine, K. J., Waldron, M. R., Cheng, C., Kharitononkov, A., et al. (2011). Plasma FGF21 is elevated by the intense lipid mobilization of lactation. *Endocrinology* 152, 4652–4661. doi: 10.1210/en.2011-1425
- Schulz, T. J., Huang, T. L., Tran, T. T., Zhang, H., Townsend, K. L., Shadrach, J. L., et al. (2011). Identification of inducible brown adipocyte progenitors residing in skeletal muscle and white fat. *Proc. Natl. Acad. Sci. U.S.A.* 108, 143–148. doi: 10.1073/pnas.1010929108
- Seale, P., Kajimura, S., Yang, W., Chin, S., Rohas, L. M., Uldry, M., et al. (2007). Transcriptional control of brown fat determination by PRDM16. *Cell Metab.* 6, 38–54. doi: 10.1016/j.cmet.2007.06.001
- Summermatter, S., Shui, G., Maag, D., Santos, G., Wenk, M. R., and Handschin, C. H. (2013). PGC-1  $\alpha$  improves glucose homeostasis in skeletal muscle in an activity-dependent manner. *Diabetes* 62, 85–95. doi: 10.2337/db12-0291
- Suomalainen, A., Elo, J. M., Pietiläinen, K. H., Hakonen, A. H., Sevastianova, K., Korpela, M., et al. (2011). FGF-21 as a biomarker for muscle-manifesting mitochondrial respiratory chain deficiencies: a diagnostic study. *Lancet Neurol.* 10, 806–818. doi: 10.1016/S1474-4422(11)70155-7
- Talukdar, S., Zhou, Y., Li, D., Rossulek, M., Dong, J., Somayaji, V., et al. (2016). A long-acting FGF21 molecule, PF-05231023, decreases body weight and improves lipid profile in non-human primates and type 2 diabetic subjects. *Cell Metab.* 23, 427–440. doi: 10.1016/j.cmet.2016.02.001
- Teodoro, J. S., Zouhar, P., Flachs, P., Bardova, K., Janovska, P., Gomes, A. P., et al. (2014). Enhancement of brown fat thermogenesis using chenodeoxycholic acid in mice. *Int. J. Obes.* 38, 1027–1034. doi: 10.1038/ijo.2013.230
- Veniant, M. M., Hale, C., Helmering, J., Chen, M. M., Stanislaus, S., Busby, J., et al. (2012). FGF21 promotes metabolic homeostasis via white adipose and leptin in mice. *PLoS One* 7:e40164. doi: 10.1371/journal.pone.0040164
- Veniant, M. M., Sivits, G., Helmering, J., Komorowski, R., Lee, J., Fan, W., et al. (2015). Pharmacologic effects of FGF21 are independent of the “browning” of white adipose tissue. *Cell Metab.* 21, 731–738. doi: 10.1016/j.cmet.2015.04.019
- Villarroya, F., Cereijo, R., Villarroya, J., and Giral, M. (2017). Brown adipose tissue as a secretory organ. *Nat. Rev. Endocrinol.* 13, 26–35. doi: 10.1038/nrendo.2016.136
- Wang, S., Liang, X., Yang, Q., Fu, X., Rogers, C. J., Zhu, M., et al. (2015). Resveratrol induces brown-like adipocyte formation in white fat through activation of AMP activated protein kinase (AMPK)  $\alpha$ 1. *Int. J. Obes.* 39, 967–976. doi: 10.1038/ijo.2015.23
- Watanabe, M., Houten, S. M., Matak, C., Christoffolete, M. A., Kim, B. W., Sato, H., et al. (2006). Bile acids induce energy expenditure by promoting intracellular thyroid hormone activation. *Nature* 439, 484–489. doi: 10.1038/nature04330
- Whittle, A. J., Carobbio, S., Martins, L., Slawik, M., Hondares, E., Vazquez, M. J., et al. (2012). BMP8B increases brown adipose tissue thermogenesis through both central and peripheral actions. *Cell* 149, 871–885. doi: 10.1016/j.cell.2012.02.066
- Wu, A. L., Kolumam, G., Stawicki, S., Chen, Y., Li, J., Zavala-Solorio, J., et al. (2011). Amelioration of type 2 diabetes by antibody-mediated activation of fibroblast growth factor receptor 1. *Sci. Transl. Med.* 3:113ra126. doi: 10.1126/scitranslmed.3002669
- Wu, J., Bostrom, P., Sparks, L. M., Ye, L., Choi, J. H., Giang, A. H., et al. (2012). Beige adipocytes are a distinct type of thermogenic fat cell in mouse and human. *Cell* 150, 366–376. doi: 10.1016/j.cell.2012.05.016
- Wu, J., Cohen, P., and Spiegelman, B. M. (2013). Adaptive thermogenesis in adipocytes: is beige the new brown? *Genes Dev.* 27, 234–250. doi: 10.1101/gad.211649.112
- Young, P., Arch, J. R., and Ashwell, M. (1984). Brown adipose tissue in the parametrial fat pad of the mouse. *FEBS Lett.* 167, 10–14. doi: 10.1016/0014-5793(84)80822-4

- Zhang, X., Yeung, D. C., Karpisek, M., Stejskal, D., Zhou, Z. G., Liu, F., et al. (2008). Serum FGF21 levels are increased in obesity and are independently associated with the metabolic syndrome in humans. *Diabetes* 57, 1246–1253. doi: 10.2337/db07-1476
- Zhang, X., Zhang, Q. X., Wang, X., Zhang, L., Qu, W., Bao, B., et al. (2016). Dietary luteolin activates browning and thermogenesis in mice through an AMPK/PGC1alpha pathway-mediated mechanism. *Int. J. Obes.* 40, 1841–1849. doi: 10.1038/ijo.2016.108
- Zhang, Y., Li, R., Meng, Y., Li, S., Donelan, W., Zhao, Y., et al. (2014). Irisin stimulates browning of white adipocytes through mitogen-activated protein kinase p38 MAP kinase and ERK MAP kinase signaling. *Diabetes* 63, 514–525. doi: 10.2337/db13-1106
- Zhang, Y., Xie, C., Wang, H., Foss, R. M., Clare, M., George, E. V., et al. (2016). Irisin exerts dual effects on browning and adipogenesis of human white adipocytes. *Am. J. Physiol. Endocrinol. Metab.* 311, E530–E541. doi: 10.1152/ajpendo.00094.2016
- Zhang, Y., Xie, Y., Berglund, E. D., et al. (2012). The starvation hormone, fibroblast growth factor-21, extends lifespan in mice. *eLife* 1:e00065. doi: 10.7554/eLife.00065
- Zhao, M., and Chen, X. (2014). Eicosapentaenoic acid promotes thermogenic and fatty acid storage capacity in mouse subcutaneous adipocytes. *Biochem. Biophys. Res. Commun.* 450, 1446–1451. doi: 10.1016/j.bbrc.2014.07.010
- Zoli, M., and Picciotto, M. R. (2012). Nicotinic regulation of energy homeostasis. *Nicotine Tob. Res.* 14, 1270–1290. doi: 10.1093/ntr/nts159
- Conflict of Interest Statement:** The authors declare that the research was conducted in the absence of any commercial or financial relationships that could be construed as a potential conflict of interest.

Copyright © 2019 Cuevas-Ramos, Mehta and Aguilar-Salinas. This is an open-access article distributed under the terms of the Creative Commons Attribution License (CC BY). The use, distribution or reproduction in other forums is permitted, provided the original author(s) and the copyright owner(s) are credited and that the original publication in this journal is cited, in accordance with accepted academic practice. No use, distribution or reproduction is permitted which does not comply with these terms.





# Secretory Proteome of Brown Adipocytes in Response to cAMP-Mediated Thermogenic Activation

Joan Villarroya<sup>1,2</sup>, Rubén Cereijo<sup>1,3</sup>, Marta Giral<sup>1,3</sup> and Francesc Villarroya<sup>1,3\*</sup>

<sup>1</sup> Departament de Bioquímica i Biomedicina Molecular and Institut de Biomedicina (IBUB), Universitat de Barcelona, Barcelona, Spain, <sup>2</sup> Infectious Diseases Unit, Hospital de la Santa Creu i Sant Pau, Barcelona, Spain, <sup>3</sup> CIBER Fisiopatología de la Obesidad y Nutrición, Madrid, Spain

## OPEN ACCESS

### Edited by:

Paula Oliver,  
Universidad de les Illes Balears, Spain

### Reviewed by:

Joan Ribot,  
Universidad de les Illes Balears, Spain  
Rushita Bagchi,  
University of Colorado Denver,  
United States

### \*Correspondence:

Francesc Villarroya  
fvillarroya@ub.edu

### Specialty section:

This article was submitted to  
Integrative Physiology,  
a section of the journal  
Frontiers in Physiology

**Received:** 28 August 2018

**Accepted:** 21 January 2019

**Published:** 07 February 2019

### Citation:

Villarroya J, Cereijo R, Giral M and  
Villarroya F (2019) Secretory Proteome  
of Brown Adipocytes in Response to  
cAMP-Mediated Thermogenic  
Activation. *Front. Physiol.* 10:67.  
doi: 10.3389/fphys.2019.00067

**Background:** The secretory properties of brown adipose tissue are thought to contribute to the association between active brown fat and a healthy metabolic status. Although a few brown adipokines have been identified, a comprehensive knowledge of the brown adipose tissue secretome is lacking.

**Methods:** Here, to examine the effects of thermogenic activation of brown adipocytes on protein secretion, we used isobaric tags for relative and absolute quantification (iTRAQ) analysis to determine how the secreted proteome of brown adipocytes (that detected in cell culture medium) differed in response to cAMP.

**Results:** Our results indicated that 56 secreted proteins were up-regulated in response to cAMP. Of them, nearly half (29) corresponded to extracellular matrix components and regulators. Several previously known adipokines, were also detected. Unexpectedly, we also found five components of the complement system. Only 15 secreted proteins were down-regulated by cAMP; of them three were ECM-related and none was related to the complement system. We observed a partial concordance between the cAMP-regulated release of proteins (both from proteomics and from antibody-based quantification of specific proteins) and the cAMP-mediated regulation of their encoding transcript for the up-regulated secreted proteins. However, a stronger concordance was seen for the down-regulated secreted proteins.

**Conclusions:** The present results highlight the need to investigate previously unrecognized processes such as the role of extracellular matrix in thermogenic activation-triggered brown fat remodeling, as well as the intriguing question of how brown adipocyte-secreted complement factors contribute to the signaling properties of active brown adipose tissue.

**Keywords:** brown adipose tissue, thermogenesis, secretome, adipokine, extracellular matrix

## INTRODUCTION

The high capacity of brown adipose tissue (BAT) for energy expenditure and oxidation of glucose and lipids is associated with protection against obesity, hyperglycemia and hyperlipidemia in rodents and possibly in humans (Bartelt et al., 2011; Giralto and Villarroya, 2017; Carobbio et al., 2018). However, the effects of BAT on metabolism may also reflect the release of bioactive factors that act in autocrine, paracrine, and even endocrine manners (Villarroya et al., 2017). The secretory activity of white fat has long been recognized and a large number of “white” adipokines have been identified. In contrast, the secretory properties of BAT have received much less research attention. Most brown adipokines were identified from the high-level expression of genes encoding putative secreted proteins, such as fibroblast growth factor-21 (FGF21) or interleukin-6 (IL-6) in active BAT (Burýsek and Houstek, 1997; Hondares et al., 2011). In some cases, brown adipokine candidates were identified by screening transcriptomic data from BAT using bioinformatic tools that can predict the “secretability” of encoded factors (Wang et al., 2014; Verdeguer et al., 2015; Cereijo et al., 2018). Other approaches have used indirect methodologies, such as signal sequence trap (Hansen et al., 2014). However, we still lack a comprehensive knowledge of the BAT secretome. Here, we use an updated iTRAQ-based proteomic analysis to provide the first report of a direct assessment of proteins secreted by brown adipocytes in response to cAMP, which is the main intracellular mediator of BAT thermogenic activity.

## MATERIALS AND METHODS

### Cell Culture

Murine C57BAT brown pre-adipocytes were supplied by Klein et al. (1999) and were obtained using protocols approved by the Institutional Animal Care and Use Committee, Joslin Diabetes Center (Boston, USA). Pre-adipocytes were cultured in DMEM (Life Technologies, Grand Island, NY, USA), 10% FBS, 1% penicillin-streptomycin, for 2–3 days. Before differentiation was induced, the plates were rinsed with PBS to remove the FBS; further culture was performed in FBS-free medium. Differentiation was induced by culturing cells overnight in DMEM plus T3 (1 nM), insulin (20 nM), IBMX (500  $\mu$ M), dexamethasone (2 mM), and indomethacin (125  $\mu$ M), and then replacing this medium with DMEM plus T3 and insulin until brown adipocytes had fully differentiated (5–6 days). Differentiated brown adipocytes were left untreated or treated with 1 mM dibutyl-*c*-AMP for 24 h. Three independent samples were used for each group. Medium was collected and cells were scrapped and collected for RNA analysis. Unless otherwise noted, reagents were from Merck Sigma-Aldrich, S. Louis, MO, USA.

### Comparative Proteomic Analysis iTRAQ

Identification of proteins with differences in abundance between cAMP-treated and non-cAMP-treated brown adipocytes was performed using the isobaric tag for relative and absolute quantitation (iTRAQ) technology (see **Supplementary Material** for detailed methodology). Three independent replicates were

prepared for each sample. Samples were resuspended in 500 mM triethyl ammonium bicarbonate/8M urea solution. Proteins were reduced with tris (2-carboxyethyl) phosphine, alkylated with iodoacetamide and digested with porcine trypsin (Promega, Madison, WI, USA). Digested peptides were labeled with 8-plex iTRAQ reagent (AB Sciex, Wien, Austria). Pooled peptides were cleaned up in two steps: C18 clean-up (reverse phase, toptip C18) and then SCX cleanup (strong cationic exchange, P200 toptip, PolySULFOETHYL A) (PolyLC, Columbia, MD, USA). Peptides were analyzed by liquid chromatography coupled to mass spectrometry using nanoAcquity (Waters, Milford, MA, USA) coupled to LTQ-Orbitrap Velos mass spectrometer (ThermoScientific, Foster City, CA, USA). Up to the 10 most abundant peptides were selected from each MS scan and then fragmented using Higher Energy Collision Dissociation. Database search was performed with Mascot search engine against SwissProt/Uniprot database. IsobariQ software (Arntzen et al., 2011) was used to perform the relative quantitation of proteins by iTRAQ. We used the annotation “extracellular” in the Gene Ontology database, TargetP 1.1 (Emanuelsson et al., 2007), and Secretome P 2.0 (Bendtsen et al., 2004) software to identify secreted proteins. Crude data from proteomics analysis are available at [www.adipoplast.org/database](http://www.adipoplast.org/database).

### Quantitative Real Time PCR

RNA was extracted (Nucleospin, Macherey-Nagel, Düren, Germany) and retrotranscribed using TaqMan Reverse Transcription Reagents (Applied Biosystems, Foster City, CA, USA). Transcript levels were determined by quantitative real-time PCR on a 7500 Real-Time PCR System (Applied Biosystems), using TaqMan assays or SyberGreen assays with specifically designed primers (PerlPrimer software) (see **Supplementary Material**). The mRNA levels of each gene of interest was normalized to 18S rRNA levels using the  $2^{-\Delta Ct}$  method.

### Specific Quantification of Secreted Proteins

Individual proteins were quantified in brown adipocyte culture medium using specific ELISA kits (see **Supplemental Table 2** for suppliers), except retinol-binding protein-4 (RBP4), which was quantified by immunoblotting, as previously described (Rosell et al., 2012).

## RESULTS

### Differentiation and Effects of cAMP in Brown Adipocytes Cultured in Serum-Free Medium

Our brown adipocyte culture protocol, adapted to allow a proteomics-based analysis of the culture medium (see section Materials and Methods), resulted in more than 90% adipogenic differentiation, as assessed by the percentage of cells exhibiting lipid droplet accumulations (**Figure 1A**), and expression of the brown adipocyte marker gene *Ucp1*. Cell culture media were collected from cAMP-treated and non-treated controls

for proteomic analysis. Transcript levels of *Ucp1* and *Fgf21*, which encodes for a thermogenically-regulated secreted protein (Hondares et al., 2011), were strongly induced in cAMP-treated brown adipocytes (Figure 1B). This validates the experimental model used to perform the proteomic analysis.

## Identification of cAMP-Regulated Secreted Proteins

A total of 71 extracellular proteins were found to differ in their abundance in cAMP-treated vs. non-treated cultures (Table 1). Fifty-six secreted proteins were induced by cAMP (Figure 1C, left). Of them, 40% (22 proteins) were components of the extracellular matrix (ECM) and 13% (7 proteins) were matricellular proteins (non-structural proteins that are present in the ECM and play regulatory roles). Among the remaining up-regulated secreted proteins, seven were extracellular enzymes, six were adipokines, and four corresponded to components of the complement system. Finally, we observed up-regulation of 10 varied proteins, including cytokines, transporters, and proteins of unknown function. Notably, fewer secreted proteins were down-regulated by cAMP (Figure 1C, right). Of these 15 proteins, five were extracellular enzymes, three were ECM-related, one was an adipokine, and six formed a heterogeneous group of proteins with multiple or unknown functions.

To ascertain whether secreted proteins underwent transcriptional regulation in response to cAMP, we measured the transcript levels of selected components of the distinct groups of differentially secreted proteins. We found that secreted proteins that were up-regulated by cAMP did not show a systematic relationship with transcript expression (Figure 1D). Among the ECM-related genes, the three tested collagen gene transcripts (*Col1a1*, *Col4a1*, and *Col4a2*) failed to show cAMP-induced up-regulation; indeed *Col1a1* was down-regulated. In contrast, the transcript level of *Lamb1* was increased by cAMP, consistently with the up-regulation of secreted laminin- $\beta$ 1 protein in cAMP-treated cultures. With respect to extracellular enzymes, the transcript levels of *Xdh* and *Ppia* were increased in response to cAMP, as observed for the corresponding secreted proteins. The analyzed adipokine-encoding gene transcripts varied: *Fabp4* was up-regulated, *Adipoq* was down-regulated, and *Rbp4* was unchanged. Varied changes were also observed for the transcripts encoding some of the other cAMP-induced secreted proteins: cAMP increased the transcript level of *Grn* (granulins), but decreased that of *Orm1* (orosomucoid). Among the transcripts encoding for secreted proteins whose abundance was reduced by cAMP treatment, we found a more consistent pattern: the transcript levels of *Efemp1*, *Lpl*, *Lbp*, and *B2m* were all significantly down-regulated in response to cAMP (Figure 1E).

Given the discordance between proteome-based detection of secreted proteins and the corresponding transcripts in some cases, levels of selected proteins from distinct functional groups were individually quantified. COL1A1, LAMB1, RBP4, and GRN proteins were confirmed to be up-regulated and LBP to be down-regulated by cAMP. However, adiponectin (ADIPOQ) and ORM1 were not confirmed to be up-regulated by cAMP,

and results were more concordant with transcript changes (Figure 1F).

## DISCUSSION

To our knowledge, this report describes the first direct assessment of the protein secretome of cultured brown adipocytes stimulated with cAMP, which triggers thermogenic activation. Thirteen of the proteins we detected with our iTRAQ-based method coincided with those identified by Hansen et al. (2014) using indirect signal sequence trap method to identify brown adipocyte-secreted proteins in response to norepinephrine (Table 1). They corresponded mainly to ECM-related factors (6) and the miscellaneous group of proteins (5). Moreover, a recent iTRAQ-based detection of proteins secreted early after induction of 3T3-L1 white adipocyte differentiation (Ojima et al., 2016) using isobutyl-methylxanthine (a phosphodiesterase inhibitor that raises intracellular cAMP) yielded results that were similar to our data. Matches were seen for 41% of the ECM-related proteins (12 of 29), 66% of the adipokines (4 of 6), and 60% of the “others” (6 of 10) (Table 1). This similarity between the two data sets may reflect the activation of common cAMP-dependent pathways in adipogenic cells.

A remarkable finding of our study is the strong representation (around 50%) of ECM-related components in the cAMP-induced secretome of brown adipocytes. A functional and flexible ECM is essential for healthy expansion of WAT (Sun et al., 2013). The thermogenic activation of BAT causes a tissue recruitment that involves hypertrophic and hyperplastic processes (Cannon and Nedergaard, 2004). The cAMP-induced secretion of ECM components, such as specific types of collagen and matricellular proteins, may be relevant to the remodeling of ECM under conditions of BAT expansion in response to thermogenic activation. Further research will be needed to explore this novel notion in BAT biology.

We identified several components of the complement system in the cAMP-induced secretome of brown adipocytes. Hansen et al. (2014) also identified several components of the complement system in their brown adipocyte secretome analysis. Interestingly, a transcriptomic analysis identified complement factor-4 as one of the top secreted protein-encoding transcripts up-regulated in human BAT vs. WAT (Svensson et al., 2011). Complement factor-D (adipsin), one of the first white adipokines identified (Cook et al., 1987), was here found to be up-regulated in the secretome of cAMP-treated brown adipocytes. Further research is warranted to ascertain the role of complement system components in the signaling that originates in brown adipocytes upon thermogenic activation.

Our study identified several brown adipokines previously reported to be regulated in response to thermogenic activation in adipose tissues, such as adiponectin (Hui et al., 2015), RBP4 (Rosell et al., 2012), angiotensinogen (Cassis, 1993), fatty acid binding protein-4 (Shu et al., 2017), and lipopolysaccharide binding protein (LBP) (Gavalda-Navarro et al., 2016). These findings further validate our proteomic analysis. However, our

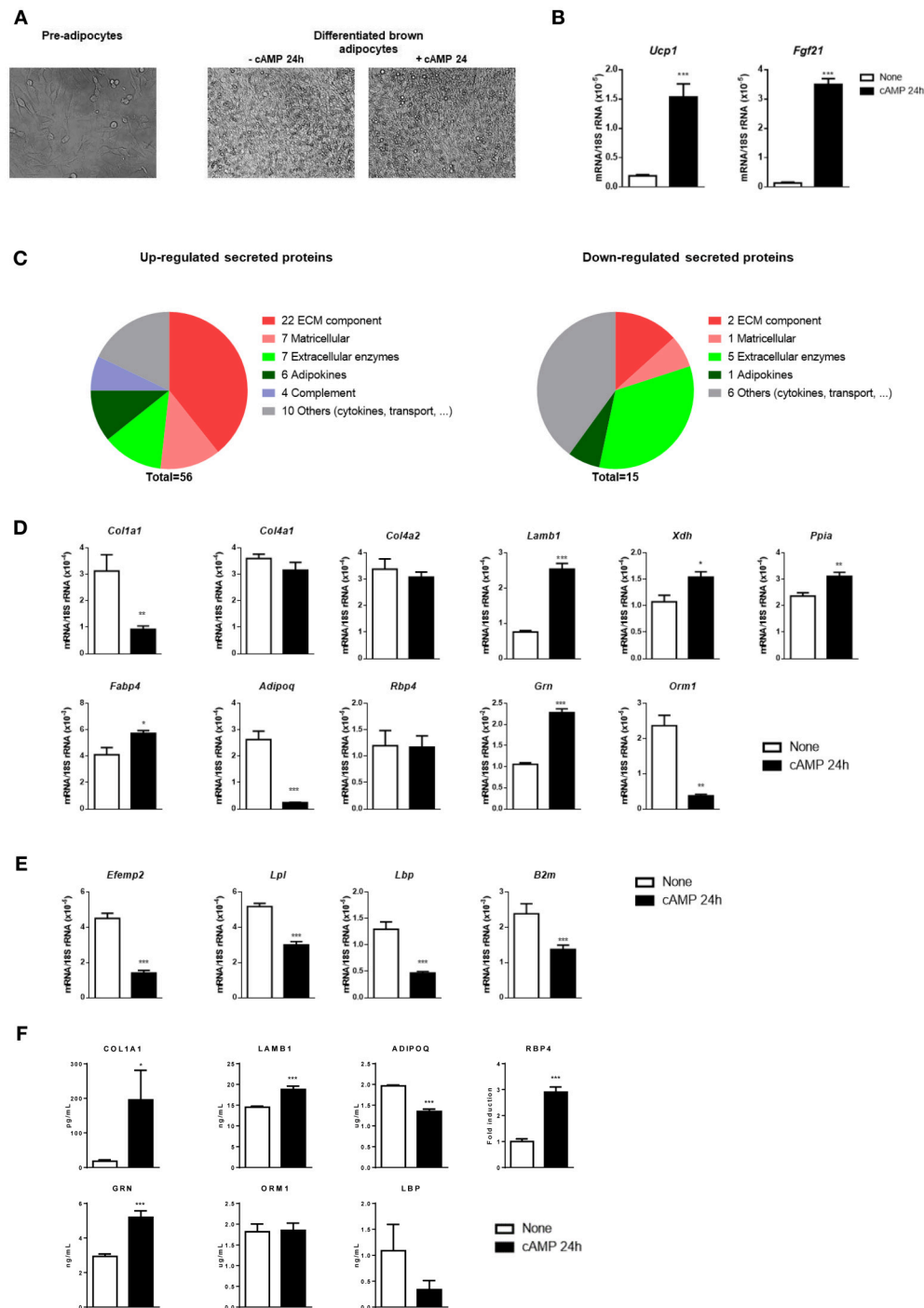


**FIGURE 1 |** Differentiation, transcript levels, and secreted proteins in cultured brown adipocytes in response to cAMP. **(A)** Representative optical microscopic images of pre-adipocytes (left), and brown adipocytes left untreated or treated with cAMP for 24 h (right). **(B)** Relative transcript levels of *Ucp1* and *Fgf21* in untreated (none) and cAMP-treated (cAMP 24 h) differentiated brown adipocytes ( $n = 6$ ). **(C)** Secreted proteins found to be up-regulated (left) and down-regulated (right) in response to cAMP were classified into six groups according to their function: ECM component, matricellular, extracellular enzymes, adipokines, complement, and others (cytokines, transport, etc). **(D)** Transcript levels corresponding to selected secreted proteins up-regulated by cAMP treatment of brown adipocytes. **(E)** Transcript levels corresponding to selected secreted proteins down-regulated by cAMP treatment of brown adipocytes. **(F)** Levels of secreted proteins in brown adipocyte culture medium individually quantified using specific antibody-based methods. Bars represent means  $\pm$  s.e.m of six samples per group. Two-tailed unpaired Student's *t*-test was used to compare means (\* $p < 0.05$ , \*\* $p < 0.01$ , \*\*\* $p < 0.001$ , cAMP vs. no treatment).



**TABLE 1** | List of secreted proteins found to be up-regulated (A) or down-regulated (B) upon cAMP treatment of brown adipocytes, categorized by their functions.

Function	UniprotKB	Gene symbol	Description	Length	cAMP-induced fold-change
<b>(A) UP REGULATED PROTEINS IN RESPONSE To cAMP</b>					
ECM component	P07356	<i>Anxa2</i>	Annexin A2	339	1.12
	Q62059-3	<i>Vcan</i>	Versican core protein	2,393	1.56
	P97927	<i>Lama4</i>	Laminin subunit alpha-4	1,816	1.36
	P02469	<i>Lamb1</i>	Laminin subunit beta-1#	1,786	1.51
	P02468	<i>Lamc1</i>	Laminin subunit gamma-1	1,607	1.40
	P08122	<i>Col4a2</i>	Collagen alpha-2(IV) chain#	1,707	1.36
	Q02788	<i>Col6a2</i>	Collagen alpha-2(VI) chain#	1,034	1.33
	P10493	<i>Nid1</i>	Nidogen-1#	1,245	1.35
	P82198	<i>Tgfb1</i>	Transforming growth factor-beta-induced protein ig-h3	693	1.29
	Q61554	<i>Fbn1</i>	Fibrillin-1#	2,871	1.28
	Q3U962	<i>Col5a2</i>	Collagen alpha-2(V) chain#	1,497	1.26
	P02463	<i>Col4a1</i>	Collagen alpha-1(IV) chain#	1,669	1.25
	P11276	<i>Fn1</i>	Fibronectin	2,477	1.25
	P11087	<i>Col1a1</i>	Collagen alpha-1(I) chain#	1,453	1.22
	Q35206	<i>Col15a1</i>	Collagen alpha-1(XV) chain	1,367	1.19
	Q05793	<i>Hspg2</i>	Basement membrane-specific heparan sulfate proteoglycan core protein (perlecan)*#	3,707	1.18
	P33434	<i>Mmp2</i>	72 kDa type IV collagenase	662	1.18
	Q04857	<i>Col6a1</i>	Collagen alpha-1(VI) chain#	1,025	1.17
	P08121	<i>Col3a1</i>	Collagen alpha-1(III) chain*#	1,464	1.12
	O08746-2	<i>Matn2</i>	Matrilin-2	956	1.07
ECM matricellular	Q61398	<i>Pcolce</i>	Procollagen C-endopeptidase enhancer 1*#	468	1.07
	O88207	<i>Col5a1</i>	Collagen alpha-1(V) chain#	1,838	1.02
	Q08879	<i>Fbln1</i>	Fibulin-1	705	1.19
	P37889-2	<i>Fbln2</i>	Fibulin-2 #	1,221	1.20
	Q62009-3	<i>Postn</i>	Periostin	838	1.20
	P70663	<i>Spard1</i>	SPARC-like protein 1	650	1.14
	P07214	<i>Sparc</i>	SPARC*	302	1.10
Extracellular enzymes	P16110	<i>Lgals3</i>	Galectin-3	264	1.11
	Q07797	<i>Lgals3bp</i>	Galectin-3-binding protein	577	1.17
	Q8BND5-2	<i>Qsox1</i>	Sulfhydryl oxidase 1	748	1.56
	P10605	<i>Ctsb</i>	Cathepsin B#	339	1.37
	P00687	<i>Amy1</i>	Alpha-amylase 1	511	1.04
	P00688	<i>Amy2</i>	Pancreatic alpha-amylase	508	1.13
	P21460	<i>Cst3</i>	Cystatin-C#	140	1.10
Adipokines	Q00519	<i>Xdh</i>	Xanthine dehydrogenase/oxidase	1,335	1.07
	P17742	<i>Ppia</i>	Peptidyl-prolyl cis-trans isomerase A#	164	1.04
	Q60994	<i>Adipoq</i>	Adiponectin#	247	1.31
	Q00724	<i>Rbp4</i>	Retinol-binding protein 4	201	1.31
	P11859	<i>Agt</i>	Angiotensinogen#	477	1.13
	P04117	<i>Fabp4</i>	Fatty acid-binding protein, adipocyte	132	1.02
	P03953-2	<i>Cfd</i>	Complement factor D (adipsin)#	259	1.01
Complement	Q9DD06	<i>Rarres2</i>	Retinoic acid receptor responder protein 2 (Chemerin)*#	162	1.01
	P01029	<i>C4b</i>	Complement C4-B	1,738	1.09
	P04186	<i>Cfb</i>	Complement factor B	761	1.06
	P48759	<i>Ptx3</i>	Pentraxin-related protein PTX3	381	1.06
	P01027	<i>C3</i>	Complement C3#	1,663	1.05

(Continued)

TABLE 1 | Continued.

Function	UniprotKB	Gene symbol	Description	Length	cAMP-induced fold-change
Others (cytokines, transport,...)	P21956-2	<i>Mfge8</i>	Lactadherin	463	1.60
	Q62356	<i>Fstl1</i>	Follistatin-related protein 1*#	306	1.34
	P28798	<i>Gm</i>	Granulins	589	1.24
	P17515	<i>Cxcl10</i>	C-X-C motif chemokine 10	98	1.20
	O88968	<i>Tcn2</i>	Transcobalamin-2	430	1.14
	Q9Z0J0	<i>Npc2</i>	Epididymal secretory protein E1 (Niemann-Pick)*#	149	1.09
	P47879	<i>Igfbp4</i>	Insulin-like growth factor-binding protein 4*#	254	1.09
	O88393	<i>Tgfb<math>\beta</math>3</i>	Transforming growth factor beta receptor type 3 (beta-glycan)#	850	1.08
	Q60590	<i>Orm1</i>	Alpha-1-acid glycoprotein 1 (orosomucoid)#	207	1.06
	P97298	<i>Serpinf1</i>	Pigment epithelium-derived factor (Serp1)#	417	1.05
<b>(B) DOWN-REGULATED PROTEINS IN RESPONSE TO cAMP</b>					
ECM component	P28653	<i>Bgn</i>	Biglycan*#	369	1.03
Matricellular	Q8BPB5	<i>Efemp1</i>	EGF-containing fibulin-like extracellular matrix protein 1*	493	1.35
Extracellular enzymes	P16045	<i>Lgals1</i>	Galectin-1	135	1.13
	Q06890	<i>Clu</i>	Clusterin	448	1.01
	P10639	<i>Txn</i>	Thioredoxin	105	1.07
	P06745	<i>Gpi</i>	Glucose-6-phosphate isomerase (neuroleukin)	558	1.06
	P11152	<i>Lpl</i>	Lipoprotein lipase*	474	1.06
	P18242	<i>Ctsd</i>	Cathepsin D	410	1.04
Adipokines	Q61805	<i>Lbp</i>	Lipopolysaccharide-binding protein	481	1.05
Others (cytokines, transport,...)	Q61646	<i>Hp</i>	Haptoglobin*	347	1.15
	P13020	<i>Gsn</i>	Gelsolin#	780	1.07
	Q61207	<i>Psap</i>	Prosaposin	557	1.07
	P01887	<i>B2m</i>	Beta-2-microglobulin#	119	1.07
	P08226	<i>ApoE</i>	Apolipoprotein E*	311	1.05
	P34884	<i>Mif</i>	Macrophage migration inhibitory factor#	115	1.01

The UniprotKB code, gene symbol, description, length (amino acids), and cAMP-induced fold-change for each detected protein are shown. \*Indicates concordance with Hansen (2014),

#Indicates concordance with Ojima et al. (2016).

secretome data did not include other known brown adipokines, such as IL-6, FGF21, or neuregulin-4 (NRG4). This is likely to reflect that such proteins are present at relatively low levels in the cell culture medium (1–10 ng/ml) (Burýsek and Houstek, 1997; Hondares et al., 2011; Rosell et al., 2014). In contrast, the levels of secreted proteins such as adiponectin or LBP exceed 100 ng/ml in the culture media of adipocyte culture systems (Díaz-Delfin et al., 2012; Moreno-Navarrete et al., 2013). The relatively low-level release of some secreted proteins by brown adipocytes may be a limitation in the ability to identify secretome components using proteomic analysis of culture media.

We found only partial concordance between the cAMP-regulated secreted proteins according to proteomics and the corresponding transcript levels. The discordance was particularly relevant for cAMP-induced ECM components and adipokines, whereas cAMP-repressed secreted factors showed more concordance. Moreover, individual quantification of a set of secreted protein candidates responsive to cAMP

confirmed most, but not all, changes detected in the proteomics assays, even in cases when transcript levels were discordant. This suggests that post-transcriptional mechanisms are involved in the cAMP-mediated regulation of protein secretion by brown adipocytes and that transcriptomic approaches may therefore be limited in their ability to predict comprehensively the BAT secretome. Moreover, our data highlight the importance of specific validation of proteomics-based findings using individual quantification of secreted protein candidates.

In conclusion, the current study opens new venues for research of the secretome of brown adipocytes. Beyond helping direct further research on novel brown adipokine candidates, our work suggests two new research foci, namely: (a) understanding the importance of the synthesis of ECM components by brown adipocytes for BAT remodeling during thermogenic adaptation, and (b) determining the roles of the complement-related proteins by brown adipocytes upon thermogenic activation.

## AUTHOR CONTRIBUTIONS

JV performed the brown adipocyte cell cultures, proteomic analytics, qRT-PCR, immunoblot, and ELISA assays. RC performed the bioinformatic analysis of secretability. MG and FV designed the study and compiled the data. FV and JV wrote the manuscript.

## FUNDING

This work was supported by grants from the Ministerio de Economía y Competitividad (MINECO), Spain (SAF2017-85722R and PI17/00420), co-financed by the European Regional Development Fund (ERDF). JV is a Juan de la Cierva post-doctoral researcher by MINECO, Spain.

## REFERENCES

- Arntzen, M. Ø., Koehler, C. J., Barsnes, H., Berven, F. S., Treumann, A., and Thiede, B. (2011). IsobaricQ: software for isobaric quantitative proteomics using iPTL, iTRAQ, and TMT. *J. Proteome Res.* 4, 913–920. doi: 10.1021/pr1009977
- Bartelt, A., Bruns, O. T., Reimer, R., Hohenberg, H., Ittrich, H., Peldschus, K., et al. (2011). Brown adipose tissue activity controls triglyceride clearance. *Nat. Med.* 17, 200–205. doi: 10.1038/nm.2297
- Bendtsen, J. D., Jensen, L. J., Blom, N., Von Heijne, G., and Brunak, S. (2004). Feature-based prediction of non-classical and leaderless protein secretion. *Protein Eng. Des. Sel.* 17, 349–356. doi: 10.1093/protein/gzh037
- Burýsek, L., and Houstek, J. (1997). beta-Adrenergic stimulation of interleukin-1alpha and interleukin-6 expression in mouse brown adipocytes. *FEBS Lett.* 411, 83–86. doi: 10.1016/S0014-5793(97)00671-6
- Cannon, B., and Nedergaard, J. (2004). Brown adipose tissue: function and physiological significance. *Physiol. Rev.* 84, 277–359. doi: 10.1152/physrev.00015.2003
- Carobbio, S., Guénant, A. C., Samuelson, I., Bahri, M., and Vidal-Puig, A. (2018). Brown and beige fat: from molecules to physiology and pathophysiology. *Biochim. Biophys. Acta Mol. Cell. Biol. Lipids* 1864, 37–50. doi: 10.1016/j.bbalip.2018.05.013
- Cassis, L. A. (1993). Role of angiotensin II in brown adipose thermogenesis during cold acclimation. *Am. J. Physiol.* 265(Pt 1), E860–E865. doi: 10.1152/ajpendo.1993.265.6.E860
- Cereijo, R., Gavalda-Navarro, A., Cairo, M., Quesada-Lopez, T., Villarroya, J., Moron-Ros, S., et al. (2018). CXCL14, a brown adipokine that mediates brown-fat-to-macrophage communication in thermogenic adaptation. *Cell Metab.* 28, 750–763.e6. doi: 10.1016/j.cmet.2018.07.015
- Cook, K. S., Min, H. Y., Johnson, D., Chaplinsky, R. J., Flier, J. S., Hunt, C. R., et al. (1987). Adipsin: a circulating serine protease homolog secreted by adipose tissue and sciatic nerve. *Science* 237, 402–405.
- Díaz-Delfin, J., Domingo, P., Mateo, M. G., Gutierrez, M. M., Domingo, J. C., Giral, M., et al. (2012). Effects of rilpivirine on human adipocyte differentiation, gene expression, and release of adipokines and cytokines. *Antimicrob. Agents Chemother.* 56, 3369–3377. doi: 10.1128/AAC.00104-12
- Emanuelsson, O., Brunak, S., von Heijne, G., and Nielsen, H. (2007). Locating proteins in the cell using TargetP, SignalP and related tools. *Nat. Protoc.* 2, 953–971. doi: 10.1038/nprot.2007.131
- Gavalda-Navarro, A., Moreno-Navarrete, J. M., Quesada-López, T., Cairó, M., Giral, M., Fernández-Real, J. M., et al. (2016). Lipopolysaccharide-binding protein is a negative regulator of adipose tissue browning in mice and humans. *Diabetologia* 59, 2208–2218. doi: 10.1007/s00125-016-4028-y
- Giral, M., and Villarroya, F. (2017). Mitochondrial uncoupling and the regulation of glucose homeostasis. *Curr. Diabetes Rev.* 13, 386–394. doi: 10.2174/1573399812666160217122707

## ACKNOWLEDGMENTS

The proteomics work was done at the Plataforma de Proteómica del Parc Científic de Barcelona, a member of ProteoRed, PRB3 and is supported by grant PT17/0019/0016, funded by Instituto de Salud Carlos III (Spain) and European Region Development Fund. Thanks are given to Dr. E. de Oliveira for support in the proteomics analysis, and to Dr. J. Klein (University of Luebeck, Germany), and Dr. A. Whittle (University of Cambridge, UK) for the supply of C57 brown pre-adipocytes.

## SUPPLEMENTARY MATERIAL

The Supplementary Material for this article can be found online at: <https://www.frontiersin.org/articles/10.3389/fphys.2019.00067/full#supplementary-material>

- Hansen, I. R. (2014). *The Secretome of Brown Adipose Tissue*. Doctoral thesis, Stockholm University, Stockholm.
- Hansen, I. R., Jansson, K. M., Cannon, B., and Nedergaard, J. (2014). Contrasting effects of cold acclimation versus obesogenic diets on chemerin gene expression in brown and white adipose tissues. *Biochim. Biophys. Acta* 1841, 1691–1699. doi: 10.1016/j.bbalip.2014.09.003
- Hondares, E., Iglesias, R., Giral, A., Gonzalez, F. J., Giral, M., Mampel, T., et al. (2011). Thermogenic activation induces FGF21 expression and release in brown adipose tissue. *J. Biol. Chem.* 286, 12983–12990. doi: 10.1074/jbc.M110.215889
- Hui, X., Gu, P., Zhang, J., Nie, T., Pan, Y., Wu, D., et al. (2015). Adiponectin enhances cold-induced browning of subcutaneous adipose tissue via promoting M2 macrophage proliferation. *Cell Metab.* 22, 279–290. doi: 10.1016/j.cmet.2015.06.004
- Klein, J., Fasshauer, M., Ito, M., Lowell, B. B., Benito, M., and Kahn, C. R. (1999). Beta(3)-adrenergic stimulation differentially inhibits insulin signaling and decreases insulin-induced glucose uptake in brown adipocytes. *J. Biol. Chem.* 274, 34795–34802. doi: 10.1074/jbc.274.49.34795
- Moreno-Navarrete, J. M., Escoté, X., Ortega, F., Serino, M., Campbell, M., Michalski, M. C., et al. (2013). A role for adipocyte-derived lipopolysaccharide-binding protein in inflammation- and obesity-associated adipose tissue dysfunction. *Diabetologia* 56, 2524–2537. doi: 10.1007/s00125-013-3015-9
- Ojima, K., Oe, M., Nakajima, I., Muroya, S., and Nishimura, T. (2016). Dynamics of protein secretion during adipocyte differentiation. *FEBS Open Bio* 6, 816–826. doi: 10.1002/2211-5463.12091
- Rosell, M., Hondares, E., Iwamoto, S., Gonzalez, F. J., Wabitsch, M., Staels, B., et al. (2012). Peroxisome proliferator-activated receptors- $\alpha$  and - $\gamma$ , and cAMP-mediated pathways, control retinol-binding protein-4 gene expression in brown adipose tissue. *Endocrinology* 153, 1162–1173. doi: 10.1210/en.2011-1367
- Rosell, M., Kaforou, M., Frontini, A., Okolo, A., Chan, Y. W., Nikolopoulou, E., et al. (2014). Brown and white adipose tissues: intrinsic differences in gene expression and response to cold exposure in mice. *Am. J. Physiol. Endocrinol. Metab.* 306, E945–E964. doi: 10.1152/ajpendo.00473.2013
- Shu, L., Hoo, R. L., Wu, X., Pan, Y., Lee, I. P., Cheong, L. Y., et al. (2017). A-FABP mediates adaptive thermogenesis by promoting intracellular activation of thyroid hormones in brown adipocytes. *Nat. Commun.* 8:14147. doi: 10.1038/ncomms14147
- Sun, K., Tordjman, J., Clément, K., and Scherer, P. E. (2013). Fibrosis and adipose tissue dysfunction. *Cell Metab.* 18, 470–477. doi: 10.1016/j.cmet.2013.06.016
- Svensson, P. A., Jernäs, M., Sjöholm, K., Hoffmann, J. M., Nilsson, B. E., Hansson, M., et al. (2011). Gene expression in human brown adipose tissue. *Int. J. Mol. Med.* 27, 227–232. doi: 10.3892/ijmm.2010.566

- Verdeguer, F., Soustek, M. S., Hatting, M., Blättler, S. M., McDonald, D., Barrow, J. J., et al. (2015). Brown adipose YY1 deficiency activates expression of secreted proteins linked to energy expenditure and prevents diet-induced obesity. *Mol. Cell. Biol.* 36, 184–196. doi: 10.1128/MCB.00722-15
- Villarroya, F., Cereijo, R., Villarroya, J., and Giralt, M. (2017). Brown adipose tissue as a secretory organ. *Nat. Rev. Endocrinol.* 13, 26–35. doi: 10.1038/nrendo.2016.136
- Wang, G. X., Zhao, X. Y., Meng, Z. X., Kern, M., Dietrich, A., Chen, Z., et al. (2014). The brown fat-enriched secreted factor Nrg4 preserves metabolic homeostasis through attenuation of hepatic lipogenesis. *Nat. Med.* 20, 1436–1443. doi: 10.1038/nm.3713

**Conflict of Interest Statement:** The authors declare that the research was conducted in the absence of any commercial or financial relationships that could be construed as a potential conflict of interest.

Copyright © 2019 Villarroya, Cereijo, Giralt and Villarroya. This is an open-access article distributed under the terms of the Creative Commons Attribution License (CC BY). The use, distribution or reproduction in other forums is permitted, provided the original author(s) and the copyright owner(s) are credited and that the original publication in this journal is cited, in accordance with accepted academic practice. No use, distribution or reproduction is permitted which does not comply with these terms.





# Neonatal Resveratrol and Nicotinamide Riboside Supplementations Sex-Dependently Affect Beige Transcriptional Programming of Preadipocytes in Mouse Adipose Tissue

Madhu Asnani-Kishnani<sup>1</sup>, Ana M. Rodríguez<sup>1,2,3</sup>, Alba Serrano<sup>1,2</sup>, Andreu Palou<sup>1,2,3</sup>, M. Luisa Bonet<sup>1,2,3\*</sup> and Joan Ribot<sup>1,2,3</sup>

## OPEN ACCESS

### Edited by:

Rita De Matteis,  
University of Urbino Carlo Bo, Italy

### Reviewed by:

Paul Thomas Pfluger,  
Helmholtz Center Munich – German  
Research Center for Environmental  
Health, Germany  
Alexander Bartelt,  
Ludwig Maximilian University  
of Munich, Germany

### \*Correspondence:

M. Luisa Bonet  
luisabonet@uib.es

### Specialty section:

This article was submitted to  
Integrative Physiology,  
a section of the journal  
Frontiers in Physiology

**Received:** 05 October 2018

**Accepted:** 24 January 2019

**Published:** 08 February 2019

### Citation:

Asnani-Kishnani M,  
Rodríguez AM, Serrano A, Palou A,  
Bonet ML and Ribot J (2019)  
Neonatal Resveratrol  
and Nicotinamide Riboside  
Supplementations Sex-Dependently  
Affect Beige Transcriptional  
Programming of Preadipocytes  
in Mouse Adipose Tissue.  
Front. Physiol. 10:83.  
doi: 10.3389/fphys.2019.00083

<sup>1</sup> Grup de Recerca Nutrigenòmica i Obesitat, Laboratori de Biologia Molecular, Nutrició i Biotecnologia, Universitat de les Illes Balears, Palma de Mallorca, Spain, <sup>2</sup> CIBER de Fisiopatología de la Obesidad y Nutrición, Palma de Mallorca, Spain, <sup>3</sup> Institut d'Investigació Sanitària Illes Balears, Palma de Mallorca, Spain

Nutritional programming of the thermogenic and fuel oxidation capacity of white adipose tissue (WAT) through dietary interventions in early life is a potential strategy to enhance future metabolic health. We previously showed that mild neonatal supplementations with the polyphenol resveratrol (RSV) and the vitamin B3 form nicotinamide riboside (NR) have sex-dependent, long-term effects on the thermogenic/oxidative phenotype of WAT of mice in adulthood, enhancing this phenotype selectively in male animals. Here, we tested the hypothesis that these dietary interventions may impact the commitment of progenitor cells resident in the developing WAT toward brown-like (beige) adipogenesis. NMRI mice received orally from postnatal day 2–20 (P2–20) a mild dose of RSV or NR, in independent experiments; control littermates received the vehicle. Sex-separated primary cultures were established at P35 from the stromovascular fraction of inguinal WAT (iWAT) and of brown adipose tissue (BAT). Expression of genes related to thermogenesis and oxidative metabolism was assessed in the differentiated cultures, and *in vivo* in the iWAT depot of young (P35) animals. Neonatal RSV and NR treatments had little impact on the animals' growth during early postnatal life and the expression of thermogenesis- and oxidative metabolism-related genes in the iWAT depot of young mice. However, the expression of brown/beige adipocyte marker genes was upregulated in the iWAT primary cultures from RSV supplemented and NR supplemented male mice, and downregulated in those from supplemented female mice, as compared to cultures derived from sex-matched control littermates. RSV supplementation had similar sex-dependent effects on the expression of thermogenesis-related genes in the BAT primary cultures. A link between the sex-dependent short-term effects of neonatal RSV and NR supplementations on primary iWAT preadipocyte differentiation observed herein and their previously reported

sex-dependent long-term effects on the thermogenic/oxidative capacity of adult iWAT is suggested. The results provide proof-of-concept that the fate of preadipocytes resident in WAT of young animals toward the beige adipogenesis transcriptional program can be modulated by specific food bioactives/micronutrients received in early postnatal life.

**Keywords:** adipose tissue, beigeing, browning, metabolic programming, sex differences, food bioactives, primary culture

## INTRODUCTION

Brown adipocytes in canonical BAT depots in mammals express uncoupling protein 1 (UCP1) and a high oxidative capacity and mitochondria content, which distinguishes them metabolically from white adipocytes in typical WAT depots. A third type of adipocytes, beige adipocytes (also called brite [brown-in-white]), are brown-like adipocytes found in WAT depots. Beige adipocytes share with brown adipocytes a common core thermogenesis gene signature including inducible UCP1 expression, which allows for the regulated dissipation as heat of the energy contained in fatty acid and glucose fuel molecules (Bartelt and Heeren, 2014). Additionally, transcripts of several markers have been identified that appear to be specific for beige adipocytes (Wu et al., 2012). The emergence of beige adipocytes in WAT is termed WAT browning or beigeing. BAT activation and WAT browning are both viewed as potential therapeutic targets in the management of obesity and related metabolic disorders such as hyperlipidemia and diabetes (Bonet et al., 2013; Harms and Seale, 2013).

The recruitment of brown and beige adipocytes responds to a variety of hormonal and diet-related stimulus including the intake of specific food bioactives (Bonet et al., 2013, 2017). This is well established in adult rodents and appears to hold for humans as well (Rossato et al., 2014; Fleckenstein-Elsen et al., 2016; Palmeri et al., 2016; Saito et al., 2016). Besides contemporary dietary intake in adulthood, exposure to food bioactives in prenatal and early postnatal life might be important. Epidemiological and experimental evidence indicates that early life nutrition can influence metabolic health in adulthood through programming effects on the developing tissues, with consequences in the long-term (Cottrell and Ozanne, 2008). The browning potential of WAT might be nutritionally programmed (Palou et al., 2013), as well as other aspects such as WAT cellularity (Lecoutre and Breton, 2014), though these aspects are still largely unexplored.

The B3 vitamin and NAD<sup>+</sup> precursor NR and the polyphenol resveratrol (RSV; 3,5,4'-trihydroxy-*trans*-stilbene) are two dietary compounds that enhance oxidative metabolism in adipose and other tissues when supplemented to adult rodents, possibly through their shared ability to activate sirtuin 1 (SIRT1) protein deacetylase (Lagouge et al., 2006; Canto et al., 2012; Alberdi et al., 2013; Andrade et al., 2014; Wang et al., 2015). Nutritional programming by RSV and NR has recently begun to be addressed (Zou et al., 2017; Ros et al., 2018; Serrano et al.,

2018). We have shown that direct treatment of newborn mouse with mild doses of RSV or NR throughout lactation leads to sex-dependent long-term effects on the WAT thermogenic/oxidative phenotype. Signs of white-to-brown fat remodeling of iWAT in adulthood including smaller adipocyte size, enrichment in multilocular adipocytes, increased immunostaining against UCP1 and the respiratory chain protein component COXIV, and higher expression levels of genes related to brown fat determination, mitochondrial oxidative metabolism and beige markers (e.g., *Prdm16*, *Ppargc1b*, *Pparg*, *Cpt1b*, *Mfn2*, and *Slc27a1*) were found selectively in the treated male mice relative to sex-matched controls (Serrano et al., 2018). In parallel with these changes in WAT, RSV, and NR treated male mice displayed in adulthood better responses to an obesogenic high-fat diet than controls, such as a delayed body weight gain, a blunted increase in the plasma leptin-to-adiponectin ratio and a decreased lipolytic response (Serrano et al., 2018). However, the mechanisms behind the early programming of WAT energy metabolism related features by neonatal RSV and NR supplementations remain unknown.

Adipose tissue is a reservoir of immature progenitor cells which are part of the tissue stromovascular fraction (SVF). These cells undergo proliferation and differentiation (adipogenesis) *in vivo* to allow continuous renewal of the adipocytes in the fat depots throughout life, as well as hyperplastic adipose tissue expansion (i.e., increased adipocyte number) under conditions of positive energy balance, and are thus very important for adipose tissue homeostasis. Importantly, primary cultures established from the SVF of WAT can be used to unveil beige adipocytes (Petrovic et al., 2010), and these cultures reflect genetic differences in the capacity for brown-like adipogenesis in animals *in vivo* (Petrov et al., 2016). It is conceivable that nutritional influences during critical windows of WAT development condition the fate of adipogenesis from adipose tissue progenitor cells and, consequently, the metabolic features of adult WAT. The early postnatal period might be especially important for WAT programming. Subcutaneous (inguinal) WAT, in particular, basically forms in rodents coincident with the suckling period, after BAT (that develops mainly during the late fetal stage), and prior to visceral WAT (Cryer and Jones, 1979; Kozak, 2011).

In this work, we tested the hypothesis that mild supplementations with RSV or NR in early postnatal life can impact the programming of beige adipogenesis in progenitor cells resident in iWAT. To this end, gene expression related to thermogenesis and oxidative metabolism was studied in corresponding primary cultures established from the tissue SVF of young mice. The studies were conducted both in male and

**Abbreviations:** BAT, brown adipose tissue; iWAT, inguinal WAT; NA, noradrenaline; NR, nicotinamide riboside; RSV, resveratrol; WAT, white adipose tissue.

female mice, in view of previous reports of sexual dimorphism in thermogenic responses (Rodriguez and Palou, 2004; Valencak et al., 2017) and our previous characterization of RSV and NR treated offspring in adulthood, which pointed to sex-dependence of treatments effects (Serrano et al., 2018).

## MATERIALS AND METHODS

### Animals and Experimental Design

Study protocols were approved by the Bioethical Committee of the University of the Balearic Islands (Ref. 3513, 26/03/2012). International standards for the use and care of laboratory animals were followed. Animals were housed at 22°C, with a 12 h light-dark cycle (lights on at 08:00), and free access to tap water and standard chow diet (type A03; 3.3 kcal/g, 8% calories from fat; Panlab, Barcelona, Spain). Virgin female NMRI mice (Charles River Laboratories, Barcelona, Spain) were mated. Each female was single-caged after mating. The morning in which newborn litters were found was designated as day 0. At day 2, litter size was adjusted to 12 pups per dam. Pups in four litters were randomly assigned to control or RSV group; in a separate experiment, pups in four additional litters were assigned to control or NR group (six pups per litter per group in both experiments). From postnatal day 2 (P2) to P20, the pups received daily orally 10–15 µL of either vehicle (water, control groups), a solution of RSV (Sigma, Madrid, Spain) or a solution of NR (Chemical Point, Diessenhofen, Germany), using a pipette. The amount of supplemented RSV was adjusted along the suckling period to meet a daily dose of 2 mg/kg body weight. RSV at 10–30 mg/kg animal/day decreases adiposity in adult rodents (Rivera et al., 2009; Alberdi et al., 2013) and we further applied a security factor considering the young age of the animals. The NR supplied ranged from 24 µg on P2 to 45 µg on P20, and was equivalent to ~15-fold the total vitamin B3 ingested daily from maternal milk, considering the vitamin B3 content found in milk of in-home mouse dams [2378 ppb (Serrano et al., 2018)] and the daily milk intake of pups throughout lactation (Kojima et al., 1998). Animals were weaned and separated by sex on P21. The studies were performed separately in male and female mice. Body weight was periodically recorded from birth. Body composition was analyzed at P34, using an Echo MRI body composition analyzer (EchoMRI, LCC, Houston, TX, United States). Naso-anal length was also measured on P34, and used to calculate Lee's obesity index (body weight in g<sup>0.33</sup> × 1000/naso-anal length in cm). Energy intake from weaning until euthanization was estimated on a per-cage basis, from the actual amount of food consumed by the animals and its caloric equivalence. The animals were euthanized on P35, by decapitation, under fed conditions, within the first 2 h of the light cycle; half of the animals in each sex and treatment group (*n* = 5–6, from four different litters) were used to establish sex-separated adipose tissue primary cultures (see below), while the other half were used for tissue sampling for molecular analyses. Interscapular BAT and WAT depots (inguinal, epididymal, and retroperitoneal) were dissected in their entirety, weighed, snap-frozen in liquid nitrogen and stored at –80°C until processed. Glucose was measured from trunk

blood using the Accu-Chek Aviva system (Roche Diagnostics). Adiposity index was calculated as the sum of all WAT depot mass divided per body weight and per cent.

### Adipocyte Primary Cultures

The SVF containing preadipocytes was obtained from iWAT depot and pooled (interscapular, cervical, and axillary) BAT depots of 35-day-old mice, following a previously described protocol (Petrovic et al., 2010). The cell pellet was suspended in culture medium (0.5 mL/animal for brown preadipocytes, 0.4 mL/animal for white preadipocytes) and seeded onto 6-well culture plates (2 mL culture medium and 0.2 mL of cell suspension per well). The culture medium was Dulbecco's modified Eagle's medium with 10% (v/v) newborn calf serum (Gibco, Thermo Fisher Scientific, Waltham, MA, United States), 4 nM insulin, 25 µg/mL sodium ascorbate, 10 mM HEPES, 4 mM glutamine, 50 units/mL penicillin, and 50 µg/mL streptomycin. From day 0 of culture, all wells were supplemented with 1 µM rosiglitazone (BioVision, Milpitas, CA, United States) to favor the recruitment of brown-like adipocytes (Petrovic et al., 2010). Medium was changed on day 1 and then every second day, except the day the cells were harvested. The cells were grown for 7 days at 37°C in an atmosphere of 8% CO<sub>2</sub> in air. Adipogenic differentiation of the cells was regularly monitored through phase contrast microscopical examination. At harvesting, the percentage of cells showing intracellular lipid accumulation was ~80% and 60% for the primary cultures established from, respectively, BAT and iWAT, as in previous reports from our group using the same primary culture protocol (Petrov et al., 2016) and without apparent differences between neonatal treatments (see representative microphotographs in **Supplementary Figures S1, S2**). Half of the cultures were exposed to 1 µM NA for the 2 h prior harvesting, to stimulate thermogenically competent cells and UCP1 expression (Petrovic et al., 2010).

### RNA Isolation, Retrotranscription, and Real-Time PCR

Total RNA was extracted using Tripure Reagent (Roche, Barcelona, Spain) according to the manufacturer's instructions, followed by a sodium acetate/ethanol precipitation to purify nucleic acids. Isolated RNA was quantified using NanoDrop ND-1000 spectrophotometer (NanoDrop Technologies Inc., Wilmington, United States) and its integrity confirmed by agarose gel electrophoresis. Total RNA (0.25 µg/reaction) was reverse-transcribed using MuLV Reverse Transcriptase and random hexamers priming (Applied Biosystems, Madrid, Spain). Diluted cDNA template was used to perform PCR amplification of selected genes, along with specific forward and reverse primers (Sigma, Madrid, Spain), and Power SYBER Green PCR Master Mix (Applied Biosystems). Primers sequences are available on request. For Real-Time PCR the Applied Biosystems StepOnePlus Real-Time PCR Systems (Applied Biosystems) was used, with the following profile: 10 min at 95°C, followed by a total of 40 two-temperature cycles (15 s at 95°C and 1 min at 60°C). To verify the purity of the products, a melting curve was produced after



each run. The threshold cycle was calculated by the instrument's software (StepOne Software v2.2.2, Applied Biosystem) and the relative expression of each mRNA was calculated according to the  $2^{-\Delta C_t}$  method, using 18S rRNA as reference gene.

## Statistical Analysis

Data are expressed as mean  $\pm$  SEM. Statistical analyses were conducted separately by treatment (RSV and NR supplementation) and sex (male and female mice). Student's *t*-test was used for single comparisons. Two-way ANOVA was used for analysis of treatments effects in primary adipocytes under basal and NA-stimulated conditions; *post hoc* comparisons were included when two-way ANOVA indicated an interactive effect between neonatal treatment and NA exposure of cultures. Threshold of significance was set at  $p < 0.05$ . IBM SPSS Statistics for Windows, version 19.0 (IBM Corp., Armonk, NY, United States) was used for the analyses.

## RESULTS

### Neonatal RSV and NR Treatments Affected Beige Adipogenesis in iWAT Primary Cultures From Young Animals

To study the influence of treatments on the commitment of WAT preadipocytes toward the beige adipogenesis transcriptional program, expression levels of markers of brown/beige adipocyte determination and thermogenic function (*Ucp1*, *Cpt1b*, *Prdm16*, *Ppargc1a*, *Ppargc1b*, *Ppara*), and of purported beige adipocyte-selective transcriptional markers (*Tmem26*, *Hoxc9*, *Slc27a1*) were compared in differentiated iWAT primary cultures from RSV and NR mice and their respective controls. *Pparg* expression was also assessed, since the encoded product, PPAR $\gamma$ , is a master adipogenic factor that is also central to WAT browning (Ohno et al., 2012).

Adipocytes differentiated from the iWAT SVF of RSV female mice showed a generalized decreased expression of transcripts of brown and beige adipocyte marker genes (namely: *Ucp1*, *Cpt1b*, *Prdm16*, *Ppargc1b*, *Ppara*, *Tmem26*, *Slc27a1*), as well as of *Pparg*, when compared to primary adipocytes from control female mice (Figure 1A). On the contrary, primary adipocytes from RSV male mice showed increased expression levels of *Ucp1* and *Slc27a1* compared with corresponding controls (Figure 1B). *Ucp1* expression is the hallmark of the brown and beige adipocyte phenotype, and *Slc27a1* encodes a fatty acid transport protein (FATP1) that is highly expressed in BAT and other tissues actively oxidizing fatty acids and that is required for BAT thermogenesis (Wu et al., 2006). Furthermore, *Slc27a1* has been related to mitochondrial function in clonal white (3T3-L1) adipocytes (Wiczner and Bernlohr, 2009), and it is the only beige adipocyte transcriptional marker (out of 6 studied) found to be induced together with classical brown adipocyte marker genes in mouse WAT primary cultures following rosiglitazone exposure (Petrov et al., 2016). Additionally, trends to increased expression levels of most other genes related to oxidative metabolism/fatty acid oxidation assayed were apparent in the primary adipocytes

derived from RSV male mice vs. controls under NA stimulated conditions (Figure 1B).

The overall picture was similar for the NR treatment. *Ucp1* mRNA levels were increased in primary iWAT adipocytes derived from NR male mice but not female mice (Figure 2). Moreover, primary iWAT adipocytes from NR female mice showed a downregulated expression of several of the brown and beige transcriptional markers assessed (*Ppargc1a*, *Ppargc1b*, *Tmem26*, *Hoxc9*), whereas those from NR male mice showed an upregulated expression of *Slc27a1* – as for the RSV treatment – and also of *Prdm16* and *Pparg* (the latter with  $p = 0.073$ , two-way ANOVA) compared to corresponding controls (Figure 2). *Prdm16* encodes a transcriptional coactivator critical for WAT browning in postnatal life (Seale et al., 2011; Cohen et al., 2014), and agonism of PPAR $\gamma$  favors WAT browning *in vivo* and beige adipogenesis in primary adipose cultures (Fukui et al., 2000; Petrovic et al., 2010), possibly through stabilization of the PRDM16 protein (Ohno et al., 2012).

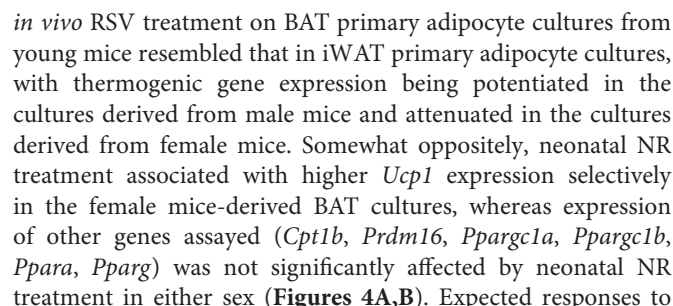
Half of the cultures were adrenergically stimulated prior harvesting to potentiate the emergence of thermogenically competent cells (Petrovic et al., 2010). Expected transcriptional responses to NA stimulation were found. In particular, *Ppargc1a* expression (encoding PGC1 $\alpha$ ) was induced by NA exposure in all iWAT primary cultures, regardless of sex of origin or neonatal treatment (Figures 1, 2). *Ucp1* expression was induced by NA exposure in the iWAT cultures from control and RSV mice regardless of sex, but not further induced by NA in the iWAT cultures from NR mice of either sex, which already overexpressed *Ucp1* compared to controls under the basal, non-stimulated, conditions (Figure 2). Apart from *Ppargc1a* and *Ucp1*, other brown/beige marker genes analyzed in iWAT primary cultures were not induced following NA exposure, but were rather unaffected or downregulated (Figures 1, 2). Down-regulation of genes in this class upon NA exposure was especially evident in the cultures derived from control male mice, and was attenuated in the cultures derived from RSV male mice (see results for *Cpt1b*, *Prdm16*, *Ppargc1b*, *Ppara*, *Hoxc9*, and *Slc27a1* expression in Figure 1B).

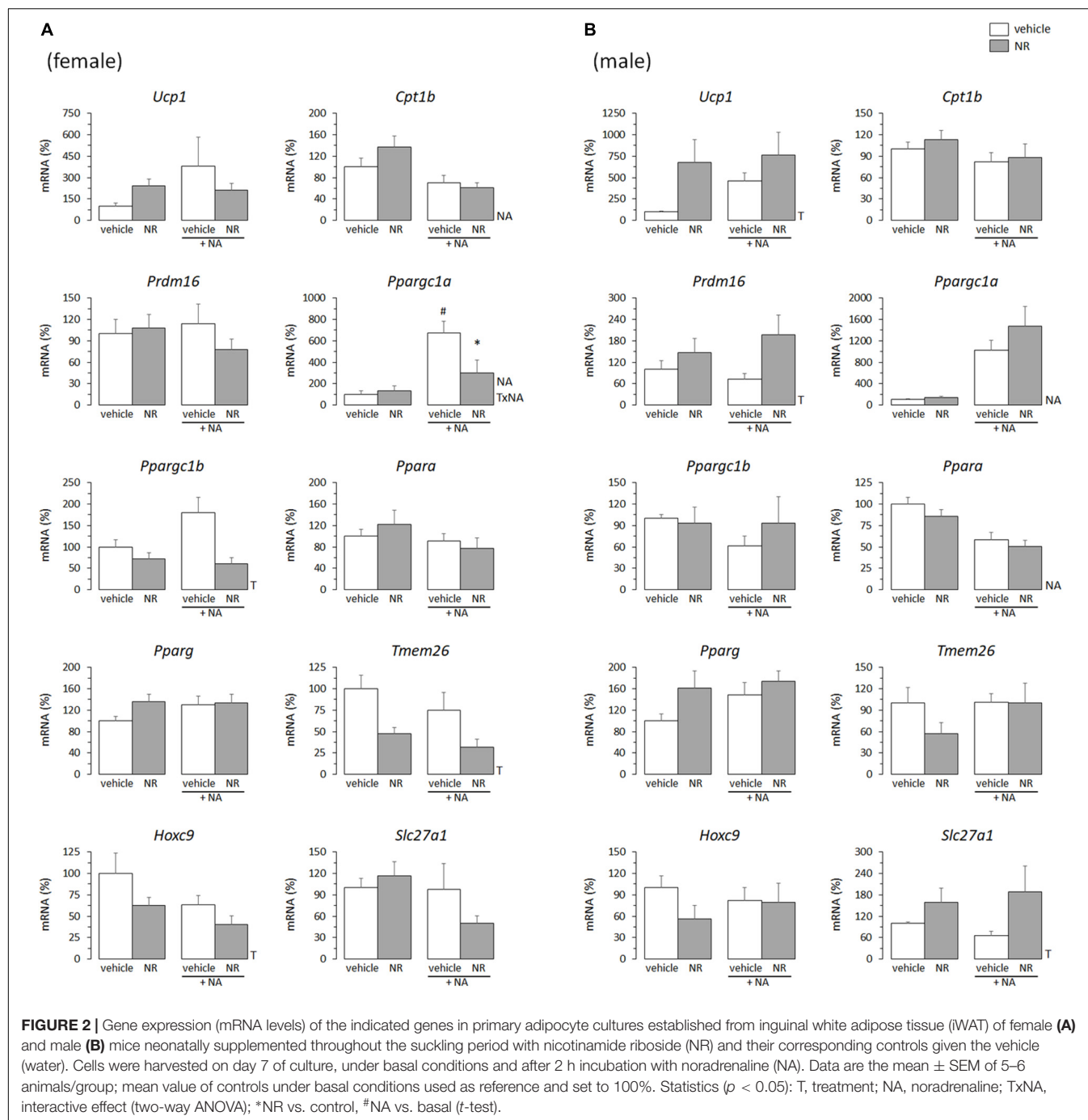
Altogether, these results indicated that the neonatal RSV and NR treatments had sex-dependent effects on the brown/beige transcriptional signature of iWAT primary cultures from young mice.

### Neonatal RSV and NR Treatments Affected Thermogenesis-Related Gene Expression in BAT Primary Cultures From Young Animals

In adult animals, it is common that the same stimuli that induce WAT browning also induce BAT recruitment (Bonet et al., 2013, 2017). Thus, effects of the *in vivo* neonatal treatments on thermogenic gene expression in primary BAT adipocytes from young mice were studied, to check for potential parallelisms between results in iWAT- and BAT-derived cultures. Compared with levels in cultures from sex-matched controls, the mRNA levels of *Ucp1*, *Cpt1b*, *Ppargc1b*, and *Ppara* were downregulated





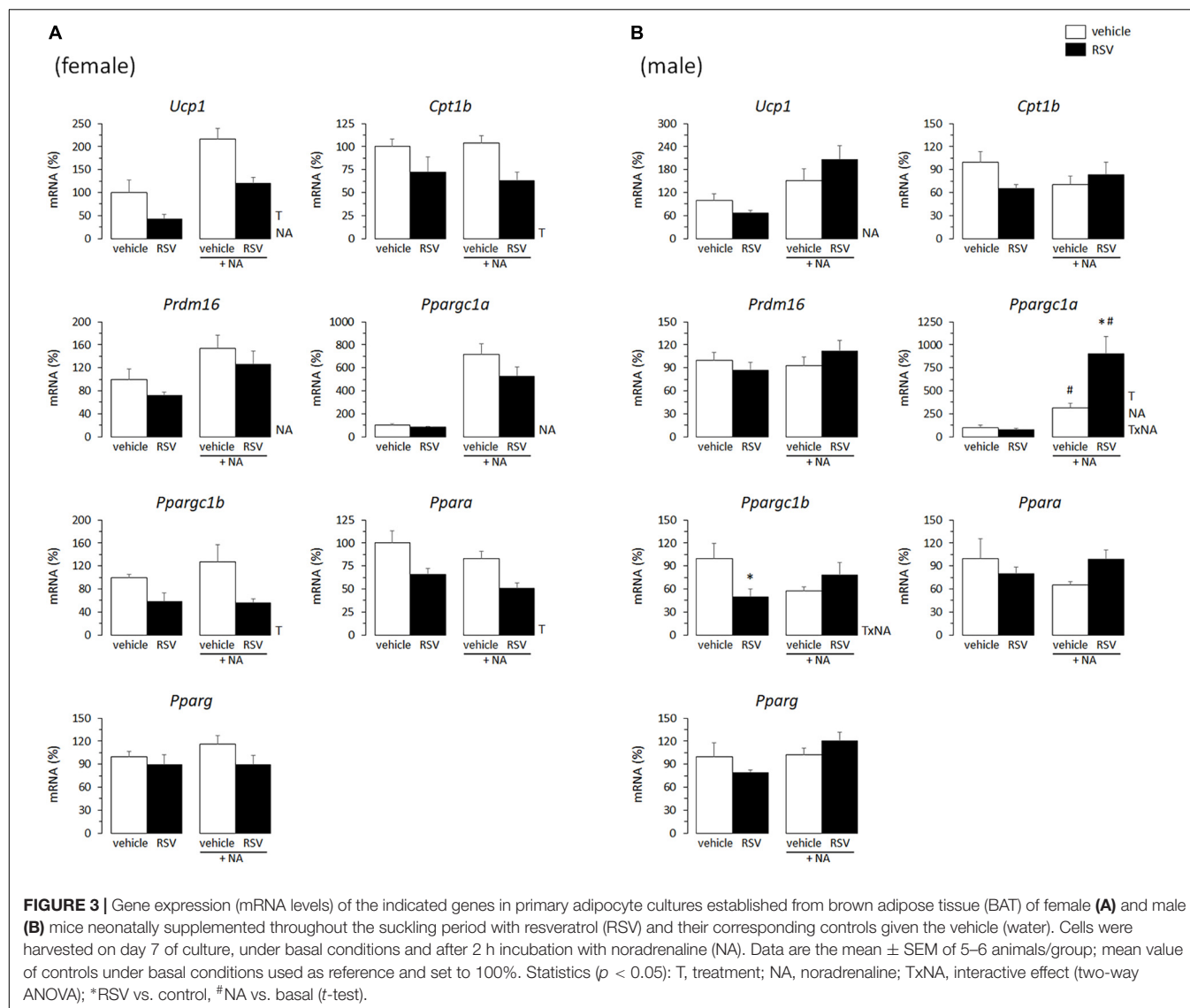


NA, namely induction of *Ucp1* and *Ppargc1a* expression, were present in all BAT primary cultures regardless of sex of origin or treatment (Figures 3, 4).

## Effects of Neonatal RSV and NR on Early Postnatal Growth

Eventual effects of treatments on early postnatal growth were evaluated by monitoring body weight evolution from birth; body length (nasal-to-anal distance), Lee index and body

composition (by EchoMRI) at P34; and tissue/organ weights at euthanization at P35. RSV treatment had no significant effect on any of these parameters, neither in male nor in female animals (Table 1). As for the NR treatment, treated male mice, but not females, were slightly but significantly heavier (by  $\sim 6\%$ ) and had higher (by  $\sim 20\%$ ) body fat content and fat/lean ratio at P34 compared to sex-matched controls (Table 2). Consistent with these body composition results, NR male mice, but not females, displayed after dissection a trend to higher gonadal WAT mass ( $p = 0.090$ ) (Table 2). Cumulative

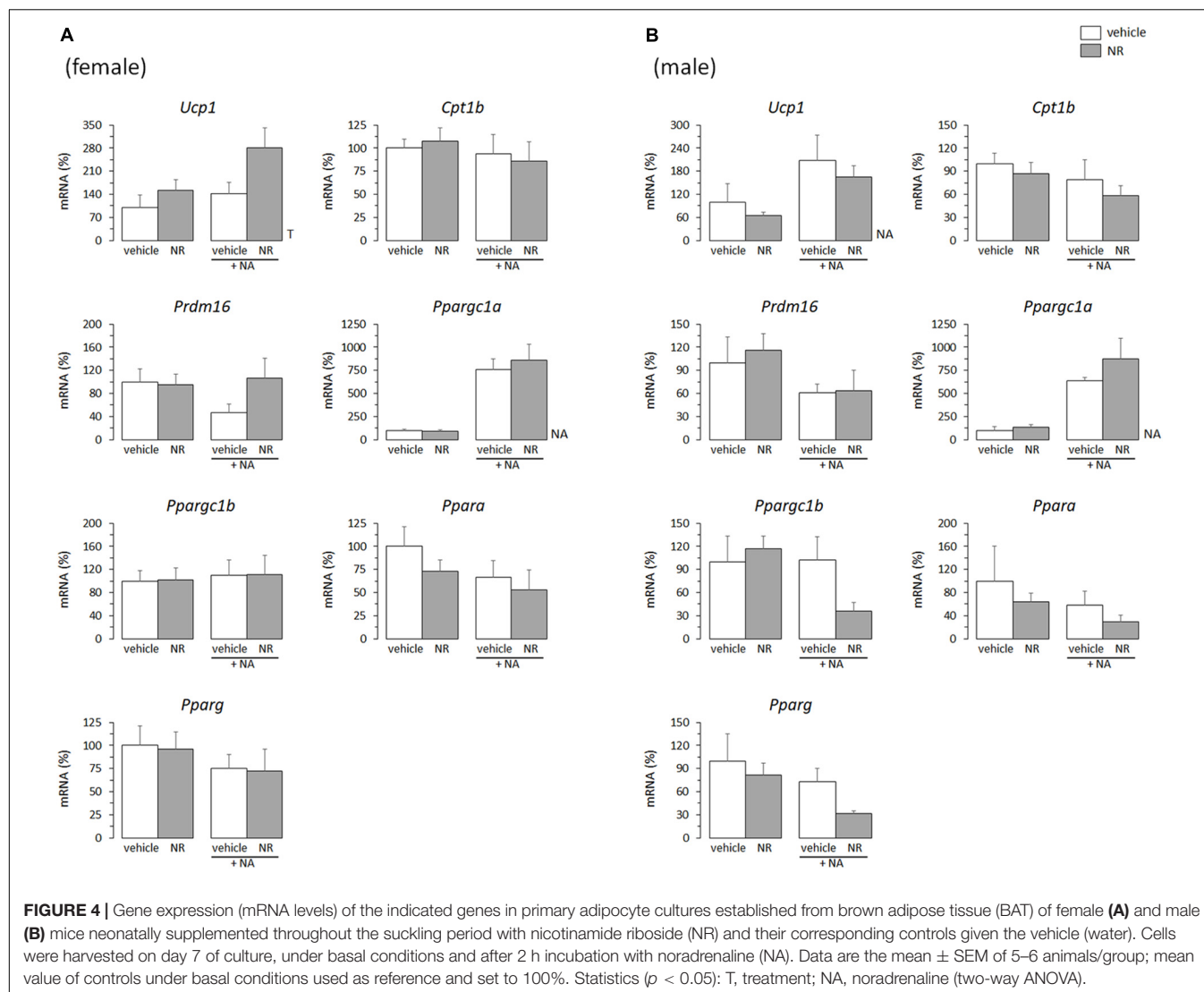


energy intake from weaning until P30 was significantly lower (by  $\sim 4\%$ ) in the NR animals of both sexes relative to sex-matched controls (Table 2), and showed a trend to be lower (also by  $\sim 4\%$ ,  $p = 0.076$ ) in the RSV male mice, but not the RSV female mice. Fed blood glucose levels at P35 were unaffected by treatments in either sex (not shown). Collectively, these results indicate that the neonatal RSV and NR supplementations applied did not compromise the animals' growth during early postnatal life, and had only a minor impact on it.

### Effects of Neonatal RSV and NR Treatments on Targeted Gene Expression in iWAT of Young Mice

The same panel of brown and beige adipocyte transcriptional markers analyzed in the iWAT primary cultures was analyzed in the iWAT depot of 35-day-old RSV and NR male mice and

their respective control littermates (Figure 5). Genes related to mitochondria biogenesis and function were additionally analyzed in the iWAT tissue, since expression of genes in this category (*Nrf1*, *Nrf2*, *Tfam*, *Tfb2m*, *Mfn2*) is increased at adult age in iWAT of RSV and NR neonatally treated male mice compared to control littermates (Serrano et al., 2018). Of the genes analyzed, the only significant difference from expression levels in controls was a greater than 2-fold increase in *Prdm16* mRNA levels in the iWAT of young NR male mice (Figure 5). *Lep*, *Mest*, and *Lpl* mRNA levels in iWAT, which were used as indicators of adipose tissue mass and expandability, were unaffected by treatments (Figure 5), in good concordance with the lack of effect of treatments on iWAT depot mass (Tables 1, 2). mRNA expression levels of a selection of genes in the above categories (*Ucp1*, *Slc27a1*, *Mfn2*, *Lpl*) were analyzed in iWAT of young (P35) female mice and found to be unaffected by treatments (data not shown).



Finally, because RSV and NR can both enhance energy metabolism through the activation of SIRT1 (Canto et al., 2012; Park et al., 2012; Price et al., 2012), transcriptional markers of SIRT1 activity were assessed in iWAT of young animals. SIRT1 represses *Ucp2* gene transcription (Bordone et al., 2006) and deacetylates FOXO1 transcription factor, resulting in higher expression levels in cells of FOXO1 target genes such as *Gadd45*, *Sod2*, and *Atgl* (Calnan and Brunet, 2008; Chakrabarti et al., 2011). Consistent with neonatal RSV and NR treatments activating SIRT1 specifically in iWAT of male mice, *Ucp2* mRNA levels were significantly decreased in iWAT of both groups of treated male mice relative to controls (Figure 5), but not in the iWAT depot of treated female mice (controls,  $100 \pm 14$  and  $100 \pm 21$ ; treated  $134 \pm 63$  and  $92 \pm 21$ , for the RSV and NR treatments, respectively). However, none of the three FOXO1 target genes analyzed was significantly induced by the experimental treatments in iWAT of young male mice, and expression of *Gadd45* was even significantly downregulated in the RSV male mice. *Sirt1* expression was also measured, and a

trend to down-regulation of its mRNA levels was apparent in the RSV male mice ( $p = 0.053$ ). Overall, from the transcriptional analysis performed, we conclude that there is little evidence of iWAT browning or SIRT1 activation in iWAT of young male mice receiving neonatal RSV or NR supplementation.

## DISCUSSION

Modulation of the browning potential of adipose tissues through the intake of food bioactives in early life is a potential, yet still largely unexplored, strategy to enhance metabolic health in later life (Palou et al., 2013). Adipose progenitor cells resident in fat depots are likely to be natural depositors of programming information from dietary and other cues in critical life stages, making the primary culture an attractive model for studies in the field of nutritional programming of adipose tissue cellular and metabolic features. Using this model, we show here that the intake of mild supraphysiological doses of RSV or NR during



**TABLE 1 |** Biometric parameters in mice receiving resveratrol (RSV) supplementation throughout lactation and their corresponding control littermates.

	Female		Male	
	Vehicle	RSV	Vehicle	RSV
<b>Body weight evolution (g)</b>				
Day 3	2.7 ± 0.09	2.7 ± 0.17	2.7 ± 0.07	2.7 ± 0.07
Day 12	7.5 ± 0.19	7.2 ± 0.18	7.5 ± 0.16	7.2 ± 0.16
Day 21	13.8 ± 0.41	13.8 ± 0.41	14.9 ± 0.43	14.7 ± 0.38
Day 30	23.7 ± 0.44	23.6 ± 0.65	27.9 ± 0.83	27.6 ± 0.67
Cumulative energy intake from day 21 to day 30 (kcal/mice)	115 ± 1.8	117 ± 0.3	143 ± 1.2	137 ± 2.2
<b>Body composition (day 34)</b>				
Body weight (g)	26.6 ± 0.55	26.3 ± 0.47	31.4 ± 0.73	30.3 ± 0.53
Fat mass (g)	4.0 ± 0.31	4.0 ± 0.23	3.8 ± 0.26	3.4 ± 0.17
Lean mass (g)	20.0 ± 0.39	19.7 ± 0.35	25.2 ± 0.59	24.5 ± 0.40
Fat mass (g/100 g bw)	14.9 ± 0.97	15.3 ± 0.81	11.9 ± 0.60	11.2 ± 0.43
Lean mass (g/100 g bw)	75.1 ± 0.79	74.9 ± 0.76	80.6 ± 1.36	81.0 ± 0.36
Ratio fat/lean mass	0.168 ± 0.013	0.172 ± 0.010	0.128 ± 0.007	0.120 ± 0.005
Naso-anal length (cm)	9.2 ± 0.09	9.2 ± 0.07	9.5 ± 0.11	9.6 ± 0.13
Lee index (g <sup>0.33</sup> 1000/cm)	326 ± 03.1	323 ± 2.2	332 ± 2.2	324 ± 3.7
<b>Final animal/tissue weights (day 35)</b>				
Body weight (g)	26.2 ± 0.47	27.1 ± 0.65	31.4 ± 0.98	31.4 ± 0.63
Inguinal WAT (g/100g bw)	1.39 ± 0.10	1.58 ± 0.15	1.11 ± 0.07	1.15 ± 0.08
Gonadal WAT (g/100g bw)	1.14 ± 0.19	1.42 ± 0.23	1.23 ± 0.15	1.32 ± 0.10
Interscapular BAT (g/100g bw)	0.60 ± 0.04	0.72 ± 0.04	0.53 ± 0.04	0.60 ± 0.05
Liver (g/100g bw)	2.79 ± 1.11	2.09 ± 1.07	3.11 ± 1.26	3.30 ± 1.34
Gastrocnemius SM (g/100 g bw)	0.80 ± 0.04	0.90 ± 0.03	0.89 ± 0.04	0.88 ± 0.04

Data on body weight evolution, energy intake, and body composition correspond to the mean ± SEM of 11–12 animals per sex and treatment (vehicle or RSV); data on final animal/tissue weights are the mean ± SEM of 5–6 animals per sex and treatment. bw, body weight; SM, skeletal muscle. No significant differences in any of the Table's parameters were revealed by Student's *t*-test.

the suckling period impacts adipocyte precursor cells resident in subcutaneous WAT of young mice and affects the commitment of these cells to the beige adipogenesis transcriptional program in a sex-dependent manner, down-regulating it in the female mice and up-regulating it in the male mice. As expected considering the rather mild dietary treatments applied, gene expression changes observed were relatively small, yet they affected different functionally related genes concertedly. Interestingly, long-term consequences of neonatal RSV and NR treatments under the same conditions as those used here include signs of iWAT-to-BAT remodeling and better responses to an obesogenic high-fat diet in adulthood selectively in the male mice (Serrano et al., 2018). A causal link between the sex-dependent effects on iWAT preadipocyte differentiation revealed here in the primary cultures and the sex-dependent long-term effects on iWAT features and benefits against metabolic challenge found *in vivo* in adulthood is thus suggested.

Our studies are first to examine nutritional programming of adipose tissue metabolic features by NR and RSV supplements given directly to the lactating pups. Programming effects of supplemental NR has not previously been addressed, to our knowledge. In the case of RSV, maternal supplementation with this compound was previously shown to enhance brown/beige adipocyte function in the male offspring of high-fat diet-fed dams, as indicated by WAT and BAT analysis and systemic measurements (Zou et al., 2017). However, in this previous study

RSV was included in the dam's diet at a rather high dose (0.2% in the diet, ~200 mg/kg body weight per day) and throughout pregnancy and lactation, whereas we here used a mild, precise dose of RSV (2 mg/kg body weight per day) supplied directly to the pups. Additionally, only effects on the male offspring of RSV-supplemented dams were previously reported (Zou et al., 2017), whereas our study included both male and female offspring, thus allowing to unveil sex-dependent effects.

Differences in WAT browning capacity due to early metabolic imprinting might be better revealed in young animals through the establishment of WAT primary cultures, which can be readily stimulated with rosiglitazone and NA in order to recruit and activate beige adipocytes in them, than through direct WAT depot analysis (especially in the absence of extra *in vivo* challenges, such as cold-exposure). In fact, whereas brown/beige gene expression was enhanced in the derived primary cultures, iWAT of young (P35) RSV and NR treated male mice did not show an obvious brown fat-like gene expression signature: out of the fifteen brown/beige markers and mitochondria-related genes assayed, only *Prdm16* in the NR-treated male group was found to be upregulated at P35 compared to levels in controls. However, up-regulation of many of these genes in the iWAT of mice neonatally treated with RSV or NR is apparent at adult age (P164), after regular diet feeding and/or high-fat diet feeding (Serrano et al., 2018). Taken together, we interpret these results as indicating that, with time—after rounds of preadipocyte

**TABLE 2 |** Biometric parameters in mice receiving nicotinamide riboside (NR) supplementation throughout lactation and their corresponding control littermates.

	Female		Male	
	Vehicle	NR	Vehicle	NR
<b>Body weight evolution (g)</b>				
Day 3	2.9 ± 0.08	2.8 ± 0.07	3.1 ± 0.07	3.1 ± 0.06
Day 12	7.1 ± 0.22	6.9 ± 0.21	7.0 ± 0.26	7.4 ± 0.21
Day 21	12.4 ± 0.37	12.0 ± 0.32	12.5 ± 0.50	13.2 ± 0.39
Day 30	19.7 ± 1.37	19.4 ± 1.21	21.3 ± 1.31	23.5 ± 1.62
Cumulative energy intake from day 21 to day 30 (kcal/mice)	128 ± 0.8	122 ± 1.6*	159 ± 1.6	153 ± 1.6*
<b>Body composition (day 34)</b>				
Body weight (g)	25.6 ± 0.38	26.1 ± 0.39	30.3 ± 0.48	32.0 ± 0.58*
Fat mass (g)	2.9 ± 0.16	2.7 ± 0.16	2.4 ± 0.16	3.0 ± 0.22*
Lean mass (g)	19.3 ± 0.34	19.7 ± 0.24	24.8 ± 0.39	25.8 ± 0.47
Fat mass (g/100 g bw)	11.4 ± 0.58	10.5 ± 0.49	7.8 ± 0.45	9.4 ± 0.60*
Lean mass (g/100 g bw)	75.2 ± 0.55	75.3 ± 0.40	81.7 ± 0.49	80.7 ± 0.68
Ratio fat/lean mass	0.152 ± 0.009	0.139 ± 0.007	0.096 ± 0.006	0.118 ± 0.009*
Naso-anal length (cm)	9.0 ± 0.10	8.9 ± 0.11	9.3 ± 0.07	9.3 ± 0.08
Lee index (g <sup>0.33</sup> 1000/cm)	328 ± 4.1	336 ± 4.4	336 ± 2.8	339 ± 3.2
<b>Final animal/tissue weights (day 35)</b>				
Body weight (g)	27.6 ± 0.82	27.4 ± 0.83	33.2 ± 0.60	35.0 ± 0.79
Inguinal WAT (g/100g bw)	1.41 ± 0.15	1.38 ± 0.15	1.08 ± 0.08	1.19 ± 0.04
Gonadal WAT (g/100g bw)	1.12 ± 0.24	0.93 ± 0.16	1.12 ± 0.14	1.47 ± 0.12
Interscapular BAT (g/100g bw)	0.60 ± 0.04	0.66 ± 0.07	0.63 ± 0.04	0.62 ± 0.03
Liver (g/100g bw)	2.18 ± 1.13	2.89 ± 1.17	3.44 ± 1.16	2.68 ± 1.44
Gastrocnemius SM (g/100 g bw)	0.88 ± 0.03	0.89 ± 0.01	0.94 ± 0.02	0.96 ± 0.03

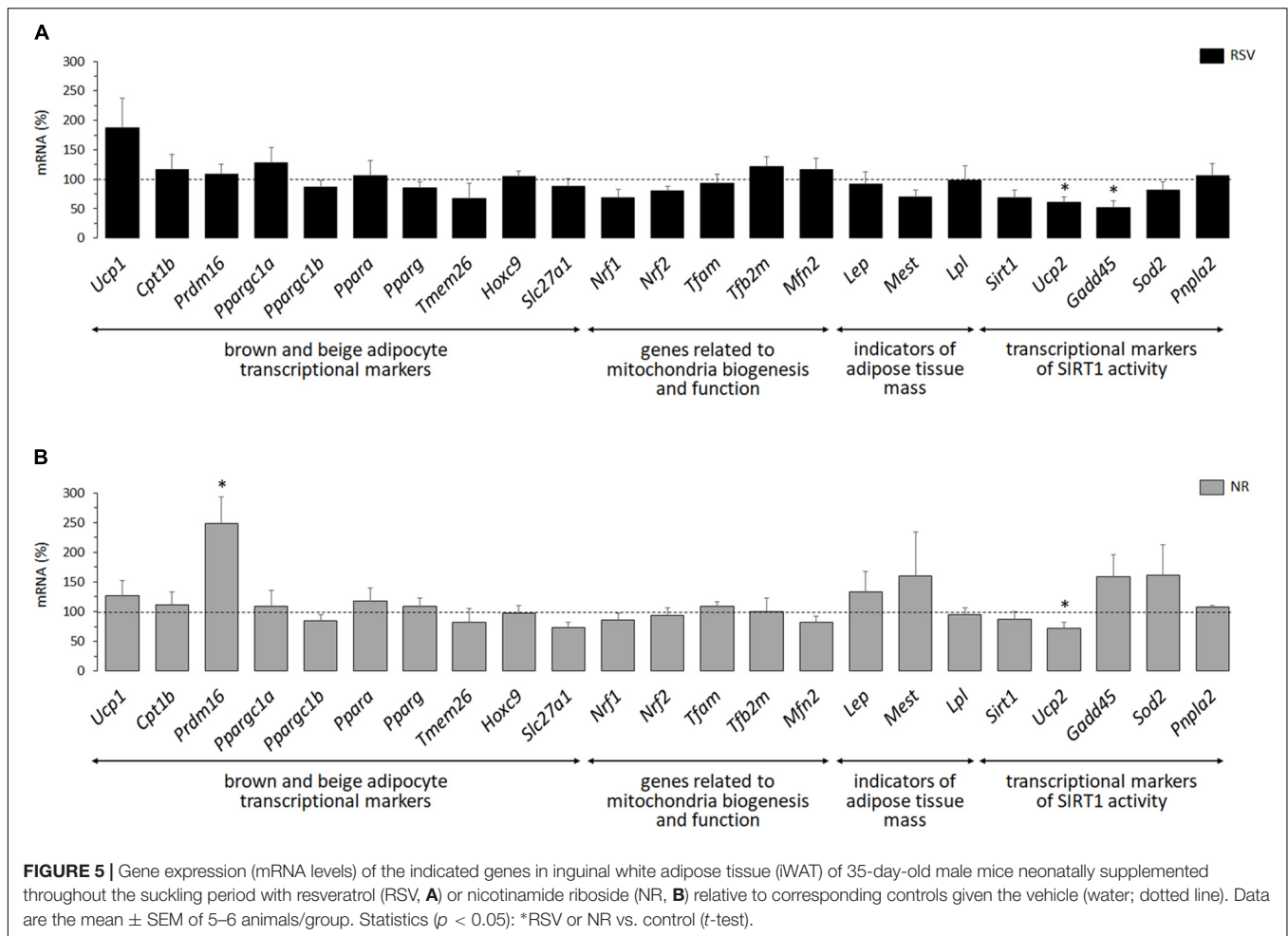
Data on body weight evolution, energy intake and body composition correspond to the mean ± SEM of 11–12 animals per sex and treatment (vehicle or RSV); data on final animal/tissue weights are the mean ± SEM of 5–6 animals per sex and treatment. bw, body weight; SM, skeletal muscle. \**p* < 0.05 vs. vehicle, Student's *t*-test.

proliferation and *de novo* adipogenesis *in vivo*, linked to aging and eventual obesogenic diet feeding—the greater commitment to brown-like adipogenesis translates into a greater appearance of BAT-like properties in the iWAT of treated male mice. In contrast, the decreased capacity for beige adipogenesis found here in iWAT primary cultures from young RSV and NR treated female mice does not translate into a generalized lower thermogenic/oxidative gene expression in the adult female iWAT, in which most of these markers are unaffected (Serrano et al., 2018). Challenging the adult animals with a strong acute pro-browning stimulus, such as cold-exposure, may be required to reveal inhibitory programming of WAT browning *in vivo*.

Whereas for iWAT of male animals there is a good concordance between observed effects of neonatal RSV and NR treatments on primary adipose cultures established at young age and observed adipose depot features at adult age, this is not the case for BAT. For instance, neonatal RSV supplementation enhanced the expression of brown marker genes in the BAT primary cultures (this work) but not in BAT of male mice in adulthood, where if anything there was decreased expression (Serrano et al., 2018). The difference may relate to the fact that our treatment period is coincident with iWAT rather than BAT development during ontogeny (Kozak, 2011). Thus, we suggest that observed effects of neonatal RSV and NR treatments on BAT preadipocyte adipogenesis in primary culture are likely a transient reflect of recent treatment, whereas effects on iWAT preadipocyte adipogenesis are likely to be persistent and of

programming nature, when the treatment is performed in the specific developmental time window of lactation.

Previous studies on the nutritional programming of adipose tissue features have mainly focused on the influence of maternal diet during pregnancy and lactation, studying factors such as maternal total energy intake (Garcia et al., 2011; Palou et al., 2015), diet macronutrient composition (Dumortier et al., 2017) or dietary fat quality (Priego et al., 2013; Kodde et al., 2017). Specific nutrients/bioactives such as RSV itself (Zou et al., 2017; Ros et al., 2018), grape seed procyanidins (del Bas et al., 2015), or leptin (Konieczna et al., 2015; Szostaczuk et al., 2017), among others, have been tested in this context mainly for their ability to counteract detrimental effects of maternal malnutrition, as in calorie restricted or high-fat diet fed dams. Early postnatal nutritional programming by specific nutrients/bioactives independently of maternal diet has been much less studied, despite its biological interest and its translational interest for the baby food market. There are studies of this kind for vitamin A (Granados et al., 2013; Musinovic et al., 2014), n-3 long-chain polyunsaturated fatty acids (Oosting et al., 2010), and leptin (Priego et al., 2010), for instance, but those studies generally focused on effects on WAT expansion, and did not specifically address effects on the WAT browning potential. Our findings are among first proof-of-concept that the fate of preadipocytes in WAT toward the beige adipogenesis transcriptional program can be influenced by the intake of specific nutrients and food bioactives in the early postnatal



life, independently of maternal diet. Another novel aspect of the present work is the use of the primary culture model, which so far has been little exploited in the field of nutritional programming, despite its potential relevance for this field. To our knowledge, only one recent report has used a similar approach, to demonstrate that neonatal overfeeding affects the differentiation capacities of adipose tissue mesenchymal stem cells (Dias et al., 2018).

Sexual dimorphism regarding the BAT thermogenic system is well-known (reviewed in Rodriguez and Palou, 2004; Valencak et al., 2017). Female rats possess more BAT of higher thermogenic capacity compared to male rats, and the same appears to be the case in humans (Valencak et al., 2017). BAT thermogenesis is more easily activated by cold in female rats (Rodriguez and Palou, 2004) and in women (van den Beukel et al., 2015) than in male counterparts, but less efficiently activated by excess palatable food intake in female than in male rats (Rodriguez and Palou, 2004). Sex differences in the capabilities for browning of WAT have also been described, with greater levels of WAT browning in female than male mice (Kim et al., 2016) and in women than in men (Barquissau et al., 2018). Our results extend sexual dimorphism of the WAT browning phenomenon to

its developmental programming in response to dietary factors. Additionally, from an operational point of view, results herein underscore that sex-dependent responses can be unveiled in primary cultures, a fact often neglected in studies using this model system.

Programming effects of RSV and NR neonatal treatments observed in this work may result from epigenetic changes in adipocyte precursor cells subsequent to treatment effects at the iWAT level and/or the central level, on neuronal circuitries impinging on the developing adipose tissue. Such actions may involve SIRT1 activation, since (i) RSV and NR can both activate SIRT1, albeit through distinct mechanisms (Canto et al., 2012; Park et al., 2012; Price et al., 2012), (ii) the activity of SIRT1 favors BAT thermogenesis and WAT browning [(Boutant and Canto, 2016) and references therein], and (iii) SIRT1 interacts with epigenetic mechanisms including DNA methylation (Ions et al., 2013). However, besides SIRT1, both RSV and NR have distinct, non-overlapping biological targets for interaction, and it is to be noted that observed effects of neonatal NR and RSV treatments, though similar, were not identical, neither in the short-term (this work) nor in the long-term (Serrano et al., 2018). Moreover, we found little evidence of activation of SIRT1 in iWAT of young treated mice, where of four transcriptional markers of SIRT1

activity assayed, only changes in *Ucp2* expression in the expected sense (Bordone et al., 2006) relative to controls were present. Further studies on the mechanisms behind programming by neonatal RSV and NR treatments of energy metabolism in adipose tissues and other key tissues in whole body energy homeostasis are warranted.

## AUTHOR CONTRIBUTIONS

MLB, JR, AMR, and AP conceived and designed the work. MA-K managed the animals. MA-K and AR established the primary cultures. MA-K and AS acquired the data. MLB and JR wrote the article. All authors analyzed and interpreted the data, revised the manuscript critically, and gave final approval of the version to be published.

## REFERENCES

- Alberdi, G., Rodriguez, V. M., Miranda, J., Macarulla, M. T., Churrua, I., and Portillo, M. P. (2013). Thermogenesis is involved in the body-fat lowering effects of resveratrol in rats. *Food Chem.* 141, 1530–1535. doi: 10.1016/j.foodchem.2013.03.085
- Andrade, J. M., Frade, A. C., Guimaraes, J. B., Freitas, K. M., Lopes, M. T., Guimaraes, A. L., et al. (2014). Resveratrol increases brown adipose tissue thermogenesis markers by increasing SIRT1 and energy expenditure and decreasing fat accumulation in adipose tissue of mice fed a standard diet. *Eur. J. Nutr.* 53, 1503–1510. doi: 10.1007/s00394-014-0655-6
- Barquissau, V., Leger, B., Beuzelin, D., Martins, F., Amri, E. Z., Pisani, D. F., et al. (2018). Caloric restriction and diet-induced weight loss do not induce browning of human subcutaneous white adipose tissue in women and men with obesity. *Cell Rep.* 22, 1079–1089. doi: 10.1016/j.celrep.2017.12.102
- Bartelt, A., and Heeren, J. (2014). Adipose tissue browning and metabolic health. *Nat. Rev. Endocrinol.* 10, 24–36. doi: 10.1038/nrendo.2013.204
- Bonet, M. L., Mercader, J., and Palou, A. (2017). A nutritional perspective on UCP1-dependent thermogenesis. *Biochimie* 134, 99–117. doi: 10.1016/j.biochi.2016.12.014
- Bonet, M. L., Oliver, P., and Palou, A. (2013). Pharmacological and nutritional agents promoting browning of white adipose tissue. *Biochim. Biophys. Acta* 1831, 969–985. doi: 10.1016/j.bbalip.2012.12.002
- Bordone, L., Motta, M. C., Picard, F., Robinson, A., Jhala, U. S., Apfeld, J., et al. (2006). Sirt1 regulates insulin secretion by repressing UCP2 in pancreatic beta cells. *PLoS Biol.* 4:e31. doi: 10.1371/journal.pbio.0040031
- Boutant, M., and Canto, C. (2016). SIRT1: a novel guardian of brown fat against metabolic damage. *Obesity* 24:554. doi: 10.1002/oby.21432
- Calnan, D. R., and Brunet, A. (2008). The FoxO code. *Oncogene* 27, 2276–2288. doi: 10.1038/ncr.2008.21
- Canto, C., Houtkooper, R. H., Pirinen, E., Youn, D. Y., Oosterveer, M. H., Cen, Y., et al. (2012). The NAD(+) precursor nicotinamide riboside enhances oxidative metabolism and protects against high-fat diet-induced obesity. *Cell Metab.* 15, 838–847. doi: 10.1016/j.cmet.2012.04.022
- Chakrabarti, P., English, T., Karki, S., Qiang, L., Tao, R., Kim, J., et al. (2011). SIRT1 controls lipolysis in adipocytes via FOXO1-mediated expression of ATGL. *J. Lipid Res.* 52, 1693–1701. doi: 10.1194/jlr.M014647
- Cohen, P., Levy, J. D., Zhang, Y., Frontini, A., Kolodin, D. P., Svensson, K. J., et al. (2014). Ablation of PRDM16 and beige adipose causes metabolic dysfunction and a subcutaneous to visceral fat switch. *Cell* 156, 304–316. doi: 10.1016/j.cell.2013.12.021
- Cottrell, E. C., and Ozanne, S. E. (2008). Early life programming of obesity and metabolic disease. *Physiol. Behav.* 94, 17–28. doi: 10.1016/j.physbeh.2007.11.017
- Cryer, A., and Jones, H. M. (1979). The early development of white adipose tissue. Effects of litter size on the lipoprotein lipase activity of four adipose-tissue depots, serum immunoreactive insulin and tissue cellularity during the first four weeks of life in the rat. *Biochem. J.* 178, 711–724. doi: 10.1042/bj1780711

## FUNDING

This work was sponsored by grants from the Spanish Government (AGL2015-67019-P to AP; Agencia Estatal de Investigación, MINECO/FEDER, EU) and Fundación Ramón Areces (to MLB). Our group is a member of the European Nutrigenomics Organization (NuGO). CIBER de Fisiopatología de la Obesidad y Nutrición (CIBEROBN) is an initiative of the ISCIII (Spanish Government).

## SUPPLEMENTARY MATERIAL

The Supplementary Material for this article can be found online at: <https://www.frontiersin.org/articles/10.3389/fphys.2019.00083/full#supplementary-material>

- del Bas, J. M., Crescenti, A., Arola-Arnal, A., Oms-Oliu, G., Arola, L., and Caimari, A. (2015). Grape seed procyanidin supplementation to rats fed a high-fat diet during pregnancy and lactation increases the body fat content and modulates the inflammatory response and the adipose tissue metabolism of the male offspring in youth. *Int. J. Obes.* 39, 7–15. doi: 10.1038/ijo.2014.159
- Dias, I., Salviano, I., Mencia, A., de Carvalho, S. N., Thole, A. A., Carvalho, L., et al. (2018). Neonatal overfeeding impairs differentiation potential of mice subcutaneous adipose mesenchymal stem cells. *Stem Cell Rev.* 14, 535–545. doi: 10.1007/s12015-018-9812-2
- Dumortier, O., Roger, E., Pisani, D. F., Casamento, V., Gautier, N., Lebrun, P., et al. (2017). Age-dependent control of energy homeostasis by brown adipose tissue in progeny subjected to maternal diet-induced fetal programming. *Diabetes Metab. Res. Rev.* 66, 627–639. doi: 10.2337/db16-0956
- Fleckenstein-Elsen, M., Dinnies, D., Jelenik, T., Roden, M., Romacho, T., and Eckel, J. (2016). Eicosapentaenoic acid and arachidonic acid differentially regulate adipogenesis, acquisition of a brite phenotype and mitochondrial function in primary human adipocytes. *Mol. Nutr. Food Res.* 60, 2065–2075. doi: 10.1002/mnfr.201500892
- Fukui, Y., Masui, S., Osada, S., Umesono, K., and Motojima, K. (2000). A new thiazolidinedione, NC-2100, which is a weak PPAR-gamma activator, exhibits potent antidiabetic effects and induces uncoupling protein 1 in white adipose tissue of KKAY obese mice. *Diabetes Metab. Res. Rev.* 49, 759–767. doi: 10.2337/diabetes.49.5.759
- Garcia, A. P., Palou, M., Sanchez, J., Priego, T., Palou, A., and Pico, C. (2011). Moderate caloric restriction during gestation in rats alters adipose tissue sympathetic innervation and later adiposity in offspring. *PLoS One* 6:e17313. doi: 10.1371/journal.pone.0017313
- Granados, N., Amengual, J., Ribot, J., Musinovic, H., Ceresi, E., von Lintig, J., et al. (2013). Vitamin A supplementation in early life affects later response to an obesogenic diet in rats. *Int. J. Obes.* 37, 1169–1176. doi: 10.1038/ijo.2012.190
- Harms, M., and Seale, P. (2013). Brown and beige fat: development, function and therapeutic potential. *Nat. Med.* 19, 1252–1263. doi: 10.1038/nm.3361
- Ions, L. J., Wakeling, L. A., Bosomworth, H. J., Hardyman, J. E., Escolme, S. M., Swan, D. C., et al. (2013). Effects of Sirt1 on DNA methylation and expression of genes affected by dietary restriction. *Age* 35, 1835–1849. doi: 10.1007/s11357-012-9485-8
- Kim, S. N., Jung, Y. S., Kwon, H. J., Seong, J. K., Granneman, J. G., and Lee, Y. H. (2016). Sex differences in sympathetic innervation and browning of white adipose tissue of mice. *Biol. Sex Differ.* 7:67. doi: 10.1186/s13293-016-0121-7
- Kodde, A., van der Beek, E. M., Phielix, E., Engels, E., Schipper, L., and Oosting, A. (2017). Supramolecular structure of dietary fat in early life modulates expression of markers for mitochondrial content and capacity in adipose tissue of adult mice. *Nutr. Metab.* 14:37. doi: 10.1186/s12986-017-0191-5
- Kojima, T., Nishimura, M., Yajima, T., Kuwata, T., Suzuki, Y., Goda, T., et al. (1998). Effect of intermittent feeding on the development of disaccharidase



- activities in artificially reared rat pups. *Comp. Biochem. Physiol. A Mol. Integr. Physiol.* 121, 289–297. doi: 10.1016/S1095-6433(98)10133-2
- Konieczna, J., Palou, M., Sanchez, J., Pico, C., and Palou, A. (2015). Leptin intake in suckling rats restores altered T3 levels and markers of adipose tissue sympathetic drive and function caused by gestational calorie restriction. *Int. J. Obes.* 39, 959–966. doi: 10.1038/ijo.2015.22
- Kozak, L. P. (2011). The genetics of brown adipocyte induction in white fat depots. *Front. Endocrinol.* 2:64. doi: 10.3389/fendo.2011.00064
- Lagouge, M., Argmann, C., Gerhart-Hines, Z., Meziane, H., Lerin, C., Daussin, F., et al. (2006). Resveratrol improves mitochondrial function and protects against metabolic disease by activating SIRT1 and PGC-1 $\alpha$ . *Cell* 127, 1109–1122. doi: 10.1016/j.cell.2006.11.013
- Lecoutre, S., and Breton, C. (2014). The cellularity of offspring's adipose tissue is programmed by maternal nutritional manipulations. *Adipocyte* 3, 256–262. doi: 10.4161/adip.29806
- Musinovic, H., Bonet, M. L., Granados, N., Amengual, J., von Lintig, J., Ribot, J., et al. (2014). beta-Carotene during the suckling period is absorbed intact and induces retinoic acid dependent responses similar to preformed vitamin A in intestine and liver, but not adipose tissue of young rats. *Mol. Nutr. Food Res.* 58, 2157–2165. doi: 10.1002/mnfr.201400457
- Ohno, H., Shinoda, K., Spiegelman, B. M., and Kajimura, S. (2012). PPAR $\gamma$  agonists induce a white-to-brown fat conversion through stabilization of PRDM16 protein. *Cell Metab.* 15, 395–404. doi: 10.1016/j.cmet.2012.01.019
- Oosting, A., Kessler, D., Boehm, G., Jansen, H. T., van de Heijning, B. J., and van der Beek, E. M. (2010). N-3 long-chain polyunsaturated fatty acids prevent excessive fat deposition in adulthood in a mouse model of postnatal nutritional programming. *Pediatr. Res.* 68, 494–499. doi: 10.1203/PDR.0b013e3181f74940
- Palmeri, R., Monteleone, J. I., Spagna, G., Restuccia, C., Raffaele, M., Vanella, L., et al. (2016). Olive leaf extract from sicilian cultivar reduced lipid accumulation by inducing thermogenic pathway during adipogenesis. *Front. Pharmacol.* 7:143. doi: 10.3389/fphar.2016.00143
- Palou, A., Pico, C., and Bonet, M. L. (2013). Nutritional potential of metabolic remodelling of white adipose tissue. *Curr. Opin. Clin. Nutr. Metab. Care* 16, 650–656. doi: 10.1097/MCO.0b013e31828365980f
- Palou, M., Priego, T., Romero, M., Szostaczuk, N., Konieczna, J., Cabrer, C., et al. (2015). Moderate calorie restriction during gestation programs offspring for lower BAT thermogenic capacity driven by thyroid and sympathetic signaling. *Int. J. Obes.* 39, 339–345. doi: 10.1038/ijo.2014.56
- Park, S. J., Ahmad, F., Philp, A., Baar, K., Williams, T., Luo, H., et al. (2012). Resveratrol ameliorates aging-related metabolic phenotypes by inhibiting cAMP phosphodiesterases. *Cell* 148, 421–433. doi: 10.1016/j.cell.2012.01.017
- Petrov, P. D., Palou, A., Bonet, M. L., and Ribot, J. (2016). Cell-autonomous brown-like adipogenesis of preadipocytes from retinoblastoma haploinsufficient mice. *J. Cell. Physiol.* 231, 1941–1952. doi: 10.1002/jcp.25299
- Petrovic, N., Walden, T. B., Shabalina, I. G., Timmons, J. A., Cannon, B., and Nedergaard, J. (2010). Chronic peroxisome proliferator-activated receptor gamma (PPAR $\gamma$ ) activation of epididymally derived white adipocyte cultures reveals a population of thermogenically competent, UCP1-containing adipocytes molecularly distinct from classic brown adipocytes. *J. Biol. Chem.* 285, 7153–7164. doi: 10.1074/jbc.M109.053942
- Price, N. L., Gomes, A. P., Ling, A. J., Duarte, F. V., Martin-Montalvo, A., North, B. J., et al. (2012). SIRT1 is required for AMPK activation and the beneficial effects of resveratrol on mitochondrial function. *Cell Metab.* 15, 675–690. doi: 10.1016/j.cmet.2012.04.003
- Priego, T., Sanchez, J., Garcia, A. P., Palou, A., and Pico, C. (2013). Maternal dietary fat affects milk Fatty Acid profile and impacts on weight gain and thermogenic capacity of suckling rats. *Lipids* 48, 481–495. doi: 10.1007/s11745-013-3764-8
- Priego, T., Sanchez, J., Palou, A., and Pico, C. (2010). Leptin intake during the suckling period improves the metabolic response of adipose tissue to a high-fat diet. *Int. J. Obes.* 34, 809–819. doi: 10.1038/ijo.2010.18
- Rivera, L., Moron, R., Zarzuelo, A., and Galisteo, M. (2009). Long-term resveratrol administration reduces metabolic disturbances and lowers blood pressure in obese Zucker rats. *Biochem. Pharmacol.* 77, 1053–1063. doi: 10.1016/j.bcp.2008.11.027
- Rodriguez, A. M., and Palou, A. (2004). Uncoupling proteins: gender-dependence and their relation to body weight control. *Int. J. Obes. Relat. Metab. Disord.* 28, 327–329. doi: 10.1038/sj.ijo.0802579
- Ros, P., Diaz, F., Freire-Regatillo, A., Argente-Arizon, P., Barrios, V., Argente, J., et al. (2018). Resveratrol intake during pregnancy and lactation modulates the early metabolic effects of maternal nutrition differently in male and female offspring. *Endocrinology* 159, 810–825. doi: 10.1210/en.2017-00610
- Rossato, M., Granzotto, M., Macchi, V., Porzionato, A., Petrelli, L., Calcagno, A., et al. (2014). Human white adipocytes express the cold receptor TRPM8 which activation induces UCP1 expression, mitochondrial activation and heat production. *Mol. Cell. Endocrinol.* 383, 137–146. doi: 10.1016/j.mce.2013.12.005
- Saito, M., Yoneshiro, T., and Matsushita, M. (2016). Activation and recruitment of brown adipose tissue by cold exposure and food ingredients in humans. *Best Pract. Res. Clin. Endocrinol. Metab.* 30, 537–547. doi: 10.1016/j.beem.2016.08.003
- Seale, P., Conroe, H. M., Estall, J., Kajimura, S., Frontini, A., Ishibashi, J., et al. (2011). Prdm16 determines the thermogenic program of subcutaneous white adipose tissue in mice. *J. Clin. Invest.* 121, 96–105. doi: 10.1172/JCI44271
- Serrano, A., Asnani-Kishnani, M., Rodriguez, A. M., Palou, A., Ribot, J., and Bonet, M. L. (2018). Programming of the beige phenotype in white adipose tissue of adult mice by mild resveratrol and nicotinamide riboside supplementations in early postnatal life. *Mol. Nutr. Food Res.* 62:e1800463. doi: 10.1002/mnfr.201800463
- Szostaczuk, N., Priego, T., Palou, M., Palou, A., and Pico, C. (2017). Oral leptin supplementation throughout lactation in rats prevents later metabolic alterations caused by gestational calorie restriction. *Int. J. Obes.* 41, 360–371. doi: 10.1038/ijo.2016.241
- Valencak, T. G., Osterrieder, A., and Schulz, T. J. (2017). Sex matters: the effects of biological sex on adipose tissue biology and energy metabolism. *Redox Biol.* 12, 806–813. doi: 10.1016/j.redox.2017.04.012
- van den Beukel, J. C., Grefhorst, A., Hoogduijn, M. J., Steenbergen, J., Mastroberardino, P. G., Dor, F. J., et al. (2015). Women have more potential to induce browning of perirenal adipose tissue than men. *Obesity* 23, 1671–1679. doi: 10.1002/oby.21166
- Wang, S., Liang, X., Yang, Q., Fu, X., Rogers, C. J., Zhu, M., et al. (2015). Resveratrol induces brown-like adipocyte formation in white fat through activation of AMP-activated protein kinase (AMPK)  $\alpha$ 1. *Int. J. Obes.* 39, 967–976. doi: 10.1038/ijo.2015.23
- Wiczor, B. M., and Bernlohr, D. A. (2009). A novel role for fatty acid transport protein 1 in the regulation of tricarboxylic acid cycle and mitochondrial function in 3T3-L1 adipocytes. *J. Lipid Res.* 50, 2502–2513. doi: 10.1194/jlr.M900218-JLR200
- Wu, J., Bostrom, P., Sparks, L. M., Ye, L., Choi, J. H., Giang, A. H., et al. (2012). Beige adipocytes are a distinct type of thermogenic fat cell in mouse and human. *Cell* 150, 366–376. doi: 10.1016/j.cell.2012.05.016
- Wu, Q., Kazantzis, M., Doege, H., Ortegon, A. M., Tsang, B., Falcon, A., et al. (2006). Fatty acid transport protein 1 is required for nonshivering thermogenesis in brown adipose tissue. *Diabetes Metab. Res. Rev.* 55, 3229–3237. doi: 10.2337/db06-0749
- Zou, T., Chen, D., Yang, Q., Wang, B., Zhu, M. J., Nathanielsz, P. W., et al. (2017). Resveratrol supplementation of high-fat diet-fed pregnant mice promotes brown and beige adipocyte development and prevents obesity in male offspring. *J. Physiol.* 595, 1547–1562. doi: 10.1113/JP273478

**Conflict of Interest Statement:** The authors declare that the research was conducted in the absence of any commercial or financial relationships that could be construed as a potential conflict of interest.

Copyright © 2019 Asnani-Kishnani, Rodríguez, Serrano, Palou, Bonet and Ribot. This is an open-access article distributed under the terms of the Creative Commons Attribution License (CC BY). The use, distribution or reproduction in other forums is permitted, provided the original author(s) and the copyright owner(s) are credited and that the original publication in this journal is cited, in accordance with accepted academic practice. No use, distribution or reproduction is permitted which does not comply with these terms.



# Mechanisms of Impaired Brown Adipose Tissue Recruitment in Obesity

Martín Alcalá<sup>1</sup>, María Calderon-Dominguez<sup>2,3</sup>, Dolors Serra<sup>2,3\*</sup>, Laura Herrero<sup>2,3\*</sup> and Marta Viana<sup>1\*</sup>

<sup>1</sup> Department of Chemistry and Biochemistry, Facultad de Farmacia, Universidad San Pablo-CEU, CEU Universities, Madrid, Spain, <sup>2</sup> Department of Biochemistry and Physiology, School of Pharmacy, Institut de Biomedicina de la Universitat de Barcelona (IBUB), Universitat de Barcelona, Barcelona, Spain, <sup>3</sup> Centro de Investigación Biomédica en Red de Fisiopatología de la Obesidad y la Nutrición (CIBEROBN), Instituto de Salud Carlos III, Madrid, Spain

## OPEN ACCESS

### Edited by:

Rita De Matteis,  
University of Urbino Carlo Bo, Italy

### Reviewed by:

Rosalba Senese,  
Università degli Studi della Campania  
Luigi Vanvitelli, Italy  
Radhika Muzumdar,  
University of Pittsburgh, United States

### \*Correspondence:

Dolors Serra  
dserra@ub.edu  
Laura Herrero  
lherrero@ub.edu  
Marta Viana  
mviana@ceu.es

### Specialty section:

This article was submitted to  
Integrative Physiology,  
a section of the journal  
Frontiers in Physiology

Received: 03 September 2018

Accepted: 25 January 2019

Published: 13 February 2019

### Citation:

Alcalá M, Calderon-Dominguez M,  
Serra D, Herrero L and Viana M  
(2019) Mechanisms of Impaired  
Brown Adipose Tissue Recruitment  
in Obesity. *Front. Physiol.* 10:94.  
doi: 10.3389/fphys.2019.00094

Brown adipose tissue (BAT) dissipates energy to produce heat. Thus, it has the potential to regulate body temperature by thermogenesis. For the last decade, BAT has been in the spotlight due to its rediscovery in adult humans. This is evidenced by over a hundred clinical trials that are currently registered to target BAT as a therapeutic tool in the treatment of metabolic diseases, such as obesity or diabetes. The goal of most of these trials is to activate the BAT thermogenic program via several approaches such as adrenergic stimulation, natriuretic peptides, retinoids, capsinoids, thyroid hormones, or glucocorticoids. However, the impact of BAT activation on total body energy consumption and the potential effect on weight loss is still limited. Other studies have focused on increasing the mass of thermogenic BAT. This can be relevant in obesity, where the activity and abundance of BAT have been shown to be drastically reduced. The aim of this review is to describe pathological processes associated with obesity that may influence the correct differentiation of BAT, such as catecholamine resistance, inflammation, oxidative stress, and endoplasmic reticulum stress. This will shed light on the thermogenic potential of BAT as a therapeutic approach to target obesity-induced metabolic diseases.

**Keywords: differentiation, BAT recruitment, preadipocyte, obesity, catecholamine, inflammation, oxidative stress, endoplasmic reticulum stress**

**Abbreviations:** 4-PBA, 4-phenyl butyric acid; ATF, Activating transcription factor; BAT, Brown adipose tissue; BIP, Binding immunoglobulin protein; BMP7 Bone morphogenic protein 7; C/EBP, CCAAT-enhancer-binding proteins; CHOP, C/EBP homologous protein; EBF2 Early B cell factor 2; EN1 Homeobox protein engrailed 1; ER, Endoplasmic reticulum; ERK, Extracellular signal-regulated kinase; EWS, Ewing sarcoma protein; FOXO (Forkhead box) proteins; GDF-3 Growth differentiation factor 3; HFD, High-fat diet; IL-1 Interleukin 1; LPS, Lipopolysaccharide; MSC, Mesenchymal cells; mTOR, Mammalian target of rapamycin; MYF5 Myogenic factor 5; NF- $\kappa$ B, Nuclear factor kappa B; NOD, Nucleotide-binding oligomerization domain-containing protein; NRF2 Nuclear factor (erythroid-derived 2)-like 2; PAX7 Paired box-protein 7; PI3K, Phosphatidylinositol-3-kinase; PPAR, Peroxisome proliferator-activated receptor; PRDM16 PR domain containing 16; TLR, Toll-like receptor; TNF- $\alpha$  Tumor necrosis factor Alpha; UCP1 Uncoupling protein 1; UPR, Unfolded protein response; WAT, White adipose tissue; XBP1 X-box binding protein 1; YBX1 Y-box binding protein 1.

## BROWN ADIPOSE TISSUE AND OBESITY

In recent years, adipose tissue has become a central focus of studies on the mechanisms involved in obesity-related diseases. In humans, this tissue is composed mainly of white adipose tissue (WAT), which stores energy in the form of triglycerides, and brown adipose tissue (BAT), which is responsible for thermogenesis. Much has been learned in the past decades about the pathophysiology of obesity in relation to WAT molecular deregulation (Gesta et al., 2007; Shoelson et al., 2007; de Heredia et al., 2012). However, little was known about these processes in BAT during obesity progression (Villarroya et al., 2018). With the rediscovery of BAT in 2009, and the fact that its mass and activity is reduced in obese and diabetic patients, a door opened for the treatment of obesity and its associated disorders (Cypess et al., 2009; Saito et al., 2009; van Marken Lichtenbelt et al., 2009; Virtanen et al., 2009; Zingaretti et al., 2009).

BAT mass and activity also change with age. In newborns, an increased BAT mass at birth has been related to decreased body fat accumulation during the first 6 months of life (Entringer et al., 2017). In adulthood, a decline of BAT mass and activity has been observed in males and females with age, and may have an impact on the accumulation of body fat (Pfannenberger et al., 2010; Yoneshiro et al., 2011).

Although a few studies have described some characteristics of BAT in a mouse model of diet-induced obesity, the molecular mechanisms involved remain unclear. Recently, it was demonstrated that BAT from obese and hyperglycemic mice shows higher levels of inflammation (macrophages and T cell infiltration), endoplasmic reticulum (ER) stress, oxidative damage, and enhanced mitochondrial respiration activity (Calderon-Dominguez et al., 2016; Alcalá et al., 2017). The results of transcriptomic studies have reported several BAT molecular networks modulated in a time-dependent mode in response to a high-fat diet (HFD). The molecular networks are associated with skeletal muscle development, regulation of ion transport, neurotransmitter secretion, the immune system, and lipid metabolism (McGregor et al., 2013; Cao et al., 2018). In addition, several microRNAs (miR) have been identified (miR-491, miR-455, miR-423-5p, miR-132-3p, miR-365-3p, and miR-30b) in obese BAT and could be novel potential pharmacological targets (Gottmann et al., 2018).

## BAT ORIGIN AND DIFFERENTIATION

Most brown adipocytes originate from precursor mesenchymal stem cells (MSC) in the somites during embryonic development. These somatic multipotent precursor cells are characterized by the expression of certain transcription factors such as myogenic factor 5 (Myf5), paired box protein 7 (Pax7), and engrailed-1 (En1) (Atit et al., 2006; Lepper and Fan, 2010; Sanchez-Gurmaches and Guertin, 2014; Wang and Scherer, 2014; Ishibashi and Seale, 2015). Skeletal myocytes, dorsal dermis, and a subset of white adipocytes in certain fat depots also arise from this lineage. Genetic lineage tracing denotes that a multistage process involves the serial activation and repression of transcription

factors, co-activators, co-repressors, and cell-cycle regulatory molecules during brown fat adipogenesis (Tapia et al., 2018).

Although the upstream factors that determine brown fat lineage remain unclear, the developmental origin of classical brown adipocytes has been studied in depth (Carobbio et al., 2013; Rosenwald and Wolfrum, 2014). Many transcription factors have been described as core regulators of brown fat development and function, such as peroxisome proliferator-activated receptor  $\gamma$  (PPAR $\gamma$ ), CCAAT/enhancer binding proteins (C/EBP $\alpha$ , C/EBP $\beta$ , C/EBP $\delta$ ), PPAR $\gamma$  coactivator 1 alpha (PGC-1 $\alpha$ ), PRD1-BF1-RIZ1 homologous domain-containing 16 (PRDM16), and even microRNAs. These factors are individually described below.

PPAR $\gamma$  has been described as a master transcription factor in the general differentiation program of brown adipocytes and induces uncoupling protein 1 (*Ucp1*) expression during adipogenesis (Tontonoz and Spiegelman, 2008). Adipocyte-specific *Ppar $\gamma$* <sup>-/-</sup> animals and the identification of mutations in the *Ppar $\gamma$*  gene in lipodystrophic patients have verified the key role of PPAR $\gamma$  in adipogenesis *in vivo* (Barak et al., 1999; Rosen et al., 1999; Agarwal and Garg, 2002; He et al., 2003). The second group of essential adipogenic transcription factors is the CCAAT/enhancer binding proteins (C/EBPs) (Lane et al., 1999). These transcription factors control the differentiation of a range of cell types and are expressed in early adipogenesis. C/EBP $\beta$  and C/EBP $\delta$  regulate the expression of C/EBP $\alpha$  and PPAR $\gamma$ , which are involved in the last stages of adipogenic differentiation. However, the mechanism that regulates brown cell lineage determination is not completely clear. Neither PPAR $\gamma$  nor C/EBPs are sufficient to induce and complete the brown adipogenic transcriptional program, although they are considered crucial transcription factors in this process (Tapia et al., 2018).

PRDM16 configures a transcriptional complex with C/EBP- $\beta$ , which controls the cell fate switch from Myf5<sup>+</sup> cells to brown preadipocytes (Kajimura et al., 2009; Sanchez-Gurmaches and Guertin, 2014). This transcriptional regulator can activate *Ppar $\gamma$*  expression and induce the thermogenic program. PRDM16 was considered critical for embryonic brown fat development (Sanchez-Gurmaches and Guertin, 2014). Nevertheless, recent studies have shown that brown fat appears in the absence of *Prdm16* expression, because of independent activation of *Ppar $\gamma$*  and *C/ebp $\alpha/\beta$*  genes during brown fat development (Ishibashi and Seale, 2015). Hence, the participation of PRDM16 in early brown adipogenesis remains unclear.

PGC-1 $\alpha$  was initially characterized as a cold-inducible co-activator of PPAR $\gamma$  (Puigserver et al., 1998). This transcription factor was indicated as a key regulator of mitochondrial biogenesis and adaptive thermogenesis. However, the expression of several brown fat-selective genes and the mass of BAT are not affected by genetic ablation of PGC-1 $\alpha$ . Hence, PGC-1 $\alpha$  does not determine the cellular specification of BAT (Sharma et al., 2014). There has been increasing interest in the differentiation of brown adipocyte by non-coding RNAs (Zhou and Li, 2014; Kajimura et al., 2015). Certain miRs, including miR-378, miR-30, and miR-26, induce brown or beige adipocyte differentiation (Karbiener et al., 2014; Pan et al., 2014; Hu et al., 2015).

Recently, the helix-loop-helix transcription factor, early B-cell factor 2 (EBF2), has been described as an essential mediator of brown adipocyte commitment and terminal differentiation (Rajakumari et al., 2013; Wang W. et al., 2014; Stine et al., 2016; Shapira et al., 2017). EBF2 has been proposed as one of the initial markers in the embryological development of brown fat cells. Moreover, this transcription factor is essential for adequate binding of PPAR $\gamma$  to *Ucp1* and other thermogenic genes (Rajakumari et al., 2013). However, the mechanism by which EBF2 activates the brown fat transcriptional program remains poorly defined.

Finally, bone morphogenetic protein 7 (BMP7) is a new critical candidate for progenitor cells to commit to brown fat lineage (Tseng et al., 2008; Schulz et al., 2013; Chen and Yu, 2018). BMP7 is expressed during the early phase of adipogenesis, and several studies revealed that it induces expression of the early regulator of brown fat fate *Pgc-1 $\alpha$* , *Prdm16* (Puigserver et al., 1998), as well as the brown adipocyte-specific genes *Ucp1*, *Dio2*, *Cidea*, *Zic1*, *Tfam*, and *Nrf-1* *in vivo* and *in vitro* (Chen and Yu, 2018). Although other BMP family members can enhance adipogenesis *in vitro*, only BMP7 initiates the brown adipogenic program. In fact, MSC fate depends on levels of BMP7 (Tseng et al., 2008). A multifunctional protein EWS (Ewing sarcoma), coupled with its binding partner Y-box binding protein 1 (YBX1), induces *Bmp7* transcription. These results indicate that EWS is also essential for early brown adipocyte lineage determination (Park et al., 2013).

## BAT QUANTIFICATION IN HUMANS

An increase in BAT mass could emerge as a promising strategy against obesity and related metabolic diseases. Approaches could entail increasing the mass of active cells by promoting differentiation and proliferation or reducing apoptosis of precursor cells.

Prior to the analysis of factors that regulate brown adipocyte recruitment in obese patients, it is important to note that we lack imaging techniques to unequivocally detect the presence of BAT in humans. The traditional combination of  $^{18}\text{F}$ -fluorodeoxyglucose and computed tomography ( $^{18}\text{F}$ -FDG PET-CT) allows visualization of the tissue from a functional perspective, since the technique is based on detecting radioactive-labeled glucose uptake by the active tissue. Other imaging techniques, recently reviewed in Ong et al. (2018), are also based on functional studies. This implies that patients classified as BAT-negative could be better defined as BAT-inactive. However, the question of whether increased BAT detection is related to preexisting BAT activation or enhanced BAT recruitment still needs to be addressed. Other techniques, such as magnetic resonance imaging (MRI) (Deng et al., 2018) or Xenon-CT (Branca et al., 2018) should be further explored (Sampath et al., 2016). MRI may have benefits over the classic PET-CT approach. For instance, PET-CT is ethically limited in the pediatric population due to ionizing radiation. In addition, the uptake of FDG might be accidentally modified by the room temperature or anesthesia. MRI measurements depend on the

hydration state of BAT, which in an obese state is similar to that of WAT and presents high intra- and inter-individual variability (Hu et al., 2013). Inert lipophilic xenon gas in Xenon-CT specifically detects BAT with a high resolution regardless of its activation state. However, it requires the use of ionizing radiation and the implementation of xenon inhalation protocols for its use in humans. Finally, validation of these new imaging methods requires the use of larger cohorts of patients to assess specificity and sensitivity.

## MECHANISMS INVOLVED IN BAT EXPANSION

### Cold/Adrenergic Stimulation

Cold-induced adrenergic stimulation is the best-studied intervention for activating the thermogenic program of BAT. Noradrenaline release stimulates UCP-1 expression and WAT lipolysis, which, together with glucose, supplies BAT with energy-rich substrates that are easily oxidizable. KO mice models lacking key genes of BAT lipolysis have been used recently to demonstrate that cold-induced thermogenesis requires WAT lipolysis rather than BAT lipolysis (Cannon and Nedergaard, 2017; Schreiber et al., 2017; Shin et al., 2017).

Coupled with this observation, an increase in brown adipocyte recruitment has been reported in rodents since the 1960s (Cameron and Smith, 1964) and more recently suggested in humans. Mild exposure to cold in humans (10°C, 2 h daily for 4 weeks or 15°C, 6 h daily for 10 days) increases the volume of active tissue as reported by  $^{18}\text{F}$ -FDG PET-CT (van der Lans et al., 2013; Blondin et al., 2014). Even in patients with non-detectable BAT prior to cold intervention, mild exposure to 17°C, 2 h daily for 6 weeks was enough to increase 2-deoxyglucose uptake and BAT activity (Yoneshiro et al., 2013). A similar result was found in a pilot study on young obese patients (Hanssen et al., 2016), although the report has two major drawbacks: a low number of subjects ( $n = 5$ ) and BAT activity was measured rather than BAT volume, as discussed above.

The molecular mechanism of cold-induced BAT recruitment has been thoroughly reviewed (Nedergaard et al., 2018). Briefly, the authors summarize how BAT recruitment in rodents exposed to cold is due to enhanced proliferation of a group of MSC within the tissue, in addition to a reduction in apoptosis (Lee et al., 2015). Unlike white subcutaneous adipocytes, which can activate a thermogenic program by sensing cold without the strict action of adrenergic stimuli (Ye et al., 2013), brown adipocyte proliferation is exclusively linked to the presence of  $\beta 1$  adrenoreceptors, which is the only subtype that is expressed in brown preadipocytes (Bronnikov et al., 1999). In addition, mature adipocyte proliferation can be stimulated by  $\beta 3$  agonists (Fukano et al., 2016). Intracellular signaling involves activation of the cAMP pathway, mediated by well-known mitogen regulators such as phosphatidylinositol-3-kinase (PI3K) (Hinoi et al., 2014), mammalian target of rapamycin (mTOR) (Labbe et al., 2016), and extracellular signal-regulated kinase (ERK1/2) (Fredriksson and Nedergaard, 2002). However, *in vitro*, the addition of inhibitors of



these pathways was unable to completely inhibit cAMP-mediated cell proliferation (Wang Y. et al., 2014).

Another interesting field of research is how cold affects brown preadipocyte differentiation. In a recent report, the authors describe an *in vitro* model to enhance brown adipocyte differentiation from an immortalized line of mouse MSC by reducing the incubation temperature from 37 to 32°C for 9 days (Velickovic et al., 2018). This could indicate that differentiation can be independent of adrenergic stimulation. However, in this model, differentiated cold-induced cells resemble a beige phenotype according to the expression levels of several beige/brown feature transcription factors.

The key role of adrenergic innervation to enhance BAT recruitment is potentially one of the reasons for the reduced amount of BAT in obese patients. Central obesity has been inversely related to plasma catecholamine levels (Wang et al., 2011). In addition, obesity is characterized by a catecholamine-resistant state, at least in WAT, with reduced expression of adrenergic receptors and a reduced response to noradrenaline-induced lipolysis (Arner, 1999; Guo et al., 2014). We suggest that this situation could also affect BAT, by hampering brown adipocyte proliferation and differentiation.

## Adipokines/Batokines

Immune cells and inflammatory cytokines play a key role in regulation of the thermogenic program of BAT, although knowledge of this process is not as well-known as in WAT. Some of the latest evidence has been thoughtfully reviewed in van den Berg et al. (2017). For instance, alternatively activated M2 macrophages have been reported to be necessary to sustain a cold-adaptive thermogenic program in BAT, probably due to the ability to synthesize catecholamines (Nguyen et al., 2011). Regulatory T cells are also required to maintain a proper adaptive response to cold. Genetic ablation of this type of immune cells impaired the expression of thermogenic markers and promoted the invasion of proinflammatory macrophages (Medrikova et al., 2015).

In obesity, BAT shows a low-degree of inflammation characterized by the M1 macrophage, T cell infiltration, regulatory T cell decline and cytokine release. However, it takes longer to appear and has a more limited extension than in white adipose depots (Fitzgibbons et al., 2011; Alcalá et al., 2017). Time-course microarrays on HFD-fed mice revealed that the upregulation of immune cell trafficking genes begins after week 8 and spikes by week 20, together with an inflammatory response (McGregor et al., 2013). The infiltration of M1 macrophages and the proinflammatory cytokines that are released promotes a decline in UCP-1 expression, which alters thermogenic activity (Sakamoto et al., 2016).

In addition, infiltrated immune cells with pro-inflammatory potential and both circulating and self-synthesized chemokines can inhibit BAT recruitment during obesity. During normal brown preadipocyte differentiation, there is a time-dependent downregulation of the expression of pattern recognition receptors such as NOD2 and TLR2, both upstream of the NF- $\kappa$ B proinflammatory pathway (Bae et al., 2014). When these receptors are activated by their corresponding agonists, brown preadipocyte differentiation and adipogenesis are inhibited in

a NF- $\kappa$ B-dependent mechanism (Bae et al., 2015). Similarly, exposure to pro-inflammatory molecules such as TNF- $\alpha$ , IL-1, LPS, or Oncostatin M, secreted by T cells and macrophages, inhibits brown differentiation *in vitro* (Mracek et al., 2004; Zoller et al., 2016; Sanchez-Infantes et al., 2017). This is achieved by downregulating key adipogenic factors such as PPAR $\gamma$ , which reproduces effects that were previously observed in white preadipocytes (Ron et al., 1992).

Inflammatory signals can also promote cellular apoptosis, which impedes the expansion of BAT. For instance, the induction of apoptosis by TNF- $\alpha$  has been traditionally described in white (Furuoka et al., 2016; Zoller et al., 2016) and brown adipocytes (Valladares et al., 2000; Miranda et al., 2010).

Finally, inflammation can inhibit brown adipocyte proliferation indirectly by inhibiting catecholamine signaling (Villarroya et al., 2018). As mentioned above, noradrenaline promotes brown adipocyte proliferation and preadipocyte differentiation. However, obesity-induced inflammation may reduce the noradrenergic tone by several potential mechanisms:

- (1) Interrupting cAMP intracellular signaling. IKK $\epsilon$  overexpression drives the activation of NF- $\kappa$ B and phosphodiesterases, which reduces the availability of cAMP (Mowers et al., 2013).
- (2) Reducing the synthesis of catecholamines. Traditionally, it was claimed that the obesity-induced phenotype shift from M2 anti-inflammatory macrophage to M1 pro-inflammatory macrophage was accompanied by loss of the capacity to express tyrosine hydroxylase (Nguyen et al., 2011), the rate-limiting step in the synthesis of noradrenaline. However, recent studies question the initial capacity of M2 macrophages to express TH (Fischer et al., 2017).
- (3) Enhancing the clearance of catecholamines. Growth differentiation factor-3 (GDF3), a member of the TGF- $\beta$  family, enhances the activity of monoamine oxidase in macrophages through activation of the inflammasome system. This promotes noradrenaline uptake and degradation (Guo et al., 2014).

## Oxidative Stress

During obesity development, mitochondrial dysfunction due to increased substrate oxidation, together with the action of other oxidases, increases the production of reactive oxygen species (ROS). As a compensatory mechanism, the expression of antioxidant enzymes is upregulated via NRF2 and FOXO, which maintains the intracellular redox state. Oxidative stress occurs when excessive production of ROS overrides the antioxidant defense, causing macromolecule oxidation. In WAT, oxidative stress is one of the mechanisms that accounts for malfunction of the adipocyte, since it has an impact on insulin signaling or inflammation, among other factors (Furukawa et al., 2004; Jankovic et al., 2014; Alcalá et al., 2015). Obese mouse BAT presented the same signs of oxidative stress: increased ROS production and a decline in antioxidant capacity (Alcalá et al., 2017).

The relevant role of oxidative stress in BAT recruitment lies in the dual effect of ROS as pro-oxidative molecules at high pathological concentrations when they surpass the antioxidant defense, and their action as second messengers in cell signaling processes at physiological levels (Jones and Sies, 2015; Castro et al., 2016).

Unfortunately, little is known about the effect of ROS on BAT differentiation. A recent report describes an increase in mRNA and protein levels of antioxidant enzymes during murine brown preadipocyte differentiation (Rebiger et al., 2016). The same was observed in white adipocytes, in which the expression of antioxidant enzymes during differentiation is also increased to prevent oxidative stress (Adachi et al., 2009; Higuchi et al., 2013). In fact, Furukawa et al. (2004) described for the first time that *in vitro* differentiation of 3T3-L1 adipocytes was accompanied by an increase in ROS formation. These results have been reproduced in other *in vitro* models of white preadipocytes (Kanda et al., 2011). The addition of extracellular H<sub>2</sub>O<sub>2</sub> shows a concentration-dependent effect on differentiation in the micromolar range. This enhances adipogenesis by acting on PPAR $\gamma$  and the C/EBP family of transcription factors (Tormos et al., 2011; Higuchi et al., 2013) to accommodate the excess of fat and accelerating cell proliferation (Lee et al., 2009).

However, to the best of our knowledge, there is little evidence of the role of ROS in the regulation of differentiation and adipogenesis in BAT, although some reports point to the role of Wnt signaling. BAT expresses Wnt10a, which is upregulated, at least *in vitro*, by the addition of H<sub>2</sub>O<sub>2</sub> (Yasuniwa et al., 2010) and Wnt10b. Wnt activation leads to impaired brown preadipocyte

differentiation and whitening of the mature brown adipocyte (Kang et al., 2005).

The incubation of preadipocytes with antioxidants led to reduced ROS formation and impaired differentiation (Calzadilla et al., 2011; Hou et al., 2012), which reflects the need to maintain a proper intracellular redox balance. Similarly, when BSO, a glutathione quencher, was added to mimic an oxidative stress situation, ROS production increased but differentiation was inhibited (Findeisen et al., 2011).

If these molecular pathways were common between white and brown preadipocytes, they would lead to changes in BAT phenotype during obesity. Changes would range from “whitening” as ROS secretion begins to a complete loss of the ability to differentiate new cells when oxidative stress is established. As a result, thermogenic capability would be completely lost.

## Endoplasmic Reticulum Stress

During obesity, the overload of protein folding requirement can trigger ER stress to activate the unfolded protein response (UPR). Briefly, the UPR tries to restore the function of the ER through three pathways: decreasing protein translation, enhancing protein folding, and triggering cellular apoptosis if the repair process fails. Key markers of UPR such as *Bip*, *Chop*, *Atf4*, or *Atf6* expression have been found to be overexpressed in BAT from HFD-fed obese mice (Alcala et al., 2017; Liu et al., 2017). However, caspase 3 was not overexpressed, which indicates that the UPR was activated for a reparative rather than a proapoptotic end. Actually, when HFD-fed mice were further induced ER stress with the administration of thapsigargin or tunicamycin,

**TABLE 1** | miRNA involved in BAT expansion.

miRNA	Effect in differentiation	Target gene	Obesity	Reference
miR-27	↓	Prdm16 Creb Ppar $\alpha$ Pgc-1 $\beta$	miR-27 expression correlates with BMI	Yu et al., 2018 Sun and Trajkovski, 2014
miR-34a	↓	Fgf21 Sirt1	miR-34a expression is increased in obesity. miR-34a overexpression protected against HFD-induced obesity	Fu et al., 2014
miR-133	↓	Prdm16	Antagonist miR-133 treatment protected against HFD-induced obesity	Yin et al., 2013
miR-155	↓	Cebp $\beta$	miR-155 KO protected against HFD-induced obesity	Gaudet et al., 2016
miR-199a-214	↓	Prdm16 Pgc-1 $\alpha$	miR-199a-214 expression reduced in genetic models of obesity. Anti-miR-199a-214 injection protected against body weight gain	He et al., 2018
miR-328	↑	Bace1	HFD-induced obesity increased miRNA-328 expression in BAT	Oliverio et al., 2016
miR-378	↑	Pde1b	miR-378 promoted BAT expansion, protecting against genetic and HFD-induced obesity	Pan et al., 2014
miR-455	↑	Runx1t1 Necdin	miRNA-455 transgenic mice (FAT455) protected against HFD-induced obesity	Zhang et al., 2015
miR-93-106b	↓	Pppar $\alpha$	HFD-induced obesity increased miRNA-93-106b expression in BAT	Wu et al., 2013

*Role in obesity.*

gene expression of caspase 3 and 12 and *Bax* was upregulated (Liu et al., 2017).

A recent report uses two approaches to inhibit UPR in brown preadipocytes: incubation with 4-phenyl butyric acid (4-PBA), an inhibitor of ER stress, and siRNA for Xbp1. Both approaches drastically reduced differentiation and adipogenesis, which indicates the key role of the activation of UPR during differentiation. Furthermore, the incubation of brown preadipocytes with capsaicin, a component of red chili peppers, stimulates brown adipogenesis as well as the expression of UPR

genes such as Xbp1 or Chop (Kida et al., 2018). More recently, Ju et al. (2018) described the role of a member of the Bcl2 family, Bcl2l13, in the differentiation of brown preadipocytes. Bcl2l13 play a key role in the regulation of mitochondrial dynamics. Silencing Bcl2l13 expression resulted in hampered brown preadipocyte differentiation due to decreased expression of mitochondrial fusion genes, biogenesis and respiratory chain complexes.

These results may suggest that reparative branches of the UPR must be activated for brown preadipocyte differentiation,

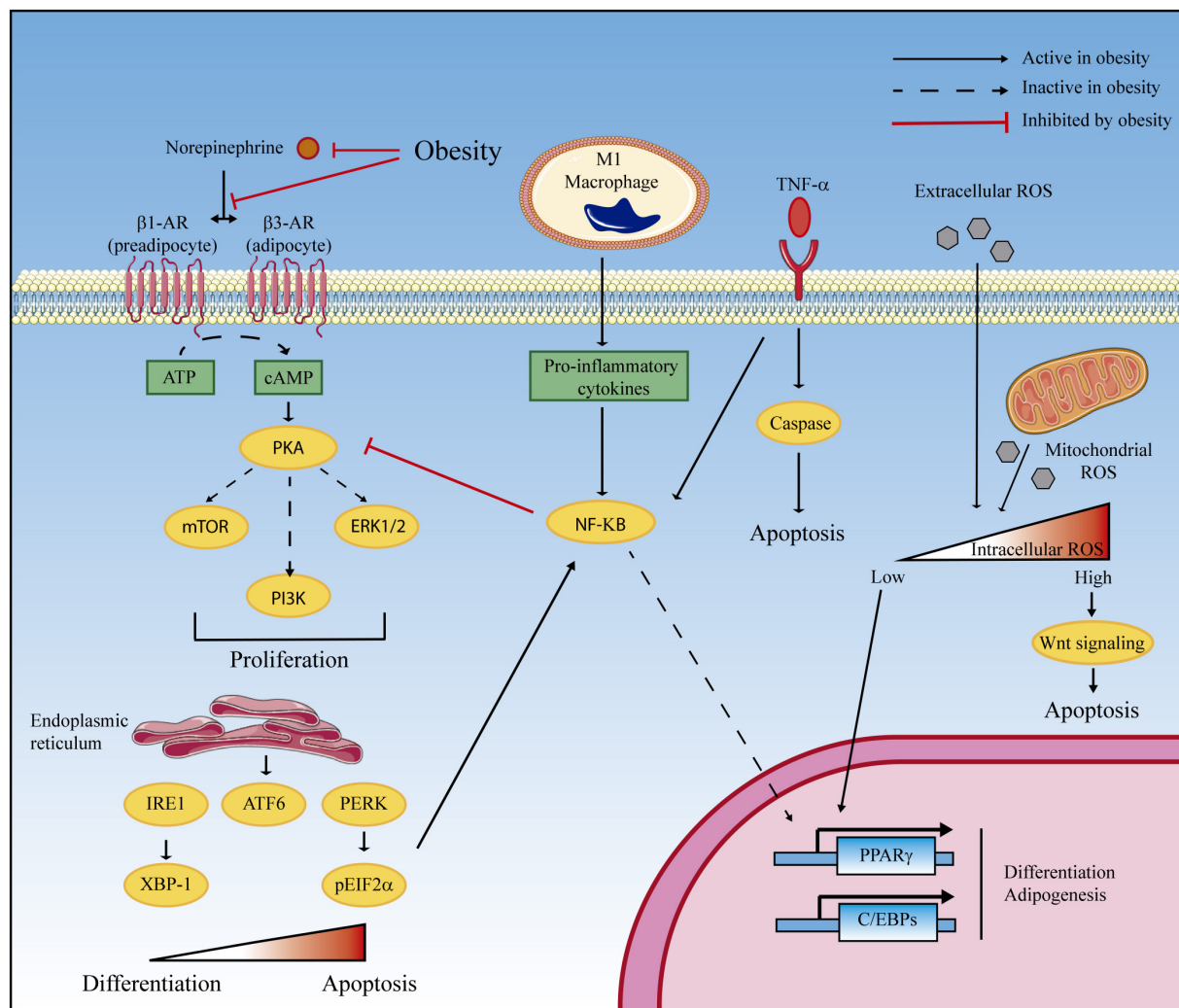


**FIGURE 1 |** Proposed mechanisms of obesity-induced BAT depletion. BAT mass and activity are minimized in obese patients due to reduced cell proliferation and preadipocyte differentiation and increased apoptosis. At least four obesity-related mechanisms can be involved. (1) Catecholamine resistance in obesity is characterized by decreased synthesis of norepinephrine and beta-adrenergic ( $\beta$ -AR) receptors and by defective intracellular signaling, which impedes PKA-mediated cell proliferation. (2) Obesity promotes the infiltration of M1 macrophages that participate in norepinephrine clearance and contribute to the synthesis of proinflammatory cytokines. NF- $\kappa$ B-mediated signaling inhibits the PKA proliferation pathway and represses PPAR $\gamma$  and C/EBPs gene expression, which inhibits differentiation and adipogenesis. In addition, TNF- $\alpha$  overexpression triggers cellular apoptosis. (3) The unfolded protein response (UPR) in the endoplasmic reticulum plays a dual role in brown adipocyte differentiation according to the intensity of the signal. While activation of the three branches of UPR (IRE-1, ATF6, and PERK) is required for differentiation, excessive UPR activation (that can be found in severe obesity) triggers proapoptotic mechanisms. (4) In a similar manner, reactive oxygen species (ROS) are also homeostatic regulators of cell differentiation and apoptosis. Physiological ROS concentrations promote C/EBP expression leading to differentiation, whereas supraphysiological concentration leads to oxidative stress and apoptosis via Wnt signaling. Artwork was obtained from Servier Medical Art, licensed under a Creative Commons Attribution 3.0 Generic License (<http://smart.servier.com/>).

in a similar manner to that previously observed in white differentiation (Sha et al., 2009). However, when ER stress is strongly induced (by chemical inducers or by long-term obesity), the apoptotic pathway can be triggered, which participates partially in BAT atrophy. BAT from obese rats has lower Bcl-2/Bax mRNA and protein ratios than the BAT of their lean littermates (Brischini et al., 1998).

## miRNA

miRNAs are a type of single-stranded mRNA with a variable size ranging from 21 to 25 nucleotides. They play a key role in the regulation of gene expression, mainly by binding to the 3'UTR of target mRNAs and blocking their translation. In the last few years, the role of several miRNAs in adipose tissue biology has been revealed (Brandao et al., 2017). More specifically, miRNA arrays were used to detect at least 25 BAT-enriched miRNA genes targeting up to 788 genes involved in brown adipocyte growth, proliferation and differentiation (Guller et al., 2015; Price and Fernandez-Hernando, 2016). However, the regulation of these miRNAs in obesity has not yet been determined. Findings regarding miRNAs and BAT expansion in obesity are summarized in **Table 1**.

## CONCLUSION

Although not completely understood yet, brown adipocyte differentiation involves a complex network of transcription factors, genes, and miRNAs that are apparently interrupted in obesity.

The relations between the pathological basis of obesity and strategies to recruit active BAT are summarized in **Figure 1**. Resistance to catecholamines and inflammatory processes directly reduce adipocyte differentiation and proliferation and can promote apoptosis. In addition, a moderate increase in ROS generation (before antioxidant defense is surpassed and oxidative stress is established) and ER stress favors brown

preadipocyte differentiation and adipogenesis. The goal would most likely be to accumulate an excess of fat, which involves brown adipocytes changing to acquire a white phenotype, and thus losing their thermogenic potential. If the obesity challenge continues and oxidative stress and ER stress are completely established, both differentiation and proliferation are inhibited, and cellular apoptosis is triggered. The decrease of BAT mass and activity in obese individuals indicates that any strategy leading to an enhancement of preadipocyte differentiation and proliferation or a reduction of apoptosis could be potentially added to the therapeutic arsenal against obesity.

## AUTHOR CONTRIBUTIONS

MA, MC-D, and MV participated in the conception of the study and in the preparation of the manuscript. LH and DS participated in the preparation of the manuscript and critically reviewed the final draft.

## FUNDING

This study was supported by the Universidad CEU San Pablo-Banco Santander (FUSP-BS-PPC-USP02/2017) to MA, the Ministry of Spain (MINECO) (Grant SAF2017-83813-C3-1-R to DS and LH cofunded by the European Regional Development Fund [ERDF]), the *Centro de Investigación Biomédica en Red de Fisiopatología de la Obesidad y la Nutrición* (CIBEROBN) (Grant CB06/03/0001 to DS), and the *Fundació La Marató de TV3* (Grant 87/C/2016 to DS).

## ACKNOWLEDGMENTS

Artwork was obtained from Servier Medical Art, licensed under a Creative Common Attribution 3.0 Generic License (<http://smart.servier.com/>).

## REFERENCES

- Adachi, T., Toishi, T., Wu, H., Kamiya, T., and Hara, H. (2009). Expression of extracellular superoxide dismutase during adipose differentiation in 3T3-L1 cells. *Redox Rep.* 14, 34–40. doi: 10.1179/135100009X392467
- Agarwal, A. K., and Garg, A. (2002). A novel heterozygous mutation in peroxisome proliferator-activated receptor-gamma gene in a patient with familial partial lipodystrophy. *J. Clin. Endocrinol. Metab.* 87, 408–411. doi: 10.1210/jcem.87.1.8290
- Alcala, M., Calderon-Dominguez, M., Bustos, E., Ramos, P., Casals, N., Serra, D., et al. (2017). Increased inflammation, oxidative stress and mitochondrial respiration in brown adipose tissue from obese mice. *Sci. Rep.* 7:16082. doi: 10.1038/s41598-017-16463-6
- Alcala, M., Sanchez-Vera, I., Sevillano, J., Herrero, L., Serra, D., Ramos, M. P., et al. (2015). Vitamin E reduces adipose tissue fibrosis, inflammation, and oxidative stress and improves metabolic profile in obesity. *Obesity* 23, 1598–1606. doi: 10.1002/oby.21135
- Arner, P. (1999). Catecholamine-induced lipolysis in obesity. *Int. J. Obes. Relat. Metab. Disord.* 23(Suppl. 1), 10–13. doi: 10.1038/sj.ijo.0800789
- Atit, R., Sgaier, S. K., Mohamed, O. A., Taketo, M. M., Dufort, D., Joyner, A. L., et al. (2006). Beta-catenin activation is necessary and sufficient to specify the dorsal dermal fate in the mouse. *Dev. Biol.* 296, 164–176. doi: 10.1016/j.ydbio.2006.04.449
- Bae, J., Chen, J., and Zhao, L. (2015). Chronic activation of pattern recognition receptors suppresses brown adipogenesis of multipotent mesodermal stem cells and brown pre-adipocytes. *Biochem. Cell Biol.* 93, 251–261. doi: 10.1139/bcb-2014-0139
- Bae, J., Ricciardi, C. J., Esposito, D., Komarnytsky, S., Hu, P., Curry, B. J., et al. (2014). Activation of pattern recognition receptors in brown adipocytes induces inflammation and suppresses uncoupling protein 1 expression and mitochondrial respiration. *Am. J. Physiol. Cell Physiol.* 306, C918–C930. doi: 10.1152/ajpcell.00249.2013
- Barak, Y., Nelson, M. C., Ong, E. S., Jones, Y. Z., Ruiz-Lozano, P., Chien, K. R., et al. (1999). PPAR gamma is required for placental, cardiac, and adipose tissue development. *Mol. Cell* 4, 585–595. doi: 10.1016/S1097-2765(00)80209-9
- Blondin, D. P., Labbe, S. M., Tinelstad, H. C., Noll, C., Kunach, M., Phoenix, S., et al. (2014). Increased brown adipose tissue oxidative capacity in cold-acclimated humans. *J. Clin. Endocrinol. Metab.* 99, E438–E446. doi: 10.1210/jc.2013-3901



- Branca, R. T., McCallister, A., Yuan, H., Aghajanian, A., Faber, J. E., Weimer, N., et al. (2018). Accurate quantification of brown adipose tissue mass by xenon-enhanced computed tomography. *Proc. Natl. Acad. Sci. U.S.A.* 115, 174–179. doi: 10.1073/pnas.1714431115
- Brandao, B. B., Guerra, B. A., and Mori, M. A. (2017). Shortcuts to a functional adipose tissue: the role of small non-coding RNAs. *Redox Biol.* 12, 82–102. doi: 10.1016/j.redox.2017.01.020
- Brischini, L., Tonello, C., Dioni, L., Carruba, M. O., and Nisoli, E. (1998). Bcl-2 and Bax are involved in the sympathetic protection of brown adipocytes from obesity-linked apoptosis. *FEBS Lett.* 431, 80–84. doi: 10.1016/S0014-5793(98)00730-3
- Bronnikov, G., Bengtsson, T., Kramarova, L., Golozoubova, V., Cannon, B., and Nedergaard, J. (1999). beta1 to beta3 switch in control of cyclic adenosine monophosphate during brown adipocyte development explains distinct beta-adrenoceptor subtype mediation of proliferation and differentiation. *Endocrinology* 140, 4185–4197. doi: 10.1210/endo.140.9.6972
- Calderon-Dominguez, M., Mir, J. F., Fucho, R., Weber, M., Serra, D., and Herrero, L. (2016). Fatty acid metabolism and the basis of brown adipose tissue function. *Adipocyte* 5, 98–118. doi: 10.1080/21623945.2015.1122857
- Calzadilla, P., Sapochnik, D., Cosentino, S., Diz, V., Dicelio, L., Calvo, J. C., et al. (2011). N-acetylcysteine reduces markers of differentiation in 3T3-L1 adipocytes. *Int. J. Mol. Sci.* 12, 6936–6951. doi: 10.3390/ijms12106936
- Cameron, I. L., and Smith, R. E. (1964). Cytological Responses of Brown Fat Tissue in Cold-Exposed Rats. *J. Cell Biol.* 23, 89–100. doi: 10.1083/jcb.23.1.89
- Cannon, B., and Nedergaard, J. (2017). What Ignites UCP1? *Cell Metab.* 26, 697–698. doi: 10.1016/j.cmet.2017.10.012
- Cao, J., Zhu, Q., Liu, L., Glazier, B. J., Hinkel, B. C., Liang, C., et al. (2018). Global transcriptome analysis of brown adipose tissue of diet-induced obese mice. *Int. J. Mol. Sci.* 19:E1095. doi: 10.3390/ijms19041095
- Carobbio, S., Rosen, B., and Vidal-Puig, A. (2013). Adipogenesis: new insights into brown adipose tissue differentiation. *J. Mol. Endocrinol.* 51, T75–T85. doi: 10.1530/JME-13-0158
- Castro, J. P., Grune, T., and Speckmann, B. (2016). The two faces of reactive oxygen species (ROS) in adipocyte function and dysfunction. *Biol. Chem.* 397, 709–724. doi: 10.1515/hsz-2015-0305
- Chen, Y. C., and Yu, Y. H. (2018). The potential of brown adipogenesis and browning in porcine bone marrow-derived mesenchymal stem cells. *J. Anim. Sci.* doi: 10.1093/jas/sky230 [Epub ahead of print].
- Cypess, A. M., Lehman, S., Williams, G., Tal, I., Rodman, D., Goldfine, A. B., et al. (2009). Identification and importance of brown adipose tissue in adult humans. *N. Engl. J. Med.* 360, 1509–1517. doi: 10.1056/NEJMoa0810780
- de Heredia, F. P., Gomez-Martinez, S., and Marcos, A. (2012). Obesity, inflammation and the immune system. *Proc. Nutr. Soc.* 71, 332–338. doi: 10.1017/S0029665112000092
- Deng, J., Neff, L. M., Rubert, N. C., Zhang, B., Shore, R. M., Samet, J. D., et al. (2018). MRI characterization of brown adipose tissue under thermal challenges in normal weight, overweight, and obese young men. *J. Magn. Reson. Imaging* 47, 936–947. doi: 10.1002/jmri.25836
- Entringer, S., Rasmussen, J., Cooper, D. M., Ikenoue, S., Waffarn, F., Wadhwa, P. D., et al. (2017). Association between supraclavicular brown adipose tissue composition at birth and adiposity gain from birth to 6 months of age. *Pediatr. Res.* 82, 1017–1021. doi: 10.1038/pr.2017.159
- Findeisen, H. M., Pearson, K. J., Gizard, F., Zhao, Y., Qing, H., Jones, K. L., et al. (2011). Oxidative stress accumulates in adipose tissue during aging and inhibits adipogenesis. *PLoS One* 6:e18532. doi: 10.1371/journal.pone.0018532
- Fischer, K., Ruiz, H. H., Jhun, K., Finan, B., Oberlin, D. J., van der Heide, V., et al. (2017). Alternatively activated macrophages do not synthesize catecholamines or contribute to adipose tissue adaptive thermogenesis. *Nat. Med.* 23, 623–630. doi: 10.1038/nm.4316
- Fitzgibbons, T. P., Kogan, S., Aouadi, M., Hendricks, G. M., Straubhaar, J., and Czech, M. P. (2011). Similarity of mouse perivascular and brown adipose tissues and their resistance to diet-induced inflammation. *Am. J. Physiol. Heart Circ. Physiol.* 301, H1425–H1437. doi: 10.1152/ajpheart.00376.2011
- Fredriksson, J. M., and Nedergaard, J. (2002). Norepinephrine specifically stimulates ribonucleotide reductase subunit R2 gene expression in proliferating brown adipocytes: mediation via a cAMP/PKA pathway involving Src and Erk1/2 kinases. *Exp. Cell Res.* 274, 207–215. doi: 10.1006/excr.2002.5470
- Fu, T., Seok, S., Choi, S., Huang, Z., Suino-Powell, K., Xu, H. E., et al. (2014). MicroRNA 34a inhibits beige and brown fat formation in obesity in part by suppressing adipocyte fibroblast growth factor 21 signaling and SIRT1 function. *Mol. Cell Biol.* 34, 4130–4142. doi: 10.1128/MCB.00596-14
- Fukano, K., Okamatsu-Ogura, Y., Tsubota, A., Nio-Kobayashi, J., and Kimura, K. (2016). Cold exposure induces proliferation of mature brown adipocyte in a ss3-adrenergic receptor-mediated pathway. *PLoS One* 11:e0166579. doi: 10.1371/journal.pone.0166579
- Furukawa, S., Fujita, T., Shimabukuro, M., Iwaki, M., Yamada, Y., Nakajima, Y., et al. (2004). Increased oxidative stress in obesity and its impact on metabolic syndrome. *J. Clin. Invest.* 114, 1752–1761. doi: 10.1172/JCI21625
- Furuoka, M., Ozaki, K., Sadatomi, D., Mamiya, S., Yonezawa, T., Tanimura, S., et al. (2016). TNF-alpha induces caspase-1 activation independently of simultaneously induced NLRP3 in 3T3-L1 cells. *J. Cell Physiol.* 231, 2761–2767. doi: 10.1002/jcp.25385
- Gaudet, A. D., Fonken, L. K., Gushchina, L. V., Aubrecht, T. G., Maurya, S. K., Periasamy, M., et al. (2016). miR-155 Deletion in Female Mice Prevents Diet-Induced Obesity. *Sci. Rep.* 6:22862. doi: 10.1038/srep22862
- Gesta, S., Tseng, Y. H., and Kahn, C. R. (2007). Developmental origin of fat: tracking obesity to its source. *Cell* 131, 242–256. doi: 10.1016/j.cell.2007.10.004
- Gottmann, P., Ouni, M., Saussenthaler, S., Roos, J., Stirn, L., Jahnert, M., et al. (2018). A computational biology approach of a genome-wide screen connected miRNAs to obesity and type 2 diabetes. *Mol. Metab.* 11, 145–159. doi: 10.1016/j.molmet.2018.03.005
- Guller, I., McNaughton, S., Crowley, T., Gilsanz, V., Kajimura, S., Watt, M., et al. (2015). Comparative analysis of microRNA expression in mouse and human brown adipose tissue. *BMC Genomics* 16:820. doi: 10.1186/s12864-015-2045-8
- Guo, T., Marmol, P., Moliner, A., Bjornholm, M., Zhang, C., Shokat, K. M., et al. (2014). Adipocyte ALK7 links nutrient overload to catecholamine resistance in obesity. *eLife* 3:e03245. doi: 10.7554/eLife.03245
- Hanssen, M. J., van der Lans, A. A., Brans, B., Hoeks, J., Jardon, K. M., Schaart, G., et al. (2016). Short-term cold acclimation recruits brown adipose tissue in obese humans. *Diabetes* 65, 1179–1189. doi: 10.2337/db15-1372
- He, L., Tang, M., Xiao, T., Liu, H., Liu, W., Li, G., et al. (2018). Obesity-associated miR-199a/214 cluster inhibits adipose browning via PRDM16-PGC-1alpha transcriptional network. *Diabetes* 67, 2585–2600. doi: 10.2337/db18-0626
- He, W., Barak, Y., Heverner, A., Olson, P., Liao, D., Le, J., et al. (2003). Adipose-specific peroxisome proliferator-activated receptor gamma knockout causes insulin resistance in fat and liver but not in muscle. *Proc. Natl. Acad. Sci. U.S.A.* 100, 15712–15717. doi: 10.1073/pnas.2536828100
- Higuchi, M., Disting, G. J., Peshvariya, H., Jiang, F., Hsiao, S. T., Chan, E. C., et al. (2013). Differentiation of human adipose-derived stem cells into fat involves reactive oxygen species and Forkhead box O1 mediated upregulation of antioxidant enzymes. *Stem Cells Dev.* 22, 878–888. doi: 10.1089/scd.2012.0306
- Hinoi, E., Iezaki, T., Fujita, H., Watanabe, T., Odaka, Y., Ozaki, K., et al. (2014). PI3K/Akt is involved in brown adipogenesis mediated by growth differentiation factor-5 in association with activation of the Smad pathway. *Biochem. Biophys. Res. Commun.* 450, 255–260. doi: 10.1016/j.bbrc.2014.05.108
- Hou, Y., Xue, P., Bai, Y., Liu, D., Woods, C. G., Yarborough, K., et al. (2012). Nuclear factor erythroid-derived factor 2-related factor 2 regulates transcription of CCAAT/enhancer-binding protein beta during adipogenesis. *Free Radic Biol. Med.* 52, 462–472. doi: 10.1016/j.freeradbiomed.2011.10.453
- Hu, F., Wang, M., Xiao, T., Yin, B., He, L., Meng, W., et al. (2015). miR-30 promotes thermogenesis and the development of beige fat by targeting RIP140. *Diabetes* 64, 2056–2068. doi: 10.2337/db14-1117
- Hu, H. H., Perkins, T. G., Chia, J. M., and Gilsanz, V. (2013). Characterization of human brown adipose tissue by chemical-shift water-fat MRI. *AJR Am. J. Roentgenol.* 200, 177–183. doi: 10.2214/AJR.12.8996
- Ishibashi, J., and Seale, P. (2015). Functions of Prdm16 in thermogenic fat cells. *Temperature* 2, 65–72. doi: 10.4161/23328940.2014.974444
- Jankovic, A., Korac, A., Srdic-Galic, B., Buzadzic, B., Otasevic, V., Stancic, A., et al. (2014). Differences in the redox status of human visceral and subcutaneous adipose tissues-relationships to obesity and metabolic risk. *Metabolism* 63, 661–671. doi: 10.1016/j.metabol.2014.01.009
- Jones, D. P., and Sies, H. (2015). The redox code. *Antioxid. Redox Signal.* 23, 734–746. doi: 10.1089/ars.2015.6247

- Ju, L., Chen, S., Alimujiang, M., Bai, N., Yan, H., Fang, Q., et al. (2018). A novel role for Bcl2l13 in promoting beige adipocyte biogenesis. *Biochem. Biophys. Res. Commun.* 506, 485–491. doi: 10.1016/j.bbrc.2018.10.034
- Kajimura, S., Seale, P., Kubota, K., Lunsford, E., Frangioni, J. V., Gygi, S. P., et al. (2009). Initiation of myoblast to brown fat switch by a PRDM16-C/EBP-beta transcriptional complex. *Nature* 460, 1154–1158. doi: 10.1038/nature08262
- Kajimura, S., Spiegelman, B. M., and Seale, P. (2015). Brown and beige fat: physiological roles beyond heat generation. *Cell Metab.* 22, 546–559. doi: 10.1016/j.cmet.2015.09.007
- Kanda, Y., Hinata, T., Kang, S. W., and Watanabe, Y. (2011). Reactive oxygen species mediate adipocyte differentiation in mesenchymal stem cells. *Life Sci.* 89, 250–258. doi: 10.1016/j.lfs.2011.06.007
- Kang, S., Bajnok, L., Longo, K. A., Petersen, R. K., Hansen, J. B., Kristiansen, K., et al. (2005). Effects of Wnt signaling on brown adipocyte differentiation and metabolism mediated by PGC-1alpha. *Mol. Cell Biol.* 25, 1272–1282. doi: 10.1128/MCB.25.4.1272-1282.2005
- Karbiener, M., Pisani, D. F., Frontini, A., Oberreiter, L. M., Lang, E., Vegiopoulos, A., et al. (2014). MicroRNA-26 family is required for human adipogenesis and drives characteristics of brown adipocytes. *Stem Cells* 32, 1578–1590. doi: 10.1002/stem.1603
- Kida, R., Noguchi, T., Murakami, M., Hashimoto, O., Kawada, T., Matsui, T., et al. (2018). Supra-pharmacological concentration of capsaicin stimulates brown adipogenesis through induction of endoplasmic reticulum stress. *Sci. Rep.* 8:845. doi: 10.1038/s41598-018-19223-2
- Labbe, S. M., Mouchiroud, M., Caron, A., Secco, B., Freinkman, E., Lamoureux, G., et al. (2016). mTORC1 is required for brown adipose tissue recruitment and metabolic adaptation to cold. *Sci. Rep.* 6:37223. doi: 10.1038/srep37223
- Lane, M. D., Tang, Q. Q., and Jiang, M. S. (1999). Role of the CCAAT enhancer binding proteins (C/EBPs) in adipocyte differentiation. *Biochem. Biophys. Res. Commun.* 266, 677–683. doi: 10.1006/bbrc.1999.1885
- Lee, H., Lee, Y. J., Choi, H., Ko, E. H., and Kim, J. W. (2009). Reactive oxygen species facilitate adipocyte differentiation by accelerating mitotic clonal expansion. *J. Biol. Chem.* 284, 10601–10609. doi: 10.1074/jbc.M808742200
- Lee, Y. H., Petkova, A. P., Konkari, A. A., and Granneman, J. G. (2015). Cellular origins of cold-induced brown adipocytes in adult mice. *FASEB J.* 29, 286–299. doi: 10.1096/fj.14-263038
- Lepper, C., and Fan, C. M. (2010). Inducible lineage tracing of Pax7-descendant cells reveals embryonic origin of adult satellite cells. *Genesis* 48, 424–436. doi: 10.1002/dvg.20630
- Liu, Z., Gu, H., Gan, L., Xu, Y., Feng, F., Saeed, M., et al. (2017). Reducing Smad3/ATF4 was essential for Sirt1 inhibiting ER stress-induced apoptosis in mice brown adipose tissue. *Oncotarget* 8, 9267–9279. doi: 10.18632/oncotarget.14035
- McGregor, R. A., Kwon, E. Y., Shin, S. K., Jung, U. J., Kim, E., Park, J. H., et al. (2013). Time-course microarrays reveal modulation of developmental, lipid metabolism and immune gene networks in intrascapular brown adipose tissue during the development of diet-induced obesity. *Int. J. Obes.* 37, 1524–1531. doi: 10.1038/ijo.2013.52
- Medrikova, D., Sijmonsma, T. P., Sowodniok, K., Richards, D. M., Delacher, M., Sticht, C., et al. (2015). Brown adipose tissue harbors a distinct sub-population of regulatory T cells. *PLoS One* 10:e0118534. doi: 10.1371/journal.pone.0118534
- Miranda, S., Gonzalez-Rodriguez, A., Revuelta-Cervantes, J., Rondonone, C. M., and Valverde, A. M. (2010). Beneficial effects of PTP1B deficiency on brown adipocyte differentiation and protection against apoptosis induced by pro- and anti-inflammatory stimuli. *Cell Signal.* 22, 645–659. doi: 10.1016/j.cellsig.2009.11.019
- Mowers, J., Uhm, M., Reilly, S. M., Simon, J., Leto, D., Chiang, S. H., et al. (2013). Inflammation produces catecholamine resistance in obesity via activation of PDE3B by the protein kinases IKKepsilon and TBK1. *eLife* 2:e01119. doi: 10.7554/eLife.01119
- Mracek, T., Cannon, B., and Housteck, J. (2004). IL-1 and LPS but not IL-6 inhibit differentiation and downregulate PPAR gamma in brown adipocytes. *Cytokine* 26, 9–15. doi: 10.1016/j.cyt.2003.12.001
- Nedergaard, J., Wang, Y., and Cannon, B. (2018). Cell proliferation and apoptosis inhibition: essential processes for recruitment of the full thermogenic capacity of brown adipose tissue. *Biochim. Biophys. Acta Mol. Cell Biol. Lipids* 1864, 51–58. doi: 10.1016/j.bbalip.2018.06.013
- Nguyen, K. D., Qiu, Y., Cui, X., Goh, Y. P., Mwangi, J., David, T., et al. (2011). Alternatively activated macrophages produce catecholamines to sustain adaptive thermogenesis. *Nature* 480, 104–108. doi: 10.1038/nature10653
- Oliverio, M., Schmidt, E., Mauer, J., Baitzel, C., Hansmeier, N., Khani, S., et al. (2016). Dicer1-miR-328-Bace1 signalling controls brown adipose tissue differentiation and function. *Nat. Cell Biol.* 18, 328–336. doi: 10.1038/ncb3316
- Ong, F. J., Ahmed, B. A., Oreskovich, S. M., Blondin, D. P., Haq, T., Konyer, N. B., et al. (2018). Recent advances in the detection of brown adipose tissue in adult humans: a review. *Clin. Sci.* 132, 1039–1054. doi: 10.1042/CS20170276
- Pan, D., Mao, C., Quattrochi, B., Friedline, R. H., Zhu, L. J., Jung, D. Y., et al. (2014). MicroRNA-378 controls classical brown fat expansion to counteract obesity. *Nat. Commun.* 5:4725. doi: 10.1038/ncomms5725
- Park, J. H., Kang, H. J., Kang, S. I., Lee, J. E., Hur, J., Ge, K., et al. (2013). A multifunctional protein, EWS, is essential for early brown fat lineage determination. *Dev. Cell* 26, 393–404. doi: 10.1016/j.devcel.2013.07.002
- Pfannenberger, C., Werner, M. K., Ripkens, S., Stef, I., Deckert, A., Schmadl, M., et al. (2010). Impact of age on the relationships of brown adipose tissue with sex and adiposity in humans. *Diabetes* 59, 1789–1793. doi: 10.2337/db10-0004
- Price, N. L., and Fernandez-Hernando, C. (2016). miRNA regulation of white and brown adipose tissue differentiation and function. *Biochim. Biophys. Acta* 1861(12 Pt B), 2104–2110. doi: 10.1016/j.bbalip.2016.02.010
- Puigserver, P., Wu, Z., Park, C. W., Graves, R., Wright, M., and Spiegelman, B. M. (1998). A cold-inducible coactivator of nuclear receptors linked to adaptive thermogenesis. *Cell* 92, 829–839. doi: 10.1016/S0092-8674(00)81410-5
- Rajakumari, S., Wu, J., Ishibashi, J., Lim, H. W., Giang, A. H., Won, K. J., et al. (2013). EBF2 determines and maintains brown adipocyte identity. *Cell Metab.* 17, 562–574. doi: 10.1016/j.cmet.2013.01.015
- Rebiger, L., Lenzen, S., and Mehmeti, I. (2016). Susceptibility of brown adipocytes to pro-inflammatory cytokine toxicity and reactive oxygen species. *Biosci. Rep.* 36:e00306. doi: 10.1042/BSR20150193
- Ron, D., Brasier, A. R., McGehee, R. E. Jr., and Habener, J. F. (1992). Tumor necrosis factor-induced reversal of adipocytic phenotype of 3T3-L1 cells is preceded by a loss of nuclear CCAAT/enhancer binding protein (C/EBP). *J. Clin. Invest.* 89, 223–233. doi: 10.1172/JCI115566
- Rosen, E. D., Sarraf, P., Troy, A. E., Bradwin, G., Moore, K., Milstone, D. S., et al. (1999). PPAR gamma is required for the differentiation of adipose tissue in vivo and in vitro. *Mol. Cell* 4, 611–617. doi: 10.1016/S1097-2765(00)80211-7
- Rosenwald, M., and Wolfrum, C. (2014). The origin and definition of brite versus white and classical brown adipocytes. *Adipocyte* 3, 4–9. doi: 10.4161/adip.26232
- Saito, M., Okamatsu-Ogura, Y., Matsushita, M., Watanabe, K., Yoneshiro, T., Nio-Kobayashi, J., et al. (2009). High incidence of metabolically active brown adipose tissue in healthy adult humans: effects of cold exposure and adiposity. *Diabetes* 58, 1526–1531. doi: 10.2337/db09-0530
- Sakamoto, T., Nitta, T., Maruno, K., Yeh, Y. S., Kuwata, H., Tomita, K., et al. (2016). Macrophage infiltration into obese adipose tissues suppresses the induction of UCP1 level in mice. *Am. J. Physiol. Endocrinol. Metab.* 310, E676–E687. doi: 10.1152/ajpendo.00028.2015
- Sampath, S. C., Sampath, S. C., Bredella, M. A., Cypess, A. M., and Torriani, M. (2016). Imaging of brown adipose tissue: state of the art. *Radiology* 280, 4–19. doi: 10.1148/radiol.2016150390
- Sanchez-Gurmaches, J., and Guertin, D. A. (2014). Adipocyte lineages: tracing back the origins of fat. *Biochim. Biophys. Acta* 1842, 340–351. doi: 10.1016/j.bbadis.2013.05.027
- Sanchez-Infantes, D., Cereijo, R., Peyrou, M., Piquer-Garcia, I., Stephens, J. M., and Villarroja, F. (2017). Oncostatin m impairs brown adipose tissue thermogenic function and the browning of subcutaneous white adipose tissue. *Obesity* 25, 85–93. doi: 10.1002/oby.21679
- Schreiber, R., Diwoky, C., Schoiswohl, G., Feiler, U., Wongsiriroj, N., Abdellatif, M., et al. (2017). Cold-induced thermogenesis depends on ATGL-mediated lipolysis in cardiac muscle, but not brown adipose tissue. *Cell Metab.* 26, 753–763.e7. doi: 10.1016/j.cmet.2017.09.004
- Schulz, T. J., Huang, P., Huang, T. L., Xue, R., McDougall, L. E., Townsend, K. L., et al. (2013). Brown-fat paucity due to impaired BMP signalling induces compensatory browning of white fat. *Nature* 495, 379–383. doi: 10.1038/nature11943
- Sha, H., He, Y., Chen, H., Wang, C., Zenno, A., Shi, H., et al. (2009). The IRE1alpha-XBP1 pathway of the unfolded protein response is required

- for adipogenesis. *Cell Metab.* 9, 556–564. doi: 10.1016/j.cmet.2009.04.009
- Shapira, S. N., Lim, H. W., Rajakumari, S., Sakers, A. P., Ishibashi, J., Harms, M. J., et al. (2017). EBF2 transcriptionally regulates brown adipogenesis via the histone reader DPf3 and the BAF chromatin remodeling complex. *Genes Dev.* 31, 660–673. doi: 10.1101/gad.294405.116
- Sharma, B. K., Patil, M., and Satyanarayana, A. (2014). Negative regulators of brown adipose tissue (BAT)-mediated thermogenesis. *J. Cell Physiol.* 229, 1901–1907. doi: 10.1002/jcp.24664
- Shin, H., Ma, Y., Chanturiya, T., Cao, Q., Wang, Y., Kadegowda, A. K. G., et al. (2017). Lipolysis in brown adipocytes is not essential for cold-induced thermogenesis in mice. *Cell Metab.* 26, 764–777.e5. doi: 10.1016/j.cmet.2017.09.002
- Shoelson, S. E., Herrero, L., and Naaz, A. (2007). Obesity, inflammation, and insulin resistance. *Gastroenterology* 132, 2169–2180. doi: 10.1053/j.gastro.2007.03.059
- Stine, R. R., Shapira, S. N., Lim, H. W., Ishibashi, J., Harms, M., Won, K. J., et al. (2016). EBF2 promotes the recruitment of beige adipocytes in white adipose tissue. *Mol. Metab.* 5, 57–65. doi: 10.1016/j.molmet.2015.11.001
- Sun, L., and Trajkovski, M. (2014). MiR-27 orchestrates the transcriptional regulation of brown adipogenesis. *Metabolism* 63, 272–282. doi: 10.1016/j.metabol.2013.10.004
- Tapia, P., Fernandez-Galilea, M., Robledo, F., Mardones, P., Galgani, J. E., and Cortes, V. A. (2018). Biology and pathological implications of brown adipose tissue: promises and caveats for the control of obesity and its associated complications. *Biol. Rev. Camb. Philos. Soc.* 93, 1145–1164. doi: 10.1111/brv.12389
- Tontonoz, P., and Spiegelman, B. M. (2008). Fat and beyond: the diverse biology of PPARgamma. *Annu. Rev. Biochem.* 77, 289–312. doi: 10.1146/annurev.biochem.77.061307.091829
- Tormos, K. V., Anso, E., Hamanaka, R. B., Eisenbart, J., Joseph, J., Kalyanaraman, B., et al. (2011). Mitochondrial complex III ROS regulate adipocyte differentiation. *Cell Metab.* 14, 537–544. doi: 10.1016/j.cmet.2011.08.007
- Tseng, Y. H., Kokkotou, E., Schulz, T. J., Huang, T. L., Winnay, J. N., Taniguchi, C. M., et al. (2008). New role of bone morphogenetic protein 7 in brown adipogenesis and energy expenditure. *Nature* 454, 1000–1004. doi: 10.1038/nature07221
- Valladares, A., Alvarez, A. M., Ventura, J. J., Roncero, C., Benito, M., and Porras, A. (2000). p38 mitogen-activated protein kinase mediates tumor necrosis factor- $\alpha$ -induced apoptosis in rat fetal brown adipocytes. *Endocrinology* 141, 4383–4395. doi: 10.1210/endo.141.12.7843
- van den Berg, S. M., van Dam, A. D., Rensen, P. C., de Winther, M. P., and Lutgens, E. (2017). Immune modulation of brown(ing) adipose tissue in obesity. *Endocr. Rev.* 38, 46–68. doi: 10.1210/er.2016-1066
- van der Lans, A. A., Hoeks, J., Brans, B., Vijgen, G. H., Visser, M. G., Vosselman, M. J., et al. (2013). Cold acclimation recruits human brown fat and increases nonshivering thermogenesis. *J. Clin. Invest.* 123, 3395–3403. doi: 10.1172/JCI68993
- van Marken Lichtenbelt, W. D., Vanhommerig, J. W., Smulders, N. M., Drossaerts, J. M., Kemerink, G. J., Bouvy, N. D., et al. (2009). Cold-activated brown adipose tissue in healthy men. *N. Engl. J. Med.* 360, 1500–1508. doi: 10.1056/NEJMoa0808718
- Velickovic, K., Lugo Leija, H. A., Bloor, I., Law, J., Sacks, H., Symonds, M., et al. (2018). Low temperature exposure induces browning of bone marrow stem cell derived adipocytes in vitro. *Sci. Rep.* 8:4974. doi: 10.1038/s41598-018-23267-9
- Villarroya, F., Cereijo, R., Gavaldà-Navarro, A., Villarroya, J., and Giral, M. (2018). Inflammation of brown/beige adipose tissues in obesity and metabolic disease. *J. Intern. Med.* 284, 492–504. doi: 10.1111/joim.12803
- Virtanen, K. A., Lidell, M. E., Orava, J., Heglind, M., Westergren, R., Niemi, T., et al. (2009). Functional brown adipose tissue in healthy adults. *N. Engl. J. Med.* 360, 1518–1525. doi: 10.1056/NEJMoa0808949
- Wang, Q., Zhang, M., Ning, G., Gu, W., Su, T., Xu, M., et al. (2011). Brown adipose tissue in humans is activated by elevated plasma catecholamines levels and is inversely related to central obesity. *PLoS One* 6:e21006. doi: 10.1371/journal.pone.0021006
- Wang, Q. A., and Scherer, P. E. (2014). The adipochaser mouse: a model tracking adipogenesis in vivo. *Adipocyte* 3, 146–150. doi: 10.4161/adip.27656
- Wang, W., Kissig, M., Rajakumari, S., Huang, L., Lim, H. W., Won, K. J., et al. (2014). Ebf2 is a selective marker of brown and beige adipogenic precursor cells. *Proc. Natl. Acad. Sci. U.S.A.* 111, 14466–14471. doi: 10.1073/pnas.1412685111
- Wang, Y., Sato, M., Guo, Y., Bengtsson, T., and Nedergaard, J. (2014). Protein kinase a-mediated cell proliferation in brown preadipocytes is independent of Erk1/2, PI3K and mTOR. *Exp. Cell Res.* 328, 143–155. doi: 10.1016/j.yexcr.2014.07.029
- Wu, Y., Zuo, J., Zhang, Y., Xie, Y., Hu, F., Chen, L., et al. (2013). Identification of miR-106b-93 as a negative regulator of brown adipocyte differentiation. *Biochem. Biophys. Res. Commun.* 438, 575–580. doi: 10.1016/j.bbrc.2013.08.016
- Yasuniwa, Y., Izumi, H., Wang, K. Y., Shimajiri, S., Sasaguri, Y., Kawai, K., et al. (2010). Circadian disruption accelerates tumor growth and angio/stromagenesis through a Wnt signaling pathway. *PLoS One* 5:e15330. doi: 10.1371/journal.pone.0015330
- Ye, L., Wu, J., Cohen, P., Kazak, L., Khandekar, M. J., Jedrychowski, M. P., et al. (2013). Fat cells directly sense temperature to activate thermogenesis. *Proc. Natl. Acad. Sci. U.S.A.* 110, 12480–12485. doi: 10.1073/pnas.1310261110
- Yin, H., Pasut, A., Soleimani, V. D., Bentzinger, C. F., Antoun, G., Thorn, S., et al. (2013). MicroRNA-133 controls brown adipose determination in skeletal muscle satellite cells by targeting Prdm16. *Cell Metab.* 17, 210–224. doi: 10.1016/j.cmet.2013.01.004
- Yoneshiro, T., Aita, S., Matsushita, M., Kayahara, T., Kameya, T., Kawai, Y., et al. (2013). Recruited brown adipose tissue as an antiobesity agent in humans. *J. Clin. Invest.* 123, 3404–3408. doi: 10.1172/JCI67803
- Yoneshiro, T., Aita, S., Matsushita, M., Okamatsu-Ogura, Y., Kameya, T., Kawai, Y., et al. (2011). Age-related decrease in cold-activated brown adipose tissue and accumulation of body fat in healthy humans. *Obesity* 19, 1755–1760. doi: 10.1038/oby.2011.125
- Yu, J., Lv, Y., Di, W., Liu, J., Kong, X., Sheng, Y., et al. (2018). MiR-27b-3p Regulation in Browning of Human Visceral Adipose Related to Central Obesity. *Obesity* 26, 387–396. doi: 10.1002/oby.22104
- Zhang, H., Guan, M., Townsend, K. L., Huang, T. L., An, D., Yan, X., et al. (2015). MicroRNA-455 regulates brown adipogenesis via a novel HIF1 $\alpha$ -AMPK-PGC1 $\alpha$  signaling network. *EMBO Rep.* 16, 1378–1393. doi: 10.15252/embr.201540837
- Zhou, J. Y., and Li, L. (2014). MicroRNAs are key regulators of brown adipogenesis. *Biochim. Biophys. Acta* 1841, 1590–1595. doi: 10.1016/j.bbali.2014.08.009
- Zingaretti, M. C., Crosta, F., Vitali, A., Guerrieri, M., Frontini, A., Cannon, B., et al. (2009). The presence of UCP1 demonstrates that metabolically active adipose tissue in the neck of adult humans truly represents brown adipose tissue. *FASEB J.* 23, 3113–3120. doi: 10.1096/fj.09-133546
- Zoller, V., Funcke, J. B., Keuper, M., Abd El Hay, M., Debatin, K. M., Wabitsch, M., et al. (2016). TRAIL (TNF-related apoptosis-inducing ligand) inhibits human adipocyte differentiation via caspase-mediated downregulation of adipogenic transcription factors. *Cell Death Dis.* 7:e2412. doi: 10.1038/cddis.2016.286

**Conflict of Interest Statement:** The authors declare that the research was conducted in the absence of any commercial or financial relationships that could be construed as a potential conflict of interest.

Copyright © 2019 Alcalá, Calderon-Dominguez, Serra, Herrero and Viana. This is an open-access article distributed under the terms of the Creative Commons Attribution License (CC BY). The use, distribution or reproduction in other forums is permitted, provided the original author(s) and the copyright owner(s) are credited and that the original publication in this journal is cited, in accordance with accepted academic practice. No use, distribution or reproduction is permitted which does not comply with these terms.



# Housing Temperature Modulates the Impact of Diet-Induced Rise in Fat Mass on Adipose Tissue Before and During Pregnancy in Rats

Layla Albustanji<sup>1†</sup>, Gabriela S. Perez<sup>1,2,3†</sup>, Enas AlHarethi<sup>1</sup>, Peter Aldiss<sup>1</sup>, Ian Bloor<sup>1</sup>, Jairza M. Barreto-Medeiros<sup>2,3</sup>, Helen Budge<sup>1</sup>, Michael E. Symonds<sup>1,4\*</sup> and Neele Dellschaft<sup>1</sup>

<sup>1</sup> Early Life Research Unit, Division of Child Health, Obstetrics, and Gynaecology, University of Nottingham, Nottingham, United Kingdom, <sup>2</sup> Graduate Program of Food Nutrition and Health, Department of Food Science, School of Nutrition, Federal University of Bahia, Salvador, Brazil, <sup>3</sup> CAPES Foundation, Ministry of Education of Brazil, Brasília, Brazil, <sup>4</sup> Nottingham Digestive Disease Centre and Biomedical Research Centre, School of Medicine, University of Nottingham, Nottingham, United Kingdom

## OPEN ACCESS

### Edited by:

Rita De Matteis,  
University of Urbino Carlo Bo, Italy

### Reviewed by:

Maria Razzoli,  
University of Minnesota Twin Cities,  
United States  
Rebecca Oelkrug,  
Universität zu Lübeck, Germany

### \*Correspondence:

Michael E. Symonds  
michael.symonds@nottingham.ac.uk

<sup>†</sup> Joint first authors

### Specialty section:

This article was submitted to  
Integrative Physiology,  
a section of the journal  
Frontiers in Physiology

**Received:** 16 October 2018

**Accepted:** 18 February 2019

**Published:** 06 March 2019

### Citation:

Albustanji L, Perez GS,  
AlHarethi E, Aldiss P, Bloor I,  
Barreto-Medeiros JM, Budge H,  
Symonds ME and Dellschaft N (2019)  
Housing Temperature Modulates  
the Impact of Diet-Induced Rise in Fat  
Mass on Adipose Tissue Before  
and During Pregnancy in Rats.  
Front. Physiol. 10:209.  
doi: 10.3389/fphys.2019.00209

**Aim:** To investigate whether housing temperature influences rat adiposity, and the extent it is modified by diet and/or pregnancy. Housing temperature impacts on brown adipose tissue, that possess a unique uncoupling protein (UCP) 1, which, when activated by reduced ambient temperature, enables rapid heat generation.

**Methods:** We, therefore, examined whether the effects of dietary induced rise in fat mass on interscapular brown fat in female rats were dependent on housing temperature, and whether pregnancy further modulates the response. Four week old rats were either maintained at thermoneutrality (27°C) or at a “standard” cool temperature (20°C), and fed either a control or obesogenic (high in fat and sugar) diet until 10 weeks old. They were then either tissue sampled or mated with a male maintained under the same conditions. The remaining dams were tissue sampled at either 10 or 19 days gestation.

**Results:** Diet had the greatest effect on fat mass at thermoneutrality although, by 19 days gestation, fat weight was similar between groups. Prior to mating, the abundance of UCP1 was higher at 20°C, but was similar between groups during pregnancy. *UCP1* mRNA followed a similar pattern, with expression declining to a greater extent in the animals maintained at 20°C.

**Conclusion:** Housing temperature has a marked influence on the effect of dietary induced rise in fat deposition that was modified through gestation. This maybe mediated by the reduction in UCP1 with housing at thermoneutrality prior to pregnancy and could subsequently impact on growth and development of the offspring.

**Keywords:** thermogenesis, brown fat, obesity, temperature, pregnancy

## INTRODUCTION

The temperature in which laboratory animals are maintained can have a pronounced impact on both metabolic and physiological homeostasis (Maloney et al., 2014). This is important when investigating adipose tissue function, as brown fat is very sensitive to ambient temperature and its activity is enhanced when rats are kept at temperatures below thermoneutrality, i.e., less than 27°C



(Gordon, 1990). Consequently, the metabolic and endocrine effects of dietary induced obesity are likely to be underestimated when animals are maintained at the standard housing temperature of 20°C, which represents a chronic cool challenge (Xiao et al., 2015; Cui et al., 2016). Furthermore, humans usually live in an environment close to their thermoneutral zone, which needs taking into account when relating rodent studies to the human situation (Maloney et al., 2014; Gordon, 2017).

Housing temperature will also be important in the interpretation of studies investigating the impact of maternal obesity on pregnancy outcomes. For example, the majority of rodent studies show little stimulatory effect of obesity on birth weight (Shankar et al., 2007; Morris and Chen, 2009) and some even show an increased incidence of intra-uterine growth retardation (Howie et al., 2009). This is important as the main consequence of maternal obesity in otherwise apparently healthy women is increased birth weight (Ruager-Martin et al., 2010). Before examining the magnitude of postnatal outcome, it is necessary to establish whether ambient temperature has comparable effects in the mother, to those which have been described primarily in male mice (Stemmer et al., 2015; Xiao et al., 2015; Cui et al., 2016).

The extent to which a dietary induced increase in fat mass prior to pregnancy modulates brown adipose tissue (BAT) remains to be established. The primary functional marker of BAT is uncoupling protein (UCP)1 (Aquila et al., 1985; Cannon and Nedergaard, 2004), that is located on the inner mitochondrial membrane. When UCP1 is stimulated, this results in the free flow of protons across the inner mitochondrial membrane (Nicholls, 1983) thereby bypassing the need to convert ADP to ATP as occurs in the mitochondria of all other tissues. In rodents fed a standard diet it has been suggested that the activity of BAT declines with pregnancy to enable the conservation of maternal energy stores (Martin et al., 1989). Not all studies have, however, found this (Frontera et al., 2005). A recent study in mice suggests the activity of BAT may decline between conception and day 14 of gestation (McIlvride et al., 2017). This conclusion was based on “*in vivo*” measurements made in terminally anaesthetized animals and did account for the reduction in BAT function it causes (Ohlson et al., 1994). The same study also suggested that removal of interscapular fat from the mother influenced fetal weight, but considered the fetus rather than the dam, as the unit of experimentation, which is incorrect (Festing, 2006). Pregnancy, and diet could also impact on the abundance of beige adipocytes, although currently temperature is considered to be the primary determinant (Wu et al., 2012).

We examined the impact of housing temperature on UCP1 in the primary BAT depot in rodents (i.e., interscapular) and the extent to which either protein or gene expression could be modulated by being maintained at a “standard” cool temperature (i.e., 20°C) or at thermoneutrality (i.e., ~27°C). In addition, we investigated whether any such response was modified by dietary induced increase in fat mass. We also determined whether primary gene markers of BAT function and growth [i.e., *UCP1*, *PGC1 $\alpha$* , and *PPAR $\gamma$*  (Puigserver et al., 1998)], plus those involved in fat transport [i.e., *FATP4*, *CD36*, and *LPL*

(Jemaa et al., 1995; Herrmann et al., 2001; Le Foll et al., 2015)] and insulin sensitivity [i.e., *IRS1* and 2 (Rondinone et al., 1997)], were modified in pregnancy. Some, but not all, of these genes are temperature sensitive in brown or beige adipocytes (Puigserver et al., 1998; Bartelt et al., 2011; Ye et al., 2013), but have yet to be examined through gestation. The same measurements were also performed in a fat depot considered to exhibit an increase in beige characteristics following cold exposure, i.e., the inguinal depot, as well as one that does not i.e., the omental fat depot (Waldén et al., 2012). We hypothesized that the impact of diet and pregnancy on adipose tissue would be amplified when animals were maintained at thermoneutrality and that this would be mediated by changes in BAT.

## MATERIALS AND METHODS

### Animals and Diets

A summary of the animal protocol is illustrated in **Supplementary Figure S1** and was undertaken under the United Kingdom Animals (Scientific Procedures) Act, 1986 with approval from the Local Ethics Committee of the University of Nottingham (Nottingham, United Kingdom).

Eighty-eight female and 16 male Sprague-Dawley rats were obtained at 4 weeks of age from Charles River Laboratories. Half of the male and female rats were immediately randomized to be housed either at a cool temperature (19–21°C) or at thermoneutrality (26–28°C). They were also randomized to receive either a low fat, low sucrose diet (L; 18% of energy from fat (soybean oil); 24% from protein; 58% from carbohydrates, of which 7% are mono- and disaccharides; 3.1 kcal/g; Harlan Teklad Global 18% Protein Rodent Diet; Teklad Diets, Madison, WI, United States) or a high fat, high sucrose diet (H; 39% of energy from fat (lard); 23% from protein; 39% from carbohydrate, of which 44% are mono- and disaccharides; 4.6 kcal/g; custom diet supplied by Abbott Nutrition, Granada, Spain; **Supplementary Table S1**), fed *ad libitum*. Food intake was measured over the course of three days before mating occurred. Starting numbers of males and females in the H groups were higher than in the L groups as we anticipated a lower fertility although this did not occur. Twelve females (3 at 20L, 2 at 20H, 2 at 27L, 5 at 27H) had reabsorbed all fetuses or failed to mate and were therefore not analyzed. Final groups were, therefore, 20L (18 females, 3 males), 20H (21 females, 5 males), 27L (19 females, 3 males), 27H (18 females, 5 males). All animals were kept in 12:12 h light:dark cycle at 40–50% humidity, and in groups of 3 females and 2 or 3 males to reduce social stress, but had no observable impact on their behavior.

Body weight was recorded three times a week. At 10 weeks of age, 6 randomly selected females of each group were euthanased and tissues were collected. The remaining females were mated with males of the same diet and temperature group. Vaginal plugs found in the morning indicated day 1 of pregnancy. Females were returned to their home cages and re-housed with the same cage mates, but because of the 4 day reproductive

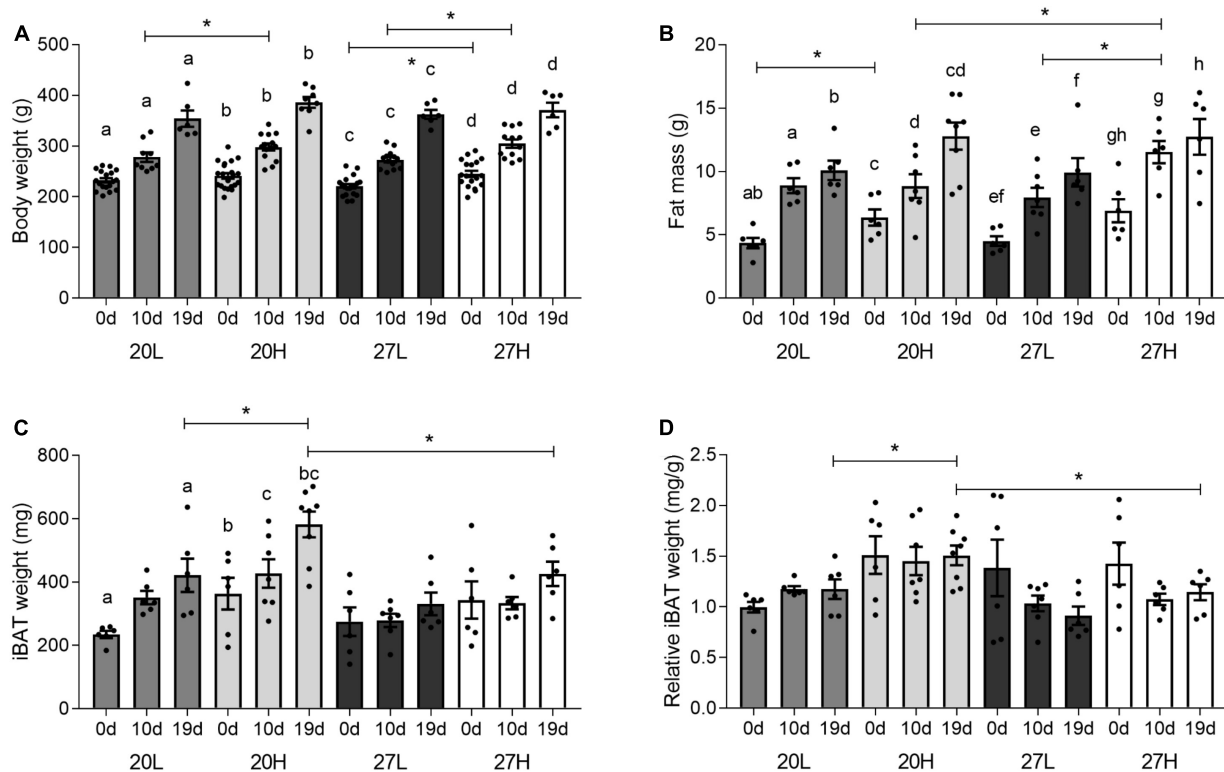


**FIGURE 1 |** Effect of housing temperature, pregnancy, and diet on body and fat mass. **(A)** body weight, **(B)** fat mass, expressed as the total sum of dissected inguinal, perirenal, omental, and gonadal adipose tissue, **(C)** total, and **(D)** relative interscapular brown fat mass of females before (0 days) and during pregnancy (10 and 19 days), when kept at either a cool temperature (20°C) or thermoneutrality (27°C), and fed a low (L) or high (H) fat and sucrose diet. Fat mass was also expressed as change from unmated **(C)**. Differences between dietary groups housed at the same temperature \* $P < 0.05$ ; for each study group columns with the same superscripts are significantly different ( $P < 0.05$ ). For body weight, unmated  $n = 18$ –21, 10 d/g  $n = 10$ –14, 19 d/g  $n = 6$ –8; for fat mass, unmated  $n = 6$ , 10 d/g  $n = 6$ –7, 19 d/g  $n = 6$ –8.

cycle of the rat, each mother did not become pregnant on the same day. This meant it was not possible to accurately measure food intake for each group of mothers through pregnancy. Females were euthanased and tissues were collected from 6 to 7 dams per group at 10 days gestation (d/g), coincident with mid-gestation, and from 6 to 8 dams per group near term i.e., 19 d/g.

## Tissue Collection

Females were not fasted before tissue collection to avoid the fasting effects on brown adipocytes. They were euthanased between 10.00 and 12.00 h by CO<sub>2</sub> asphyxiation and subsequent cervical dislocation. A blood sample was collected into EDTA tubes after cardiac puncture, and interscapular, inguinal, omental (mesenteric), perirenal and gonadal adipose depots were collected and weighed. Blood was centrifuged at 4°C (15 min at 2000g) and plasma aliquoted and stored at  $-80^{\circ}\text{C}$  until analysis. The interscapular adipose depot was halved, with one half snap frozen in liquid nitrogen and stored at  $-80^{\circ}\text{C}$  until analysis, and the other half fixed in 4% formaldehyde in 0.9% saline before dehydration and blocking in paraffin. An aliquot of the remaining adipose tissues was snap frozen in liquid nitrogen and stored at  $-80^{\circ}\text{C}$  until analysis.

## Plasma Metabolites and Hormones

Plasma was thawed gently on ice. Plasma concentrations of glucose (GAGO-20, Sigma-Aldrich, Gillingham, United Kingdom), triglycerides (GPO DAOS method, Wako, Neuss, Germany), non-esterified fatty acids [NEFA-HR(2), Wako, Neuss, Germany], insulin (80-INSRT-E01, Alpcos, Salem, NH, United States), corticosterone (K014-H1, Arbor Assays, Ann Arbor, MI, United States) and leptin (EZRL-83K, Merck, Darmstadt, Germany) were measured with commercial assays, respectively, following manufacturer's instructions.

## UCP1 Immunohistochemistry

Paraffin-blocked interscapular adipose tissue were sectioned to 6  $\mu\text{m}$  and applied to Superfrost Plus slides (Thermo Fisher Scientific, Wilmingont, DE, United States). Slides were processed in a Bond Max IHC stainer (Leica Biosystems, Milton Keynes, United Kingdom) with rabbit anti-UCP1 antibody (ab10983, Abcam, Cambridge, United Kingdom; 1:3000), and compared to negative control slides without primary antibody applied. Slides were viewed and photographed at 10 $\times$  magnification (Nikon Eclipse 90i, Nikon, Tokyo, Japan; with Hamamatsu ORCA-ER camera, Hamamatsu, Hamamatsu City, Japan). A minimum of five images per sample were analyzed with Fiji-native methods,

**TABLE 1 |** Plasma metabolites hormones of females before and during pregnancy, when kept at either a cool temperature (20°C) or thermoneutrality (27°C), and fed a low (L) or high (H) fat and sucrose diet.

Plasma measurement	Pregnancy time point (d/g)	20L	20H	27L	27H	ANOVA
Glucose ( $\mu\text{g ml}^{-1}$ )	0	24 $\pm$ 4 <sup>ac</sup>	28 $\pm$ 5	47 $\pm$ 6 <sup>c</sup>	40 $\pm$ 4	0.009
	10	48 $\pm$ 9 <sup>ab</sup>	38 $\pm$ 6	43 $\pm$ 9	35 $\pm$ 3	N.S.
	19	22 $\pm$ 2 <sup>b</sup>	35 $\pm$ 9	28 $\pm$ 4	30 $\pm$ 4	N.S.
	ANOVA	0.008	N.S.	N.S.	N.S.	
Triglycerides (mg dl <sup>-1</sup> )	0	95 $\pm$ 14 <sup>a</sup>	118 $\pm$ 19 <sup>c</sup>	82 $\pm$ 17 <sup>e</sup>	127 $\pm$ 28 <sup>g</sup>	N.S.
	10	106 $\pm$ 19 <sup>ab</sup>	107 $\pm$ 14 <sup>cd</sup>	130 $\pm$ 20 <sup>ef</sup>	143 $\pm$ 27 <sup>gh</sup>	N.S.
	19	245 $\pm$ 35 <sup>b</sup>	300 $\pm$ 36 <sup>d</sup>	320 $\pm$ 58 <sup>f</sup>	227 $\pm$ 26 <sup>h</sup>	N.S.
	ANOVA	0.008	0.006	0.002	0.0387	
NEFA (mmol l <sup>-1</sup> )	0	0.17 $\pm$ 0.02	0.24 $\pm$ 0.05	0.31 $\pm$ 0.06	0.21 $\pm$ 0.03	N.S.
	10	0.15 $\pm$ 0.02	0.17 $\pm$ 0.02 <sup>a</sup>	0.15 $\pm$ 0.01	0.20 $\pm$ 0.03	N.S.
	19	0.22 $\pm$ 0.03	0.33 $\pm$ 0.02 <sup>a</sup>	0.24 $\pm$ 0.04	0.31 $\pm$ 0.04	N.S.
	ANOVA	N.S.	0.010	N.S.	N.S.	
Insulin (ng ml <sup>-1</sup> )	0	0.95 $\pm$ 0.12 <sup>a</sup>	1.77 $\pm$ 0.21 <sup>a</sup>	0.97 $\pm$ 0.14	1.67 $\pm$ 0.62	0.040
	10	1.24 $\pm$ 0.35	0.96 $\pm$ 0.10	1.17 $\pm$ 0.24	1.92 $\pm$ 0.23	N.S.
	19	1.24 $\pm$ 0.30	1.84 $\pm$ 0.45	3.58 $\pm$ 1.12	1.53 $\pm$ 0.46	N.S.
	ANOVA	N.S.	N.S.	N.S.	N.S.	
Corticosterone (ng ml <sup>-1</sup> )	0	169 $\pm$ 52	106 $\pm$ 35	450 $\pm$ 171	107 $\pm$ 23	N.S.
	10	68 $\pm$ 20	180 $\pm$ 100	32 $\pm$ 7 <sup>a</sup>	148 $\pm$ 94	N.S.
	19	111 $\pm$ 18	159 $\pm$ 25	242 $\pm$ 112 <sup>a</sup>	178 $\pm$ 46	N.S.
	ANOVA	N.S.	N.S.	0.016	N.S.	
Leptin (ng ml <sup>-1</sup> )	0	3.2 $\pm$ 0.4 <sup>ab</sup>	4.7 $\pm$ 0.6 <sup>c</sup>	3.4 $\pm$ 0.8 <sup>de</sup>	4.4 $\pm$ 0.2 <sup>fg</sup>	N.S.
	10	5.5 $\pm$ 0.6 <sup>a</sup>	7.1 $\pm$ 1.1	5.6 $\pm$ 0.7 <sup>d</sup>	11.0 $\pm$ 2.1 <sup>f</sup>	N.S.
	19	6.9 $\pm$ 0.7 <sup>b</sup>	7.8 $\pm$ 1.2 <sup>c</sup>	8.2 $\pm$ 1.7 <sup>e</sup>	9.1 $\pm$ 1.6 <sup>g</sup>	N.S.
	ANOVA	0.002	0.047	0.029	0.023	

*P* values given are the statistically significant outcomes of comparisons (ANOVA or Kruskal-Wallis, indicated as "ANOVA"). If data within one outcome carry the same superscripts they are statistically different ( $P < 0.05$ ). For all plasma measurements, unmated  $n = 5-6$ , 10 d/g  $n = 6-7$ , 19 d/g  $n = 5-8$ .

(Schindelin et al., 2012) using Weka segmentation (Arganda-Carreras et al., 2017).

## Gene Expression Analysis

Adipose tissues were homogenized using a Dispomix (Wiltex, Etten-Leur, Netherlands), and RNA was extracted from 50 to 100 mg of tissue using TRI reagent (Sigma-Aldrich, Gillingham, United Kingdom) and chloroform (Thermo Fisher Scientific, Wilmington, DE, United States) within the Qiagen RNeasy kit (Hilden, Germany) with gDNA eliminator columns. Concentration and purity of eluted RNA was measured on a Nanodrop spectrometer (Thermo Fisher Scientific, Wilmington, DE, United States). One  $\mu\text{g}$  of RNA was reverse transcribed to cDNA with the High Capacity RNA-t-cDNA kit (Applied Biosystems, Thermo Fisher Scientific, Wilmington, DE, United States).

Gene expression was measured using fast SYBR Green (Applied Biosystems, Thermo Fisher Scientific, Wilmington, DE, United States) in StepOnePlus Real-Time PCR system (Applied Biosystems, Thermo Fisher Scientific, Wilmington, DE, United States). Specificity of primers (Sigma-Aldrich, Gillingham, United Kingdom; working concentration 250 nM) was confirmed by sequencing PCR product (primers are listed in **Supplementary Table S2**). Gene expression was assessed for the following pathways:

- Thermogenesis: *UCP1*, peroxisome proliferator activated receptor gamma (*PPARG*), *PPARG* coactivator 1 alpha (*PGC1a*), leptin, beta-3 adrenergic receptor (*B3AR*), vascular endothelial growth factor A (*VEGFA*), capsaicin receptor (*TRPV1*), hydroxysteroid 11 beta dehydrogenase (*BHSD11*), voltage-dependent anion channel 1 (*VDAC*), ATPase sarcoplasmic/endoplasmic reticulum  $\text{Ca}^{2+}$  (*SERCA2B*), ryanodine receptor 2 (*RyR2*);
- Insulin sensitivity and energy sensing: insulin receptor substrates 1 and 2 (*IRS1+2*), mammalian target or rapamycin (*mTOR*), transcription factor 7 like 2 (*TCF7L2*);
- Fat transport: fatty acid transport protein 4 (*FATP4*), fatty acid binding protein 4 (*FABP4*), fatty acid translocase (*CD36*), lipoprotein lipase (*LPL*), adipose triglyceride lipase (*ATGL*);
- Immune response: tumor necrosis factor (*TNF*), interleukin 6 (*IL6*), monocyte chemotactic protein 1 (*MCP1*), adhesion G protein-coupled receptor E1 (*EMR1*);

Gene expression was normalized to the geometric mean of housekeeping genes TATA-box binding protein (*TBP*) and tyrosine 3-monooxygenase/tryptophan 5-monooxygenase activation protein (*YWHAZ*) throughout, and was calculated using the  $2^{-\Delta\Delta\text{Ct}}$  method (Livak and Schmittgen, 2001).



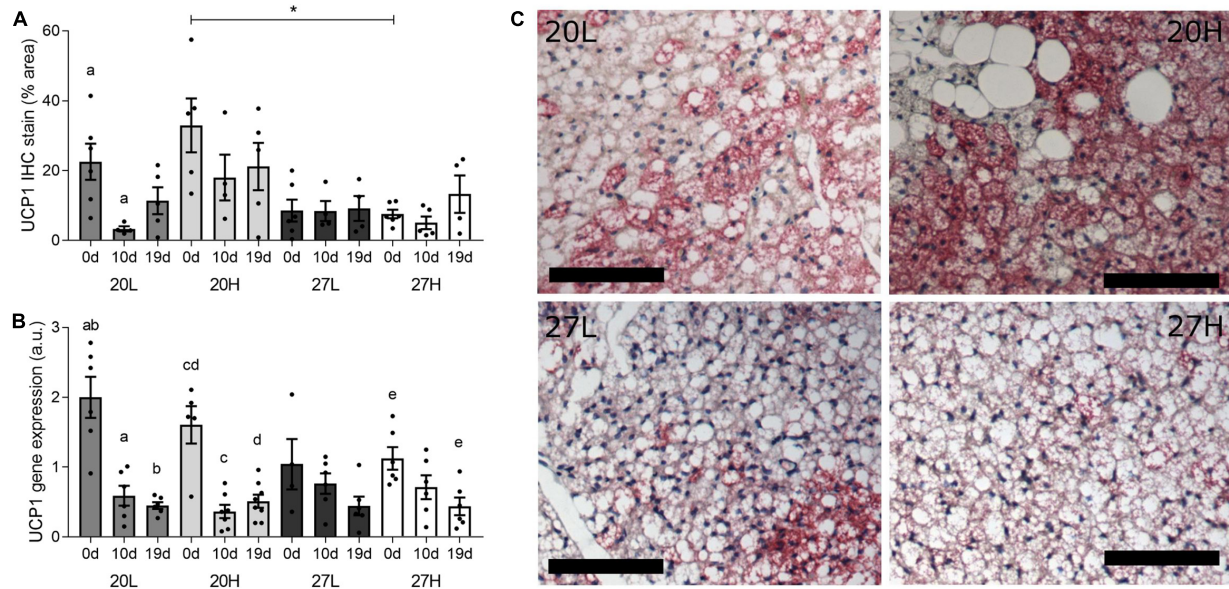


**FIGURE 2 |** Effect of housing temperature, pregnancy and diet on uncoupling protein (UCP)1. **(A)** UCP1 protein, **(B)** UCP1 mRNA abundance, and **(C)** representative histological images of interscapular adipose tissue of females before (0 d/g) and during pregnancy (10 and 19 d/g), when kept at either a cool temperature (20°C) or thermoneutrality (27°C), and fed a low (L) or high (H) fat and sucrose diet. Differences between dietary groups housed at the same temperature \* $P < 0.05$ ; for each study group columns with the same superscripts are significantly different ( $P < 0.05$ ). For interscapular adipose tissue mass, unmated  $n = 6$ , 10 d/g  $n = 6-7$ , 19 d/g  $n = 6-8$ ; for UCP1 protein, unmated  $n = 5-6$ , 10 d/g  $n = 4-6$ , 19 d/g  $n = 4-6$ . Representative anti-UCP1 immunohistochemistry images of interscapular adipose tissue **(C)** from unmated females of the 20L (top left), 20H (top right), 27L (bottom left), and 27H groups (bottom right), with size bars indicating 100 μm.

## Statistical Analysis

All statistical analyses were carried out in SPSS (Version 22, IBM, Portsmouth, United Kingdom) and Graphpad (Version 6, GraphPad Software, La Jolla, CA, United States). Data was tested for normality using a Kolmogorov-Smirnov test. If normally distributed, data was analyzed (i) with two-way ANOVAs with LSD *post hoc* comparisons (20L vs. 20H, 27L vs. 27H, 20L vs. 27L, and 20H vs. 27H) within each of the three time points (0, 10, and 19 d/g) to test for changes due to the interventions, and (ii) with one-way ANOVAs with *a priori* comparisons (0 vs. 10 or 19, and 10 vs. 19 d/g) within each interventional group to test for changes with pregnancy. If data was not normally distributed, Kruskal-Wallis tests with equivalent Mann-Whitney tests were carried out.

## RESULTS

### Body Weight and Fat Mass

Before mating, body weight was only higher due to the H diet when animals were kept at thermoneutrality, whereas fat mass was higher due to the H diet only at the low temperature (Figure 1). Body weight and fat mass increased with pregnancy in all interventional groups. By 10 d/g, body weight was higher with the H diet regardless of temperature, whereas fat mass was only raised in those dams maintained at thermoneutrality. Body weight and fat mass were similar between groups by 19 d/g. Fetal weight was not different between any of the groups, at

either sampling gestations and increased with gestation e.g., 20H:  $88 \pm 2$  mg at 10 d/g;  $135 \pm 3$  mg at 19 d/g.

### Metabolic and Endocrine Profiles

Before mating, plasma glucose concentrations were notably higher in animals maintained at thermoneutrality but were similar between groups through pregnancy (Table 1). Plasma triglyceride and leptin increased with gestation in all groups, whereas NEFA concentrations were only increased at 19 d/g in the 20H group. Insulin was raised with the H diet before mating, but this only reached statistical significance for animals raised at 20°C. Although insulin concentrations were similar between groups through pregnancy there was high variability. Corticosterone was similar between groups, although mean values were highest in the 27L group, this difference was not significant. It was low in the 27L group at 10 d/g to increase by 19 d/g. Food intake, measured just before mating, was higher in the H diet group only when animals were kept at thermoneutrality when consumption of the L diet was reduced [20L:  $57 \pm 3$ ; 20H  $67 \pm 3$ ; 27L:  $45 \pm 3$ ; 27H:  $66 \pm 5$  kcal/d ( $P < 0.05$ )].

### Interscapular Adipose Depot Weight, UCP1 Protein, and Gene Expression

Interscapular adipose mass was similar between unmated animals (Figures 1C,D), but during pregnancy it was lower in animals at thermoneutrality, in which there was a smaller rise with gestation compared with those kept at a 20°C. Additionally, at 19 d/g, 20H



**TABLE 2 |** Interscapular gene expression measurements of genes of thermogenic, energy regulatory, and fat transport pathways of females before and during pregnancy, when kept at either a cool temperature (20°C) or thermoneutrality (27°C), and fed a low (L) or high (H) fat and sucrose diet.

Gene	Pregnancy time point (d/g)	20L	20H	27L	27H	ANOVA
<b>Thermogenesis</b>						
B3AR	0	0.89 ± 0.06	0.84 ± 0.06 <sup>a</sup>	0.90 ± 0.15	0.71 ± 0.10	N.S.
	10	0.62 ± 0.09	0.46 ± 0.06 <sup>ab</sup>	0.67 ± 0.05	0.64 ± 0.11	N.S.
	19	0.73 ± 0.08	0.65 ± 0.08 <sup>b</sup>	0.73 ± 0.13	0.47 ± 0.06	N.S.
	ANOVA	N.S.	0.006	N.S.	N.S.	
SERCA2B	0	0.49 ± 0.18	0.58 ± 0.16 <sup>a</sup>	0.41 ± 0.09	0.43 ± 0.12	N.S.
	10	0.32 ± 0.17	0.20 ± 0.16 <sup>ab</sup>	0.17 ± 0.07	0.31 ± 0.14	N.S.
	19	0.32 ± 0.12	0.56 ± 0.17 <sup>b</sup>	0.48 ± 0.16	0.28 ± 0.10	N.S.
	ANOVA	N.S.	0.028	N.S.	N.S.	
TRPV1	0	0.58 ± 0.09 <sup>a</sup>	0.57 ± 0.06 <sup>c</sup>	0.75 ± 0.16	0.86 ± 0.18 <sup>f</sup>	N.S.
	10	1.73 ± 0.39 <sup>ab</sup>	1.75 ± 0.26 <sup>cd</sup>	1.62 ± 0.54 <sup>e</sup>	1.17 ± 0.13 <sup>g</sup>	N.S.
	19	0.61 ± 0.05 <sup>b</sup>	0.72 ± 0.16 <sup>d</sup>	0.45 ± 0.05 <sup>e</sup>	0.46 ± 0.06 <sup>fg</sup>	N.S.
	ANOVA	0.011	0.006	0.013	0.004	
BHSD11	0	0.41 ± 0.05 <sup>ab</sup>	0.30 ± 0.05 <sup>de</sup>	0.64 ± 0.13 <sup>bi</sup>	0.64 ± 0.05 <sup>ek</sup>	0.020
	10	0.61 ± 0.26	0.27 ± 0.05 <sup>fg</sup>	0.50 ± 0.09 <sup>j</sup>	0.53 ± 0.05 <sup>gl</sup>	0.014
	19	0.73 ± 0.07 <sup>ac</sup>	0.92 ± 0.13 <sup>dth</sup>	2.80 ± 0.23 <sup>cij</sup>	3.11 ± 0.51 <sup>hkl</sup>	<0.001
	ANOVA	0.032	0.001	0.003	0.003	
<b>Insulin sensitivity and energy sensing</b>						
TCF7L2	0	0.65 ± 0.04 <sup>ab</sup>	0.70 ± 0.07 <sup>c</sup>	0.70 ± 0.09 <sup>d</sup>	0.67 ± 0.11 <sup>e</sup>	N.S.
	10	1.24 ± 0.20 <sup>a</sup>	1.14 ± 0.11 <sup>c</sup>	0.95 ± 0.12	0.80 ± 0.13	N.S.
	19	1.62 ± 0.14 <sup>b</sup>	1.53 ± 0.15 <sup>c</sup>	1.33 ± 0.19 <sup>d</sup>	2.80 ± 1.06 <sup>e</sup>	N.S.
	ANOVA	0.001	0.001	0.020	0.030	
mTOR	0	0.27 ± 0.03 <sup>a</sup>	0.28 ± 0.02 <sup>b</sup>	0.26 ± 0.03 <sup>c</sup>	0.24 ± 0.03 <sup>d</sup>	N.S.
	10	0.91 ± 0.06 <sup>a</sup>	1.00 ± 0.11 <sup>b</sup>	1.08 ± 0.08 <sup>c</sup>	0.85 ± 0.07 <sup>de</sup>	N.S.
	19	0.55 ± 0.04 <sup>a</sup>	0.43 ± 0.03 <sup>b</sup>	0.43 ± 0.06 <sup>c</sup>	0.34 ± 0.06 <sup>e</sup>	N.S.
	ANOVA	<0.001	<0.001	0.002	0.003	
IRS1	0	0.92 ± 0.14	0.81 ± 0.04	0.66 ± 0.14	0.66 ± 0.06 <sup>d</sup>	N.S.
	10	1.00 ± 0.11	0.86 ± 0.09	0.75 ± 0.12	0.76 ± 0.04 <sup>e</sup>	N.S.
	19	0.67 ± 0.05 <sup>a</sup>	0.65 ± 0.05 <sup>b</sup>	0.49 ± 0.07 <sup>ac</sup>	0.31 ± 0.05 <sup>bcde</sup>	0.001
	ANOVA	N.S.	N.S.	N.S.	<0.001	
IRS2	0	0.096 ± 0.014 <sup>ab</sup>	0.052 ± 0.004 <sup>bd</sup>	0.124 ± 0.020 <sup>fg</sup>	0.055 ± 0.012 <sup>fi</sup>	0.008
	10	0.069 ± 0.019 <sup>c</sup>	0.058 ± 0.008 <sup>e</sup>	0.088 ± 0.024 <sup>h</sup>	0.058 ± 0.006 <sup>j</sup>	N.S.
	19	1.01 ± 0.16 <sup>ac</sup>	0.98 ± 0.14 <sup>de</sup>	1.24 ± 0.21 <sup>fh</sup>	0.97 ± 0.23 <sup>ij</sup>	N.S.
	ANOVA	0.002	0.001	0.003	0.006	
<b>Fat transport</b>						
CD36	0	0.98 ± 0.10	0.92 ± 0.10	0.83 ± 0.04 <sup>c</sup>	0.80 ± 0.08 <sup>e</sup>	N.S.
	10	0.67 ± 0.09	0.78 ± 0.10	0.84 ± 0.07 <sup>d</sup>	0.89 ± 0.07 <sup>f</sup>	N.S.
	19	0.85 ± 0.12 <sup>a</sup>	1.00 ± 0.04 <sup>b</sup>	1.16 ± 0.06 <sup>acd</sup>	1.12 ± 0.04 <sup>bef</sup>	0.006
	ANOVA	N.S.	N.S.	0.001	0.012	
ATGL	0	1.40 ± 0.15 <sup>ab</sup>	1.14 ± 0.04	1.28 ± 0.14 <sup>d</sup>	0.85 ± 0.11 <sup>d</sup>	0.020
	10	0.90 ± 0.14 <sup>a</sup>	0.83 ± 0.14	1.15 ± 0.09	1.07 ± 0.12	N.S.
	19	0.91 ± 0.05 <sup>bc</sup>	0.90 ± 0.07	1.51 ± 0.12 <sup>ce</sup>	1.03 ± 0.12 <sup>e</sup>	<0.001
	ANOVA	0.015	N.S.	N.S.	N.S.	
LPL	0	0.91 ± 0.08 <sup>a</sup>	0.86 ± 0.07	0.79 ± 0.07 <sup>c</sup>	0.64 ± 0.07	N.S.
	10	1.03 ± 0.04 <sup>b</sup>	0.89 ± 0.07	1.05 ± 0.10 <sup>cd</sup>	0.72 ± 0.07 <sup>d</sup>	0.016
	19	0.59 ± 0.04 <sup>ab</sup>	0.68 ± 0.05	0.53 ± 0.06 <sup>c</sup>	0.53 ± 0.07	N.S.
	ANOVA	<0.001	N.S.	0.001	N.S.	
FATP4	0	0.59 ± 0.04 <sup>ab</sup>	0.56 ± 0.03	0.62 ± 0.05 <sup>cd</sup>	0.59 ± 0.04 <sup>ef</sup>	N.S.
	10	0.92 ± 0.06 <sup>a</sup>	0.86 ± 0.05	1.00 ± 0.05 <sup>c</sup>	0.89 ± 0.04 <sup>e</sup>	N.S.
	19	0.85 ± 0.10 <sup>b</sup>	0.87 ± 0.14	1.32 ± 0.15 <sup>d</sup>	1.17 ± 0.15 <sup>f</sup>	N.S.
	ANOVA	0.016	N.S.	0.001	0.002	

*P* values given are the statistically significant outcomes of comparisons (ANOVA or Kruskal-Wallis, indicated as "ANOVA"). If data within one outcome carry the same superscripts they are statistically different ( $P < 0.05$ ). For all interscapular gene expression, unmated  $n = 5-6$ , 10 d/g  $n = 5-7$ , 19 d/g  $n = 6-8$ . B3AR, beta-3 adrenergic receptor; SERCA2B, ATPase sarcoplasmic/endoplasmic reticulum Ca<sup>2+</sup>; TRPV1, capsaicin receptor; BHSD11, hydroxysteroid 11 beta dehydrogenase; TCF7L2, transcription factor 7 like 2; mTOR, mammalian target or rapamycin; IRS1+2, insulin receptor substrates 1 and 2; CD36, fatty acid translocase; ATGL, adipose triglyceride lipase; LPL, lipoprotein lipase; FATP4, fatty acid transport protein 4.

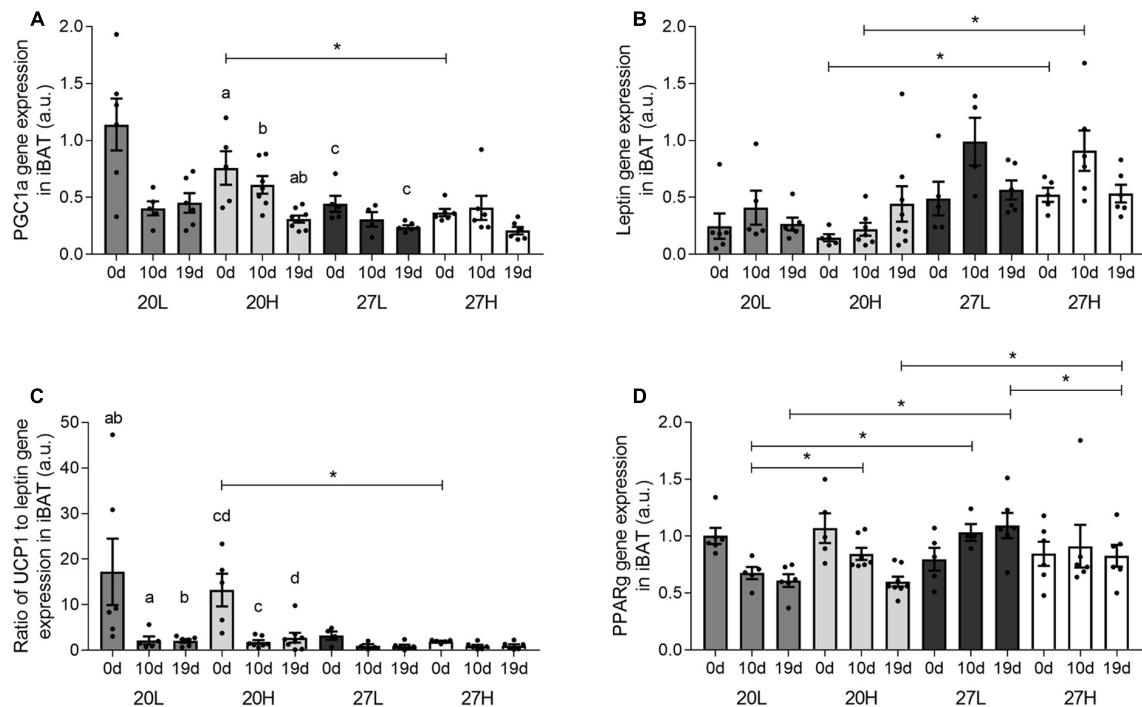


**FIGURE 3 |** Effect of housing temperature, pregnancy, and diet on interscapular gene expression. **(A)** *PGC1α*, **(B)** *leptin*, **(C)** the ratio of *UCP1* to *leptin* gene expression, and **(D)** *PPARγ* of females before (0 days) and during pregnancy (10 and 19 days), when kept at either a cool temperature (20°C) or thermoneutrality (27°C), and fed a low (L) or high (H) fat and sucrose diet. Differences between dietary groups housed at the same temperature \* $P < 0.05$ ; for each study group columns with the same superscripts are significantly different ( $P < 0.05$ ). For all interscapular gene expression, unmated  $n = 5-6$ , 10 d/g  $n = 5-7$ , 19 d/g  $n = 6-8$ .

animals had a greater interscapular fat mass than 20L, whereas diet had no effect at thermoneutrality.

Uncoupling protein 1 protein was more abundant in unmated animals fed the H diet at 20°C than at thermoneutrality (Figure 2). In contrast, *UCP1* gene expression was similar between groups and declined with gestation, and was accompanied with similar changes in *PGC1α* (Figure 3). There was also a higher gene expression of *PGC1α* in 20H compared with 27H groups prior to mating. Gene expression of leptin, a marker of white fat, was higher before, and in mid-pregnancy, in the 27H, compared with the 20H group. When comparing the ratio of *UCP1* and *leptin* gene expression, i.e., the main genes characteristic of brown and white adipocytes, respectively, the ratio of gene expression was markedly higher in unmated animals at 20°C, and then declined to similar mean values for all groups through pregnancy. *PPARγ* gene expression also declined with pregnancy in the animals kept at 20°C, irrespective of diet.

Other thermogenic genes examined i.e., *B3AR* and *SERCA2B* were unaffected by pregnancy, diet, or temperature, whilst *TRPV1* gene expression was higher at 10 than 19 d/g (Table 2). Gene expression of *BHSD11* was consistently higher in 27H than 20H groups and higher in 27L than 20L at 19 d/g, as it rose substantially by the end of pregnancy in those dams maintained at thermoneutrality. Energy sensing genes i.e., *TCFL2* and *mTOR* were consistently upregulated through pregnancy but were not affected by diet or temperature. *IRS1* gene expression

was lower at thermoneutrality at 19 d/g regardless of diet, and was downregulated with pregnancy in the 27H group, whilst *IRS2* was reduced with the H diet prior to pregnancy. Subsequently, there was no difference between groups as mRNA abundance increased up to 10 d/g and was similar between all groups by term. Of the genes involved in fat transport, *CD36* showed an increase in late pregnancy, but only at thermoneutrality. *ATGL* expression was higher in 27L than 27H, a difference that was not present at 20°C, as it was downregulated with pregnancy in the 20L group. At both environmental housing temperatures, *LPL* peaked at 10 d/g in those dams fed the control diet. *FATP4* gene expression increased with pregnancy regardless of any intervention.

## Inguinal and Omental Adipose Depots

*UCP1* mRNA was undetectable in the inguinal (or omental) depot. *PPARG* and *IRS2* gene expression declined through gestation in all groups (Table 3), whilst *B3AR* was undetectable at the end of pregnancy. *Leptin* gene expression declined by mid gestation in the 20L group only, whilst *FABP4* only decreased with gestation in the 27L group.

There were few differences in gene expression between groups in omental fat (Table 4). In contrast to the inguinal depot, *B3AR* was expressed throughout pregnancy, though declined by 19 d/g. *RXR2* gene expression was also higher in unmated animals and declined with pregnancy in all groups except 20L. Gene expression of *IRS2* was high before mating in the animals kept at thermoneutrality

**TABLE 3 |** Inguinal adipose tissue gene expression measurements of genes of thermogenic, energy regulatory and fat transport pathways of females before and during pregnancy, when kept at either a cool temperature (20°C) or thermoneutrality (27°C), and fed a low (L) or high (H) fat and sucrose diet.

Gene	Pregnancy time point (d/g)	20L	20H	27L	27H	ANOVA
<b>Thermogenesis</b>						
PPARG	0	1.02 ± 0.15 <sup>a</sup>	0.71 ± 0.09 <sup>b</sup>	0.84 ± 0.12 <sup>d</sup>	0.89 ± 0.16 <sup>d</sup>	N.S.
	10	0.78 ± 0.11	0.59 ± 0.13 <sup>c</sup>	0.72 ± 0.04 <sup>e</sup>	0.76 ± 0.12 <sup>e</sup>	N.S.
	19	0.50 ± 0.07 <sup>a</sup>	0.29 ± 0.05 <sup>bc</sup>	0.46 ± 0.08 <sup>de</sup>	0.39 ± 0.04 <sup>de</sup>	N.S.
	ANOVA	0.020	0.009	0.016	0.025	
B3AR	0	0.75 ± 0.14 <sup>a</sup>	0.59 ± 0.09	0.91 ± 0.13	0.79 ± 0.13	N.S.
	10	0.30 ± 0.06 <sup>a</sup>	0.42 ± 0.10	0.57 ± 0.10	0.63 ± 0.12	N.S.
	19	N.D.	N.D.	N.D.	N.D.	N.S.
	ANOVA	0.020	N.S.	N.S.	N.S.	
LEPTIN	0	0.50 ± 0.16 <sup>a</sup>	0.31 ± 0.09	0.47 ± 0.13	0.20 ± 0.05	N.S.
	10	0.11 ± 0.03 <sup>ab</sup>	0.13 ± 0.02	0.23 ± 0.05	0.19 ± 0.03	N.S.
	19	0.26 ± 0.04 <sup>b</sup>	0.20 ± 0.05	0.21 ± 0.06	0.25 ± 0.04	N.S.
	ANOVA	0.021	N.S.	N.S.	N.S.	
<b>Insulin sensitivity and energy sensing</b>						
IRS2	0	0.45 ± 0.04 <sup>a</sup>	0.47 ± 0.08 <sup>b</sup>	0.56 ± 0.03 <sup>d</sup>	0.55 ± 0.19 <sup>e</sup>	N.S.
	10	0.21 ± 0.03 <sup>a</sup>	0.32 ± 0.06 <sup>c</sup>	0.26 ± 0.04 <sup>d</sup>	0.17 ± 0.02 <sup>ef</sup>	N.S.
	19	1.26 ± 0.20 <sup>a</sup>	1.32 ± 0.16 <sup>bc</sup>	1.23 ± 0.21 <sup>d</sup>	1.07 ± 0.10 <sup>f</sup>	N.S.
	ANOVA	0.001	0.001	<0.001	0.002	
<b>Fat transport</b>						
FABP4	0	0.59 ± 0.20	0.37 ± 0.07	0.69 ± 0.22 <sup>a</sup>	0.38 ± 0.06	N.S.
	10	0.18 ± 0.04	0.18 ± 0.04	0.27 ± 0.05 <sup>ab</sup>	0.28 ± 0.05	N.S.
	19	0.29 ± 0.03	0.20 ± 0.03	0.30 ± 0.05 <sup>b</sup>	0.29 ± 0.04	N.S.
	ANOVA	N.S.	N.S.	0.023	N.S.	

*P* values given are the statistically significant outcomes of comparisons (ANOVA or Kruskal-Wallis, indicated as "ANOVA"). If data within one outcome carry the same superscripts they are statistically different ( $P < 0.05$ ). For all inguinal AT gene expression, unmated  $n = 6$ , 10 d/g  $n = 5-7$ , 19 d/g  $n = 6-8$ . PPARG, peroxisome proliferator activated receptor gamma; B3AR, beta-3 adrenergic receptor; IRS2, insulin receptor substrate 2; FABP4, fatty acid binding protein 4.

and declined during pregnancy. *FATP4* gene expression increased at 10 d/g but then decreased by 19 d/g, a pattern that is also seen for *FABP4* in 27L but no other groups. Expression of genes of the immune response pathways were not affected, with the exception of a reduction in *MCPI* through pregnancy.

## DISCUSSION

This is the first study to investigate the impact of housing temperature on a dietary induced rise in fat mas followed by pregnancy and further demonstrates its impact on metabolic outcomes (Maloney et al., 2014; Gordon, 2017). Ambient temperature modulated the effect of a diet that persisted into pregnancy. This could be explained, in part, by reduced UCP1 protein and increased food intake before pregnancy. Irrespective of diet, unmated females maintained at thermoneutrality had raised glucose, that could be mediated by a lower rate of thermogenesis, especially in BAT (Zingaretti et al., 2009). However, the effect of temperature on plasma glucose did not persist into pregnancy, possibly due to the concomitant metabolic adaptations (Bell and Bauman, 1997), and/or due to changes in UCP1. These findings complement the effect of housing at thermoneutrality demonstrated in male mice, in which UCP1 abundance is reduced, whereas effects

on glucose, and insulin diminish with time (Xiao et al., 2015; Small et al., 2018). Moreover, the raised maternal glucose at the time of mating could impact on embryo development without an immediate impact on fetal growth (Lewis et al., 2013). Ideally, we would also have made additional measurements on UCP1 but with the limited amount of tissue available meant we could only undertake measures of gene expression and histology.

Overall, there was a decrease in *UCP1* and *PGC1α* gene expression within BAT through gestation which was more pronounced at 20°C than at thermoneutrality. No other gene examined showed a comparable response, which was accompanied with a transient decline in UCP1 protein at 20°C, but not thermoneutrality. A recent study in mice (McIlvride et al., 2017) suggested that UCP1 protein decreased with gestation, although this was based on a single immunohistochemistry slide, without quantification. The same study also suggested that the thermogenic response was reduced with gestation, but this was measured in terminally anaesthetized animals, that suppresses BAT function (Ohlson et al., 1994) and potentially confounding effects of this procedure in pregnancy cannot be ruled out. A further report suggested UCP1 protein declines with pregnancy in mice (Qiao et al., 2018). These measurements were, however, made in total protein homogenates, rather than mitochondrial preparations which is where UCP1 resides (Aquila et al., 1985) and is known to decline with gestation

**TABLE 4 |** Omental adipose tissue gene expression measurements of genes of thermogenic, energy regulatory, fat transport, and immune response pathways of females before and during pregnancy, when kept at either a cool temperature (20°C) or thermoneutrality (27°C), and fed a low (L) or high (H) fat and sucrose diet.

Gene	Pregnancy time point (d/g)	20L	20H	27L	27H	ANOVA
<b>Thermogenesis</b>						
B3AR	0	0.23 ± 0.12	0.62 ± 0.22	0.47 ± 0.14	0.99 ± 0.27	N.S.
	10	0.78 ± 0.37	1.46 ± 0.51	1.37 ± 0.34 <sup>a</sup>	1.00 ± 0.29	N.S.
	19	0.45 ± 0.11	0.40 ± 0.15	0.32 ± 0.14 <sup>a</sup>	0.33 ± 0.06	N.S.
	ANOVA	N.S.	N.S.	0.028	N.S.	
RYR2	0	1.17 ± 0.38	2.16 ± 0.46 <sup>a</sup>	1.92 ± 0.49 <sup>b</sup>	2.34 ± 0.56 <sup>d</sup>	N.S.
	10	0.83 ± 0.15	1.09 ± 0.20	1.09 ± 0.22 <sup>c</sup>	0.85 ± 0.19	N.S.
	19	0.73 ± 0.18	0.61 ± 0.10 <sup>a</sup>	0.40 ± 0.09 <sup>bc</sup>	0.50 ± 0.11 <sup>d</sup>	N.S.
	ANOVA	N.S.	0.017	0.007	0.021	
LEPTIN	0	0.22 ± 0.15	0.38 ± 0.14	0.24 ± 0.16	0.65 ± 0.13	N.S.
	10	0.56 ± 0.23	0.62 ± 0.19	0.60 ± 0.16	0.95 ± 0.28	N.S.
	19	0.50 ± 0.13	0.42 ± 0.13	0.46 ± 0.21	0.53 ± 0.19	N.S.
	ANOVA	N.S.	N.S.	N.S.	N.S.	
TRPV1	0	1.62 ± 1.10	2.45 ± 1.08	0.91 ± 0.25 <sup>a</sup>	2.65 ± 0.89	N.S.
	10	2.25 ± 0.84	2.29 ± 0.95	3.78 ± 0.58 <sup>a</sup>	3.17 ± 0.93	N.S.
	19	4.67 ± 0.85	2.56 ± 0.56	2.22 ± 0.68	3.18 ± 0.85	N.S.
	ANOVA	N.S.	N.S.	0.012	N.S.	
VEGFA	0	1.24 ± 0.61	1.62 ± 0.63	1.08 ± 0.22	2.22 ± 0.59 <sup>a</sup>	N.S.
	10	0.84 ± 0.35	1.10 ± 0.33	1.91 ± 0.68	0.86 ± 0.23	N.S.
	19	0.94 ± 0.20	0.88 ± 0.19	0.60 ± 0.18	0.61 ± 0.07 <sup>a</sup>	N.S.
	ANOVA	N.S.	N.S.	N.S.	0.048	
SERCA2B	0	0.23 ± 0.10	0.62 ± 0.21	0.68 ± 0.37	1.38 ± 0.45	N.S.
	10	0.28 ± 0.11	0.76 ± 0.31	0.62 ± 0.12	0.60 ± 0.29	N.S.
	19	0.51 ± 0.14	0.32 ± 0.10	0.30 ± 0.10	0.45 ± 0.17	N.S.
	ANOVA	N.S.	N.S.	N.S.	N.S.	
VDAC	0	2.03 ± 0.90	3.43 ± 1.05	1.86 ± 0.44	3.34 ± 0.85	N.S.
	10	3.01 ± 0.94	2.95 ± 0.92	4.67 ± 0.83	4.50 ± 1.28	N.S.
	19	4.68 ± 0.73	3.37 ± 0.70	2.88 ± 0.77	3.40 ± 0.77	N.S.
	ANOVA	N.S.	N.S.	N.S.	N.S.	
<b>Insulin sensitivity and energy sensing</b>						
IRS1	0	0.38 ± 0.13	0.62 ± 0.24	0.68 ± 0.24	1.44 ± 0.56	N.S.
	10	0.67 ± 0.26	0.84 ± 0.25	0.99 ± 0.20	0.57 ± 0.16	N.S.
	19	0.76 ± 0.16	0.61 ± 0.15	0.52 ± 0.23	0.51 ± 0.10	N.S.
	ANOVA	N.S.	N.S.	N.S.	N.S.	
IRS2	0	1.02 ± 0.23	0.56 ± 0.23	2.01 ± 0.40 <sup>ab</sup>	1.97 ± 0.61 <sup>c</sup>	N.S.
	10	0.91 ± 0.27	0.78 ± 0.17	0.78 ± 0.17 <sup>a</sup>	0.64 ± 0.15	N.S.
	19	0.73 ± 0.16	0.89 ± 0.14	0.63 ± 0.13 <sup>b</sup>	0.57 ± 0.10 <sup>c</sup>	N.S.
	ANOVA	N.S.	N.S.	0.007	0.047	
<b>Fat transport</b>						
FATP4	0	0.23 ± 0.04	0.19 ± 0.03	0.23 ± 0.02 <sup>b</sup>	0.27 ± 0.02 <sup>d</sup>	N.S.
	10	0.35 ± 0.07 <sup>a</sup>	0.30 ± 0.05	0.75 ± 0.34 <sup>bc</sup>	1.51 ± 0.87 <sup>de</sup>	N.S.
	19	0.15 ± 0.01 <sup>a</sup>	0.20 ± 0.03	0.17 ± 0.03 <sup>c</sup>	0.14 ± 0.02 <sup>a</sup>	N.S.
	ANOVA	0.023	N.S.	0.018	0.015	
FABP4	0	0.48 ± 0.30	1.35 ± 0.52	0.46 ± 0.16 <sup>a</sup>	1.01 ± 0.19	N.S.
	10	0.51 ± 0.20	1.38 ± 0.49	1.91 ± 0.20 <sup>ab</sup>	1.48 ± 0.42	N.S.
	19	1.18 ± 0.23	0.62 ± 0.23	0.62 ± 0.21 <sup>b</sup>	0.89 ± 0.26	N.S.
	ANOVA	N.S.	N.S.	<0.001	N.S.	
<b>Immune response</b>						
EMR1	0	0.72 ± 0.16	0.72 ± 0.16	0.61 ± 0.09	0.82 ± 0.15 <sup>ab</sup>	N.S.
	10	0.79 ± 0.25	0.67 ± 0.17	0.85 ± 0.15	0.37 ± 0.10 <sup>a</sup>	N.S.
	19	0.64 ± 0.06	0.79 ± 0.20	0.50 ± 0.14	0.40 ± 0.05 <sup>b</sup>	N.S.
	ANOVA	N.S.	N.S.	N.S.	0.016	

(Continued)



TABLE 4 | Continued

Gene	Pregnancy time point (d/g)	20L	20H	27L	27H	ANOVA
TNF	0	1.26 ± 0.24	0.77 ± 0.25	1.11 ± 0.33	0.65 ± 0.20	N.S.
	10	0.90 ± 0.24	0.59 ± 0.17	0.42 ± 0.11	0.50 ± 0.22	N.S.
	19	0.44 ± 0.14	1.09 ± 0.31	0.76 ± 0.12	0.59 ± 0.19	N.S.
	ANOVA	N.S.	N.S.	N.S.	N.S.	
IL6	0	0.036 ± 0.013 <sup>ab</sup>	0.024 ± 0.006	0.019 ± 0.005	0.012 ± 0.002	N.S.
	10	0.010 ± 0.003 <sup>a</sup>	0.012 ± 0.003	0.010 ± 0.002	0.009 ± 0.002	N.S.
	19	0.012 ± 0.003 <sup>b</sup>	0.016 ± 0.004	0.014 ± 0.003	0.015 ± 0.006	N.S.
	ANOVA	0.017	N.S.	N.S.	N.S.	
MCP1	0	2.76 ± 0.92 <sup>a</sup>	4.80 ± 1.04 <sup>ef</sup>	2.93 ± 0.30 <sup>gh</sup>	2.85 ± 0.70 <sup>ij</sup>	N.S.
	10	0.47 ± 0.06 <sup>a</sup>	0.57 ± 0.07 <sup>e</sup>	0.59 ± 0.07 <sup>g</sup>	0.43 ± 0.09 <sup>j</sup>	N.S.
	19	1.12 ± 0.14 <sup>abcd</sup>	0.66 ± 0.06 <sup>bf</sup>	0.71 ± 0.09 <sup>ch</sup>	0.51 ± 0.05 <sup>dj</sup>	0.005
	ANOVA	0.003	0.002	0.002	0.012	

*P* values given are the statistically significant outcomes of comparisons (ANOVA or Kruskal-Wallis, indicated as "ANOVA"). If data within one outcome carry the same superscripts they are statistically different ( $P < 0.05$ ). For all omental AT gene expression, unmated  $n = 5-6$ , 10 d/g  $n = 5-7$ , 19 d/g  $n = 6-8$ . B3AR, beta-3 adrenergic receptor; RYR2, ryanodine receptor 2; TRPV1, capsaicin receptor; VEGFA, vascular endothelial growth factor A; SERCA2B, ATPase sarcoplasmic/endoplasmic reticulum Ca<sup>2+</sup>; VDAC, voltage-dependent anion channel 1; IRS1+2, insulin receptor substrates 1 and 2; FATP4, fatty acid transport protein 4; FABP4, fatty acid binding protein 4; EMR1, adhesion G protein-coupled receptor E1; TNF, tumor necrosis factor; IL6, interleukin 6; MCP1, monocyte chemoattractant protein 1.

(Frontera et al., 2005). In the present study, the lack of any quantitative, sustained change in UCP1 protein with gestation is indicative of maintained function, given it is the protein and not mRNA that determines heat production from UCP1 (Nedergaard and Cannon, 2013).

We observed modest temperature dependent changes in gene expression of some BAT markers by late gestation e.g., a decline in *PPARγ* was only seen at 20°C, whilst *CD36* and *BHSD11* were raised considerably more substantially at thermoneutrality. It is likely that the maternal endocrine adaptations with gestation mediate these responses and could include changes in the prolactin-growth hormone axis as well as steroid hormones (Napso et al., 2018). The largest relative change in gene expression with gestation within BAT we observed was for *leptin*, and this was confined to those dams kept at thermoneutrality. The extent to which such an adaptation could impact on BAT function has yet to be established, although recent *in vitro* studies suggest an increase in leptin co-localisation within the nucleus that co-regulates the appearance of UCP1 with cold exposure (Velickovic et al., 2018). Interestingly, the increase in *leptin* gene expression was confined to BAT and was not seen within the inguinal fat depot that did not express *UCP1*. As inguinal fat has been considered to be an important beige depot, the absence of *UCP1* gene expression suggests such adaptations may be confined to males, or that lower ambient temperatures are required in females (Waldén et al., 2012). Neither the inguinal and omental fat depots expressed UCP1 mRNA and were both unresponsive to changes in housing temperature. Taken together these findings emphasize the importance of the presence of UCP1 in modulating the effect of temperature on adipose function.

In conclusion, housing temperature determines the effect of dietary induced obesity on fat deposition, although this response was modified through gestation. This adaptation maybe mediated by reduced UCP1 content of brown fat seen with the H diet prior to pregnancy.

## DATA AVAILABILITY

All datasets generated for this study are included in the manuscript and/or the **Supplementary Files**.

## AUTHOR CONTRIBUTIONS

MS, HB, and ND conceived and designed the study, interpreted the data, refined the manuscript, and critiqued the output for intellectual content. MS, ND, LA, and GP conducted the animal study. LA, GP, EA, IB, PA, and ND undertook the laboratory analyses. LA and GP equally wrote the first manuscript draft. All authors reviewed the final manuscript.

## FUNDING

This work was funded by the EU-CASCADE fellowship scheme funded by the EU's 7th FP PCOFUND-GA-2012-600181 (ND), the British Heart Foundation (Grant No. FS/15/4/31184/) (PA), and by the Coordenação de Aperfeiçoamento de Pessoal de Nível Superior, Brasil (CAPES) – Finance Code 001. GP was the recipient of a doctoral fellowship from the CAPES.

## ACKNOWLEDGMENTS

The authors would like to thank the University of Nottingham's Biomedical Support Unit for their skilled maintenance of the animals.

## SUPPLEMENTARY MATERIAL

The Supplementary Material for this article can be found online at: <https://www.frontiersin.org/articles/10.3389/fphys.2019.00209/full#supplementary-material>

## REFERENCES

- Aquila, H., Link, T. A., and Klingenberg, M. (1985). The uncoupling protein from brown fat mitochondria is related to the mitochondrial ADP/ATP carrier. Analysis of sequence homologies and of folding of the protein in the membrane. *EMBO J.* 4, 2369–2376.
- Arganda-Carreras, I., Kaynig, V., Rueden, C., Eliceiri, K. W., Schindelin, J., Cardona, A., et al. (2017). Trainable Weka Segmentation: a machine learning tool for microscopy pixel classification. *Bioinformatics* 33, 2424–2426. doi: 10.1093/bioinformatics/btx180
- Bartelt, A., Bruns, O. T., Reimer, R., Hohenberg, H., Itrich, H., Peldschus, K., et al. (2011). Brown adipose tissue activity controls triglyceride clearance. *Nat. Med.* 17, 200–205. doi: 10.1038/nm.2297
- Bell, A. W., and Bauman, D. E. (1997). Adaptations of glucose metabolism during pregnancy and lactation. *J. Mammary Gland Biol. Neoplasia* 2, 265–278.
- Cannon, B., and Nedergaard, J. (2004). Brown adipose tissue: function and physiological significance. *Physiol. Rev.* 84, 277–359. doi: 10.1152/physrev.00015.2003
- Cui, X., Nguyen, N. L. T., Zarebidaki, E., Cao, Q., Li, F., Zha, L., et al. (2016). Thermoneutrality decreases thermogenic program and promotes adiposity in high-fat diet-fed mice. *Physiol. Rep.* 4:e12799. doi: 10.14814/phy2.12799
- Festing, M. F. W. (2006). Design and statistical methods in studies using animal models of development. *ILAR J.* 47, 5–14.
- Frontera, M., Pujol, E., Rodríguez-Cuenca, S., Català-Niell, A., Roca, P., García-Palmer, F., et al. (2005). Rat brown adipose tissue thermogenic features are altered during mid-pregnancy. *Cell. Physiol. Biochem.* 15, 203–210. doi: 10.1159/000086407
- Gordon, C. J. (1990). Thermal biology of the laboratory rat. *Physiol. Behav.* 47, 963–991. doi: 10.1016/0031-9384(90)90025-Y
- Gordon, C. J. (2017). The mouse thermoregulatory system: its impact on translating biomedical data to humans. *Physiol. Behav.* 179, 55–66. doi: 10.1016/j.physbeh.2017.05.026
- Herrmann, T., Buchkremer, F., Gosch, I., Hall, A. M., Bernlohr, D. A., and Stremmel, W. (2001). Mouse fatty acid transport protein 4 (FATP4): characterization of the gene and functional assessment as a very long chain acyl-CoA synthetase. *Gene* 270, 31–40. doi: 10.1016/S0378-1119(01)00489-9
- Howie, G. J., Sloboda, D. M., Kamal, T., and Vickers, M. H. (2009). Maternal nutritional history predicts obesity in adult offspring independent of postnatal diet: maternal high fat nutrition and obesity in offspring. *J. Physiol.* 587, 905–915. doi: 10.1113/jphysiol.2008.163477
- Jemaa, R., Tuzet, S., Portos, C., Betoulle, D., Apfelbaum, M., and Fumeron, F. (1995). Lipoprotein lipase gene polymorphisms: associations with hypertriglyceridemia and body mass index in obese people. *Int. J. Obes. Relat. Metab. Disord. J. Int. Assoc. Study Obes.* 19, 270–274.
- Le Foll, C., Dunn-Meynell, A. A., and Levin, B. E. (2015). Role of FAT/CD36 in fatty acid sensing, energy, and glucose homeostasis regulation in DIO and DR rats. *Am. J. Physiol. Regul. Integr. Comp. Physiol.* 308, R188–R198. doi: 10.1152/ajpregu.00367.2014
- Lewis, R. M., Demmelmair, H., Gaillard, R., Godfrey, K. M., Hauguel-de Mouzon, S., Huppertz, B., et al. (2013). The placental exposome: placental determinants of fetal adiposity and postnatal body composition. *Ann. Nutr. Metab.* 63, 208–215. doi: 10.1159/000355222
- Livak, K. J., and Schmittgen, T. D. (2001). Analysis of relative gene expression data using real-time quantitative PCR and the 2- $\Delta\Delta$ CT Method. *Methods* 25, 402–408. doi: 10.1006/meth.2001.1262
- Maloney, S. K., Fuller, A., Mitchell, D., Gordon, C., and Overton, J. M. (2014). Translating animal model research: does it matter that our rodents are cold? *Physiology* 29, 413–420. doi: 10.1152/physiol.00029.2014
- Martin, I., Giral, M., Viñas, O., Iglesias, R., Mampel, T., and Villarroja, F. (1989). Adaptive decrease in expression of the mRNA for uncoupling protein and subunit II of cytochrome c oxidase in rat brown adipose tissue during pregnancy and lactation. *Biochem. J.* 263, 965–968. doi: 10.1042/bj2630965
- McIlvride, S., Mushtaq, A., Papacleovoulou, G., Hurling, C., Steel, J., Jansen, E., et al. (2017). A progesterone-brown fat axis is involved in regulating fetal growth. *Sci. Rep.* 7:10671. doi: 10.1038/s41598-017-10979-7
- Morris, M. J., and Chen, H. (2009). Established maternal obesity in the rat reprograms hypothalamic appetite regulators and leptin signaling at birth. *Int. J. Obes.* 33, 115–122. doi: 10.1038/ijo.2008.213
- Napso, T., Yong, H. E. J., Lopez-Tello, J., and Sferruzzi-Perri, A. N. (2018). The role of placental hormones in mediating maternal adaptations to support pregnancy and lactation. *Front. Physiol.* 9:1091. doi: 10.3389/fphys.2018.01091
- Nedergaard, J., and Cannon, B. (2013). UCP1 mRNA does not produce heat. *Biochim. Biophys. Acta BBA* 1831, 943–949. doi: 10.1016/j.bbali.2013.01.009
- Nicholls, D. G. (1983). The thermogenic mechanism of brown adipose tissue. *Biosci. Rep.* 3, 431–441. doi: 10.1007/BF01121954
- Ohlson, K. B., Mohell, N., Cannon, B., Lindahl, S. G., and Nedergaard, J. (1994). Thermogenesis in brown adipocytes is inhibited by volatile anesthetic agents. A factor contributing to hypothermia in infants? *Anesthesiology* 81, 176–183.
- Puigserver, P., Wu, Z., Park, C. W., Graves, R., Wright, M., and Spiegelman, B. M. (1998). A cold-inducible coactivator of nuclear receptors linked to adaptive thermogenesis. *Cell* 92, 829–839. doi: 10.1016/S0092-8674(00)81410-5
- Qiao, L., Lee, S., Nguyen, A., Hay, W. W. Jr., and Shao, J. (2018). The regulatory effects of brown adipose tissue thermogenesis on maternal metabolic adaptation, placental efficiency, and fetal growth in mice. *Am. J. Physiol. Endocrinol. Metab.* 315, E1224–E1231. doi: 10.1152/ajpendo.00192.2018
- Rondinone, C. M., Wang, L.-M., Lonroth, P., Wesslau, C., Pierce, J. H., and Smith, U. (1997). Insulin receptor substrate (IRS) 1 is reduced and IRS-2 is the main docking protein for phosphatidylinositol 3-kinase in adipocytes from subjects with non-insulin-dependent diabetes mellitus. *Proc. Natl. Acad. Sci.* 94, 4171–4175. doi: 10.1073/pnas.94.8.4171
- Ruager-Martin, R., Hyde, M. J., and Modi, N. (2010). Maternal obesity and infant outcomes. *Early Hum. Dev.* 86, 715–722. doi: 10.1016/j.earlhumdev.2010.08.007
- Schindelin, J., Arganda-Carreras, I., Frise, E., Kaynig, V., Longair, M., Pietzsch, T., et al. (2012). Fiji: an open-source platform for biological-image analysis. *Nat. Methods* 9, 676–682. doi: 10.1038/nmeth.2019
- Shankar, K., Harrell, A., Liu, X., Gilchrist, J. M., Ronis, M. J. J., and Badger, T. M. (2007). Maternal obesity at conception programs obesity in the offspring. *AJP Regul. Integr. Comp. Physiol.* 294, R528–R538. doi: 10.1152/ajpregu.00316.2007
- Small, L., Gong, H., Yassmin, C., Cooney, G. J., and Brandon, A. E. (2018). Thermoneutral housing does not influence fat mass or glucose homeostasis in C57BL/6 mice. *J. Endocrinol.* 239, 313–324. doi: 10.1530/JOE-18-0279
- Stemmer, K., Kotzbeck, P., Zani, F., Bauer, M., Neff, C., Müller, T. D., et al. (2015). Thermoneutral housing is a critical factor for immune function and diet-induced obesity in C57BL/6 nude mice. *Int. J. Obes.* 39, 791–797. doi: 10.1038/ijo.2014.187
- Velickovic, K., Lugo Leija, H. A., Bloor, I., Law, J., Sacks, H., Symonds, M., et al. (2018). Low temperature exposure induces browning of bone marrow stem cell derived adipocytes in vitro. *Sci. Rep.* 8:4974. doi: 10.1038/s41598-018-23267-9
- Waldén, T. B., Hansen, I. R., Timmons, J. A., Cannon, B., and Nedergaard, J. (2012). Recruited vs. nonrecruited molecular signatures of brown, “brite,” and white adipose tissues. *Am. J. Physiol. Endocrinol. Metab.* 302, E19–E31. doi: 10.1152/ajpendo.00249.2011
- Wu, J., Boström, P., Sparks, L. M., Ye, L., Choi, J. H., Giang, A.-H., et al. (2012). Beige adipocytes are a distinct type of thermogenic fat cell in mouse and human. *Cell* 150, 366–376. doi: 10.1016/j.cell.2012.05.016
- Xiao, C., Goldhof, M., Gavrilova, O., and Reitman, M. L. (2015). Anti-obesity and metabolic efficacy of the  $\beta$ 3-adrenergic agonist, CL316243, in mice at thermoneutrality compared to 22°C: effect of CL316243 at thermoneutrality. *Obesity* 23, 1450–1459. doi: 10.1002/oby.21124
- Ye, L., Wu, J., Cohen, P., Kazak, L., Khandekar, M. J., Jedrychowski, M. P., et al. (2013). Fat cells directly sense temperature to activate thermogenesis. *Proc. Natl. Acad. Sci.* 110, 12480–12485. doi: 10.1073/pnas.1310261110
- Zingaretti, M. C., Crosta, F., Vitali, A., Guerrieri, M., Frontini, A., Cannon, B., et al. (2009). The presence of UCP1 demonstrates that metabolically active adipose tissue in the neck of adult humans truly represents brown adipose tissue. *FASEB J. Off. Publ. Fed. Am. Soc. Exp. Biol.* 23, 3113–3120. doi: 10.1096/fj.09-133546

**Conflict of Interest Statement:** The authors declare that the research was conducted in the absence of any commercial or financial relationships that could be construed as a potential conflict of interest.

Copyright © 2019 Albustanji, Perez, AlHarethi, Aldiss, Bloor, Barreto-Medeiros, Budge, Symonds and Dellschaft. This is an open-access article distributed under the terms of the Creative Commons Attribution License (CC BY). The use, distribution or reproduction in other forums is permitted, provided the original author(s) and the copyright owner(s) are credited and that the original publication in this journal is cited, in accordance with accepted academic practice. No use, distribution or reproduction is permitted which does not comply with these terms.



# Important Trends in UCP3 Investigation

Elena E. Pohl<sup>1\*†</sup>, Anne Rupprecht<sup>1,2\*†</sup>, Gabriel Macher<sup>1</sup> and Karolina E. Hilse<sup>1</sup>

<sup>1</sup> Institute of Physiology, Pathophysiology and Biophysics, University of Veterinary Medicine, Vienna, Austria, <sup>2</sup> Institute of Pharmacology and Toxicology, Rostock University Medical Center, Rostock, Germany

## OPEN ACCESS

### Edited by:

Rita De Matteis,  
University of Urbino Carlo Bo, Italy

### Reviewed by:

Denis Richard,  
Laval University, Canada  
Mary-Ellen Harper,  
University of Ottawa, Canada

### \*Correspondence:

Elena E. Pohl  
elena.pohl@vetmeduni.ac.at  
Anne Rupprecht  
anne.rupprecht@med.uni-rostock.de

<sup>†</sup> These authors have contributed  
equally to this work

### Specialty section:

This article was submitted to  
Integrative Physiology,  
a section of the journal  
Frontiers in Physiology

Received: 11 November 2018

Accepted: 04 April 2019

Published: 30 April 2019

### Citation:

Pohl EE, Rupprecht A, Macher G  
and Hilse KE (2019) Important Trends  
in UCP3 Investigation.  
Front. Physiol. 10:470.  
doi: 10.3389/fphys.2019.00470

Membrane uncoupling protein 3 (UCP3), a member of the mitochondrial uncoupling protein family, was discovered in 1997. UCP3's properties, such as its high homology to other mitochondrial carriers, especially to UCP2, its short lifetime and low specificity of UCP3 antibodies, have hindered progress in understanding its biological function and transport mechanism over decades. The abundance of UCP3 is highest in murine brown adipose tissue (BAT, 15.0 pmol/mg protein), compared to heart (2.7 pmol/mg protein) and the gastrocnemius muscle (1.7 pmol/mg protein), but it is still 400-fold lower than the abundance of UCP1, a biomarker for BAT. Investigation of UCP3 reconstituted in planar bilayer membranes revealed that it transports protons only when activated by fatty acids (FA). Although purine nucleotides (PN) inhibit UCP3-mediated transport, the molecular mechanism differs from that of UCP1. It remains a conundrum that two homologous proton-transporting proteins exist within the same tissue. Recently, we proposed that UCP3 abundance directly correlates with the degree of FA  $\beta$ -oxidation in cell metabolism. Further development in this field implies that UCP3 may have dual function in transporting substrates, which have yet to be identified, alongside protons. Evaluation of the literature with respect to UCP3 is a complex task because (i) UCP3 features are often extrapolated from its "twin" UCP2 without additional proof, and (ii) the specificity of antibodies against UCP3 used in studies is rarely evaluated. In this review, we primarily focus on recent findings obtained for UCP3 in biological and biomimetic systems.

**Keywords: proton transport, uncoupling protein expression pattern, fatty acid beta-oxidation, cell metabolism, mitochondria**

## INTRODUCTION

The role of brown adipose tissue (BAT) in obesity was suggested 40 years ago based on the ability of brown fat mitochondria to dissipate energy as heat (Parascandola, 1974; Himms-Hagen, 1979; Harper et al., 2001). However, until 2009 BAT was only linked to hibernating mammals and newborns (Heaton, 1972; Spiegelman and Flier, 2001). The discovery of active BAT in human adults and identification of a third type of fat cells – beige or brite adipocytes (brite adipose tissue, BrAT) (Petrovic et al., 2010; Wu et al., 2012) – reintroduced BAT into research focus as a target for the treatment of obesity and other metabolic disorders (Cypess et al., 2009; Virtanen et al., 2009; Chondronikola and Sidossis, 2018).

Uncoupling protein 1 (UCP1, previously called thermogenin) is a main player in the energy dissipation process in BAT (**Figure 1**) and BrAT (Shabalina et al., 2013). It is the most investigated

member of the uncoupling protein subfamily that belongs to the mitochondrial anion transporters superfamily (SLC25, for review; Palmieri, 2013). UCP subfamily formally comprises five members (UCP1-UCP5). UCP1 was discovered in the mid-1970s in the mitochondria of hamster, rat and guinea pig BAT by several groups (for reviews Nicholls, 2017; Ricquier, 2017). It is regarded by several groups as the only “true” uncoupling protein (Nedergaard et al., 1999; Ricquier, 2011; Nicholls, 2017) because it dissipates the proton gradient over the inner mitochondrial membrane (IMM) to produce a remarkable amount of heat if upregulated in mammals under cold acclimation conditions.

The function of another member of the UCP family that was found in BAT, UCP3, has also been increasingly associated with obesity and diabetes (Harper et al., 2002; Costford et al., 2008; Holloway et al., 2009). However, results from different research groups are often contradicting and largely affected by the usage of non-specific antibodies. The underlying mechanisms of UCP3 functioning are obscure. UCP3 was long time handled as a twin of UCP2 due to their very high homology and history of their discovery. Meanwhile, it has become clear that their biological and transport functions differ considerably. The most intriguing issue is that UCP3, which is preferentially investigated in skeletal muscle and heart, is much more abundant in BAT [Hilse et al., 2016b; see section below]. However, UCP3 role in BAT and BrAT remains enigmatic due to the high abundance of UCP1.

In this review, we outline current knowledge on UCP3 expression and transport functions. We discuss its putative involvement in BAT functions, its interplay with UCP1 and its role in other tissues. Because several excellent reviews about different aspects of UCP1 physiology have appeared in recent years (Betz and Enerback, 2018; Gaudry et al., 2018; Jezek et al., 2018; Chouchani et al., 2019), we primarily concentrate on controversial issues in UCP1 research. We especially focus on protein expression studies and functional investigations of reconstituted UCPs.

## UCP3 IS A MEMBER OF THE UNCOUPLING PROTEIN SUBFAMILY

The ways how members of the mitochondrial UCP subfamily were discovered are strikingly different. UCP1 was identified due to its high protein amount in BAT, which was visible on a Coomassie stained SDS gel loaded with mitochondrial protein obtained from BAT (Ricquier and Kader, 1976; Heaton et al., 1978). UCP3 (similar to UCP2, UCP4, and UCP5) was identified through screening cDNA libraries for candidates with homology to UCP1 (Boss et al., 1997; Fleury et al., 1997; Sanchis et al., 1998; Mao et al., 1999; Hagenauer et al., 2005).

The debates, whether UCP3, alongside with other “minor” proteins, truly belongs to the uncoupling family started shortly after they were discovered (Nedergaard and Cannon, 2003). This issue remains unsettled until now (Nicholls, 2017). The main reason for that is the discrepancy between UCP3’s ability to transport protons

(Macher et al., 2018) and its low expression levels (compared to UCP1, see section below) to perform essential uncoupling.

## EXPRESSION PATTERN OF UCP3 – NEW HINTS FOR ITS PUTATIVE FUNCTION(S)

### Expression of UCP3 at mRNA Level

UCP3 was first identified by screening a human skeletal muscle cDNA library. These initial studies revealed different patterns of UCP3 mRNA expression in human and rat (Boss et al., 1997; Gong et al., 1997; Vidal-Puig et al., 1997). In rats, UCP3 mRNA was mostly present in BAT, followed by muscles with glycolytic (tensor fascia latae, tibialis anterior), mixed (gastrocnemius) and slow-twitch oxidative (soleus muscle) metabolism. UCP3 mRNA at much lower levels was also described in rat heart, lung and WAT (Alan et al., 2009). In humans, UCP3 mRNA was reported primarily in skeletal muscle and in trace quantities in the heart (Boss et al., 1997; Gong et al., 1997; Vidal-Puig et al., 1997). Differences in UCP3 mRNA distribution patterns were also detected between mouse and rat (Alan et al., 2009).

### Pitfalls in the Investigation of UCP Protein Expression

#### Discrepancy Between UCP3 Gene and Protein Expression Levels

Several unique features of UCP3, and other UCPs, complicate analysis of their expression patterns. These features are most evident for UCP2, which is regulated on multiple levels: transcriptional, translational and posttranslational (Donadelli et al., 2014). An upstream open-reading frame (uORF) regulates translation of UCP2 and is only overcome in the presence of glutamine (Hurtaud et al., 2006, 2007). This leads to a strong discrepancy between protein and mRNA expression (Pecqueur et al., 2001; Rupprecht et al., 2012, 2014), making evaluation of protein levels very important for understanding of protein’s function. UCP3 and UCP5 also possess this type of uORF (Pecqueur et al., 2001). Although the discrepancy between UCP3 and *ucp3* expression levels is less obvious (Hilse et al., 2016b), it should be considered. UCP5 expression seems to be below the detection level of western blot sensitivity. Furthermore, the ratio of UCP5 mRNA to the housekeeping gene GAPDH is very low compared to UCP2/GAPDH or UCP4/GAPDH (Rupprecht et al., 2014; Smorodchenko et al., 2017).

### Unusually Short Lifetime of UCP3

The half-life of most mitochondrial inner-membrane proteins is approximately 12 days in liver mitochondria (Brunner and Neupert, 1968). UCP3 and UCP2 share an unusually short half-life of approximately 30 min (Rousset et al., 2007; Azzu et al., 2010). In contrast to UCP1, which has a half-life of 30 h (Puigserver et al., 1992), both UCP3 and UCP2 are quickly degraded by the cytosolic proteasome (Azzu and Brand, 2010). This feature allows a very rapid adjustment of protein levels. Therefore, evaluation of data based only on RNA expression should be assessed with caution.



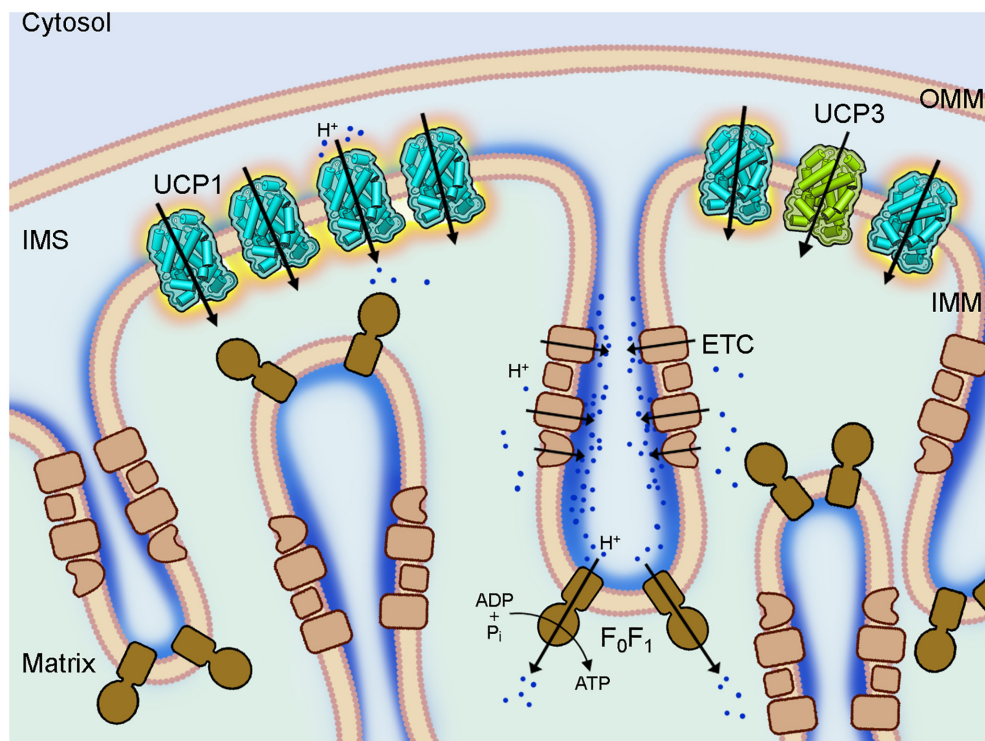


**FIGURE 1 |** Coupling and uncoupling in mitochondria of brown adipose tissue. A section of a brown fat mitochondrion with outer mitochondrial membrane (OMM), intermembrane space (IMS) and cristae of the inner mitochondrial membrane (IMM) is shown. The complexes of the electron transport chain (ETC, beige) shuttle protons (dark blue) across the IMM and create a proton gradient, which conserved energy drives the ATP synthesis by the ATP synthase ( $F_0F_1$ , brown) in the cristae. Uncoupling protein 1 (UCP1, light blue), which is largely present in brown fat mitochondria IMM short-circuits the coupling of ETC and  $F_0F_1$  by mediating a proton leak and dissipating the conserved energy as heat. The homologous UCP3 (green) with a similar proton transport activity is also present in the IMM but at much lower amount and its biological function is still unknown.

### Poor Specificity of Commercial Antibodies Against Uncoupling Proteins

A serious issue contributing to divergent results regarding expression patterns of uncoupling proteins in general, and UCP3 in particular, is high homology within the UCP subfamily (Figure 2A and Table 1). Moreover, homology between UCPs and other mitochondrial carriers is approximately 20% and molecular weights vary between only 30 and 36 kDa for most carriers (Table 1). This considerably hampers the design and evaluation of specific antibodies.

Full-length proteins are rarely used as immunogen because of high levels of homologous sequences between mitochondrial membrane proteins and difficulties with production of pure and correctly folded protein in sufficient amounts. Thus, antibodies are typically produced against a specific peptide from the target protein (Smorodchenko et al., 2009; Hilse et al., 2016b). This requires selection of a sequence that (i) shows the lowest homology to other proteins, (ii) has low hydrophobicity and is, therefore, not located in the membrane. Most antibodies against UCPs that are commercially available and/or used in studies are polyclonal. The documented antibody specificity to the target peptide is not sufficient for its proper evaluation. As a positive control, use of the full recombinant protein or tissue/cells with known prominent UCP3 expression (see section below) is

crucial. Importantly, additional validation is required showing that the antibody does not detect other proteins. Cells or tissues from corresponding knockout (KO) mice or cellular knockdown models are the best choice for negative controls. Additionally, glutamine deprivation decreases UCP2 protein level and can be used as a negative control for antibody evaluation (Zimmermann et al., 2017; Rupprecht et al., 2019). Unfortunately, no such controls have been identified for UCP3.

The Ricquier group demonstrated poor specificity of commercially available antibodies in 2001 (Pecqueur et al., 2001). Unfortunately, antibody specificity and evaluation prior to use have not improved during the subsequent years, largely contributing to the confusion surrounding expression patterns and functions of UCP, particularly UCP3.

### Expression Pattern of UCP3 at Protein Level

The general consensus is that UCP3 protein expression is limited to skeletal muscles (SkM), heart, BAT and BrAT. Increased levels of UCP3 observed in WAT of mice housed at room temperature (Shabalina et al., 2013; Hilse et al., 2016b) are thought to originate from BrAT. Relative UCP3 abundance between tissues seems to depend strongly on the investigated

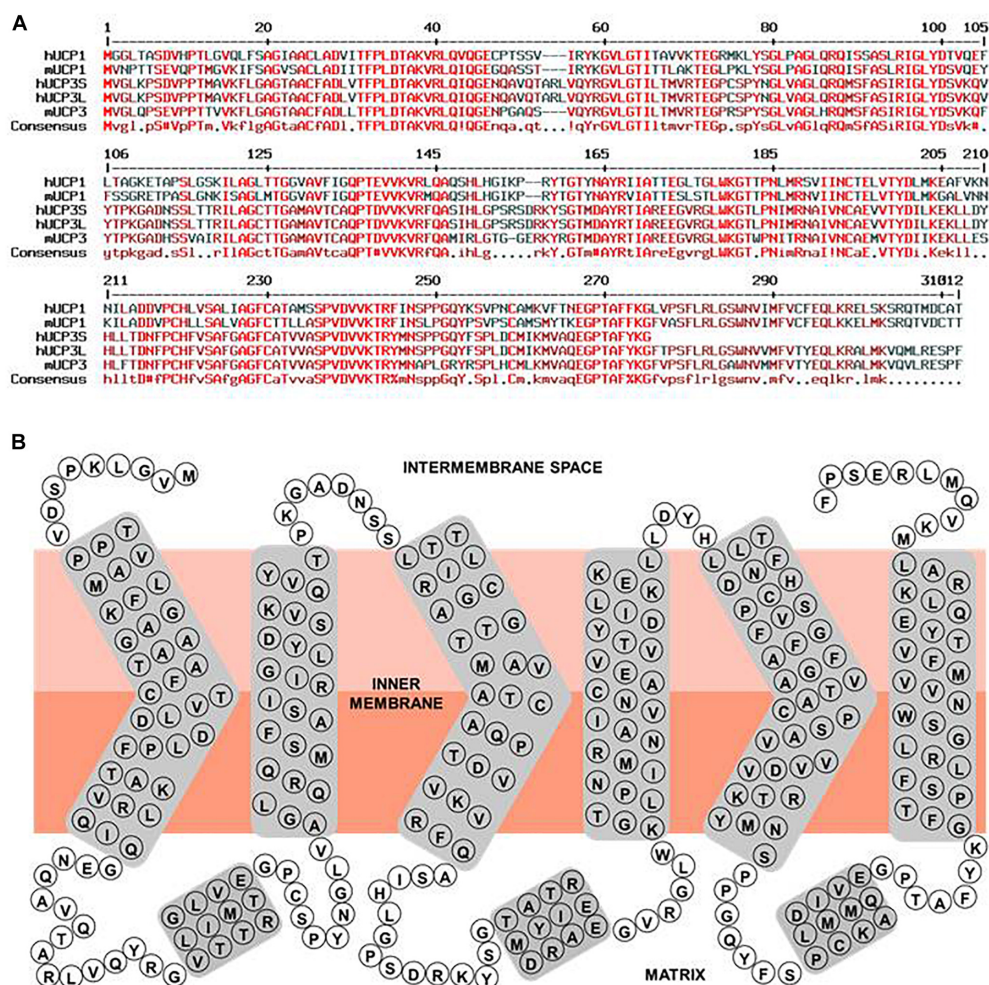


**FIGURE 2 |** Human UCP3 primary sequence characteristics. **(A)** Multiple sequence alignment of hUCP1, hUCP3S, hUCP3L, mUCP1, and mUCP3. Amino acid sequences of human UCP1 (NP\_068605.1), mouse UCP1 (NP\_033489.1), human UCP3 short isoform (NP\_073714.1), human UCP3 long isoform, and mouse UCP3 (NP\_033490.1) were compared with respect to homology using “Multiple sequence alignment with hierarchical clustering” (Corpet, 1988). Red, dark red and black colored residues indicate homologous, similar and different residues between the proteins, respectively. **(B)** Simple scheme of the structure of the human UCP3 long isoform based on its homology to ANT and ANT crystallographic structure (Pebay-Peyroula et al., 2003).

species. UCP3 quantification in mouse tissues using recombinant protein revealed that BAT contains eight times more UCP3 than any SkM under physiological conditions (Hilse et al., 2016b).

UCP3 levels are much lower than those of UCP1 but are comparable to other mitochondrial carriers. Except for adenine nucleotide translocator (ANT, AAC) and UCP1, all members of the SLC25 family are present at concentrations less than 20 pmol/mg of total protein (Palmieri, 2013). Quantitative analysis based on western blot using recombinant protein for calibration revealed that UCP3 is present at 15.0, 1.7, 1.1, and 2.7 pmol/mg protein in BAT, gastrocnemius muscle, scapular muscle and heart, respectively (Hilse et al., 2016b). At 15.0 pmol/mg protein, maximal levels of UCP2 were detected in stimulated T-cells (Rupprecht et al., 2012). In contrast, UCP1 is present in BAT of mice not adapted to cold at nearly 4 nmol/mg protein, being 400-fold more abundant than UCP3 (Hilse et al., 2016b). Consequently, only UCP1 can be purified

from tissue, whereas UCP3 and other mitochondrial carriers are typically overexpressed in heterologous systems, such as *E. coli*, yeast, mammalian cells, insects, etc. for further investigation in biomimetic systems (Hirschberg et al., 2011).

## UCP3 Abundance and Fatty Acid Oxidation – A New Concept

Analysis of UCP3 protein expression pattern in mice (BAT >> heart > muscles) implies that its presence correlates with a definite type of cellular metabolism – FA  $\beta$ -oxidation (FAO). BAT mitochondria have a high capacity for utilizing free long-chain FA as a substrate for  $\beta$ -oxidation (Cannon and Nedergaard, 2004). Although both, FA and glucose can be used for immediate energetic supply, FAs from internal stores are preferentially used (Bargut et al., 2016). In contrast, SkM use glucose/glycogen in a resting state and during short

**TABLE 1** | Homology of human mitochondrial transporters.

Protein name	MW (kDa)	Homology (%)								
		UCP1	UCP2	UCP3	UCP4	UCP5	UCP6	DIC	OGC	ANT1
UCP1	33.0	100	59	59	32	34	35	34	33	23
Slc25a7										
UCP2	33.2	59	100	72	34	38	38	37	33	29
Slc25a8										
UCP3	34.2	59	72	100	35	37	38	37	34	26
Slc25a9										
UCP4	36.1	32	34	35	100	40	39	29	31	23
Slc25a27										
UCP5 (BMCP1)	40.1	34	38	37	40	100	80	30	38	30
Slc25a14										
UCP6 (KMCP1)	32.5	35	38	38	39	80	100	31	35	28
Slc25a30										
DIC	32.1	34	37	37	29	30	31	100	38	28
Slc25a10										
OGC	34.1	33	33	34	31	38	35	38	100	25
Slc25a11										
ANT1	33.1	23	29	26	23	30	28	28	25	100
Slc25a4										
CIC	34.0	25	27	26	20	24	24	27	26	23
Slc25a1										
PiC	40.1	26	24	26	26	24	21	26	24	23
Slc25a3										
CAC	32.9	28	28	28	26	25	26	23	24	24
Slc25a20										
GC1	34.5	26	25	25	21	27	26	24	24	24
Slc25a22										
AGC1 (Aralar)	74.8	29	27	27	25	28	28	26	29	30
Slc25a12										
APC2	52.4	26	31	30	22	28	31	27	26	28
Slc25a23										

activity, whereas they break down lipids and even proteins during prolonged exercise (Egan and Zierath, 2013). Indeed, increased UCP3 mRNA in response to prolonged muscular contraction has been reported by several groups (Cortright et al., 1999; Zhou et al., 2000). At protein level, UCP3 was also proposed to be positively affected by exercise (Zhou et al., 2000; Ljubicic et al., 2004).

The correlation between UCP3 levels and degree of FAO was investigated in murine heart (Hilse et al., 2018). This model has the advantage that cardiomyocyte metabolism gradually changing at different stages of maturity from predominantly glycolysis in embryonic heart to FAO in adult hearts (Lopaschuk and Jaswal, 2010). Notably, both UCP3 abundance and dominance of FAO reach a maximum in 2 months old mice and decline again in old mice that increasingly utilize carbohydrates.

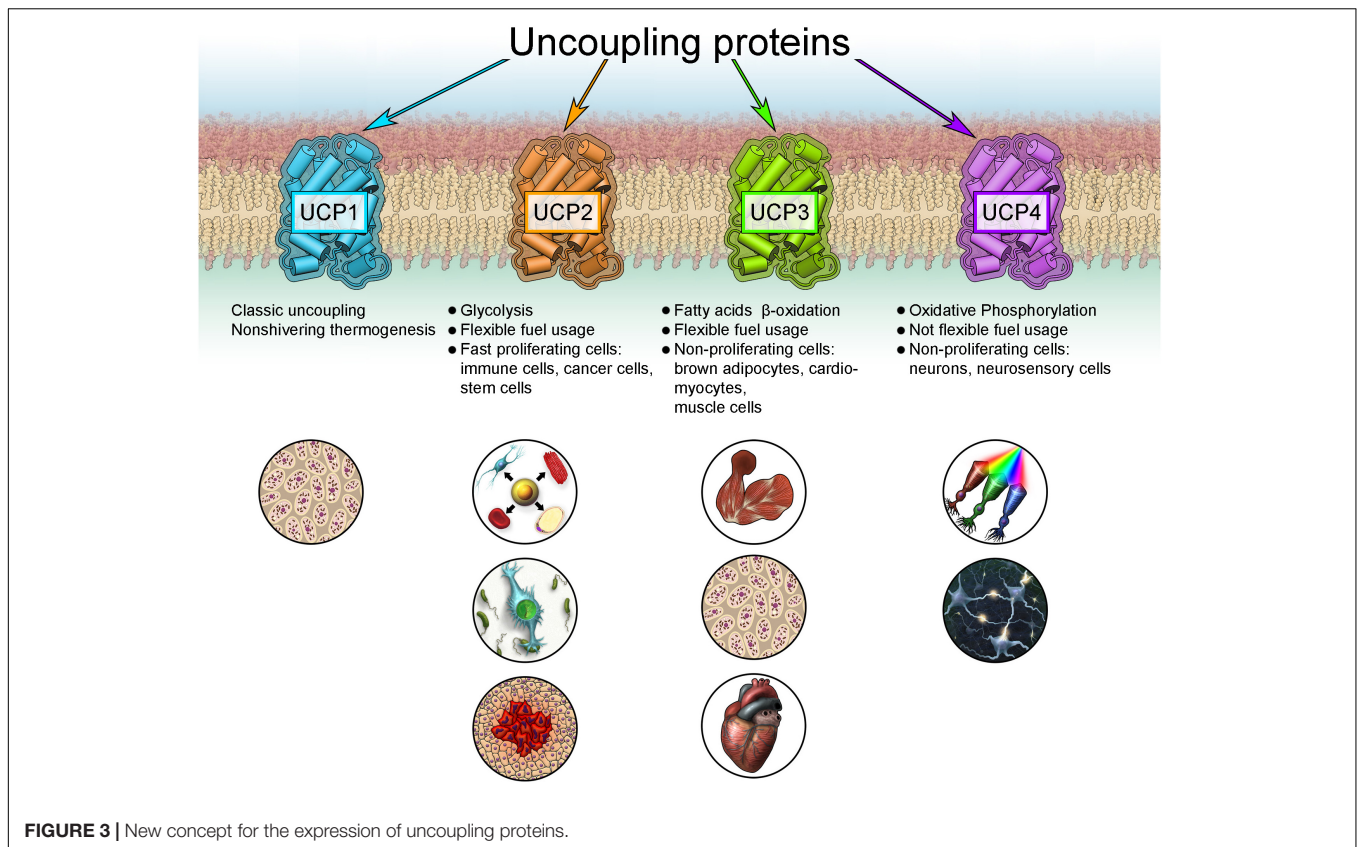
Increases in *ucp3* gene expression, which are induced by augmented lipid levels in blood plasma, e.g., during fasting/starvation, high fat diet (HFD), cold exposure (Matsuda et al., 1997; Millet et al., 1997; Cadenas et al., 1999) and after direct FA supply (Weigle et al., 1998), further support the correlation between FAO and UCP3 abundance. At the protein level, UCP3 was characterized under HFD conditions, revealing a 2.5-fold increase in UCP3 in the heart of wild type (wt) mice fed with HFD

(Boudina et al., 2012). Increased abundance of skeletal muscle UCP3 protein was also shown in mice under caloric restriction (Bevilacqua et al., 2005), implying again that UCP3 is sensitive to increased lipid levels in the blood independently of lipid origin (exogenous or endogenous).

FAO-dependent UCP3 expression fits into the new concept of cell metabolism-specific UCP expression, originally proposed for UCP2 and UCP4 (Rupprecht et al., 2014). UCP2 is primarily identified in cells with high synthetic and proliferative activity, such as pluripotent stem, cancer and immune cells, including microglia in the brain (Figure 3). These cells support their metabolism mainly by aerobic glycolysis. This cell and tissue distribution is further supported by several studies using validated UCP2 antibodies (Pecqueur et al., 2001, 2009; Yu et al., 2013). In contrast, UCP4 protein is abundant in highly active cells with low proliferation potential that rely on a stable supply of glucose, such as neurons and neurosensory cells (Mao et al., 1999; Liu et al., 2006; Smorodchenko et al., 2009, 2011, 2017; Rupprecht et al., 2014).

Because the preferred metabolism of most cells and tissues depends on many physiological conditions that may change under pathological conditions, this concept may partly explain controversial reports concerning UCP expression, particularly





for UCP2 in brain, heart, etc. During inflammation or allergic reaction, activated lymphocytes or mast cells massively invade the affected organ, potentially yielding false positive results for expression of UCP2 in inflamed organs (Smorodchenko et al., 2017). It was shown that UCP2 is highly abundant in embryonic heart and during early stages of heart development, coinciding with the glycolytic type of cardiomyocyte metabolism (Hilse et al., 2018). The ubiquitous presence of UCP2 mRNA may be required for rapid protein production to adapt to changing metabolic conditions, for instance, facilitating rapid proliferation in activated immune and cancer cells (Rupprecht et al., 2012, 2014).

## TRANSPORT FUNCTION OF UCP3 AND ITS REGULATION

### Short Description of UCP3 Structure

To date, only the 3D crystallographic structure of adenine nucleotide translocase (ANT) has been solved among all mitochondrial carriers (Pebay-Peyroula et al., 2003). The NMR structure of UCP2 obtained in the presence of dodecylphosphocholine (Berardi et al., 2011) is under discussion with regard to its physiological relevance (Zoonens et al., 2013). The structures of other mitochondrial carriers have been modeled based on their homology to the ANT (Table 1).

UCP3 is a typical mitochondrial carrier with a 312 amino acid peptide chain in mouse, arranged in six transmembrane

domains that are connected by three long matrix loops and two shorter intermembrane (IMS) space loops (Figure 2B). N- and C-termini are located in the IMS. The protein displays a tripartite structure. Each part is composed of two transmembrane helices joined by a matrix loop comprising approximately 100 amino acids with the highly conserved mitochondrial carrier motif PX[D/E]XX[K/R]. UCP3 has 59% homology to UCP1 (Table 1). Two splice variants of UCP3 have been discovered in human (Solanes et al., 1997). The long form has a length of 312 amino acids (aa) and a molecular weight (MW) of 34.2 kDa. The short isoform is missing sixth helices. It has a length of 275 amino acids and MW = 29.8 kDa. The relevance of splice variants is still uncertain.

### Fatty Acid-Activated Proton Transport Is a Function of UCP3 Verified in Biomimetic Systems

Whereas measurements of the enhanced proton leak led directly to the discovery of UCP1 (Nicholls, 2017), the conclusion about UCP3 proton-transporting function was first derived from measurements of mitochondrial potential,  $\Phi_m$ , in yeast overexpressing UCP3 (Gong et al., 1997). This result was questioned in studies employing KO mice and isolated mitochondria (Thompson and Kim, 2004; Lombardi et al., 2010; Nabben et al., 2011b; Georgiadi et al., 2012; Lee et al., 2013).

Direct proof for UCP3's ability to transport protons in the presence of FA was obtained in biomimetic systems – liposomes



and planar bilayer membranes (Zackova et al., 2003; Macher et al., 2018).  $H^+$  transport rate of reconstituted recombinant UCP3 (2.6/s; Macher et al., 2018) was similar to UCP2 (4.5/s; Beck et al., 2007) but was fivefold lower than that of UCP1 (13.5/s; Urbankova et al., 2003). The difference between UCP1 and UCP3 would only be relevant at high protein concentrations, such during cold acclimation. Proton transport rates estimated for UCP1 using other models range from 1 to 700/s (reviewed in Hirschberg et al., 2011).

It was directly shown both in isolated mitochondria (reviewed in Ricquier, 2017) and in reconstituted systems (Urbankova et al., 2003; Klingenberg, 2017) that UCP1-mediated proton transport is activated only in the presence of free long-chain FA. Indirect evidence is obtained from experiments with UCP3 KO mice, showing a lack of effect on basal proton conductance of isolated mouse mitochondria (Cadenas et al., 2002). In mitochondrial membranes, free FAs are produced by PLA2 from phospholipids in sufficient amounts to activate UCPs (Jezek et al., 2015). In the venous blood, free FA concentrations vary from  $\sim 0.25$ – $3.0$  mmol/l, depending on food supply and exercise. Their levels significantly increase under pathological conditions, such as obesity and diabetes (Hamilton and Kamp, 1999) or locally. Typically, saturated FAs (myristic, palmitic, stearic) are added in micromolar concentrations to mitochondria to activate UCP1-UCP3 to avoid interference with cellular pathways or FA oxidation. Direct comparison of UCP3 activation in response to different FAs comes from experiments using biomimetic systems (Zackova et al., 2003; Macher et al., 2018). Activation efficiency increases with increased FA unsaturation and chain length in the order of palmitic < oleic < eicosatrienoic < linoleic < retinoic < arachidonic acids as shown for UCP1 and UCP2 (Zackova et al., 2003; Beck et al., 2007). The strongest activation for UCP3 was obtained in the presence of arachidonic acid (Macher et al., 2018).

Several other molecules have been proposed as direct activators of UCP1 and UCP3 (for review Crichton et al., 2017). However, reports that coenzyme Q10, superoxide and  $H_2O_2$  activate these proteins in the absence of free FAs have not been confirmed (Jaburek and Garlid, 2003; Esteves et al., 2004; Lombardi et al., 2008).

The lipid oxidation products hydroxynonenal (HNE) and oxononenal (ONE) do not activate UCPs directly but strongly enhance the proton transport (Malingriaux et al., 2013; Jovanovic et al., 2015) if directly added to the UCP reconstituted in bilayer membrane in the presence of FA (this situation corresponds to local production of reactive aldehydes under oxidative stress). Interestingly, this effect was only recorded if membranes contained phosphatidylethanolamine (PE). The formation of HNE-PE and ONE-PE adducts, but not direct binding to the positively charged amino acids of the protein, was responsible for this effect (Jovanovic et al., 2015).

Interaction of UCP3 with HNE was investigated in SkM and heart in connection with its putative ROS-regulating role (Echtay et al., 2003; Aguirre and Cadenas, 2010; Nabben et al., 2011b; Lopez-Bernardo et al., 2015). No consensus has been achieved on whether HNE directly influences UCP3 and UCP2 activity. Our own results demonstrated that HNE added to UCP2-expressing

neuroblastoma cells leads to decreased mitochondrial potential. The latter, however, does not depend on the presence of UCP2 (Zimmermann et al., 2017). ROS regulation can also occur indirectly via reversible glutathionylation on cysteine residues in UCP3 (Mailloux et al., 2011).

Transmembrane potential,  $\Phi_m$  is an important factor for UCP activation. Protein activity in the presence of FA increases non-linearly at physiologically relevant potentials 130–220 mV (Rupprecht et al., 2010), implying that  $\Phi_m$  is crucial for regulation of UCP-mediated proton leak at constant free FA levels. Recent research revealed that UCPs are very sensitive to alteration of physico-chemical membrane parameters, such as surface potential and membrane fluidity (Malingriaux et al., 2013; Jovanovic et al., 2015). Interestingly, alteration of dipole potential in the presence of phloretin (Pohl, 2005) did not affect the proton activity of UCP1 (Jovanovic et al., 2015).

Conductance of membranes reconstituted with FA and UCP strongly depends on pH. The  $pK_a$  of the FA carboxyl group depends on FA structure and shifts from approximately 4.75 to 6.5–7.5 upon FA incorporation in the membrane (Hamilton, 1998; Pohl et al., 2008; Pashkovskaya et al., 2018). Maximum UCP activity was measured at pH values that coincide with  $pK_a$  values of the activating FA (Rupprecht et al., 2010).

## Putative Mechanisms of UCP3-Mediated Proton Transport

It is still unclear how FAs activate the protonophoric activity of UCPs. Although the discussion is mainly based on experiments performed with UCP1, the conclusions are typically extended to UCP3.

Basically, all existing models can be divided in two groups according to the roles attributed to FA and UCP (**Figure 4**). The *fatty acid cycling* hypothesis, introduced by Garlid et al. (1998) and Skulachev (1991), regards the protein as an anion transporter. Proton transport is performed by FA in its neutral form through a so-called “flip-flop” mechanism (Kamp and Hamilton, 1992). This concept is in agreement with classification of UCPs as mitochondrial anion transporters. Classical support for this hypothesis comes from experiments with sulfonated FA homologs, which cannot be protonated and therefore do not activate UCP1 (Garlid et al., 1996) or UCP2 (Berardi and Chou, 2014). The dependence of  $H^+$  transport rate on FA saturation, FA chain length (Beck et al., 2007) and fluidity of the membrane (Jovanovic et al., 2015) indicates that  $FA^-$  transport likely occurs at the protein-lipid interface.

In the second group of hypotheses (**Figure 4**) UCPs (mainly discussed for UCP1) are regarded as proton transporters that function in complex with FAs. The *FA buffering* model (for review Klingenberg, 2017) postulates that FAs bind in the protein cavity that makes their carboxyl groups available for protons to translocate from the IMS to the mitochondrial matrix through the channel (Klingenberg and Huang, 1999; Klingenberg, 2010). The recently proposed *FA shuttle* model may be regarded as a modification. It states that FA anion binds inside the pore from the cytosolic side of UCP1 and transfers protons by shuttling from the cytosolic to matrix side (for review Bertholet and

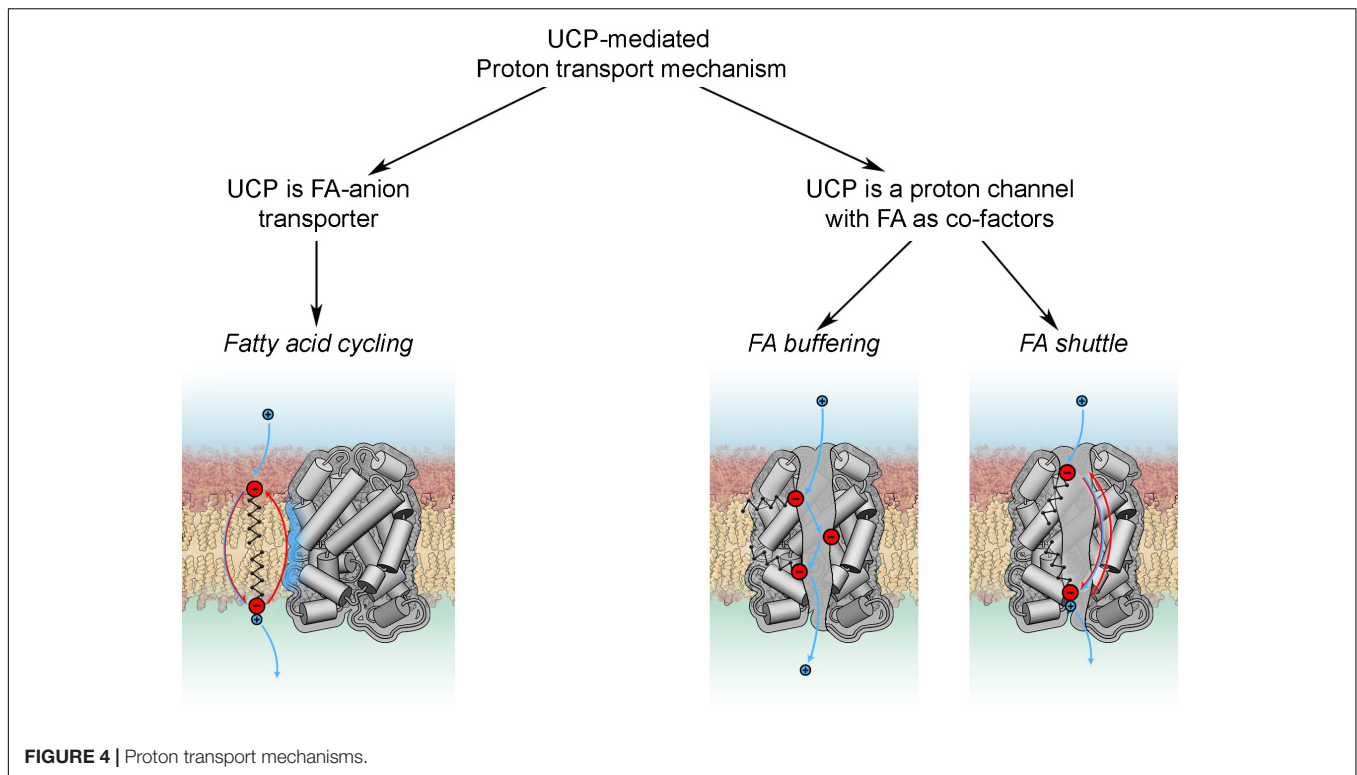


**FIGURE 4 |** Proton transport mechanisms.

Kirichok, 2017). This model is based on the inability of UCP1 to bind FAs on the matrix side, which was demonstrated in patch-clamp experiments on mitoplasts (Fedorenko et al., 2012). This contradicts the well-established view that FA binding to protein occurs from the matrix side. A further shortcoming of this model is the assumption that hydrophobic interaction of FA with the protein is much stronger than with membrane lipids. Several experiments, such as the addition of alkylsulfonates and establishment of a FA gradient, cannot be unambiguously interpreted in favor of the FA shuttle model, as comprehensively discussed in Jezek et al. (2018). Both models, FA buffering and FA shuttle, fail to explain the dependency of UCP proton transport rates on FA structure (Zackova et al., 2003; Beck et al., 2007) and membrane fluidity (Beck et al., 2007).

### Comparison of UCP1 and UCP3 Inhibition by Purine Nucleotides (PN)

It is generally accepted that the protonophoric activity of UCP1 and UCP3 is inhibited by PN. The mechanism of UCP1 inhibition was proposed by Garlid's and Klingenberg's groups 20 years ago (Modriansky et al., 1997; Klingenberg, 2010). Three arginine residues, R84\*, R183\*, and R277\*, located in the UCP1 funnel, were postulated to be crucial for the interaction with the PN phosphate groups and protein inhibition. According to this model, PN binding to UCP1 occurs in three steps: (1) the  $\beta$ -phosphate of PN binds to R183\* to form the loose conformation; (2) either the  $\gamma$ -phosphate (ATP, GTP) or  $\beta$ -phosphate (ADP, GDP) binds to R84\* to generate a tight conformation, and finally, (3)

$\alpha$ -phosphate binds to R277\*, triggering protein conformational change and inhibition. Thus, binding strengths and inhibition of di- and triphosphates were supposed to be identical, while monophosphates are unable to bind.

Recently, we compared binding forces between different nucleotides and UCP1-UCP3 at the single molecule level using a combination of recognition imaging and force spectroscopy (Koehler et al., 2017). We revealed that bond lifetimes of both mUCP3-PN and mUCP1-PN interactions decreased in proportion to the degree of PN phosphorylation. These results are in agreement with the overall strength of PN inhibition that decreases in the order ATP > ADP > AMP in electrophysiological experiments (Macher et al., 2018).

For the first time, the combination of recognition and force modes of atomic force microscopy (AFM) (Koehler et al., 2017) have allowed estimation of the depth of the nucleotide binding side from the membrane surface. It was shown to be 1.27 nm (Zhu et al., 2013). Nucleotides were able to bind to UCP1 from both the intermembrane and matrix sides. However, only binding from the intermembrane side led to protein inhibition. This finding explains why UCPs may still exhibit protonophoric activity, even at high PN concentrations permanently present in the mitochondria.

We demonstrated that UCP3 reconstituted in bilayer membranes is completely inhibited by all PNs, regardless of phosphorylation, but IC<sub>50</sub> increases as phosphorylation decreases. This contradicts the previous assumption that diphosphate-PNs are the most potent inhibitors of UCP3 (Echtay et al., 1999; Zackova et al., 2003). However, observations of UCP3 helical content using circular dichroism (CD) (Ivanova

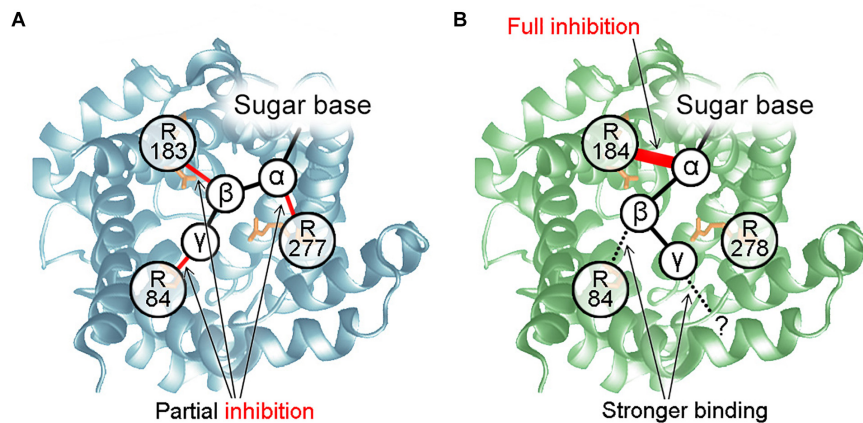


**FIGURE 5 |** Mechanisms of UCP-PN interaction and inhibition. **(A)** PN inhibition mechanism for UCP1. The  $\alpha$ -,  $\beta$ -, and  $\gamma$ -phosphate of PNs bind to R277, R183, and R84, respectively. R84 does not interact with the  $\beta$ -phosphate of diphosphate-PNs. The three P-R bonds additively contribute to maximum inhibition but interact independently. None of them is essential for inhibition or PN binding. **(B)** Mechanism of UCP3 inhibition by PNs. R184 and R84 bind to the  $\alpha$ - and  $\beta$ -phosphate of PNs. Interaction between R184 and the PN  $\alpha$ -phosphate is essential for protein inhibition and may induce a conformational change. Interaction of R84 with the  $\beta$ -phosphate increases binding strength. Instead of R278, another residue is proposed to be a part of the UCP3 PN-binding-pocket, which binds to the  $\gamma$ -phosphate of PN.

et al., 2010) support that triphosphate-PNs exert the strongest effect on UCP1/UCP3 conformation. Experiments with mutated arginines allowed us to propose a mechanism for UCP3 inhibition (Figure 5). It postulates that the interaction between R183 and  $\alpha$ -phosphate of PN is essential for UCP3 inhibition and, by itself, causes full inhibition. The  $IC_{50}$  of inhibition is further decreased by bond formation between arginines and PN  $\beta$ - and  $\gamma$ -phosphates. In contrast to its important role in UCP1 inhibition, R277 is not a part of the UCP3-PN binding-pocket. R84 interacts with the  $\beta$ -phosphate of PN, while the residue that binds the  $\gamma$ -phosphate remains unknown (Macher et al., 2018).

We also re-evaluated the mechanism of inhibition for UCP1. We first revealed that interaction between the  $\alpha$ -phosphate of AMP and arginine is sufficient for binding and partial inhibition of UCP1. We further proposed that each arginine-phosphate interaction contributes equally and additively to maximum inhibition, resulting in complete inhibition in the case of three interactions ( $\alpha$ -,  $\beta$ -, and  $\gamma$ - phosphates, Figure 5). In contrast, it was shown earlier, that site-directed mutagenesis of R277 completely abolishes GDP inhibition of proton transport by UCP1 (Murdza-Inglis et al., 1994).

### Other Inhibitors of UCP3

It is very likely that molecules capable of binding to the above mentioned arginines, might be putative inhibitors of UCP3. For example, genipin was described as a specific inhibitor of UCP2 (Zhang et al., 2006). Recently, we have shown that genipin also decreases the protonophoric activity of UCP1 and UCP3 (Kreiter et al., 2018). Several chromane derivatives inhibit UCP1 and UCP2 (Rial et al., 2011), but have not been tested on UCP3. Organic phosphate,  $P_i$ , decreases the activity of UCP1, UCP2, and UCP3 reconstituted in planar bilayer membranes up to 60% (Macher et al., 2018). Inhibition by  $P_i$  was independent of the presence of arginine residues in the PN-binding pocket, implying a different molecular mechanism from that of PNs.

### PUTATIVE BIOLOGICAL FUNCTIONS OF UCP3

Meanwhile UCP3 was proposed to be involved in all relevant pathophysiological states. Several studies have identified polymorphism of UCP genes that are associated with fat metabolism, obesity and diabetes (for review Jia et al., 2009).

### Conclusions From UCP3 KO Mice and Cells Overexpressing UCP3

With the creation of the UCP1 KO mouse (Enerback et al., 1997), the function of UCP1 as a molecular basis of non-shivering thermogenesis was verified. UCP1 KO mice were shown to rely on shivering for thermoregulation (Golozoubova et al., 2001). In contrast, UCP3 KO mice did not contribute to uncovering the precise function of UCP3 (Gong et al., 2000; Vidal-Puig et al., 2000). UCP3 KO mice showed no obvious phenotype or changes in general behavior compared to their wt littermates under physiological conditions. Analysis of isolated mitochondria revealed a more uncoupled state with simultaneous increase in ROS production. Despite these changes, UCP3's contribution to weight regulation, FA oxidation and non-shivering thermogenesis was not substantial. Even under challenging conditions as high-fat diet, fasting, stress, cold exposure and thyroid hormone treatment UCP3 KO mice were indistinguishable from wt littermates. Double KO mouse (UCP1/UCP3 dKO) revealed the same phenotype as a single UCP1 KO mouse (Gong et al., 2000).

Investigation the physiological role of UCP3 in skeletal muscle by challenging UCP3 KO mice did not lead to conclusive results. A protective role of UCP3 during lipotoxicity was not confirmed (Nabben et al., 2011a), but was later found to be relevant in the heart (Nabben et al., 2014). UCP3 was not required during fasting in skeletal muscle, and FA anion export occurred



independently of UCP3 (Seifert et al., 2008). In contrast, UCP3 was suggested to protect mitochondria against lipid-induced damage by transporting FA anions out of the mitochondria based on experiments involving short and long-term high-fat diet (Schrauwen et al., 2002; Costford et al., 2008).

One possible reason for the failure to detect a UCP3 KO phenotype could be the lack of a relevant trigger, as represented by cold adaptation in UCP1 KO mice. Second, it has to be considered that an organism with a complete protein KO has to adapt to modified circumstances, especially before birth. It is well known that essential life processes have several back-up pathways. The involvement of UCP3 in FA metabolism suggests a possible metabolic adaptation by preferential utilization of other metabolic pathways (e.g., glycolysis). The high homology between mitochondrial carriers, especially UCPs, has prompted a “take over” hypothesis (Nedergaard and Cannon, 2003). However, for UCP1, UCP2, and UCP3 this hypothesis was refuted (Hilse et al., 2016b). Instead, dependence of UCP3 expression on UCP1 presence has been observed (Hilse et al., 2016b).

Mouse overexpressing UCP3 (UCP3 Tg) in skeletal muscle was created in the same year as KO mouse (Clapham et al., 2000). The original Tg mice exhibited a 20-fold increase in UCP3 over normal levels. Subsequently, their phenotypic characteristics were attributed to high proton leak caused by the non-physiological levels of UCP3. Successive studies involved mice that overexpressed UCP3 in skeletal muscle at lower levels (2–3-fold greater than wt mice). This mice exhibited a hyperphagic and lean phenotype with a shift toward FA transport and oxidation (Bezaire et al., 2005). Overall analysis of these mice revealed decreased body weight, as well as epididymal white adipose tissue (eWAT) and BAT deposits. Increased insulin sensitivity and impaired tolerance to glucose provided further hints of changes occurring in the whole organism (Costford et al., 2006). Moreover, caloric restriction had a higher impact on muscle loss in UCP3 Tg than in wt mice (Estey et al., 2012). This finding suggests that UCP3 overexpression in muscle imitates strong exercise, as these tissues exhibited decreased markers of incomplete  $\beta$ -oxidation (Aguer et al., 2013), once again connecting UCP3 function to FAO.

Importantly, the ectopic and entopic overexpression of mitochondrial carriers also faces serious problems. The described changes may be caused by experimental artifacts. When ectopically overexpressed in HEK cells, the oxoglutarate carrier was shown to cause strong mitochondrial uncoupling due to incorrect assembly into the membrane (Yu et al., 2001). On the other side, if protein function is associated with a definite type of metabolism (FAO in case of UCP3), only a matching host metabolism would deliver reliable insight into UCP3 function.

## Evidences for and Against UCP3 Involvement in Thermogenesis

Because UCP1 and UCP3 are both localized in BAT and transport protons, the first idea is that the thermogenic function of UCP1 may be taken over by its “sister” protein. Due to the similarity of their proton transport rates (Urbankova et al.,

2003; Macher et al., 2018), only strongly upregulated UCP3 can substitute for UCP1 under cold acclimation conditions. However, the abundance of UCP1 increases sevenfold (Kalinovich et al., 2017), whereas UCP3 only triples its levels (Hilse et al., 2016b). Since it is nearly 400 times less abundant than UCP1, UCP3 cannot play a thermogenic role. As mentioned previously, KO of UCP3 and UCP1/UCP3 dKO did not support a thermogenic function of UCP3 (Gong et al., 2000; Vidal-Puig et al., 2000). Interestingly, the abundance of UCP3 decreases if UCP1 is knocked out (Hilse et al., 2016b), indicating a direct correlation between UCP3 and UCP1 expression. UCP3 expression in BAT, in contrast to heart and muscles, can also be induced by cold exposure, similar to UCP1. However, although UCP3 levels tripled (Hilse et al., 2016b), its levels still remained very low compared to UCP1 (128.4 ng/mg of total cellular protein) in BAT of non-cold-acclimated mice (Rupprecht et al., 2012). Notably, UCP1<sup>-/-</sup> mice revealed a decreased expression of UCP3 in BAT, which was even further decreased in response to cold exposure. In contrast, UCP3 expression in heart and skeletal tissues was unaffected by cold exposure. These observations give an important hint that specific (non-protonophoric) UCP3 transport function is only required in full functioning and activated BAT. Furthermore, a connection to the previously elucidated UCP1-independent thermogenic process (for review Kazak et al., 2015) can be denied.

Recently it was reported that both UCP1 and UCP3 are important for mammalian thermoregulation (Riley et al., 2016). Riley et al. demonstrated that noradrenaline-induced hyperthermia relays on UCP1 presence, whereas lipopolysaccharide thermogenesis requires skeletal muscle UCP3 using UCP3 KO, UCP1 KO, and UCP1/UCP3 dKO mice. This unexpected conclusion remains to be verified.

## Putative Involvement of UCP3 in ROS-Regulation

Members of the uncoupling protein family have long been hypothesized to reduce oxidative stress through mild uncoupling (Brand et al., 2004; Mailloux and Harper, 2011; Jezek et al., 2018). This hypothesis is based on UCPs' ability to transport protons, allowing for the regulation of membrane potential dependent superoxide anion generation from the electron transport chain (mild uncoupling, Skulachev, 1998). The presence of uncoupling proteins, such as UCP4, in the inner boundary membrane supports the mild uncoupling hypothesis (Klotzsch et al., 2015). In particular, UCP2 and UCP3 are often described as regulators of ROS (Krauss et al., 2005). ROS play a regulatory role in several cellular processes or lead to oxidative stress and damage. ROS are discussed in the regulation of the thermogenesis (Chouchani et al., 2017). Increased ROS was observed in both UCP3 KO (Vidal-Puig et al., 2000) and UCP3 Tg mice (Nabben et al., 2008). In the heart, UCP3 is described as cardioprotective because of its suggested anti-oxidative function (Cadenas, 2018). The hypothesis concerning the anti-oxidative function of UCP3 is controversially discussed (Shabalina and Nedergaard, 2011). The main arguments against this hypothesis are (i) the confinement of UCP3 to limited tissues and (ii)



the missing correlation between UCP3 expression and ROS production. No correlation of UCP3 levels with the expression of respiratory chain complexes, the main source of ROS, was found (Hilse et al., 2018). This renders the involvement of UCP3 in ROS regulation doubtful. Of note, mild uncoupling can also be mediated by other mitochondrial carriers, e.g., ANT (Andreyev et al., 1989).

### UCP3 Involvement in Cell Metabolism

It is important to note that all proposed functions for UCP3 are highly dependent on cellular energy metabolism. Reduced cold tolerance in hamsters due to a lack of UCP3 was accompanied by reduced metabolic gene expression in BAT (Nau et al., 2007). Noteworthy, UCP3 gene expression is controlled by PPARs, fundamental nuclear receptors for cellular energy metabolism (Villarroya et al., 2007). FAs during fasting or HFD were shown to increase UCP3 mRNA. Our recent results demonstrated that UCP3 protein expression increases during food deprivation in all organs (BAT, He, SkM; Hilse et al., 2016a). The observed phenotype of UCP3 overexpressing mice indicates putative involvement of UCP3 in (FA) metabolism (Clapham et al., 2000; Thompson and Kim, 2004; Bezaire et al., 2005). Muscle cells overexpressing UCP3 exhibit a shift to FAO (Garcia-Martinez et al., 2001). A direct correlation between UCP3 and  $\beta$ -oxidation type of cellular metabolism was observed during heart development (Hilse et al., 2018). UCP3 expression reaches its peak with increasing density of mitochondrial cristae, appearance of lipid drops and formation of multiple connections between mitochondria and lipid drops. The role of UCP3 in FAO may be mediated by an additional transport function, e.g., FA transport into the mitochondrial matrix to support FAO. Other groups have proposed transport of FA out of the mitochondria, implying a protective role of UCP3 against triglyceride accumulation (Goglia and Skulachev, 2003; Schrauwen et al., 2006). It has to be mentioned that FAO is another source of ROS production (St-Pierre et al., 2002).

Few comparative investigations of UCP1 and UCP3 exist. One of them describes that training enhances the relationship between UCP1/UCP3 mRNA levels, which could result in higher energy efficiency, but not under a high sugar diet (de Queiroz et al., 2012). In contrast, Shabalina et al. reported that UCP3 expression in SkM increases to compensate for UCP1 KO (Shabalina et al., 2010). We recently found that UCP3 expression in BAT, which is induced by food deprivation, is diminished by knocking out UCP1. In contrast, HFD does not affect UCP3 levels although UCP1 is increased (Hilse et al., 2016a).

### Other Putative Functions

UCP3 is associated with contractile heart function (Ozcan et al., 2013; Harmanecy et al., 2015; Motloch et al., 2016). However, the electrical activity was shown to be independent from UCP3 presence (Hilse et al., 2018).

Together, UCP2 and UCP3 were suggested to regulate mitochondrial calcium uptake (Trenker et al., 2007; Waldeck-Weiermair et al., 2011). These studies

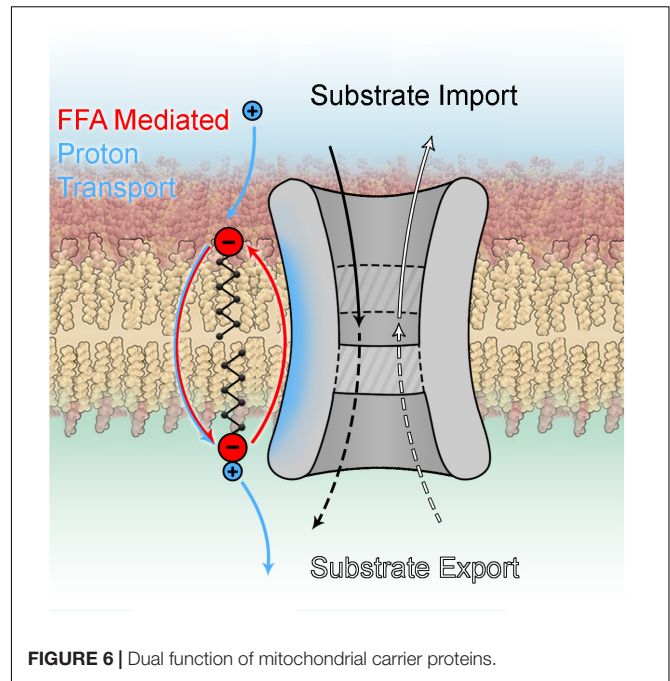


**FIGURE 6 |** Dual function of mitochondrial carrier proteins.

are controversial and have been discussed elsewhere. Direct transport was disproven (Brookes et al., 2008), but influence on calcium homeostasis by a specific metabolite transport function cannot be excluded (Bouillaud et al., 2016).

### UCP3 AS A MARKER FOR FA OXIDATION

The presence of UCP3 protein in BAT, heart and muscles, as well as its changing expression pattern during organ development, cell differentiation or physiological state (as exercising muscles), clearly reflect FAO type of the cell metabolism (Hilse et al., 2016b). This observation allows to use UCP3 as a marker for cellular metabolic state. The expression ratio of UCP3 to UCP2 might be important as a diagnostic criterion for the severity of heart failure or the degree of cardiomyocyte differentiation after stem cell transplantation (Hilse et al., 2018). Furthermore, the direct correlation of UCP1 and UCP3 expression makes UCP3 suitable as a protein marker in BAT and BrAT (Shabalina et al., 2013).

### CONCLUSION

- (1) It has been verified that UCP3 transports protons with a rate comparable to UCP1. However, it seems very likely that its protonophoric function may be additional to another as yet unknown transport function (**Figure 6**) similar to other members of this family, including the oxoglutarate carrier (Yu et al., 2001), ANT (Andreyev et al., 1989), the phosphate carrier and even UCP2 (Vozza et al., 2014). This idea was already proposed by

- Nedergaard and Cannon (2003) but did not gain much attraction due to a lack of mechanistic insight.
- (2) There are significant differences in inhibition by PN between UCP3 and UCP1. Maximum inhibition of UCP1 decreases with decreasing PN phosphorylation, while all PNs can fully inhibit UCP3. This is caused by different interaction mechanisms between PNs and arginine residues in UCP1 and UCP3. Increased free FA concentrations decrease the effect of all PNs on UCP1. In contrast, FAs affect only ATP-mediated inhibition in UCP3.
  - (3)  $P_i$  is a new inhibitor of UCP1 and UCP3 that causes partial inhibition while utilizing a mechanism distinct from that of PNs.
  - (4) UCP3 tissue distribution shows a clear dependence on cell metabolism, directly correlating with a preference for FAO. Expression of this protein is adaptive in nature, emerging short-term during metabolic

necessity. Hence, drawing conclusions about UCP3 function based solely on mRNA data is not feasible. KO models have limited potential for the exploration of UCP3 function because mice may adapt their metabolism to the existing nutrition supply.

## AUTHOR CONTRIBUTIONS

EP and AR contributed to the conceptualization and wrote the original draft. KH, AR, and especially GM contributed to the visualization. EP acquired funding. All authors reviewed and edited the draft.

## FUNDING

This work was supported by Austrian Science Fund (FWF, P25357-820 to EP).

## REFERENCES

- Aguer, C., Fiehn, O., Seifert, E. L., Bezaire, V., Meissen, J. K., Daniels, A., et al. (2013). Muscle uncoupling protein 3 overexpression mimics endurance training and reduces circulating biomarkers of incomplete beta-oxidation. *FASEB J.* 27, 4213–4225. doi: 10.1096/fj.13-234302
- Aguirre, E., and Cadenas, S. (2010). GDP and carboxyatractylate inhibit 4-hydroxynonenal-activated proton conductance to differing degrees in mitochondria from skeletal muscle and heart. *Biochim. Biophys. Acta* 1797, 1716–1726. doi: 10.1016/j.bbabi.2010.06.009
- Alan, L., Smolkova, K., Kronusova, E., Santorova, J., and Jezek, P. (2009). Absolute levels of transcripts for mitochondrial uncoupling proteins UCP2, UCP3, UCP4, and UCP5 show different patterns in rat and mice tissues. *J. Bioenergy Biomembr.* 41, 71–78. doi: 10.1007/s10863-009-9201-2
- Andreyev, A. Y., Bondareva, T. O., Dedukhova, V. I., Mokhova, E. N., Skulachev, V. P., Tsofina, L. M., et al. (1989). The ATP/ADP-antiporter is involved in the uncoupling effect of fatty acids on mitochondria. *Eur. J. Biochem.* 182, 585–592. doi: 10.1111/j.1432-1033.1989.tb14867.x
- Azzu, V., and Brand, M. D. (2010). The on-off switches of the mitochondrial uncoupling proteins. *Trends Biochem. Sci.* 35, 298–307. doi: 10.1016/j.tibs.2009.11.001
- Azzu, V., Mookerjee, S. A., and Brand, M. D. (2010). Rapid turnover of mitochondrial uncoupling protein 3. *Biochem. J.* 426, 13–17. doi: 10.1042/bj20091321
- Bargut, T. C., Aguila, M. B., and Mandarim-de-Lacerda, C. A. (2016). Brown adipose tissue: updates in cellular and molecular biology. *Tissue Cell* 48, 452–460. doi: 10.1016/j.tice.2016.08.001
- Beck, V., Jaburek, M., Demina, T., Rupprecht, A., Porter, R. K., Jezek, P., et al. (2007). Polyunsaturated fatty acids activate human uncoupling proteins 1 and 2 in planar lipid bilayers. *FASEB J.* 21, 1137–1144. doi: 10.1096/fj.06-7489com
- Berardi, M. J., and Chou, J. J. (2014). Fatty acid flippase activity of UCP2 is essential for its proton transport in mitochondria. *Cell Metab.* 20, 541–552. doi: 10.1016/j.cmet.2014.07.004
- Berardi, M. J., Shih, W. M., Harrison, S. C., and Chou, J. J. (2011). Mitochondrial uncoupling protein 2 structure determined by NMR molecular fragment searching. *Nature* 476, 109–113. doi: 10.1038/nature10257
- Bertholet, A. M., and Kirichok, Y. (2017). UCP1: a transporter for H<sup>+</sup> and fatty acid anions. *Biochimie* 134, 28–34. doi: 10.1016/j.biochi.2016.10.013
- Betz, M. J., and Enerback, S. (2018). Targeting thermogenesis in brown fat and muscle to treat obesity and metabolic disease. *Nat. Rev. Endocrinol.* 14, 77–87. doi: 10.1038/nrendo.2017.132
- Bevilacqua, L., Ramsey, J. J., Hagopian, K., Weindruch, R., and Harper, M. E. (2005). Long-term caloric restriction increases UCP3 content but decreases proton leak and reactive oxygen species production in rat skeletal muscle mitochondria. *Am. J. Physiol. Endocrinol. Metab.* 289, E429–E438.
- Bezaire, V., Spriet, L. L., Campbell, S., Sabet, N., Gerrits, M., Bonen, A., et al. (2005). Constitutive UCP3 overexpression at physiological levels increases mouse skeletal muscle capacity for fatty acid transport and oxidation. *FASEB J.* 19, 977–979. doi: 10.1096/fj.04-2765fje
- Boss, O., Samec, S., Paoloni-Giacobino, A., Rossier, C., Dulloo, A., Seydoux, J., et al. (1997). Uncoupling protein-3: a new member of the mitochondrial carrier family with tissue-specific expression. *FEBS Lett.* 408, 39–42. doi: 10.1016/s0014-5793(97)00384-0
- Boudina, S., Han, Y. H., Pei, S., Tidwell, T. J., Henrie, B., Tuinei, J., et al. (2012). UCP3 regulates cardiac efficiency and mitochondrial coupling in high fat-fed mice but not in leptin-deficient mice. *Diabetes Metab. Res. Rev.* 61, 3260–3269. doi: 10.2337/db12-0063
- Bouillaud, F., Alves-Guerra, M. C., and Ricquier, D. (2016). UCPs, at the interface between bioenergetics and metabolism. *Biochim. Biophys. Acta* 1863, 2443–2456. doi: 10.1016/j.bbamcr.2016.04.013
- Brand, M. D., Affourtit, C., Esteves, T. C., Green, K., Lambert, A. J., Miwa, S., et al. (2004). Mitochondrial superoxide: production, biological effects, and activation of uncoupling proteins. *Free Radic. Biol. Med.* 37, 755–767. doi: 10.1016/j.freeradbiomed.2004.05.034
- Brookes, P. S., Parker, N., Buckingham, J. A., Vidal-Puig, A., Halestrap, A. P., Gunter, T. E., et al. (2008). UCPs—unlikely calcium porters. *Nat. Cell Biol.* 10, 1235–1237. doi: 10.1038/ncb1108-1235
- Brunner, G., and Neupert, W. (1968). Turnover of outer and inner membrane proteins of rat liver mitochondria. *FEBS Lett.* 1, 153–155. doi: 10.1016/0014-5793(68)80045-6
- Cadenas, S. (2018). ROS and redox signaling in myocardial ischemia-reperfusion injury and cardioprotection. *Free Radic. Biol. Med.* 117, 76–89. doi: 10.1016/j.freeradbiomed.2018.01.024
- Cadenas, S., Buckingham, J. A., Samec, S., Seydoux, J., Din, N., and Dulloo, A. G. (1999). UCP2 and UCP3 rise in starved rat skeletal muscle but mitochondrial proton conductance is unchanged. *FEBS Lett.* 462, 257–260. doi: 10.1016/s0014-5793(99)01540-9
- Cadenas, S., Echta, K. S., Harper, J. A., Jekabsons, M. B., Buckingham, J. A., Grau, E., et al. (2002). The basal proton conductance of skeletal muscle mitochondria from transgenic mice overexpressing or lacking uncoupling protein-3. *J. Biol. Chem.* 277, 2773–2778. doi: 10.1074/jbc.m109736200
- Cannon, B., and Nedergaard, J. (2004). Brown adipose tissue: function and physiological significance. *Physiol. Rev.* 84, 277–359. doi: 10.1152/physrev.00015.2003

- Chondronikola, M., and Sidossis, L. S. (2018). Brown and beige fat: from molecules to physiology. *Biochim. Biophys. Acta Mol. Cell. Biol. Lipids* 1864, 91–103. doi: 10.1016/j.bbalip.2018.05.014
- Chouchani, E. T., Kazak, L., and Spiegelman, B. M. (2017). Mitochondrial reactive oxygen species and adipose tissue thermogenesis: bridging physiology and mechanisms. *J. Biol. Chem.* 292, 16810–16816. doi: 10.1074/jbc.r117.789628
- Chouchani, E. T., Kazak, L., and Spiegelman, B. M. (2019). New advances in adaptive thermogenesis: UCP1 and beyond. *Cell Metab.* 29, 27–37. doi: 10.1016/j.cmet.2018.11.002
- Clapham, J. C., Arch, J. R., Chapman, H., Haynes, A., Lister, C., Moore, G. B., et al. (2000). Mice overexpressing human uncoupling protein-3 in skeletal muscle are hyperphagic and lean. *Nature* 406, 415–418. doi: 10.1038/35019082
- Corpet, F. (1988). Multiple sequence alignment with hierarchical clustering. *Nucleic Acids Res.* 16, 10881–10890. doi: 10.1093/nar/16.22.10881
- Cortright, R. N., Zheng, D., Jones, J. P., Fluckey, J. D., DiCarlo, S. E., Grujic, D., et al. (1999). Regulation of skeletal muscle UCP-2 and UCP-3 gene expression by exercise and denervation. *Am. J. Physiol.* 276, E217–E221.
- Costford, S. R., Chaudhry, S. N., Crawford, S. A., Salkhordeh, M., and Harper, M. E. (2008). Long-term high-fat feeding induces greater fat storage in mice lacking UCP3. *Am. J. Physiol. Endocrinol. Metab.* 295, E1018–E1024.
- Costford, S. R., Chaudhry, S. N., Salkhordeh, M., and Harper, M. E. (2006). Effects of the presence, absence, and overexpression of uncoupling protein-3 on adiposity and fuel metabolism in congenic mice. *Am. J. Physiol. Endocrinol. Metab.* 290, E1304–E1312.
- Crichton, P. G., Lee, Y., and Kunji, E. R. (2017). The molecular features of uncoupling protein 1 support a conventional mitochondrial carrier-like mechanism. *Biochimie* 134, 35–50. doi: 10.1016/j.biochi.2016.12.016
- Cypess, A. M., Lehman, S., Williams, G., Tal, I., Rodman, D., Goldfine, A. B., et al. (2009). Identification and importance of brown adipose tissue in adult humans. *N. Engl. J. Med.* 360, 1509–1517. doi: 10.1056/nejmoa0810780
- de Queiroz, K. B., Rodovalho, G. V., Guimaraes, J. B., de Lima, D. C., Coimbra, C. C., Evangelista, E. A., et al. (2012). Endurance training blocks uncoupling protein 1 up-regulation in brown adipose tissue while increasing uncoupling protein 3 in the muscle tissue of rats fed with a high-sugar diet. *Nutr. Res.* 32, 709–717. doi: 10.1016/j.nutres.2012.06.020
- Donadelli, M., Dando, I., Fiorini, C., and Palmieri, M. (2014). UCP2, a mitochondrial protein regulated at multiple levels. *Cell. Mol. Life Sci.* 71, 1171–1190. doi: 10.1007/s00018-013-1407-0
- Echtay, K. S., Esteves, T. C., Pakay, J. L., Jakabsons, M. B., Lambert, A. J., Portero-Otin, M., et al. (2003). A signalling role for 4-hydroxy-2-nonenal in regulation of mitochondrial uncoupling. *EMBO J.* 22, 4103–4110. doi: 10.1093/emboj/cdg412
- Echtay, K. S., Liu, Q., Caskey, T., Winkler, E., Frischmuth, K., Bienengraber, M., et al. (1999). Regulation of UCP3 by nucleotides is different from regulation of UCP1. *FEBS Lett.* 450, 8–12. doi: 10.1016/s0014-5793(99)00460-3
- Egan, B., and Zierath, J. R. (2013). Exercise metabolism and the molecular regulation of skeletal muscle adaptation. *Cell Metab.* 17, 162–184. doi: 10.1016/j.cmet.2012.12.012
- Enerback, S., Jacobsson, A., Simpson, E. M., Guerra, C., Yamashita, H., Harper, M. E., et al. (1997). Mice lacking mitochondrial uncoupling protein are cold-sensitive but not obese. *Nature* 387, 90–94. doi: 10.1038/387090a0
- Esteves, T. C., Echtay, K. S., Jonassen, T., Clarke, C. F., and Brand, M. D. (2004). Ubiquinone is not required for proton conductance by uncoupling protein 1 in yeast mitochondria. *Biochem. J.* 379, 309–315. doi: 10.1042/bj20031682
- Estey, C., Seifert, E. L., Aguer, C., Moffat, C., and Harper, M. E. (2012). Calorie restriction in mice overexpressing UCP3: evidence that prior mitochondrial uncoupling alters response. *Exp. Gerontol.* 47, 361–371. doi: 10.1016/j.exger.2012.02.008
- Fedorenko, A., Lishko, P. V., and Kirichok, Y. (2012). Mechanism of fatty-acid-dependent UCP1 uncoupling in brown fat mitochondria. *Cell* 151, 400–413. doi: 10.1016/j.cell.2012.09.010
- Fleury, C., Neverova, M., Collins, S., Raimbault, S., Champigny, O., Levi-Meyrueis, C., et al. (1997). Uncoupling protein-2: a novel gene linked to obesity and hyperinsulinemia. *Nat. Genet.* 15, 269–272. doi: 10.1038/ng0397-269
- Garcia-Martinez, C., Sibille, B., Solanes, G., Darimont, C., Mace, K., Villarroya, F., et al. (2001). Overexpression of UCP3 in cultured human muscle lowers mitochondrial membrane potential, raises ATP/ADP ratio, and favors fatty acid vs. glucose oxidation. *FASEB J.* 15, 2033–2035. doi: 10.1096/fj.00-0828fje
- Garlid, K. D., Jaburek, M., and Jezek, P. (1998). The mechanism of proton transport mediated by mitochondrial uncoupling proteins. *FEBS Lett.* 438, 10–14. doi: 10.1016/s0014-5793(98)01246-0
- Garlid, K. D., Orosz, D. E., Modriansky, M., Vassanelli, S., and Jezek, P. (1996). On the mechanism of fatty acid-induced proton transport by mitochondrial uncoupling protein. *J. Biol. Chem.* 271, 2615–2620. doi: 10.1074/jbc.271.5.2615
- Gaudry, M. J., Campbell, K. L., and Jastroch, M. (2018). Evolution of UCP1. 251, 127–141. doi: 10.1007/164\_2018\_116
- Georgiadi, A., Boekschoten, M. V., Muller, M., and Kersten, S. (2012). Detailed transcriptomics analysis of the effect of dietary fatty acids on gene expression in the heart. *Physiol. Genomics* 44, 352–361. doi: 10.1152/physiolgenomics.00115.2011
- Goglia, F., and Skulachev, V. P. (2003). A function for novel uncoupling proteins: antioxidant defense of mitochondrial matrix by translocating fatty acid peroxides from the inner to the outer membrane leaflet. *FASEB J.* 17, 1585–1591. doi: 10.1096/fj.03-0159hyp
- Golozoubova, V., Hohtola, E., Matthias, A., Jacobsson, A., Cannon, B., and Nedergaard, J. (2001). Only UCP1 can mediate adaptive nonshivering thermogenesis in the cold. *FASEB J.* 15, 2048–2050. doi: 10.1096/fj.00-0536fje
- Gong, D. W., He, Y., Karas, M., and Reitman, M. (1997). Uncoupling protein-3 is a mediator of thermogenesis regulated by thyroid hormone, beta3-adrenergic agonists, and leptin. *J. Biol. Chem.* 272, 24129–24132. doi: 10.1074/jbc.272.39.24129
- Gong, D. W., Monemdjou, S., Gavrilova, O., Leon, L. R., Marcus-Samuels, B., Chou, C. J., et al. (2000). Lack of obesity and normal response to fasting and thyroid hormone in mice lacking uncoupling protein-3. *J. Biol. Chem.* 275, 16251–16257. doi: 10.1074/jbc.m910177199
- Haguenauer, A., Raimbault, S., Masscheleyn, S., Gonzalez-Barroso Mdel, M., Criscuolo, F., Plamondon, J., et al. (2005). A new renal mitochondrial carrier, KMCP1, is up-regulated during tubular cell regeneration and induction of antioxidant enzymes. *J. Biol. Chem.* 280, 22036–22043. doi: 10.1074/jbc.m412136200
- Hamilton, J. A. (1998). Fatty acid transport: difficult or easy? *J. Lipid Res.* 39, 467–481.
- Hamilton, J. A., and Kamp, F. (1999). How are free fatty acids transported in membranes? Is it by proteins or by free diffusion through the lipids? *Diabetes* 48, 2255–2269. doi: 10.2337/diabetes.48.12.2255
- Harmancey, R., Haight, D. L., Watts, K. A., and Taegtmeyer, H. (2015). Chronic hyperinsulinemia causes selective insulin resistance and down-regulates uncoupling protein 3 (UCP3) through the activation of sterol regulatory element-binding protein (SREBP)-1 transcription factor in the mouse heart. *J. Biol. Chem.* 290, 30947–30961. doi: 10.1074/jbc.m115.673988
- Harper, J. A., Dickinson, K., and Brand, M. D. (2001). Mitochondrial uncoupling as a target for drug development for the treatment of obesity. *Obes. Rev.* 2, 255–265. doi: 10.1046/j.1467-789x.2001.00043.x
- Harper, M. E., Dent, R., Monemdjou, S., Bezaire, V., Van Wyck, L., Wells, G., et al. (2002). Decreased mitochondrial proton leak and reduced expression of uncoupling protein 3 in skeletal muscle of obese diet-resistant women. *Diabetes Metab. Res. Rev.* 51, 2459–2466. doi: 10.2337/diabetes.51.8.2459
- Heaton, G. M., Wagenvoort, R. J., Kemp, A. Jr., and Nicholls, D. G. (1978). Brown-adipose-tissue mitochondria: photoaffinity labelling of the regulatory site of energy dissipation. *Eur. J. Biochem.* 82, 515–521. doi: 10.1111/j.1432-1033.1978.tb12045.x
- Heaton, J. M. (1972). The distribution of brown adipose tissue in the human. *J. Anat.* 112, 35.
- Hilse, K. E., Kalinovich, A. V., Rupprecht, A., Smorodchenko, A., Zeitz, U., Staniek, K., et al. (2016a). Functions of UCP1 and UCP3 in brown adipose tissue – Together or apart? *Biochim. Biophys. Acta (BBA) – Bioenerget.* 1857, e94. doi: 10.1016/j.bbabio.2016.04.186
- Hilse, K. E., Kalinovich, A. V., Rupprecht, A., Smorodchenko, A., Zeitz, U., Staniek, K., et al. (2016b). The expression of UCP3 directly correlates to UCP1 abundance in brown adipose tissue. *Biochim. Biophys. Acta* 1857, 72–78. doi: 10.1016/j.bbabio.2015.10.011
- Hilse, K. E., Rupprecht, A., Egerbacher, M., Bardakji, S., Zimmermann, L., Wolczyn, A. E. M. S., et al. (2018). The expression of uncoupling protein 3 coincides with the fatty acid oxidation type of metabolism in adult murine heart. *Front. Physiol.* 9:47. doi: 10.3389/fphys.2018.00747



- Himms-Hagen, J. (1979). Obesity may be due to a malfunctioning of brown fat. *Can. Med. Assoc. J.* 121:1361.
- Hirschberg, V., Fromme, T., and Klingenspor, M. (2011). Test systems to study the structure and function of uncoupling protein 1: a critical overview. *Front. Endocrinol. (Lausanne)* 2:63. doi: 10.3389/fendo.2011.00063
- Holloway, G. P., Jain, S. S., Bezaire, V., Han, X. X., Glatz, J. F., Luiken, J. J., et al. (2009). FAT/CD36-null mice reveal that mitochondrial FAT/CD36 is required to upregulate mitochondrial fatty acid oxidation in contracting muscle. *Am. J. Physiol. Regul. Integr. Compar. Physiol.* 297, R960–R967.
- Hurtaud, C., Gelly, C., Bouillaud, F., and Levi-Meyrueis, C. (2006). Translation control of UCP2 synthesis by the upstream open reading frame. *Cell. Mol. Life Sci.* 63, 1780–1789. doi: 10.1007/s00018-006-6129-0
- Hurtaud, C., Gelly, C., Chen, Z., Levi-Meyrueis, C., and Bouillaud, F. (2007). Glutamine stimulates translation of uncoupling protein 2 mRNA. *Cell. Mol. Life Sci.* 64, 1853–1860. doi: 10.1007/s00018-007-7039-5
- Ivanova, M. V., Hoang, T., McSorley, F. R., Krnac, G., Smith, M. D., and Jelokhani-Niaraki, M. (2010). A comparative study on conformation and ligand binding of the neuronal uncoupling proteins. *Biochemistry* 49, 512–521. doi: 10.1021/bi901742g
- Jaburek, M., and Garlid, K. D. (2003). Reconstitution of recombinant uncoupling proteins: UCP1, -2, and -3 have similar affinities for ATP and are unaffected by coenzyme Q10. *J. Biol. Chem.* 278, 25825–25831. doi: 10.1074/jbc.m302126200
- Jezek, J., Dlakova, A., Zelenka, J., Jaburek, M., and Jezek, P. (2015). H(2)O(2)-activated mitochondrial phospholipase iPLA(2)gamma prevents lipotoxic oxidative stress in synergy with UCP2, amplifies signaling via G-protein-coupled receptor GPR40, and regulates insulin secretion in pancreatic beta-cells. *Antioxid. Redox Signal.* 23, 958–972. doi: 10.1089/ars.2014.6195
- Jezek, P., Holendova, B., Garlid, K. D., and Jaburek, M. (2018). Mitochondrial uncoupling proteins: subtle regulators of cellular redox signaling. *Antioxid. Redox Signal.* 29, 667–714. doi: 10.1089/ars.2017.7225
- Jia, J. J., Zhang, X., Ge, C. R., and Jois, M. (2009). The polymorphisms of UCP2 and UCP3 genes associated with fat metabolism, obesity and diabetes. *Obes. Rev.* 10, 519–526. doi: 10.1111/j.1467-789x.2009.00569.x
- Jovanovic, O., Pashkovskaya, A. A., Annibal, A., Vazdar, M., Burchardt, N., Sansone, A., et al. (2015). The molecular mechanism behind reactive aldehyde action on transmembrane translocations of proton and potassium ions. *Free Radic. Biol. Med.* 89, 1067–1076. doi: 10.1016/j.freeradbiomed.2015.10.422
- Kalinovich, A. V., de Jong, J. M., Cannon, B., and Nedergaard, J. (2017). UCP1 in adipose tissues: two steps to full browning. *Biochimie* 134, 127–137. doi: 10.1016/j.biochi.2017.01.007
- Kamp, F., and Hamilton, J. A. (1992). pH gradients across phospholipid membranes caused by fast flip-flop of un-ionized fatty acids. *Proc. Natl. Acad. Sci. U.S.A.* 89, 11367–11370. doi: 10.1073/pnas.89.23.11367
- Kazak, L., Chouchani, E. T., Jedrychowski, M. P., Erickson, B. K., Shinoda, K., Cohen, P., et al. (2015). A creatine-driven substrate cycle enhances energy expenditure and thermogenesis in beige fat. *Cell* 163, 643–655. doi: 10.1016/j.cell.2015.09.035
- Klingenberg, M. (2010). Wanderings in bioenergetics and biomembranes. *Biochim. Biophys. Acta* 1797, 579–594. doi: 10.1016/j.bbabi.2010.02.012
- Klingenberg, M. (2017). UCP1 – A sophisticated energy valve. *Biochimie* 134, 19–27. doi: 10.1016/j.biochi.2016.10.012
- Klingenberg, M., and Huang, S. G. (1999). Structure and function of the uncoupling protein from brown adipose tissue. *Biochim. Biophys. Acta* 1415, 271–296. doi: 10.1016/s0005-2736(98)00232-6
- Klotzsch, E., Smorodchenko, A., Lofler, L., Moldzio, R., Parkinson, E., Schutz, G. J., et al. (2015). Superresolution microscopy reveals spatial separation of UCP4 and F0F1-ATP synthase in neuronal mitochondria. *Proc. Natl. Acad. Sci. U.S.A.* 112, 130–135. doi: 10.1073/pnas.1415261112
- Koehler, M., Macher, G., Rupprecht, A., Zhu, R., Gruber, H. J., Pohl, E. E., et al. (2017). Combined recognition imaging and force spectroscopy: a new mode for mapping and studying interaction sites at low lateral density. *Sci. Adv. Mater.* 9, 128–134. doi: 10.1166/sam.2017.3066
- Krauss, S., Zhang, C. Y., and Lowell, B. B. (2005). The mitochondrial uncoupling-protein homologues. *Nat. Rev. Mol. Cell Biol.* 6, 248–261. doi: 10.1038/nrm1592
- Kreiter, J., Rupprecht, A., Zimmermann, L., Fedorova, M., Moschinger, M., Rokitskaya, T. I., et al. (2018). Genipin lacks the specificity for UCP2 inhibition. *Biophys. J.* 114, 658a. doi: 10.1016/j.bpj.2017.11.3556
- Lee, M. S., Kim, I. H., and Kim, Y. (2013). Effects of eicosapentaenoic acid and docosahexaenoic acid on uncoupling protein 3 gene expression in C(2)C(12) muscle cells. *Nutrients* 5, 1660–1671. doi: 10.3390/nu5051660
- Liu, D., Chan, S. L., de Souza-Pinto, N. C., Slevin, J. R., Wersto, R. P., Zhan, M., et al. (2006). Mitochondrial UCP4 mediates an adaptive shift in energy metabolism and increases the resistance of neurons to metabolic and oxidative stress. *Neuromol. Med.* 8, 389–414. doi: 10.1385/nmm%3A8%3A3%3A389
- Ljubcic, V., Adhietty, P. J., and Hood, D. A. (2004). Role of UCP3 in state 4 respiration during contractile activity-induced mitochondrial biogenesis. *J. Appl. Physiol.* 97, 976–983. doi: 10.1152/japplphysiol.00336.2004
- Lombardi, A., Busiello, R. A., Napolitano, L., Cioffi, F., Moreno, M., de Lange, P., et al. (2010). UCP3 translocates lipid hydroperoxide and mediates lipid hydroperoxide-dependent mitochondrial uncoupling. *J. Biol. Chem.* 285, 16599–16605. doi: 10.1074/jbc.m110.102699
- Lombardi, A., Grasso, P., Moreno, M., de Lange, P., Silvestri, E., Lanni, A., et al. (2008). Interrelated influence of superoxides and free fatty acids over mitochondrial uncoupling in skeletal muscle. *Biochim. Biophys. Acta* 1777, 826–833. doi: 10.1016/j.bbabi.2008.04.019
- Lopaschuk, G. D., and Jaswal, J. S. (2010). Energy metabolic phenotype of the cardiomyocyte during development, differentiation, and postnatal maturation. *J. Cardiovasc. Pharmacol.* 56, 130–140. doi: 10.1097/fjc.0b013e3181e74a14
- Lopez-Bernardo, E., Anedda, A., Sanchez-Perez, P., Acosta-Iborra, B., and Cadenas, S. (2015). 4-Hydroxynonenal induces Nrf2-mediated UCP3 upregulation in mouse cardiomyocytes. *Free Radic. Biol. Med.* 88, 427–438. doi: 10.1016/j.freeradbiomed.2015.03.032
- Macher, G., Koehler, M., Rupprecht, A., Kreiter, J., Hinterdorfer, P., and Pohl, E. E. (2018). Inhibition of mitochondrial UCP1 and UCP3 by purine nucleotides and phosphate. *Biochim. Biophys. Acta* 1860, 664–672. doi: 10.1016/j.bbamem.2017.12.001
- Mailloux, R. J., and Harper, M. E. (2011). Uncoupling proteins and the control of mitochondrial reactive oxygen species production. *Free Radic. Biol. Med.* 51, 1106–1115. doi: 10.1016/j.freeradbiomed.2011.06.022
- Mailloux, R. J., Seifert, E. L., Bouillaud, F., Aguer, C., Collins, S., and Harper, M. E. (2011). Glutathionylation acts as a control switch for uncoupling proteins UCP2 and UCP3. *J. Biol. Chem.* 286, 21865–21875. doi: 10.1074/jbc.m111.240242
- Malingrux, E. A., Rupprecht, A., Gille, L., Jovanovic, O., Jezek, P., Jaburek, M., et al. (2013). Fatty acids are key in 4-hydroxy-2-nonenal-mediated activation of uncoupling proteins 1 and 2. *PLoS One* 8:e77786. doi: 10.1371/journal.pone.0077786
- Mao, W., Yu, X. X., Zhong, A., Li, W., Brush, J., Sherwood, S. W., et al. (1999). UCP4, a novel brain-specific mitochondrial protein that reduces membrane potential in mammalian cells. *FEBS Lett.* 443, 326–330. doi: 10.1016/s0014-5793(98)01713-x
- Matsuda, J., Hosoda, K., Itoh, H., Son, C., Doi, K., Tanaka, T., et al. (1997). Cloning of rat uncoupling protein-3 and uncoupling protein-2 cDNAs: their gene expression in rats fed high-fat diet. *FEBS Lett.* 418, 200–204. doi: 10.1016/s0014-5793(97)01381-1
- Millet, L., Vidal, H., Andreelli, F., Larrouy, D., Riou, J. P., Ricquier, D., et al. (1997). Increased uncoupling protein-2 and -3 mRNA expression during fasting in obese and lean humans. *J. Clin. Invest.* 100, 2665–2670. doi: 10.1172/jci119811
- Modriansky, M., Murdza, I. D., Patel, H. V., Freeman, K. B., and Garlid, K. D. (1997). Identification by site-directed mutagenesis of three arginines in uncoupling protein that are essential for nucleotide binding and inhibition. *J. Biol. Chem.* 272, 24759–24762. doi: 10.1074/jbc.272.40.24759
- Motloch, L. J., Gebing, T., Reda, S., Schwaiger, A., Wolny, M., and Hoppe, U. C. (2016). UCP3 regulates single-channel activity of the cardiac mCa1. *J. Membr. Biol.* 249, 577–584. doi: 10.1007/s00232-016-9913-2
- Murdza-Inglis, D. L., Modriansky, M., Patel, H. V., Woldegiorgis, G., Freeman, K. B., and Garlid, K. D. (1994). A single mutation in uncoupling protein of rat brown adipose tissue mitochondria abolishes GDP sensitivity of H<sup>+</sup> transport. *J. Biol. Chem.* 269, 7435–7438.
- Nabben, M., Hoeks, J., Briede, J. J., Glatz, J. F., Moonen-Kornips, E., Hesselink, M. K., et al. (2008). The effect of UCP3 overexpression on mitochondrial ROS production in skeletal muscle of young versus aged mice. *FEBS Lett.* 582, 4147–4152. doi: 10.1016/j.febslet.2008.11.016
- Nabben, M., Hoeks, J., Moonen-Kornips, E., van, B. D., Briede, J. J., Hesselink, M. K., et al. (2011a). Significance of uncoupling protein 3 in mitochondrial



- function upon mid- and long-term dietary high-fat exposure. *FEBS Lett.* 585, 4010–4017. doi: 10.1016/j.febslet.2011.11.012
- Nabben, M., Shabalina, I. G., Moonen-Kornips, E., van, B. D., Cannon, B., Schrauwen, P., et al. (2011b). Uncoupled respiration, ROS production, acute lipotoxicity and oxidative damage in isolated skeletal muscle mitochondria from UCP3-ablated mice. *Biochim. Biophys. Acta* 1807, 1095–1105. doi: 10.1016/j.bbabo.2011.04.003
- Nabben, M., van Bree, B. W., Lenaers, E., Hoeks, J., Hesselink, M. K., Schaart, G., et al. (2014). Lack of UCP3 does not affect skeletal muscle mitochondrial function under lipid-challenged conditions, but leads to sudden cardiac death. *Basic Res. Cardiol.* 109:447.
- Nau, K., Fromme, T., Meyer, C. W., von, P. C., Heldmaier, G., and Klingenspor, M. (2007). Brown adipose tissue specific lack of uncoupling protein 3 is associated with impaired cold tolerance and reduced transcript levels of metabolic genes. *J. Compar. Physiol. B* 178, 269–277. doi: 10.1007/s00360-007-0219-7
- Nedergaard, J., and Cannon, B. (2003). The 'novel' 'uncoupling' proteins UCP2 and UCP3: what do they really do? Pros and cons for suggested functions. *Exp. Physiol.* 88, 65–84. doi: 10.1113/eph8802502
- Nedergaard, J., Matthias, A., Golozoubova, V., Jacobsson, A., and Cannon, B. (1999). UCP1: the original uncoupling protein—and perhaps the only one? New perspectives on UCP1, UCP2, and UCP3 in the light of the bioenergetics of the UCP1-ablated mice. *J. Bioenergy Biomembr.* 31, 475–491.
- Nicholls, D. G. (2017). The hunt for the molecular mechanism of brown fat thermogenesis. *Biochimie* 134, 9–18. doi: 10.1016/j.biochi.2016.09.003
- Ozcan, C., Palmeri, M., Horvath, T. L., Russell, K. S., and Russell, R. R. III (2013). Role of uncoupling protein 3 in ischemia-reperfusion injury, arrhythmias, and preconditioning. *Am. J. Physiol. Heart Circ. Physiol.* 304, H1192–H1200.
- Palmieri, F. (2013). The mitochondrial transporter family SLC25: identification, properties and physiopathology. *Mol. Aspects Med.* 34, 465–484. doi: 10.1016/j.mam.2012.05.005
- Parascandola, J. (1974). Dinitrophenol and bioenergetics: an historical perspective. *Mol. Cell. Biochem.* 5, 69–77. doi: 10.1007/bf01874175
- Pashkovskaya, A. A. V., Vazdar, M., Zimmermann, L., Jovanovic, O., Pohl, P., and Pohl, E. E. (2018). Mechanism of long-chain free fatty acid protonation at the membrane-water interface. *Biophys. J.* 114, 2142–2151. doi: 10.1016/j.bpj.2018.04.011
- Pebay-Peyroula, E., Dahout-Gonzalez, C., Kahn, R., Trezeguet, V., Lauquin, G. J., and Brandolin, G. (2003). Structure of mitochondrial ADP/ATP carrier in complex with carboxyatractylide. *Nature* 426, 39–44. doi: 10.1038/nature02056
- Pecqueur, C., Alves-Guerra, C., Ricquier, D., and Bouillaud, F. (2009). UCP2, a metabolic sensor coupling glucose oxidation to mitochondrial metabolism? *IUBMB Life* 61, 762–767. doi: 10.1002/iub.188
- Pecqueur, C., Alves-Guerra, M. C., Gelly, C., Levi-Meyrueis, C., Couplan, E., Collins, S., et al. (2001). Uncoupling protein 2, in vivo distribution, induction upon oxidative stress, and evidence for translational regulation. *J. Biol. Chem.* 276, 8705–8712. doi: 10.1074/jbc.m006938200
- Petrovic, N., Walden, T. B., Shabalina, I. G., Timmons, J. A., Cannon, B., and Nedergaard, J. (2010). Chronic peroxisome proliferator-activated receptor gamma (PPARgamma) activation of epididymally derived white adipocyte cultures reveals a population of thermogenically competent, UCP1-containing adipocytes molecularly distinct from classic brown adipocytes. *J. Biol. Chem.* 285, 7153–7164. doi: 10.1074/jbc.m109.053942
- Pohl, E. E. (2005). Dipole potential of bilayer membranes. *Adv. Planar Lipid Bilayers Liposomes* 1, 77–100. doi: 10.1016/s1554-4516(05)01002-1
- Pohl, E. E., Voltchenko, A. M., and Rupprecht, A. (2008). Flip-flop of hydroxy fatty acids across the membrane as monitored by proton-sensitive microelectrodes. *Biochim. Biophys. Acta* 1778, 1292–1297. doi: 10.1016/j.bbame.2008.01.025
- Puigserver, P., Herron, D., Gianotti, M., Palou, A., Cannon, B., and Nedergaard, J. (1992). Induction and degradation of the uncoupling protein thermogenin in brown adipocytes in vitro and in vivo. Evidence for a rapidly degradable pool. *Biochem. J.* 284(Pt 2), 393–398. doi: 10.1042/bj2840393
- Rial, E., Rodriguez-Sanchez, L., Aller, P., Guisado, A., Mar Gonzalez-Barroso, M., Gallardo-Vara, E., et al. (2011). Development of chromanes as novel inhibitors of the uncoupling proteins. *Chem. Biol.* 18, 264–274. doi: 10.1016/j.chembiol.2010.12.012
- Ricquier, D. (2011). Uncoupling protein 1 of brown adipocytes, the only uncoupler: a historical perspective. *Front. Endocrinol. (Lausanne)* 2:85. doi: 10.3389/fendo.2011.00085
- Ricquier, D. (2017). UCP1, the mitochondrial uncoupling protein of brown adipocyte: a personal contribution and a historical perspective. *Biochimie* 134, 3–8. doi: 10.1016/j.biochi.2016.10.018
- Ricquier, D., and Kader, J. C. (1976). Mitochondrial protein alteration in active brown fat: a sodium dodecyl sulfate-polyacrylamide gel electrophoretic study. *Biochem. Biophys. Res. Commun.* 73, 577–583. doi: 10.1016/0006-291x(76)90849-4
- Riley, C. L., Dao, C., Kenaston, M. A., Muto, L., Kohno, S., Nowinski, S. M., et al. (2016). The complementary and divergent roles of uncoupling proteins 1 and 3 in thermoregulation. *J. Physiol.* 594, 7455–7464. doi: 10.1113/jp272971
- Rousset, S., Mozo, J., Dujardin, G., Emre, Y., Masscheleyn, S., Ricquier, D., et al. (2007). UCP2 is a mitochondrial transporter with an unusual very short half-life. *FEBS Lett.* 581, 479–482. doi: 10.1016/j.febslet.2007.01.010
- Rupprecht, A., Brauer, A. U., Smorodchenko, A., Goyn, J., Hilse, K. E., Shabalina, I. G., et al. (2012). Quantification of uncoupling protein 2 reveals its main expression in immune cells and selective up-regulation during T-cell proliferation. *PLoS One* 7:e41406. doi: 10.1371/journal.pone.0041406
- Rupprecht, A., Moldzio, R., Mödl, B., and Pohl, E. E. (2019). Glutamine regulates mitochondrial uncoupling protein 2 to promote glutaminolysis in neuroblastoma cells. *Biochim. Biophys. Acta (BBA) – Bioenerget.* 1860, 391–401. doi: 10.1016/j.bbabo.2019.03.006
- Rupprecht, A., Sittner, D., Smorodchenko, A., Hilse, K. E., Goyn, J., Moldzio, R., et al. (2014). Uncoupling protein 2 and 4 expression pattern during stem cell differentiation provides new insight into their putative function. *PLoS One* 9:e88474. doi: 10.1371/journal.pone.0088474
- Rupprecht, A., Sokolenko, E. A., Beck, V., Ninnemann, O., Jaburek, M., Trimbuch, T., et al. (2010). Role of the transmembrane potential in the membrane proton leak. *Biophys. J.* 98, 1503–1511. doi: 10.1016/j.bpj.2009.12.4301
- Sanchis, D., Fleury, C., Chomiki, N., Goubert, M., Huang, Q., Neverova, M., et al. (1998). BMCP1, a novel mitochondrial carrier with high expression in the central nervous system of humans and rodents, and respiration uncoupling activity in recombinant yeast. *J. Biol. Chem.* 273, 34611–34615. doi: 10.1074/jbc.273.51.34611
- Schrauwen, P., Hinderling, V., Hesselink, M. K., Schaart, G., Kornips, E., Saris, W. H., et al. (2002). Etomoxir-induced increase in UCP3 supports a role of uncoupling protein 3 as a mitochondrial fatty acid anion exporter. *FASEB J.* 16, 1688–1690. doi: 10.1096/fj.02-0275fje
- Schrauwen, P., Hoeks, J., and Hesselink, M. K. (2006). Putative function and physiological relevance of the mitochondrial uncoupling protein-3: involvement in fatty acid metabolism? *Prog. Lipid Res.* 45, 17–41. doi: 10.1016/j.plipres.2005.11.001
- Seifert, E. L., Bezaire, V., Estey, C., and Harper, M. E. (2008). Essential role for uncoupling protein-3 in mitochondrial adaptation to fasting but not in fatty acid oxidation or fatty acid anion export. *J. Biol. Chem.* 283, 25124–25131. doi: 10.1074/jbc.m803871200
- Shabalina, I. G., Hoeks, J., Kramarova, T. V., Schrauwen, P., Cannon, B., and Nedergaard, J. (2010). Cold tolerance of UCP1-ablated mice: a skeletal muscle mitochondria switch toward lipid oxidation with marked UCP3 up-regulation not associated with increased basal, fatty acid- or ROS-induced uncoupling or enhanced GDP effects. *Biochim. Biophys. Acta* 1797, 968–980. doi: 10.1016/j.bbabo.2010.02.033
- Shabalina, I. G., and Nedergaard, J. (2011). Mitochondrial ('mild') uncoupling and ROS production: physiologically relevant or not? *Biochem. Soc. Trans.* 39, 1305–1309. doi: 10.1042/bst0391305
- Shabalina, I. G., Petrovic, N., de Jong, J. M., Kalinovich, A. V., Cannon, B., and Nedergaard, J. (2013). UCP1 in brite/beige adipose tissue mitochondria is functionally thermogenic. *Cell Rep.* 5, 1196–1203. doi: 10.1016/j.celrep.2013.10.044
- Skulachev, V. P. (1991). Fatty acid circuit as a physiological mechanism of uncoupling of oxidative phosphorylation. *FEBS Lett.* 294, 158–162. doi: 10.1016/0014-5793(91)80658-p
- Skulachev, V. P. (1998). Uncoupling: new approaches to an old problem of bioenergetics. *Biochim. Biophys. Acta* 1363, 100–124. doi: 10.1016/s0005-2728(97)00091-1

- Smorodchenko, A., Rupprecht, A., Fuchs, J., Gross, J., and Pohl, E. E. (2011). Role of mitochondrial uncoupling protein 4 in rat inner ear. *Mol. Cell. Neurosci.* 47, 244–253. doi: 10.1016/j.mcn.2011.03.002
- Smorodchenko, A., Rupprecht, A., Sarilova, I., Ninnemann, O., Brauer, A. U., Franke, K., et al. (2009). Comparative analysis of uncoupling protein 4 distribution in various tissues under physiological conditions and during development. *Bba-Biomembranes* 1788, 2309–2319. doi: 10.1016/j.bbamem.2009.07.018
- Smorodchenko, A., Schneider, S., Rupprecht, A., Hilse, K., Sasgary, S., Zeitze, U., et al. (2017). UCP2 up-regulation within the course of autoimmune encephalomyelitis correlates with T-lymphocyte activation. *Biochim. Biophys. Acta* 1863, 1002–1012. doi: 10.1016/j.bbadis.2017.01.019
- Solanes, G., Vidal-Puig, A., Grujic, D., Flier, J. S., and Lowell, B. B. (1997). The human uncoupling protein-3 gene. Genomic structure, chromosomal localization, and genetic basis for short and long form transcripts. *J. Biol. Chem.* 272, 25433–25436. doi: 10.1074/jbc.272.41.25433
- Spiegelman, B. M., and Flier, J. S. (2001). Obesity and the regulation of energy balance. *Cell* 104, 531–543.
- St-Pierre, J., Buckingham, J. A., Roeback, S. J., and Brand, M. D. (2002). Topology of superoxide production from different sites in the mitochondrial electron transport chain. *J. Biol. Chem.* 277, 44784–44790. doi: 10.1074/jbc.m207217200
- Thompson, M. P., and Kim, D. (2004). Links between fatty acids and expression of UCP2 and UCP3 mRNAs. *FEBS Lett.* 568, 4–9. doi: 10.1016/j.febslet.2004.05.011
- Trenker, M., Malli, R., Fertsch, I., Levak-Frank, S., and Graier, W. F. (2007). Uncoupling proteins 2 and 3 are fundamental for mitochondrial Ca<sup>2+</sup> uniport. *Nat. Cell Biol.* 9, 445–452. doi: 10.1038/ncb1556
- Urbankova, E., Voltchenko, A., Pohl, P., Jezek, P., and Pohl, E. E. (2003). Transport kinetics of uncoupling proteins. Analysis of UCP1 reconstituted in planar lipid bilayers. *J. Biol. Chem.* 278, 32497–32500. doi: 10.1074/jbc.m303721200
- Vidal-Puig, A., Solanes, G., Grujic, D., Flier, J. S., and Lowell, B. B. (1997). UCP3: an uncoupling protein homologue expressed preferentially and abundantly in skeletal muscle and brown adipose tissue. *Biochem. Biophys. Res. Commun.* 235, 79–82. doi: 10.1006/bbrc.1997.6740
- Vidal-Puig, A. J., Grujic, D., Zhang, C. Y., Hagen, T., Boss, O., Ido, Y., et al. (2000). Energy metabolism in uncoupling protein 3 gene knockout mice. *J. Biol. Chem.* 275, 16258–16266. doi: 10.1074/jbc.m910179199
- Villarroya, F., Iglesias, R., and Giral, M. (2007). PPARs in the control of uncoupling proteins gene expression. *PPAR Res.* 2007:74364.
- Virtanen, K. A., Lidell, M. E., Orava, J., Heglind, M., Westergren, R., Niemi, T., et al. (2009). Functional brown adipose tissue in healthy adults. *N. Engl. J. Med.* 360, 1518–1525.
- Vozza, A., Parisi, G., De Leonardi, F., Lasorsa, F. M., Castegna, A., Amorese, D., et al. (2014). UCP2 transports C4 metabolites out of mitochondria, regulating glucose and glutamine oxidation. *Proc. Natl. Acad. Sci. U.S.A.* 111, 960–965. doi: 10.1073/pnas.1317400111
- Waldeck-Weiermair, M., Jean-Quartier, C., Rost, R., Khan, M. J., Vishnu, N., Bondarenko, A. I., et al. (2011). The leucine zipper EF hand-containing transmembrane protein 1 (LETM1) and uncoupling proteins- 2 and 3 (UCP2/3) contribute to two distinct mitochondrial Ca<sup>2+</sup> uptake pathways. *J. Biol. Chem.* 286, 28444–28555.
- Weigle, D. S., Selfridge, L. E., Schwartz, M. W., Seeley, R. J., Cummings, D. E., Havel, P. J., et al. (1998). Elevated free fatty acids induce uncoupling protein 3 expression in muscle: a potential explanation for the effect of fasting. *Diabetes Metab. Res. Rev.* 47, 298–302. doi: 10.2337/diab.47.2.298
- Wu, J., Bostrom, P., Sparks, L. M., Ye, L., Choi, J. H., Giang, A. H., et al. (2012). Beige adipocytes are a distinct type of thermogenic fat cell in mouse and human. *Cell* 150, 366–376. doi: 10.1016/j.cell.2012.05.016
- Yu, W. M., Liu, X., Shen, J. H., Jovanovic, O., Pohl, E. E., Gerson, S. L., et al. (2013). Metabolic regulation by the mitochondrial phosphatase PTPMT1 is required for hematopoietic stem cell differentiation. *Cell Stem Cell* 12, 62–74. doi: 10.1016/j.stem.2012.11.022
- Yu, X. X., Lewin, D. A., Zhong, A., Brush, J., Schow, P. W., Sherwood, S. W., et al. (2001). Overexpression of the human 2-oxoglutarate carrier lowers mitochondrial membrane potential in HEK-293 cells: contrast with the unique cold-induced mitochondrial carrier CGI-69. *Biochem. J.* 353, 369–375. doi: 10.1042/bj3530369
- Zackova, M., Skobisova, E., Urbankova, E., and Jezek, P. (2003). Activating omega-6 polyunsaturated fatty acids and inhibitory purine nucleotides are high affinity ligands for novel mitochondrial uncoupling proteins UCP2 and UCP3. *J. Biol. Chem.* 278, 20761–20769. doi: 10.1074/jbc.m212852000
- Zhang, C. Y., Parton, L. E., Ye, C. P., Krauss, S., Shen, R., Lin, C. T., et al. (2006). Genipin inhibits UCP2-mediated proton leak and acutely reverses obesity- and high glucose-induced beta cell dysfunction in isolated pancreatic islets. *Cell Metab.* 3, 417–427. doi: 10.1016/j.cmet.2006.04.010
- Zhou, M., Lin, B. Z., Coughlin, S., Vallega, G., and Pilch, P. F. (2000). UCP-3 expression in skeletal muscle: effects of exercise, hypoxia, and AMP-activated protein kinase. *Am. J. Physiol. Endocrinol. Metab.* 279, E622–E629.
- Zhu, R., Rupprecht, A., Ebner, A., Haselgrubler, T., Gruber, H. J., Hinterdorfer, P., et al. (2013). Mapping the nucleotide binding site of uncoupling protein 1 using atomic force microscopy. *J. Am. Chem. Soc.* 135, 3640–3646. doi: 10.1021/ja312550k
- Zimmermann, L., Moldzio, R., Vazdar, K., Krewenka, C., and Pohl, E. E. (2017). Nutrient deprivation in neuroblastoma cells alters 4-hydroxynonenal-induced stress response. *Oncotarget* 8, 8173–8188.
- Zoonens, M., Comer, J., Masscheleyn, S., Pebay-Peyroula, E., Chipot, C., Miroux, B., et al. (2013). Dangerous liaisons between detergents and membrane proteins. The case of mitochondrial uncoupling protein 2. *J. Am. Chem. Soc.* 135, 15174–15182. doi: 10.1021/ja407424v

**Conflict of Interest Statement:** The authors declare that the research was conducted in the absence of any commercial or financial relationships that could be construed as a potential conflict of interest.

Copyright © 2019 Pohl, Rupprecht, Macher and Hilse. This is an open-access article distributed under the terms of the Creative Commons Attribution License (CC BY). The use, distribution or reproduction in other forums is permitted, provided the original author(s) and the copyright owner(s) are credited and that the original publication in this journal is cited, in accordance with accepted academic practice. No use, distribution or reproduction is permitted which does not comply with these terms.



# Cold Induced Depot-Specific Browning in Ferret Aortic Perivascular Adipose Tissue

Bàrbara Reynés<sup>1,2,3</sup>, Evert M. van Schothorst<sup>4</sup>, Jaap Keijer<sup>4</sup>, Enzo Ceresi<sup>1,2,3</sup>, Paula Oliver<sup>1,2,3\*</sup> and Andreu Palou<sup>1,2,3</sup>

<sup>1</sup> Laboratory of Molecular Biology, Nutrition and Biotechnology, Universitat de les Illes Balears, Palma, Spain, <sup>2</sup> CIBER de Fisiopatología de la Obesidad y Nutrición, Madrid, Spain, <sup>3</sup> Institut d'Investigació Sanitària Illes Balears, Palma, Spain, <sup>4</sup> Human and Animal Physiology, Wageningen University and Research, Wageningen, Netherlands

## OPEN ACCESS

### Edited by:

Jean-Pierre Montani,  
Université de Fribourg, Switzerland

### Reviewed by:

Vicente Lahera,  
Complutense University of Madrid,  
Spain

Marion Peyrou,  
University of Barcelona, Spain  
Shingo Kajimura,  
University of California,  
San Francisco, United States

### \*Correspondence:

Paula Oliver  
paula.oliver@uib.es

### Specialty section:

This article was submitted to  
Integrative Physiology,  
a section of the journal  
Frontiers in Physiology

Received: 11 November 2018

Accepted: 29 August 2019

Published: 18 September 2019

### Citation:

Reynés B, van Schothorst EM,  
Keijer J, Ceresi E, Oliver P and  
Palou A (2019) Cold Induced  
Depot-Specific Browning in Ferret  
Aortic Perivascular Adipose Tissue.  
Front. Physiol. 10:1171.  
doi: 10.3389/fphys.2019.01171

Brown adipose tissue is responsible for facultative thermogenesis to produce heat and increase energy expenditure in response to proper stimuli, e.g., cold. Acquisition of brown-like features (browning) in perivascular white adipose tissue (PVAT) may protect against obesity/cardiovascular disease. Most browning studies are performed in rodents, but translation to humans would benefit from a closer animal model. Therefore, we studied the browning response of ferret thoracic aortic PVAT (tPVAT) to cold. We performed global transcriptome analysis of tPVAT of 3-month-old ferrets acclimatized 1 week to 22 or 4°C, and compared the results with those of inguinal subcutaneous adipose tissue. Immunohistochemistry was used to visualize browning. Transcriptome data revealed a stronger cold exposure response of tPVAT, including increased expression of key brown/brite markers, compared to subcutaneous fat. This translated into a clear white-to-brown remodeling of tPVAT, with the appearance of multilocular highly UCP1-stained adipocytes. The pathway most affected by cold exposure in tPVAT was immune response, characterized by down-regulation of immune-related genes, with cardio protective implications. On the other hand, subcutaneous fat responded to cold by increasing energy metabolism based on increased expression of fatty acid oxidation and tricarboxylic acid cycle genes, concordant with lower inguinal adipose tissue weight in cold-exposed animals. Thus, ferret tPVAT responds to cold acclimation with a strong induction of browning and immunosuppression compared to subcutaneous fat. Our results present ferrets as an accessible translational animal model displaying functional responses relevant for obesity and cardiovascular disease prevention.

**Keywords:** adipose tissue, browning, cardiovascular disease, cold exposure, inflammation, thermogenesis

## INTRODUCTION

Adipose tissue has different biological functions, including adaptation to low ambient temperatures (Cinti, 2005). It is well known that cold acclimation, via beta-adrenergic stimulation, induces fatty acid catabolism in white adipose tissue (WAT), promoting both triacylglycerol lipolysis and fatty acid beta-oxidation, while decreasing fatty acid synthesis (Palou et al., 1998; Choe et al., 2016). In parallel, cold exposure activates brown adipose tissue (BAT), which uses circulating free fatty acids produced by catabolic lipid metabolism of WAT to produce heat representing non-shivering or facultative thermogenesis (Cannon and Nedergaard, 2004; Cinti, 2005). This process

is mediated by the uncoupling protein 1 (UCP1) (Cannon and Nedergaard, 2004) present in the inner mitochondrial membrane of brown adipocytes, which acts as a proton conductor, dissipating the proton gradient generated by the respiratory chain as heat (Palou et al., 1998). Moreover, it is well known that cold exposure not only activates BAT but also results in a remarkable induction of UCP1-positive brown fat-like adipocytes in WAT, the so-called beige or brite cells (Ishibashi and Seale, 2010; Petrovic et al., 2010). This process, known as browning is widely characterized in rodents (Cousin et al., 1992; García-Ruiz et al., 2015) and could contribute to energy dissipation as heat. It is therefore not surprising that the detection in humans of cold inducible metabolically active brown fat has provoked an interest in the activation of brown and brite adipocytes as a potential anti-obesity therapeutic strategy (Nedergaard et al., 2007; Seale et al., 2011; Saito, 2013; Lee et al., 2014). BAT of adult humans is not well defined and is present in a dispersed manner in cervical, supraclavicular and paravertebral regions (Nedergaard et al., 2007). It has been proposed that, in humans, brown adipocytes could be, in fact, beige adipocytes, arising as result of WAT browning in response to proper stimuli (Wu et al., 2012).

Excess fat deposition around blood vessels, particularly the heart and coronary arteries is related to increased cardiovascular risk (Montani et al., 2004). In contrast, browning of this aortic perivascular adipose tissue (PVAT) has been related to an improved cardiovascular health (Aldiss et al., 2017; Xiong et al., 2017; Villarroya et al., 2018). Due to the difficulties of performing human studies, rodents are the most widely used species for thermogenic research (Bonet et al., 2013). Human thoracic PVAT (tPVAT) is comprised of brite adipocytes and, thus, has browning capacity (Chatterjee et al., 2009). However, in contrast to humans, rodent tPVAT presents more similarities with classical BAT, and its gene expression pattern and morphology is closer to that of BAT than to WAT (Fitzgibbons et al., 2011; Tran et al., 2018). Moreover, it has recently been reported that humans and mice present opposing browning gene expression patterns in visceral and subcutaneous adipose tissue depots (Zuriaga et al., 2017). In addition, contrary to what happens in humans, rodents possess a well-defined BAT, mainly located in the interscapular region. This fact could interfere when using this animal model to evaluate the relevance of browning itself, as most of the stimuli known to activate adipose tissue remodeling, usually also stimulate BAT thermogenesis (Bonet et al., 2013). Given the importance of understanding browning in humans, and because of the differences between human and rodent PVAT, there is an urgent need for another animal model that is closer to humans to perform BAT/browning studies.

Ferrets (*Mustela putorius furo*) is an animal model used in different research areas, e.g., immunology, due to their closer resemblance to humans than the most widely used rodents (Oh and Hurt, 2016; Stittelaar et al., 2016). Ferrets are closer to humans in terms of thermal environment, as the thermoneutral temperature for *Mustela putorius* has been established at 25°C (Korhonen et al., 1983), lower to that of rodents (28°C), and closer to that of non-naked humans (23°C) (Speakman and Keijer, 2012). This is of interest for thermogenic research, however, to our knowledge, our group is the only one studying

browning phenomenon in this animal model. We have previously described that, unlike rodents, but similar to what is described in humans, adult ferrets do not present a well-defined BAT (Fuster et al., 2009; Sánchez et al., 2009). Noteworthy, these animals present dispersed multilocular adipocytes with modest levels of UCP1 in different adipose tissue depots, which increase by cold exposure and dietary stimuli, mainly in the retroperitoneal depot (Fuster et al., 2009; Sánchez et al., 2009). These data point to ferrets as an interesting alternative model to rodents to be used in studies of thermogenesis, as we have reported in a revision on white adipose tissue browning (Bonet et al., 2013). Moreover, we have previously shown in ferrets that cold exposure induces immunosuppression in tPVAT and in peripheral blood mononuclear cells (Reynés et al., 2017), which has been related with cardiovascular protection (Li et al., 2017). Given the relevance of PVAT for cardiovascular disease in humans and given our previous results, we here analyze, in the same set of animals, the browning response of this depot in the ferret to cold exposure, which is the main thermogenic stimulus. Moreover, using global gene expression analysis, we compared tPVAT to subcutaneous inguinal white adipose tissue (IAT) of ferrets acclimatized to 22 or 4°C during 1 week. We selected the IAT to compare because it is the one traditionally used for browning research in rodents (Wang and Yang, 2017), but according to our previous studies, in ferrets it could have a different cold-response adaptation, not related to browning (Fuster et al., 2009). Our study was complemented with morphological analysis to visualize functional adipose tissue responses.

## MATERIALS AND METHODS

### Animal Procedure

Animal experiments followed in this study was reviewed and approved by the Bioethical Committee of the University of the Balearic Islands, and animal procedures followed the guidelines from the Directive 2010/63/EU of the European Parliament on the protection of animals used for scientific purposes. Three month-old male ferrets (*Mustela putorius furo* from Cunipic, Lleida, Spain) were distributed into two groups ( $n = 7$ ): a control group, acclimatized to room temperature ( $22 \pm 2^\circ\text{C}$ ), and a cold group, acclimatized to 4°C for 1 week. Ferrets are cold-exposed mammals in their natural environment, and while the optimum range recommended by the Council of Europe Convention for housing of ferrets is 15 to 22°C, they can live at ambient temperatures between 3 and 17°C (Fox, 1998). Thus, 1 week of cold exposure to 4°C is a strong cold stimulus, but not extreme for these animals. Thermoneutrality for polecats (*Mustela putorius*) is established at 25°C (Korhonen et al., 1983) and, therefore, we worked slightly below the thermoneutral temperature, which could be considered closer to the comfort zone. The animals were weighed before and after cold exposure. Due to logistic reasons, cold-exposed animals were housed individually to avoid huddling behavior to stay warm, and although they could see and smell each other, isolation could be considered as a potential confounding factor. All animals were exposed to a light/dark cycle of 12 h and had



free access to water and diet (Gonzalo Zaragoza Manresa SL, Alicante, Spain). Ferrets were anesthetized using 10 mg/kg of Ketamine hydrochloride (Imalgène 1000, Merial Laboratorios SA, Lyon, France) and 80 mg/kg medetomidine (Domtor, Orion Pharma, Espoo, Finland), arterial blood was collected from the left ventricle and animals died by exsanguination. Afterward, thoracic perivascular, inguinal, interscapular and retroperitoneal adipose tissues were rapidly removed and weighed, frozen in liquid nitrogen, and stored at  $-80^{\circ}\text{C}$  until RNA analysis.

## Measurement of Circulating Parameters (Glucose and Free Fatty Acid)

Blood glucose concentration was measured using an Accu-Chek Glucometer (Roche Diagnostics, Barcelona, Spain) in blood obtained from the neck at the moment of sacrifice. Non-esterified free fatty acids (NEFA) levels were measured in serum using an enzymatic colorimetric NEFA-HR2 kit (from WAKO, Neuss, Germany).

## Histological Analysis

tPVAT and IAT samples were fixed by immersion in 4% paraformaldehyde in 0.1 M sodium phosphate buffer, pH 7.4, overnight at  $4^{\circ}\text{C}$ , washed in phosphate buffer, dehydrated in a graded series of ethanol, cleared in xylene and embedded in paraffin blocks for light microscopy. Five-micrometer-thick sections of tissue were cut with a microtome and mounted in slides. The area of white adipocytes was measured in hematoxylin/eosin stained section. Images from light microscopy were digitalized and the area of at least 200 cells of each section was determined using Axion Vision Software (Carl Zeiss, S.A., Barcelona, Spain).

## Immunohistochemistry Analysis of UCP1 in Aortic Perivascular and Inguinal Adipose Tissue

Five-micrometers sections of adipose tissue of the different experimental groups were immunostained by means of the avidin-biotin technique (Hsu et al., 1981). Briefly, tissue sections were incubated with 5%  $\text{H}_2\text{O}_2$  in water for 15 min to block endogenous peroxidase and then with normal goat serum 2% in PBS pH 7.3 to block unspecific sites and then overnight at  $4^{\circ}\text{C}$  with primary rabbit polyclonal UCP1 antibody (GeneTex International Corporation, CA, United States) diluted 1:370 in PBS overnight at  $4^{\circ}\text{C}$ . The primary antibody that was used cross-reacts with rat UCP1, and has been previously validated for ferrets (Fuster et al., 2009; Sánchez et al., 2009). Sections were then incubated with the corresponding biotinylated anti-rabbit IgG secondary antibody (Vector Laboratories, Burlingame, CA, United States), diluted 1:200, and finally with ABC complex (Vectastain ABC kit, Vector, CA, United States). Peroxidase activity was revealed with Sigma Fast 3,3'-diaminobenzidine (Sigma-Aldrich, St. Louis, MO, United States) as substrate. Finally, sections were counterstained with hematoxylin and mounted in Eukitt (Kindler, Freiburg, Germany). Images were acquired with a Zeiss Axioskop 2 microscope equipped with AxioCam ICC3 digital camera and AxioVision 40V

4.6.3.0 Software (Carl Zeiss, S.A., Barcelona, Spain). White adipocytes, cells of the aorta, lymph nodes and nerves were not stained, confirming the specificity of the staining for multilocular/brite adipocytes.

## Total RNA Isolation

Total RNA from tPVAT and IAT samples was extracted using Tripure Reagent (Roche Diagnostics, Barcelona, Spain). RNA samples were purified with E.Z.N.A. MicroElute RNA Clean Up (Omega Bio-tek, VT, United States), and with 3M sodium acetate and absolute ethanol. RNA yield was quantified using a NanoDrop ND 1000 spectrophotometer (NanoDrop Technologies, Wilmington, DE, United States) and the integrity was measured on an Agilent 2100 Bioanalyzer with RNA 6000 Nano chips (Agilent Technologies, South Queensferry, United Kingdom).

## Microarray Processing

A whole genome ferret-specific gene expression microarray was designed by the Genomics and Translational Genetics Service of the Príncipe Felipe Research Center (Valencia, Spain). The microarray was designed as a  $2 \times 400$  k G4861A (AMADID-064079) Agilent array (Agilent Technologies, Inc., Santa Clara, CA, United States).

For the microarray analysis, we used tPVAT and IAT RNA samples of control ( $n = 7$ ) and cold-exposed ferrets ( $n = 6$ ). For microarray hybridization 0.2  $\mu\text{g}$  RNA of each sample was reverse transcribed using the Agilent Low Input Quick Amp Labeling kit (Agilent), according to the manufacturer's protocol, with some modifications (all materials and reagents were from Agilent Technologies, Palo Alto, CA, United States). Half of the cDNA sample (5  $\mu\text{l}$ ) was used for linear RNA amplification and labeling with Cy5 or Cy3. All reactions were performed using half of the amounts indicated by the manufacturer (as previously described in van Schothorst et al., 2007). Briefly, a transcription master mix was prepared (0.375  $\mu\text{l}$  nuclease-free water; 1.6  $\mu\text{l}$  5X Transcription buffer; 0.3  $\mu\text{l}$  0.1 M DTT; 0.5  $\mu\text{l}$  NTP mix; 0.115  $\mu\text{l}$  T7 RNA Polymerase Blend and 0.12 cyanine 3-CTP or cyanine 5-CTP per sample) and added to 5  $\mu\text{l}$  cDNA. *In vitro* transcription and labeling were carried out at  $40^{\circ}\text{C}$  for 2 h. The labeled cRNA samples were purified using Qiagen RNeasy minispin columns (Qiagen, Venlo, Netherlands). Dye incorporation and cRNA concentration was measured using the microarray measurement of the Nanodrop spectrophotometer (NanoDrop Technologies). Yield of each individual sample was at least 1.875 ng and specific activity 6.0 pmol Cy3 or Cy5 per  $\mu\text{g}$  cRNA. All approved high quality Cy5 cRNAs were pooled to serve as standard reference pool; the pool consisted of RNA isolated from different tissues to increase signal distribution over all probes. This pool included 10 samples from peripheral blood mononuclear cells samples of control and cold-exposed ferrets. Hybridization was performed by preparing a cRNA target solution containing 1.875 ng Cy3-labeled cRNA, 1.875 ng Cy5-labeled pool cRNA, 25  $\mu\text{l}$  of 10X blocking agent, 5  $\mu\text{l}$  25X Fragmentation Buffer in a total volume of 125  $\mu\text{l}$ . The samples were incubated at  $60^{\circ}\text{C}$  for 30 min, and then immediately cooled on ice for 1 min. After that, 125  $\mu\text{l}$  2x GEx hybridization buffer HI-RPM was added and hybridized

on the Agilent arrays (Agilent Technologies, Inc., Santa Clara, CA, United States), for 17 h at 65°C in Agilent hybridization chambers in an Agilent hybridization oven rotating at 10 rpm. After hybridization, the arrays were subsequently washed with GE wash buffer 1, for 1 min at room temperature, and GE wash buffer 2, for 1 min at approximately 37°C, according to manufacturer's protocol (Agilent Technologies).

## Normalization and Transcriptome Data Analysis

The arrays were scanned with an Agilent Microarray Scanner (Agilent Technologies Scanner G2505C, Agilent Technologies) with a Profile AgilentG3\_GX\_2Color. Median density values and background values of each spot were extracted for both the experimental samples (Cy3) and the reference samples (Cy5). Quality control for every microarray was performed visually by using 'Quality control graphs' from Feature extraction and M-A plots and box plots, which were made using limmaGUI in R (Wettenhall and Smyth, 2004). Data were imported into GeneMaths XT 2.12 (Applied Mathematics, Sint-Martens-Latem, Belgium) for background correction and normalization. Target signals with an average intensity twice above the background were selected to increase accuracy of the data. Normalization and data analysis were performed as published (Pellis et al., 2003). In addition to the set of 26 microarray from adipose tissue samples, 10 microarray from peripheral blood cells, performed at the same time, were also included for normalization. Blood samples data analyses are not included in the present work. After normalization procedure, sequences were averaged per unique sequence (45,328 sequences of 300,577 detected probes, which corresponded to 19,282 genes). To select unique genes we considered those sequences with higher statistical differences between the cold vs. control group of IAT assessed by Student's *t*-test in GeneMaths XT. Statistical differences in tPVAT between the cold and control groups was also assessed by Student's *t*-test in GeneMaths XT, and statistical differences between tPVAT and IAT were assessed by Student's *t*-test in Microsoft Excel; the generated *p*-values were used to obtain insight into significantly affected genes. Fold change calculations were performed in Microsoft Excel. In order to compare gene expression pattern at control temperature of the two studied adipose tissues, we selected the genes with fold change > 2, using a significance threshold of  $p < 0.01$ . For analysis of the effect of cold exposure, genes with the highest or the lowest fold change, with a threshold of  $p < 0.05$ , were selected from both tissues. Moreover, all sequences were used to perform pathway analysis using MetaCore™ (GeneGo, St. Joseph, MI, United States) to determine the effect of cold exposure. In addition, the top 50 up- and down-regulated genes were manually classified into biological processes using available databases (Genecards, NCBI, WikiPathways, PubMed). Microarray data has been deposited in NCBI Gene Expression Omnibus (GEO) under accession number GSE62353 for tPVAT and GSE62351 for IAT datasets.

Volcano plots of the microarray data were made using GraphPad Prism version 6 (Graphpad Software, San Diego, CA, United States). Principal component analysis was made

using SPSS for windows (version 15.0; SPSS, Chicago, IL, United States).

## Reverse Transcription Quantitative Real-Time Polymerase Chain Reaction (RT-qPCR) Analysis

To validate microarray data for the IAT samples we analyzed mRNA expression of selected genes by RT-qPCR. The microarray confirmation for tPVAT microarray data was previously reported (Reynés et al., 2017). In IAT the following genes were analyzed: *Col3a1*, *Cpt2*, *Fabp3*, *Idh3b*, *Lum*, *Sucla2*, and *Ucp3*. These genes were selected based on their relevant biological function and/or because they are included in the top regulated genes. Fifty ng of total RNA from IAT was reverse transcribed to cDNA using iScript cDNA synthesis kit (BIO-RAD, Madrid, Spain) at 25°C for 5 min, 42°C for 30 min, and 85°C for 5 min, in an Applied Biosystems 2720 Thermal Cycler (Applied Biosystems, Madrid, Spain). Each PCR was performed from diluted (1/10) cDNA template, forward and reverse primers (5 μM), and Power SYBER Green PCR Master Mix (Applied Biosystems) in a total volume of 11 μl, with the following profile: 10 min at 95°C, followed by a total of 40 temperature cycles (15 s at 95°C and 1 min at 60°C). In order to verify the purity of the products, a melting curve was produced after each run according to the manufacturer's instructions. The threshold cycle (Ct) was calculated using the instrument's software (StepOne Software v2.0, from Applied Biosystems) and the relative expression of each mRNA was calculated as a percentage of controls rats, using the Pfaffl's method (Pfaffl, 2001).

For the genes used to validate the microarray analysis, data were normalized against the reference gene Apolipoprotein O (*ApoO*). *ApoO* was chosen because our microarray data showed equal expression over all microarrays in control and cold-exposed ferrets. Primers for the different genes are described in **Table 1** and were obtained from Sigma Genosys (Sigma-Aldrich Química SA, Madrid, Spain).

## Statistical Analysis

Data of body weight, adiposity, serum parameters and the confirmatory results of the microarray data are expressed as the mean ± SEM. Differences between groups were analyzed using Student's *t*-test. All analyses were performed with SPSS for windows (version 15.0; SPSS, Chicago, IL, United States). Threshold of significance was defined at  $p$ -value < 0.05. The statistical analysis of the microarray data has been indicated in the microarray data analysis section.

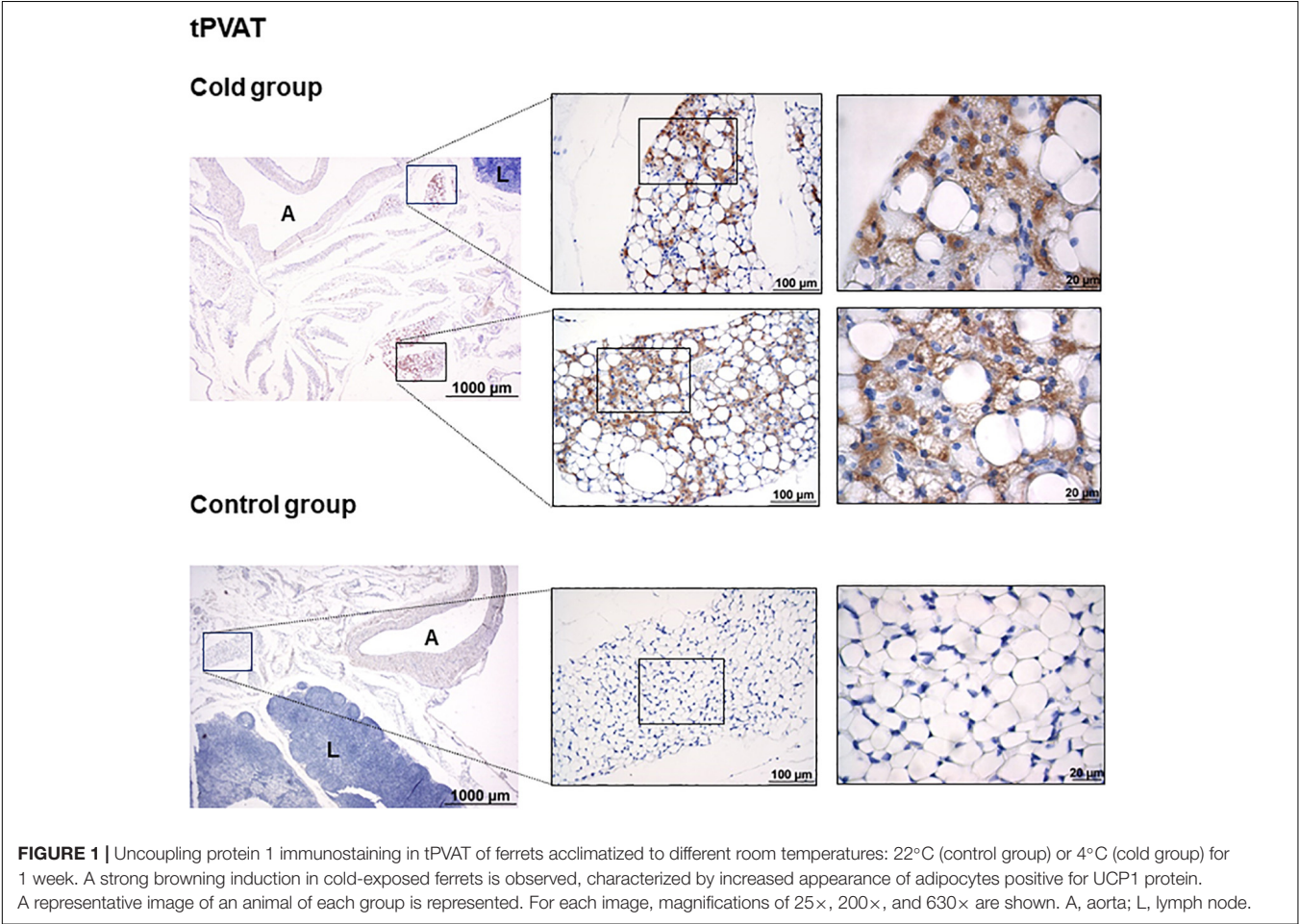
## RESULTS

### Cold Exposure Induced Fat Mass Mobilization in Ferrets

As we previously reported using the same set of animals (Reynés et al., 2017), cold exposure decreased the mass of the inguinal, retroperitoneal and interscapular white adipose tissues in cold-exposed ferrets (58% decrease in the IAT, and 74% decrease both

**TABLE 1 |** Nucleotide sequences of primers and amplicon size used for RT-qPCR amplification.

Gene	Forward primer (5'–3')	Reverse primer (5'–3')	Amplicon size (bp)
<i>Col3a1</i>	GCTGTTGAGGGAGGATGTT	ATTAGGAGGACGAGGAGGAG	222
<i>Cpt2</i>	CATTCAACCCTGACCCAAAG	AGGAAGGCACAAAGCGTATG	186
<i>Fabp3</i>	CTCGGTGTGGGTTTTGCTAC	ACGGTGGACTTGACCTTCCT	185
<i>Idh3b</i>	GGGAGCAGACAGAAGGAGAA	GGAACAATCCATCCCCAAG	198
<i>Lum</i>	GCCTATTTTCATCACAAAGCACAG	CCCATTCTTTTTGGCACATT	186
<i>Sucla2</i>	CAGGAAGATGAAAGGGAGAAA	TCTGTACTTGATGGACTGTGG	191
<i>Ucp3</i>	GCGAGCAACAGGAAATACAG	CAAAGGCAGAGATGAAGTGG	217
<i>Apoo</i> (Reference gene)	TGGTGTTATCGGTTTTGCTG	CTTCACATTCTCTGGCTTTTG	235



in the interscapular and retroperitoneal depots). This lower fat mass content was not translated into a statistically significant lower body weight, however, these animals attained a 16% lower body weight gain compared to control animals during the week in which they were exposed to 4°C, in accord with the lower adiposity. Specifically, animals of the cold-exposed group weighed  $559 \pm 31$  g before and  $510 \pm 36$  g after cold exposure; while those of the control group weighed  $581 \pm 51$  g and  $623 \pm 60$  g, before and after this week, respectively. Moreover, cold exposure induced an increase in circulating NEFA levels ( $0.955 \pm 0.078$  mM in cold-exposed animals vs.  $0.619 \pm 0.085$  mM in the control group, Student's *t*-test,  $p < 0.05$ ).

Circulating glucose levels were also analyzed, but they were not affected by cold acclimation (data not shown).

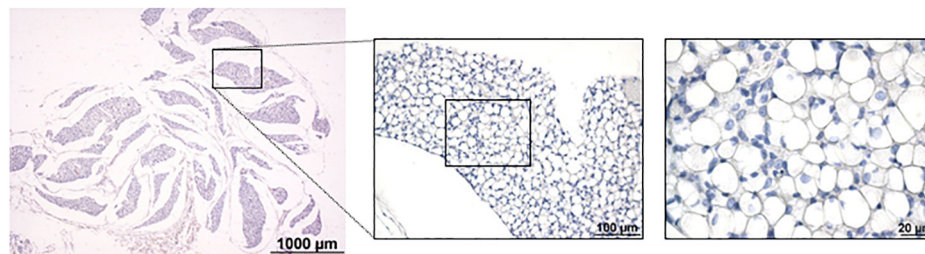
**Cold Exposure Induced the Appearance of UCP1-Positive Adipocytes in tPVAT**

As shown in **Figure 1**, immunohistochemical analysis revealed that cold exposure induced a remodeling of the tPVAT, with the appearance of multilocular adipocytes highly stained for UCP1 in sparse lobules within the adipose depot. This is similar to what occurred in the retroperitoneal adipose tissue, which, according to our previous data, is a depot with a high degree of browning



## IAT

### Cold group



### Control group

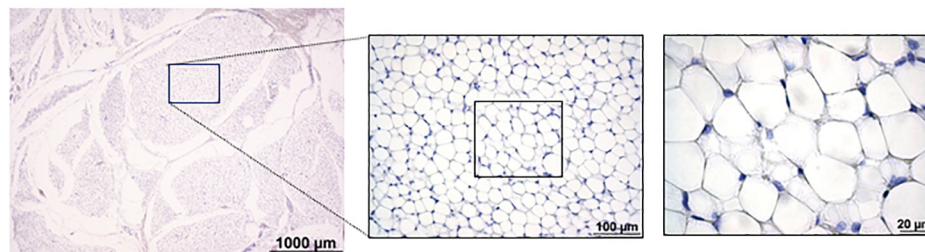


**FIGURE 2 |** Uncoupling protein 1 immunostaining in IAT of ferrets acclimatized to different room temperatures: 22°C (control group) or 4°C (cold group) for 1 week. No appearance of UCP1 positive cells was observed as result of cold exposure. A representative image of an animal of each group is represented. For each image, magnifications of 25×, 200×, and 630× are shown.

in response to proper stimuli, such as cold or diet (Fuster et al., 2009; Sánchez et al., 2009). Interestingly, cold-induced browning was not observed in the IAT (**Figure 2**); the complete area of the different sections was analyzed. In spite of the lower mass of the IAT, morphometric analysis performed in this tissue did not show a significant smaller cell size of the unilocular adipocytes as result of cold exposure ( $331 \pm 68$  vs.  $497 \pm 54 \mu\text{m}^2$ , in cold-exposed and control ferrets, respectively; Student's *t*-test, *p*-value < 0.1).

## Differential Gene Expression Pattern Between tPVAT and IAT Was Diminished as Result of Cold Exposure

To gain a global view of the molecular basis of biologic differences between tPVAT and IAT in ferrets, we performed a whole genome transcriptome analysis. A total of 19,282 genes were expressed, of which 3,090, representing 16%, being differentially expressed between tPVAT and IAT (Student's *t*-test, *p*-value < 0.01, with an absolute fold change  $\geq 2$ ). Expression of 1,640 genes was higher and of 1,450 lower in tPVAT vs. IAT (**Figure 3A**). One week of exposure to 4°C decreased the gene expression differences between both adipose tissue depots to 1,623 genes, equaling 8%; with only 525 genes being higher and 1,098 lower expressed in tPVAT vs. IAT (**Figure 3A**). Volcano plots clearly show how the differences between both adipose tissue depots were reduced by

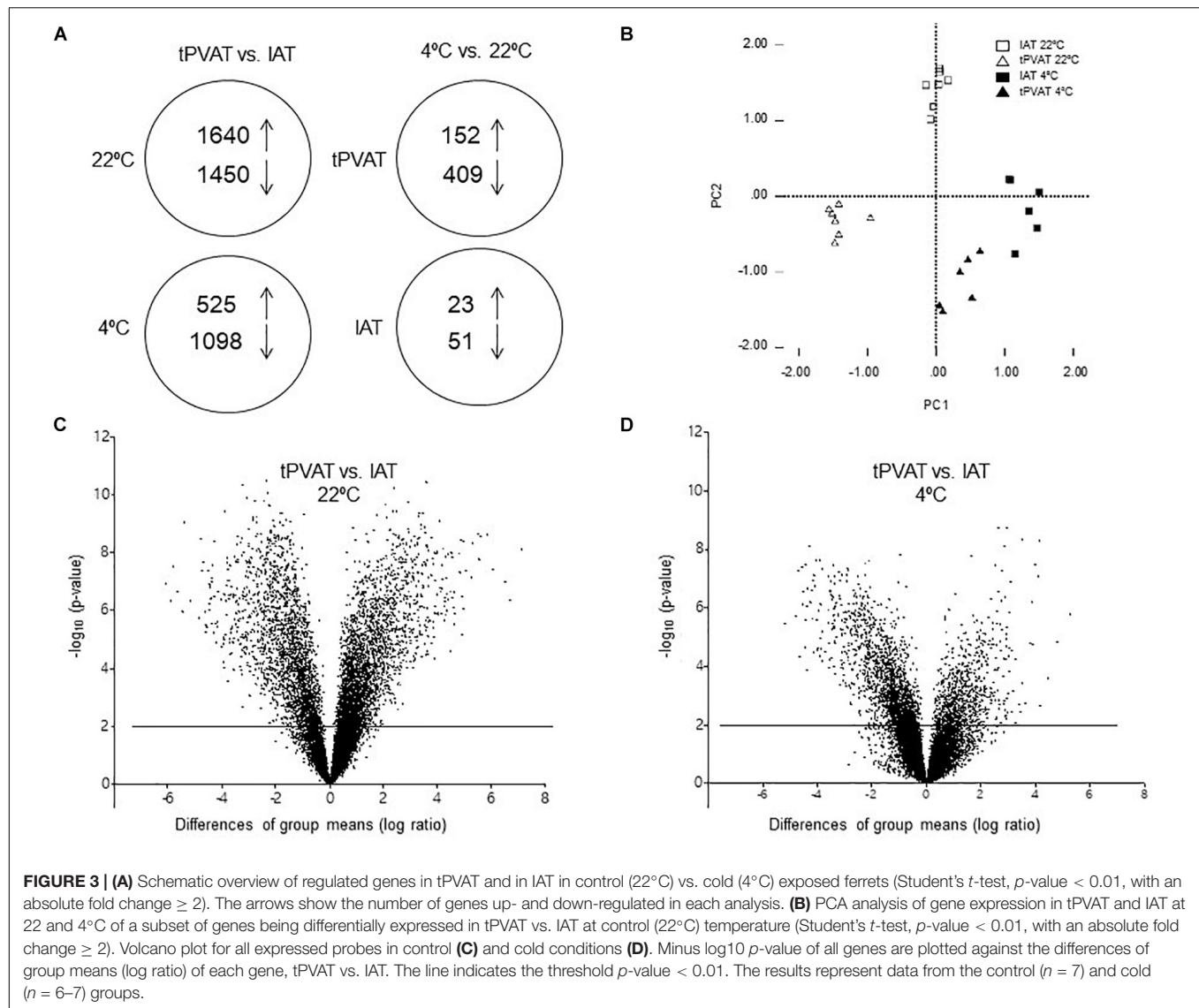
cold exposure (**Figures 3C,D**). This is also observed by PCA analysis (**Figure 3B**), which also shows that tPVAT and IAT at 22°C have indeed a clearly different gene expression profile, which becomes more similar profile due to cold exposure.

In spite of the importance of UCP1 in adaptive thermogenesis and of the increase of UCP1-positive stained adipocytes in tPVAT of cold-exposed animals, its mRNA expression was not altered—as measured by microarray analysis—by cold exposure in tPVAT and IAT. Therefore, we focused our attention on a battery of relevant genes known as brown adipocyte markers or involved in the thermogenic response (see **Table 2**). Interestingly, most of these genes, such as *Cidea*, *Ebf3*, *Fabp3*, *Ppara*, and *Ppargc1a* had a higher expression in IAT than in tPVAT in control and cold-exposed animals, suggesting a brite nature of IAT. However, cold acclimation particularly increased the expression in tPVAT of *Ebf3*, *Fabp4*, *Fndc5*, *Pdk4* and *Ppargc1b*, known brown/thermogenic markers.

## Cold Exposure Induced a Higher Gene Expression Response in tPVAT Than in IAT

Our microarray data show that cold exposure produced a higher impact on gene expression in tPVAT than in IAT. Thus, 561 in tPVAT vs. 74 in IAT from a total of 19,282 genes changed





expression in the cold condition (Figure 3A). The impact of cold exposure on transcriptional changes is illustrated in Figures 4A,C using Volcano Plots, which shows that tPVAT is primarily affected.

To obtain a more detailed view on the impact of cold exposure, we manually classified the top 50 up- and down-regulated genes of each tissue into different metabolic pathways (Student's *t*-test,  $p\text{-value} < 0.05$ ) (Supplementary Tables). Results, represented in Figures 4B,D, show that cold exposure induced different gene expression adaptations in tPVAT compared to IAT. In tPVAT, up-regulated genes as result of cold exposure were involved in different metabolic pathways, while the down-regulated genes were mainly involved in immune response and cell cycle (Figure 4B). For IAT, the top up-regulated genes were also involved in many different processes; however, the top down-regulated genes were mainly genes involved in structure/cytoskeleton organization, and in cell differentiation and development (Figure 4D). Additionally, a MetaCore

pathway analysis was performed taking all probes significantly affected by cold exposure into account (Student's *t*-test,  $p < 0.05$  for cold vs. control). Table 3 shows the top 10 pathways affected in each adipose tissue. In tPVAT the top regulated pathways were cell cycle, cell differentiation and development, immune response, protein metabolism and transcriptional regulation (Table 3A), coincident with the manual classification (Figure 4B). In the IAT, the most affected pathways were cell adhesion, cytoskeleton, immune response, energy metabolism and muscle contraction (Table 3B). We were particularly interested in the differential response observed for energy metabolism (including tricarboxylic acid –TCA– cycle and fatty acid beta-oxidation), which appeared as one of the affected pathways in response to cold exposure in the IAT but not in the tPVAT. In order to further study this differential response we manually compared the expression of genes involved in the tricarboxylic acid cycle and in fatty acid beta-oxidation in both adipose tissue depots. Our results show that most of the

**TABLE 2 |** Comparison of gene expression of brown/brite adipocyte markers in tPVAT vs. IAT and in cold vs. control temperature (Student's *t*-test).

Gene symbol	tPVAT vs. IAT				4°C vs. 22°C			
	22°C		4°C		IAT		tPVAT	
	<i>p</i> -value	Fold change	<i>p</i> -value	Fold change	<i>p</i> -value	Fold change	<i>p</i> -value	Fold change
<i>Cidea</i>	< 0.001	−8.98	< 0.001	−11.0	< 0.05	+1.69	0.35	+1.38
<i>Ebf3</i>	< 0.001	−4.60	< 0.001	−3.11	0.45	−1.12	< 0.05	+1.32
<i>Fabp3</i>	< 0.001	−5.84	< 0.001	−8.87	< 0.05	+3.10	0.12	+2.04
<i>Fgf21</i>	0.68	+1.09	0.38	−1.19	0.92	−1.02	0.16	−1.33
<i>Fndc5</i>	< 0.001	−1.97	0.08	+1.49	< 0.01	−1.95	< 0.05	+1.50
<i>Pdk4</i>	< 0.01	−5.85	0.22	−1.79	0.17	+1.75	< 0.01	+5.73
<i>Ppara</i>	< 0.001	−4.03	< 0.01	−2.69	0.83	+1.03	0.08	+1.55
<i>Ppargc1a</i>	< 0.001	−4.49	< 0.001	−4.76	0.16	+1.36	0.30	+1.28
<i>Ppargc1b</i>	< 0.001	−2.98	< 0.05	−1.81	0.56	−1.13	< 0.05	+1.46
<i>Prdm16</i>	0.53	+1.14	0.91	−1.02	0.67	+1.10	0.73	−1.07
<i>Tbx15</i>	0.30	−1.25	0.61	−1.23	0.91	+1.03	0.90	+1.04
<i>Ucp1</i>	0.92	−1.02	0.81	−1.20	0.13	+1.78	0.50	+1.51

*p*-value is indicated. Fold change: + indicates up-regulated and −indicates down-regulated genes. Bold indicates statistical significance. The results represent data from the control (*n* = 7) and cold (*n* = 6–7) groups.

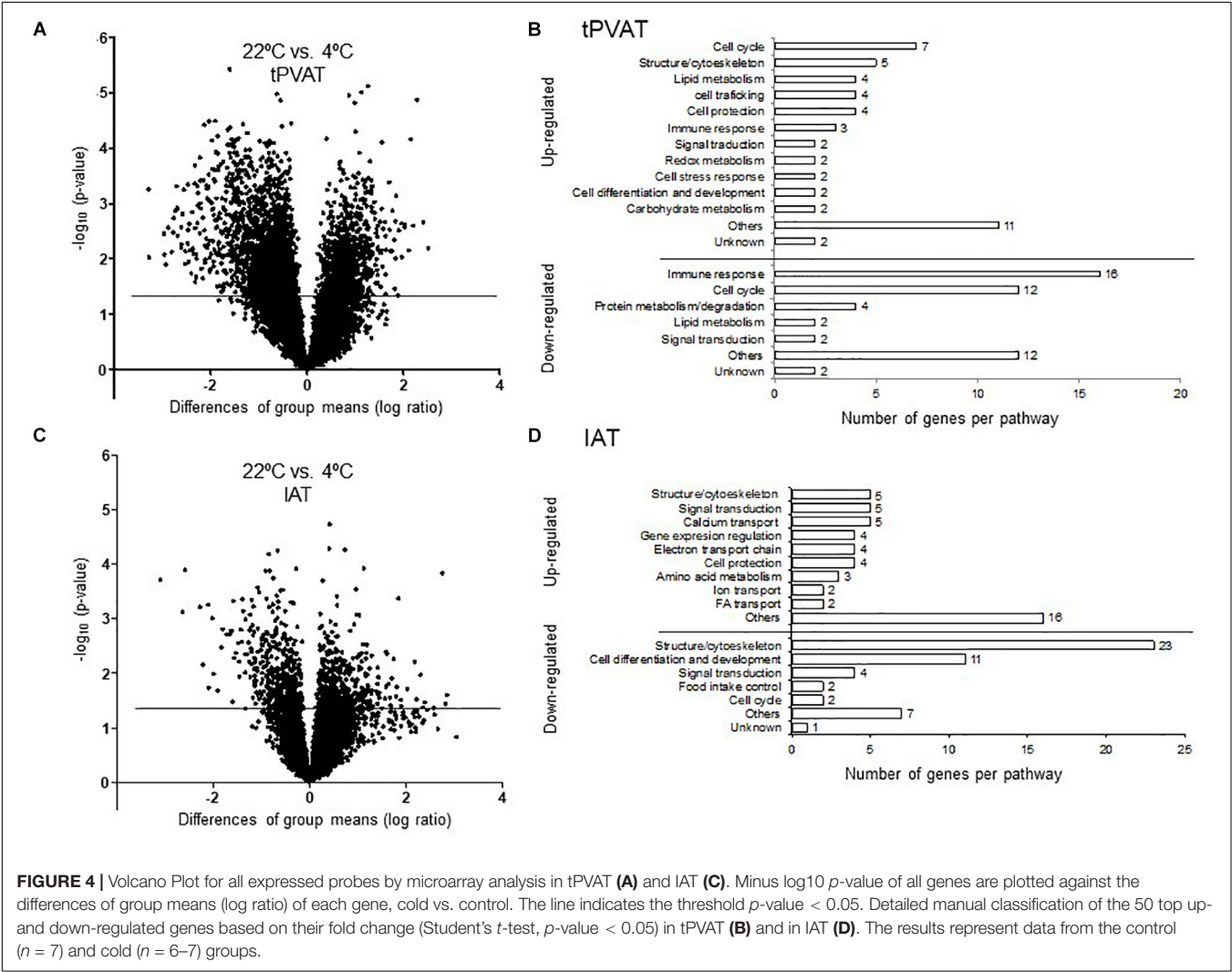


**TABLE 3 |** Top 10 regulated pathways analyzed by MetaCore™ in the tPVAT (A) and IAT (B).

Top 10 pathways	p-value
<b>(A) tPVAT</b>	
<b>Cell cycle</b>	
DNA damage ATM/ATR regulation of G1/S checkpoint	6.05E-09
Role of APC in cell cycle regulation	6.15E-10
Spindle assembly and chromosome separation	9.94E-12
Start of DNA replication in early S phase	4.37E-12
The metaphase checkpoint	7.02E-13
Transition and termination of DNA replication	3.67E-07
<b>Cell differentiation and development</b>	
Development WNT signaling pathway	7.48E-08
<b>Immune response</b>	
Inhibitory PD-1 signaling in T cells	3.93E-07
<b>Metabolism</b>	
Protein folding and maturation POMC processing	1.08E-11
<b>Transcriptional regulation</b>	
Transcriptional epigenetic regulation of gene expression	6.42E-08
<b>(B) IAT</b>	
<b>Cell adhesion</b>	
Integrin-mediated cell adhesion and migration	1.90E-04
<b>Cytoskeleton</b>	
Cytoskeleton remodeling	6.75E-04
Regulation of actin cytoskeleton by Rho GTPases	9.01E-04
Role of PKA in cytoskeleton reorganization	3.52E-04
<b>Immune response</b>	
Platelet activating factor/PTAFR pathway signaling	5.00E-04
<b>Energy metabolism</b>	
Lysine metabolism	1.54E-04
Mitochondrial unsaturated fatty acid beta-oxidation	7.41E-04
Propionate metabolism	2.99E-04
Tricarboxylic acid cycle	2.94E-04
<b>Muscle contraction</b>	
Relaxing signaling pathway	1.10E-03

Regulated pathways were classified into: cell cycle, cell differentiation and development, immune response, metabolism and transcriptional regulation in the tPVAT; and cell adhesion, cytoskeleton, immune response, energy metabolism and muscle contraction in the IAT; p-values are given.

up-regulated genes in IAT were down-regulated or not affected in tPVAT (Figure 5). A more detailed interpretation of these data can be found in the discussion section.

## Confirmation of Microarray Data Results by RT-qPCR

Real-time polymerase chain reaction was performed on total RNA from IAT samples in order to confirm the microarray data; the tPVAT microarray confirmation was previously reported (Reynés et al., 2017). We selected 7 genes, 2 involved in the TCA cycle: *Idh3b* and *Sucl2*; 2 involved in cytoskeleton organization and cell adhesion: *Col3a1* and *Lum*; 2 involved in fatty acid metabolism and transport: *Cpt2* and *Fabp3*; and *Ucp3*, which

has been proposed as a potential alternative uncoupler. RT-qPCR confirmed the microarray data for all genes analyzed (Table 4).

## DISCUSSION

Perivascular white adipose tissue in humans exerts a paracrine-based protective action, which changes to a detrimental role in the pathogenesis of obesity and metabolic syndrome, contributing to perivascular inflammation and, thus, to cardiovascular risk (Payne et al., 2012; Mazurek and Opolski, 2015; Aldiss et al., 2017). However, PVAT browning has been linked to a cardioprotection (Aldiss et al., 2017; Xiong et al., 2017; Villarroja et al., 2018), in relation to a decrease in pro-inflammatory signals, associated with a BAT-like phenotype in PVAT (Villarroja et al., 2018). Human tPVAT is a white adipose tissue, which possesses some brown adipocyte features, such as expression of brown-adipocyte specific genes (Chatterjee et al., 2009). This is in contrast to what is described in rodents, classically used as models to study thermogenesis, in which tPVAT presents a gene expression pattern and possess a morphology closer to BAT (Fitzgibbons et al., 2011; Tran et al., 2018). Previous studies of our group suggested that ferrets could be a useful animal model for thermogenesis and browning studies, as their adipose tissue is closer to that of humans (Fuster et al., 2009). As in humans, ferrets do not possess a well-defined BAT, but white adipose tissue depots with scarce brown-like adipocytes that increase in response to thermogenic stimuli, such as cold or dietary factors (Fuster et al., 2009; Sánchez et al., 2009). Due to the importance of PVAT browning for cardiovascular health, we have here studied the thoracic aortic PVAT of ferrets and its response to cold acclimation in detail. We focused on the thoracic region of the aorta because is the one with the greater thermogenic capacity reported in humans and rodents (Chatterjee et al., 2009; Fitzgibbons et al., 2011; Tran et al., 2018). In our study, we have compared tPVAT to the inguinal subcutaneous adipose tissue, the adipose tissue depot with a higher browning potential in rodents (Wang and Yang, 2017), for perspective and to obtain insight in tissue-specific adaptations to a low ambient temperature.

Cold exposure recruits and activates BAT, and induces browning in WAT depots (Palou et al., 1998; Bonet et al., 2013). According to our data, no browning is observed in the immunohistochemical analysis upon cold acclimation in the IAT. This is in sharp contrast with tPVAT, where cold exposure induces evident browning, with the appearance of multilocular brite adipocytes intensely stained for UCP1, suggesting an increased thermogenic capacity in this adipose tissue depot in ferrets. This would be probably related to the physiological need to maintain blood temperature at systemic level. This relevant tPVAT browning is similar to that previously reported by our group in the retroperitoneal adipose tissue of ferrets, in which multilocular UCP1-positive adipocytes appeared and UCP1 protein levels increased in response to cold exposure (Fuster et al., 2009) or to nutritional treatment (Sánchez et al., 2009).

Global transcriptome analysis, performed in the tPVAT and IAT, revealed a substantial difference in gene expression between

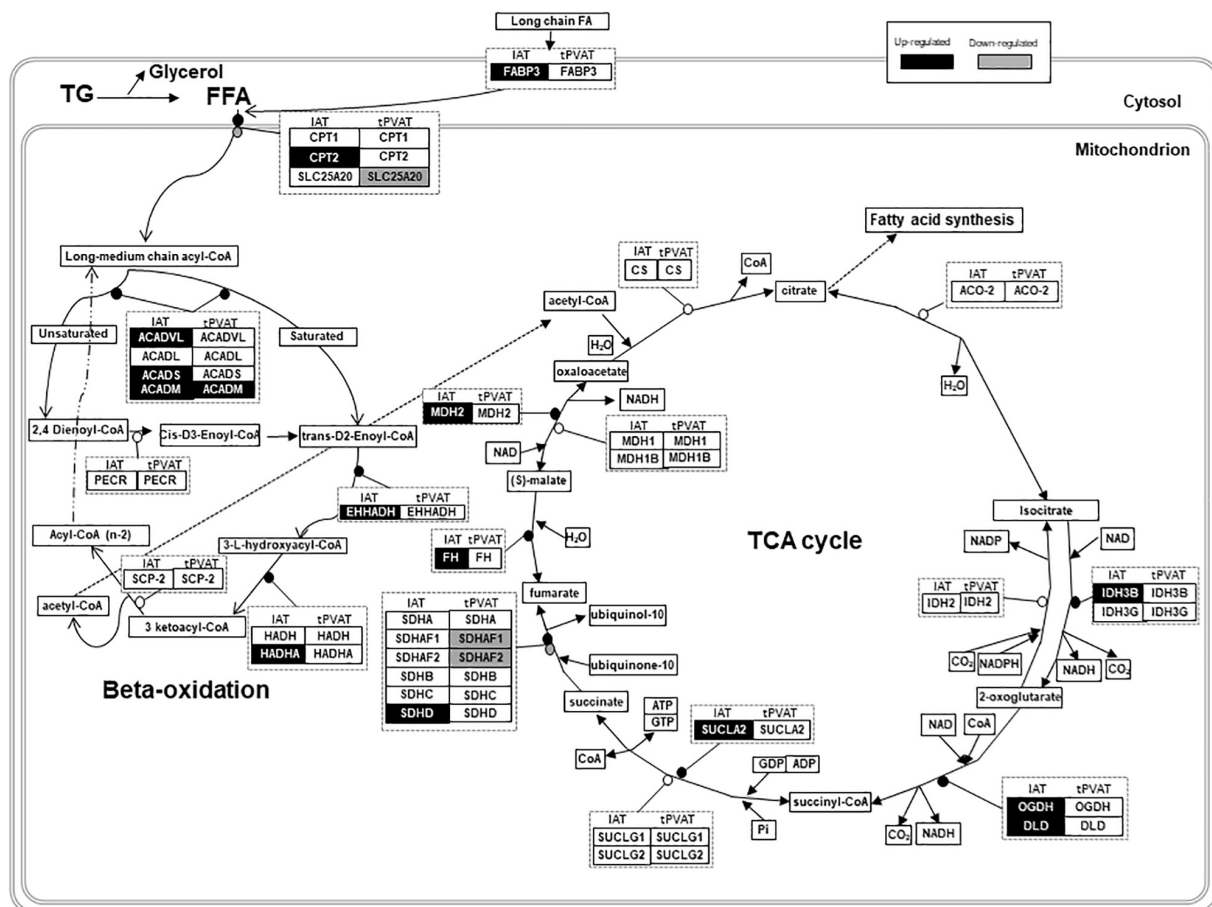


**FIGURE 5 |** Schematic overview of gene expression regulation of fatty acid oxidation and tricarboxylic acid (TCA) cycle in tPVAT and IAT. Up-regulated genes are marked in black and down-regulated are marked in gray (Student's *t*-test, *p*-value < 0.05). Source: WikiPathways (adapted). According to the license terms of WikiPathways, users are free to use the pathway images in presentations, documents, websites and publications; as well as to use the pathway data in analyses, qualitative or quantitative, while citing or giving appropriate attribution ([https://www.wikipathways.org/index.php/WikiPathways:License\\_Terms](https://www.wikipathways.org/index.php/WikiPathways:License_Terms)). ACADL, Acyl-CoA Dehydrogenase, Long Chain; ACADM, Acyl-CoA Dehydrogenase, C-4 To C-12 Straight Chain; ACADS, Acyl-CoA Dehydrogenase, C-2 To C-3 Short Chain; ACADVL, Acyl-CoA Dehydrogenase, Very Long Chain; ACO-2, Aconitase; CPT1, Carnitine Palmitoyltransferase 1; CPT2, Carnitine Palmitoyltransferase 2; CS, Citrate Synthase; DLD, Dihydropyrimidine Dehydrogenase; EHHADH, Enoyl-CoA Hydratase And 3-Hydroxyacyl CoA; FFA, Free Fatty Acids; FABP3, Fatty Acid Binding Protein 3; FH, Fumarate Hydratase; HADH, Hydroxyacyl-CoA Dehydrogenase; HADHA, Hydroxyacyl-CoA Dehydrogenase/3-Ketoacyl-CoA; IDH2, Isocitrate Dehydrogenase (NADP(+)) 2, Mitochondrial; IDH3B, Isocitrate Dehydrogenase 3 (NAD(+)) Beta; IDH3G, Isocitrate Dehydrogenase 3 (NAD(+)) Gamma; MDH1, Malate Dehydrogenase 1; MDH1B, Malate Dehydrogenase 1B; MDH2, Malate Dehydrogenase 2; NAD, Nicotinamide Adenine Dinucleotide; OGDH, Oxoglutarate Dehydrogenase; PEGR, Peroxisomal *Trans*-2-Enoyl-CoA Reductase; SCP-2, Sterol Carrier Protein 2; SDHA, Succinate Dehydrogenase Complex Flavoprotein Subunit A; SDHAF1, Succinate Dehydrogenase Complex Assembly Factor 1; SDHAF2, Succinate Dehydrogenase Complex Assembly Factor 2; SDHB, Succinate Dehydrogenase Complex Iron Sulfur Subunit B; SDHC, Succinate Dehydrogenase Complex Subunit C; SDHD, Succinate Dehydrogenase Complex Subunit D; SLC25A20, Solute Carrier Family 25 Member 20; SUCLA2, Succinate-CoA Ligase ADP-Forming Beta Subunit; SUCLG1, Succinate-CoA Ligase Alpha Subunit; SUCLG2, Succinate-CoA Ligase GDP-Forming Beta Subunit; TG, Triglycerides.

both adipose depots, with 16% of the genes differentially expressed in animals acclimated to control temperature. However, this gene expression difference was ameliorated to 8% when comparing both adipose depots in cold-exposed animals. The closer resemblance in the cold between both adipose depots is in part due to the induction of browning in tPVAT. Already at 22°C IAT expressed higher levels than tPVAT of key brown/brite markers, showing a more noticeable brite signature. However, cold exposure increased mRNA expression of several markers, such as *Ebf3*, *Fabp4*, *Fndc5*, *Pdk4* and *Ppargc1b*, specifically in the tPVAT, which appeared more sensitive to browning induction in

response to cold, as evidenced by immunohistochemical analysis that showed a prominent appearance of UCP1-positive brite cells in this tissue. Increased similarity between tPVAT and IAT in cold-exposed animals was also due to convergence of gene expression. For example, mRNA levels of *Fndc5*, a gene coding for the precursor of irisin, which is a browning inducer (Boström et al., 2012), decreased because of cold exposure in the IAT but increased in the tPVAT. However, the most highly affected pathway in tPVAT was not related to lipid metabolism, but to immune response, with immune-related genes as the most down-regulated in this depot. A down-regulation of immune response



**TABLE 4 |** Real-time polymerase chain reaction confirmation of microarray data.

Gene symbol	Gene name	Sequence ID	Microarray		RT-qPCR	
			FC	p-value	FC	p-value
<i>Col3a1</i>	Collagen, Type III, Alpha 1	XM_004763363.1	−8.58	0.0002	−1.70	0.0050
<i>Cpt2</i>	Carnitine palmitoyl transferase 2	XM_004774429.1	+ 1.42	0.0300	+ 1.48	0.0054
<i>Fabp3</i>	Fatty acid binding protein 3, muscle and heart	XM_004740951.1	+ 3.10	0.0157	+ 4.98	0.0017
<i>Idh3b</i>	Isocitrate dehydrogenase 3 (NAD +) beta	XM_004772915.1	+ 1.58	0.0060	+ 3.31	0.0000
<i>Lum</i>	Lumican	XM_004748555.1	−6.00	0.0001	−1.90	0.0026
<i>Sucla2</i>	Cuccinate-CoA ligase, ADP-forming, beta subunit	XM_004759183.1	+ 1.69	0.0090	+ 1.55	0.0103
<i>Ucp3</i>	Uncoupling protein 3	XM_004768064.1	+ 3.03	0.0044	+ 4.18	0.0020

Fold change (FC), + indicates up-regulated and − indicates down-regulated genes. p-values of microarray and RT-qPCR data are given (Student's t-test). The results represent data from the control (n = 7) and cold (n = 6–7) groups.

could be explained by its energy demanding nature (French et al., 2009). We previously proposed that the cold exposure-induced immunosuppression in tPVAT, also evidenced in immune cells, could modulate vascular inflammation decreasing cardiovascular risk (Reynés et al., 2017), a notion that was recently confirmed in rats (Li et al., 2017). In addition to down-regulation of immune response genes in tPVAT, using specific cold sensitive transgenic mice, it was shown that PVAT-dependent thermogenesis prevented atherosclerosis development (Xiong et al., 2017). Thus, our ferret data suggest that the increased browning and decreased inflammation in tPVAT may have a functional cardioprotective role. This assumption is supported by the concept that inflammatory adipocyte-derived factors from a dysfunctional PVAT have been related to cardiovascular risk (Nosalski and Guzik, 2017). Therefore, a lower fat mass (due to browning induction and/or increased white adipose tissue lipolysis), as well as immune-suppression, would be related to a lower production of inflammatory signals acting on vascular endothelia with a consequent protection from vascular inflammation, cumulatively having a protective role.

Besides thermogenic stimulation, it is widely known that cold acclimation induces an increased metabolic rate, evidenced by enhanced lipid catabolism (lipolysis and beta-oxidation), which occurs especially in WAT, providing increased serum NEFA levels (Trayhurn, 2005). In fact, MetaCore pathway analysis performed using all the differentially expressed genes ( $p$ -value < 0.05) revealed that energy metabolism, including TCA cycle and fatty acid beta-oxidation, increased in IAT of the cold group, a pattern which was not so clearly evident in tPVAT (see scheme in **Figure 5**). Thus, in IAT, cold exposure up-regulated genes involved in beta-oxidation (*Acadm*, *Acads*, *Acadvl*, *Cpt2*, *Ehhadh* and *Hadha*), and in the TCA cycle (*Dld*, *Fh*, *Idh3b*, *Mdh2*, *Ogdh*, *Sucla2* and *Sdh*). Related to this, between the top up-regulated genes as result of cold acclimation in the IAT, we also found genes involved in long chain fatty acid transport into the adipocytes (*Fabp3*), and genes of the mitochondrial electron transport chain (such as cytochrome c complex) and oxidative phosphorylation (*Slc25a4*). Altogether, these cold exposure adaptations reflect an increased use of fatty acids in IAT, which is not so evident in tPVAT.

Notably, associated with the increased capacity for lipid catabolism observed in IAT, cold acclimation induced a lower

mass of the whole depot. Interestingly, it has been reported, in rodents, that during adaptation to cold, and in connection to the decreased adipocyte size resulting from increased lipolysis, there is an expansion of extracellular space (Suter, 1969). Our data in ferret IAT go in the same direction, as 23 of the 50 down-regulated genes by cold exposure were related to cell structure and cytoskeleton organization, reflecting structural adaptations in this tissue and resembling adipose tissue adaptations as seen after massive weight loss (Roumans et al., 2017; Vink et al., 2017). Particularly, 32% of these down-regulated genes encoded for collagen or collagen-related pathways. Two of these are *Col6a3* and *Lum* that, besides their structure-related functions, have also been related with obesity development (Takahashi et al., 1993; Nakajima et al., 1998; Khan et al., 2009). *Col6a3* encodes a collagen type highly expressed in WAT that possesses an important role in adipocyte physiology and is positively correlated with the dysregulation of human adipose tissue in obesity (Khan et al., 2009). Absence of *Col6a3* is associated with lower body weight and fat mass, and with an improved metabolic phenotype (Nakajima et al., 1998; Khan et al., 2009). *Lum*, which encodes lumican, a proteoglycan identified to bind fibrillar collagen VI, is positively correlated with obesity (Khan et al., 2009). Moreover, interestingly, it has been recently reported that reduced adipose tissue fibrosis mediated by a cold-inducible transcription factor improves glucose homeostasis with independence of UCP1-mediated thermogenesis (Hasegawa et al., 2018). Thus, taken together, our results suggest that the reduction of IAT mass in cold-exposed animals is accompanied with a decreased presence of extracellular matrix components, as collagen and the proteoglycans, which could be a signal of an improved metabolic state because of cold exposure.

We conclude that acclimation to cold reduces the gene expression differences between tPVAT and IAT, with both adipose tissues responding to cold exposure in a depot-specific manner. Thoracic aortic PVAT is particularly sensitive to cold exposure, as evidenced by a higher gene expression response of brown/brite markers in comparison to the IAT, and by the dramatic morphologic remodeling of the tissue, with the appearance of abundant UCP1-positive stained brite adipocytes. Moreover, cold exposure induced a drastic immunosuppression in this PVAT depot, which is considered to contribute to an improved

cardiovascular health. On the other hand, the IAT follows a different cold-exposure adaptation pattern, not only related to increased browning, but with increased fatty acid mobilization as well as an increased TCA cycle, which is translated into lower mass of this adipose depot. This is not coincident with what is reported in rodents, where IAT is the adipose tissue that is most susceptible to browning (Petrov et al., 2015). However, results showing induction of browning in comparison to subcutaneous fat go in the same direction as data obtained in humans, indicating that adipocytes surrounding the aorta present markers of major thermogenic activity than adipocytes coming from subcutaneous adipose tissue (Vargas et al., 2018). Thus, our current data reinforce the use of ferret as an interesting animal model to mimic human browning in comparison to rodents.

In summary, the most relevant result from our study is the higher browning capacity of tPVAT in response to cold exposure in ferrets, which is accompanied by a profound immunosuppression in this depot. Taking into consideration the known protective cardiovascular effect of both aspects this animal model appears as very promising to perform cardiovascular disease research more likely to be extrapolated to humans than research performed with rodents.

## ETHICS STATEMENT

This study was carried out in accordance with the recommendations of Directive 2010/63/EU of the European Parliament on the protection of animals used for scientific purposes. The protocol was approved by the Bioethical Committee of the University of the Balearic Islands.

## REFERENCES

- Aldiss, P., Davies, G., Woods, R., Budge, H., Sacks, H. S., and Symonds, M. E. (2017). 'Browning' the cardiac and peri-vascular adipose tissues to modulate cardiovascular risk. *Int. J. Cardiol.* 228, 265–274. doi: 10.1016/j.ijcard.2016.11.074
- Bonet, M. L., Oliver, P., and Palou, A. (2013). Pharmacological and nutritional agents promoting browning of white adipose tissue. *Biochim. Biophys. Acta* 1831, 969–985. doi: 10.1016/j.bbalip.2012.12.002
- Boström, P., Wu, J., Jedrychowski, M. P., Korde, A., Ye, L., Lo, J. C., et al. (2012). A PGC1- $\alpha$ -dependent myokine that drives brown-fat-like development of white fat and thermogenesis. *Nature* 481, 463–468. doi: 10.1038/nature10777
- Cannon, B., and Nedergaard, J. (2004). Brown adipose tissue: function and physiological significance. *Physiol. Rev.* 84, 277–359. doi: 10.1152/physrev.00015.2003
- Chatterjee, T. K., Stoll, L. L., Denning, G. M., Harrelson, A., Blomkalns, A. L., Idelman, G., et al. (2009). Proinflammatory phenotype of perivascular adipocytes: influence of high-fat feeding. *Circ. Res.* 104, 541–549. doi: 10.1161/CIRCRESAHA.108.182998
- Choe, S. S., Huh, J. Y., Hwang, I. J., Kim, J. I., and Kim, J. B. (2016). Adipose tissue remodeling: its role in energy metabolism and metabolic disorders. *Front. Endocrinol.* 7:30.
- Cinti, S. (2005). The adipose organ. *Prostaglandins Leukot Essent Fatty Acids* 73, 9–15.
- Cousin, B., Cinti, S., Morroni, M., Raimbault, S., Ricquier, D., Pénicaud, L., et al. (1992). Occurrence of brown adipocytes in rat white adipose tissue: molecular and morphological characterization. *J. Cell Sci.* 103(Pt 4), 931–942.
- Fitzgibbons, T. P., Kogan, S., Aouadi, M., Hendricks, G. M., Straubhaar, J., and Czech, M. P. (2011). Similarity of mouse perivascular and brown adipose tissues

## AUTHOR CONTRIBUTIONS

AP and PO conceived and designed the experiments. BR, EC, and PO carried out experimental procedures. BR, ES, JK, EC, PO, and AP participated in the data analysis and interpretation. BR and PO wrote the manuscript. All authors revised the definitive version, read and approved the final manuscript.

## FUNDING

This work was supported by the Spanish Government: INTERBIOBES-AGL2015-67019-P (MINECO/FEDER, EU) and by the University of the Balearic Islands (BIOTERM, FA42/2016).

## ACKNOWLEDGMENTS

CIBER de Fisiopatología de la Obesidad y Nutrición is an initiative of the ISCIII. Laboratory of Molecular Biology, Nutrition and Biotechnology as well as Human and Animal Physiology are members of the European Research Network of Excellence NuGO (The European Nutrigenomics Organization, EU Contract: FOOD-CT-2004-506360 NUGO).

## SUPPLEMENTARY MATERIAL

The Supplementary Material for this article can be found online at: <https://www.frontiersin.org/articles/10.3389/fphys.2019.01171/full#supplementary-material>

- and their resistance to diet-induced inflammation. *Am. J. Physiol. Heart Circ. Physiol.* 301, H1425–H1437. doi: 10.1152/ajpheart.00376.2011
- Fox, J. G. (1998). *Biology and Disease of the Ferret*. Philadelphia, PA: Lea & Febiger.
- French, S. S., Moore, M. C., and Demas, G. E. (2009). Ecological immunology: the organism in context. *Integr. Comp. Biol.* 49, 246–253. doi: 10.1093/icb/icip032
- Fuster, A., Oliver, P., Sánchez, J., Picó, C., and Palou, A. (2009). UCP1 and oxidative capacity of adipose tissue in adult ferrets (*Mustela putorius furo*). *Comp. Biochem. Physiol. A Mol. Integr. Physiol.* 153, 106–112. doi: 10.1016/j.cbpa.2009.01.007
- García-Ruiz, E., Reynés, B., Díaz-Rúa, R., Ceresi, E., Oliver, P., and Palou, A. (2015). The intake of high-fat diets induces the acquisition of brown adipocyte gene expression features in white adipose tissue. *Int. J. Obes.* 115, 1887–1895. doi: 10.1038/ijo.2015.112
- Hasegawa, Y., Ikeda, K., Chen, Y., Alba, D. L., Stifler, D., Shinoda, K., et al. (2018). Repression of adipose tissue fibrosis through a PRDM16-GTF2IRD1 complex improves systemic glucose homeostasis. *Cell Metab.* 27(1) 18:e186. doi: 10.1016/j.cmet.2017.12.005
- Hsu, S. M., Raine, L., and Fanger, H. (1981). Use of avidin-biotin-peroxidase complex (ABC) in immunoperoxidase techniques: a comparison between ABC and unlabeled antibody (PAP) procedures. *J. Histochem. Cytochem.* 29, 577–580. doi: 10.1177/29.4.6166661
- Ishibashi, J., and Seale, P. (2010). Medicine. beige can be slimming. *Science* 328, 1113–1114. doi: 10.1126/science.1190816
- Khan, T., Muise, E. S., Iyengar, P., Wang, Z. V., Chandalia, M., Abate, N., et al. (2009). Metabolic dysregulation and adipose tissue fibrosis: role of collagen VI. *Mol. Cell. Biol.* 29, 1575–1591. doi: 10.1128/MCB.01300-08
- Korhonen, H., Harri, M., and Asikainen, J. (1983). Thermoregulation of polecat and raccoon dog: a comparative study with stoat, mink and blue fox. *Comp.*

- Biochem. Physiol. A Comp. Physiol.* 74, 225–230. doi: 10.1016/0300-9629(83)90592-3
- Lee, P., Werner, C. D., Kebebew, E., and Celi, F. S. (2014). Functional thermogenic beige adipogenesis is inducible in human neck fat. *Int. J. Obes.* 38, 170–176. doi: 10.1038/ijo.2013.82
- Li, R. M., Chen, S. Q., Zeng, N. X., Zheng, S. H., Guan, L., Liu, H. M., et al. (2017). Browning of abdominal aorta perivascular adipose tissue inhibits adipose tissue inflammation. *Metab. Syndr. Relat. Disord.* 15, 450–457. doi: 10.1089/met.2017.0074
- Mazurek, T., and Opolski, G. (2015). Pericoronary adipose tissue: a novel therapeutic target in obesity-related coronary atherosclerosis. *J. Am. Coll. Nutr.* 34, 244–254. doi: 10.1080/07315724.2014.933685
- Montani, J. P., Carroll, J. F., Dwyer, T. M., Antic, V., Yang, Z., and Dulloo, A. G. (2004). Ectopic fat storage in heart, blood vessels and kidneys in the pathogenesis of cardiovascular diseases. *Int. J. Obes. Relat. Metab. Disord.* 28(Suppl. 4), S58–S65.
- Nakajima, I., Yamaguchi, T., Ozutsumi, K., and Aso, H. (1998). Adipose tissue extracellular matrix: newly organized by adipocytes during differentiation. *Differentiation* 63, 193–200. doi: 10.1111/j.1432-0436.1998.00193.x
- Nedergaard, J., Bengtsson, T., and Cannon, B. (2007). Unexpected evidence for active brown adipose tissue in adult humans. *Am. J. Physiol. Endocrinol. Metab.* 293, E444–E452.
- Nosalski, R., and Guzik, T. J. (2017). Perivascular adipose tissue inflammation in vascular disease. *Br. J. Pharmacol.* 174, 3496–3513. doi: 10.1111/bph.13705
- Oh, D. Y., and Hurt, A. C. (2016). Using the Ferret as an animal model for investigating influenza antiviral effectiveness. *Front. Microbiol.* 7:80. doi: 10.3389/fmicb.2016.00080
- Palou, A., Picó, C., Bonet, M. L., and Oliver, P. (1998). The uncoupling protein, thermogenin. *Int. J. Biochem. Cell Biol.* 30, 7–11. doi: 10.1016/s1357-2725(97)00065-4
- Payne, G. A., Kohr, M. C., and Tune, J. D. (2012). Epicardial perivascular adipose tissue as a therapeutic target in obesity-related coronary artery disease. *Br. J. Pharmacol.* 165, 659–669. doi: 10.1111/j.1476-5381.2011.01370.x
- Pellis, L., Franssen-van Hal, N. L., Burema, J., and Keijer, J. (2003). The intraclass correlation coefficient applied for evaluation of data correction, labeling methods, and rectal biopsy sampling in DNA microarray experiments. *Physiol. Genom.* 16, 99–106. doi: 10.1152/physiolgenomics.00111.2003
- Petrov, P. D., Ribot, J., Palou, A., and Bonet, M. L. (2015). Improved metabolic regulation is associated with retinoblastoma protein gene haploinsufficiency in mice. *Am. J. Physiol. Endocrinol. Metab.* 308, E172–E183. doi: 10.1152/ajpendo.00308.2014
- Petrovic, N., Walden, T. B., Shabalina, I. G., Timmons, J. A., Cannon, B., and Nedergaard, J. (2010). Chronic peroxisome proliferator-activated receptor gamma (PPARGamma) activation of epididymally derived white adipocyte cultures reveals a population of thermogenically competent. UCP1-containing adipocytes molecularly distinct from classic brown adipocytes. *J. Biol. Chem.* 285, 7153–7164. doi: 10.1074/jbc.M109.053942
- Pfaffl, M. W. (2001). A new mathematical model for relative quantification in real-time RT-PCR. *Nucleic Acids Res.* 29:e45.
- Reynés, B., van Schothorst, E. M., García-Ruiz, E., Keijer, J., Palou, A., and Oliver, P. (2017). Cold exposure down-regulates immune response pathways in ferret aortic perivascular adipose tissue. *Thromb. Haemost.* 117, 981–991. doi: 10.1160/TH16-12-0931
- Roumans, N. J. T., Vink, R. G., Bouwman, F. G., Fazlzadeh, P., van Baak, M. A., and Mariman, E. C. M. (2017). Weight loss-induced cellular stress in subcutaneous adipose tissue and the risk for weight regain in overweight and obese adults. *Int. J. Obes.* 41, 894–901. doi: 10.1038/ijo.2016.221
- Saito, M. (2013). Brown adipose tissue as a regulator of energy expenditure and body fat in humans. *Diabetes Metab. J.* 37, 22–29. doi: 10.4093/dmj.2013.37.1.22
- Sánchez, J., Fuster, A., Oliver, P., Palou, A., and Picó, C. (2009). Effects of beta-carotene supplementation on adipose tissue thermogenic capacity in ferrets (*Mustela putorius furo*). *Br. J. Nutr.* 102, 1686–1694. doi: 10.1017/S0007114509991024
- Seale, P., Conroe, H. M., Estall, J., Kajimura, S., Frontini, A., Ishibashi, J., et al. (2011). Prdm16 determines the thermogenic program of subcutaneous white adipose tissue in mice. *J. Clin. Invest.* 121, 96–105. doi: 10.1172/JCI44271
- Speakman, J. R., and Keijer, J. (2012). Not so hot: optimal housing temperatures for mice to mimic the thermal environment of humans. *Mol. Metab.* 2, 5–9. doi: 10.1016/j.molmet.2012.10.002
- Stittelaar, K. J., de Waal, L., van Amerongen, G., Veldhuis Kroeze, E. J., Fraaij, P. L., van Baalen, C. A., et al. (2016). Ferrets as a novel animal model for studying human respiratory syncytial virus infections in immunocompetent and immunocompromised hosts. *Viruses* 8:E168. doi: 10.3390/v8060168
- Suter, E. R. (1969). The fine structure of brown adipose tissue. I. Cold-induced changes in the rat. *J. Ultrastruct. Res.* 26, 216–241.
- Takahashi, T., Cho, H. I., Kublin, C. L., and Cintron, C. (1993). Keratan sulfate and dermatan sulfate proteoglycans associate with type VI collagen in fetal rabbit cornea. *J. Histochem. Cytochem.* 41, 1447–1457. doi: 10.1177/41.10.8245404
- Tran, K. V., Fitzgibbons, T., Min, S. Y., DeSouza, T., and Corvera, S. (2018). Distinct adipocyte progenitor cells are associated with regional phenotypes of perivascular aortic fat in mice. *Mol. Metab.* 9, 199–206. doi: 10.1016/j.molmet.2017.12.014
- Trayhurn, P. (2005). Endocrine and signalling role of adipose tissue: new perspectives on fat. *Acta Physiol. Scand.* 184, 285–293. doi: 10.1111/j.1365-201x.2005.01468.x
- van Schothorst, E. M., Pagmantidis, V., de Boer, V. C., Hesketh, J., and Keijer, J. (2007). Assessment of reducing RNA input for agilent oligo microarrays. *Anal. Biochem.* 363, 315–317. doi: 10.1016/j.ab.2007.01.016
- Vargas, D., Lopez, C., Acero, E., Benítez, E., Wintaco, A., Camacho, J., et al. (2018). Thermogenic capacity of human periaortic adipose tissue is transformed by body weight. *PLoS One* 13:e0194269. doi: 10.1371/journal.pone.0194269
- Villarroya, F., Cereijo, R., Gavalda-Navarro, A., Villarroya, J., and Giral, M. (2018). Inflammation of brown/beige adipose tissues in obesity and metabolic disease. *J. Intern. Med.* 284, 492–504. doi: 10.1111/joim.12803
- Vink, R. G., Roumans, N. J., Fazlzadeh, P., Tareen, S. H., Boekschoten, M. V., van Baak, M. A., et al. (2017). Adipose tissue gene expression is differentially regulated with different rates of weight loss in overweight and obese humans. *Int. J. Obes.* 41, 309–316. doi: 10.1038/ijo.2016.201
- Wang, S., and Yang, X. (2017). Inter-organ regulation of adipose tissue browning. *Cell Mol. Life Sci* 74, 1765–1776. doi: 10.1007/s00018-016-2420-x
- Wettenhall, J. M., and Smyth, G. K. (2004). limmaGUI: a graphical user interface for linear modeling of microarray data. *Bioinformatics* 20, 3705–3706. doi: 10.1093/bioinformatics/bth449
- Wu, J., Boström, P., Sparks, L. M., Ye, L., Choi, J. H., Giang, A. H., et al. (2012). Beige adipocytes are a distinct type of thermogenic fat cell in mouse and human. *Cell* 150, 366–376. doi: 10.1016/j.cell.2012.05.016
- Xiong, W., Zhao, X., Garcia-Barrio, M. T., Zhang, J., Lin, J., Chen, Y. E., et al. (2017). MitoNEET in perivascular adipose tissue blunts atherosclerosis under mild cold condition in mice. *Front. Physiol.* 8:1032. doi: 10.3389/fphys.2017.01032
- Zuriaga, M. A., Fuster, J. J., Gokce, N., and Walsh, K. (2017). Humans and mice display opposing patterns of "Browning" gene expression in visceral and subcutaneous white adipose tissue depots. *Front. Cardiovasc. Med.* 4:27. doi: 10.3389/fcvm.2017.00027

**Conflict of Interest Statement:** The authors declare that the research was conducted in the absence of any commercial or financial relationships that could be construed as a potential conflict of interest.

Copyright © 2019 Reynés, van Schothorst, Keijer, Ceresi, Oliver and Palou. This is an open-access article distributed under the terms of the Creative Commons Attribution License (CC BY). The use, distribution or reproduction in other forums is permitted, provided the original author(s) and the copyright owner(s) are credited and that the original publication in this journal is cited, in accordance with accepted academic practice. No use, distribution or reproduction is permitted which does not comply with these terms.

# Advantages of publishing in Frontiers



## OPEN ACCESS

Articles are free to read  
for greatest visibility  
and readership



## FAST PUBLICATION

Around 90 days  
from submission  
to decision



## HIGH QUALITY PEER-REVIEW

Rigorous, collaborative,  
and constructive  
peer-review



## TRANSPARENT PEER-REVIEW

Editors and reviewers  
acknowledged by name  
on published articles

## Frontiers

Avenue du Tribunal-Fédéral 34  
1005 Lausanne | Switzerland

**Visit us:** [www.frontiersin.org](http://www.frontiersin.org)

**Contact us:** [info@frontiersin.org](mailto:info@frontiersin.org) | +41 21 510 17 00



## REPRODUCIBILITY OF RESEARCH

Support open data  
and methods to enhance  
research reproducibility



## DIGITAL PUBLISHING

Articles designed  
for optimal readership  
across devices



## FOLLOW US

@frontiersin



## IMPACT METRICS

Advanced article metrics  
track visibility across  
digital media



## EXTENSIVE PROMOTION

Marketing  
and promotion  
of impactful research



## LOOP RESEARCH NETWORK

Our network  
increases your  
article's readership